

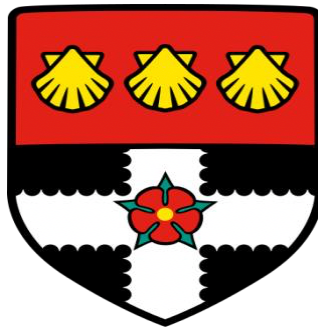
The University of Reading

Investigation of the FetMP-FetABCDEF (Ftr1-P19) Iron-Uptake

System of *Campylobacter jejuni*

A thesis submitted for the degree of Doctor of Philosophy in Microbiology

by
Dhama AlSallami



**Division of Microbiology
School of Biological Sciences
The University of Reading
Reading**

UK

July 2019

Declaration

I confirm that this is my own work and the use of all material from other sources has been properly and fully acknowledged

Dhama AlSallami

Signed:

Date:

Abstract

C. jejuni is the major cause of human gastroenteritis worldwide (including industrialized nations) inducing mild to acute infection and, in some cases, Guillain–Barré syndrome or reactive arthritis. Infection is largely foodborne, and chickens are considered to be the major source. Chicken gut colonisation by *C. jejuni* depends upon its iron-acquisition ability, as previously shown for *feo* mutants (impaired for ferrous iron uptake). In addition to the well-characterised FeoAB system, *C. jejuni* carries a second potential ferrous-iron transporter that is encoded by the Fe-Fur regulated *ftr-p19* genes. P19 is a periplasmic, Cu-containing and iron-binding protein thought to deliver iron to Ftr1 (an inner-membrane ferric permease) for high-affinity iron import.

Bioinformatic analysis indicated that the *ftr1-p19* genes are adjacent to a set of six conserved and Fe-Fur regulated genes (*cj1660-5*) of unknown function, that are predicted to contribute to Ftr1-p19 mediated iron uptake. The *cj1660-5* genes encode a predicted ATP-dependent periplasmic-mechanotransducer system of unclear purpose, two membrane anchored periplasmic thioredoxins and a potential inner-membrane-embedded electron-translocation factor. Gene context analysis showed that *ftr1-p19-cj1665*-like gene clusters are common in bacteria, and are particularly well conserved in *Campylobacter*, *Yersinia* and *Bifidobacterium* species. These observations suggest an important and potentially novel role for the *cj1660-5*-encoded components in bacterial iron uptake. The aim here was to further explore the functions of the P19 system (in particular the *cj1660-5* components) in iron uptake by *C. jejuni*.

The *ftr1-p19* and *cj1660-5* genes of *C. jejuni* NCTC 11168 were expressed in *E. coli* JC32 (an iron-transport-deficient strain), both individually and in combination, using the compatible pBADrha and pBADara vectors. Both the *ftr1-p19* and *cj1660-5* genes were found to enhance the iron-restricted growth of JC32 (with respect to vector controls) but this

effect was only observed at acidic pH. Inactivation of *ftr1*, *cj1660* and *cj1663* (substitution with a *cat* cassette) resulted in a significant growth inhibition for all three *C. jejuni* mutants in Muller-Hinton broth (low iron) at acidic pH, which was reversed with addition of iron or in rich medium. Complementing plasmids carrying *ftr1-p19* or *cj1660-5* were generated using pMA1 and these elicited a reversal of the iron-restriction phenotype of the mutants. Thus, the results generated here strongly indicate a role for Cj1660-5, as well as Ftr1, in iron uptake in *C. jejuni*. This finding is consistent with recently published research by another group. Chicken gut (caecum) colonisation experiments with 20-day-old chickens were performed using a highly motile and strongly colonising strain (PT14). The results showed weak colonisation levels at 3 dpi for all three mutants, but at 7 dpi the *cj1660* and *cj1663* mutants had adapted to show colonisation levels similar to those of the wildtype. The *ftr1* mutant retained a lower colonisation level than the wildtype at 7 dpi but had increased levels with respect to those at 3 dpi. It is suggested that the low colonisation levels seen at 3 dpi are due to the reduced growth (extended lag phase) of the mutants under iron restriction (as seen *in vitro*) and that by 7 dpi the *cj1660* and *cj1663* mutants have had sufficient time to overcome their growth lag such that a normal colonisation levels are achieved.

qRT-PCR was used to test the iron and Fur dependence of the expression of the *ftr1-cj1665* cluster, and their cotranscription potential. The results suggest that the genes are indeed expressed as a co-transcript and that they are subject to a high degree of induction (by 100-2200-fold) under low-iron conditions. This expression effect was strongly dependent on Fur. The Fur-dependent induction under low-iron conditions is consistent with previous reports. However, the *fur* mutant strain showed downregulation the *ftr1-cj1665* genes iron sufficient and deficient conditions suggesting that these genes are subject apoFur activation. This is in contrast to several previous reports that are consistent with an Fe-Fur repression mode of regulation (although Fur is considered to act as an activator in some instances in *C. jejuni*).

The reason for this difference in Fur control, as found here, is unclear and requires further investigation.

In conclusion, this work provides clear evidence that the *ftr1-cj1665* gene cluster has a role as an iron transport system under low pH and is therefore required for normal low-iron growth *in vitro* and is necessary for optimal colonisation of the chicken gut. Further work is necessary to determine precisely how the Cj1660-5 components contribute to iron acquisition, and the role played by the Ftr1-Cj1665 system in iron uptake with respect to that of other iron transporters (particularly FeoAB) in *C. jejuni*.

POSTER/ ORAL PRESENTATION

1. The Postgraduate Symposium, University of Reading, 26 May 2016. (oral)
Investigation of the FetMP-FetABCDEF (Ftr1-P19) Iron-Uptake System of *Campylobacter jejuni*. Dhama Alsallami and Simon C. Andrews.
2. The Postgraduate Symposium, University of Reading, 13 June 2017. (oral).
Investigation of the FetMP-FetABCDEF (Ftr1-P19) Iron-Uptake System of *Campylobacter jejuni*. Dhama Alsallami and Simon C. Andrews.
3. The Annual Microbiology Society conference in Birmingham, 10-13 April 2018.
(poster). Investigation of the FetMP-FetABCDEF (Ftr1-P19) Iron-Uptake System of *Campylobacter jejuni*. Dhama Alsallami, Simon C. Andrews and Sheila MacIntyre.
4. The Annual Microbiology Society conference in Belfast, 8-11 April 2019.
(poster) Investigation of the FetMP-FetABCDEF (Ftr1-P19) Iron-Uptake System of *Campylobacter jejuni*. Dhama Alsallami, Simon C. Andrews, Ian Connerton and Sheila MacIntyre.

Dedication

- To my mother and my father for their support and praying for me.
- My husband for his continuous support and patience.
- My children for their pure love and patience.
- My friends and my colleagues in the lab for all their help and support.

Acknowledgements

(In the name of Allah, the most beneficent, the most merciful and Allah's peace and blessings be upon his messenger)

Firstly, I give thanks to Allah who has given me my health and the ability to accomplish this work.

I would like to express my deepest gratitude to my advisor prof Simon Andrews for his continuous support, patience, valuable guidance, motivation, immense knowledge, and full support during the course of this study. I want to say that I feel very fortunate and honoured to have had the opportunity to work with you.

I would also like to thank my supervisory committee members, Dr. Sheila MacIntyre for her advice, guidance, and support as my second supervisor, Dr. Simon Clark and Dr. Gemma Walton for their insightful comments as a postgraduate committee.

My sincere thanks also go to Mr. Simon Fiest, Mr. Kevan, Mrs. Jay and Mr. Jordan, all CSS family who gave access to the laboratory and research facilities. Without their precious support it would not be possible to conduct this research.

I would like to express a special appreciation to my beloved husband, Amjed Alsultan for his continued love, encouragement, and support throughout the duration of this study. My deep thanks go to little kids for their patience. Also, special thanks to my big family, my parents and my sisters for their support and encouragement.

I would also like to express a special appreciation my sponsor the higher committee for education development in Iraq (HCED) for sponsoring my PhD study. Many thanks to the microbiology society for funding me to attend their annual conferences. Special thanks go out to all members of Professor Ian Connerton's laboratory at Nottingham University, especially Ian Connerton himself and Phillippa Connerton, for including me and guiding me during our collaborative chicken trial. I gratefully acknowledge Dr. Anisha in food bioscience for her effort and knowledge to analyse my NMR samples. Many thanks to the technician Ann in the soil department for ICP analysis of my samples with her master student.

Finally, I would like to thank all current and previous members of Prof. Simon Andrew's iron research lab and other labs in the building, especially; Aida Allawatti, Othman Mohammed, Salem Al-aidy, Rana Hilmi, Christopher Moon, Abdul- Ameer Ghareeb, Fawzi Issa, Nancy Elhalfawy, Marwa, Arvind, Afrah, Fawzih Al-Zahrani, Ameena Alutaibi, Noora, Kang, Andrea, Sheama, Liuis, Xara, Fawzia, Atika, Auraquazeb for their scientific criticized discussions and being incessantly supporting and helping me to overcome difficulties during my PhD.

List of Contents	Page
Abstract	iii
Chapter 1: Literature Review	
1.1: Campylobacter	1
1.2: <i>Campylobacter</i> history and taxonomy	4
1.3: <i>Campylobacter</i> genome	6
1.4: <i>Campylobacter</i> metabolism	8
1.5.1: Motility and chemotaxis	11
1.5.2: Adhesion and invasion	13
1.5.3: Bacterial Toxins	16
1.6: Niche and epidemiology of <i>Campylobacter</i>	18
1.7: Iron uptake in <i>Campylobacter</i>	21
1.7.1: Iron	21
1.7.2: The ferrous (Feo) iron uptake system	22
1.7.2.1: General overview	22
1.7.2.2: FeoAB of <i>C. jejuni</i>	23
1.7.3: Siderophore-dependent iron uptake	24
1.7.3.1: General overview	24
1.7.3.2: Utilisation of ferri-siderophores by <i>C. jejuni</i>	26
1.7.4. Heam utilisation	27
1.7.5. Transferrin and lactoferrin utilisation	27
1.7.6: Ftr-P19 (FetM-FetP) iron uptake system of <i>C. jejuni</i>, and related systems	28

1.8: Iron storage in <i>Campylobacter</i>	33
1.9: Iron regulation in <i>Campylobacter</i>	34
1.9.1. General overview	34
1.9.2. Fur in <i>C jejuni</i>	36
1.10: Redox stress and oxygen tolerance in <i>Campylobacter</i>	37
1.11: Aims and objectives of this study	41
Chapter 1 Figures	
Figure 1.1: Sources of <i>Campylobacter jejuni</i> infection	4
Figure 1.2: <i>C. jejuni</i> genome in circular representation	8
Figure 1.3: Overview of <i>Campylobacter</i> colonisation stages in human intestines	18
Figure 1.4: Organisation of the <i>feoAB</i> operon of <i>C. jejuni</i> NCTC 11168	23
Figure 1.5: Iron-uptake systems of <i>C. jejuni</i>	28
Figure 1.6: Structure of P19 from <i>C. jejuni</i>	30
Figure 1.7: The <i>p19</i> gene cluster in <i>C. jejuni</i> subsp. <i>jejuni</i> serotype O:2 (strain ATCC 700819/ NCTC 11168)	33
Figure 1.8: Schematic description of Fur and RyhB regulation in <i>E. coli</i>	36
Figure 1.9: Schematic figure of CosR (the oxidative stress regulator), Fur (the ferric uptake regulator) and PerR (the peroxide resistance regulator) control in <i>C. jejuni</i>	40

Chapter 2: Materials and Methods	
2.1. Chemicals	42
2.2. Enzymes	42
2.3. DNA marker	42
2.4. Antibiotics	43
2.5. Microbiological media	44
2.5.1. Lysogeny broth medium (LB)	44
2.5.2. M9 minimal medium	44
2.5.3. Blood agar	45
2.5.4. Brain Heart Infusion medium	45
2.5.5. Muller-Hinton medium	45
2.5.6. Dulbecco's Modified Eagle Medium	45
2.5.7. SOC media	45
2.6. Centrifugation	46
2.7. Bacterial strains	46
2.8. Plasmids	51
2.9. Primers used in this study for PCR amplification and sequencing	53
2.10. Harvesting and stocking of <i>C. jejuni</i> strains	61
2.11. DNA manipulation and analysis methods	61
2.11.1. Extraction of genomic DNA	61
2.11.2. Polymerase chain reaction	61

2.11.3. Purification of PCR products	62
2.11.4. Isolation of plasmid DNA (minipreps)	62
2.11.5. Restriction digestion	62
2.11.6. Estimation of DNA concentration	63
2.11.7. In-Fusion cloning	63
2.11.8. Cloning using the CloneJET PCR Cloning Kit	63
2.11.9. Blunting reaction	64
2.11.10. Ligation reaction	64
2.12. Agarose gel electrophoresis	64
2.13. RNA extraction	65
2.13.1. Extraction of total RNA from <i>C. jejuni</i>	65
2.13.2. Synthesis of cDNA	66
2.13.3. Quantitative PCR (qPCR)	67
2.14. Preparation of competent cells	69
2.14.1. Preparation of chemically competent cells from <i>E. coli</i> strains	69
2.14.2. Preparation of electro competent cells from <i>C. jejuni</i> strains	70
2.15. Using of DNA to transform into the competent cells	71
2.15.1. Transformation into competent <i>E. coli</i> strains	71
2.15.2. Transformation into <i>E. coli</i> Stellar competent cells	71
2.15.3. Transformation into the <i>C. jejuni</i> electro-competent cells by electroporation	71

2.15.4. Transformation into the <i>C. jejuni</i> by bi-parental conjugation	72
2.16. Gene inactivation (knockout)	73
2.16.1. Gene amplification and ligation	73
2.16.2. Inverse PCR and gene deletion	73
2.16.3. The PCR amplification of <i>cat</i> cassette	73
2.16.4. Cloning of the <i>cat</i> cassette into the deletion sites	74
2.17. Phenotypic studies with complemented <i>E. coli</i> strains	74
2.17.1. Serial dilutions tests on M9 agar plates	74
2.17.2. Growth test for <i>E. coli</i> under aerobic conditions	75
2.17.3. Growth test of <i>E. coli</i> under low-oxygen conditions	75
2.18. <i>Campylobacter</i> growth assay	76
2.18.1. Preparation of standardised cultures	76
2.18.2. Viable cell count (CFU)	76
2.18.3. <i>Campylobacter</i> motility test	77
2.18.4. Microtiter plate growth assay	77
2.18.5. Growth in flasks with shaking	77
2.19. Preparation of NMR metabolomics samples	78
2.20. Preparation of ICP-OES samples	78
2.21. Colonisation of chickens with <i>C. jejuni</i>	78
2.21.1. Chicken trial	78

2.21.2. Processing of samples	79
2.21.3. Draft genome sequencing	80
2.22. Bioinformatic analysis	80
2.22.1. Initial analysis of the gene locus of <i>frt1-p19</i> cluster in <i>C. jejuni</i> NCTC 11168	80
2.22.2. Using Gene Context Tool 3 database	81
2.22.3. Using Geneious prime software	81
2.22.4. Sanger sequencing and analysis of resulting nucleotide-sequence data	81
2.23. Statistical analysis	81
Chapter 2 Figures	
Figure 2.1. GeneRuler 1 kb DNA ladder	42
Chapter 2 Tables	
Table 2.1: Antibiotics used in this work	43
Table 2.2. Bacterial strain used in this study	46
Table 2.3. Plasmids used in this study	51
Table 2.4. Primers used for amplification and cloning of wildtype genes into pBAD_{rha} and pBAD_{ara} plasmids, and for sequencing	54
Table 2.5. Primers used for generation of knockout constructs	56
Table 2.6. Primers used for generation of complementation constructs	60
Table 2.7. Primers used to confirm <i>C. jejuni</i> AS230 Δfur	60
Table 2.8. Primers used in qRT-PCR	68

Chapter 3: Bioinformatics analysis of the P19 system of *C. jejuni*

3.1. Introduction	83
3.2. Initial analysis of the gene locus of the <i>ftr1-p19</i> cluster in <i>C. jejuni</i>	84
3.3. <i>p19</i> gene cluster distribution and organisation	87
3.4. Ftr1-P19 (FetMP) functional analysis	94
3.4.1. P19 protein	95
3.4.2. Ftr1 (iron permease)	98
3.5. Cj1660-65 and homologues	106
3.5.1. Cj1660 – an integral membrane protein associated with ABC transporters	106
3.5.2. Cj1661 and Cj1662 – noncanonical ABC transport system permease subunits	112
3.5.3. ABC transporter ATP-binding cassette protein (Cj1663)	117
3.5.4. Thioredoxin proteins	118
3.6. Discussion and Conclusion	122
3.6.1. Gene organisation and taxonomic distribution	122
3.6.2. P19	123
3.6.3. Ftr1	123
3.6.4. The DUF2318-YHS protein	124
3.6.5. The ABC-associated extra-cytoplasmic mechanotransducer components	125
3.6.6. Membrane-anchored, periplasmic thioredoxins	126
3.6.7. A model for Cj1660-5 (FetA-F)	127

Chapter 3 Figures

Figure 3.1. Physical map and genetic organisation of the <i>fetMP-fetABCDEF</i> region of <i>Campylobacter jejuni</i> (subsp. <i>jejuni</i> NCTC 11168; ATCC 700819)	85
Figure 3.2. Nucleotide sequence of the <i>fetMP-fetABCDEF</i> locus of <i>Campylobacter jejuni</i> NCTC 11168	86
Figure 3.3. Gene Context Tool comparison of selected bacterial genome regions containing <i>p19</i> homologues	93
Figure 3.4. A physical map of <i>ftr1-p19</i> and <i>fetA-F</i> locus of <i>C. jejuni</i> NCTC 11168 combined with predicted functional motif data of translation products	94
Figure 3.5. Alignment of amino acid sequence of P19 proteins	96
Figure 3.6. Phylogenetic tree of P19 proteins	97
Figure 3.7. Two-dimension plot of the predicted membrane topology of Ftr1 from <i>C. jejuni</i> NCTC 11168	99
Figure 3.8. Domain organisation of FTR1 domain proteins	100
Figure 3.9. Multiple amino acid sequence alignment of Ftr1-like proteins	101
Figure 3.10. Phylogenetic tree of FTR1 domains	102
Figure 3.11. Multiple amino acid sequence alignment of the N-terminal domain of <i>C. jejuni</i> Ftr1 (residues 1-300) with homologues	103
Figure 3.12. Phylogenetic tree of the N-terminal domain of FTR1 proteins in the DO2 group	105
Figure 3.13. Two-dimension plot of <i>C. jejuni</i> NCTC 11168 Cj1660 membrane topology	105
Figure 3.14. Domain organisation of Cj1660	108

Figure 3.15. Multiple sequence alignment of the DUF2318 domain of Cj1660 and selected homologues	109
Figure 3.16. Phylogenetic tree of the DUF2318 domain region of Cj1660 and related proteins from a range of taxonomic groups	110
Figure 3.17. Multiple alignment (A) and phylogenetic tree (B) for YHS domain proteins and the YHS domain of Cj1660	111
Figure 3.18. Pairwise alignment of Cj1661 and Cj1662	112
Figure 3.19. Domain organisation and topology plot of Cj1661 and Cj1662	113
Figure 3.20. The most common MacB_PCD domain architectures	113
Figure 3.21. Domain organisation and topology of the MacB protein of <i>Aggregatibacter actinomycetemcomitans</i>	116
Figure 3.22. Multiple alignment and phylogenetic tree of the FtsX domain of functionally defined MacB-like proteins	117
Figure 3.23. Predicted signal cleavage sites for Cj1664 (A) and Cj1665 (B)	119
Figure 3.24. Location of the <i>lolA</i> and <i>lolC/E</i> genes of <i>C. jejuni</i> NCTV 11168	120
Figure 3.25. Dot plot (A) and pairwise comparison (B) of the Cj1664 and Cj1665 full-length amino acid sequences	121
Figure 3.26: Schematic representation of the common gene organisations associated with <i>p19</i>	122
Figure 3.27: Model indicating the potential functions of the Cj1660-5 proteins in assisting Ftr1-P19-mediated iron uptake in <i>C. jejuni</i>	128
Chapter 4: Phenotypic studies of iron-transporter-deficient <i>E. coli</i> complemented with the FetMP-FetABCDEF iron transporter from <i>C. jejuni</i> NCTC 11168	
4.1. Introduction	129

4.2. Generation of plasmids carrying iron transport genes from <i>C. jejuni</i>	130
4.3. Complementation of iron-uptake mutant <i>E. coli</i> JC32 by <i>fetMP</i> and <i>fetA-F</i> from <i>C. jejuni</i> on solid media	141
4.3.1. Complementation of iron-uptake mutant, <i>E. coli</i> JC32, with <i>fetMP</i>	141
4.3.2. Complementation of iron-uptake mutant <i>E. coli</i> JC32 by <i>fetA-F</i>	143
4.3.3. Complementation of iron-uptake mutant <i>E. coli</i> JC32 by both <i>fetMP</i> and <i>fetA-F</i>	145
4.4. Complementation of iron-uptake mutant phenotype <i>E. coli</i> JC32 by <i>fetMP</i> and <i>fetA-F</i> from <i>C. jejuni</i> in liquid medium	147
4.4.1. <i>fetMP</i> enhances low-iron growth under acidic pH	147
4.4.2. <i>fetA-F</i> enhances growth of <i>E. coli</i> JC32 under acidic pH	152
4.4.3. Can <i>fetMP</i> and <i>fetA-F</i> act together to enhance growth of JC32 under acidic pH?	154
4.4.4 Complementation of JC32 with two plasmids - a vector control together with a <i>fetMP</i> or <i>fetA-F</i> -carrying plasmid	157
4.4.4.1. Aerobic growth	157
4.4.4.2. Low-oxygen growth	160
4.5. Discussion	163
Chapter 4 Figures	
Figure 4.1. Agarose gel (0.7%) electrophoretic analysis of genomic DNA from <i>C. jejuni</i> NCTC 11168	131
Figure 4.2. Gel electrophoretic analysis of the <i>fetMP</i> PCR product	131

Figure 4.3. Gel electrophoretic analysis of the <i>fetA-F</i> PCR product	132
Figure 4.4. Gel electrophoretic analysis of digested and undigested pBADrha	133
Figure 4.5. Gel electrophoretic analysis of undigested pBADara	134
Figure 4.6. Gel electrophoretic analysis of digested pBADara	134
Fig 4.7. Gel electrophoretic analysis of cut and uncut pBADrha plasmid DNA potentially carrying <i>ftr1-p19</i> (<i>fetMP</i>)	135
Fig 4.8. Gel electrophoretic analysis of cut and uncut pBADrha plasmid DNA potentially carrying <i>fetA-F</i>	136
Figure 4.9. Restriction map of A: pBADrha-<i>fetMP</i> and B: pBADrha-<i>fetA-F</i>	137
Figure 4.10. Gel electrophoretic analysis of cut and uncut pBADara plasmid DNA potentially carrying <i>fetMP</i>	138
Figure 4.11. Gel electrophoretic analysis of uncut and cut pBADara plasmid DNA potentially carrying <i>fetA-F</i>	139
Figure 4.12. Restriction map of A: pBADara-<i>fetMP</i> and B: pBADara-<i>fetA-F</i>	140
Figure 4.13. Growth of <i>fetMP</i>-complemented <i>E. coli</i> JC32 on M9 agar plates under high-iron conditions	142
Figure 4.14. Growth of <i>fetMP</i>-complemented <i>E. coli</i> JC32 on M9 agar plates under low iron conditions (1 μM DTPA)	142
Figure 4.15. Growth of <i>fetMP</i>-complemented <i>E. coli</i> JC32 on M9 agar plates under low iron conditions (4 μM DTPA)	143
Figure 4.16. Growth of <i>fetA-F</i>-complemented <i>E. coli</i> JC32 on M9 agar plates under high iron conditions	144
Figure 4.17. Growth of <i>fetA-F</i>-complemented <i>E. coli</i> JC32 on M9 agar plates under low iron conditions	144

Figure 4.18. Growth of <i>fetABCDEF</i> -complemented <i>E. coli</i> JC32 on M9 agar plates under low iron conditions	145
Figure 4.19. Growth of <i>fetMP/fetABCDEF</i> complemented <i>E. coli</i> JC32 on M9 agar plates under high-iron conditions	146
Figure 4.20. Growth of <i>fetMP/fetA-F</i> complemented <i>E. coli</i> JC32 on M9 agar plates under low iron (1 μ M DTPA)	146
Figure 4.21. Effect of <i>fetMP</i> on growth of JC32 under iron restriction at pH 5-9	150
Figure 4.22. Effect of <i>fetMP</i> on growth of JC32 under iron restriction at pH 5	151
Figure 4.23. Effect of <i>fetA-F</i> on growth of JC32 under iron restriction at pH 5-9	153
Figure 4.24. Effect of <i>fetA-F</i> on growth of JC32 under iron restriction at pH 5	154
Figure 4.25. Effect of complementation with both <i>fetMP</i> and <i>fetA-F</i> on growth of JC32 under iron restriction at pH 5	155
Figure 4.26. Effect of <i>rha-fetMP</i> or <i>ara-fetA-F</i> , along with a compatible pBAD vector, on the growth of JC32 under iron restriction	159
Figure 4.27. Effect of <i>rha-fetMP</i> or <i>ara-fetA-F</i> , along with the corresponding compatible pBAD vector, on the growth of JC32 under iron restriction and low-oxygen conditions, at pH 6	162
Chapter 5: Targeted mutation on the P19 system	
5.1. Introduction	167
5.2. Generation of a Δ <i>ftr1</i> mutant	168
5.2.1. Amplification the DNA of interest and cloning into the pJET 1.2 plasmid	168
5.2.2. The <i>ftr1</i> deletion by inverse PCR	170
5.2.3. Cloning of the <i>cat</i> cassette into the pJET- Δ <i>ftr1</i> deletion site	172

5.2.4. Transformation of pJET-Δ<i>ftr1</i>::<i>cat</i> into the <i>C. jejuni</i>	173
5.3. Generation of a Δ<i>cj1660</i> mutant	175
5.4. Generation of a Δ<i>cj1663</i> mutant	179
5.5. Construction of the <i>ftr1-p19</i> and <i>cj1660-65</i> complementation plasmids	182
5.6. Phenotypic studies of the <i>C. jejuni</i> NCTC 11168 mutants	186
5.6.1. Growth of the mutant strains in the minimal media	186
5.6.2. Growth of the mutant strains in iron-rich media	191
5.6.3. Effect of pH on the low-iron growth of the mutant strains	194
5.6.4. Growth of the mutant strains with iron chelator and iron reductant	198
5.7. Genetic complementation	201
5.8. Discussion	204

Chapter 5 Figures

Figure 5.1: Agarose gel (0.7%) electrophoretic analysis of *ftr1* PCR product with 1 kb upstream and 1 kb downstream region of *C. jejuni* NCTC 11168 169

Figure 5.2: Gel electrophoretic analysis of (pJET-*ftr1*) plasmid before and after digestion by *Bgl*III enzyme 169

Figure 5.3: Agarose gel (0.7%) electrophoretic analysis of inverse PCR product of pJET- Δ *ftr1* 170

Figure 5.4: Gel electrophoretic analysis of pVA35 vector (3811 bp), Cm^R plasmid extracted from *E. coli* Top10 171

Figure 5.5: Gel electrophoretic analysis of the *cat* gene (896 bp, 40 ng) PCR product 171

Figure 5.6: Gel electrophoretic analysis of <i>AsiSI</i>-digested pJETΔ<i>ftr1::cat</i>	
candidates	172
Figure 5.7: Diagram describing the strategy for generation of the gene knockout plasmids	173
Figure 5.8: Gel electrophoresis analysis of an Δ<i>ftr1::Cm^R</i> mutant of <i>C. jejuni</i> NCTC 11168 using <i>ftr1</i> F and <i>cat</i> R primers	174
Figure 5.9: Diagram describing the strategy for PCR-confirmation of the mutations in the <i>C. jejuni</i> chromosome	174
Figure 5.10: pJET1-Δ<i>ftr1::cat</i> map	175
Figure 5.11: Gel electrophoresis analysis of PCR product of <i>cj1660</i> with 1 kb upstream and downstream regions	176
Figure 5.12: Gel electrophoresis analysis of pJET-<i>cj1660</i> candidate plasmids digested with <i>Bgl</i>II	176
Figure 5.13: Gel electrophoresis analysis of inverse PCR of pJET-<i>cj1660</i>	177
Figure 5.14.: Gel electrophoresis of pJET-Δ<i>cj1660::cat</i> candidate digested with <i>AsiSI</i>	177
Figure 5.15: Gel electrophoresis analysis of PCR amplified Δ<i>cj1660::Cm^R</i> in <i>C. jejuni</i>	178
Figure 5.16: pJET-Δ<i>cj1660::cat</i> plasmid map	178
Figure 5.17: Gel electrophoresis analysis of the <i>cj1663</i> PCR product with 1 kb flanking DNA	179

Figure 5.18: Gel electrophoretic analysis pJET-<i>cj1663</i> candidates digest with <i>Bgl</i>III	180
Figure 5.19: Gel electrophoretic analysis of the pJET-Δ1663 product	180
Figure 5.20: Gel electrophoretic analysis of pJET-Δ1663::<i>cat</i> digested with <i>Asi</i>SI	181
Figure 5.21: Gel electrophoresis analysis of PCR products derived from candidate Δ<i>cj1663</i>::Cm^R mutants	181
Figure 5.22: pJET-Δ<i>cj1663</i>::<i>cat</i> plasmid map	182
Figure 5.23: Gel electrophoresis analysis of the pMA1 vector	183
Figure 5.24: Gel electrophoresis analysis of the <i>ftr1-p19</i> PCR product with <i>Kpn</i>I and <i>Xho</i>I restriction sites included for subsequent cloning into the pMA1 shuttle vector	183
Figure 5.25: Gel electrophoresis analysis of the <i>ftr1-p19</i> PCR product pMA1-<i>ftr1-p19</i>	184
Figure 5.26: pMA1-<i>ftr1-p19</i> (<i>fetMP</i>) plasmid map	184
Figure 5.27: Gel electrophoretic analysis of the <i>cj1660-65</i> PCR product with <i>Kpn</i>I and <i>Xho</i>I sites included	185
Figure 5.28: Gel electrophoretic analysis of the confirmation of the identity of pMA1-<i>cj1600-5</i> candidate by PCR	185
Figure 5.29: pMA1-<i>cj1660-65</i> (<i>fetA-F</i>) plasmid map	186
Figure 5.30: Microaerophilic growth comparisons of <i>C. jejuni</i> NCTC 11168 mutant and wildtype strains	191
Figure 5.31: Microaerophilic growth of <i>C. jejuni</i> NCTC 11168 wild type and mutant strains under iron-rich conditions	193

Figure 5.32: Microaerophilic growth curve of the <i>C. jejuni</i> NCTC 11168 wildtype and mutant strains in M-H broth medium buffered at pH 6, 7 and 8 with 25 mM MES-HEPES	197
Figure 5.33: Microaerophilic growth of <i>C. jejuni</i> in BHI broth medium with desferrioxamine chelator	199
Figure 5.34: Microaerophilic growth of <i>C. jejuni</i> in M-H broth medium with ascorbate	201
Figure 5.35: Complementation of the <i>C. jejuni</i> NCTC 11168 mutants with plasmid-borne <i>ptr1-p19</i> or <i>cj1600-5</i>	203
Chapter 6: Gut colonisation with <i>C. jejuni</i> in chicken	
6.1. Introduction	207
6.2. Generation of the mutations in <i>C. jejuni</i> PT14	208
6.3. PT14 mutant phenotypes	212
6.4. The chicken trials	214
6.4.1. Variation in the efficiency of chicken colonisation by the <i>C. jejuni</i> strains	214
6.4.1.1. 3 dpi	214
6.4.1.2. 7 dpi	215
6.4.1.3. Conclusion	216
6.4.2. Variation in the body weights of chickens following colonisation by the <i>C. jejuni</i> strains	219
6.4.3. Confirmation of the presence of the mutant genes in the recovered strains	221
6.5. Discussion	224

Chapter 6 Figures

Figure 6.1.: Zones of growth for <i>C. jejuni</i> NCTC 11168 on 0.4% agar M-H plates	209
Figure 6.2: Gel electrophoresis of the PCR amplification product of the Δ <i>ftr1::cat</i> mutation in <i>C. jejuni</i> PT14	210
Figure 6.3: Gel electrophoresis of the PCR amplification product of the Δ <i>cj1660::cat</i> mutation in <i>C. jejuni</i> PT14	210
Figure 6.4: Gel electrophoresis of the PCR amplification product of the Δ <i>cj1663::cat</i> mutation in <i>C. jejuni</i> PT14	211
Figure 6.5: Zones of growth for <i>C. jejuni</i> PT14 mutant strains on 0.4% agar M-H plates	212
Figure 6.6: Microaerophilic growth of <i>C. jejuni</i> PT14 mutants in M-H medium at 37 °C	213
Figure 6.7: Recovery of <i>C. jejuni</i> strains from the caecum of chickens at 3- and 7-days postchallenge	218
Figure 6.8: Body weight of the infected and control chickens over 27 days	220
Figure 6.9: Gel electrophoretic analysis of the PCR products confirming the identity of the mutants in the strains recovered from the chicken cecum contents at 3 dpi	221
Figure 6.10: Gel electrophoretic analysis of the PCR products confirming the identity of the mutants in the strains recovered from the chicken cecum contents at 7 dpi	222
Figure 6.11: The figure from IGV (Integrative Genomics Viewer) shows the deletion regions in the <i>C. jejuni</i> genomes of the mutant strains	223
Chapter 7: Iron- and Fur-regulation of <i>ftr1-p19/fetA-F</i> expression	
7.1. Introduction	227
7.2. Quantitative RT-PCR (qRT-PCR) analysis	229
7.3. Control transcripts	233
7.4. Generation of standard curve	234

7.5. Results	235
7.6. Discussion	240
Chapter 7 Figures	
Fig. 7.1. Transcriptional organisation of the <i>ftr1-p19/fetA-F</i> locus	229
Figure 7.2: Genetic map of <i>ftr1</i> cluster showing the amplified intergenic regions between neighbouring genes	231
Figure 7.3: Gel electrophoresis of PCR products generated in order to test the qPCR primers with the genomic DNA of <i>C. jejuni</i> NCTC 11168 as template	232
Figure 7.4: Gel electrophoresis of RNA samples extracted from <i>C. jejuni</i> NCTC 11168 grown in M-H medium	232
Figure 7.5: Gel electrophoresis of PCR products obtained using isolated total RNA as template to demonstrate lack of DNA contamination	233
Figure 7.6: Standard curve charts of the efficiency of the qPCR for each pair of primers	235
Figure 7.7: Effect of +/- Fe on relative expression in a wildtype and Δfur background	238
Chapter 7 Tables	
Table 7.1: Fold differences and <i>P</i> values for expression levels of each <i>p19</i> target between the wildtype and Δfur in the absence of iron	239
Chapter 8: General discussion	
8.1. Introduction	243
8.2. Gene organisation of p19 system	245
8.3. Bioinformatic analysis of the Ftr1-P19 and cj1660-5 components	245

8.4. Complementation of an iron-uptake deficient <i>E. coli</i> strain	247
8.5. The Ftr1-p19 and Cj1660-5 systems enhanced <i>in vitro</i> growth of <i>C. jejuni</i> under iron restriction	248
8.6 Inactivation of <i>ftr1</i>, <i>cj1660</i> or <i>cj1665</i> results in weak chicken gut colonisation	249
8.7. The <i>ftr1-cj1665</i> genes are highly induced by iron restriction in a Fur-dependent manner and form a co-transcript	250
8.8. Recent work by others on the Ftr1 system of <i>C. jejuni</i> strain 81-176	251
8.9. Future work	252
References	254
Appendix	293

Chapter 1: Literature Review

1.1: *Campylobacter*

Campylobacter spp. are spiral or curved, small, Gram-negative bacteria. They have a polar flagellum on one or both ends of their cell. They are oxidase and catalase positive, and negative for urease. *Campylobacter* spp. are microaerophilic. They need a low concentration of oxygen in the surrounding environment at about 3-15%, also require carbon dioxide at 3-10%, and are generally cultured in an atmosphere of 5% O₂, 10% CO₂ with 85% N₂ (van Vliet and Ketley, 2001; Hoffman and Goodman, 1982). There are around 26 different species in the *Campylobacter* genus (Murphy *et al.*, 2017). They grow optimally at temperatures between 37-42 °C, the more thermophilic species of *Campylobacter* like *C. coli* and *C. jejuni* require temperatures of 34-44 °C to grow and reproduce (van Vliet and Ketley, 2001). *C. jejuni* is unable to grow at less than 30 °C or more than 47 °C but has been shown to respire and exhibit motility at 4 °C (Humphrey and Cruickshank, 1985). *C. jejuni* also changes shape from spiral to coccoid under stress conditions, including in stationary phase. The coccoid form has been termed as 'viable but non-culturable' (VBNC). It has been suggested that the VBNC state might be an evolutionary strategy to survive between hosts, but there is still debate regarding the ability of these forms to grow again (Murphy *et al.*, 2006; He and Chen, 2010).

In the 1980s, it became apparent that *C. jejuni* is one of the predominant food-borne enteric pathogens in developed countries and also causes water-borne infection of humans. *C. jejuni* is a commensal in many animals, especially birds, but colonisation by this pathogen in the human intestinal mucosa results in digestive tract disease. *Campylobacter* and *Salmonella* are both very common causes of zoonotic disease in humans primarily due to transmission from chickens (Humphrey *et al.*, 2006; Wagenaar *et al.*, 2008; Man, 2011). Infection in humans

results from consumption of contaminated food or water. Consumption of infected and incompletely cooked chicken meat is a particularly common cause of *C. jejuni* infection in humans (see Fig. 1.1). Intestinal infection by *C. jejuni* causes watery or bloody diarrhoea arising from inflammation of the mucosa of the intestine. Diarrhoea may also result from infection with *C. coli* (Sanyal *et al.*, 1984; Koenraad *et al.*, 1997; Poly and Guerry, 2008). *C. jejuni* is normally found in the gastrointestinal tract of many wild and domesticated animal species, including pets and food animals like poultry and cattle (Lastovica *et al.*, 2014). *C. jejuni* is estimated to be responsible for about 14% of diarrheal disease cases, which is more than 400 million cases of campylobacteriosis annually in the world (Duong and Konkel, 2009). In addition, infection with certain serotypes of *C. jejuni* can result in development of Guillain-Barré Syndrome (GBS). GBS appears five days to two weeks after infection and causes neurological illness, which can lead to difficulties with movement and arthritis arising due to auto-immune damage to the peripheral nervous system (Kuroki *et al.*, 1991; Nachamkin *et al.*, 1998). The lipooligosaccharide (LOS) structure in certain serotypes of *C. jejuni* appears to be involved in development of GBS. Antibodies raised during the immune response to sialylated LOS molecules of some *C. jejuni* strains cross-react with gangliosides of the peripheral nerves of the patient resulting in nerve damage (Yuki *et al.*, 1993; Bersudsky *et al.*, 2000).

The epidemiology of *C. jejuni* is complex due to the large number of sporadic cases (Silva *et al.*, 2011), the range of animal and environmental reservoirs (Whiley *et al.*, 2013), and many potential routes for introduction of *C. jejuni* into the food chain (Pintar *et al.*, 2016). In poultry, the epidemiology of *C. jejuni* colonisation of the chickens themselves is still not fully understood. Transmission among chickens occurs by horizontal transfer of the bacteria. It has been proposed that a primary route of flock infection by *C. jejuni* is from the environment potentially from many different sources. As well as other chickens, farm animals,

contaminated housing and water source, wild birds and flies have all been implicated (Sahin *et al.*, 2002; Buhr *et al.*, 2002). There is evidence that *C. jejuni* can also colonise the eggshell at 37, 40 and 42°C (Allen and Griffiths, 2001). Hence, *C. jejuni* can also be transmitted between chickens and through the food chain via contamination of the egg surface. Otherwise, there is little evidence of vertical transmission of *C. jejuni* from the hen to the egg, as has been characterised for *Salmonella* (Cox *et al.*, 2012; Agunos *et al.*, 2014; Wagenaar *et al.*, 2013).

The epidemiological evidence indicates that not all *C. jejuni* strains and serotypes have an equal risk to human health. For example, the strains associated with GBS syndrome were shown to have the sialyltransferase gene (*cst-II*) were (Yuki and Koga 2006) and there is strain associated variation in severity of gastroenteritis. Since, *C. jejuni* isolates vary in virulence, Penner serotyping, which is based primarily on capsular polysaccharide (CPS), was used to classify serotypes commonly associated with diarrhoeal disease. In a systematic review, Pike *et al* (2013) identified that while there was extensive heterogeneity in serotypes associated with clinical cases three serotypes (HS1/44, HS2 and HS4 complex) predominated globally. The virulent clinical *C. jejuni* isolate used as reference strain for many studies, NCTC11168, belongs to serotype HS2, while another well-studied highly virulent strain, *C. jejuni* 81-176 (Hofreuter *et al.*, 2006) belongs to group HS23/36. In addition to properties of the bacterial strain, the ingested dose of virulent strains will influence the outcome and severity of disease and an additional important factor influencing the outcome of disease is the host immune response (Havelaar *et al.*, 2009). The innate and adaptive immunity of the host plays a critical role in development of *C. jejuni* pathogenicity. This is because infection by enteric bacteria causes a proinflammatory host response by activation of receptors in the immune cells and the intestinal mucosa. Such receptors are the Toll-like receptors (TLR) and Nod-like receptors which cause release of antimicrobial peptides, proinflammatory

chemokines and cytokines (Zilbauer *et al.* 2005). For example, lipooligosaccharide of *C. jejuni* causes stimulation of cytokine and interleukin production (Hu and Hickey 2005; MacCallum *et al.* 2006; Hu *et al.* 2006; Borrmann *et al.* 2007). Use of antibiotics by the farming industry, as well as prolonged treatment with macrolides, fluoroquinolones and aminoglycosides for *C. jejuni* infection, when required, has contributed to widespread occurrence of antibiotic resistance in *C. jejuni* (Skirrow, 1977; Ge *et al.*, 2013).

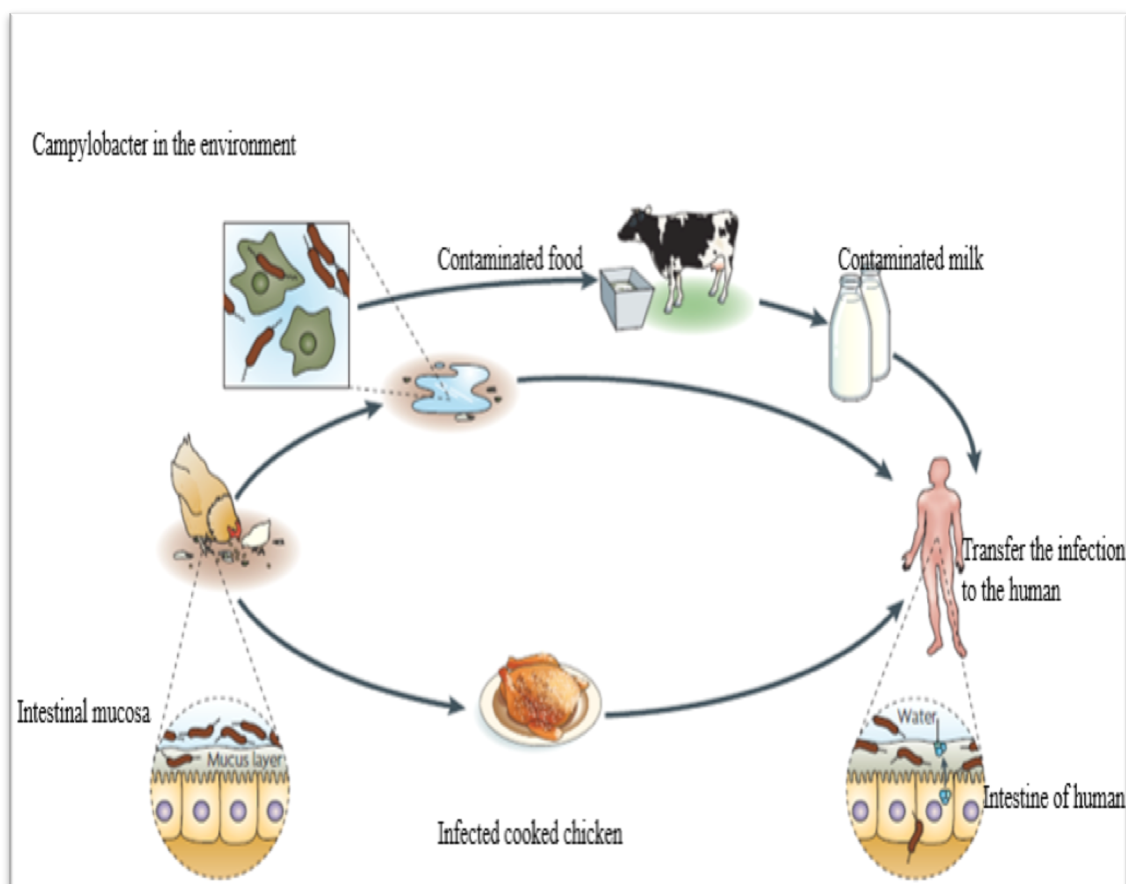


Figure 1.1: Sources of *Campylobacter jejuni* infection. Environmental reservoir can lead to human infection by *C. jejuni* by colonisation of the intestinal mucosa and transmission through the faecal-oral route within chicken flocks. *C. jejuni* can enter water sources to cause infection to humans directly or indirectly, and by consumption of infected milk or meat. From Young *et al.* (2007).

1.2: *Campylobacter* history and taxonomy

The first identification of *Campylobacter* was in 1913 from an aborted foetus isolated from an ovine source by Stockman and McFadyean (1913), where vibrio-like organisms were found. In 1957, a bacterium was isolated from an aborted bovine foetus, then the same species was isolated from humans. This was identified as *Vibrio fetus*. Also, *C. coli* and *C. jejuni* were isolated from faecal samples of cattle with diarrhoea and from blood cultures of humans with enteritis infections, and *C. sputorum* was isolated from sputum of people infected with bronchitis (King, 1957). In addition, *Vibrio fetus* was isolated from bovine vagina and semen, as well as from blood cultures of women who had suffered abortion (Butzler, 2004; Skirrow, 2006). In 1963, Sebal and Veron identified two different species of this vibrio, *Vibrio bubulus* and *Vibrio fetus*, and subsequently revised the associated classification, transferring these species from *Vibrio* into a new genus called ‘*Campylobacter*’, which included *C. jejuni* and *C. coli* (Sebald, 1963). A technique based on filtration was identified to facilitate isolation of *Campylobacter* cells from faeces of humans with diarrhoea and from veterinary sources. *Campylobacter* are small slender bacteria and pass through a 0.65 µm membrane (Skirrow, 2006; Butzler, 2004). This technique was the method used to isolate many catalase-negative *Campylobacter* strains mainly identified as *C. jejuni* and *C. coli* (Bolton *et al.*, 1988). In the 1970s, Skirrow identified antibiotics that aided greatly in selection of *Campylobacter* spp. especially *C. jejuni* and *C. coli* which are highly resistant (*in vitro*) to polymyxin B, trimethoprim and vancomycin antibiotics (Skirrow, 1977). Selective antibiotic media have been further developed, for example, modified charcoal-cefoperazone-deoxycholate agar (mCCDA) contains the cephalosporin antibiotic, cefoperazone, which is now used in selective isolation of *C. jejuni*, *C. coli*, *C. upsaliensis* and *C. lari* (Engberg *et al.*, 2000; Chon *et al.*, 2012).

Establishment of the *Campylobacter* genus was created on the basis of the distinctive features of the corresponding species: low G+C DNA content; non-fermentative metabolism; a need for a microaerophilic environment for growth and 16S rRNA gene sequence data (King, 1957; Chan and Taylor, 1990) The gastric pathogen, *Helicobacter pylori* was initially classified as *Campylobacter pylori* by Marshall and Warren in 1983. However, based on both phenotypic differences and 16S rRNA sequence data, the genus *Helicobacter* was subsequently generated in 1989 by Goodwin *et al.* (Goodwin *et al.*, 1989) with *H. pylori*, a microaerobic, curved and flagellated pathogen that causes gastric and peptic ulcers, as the first species (Chan and Taylor, 1990; Owen, 1998). Goodwin *et al.* also argued that there are significant genotypic and phenotypic differences not just between different species of *Campylobacter* but also among strains of the same species (Goodwin *et al.*, 1989). The *Campylobacter* and *Arcobacter* were finally placed in a new family called *Campylobacteriaceae* because of the similarities between them at the genetic level such as cellular fatty acid content and G+C DNA content (Paster *et al.*, 1991). *Campylobacter* spp. are now classified in the kingdom of Bacteria, phylum of Proteobacteria, class of Epsilonproteobacteria, order of Campylobacteriales, and the family of *Campylobacteriaceae*.

1.3: *Campylobacter jejuni* genome

The first reported sequence and annotation of the *C. jejuni* genome was in 2000 (strain NCTC 11168; Parkhill *et al.*, 2000) and the re-annotated sequence was published in 2007 (Gundogdu *et al.*, 2007). The chromosome was found to consist of a single circular chromosome of 1,641,481 bp with a low G+C content (30.6%) (see Fig. 1.2). Many of the genes that were updated related to lipooligosaccharide structure, the capsule and glycosylation. Strain comparison showed that *C. jejuni* is highly genetically variable and this can be attributed to natural transformation mediating exchange of genes between different strains. *C. jejuni* is able to take up DNA from the environment and combine it with the

genome irrespective of the growth phase (Sheppard *et al.*, 2008; Wang and Taylor, 1990). However, the source of the acquired DNA is important as efficient transformation is methylation dependent and DNA from PCR or propagated in *E. coli* is transformed much more poorly (Beauchamp *et al.*, 2017). A number of hypervariable sequences have been identified in *C. jejuni*, and these are within genes responsible for structure and modification of the bacterial cell surface with an expected role in *C. jejuni* survival in the host. Hypervariable cell surface structures, commonly affected by hypervariability of gene sequences include lipooligosaccharide, capsular polysaccharide and flagellum (Parkhill *et al.*, 2000; Gundogdu *et al.*, 2007; Fouts *et al.*, 2005).

Parkhill *et al.* (2000) discovered that there are very few repeat sequences in the whole genome of *C. jejuni* NCTC 11168 aside from the three repeats of the rRNA operon each of which has 5S, 16S and 23S rRNA (Phongsisay *et al.*, 2007). Amino acids are the preferred energy source for *C. jejuni*, and this was reflected in the number of genes encoding amino acid transport and catabolic enzymes. In contrast and reflecting the general inability of *C. jejuni* to utilise carbohydrate, possession of genes encoding enzymes of the Embden-Meyerhof-Parnas (EMP) pathway was incomplete. Genes for both glucokinase and 6-phosphofructokinase genes were absent from the NCTC11168 genome (Parkhill *et al.*, 2000; Velayudhan and Kelly, 2002). Comparison between the genome sequences of *C. jejuni* NCTC11168 and the phylogenetically related pathogen, *H. pylori*, identified that 55.4% of *C. jejuni* genes have orthologues in *H. pylori*, primarily relating to housekeeping function (Parkhill *et al.*, 2000). Subsequently, the complete genome sequences for two other highly virulent strains, *C. jejuni* 81116 and 81-176, was published, revealing the presence of two plasmids, pVir and pTet and identifying several unique genes involved in metabolism that contribute to virulence (Hofreuter *et al.*, 2006; Pearson *et al.*, 2007). More recently multilocus sequence typing (MLST) and whole genome sequencing (WGS) (Sheppard *et al.*,

2013; Sheppard and Maiden, 2015) has been used to investigate the phylogenetic relationship of *C. jejuni/coli* strains from different sources and to identify both metabolic features and virulence determinants that might contribute to virulence in humans and colonisation of poultry and animals. These studies have highlighted the wide genetic diversity in *C. jejuni* and *C. coli* and provided evidence for host-specificity of some but not all *C. jejuni* genotypes (Sheppard *et al.*, 2011; Sheppard *et al.*, 2014).

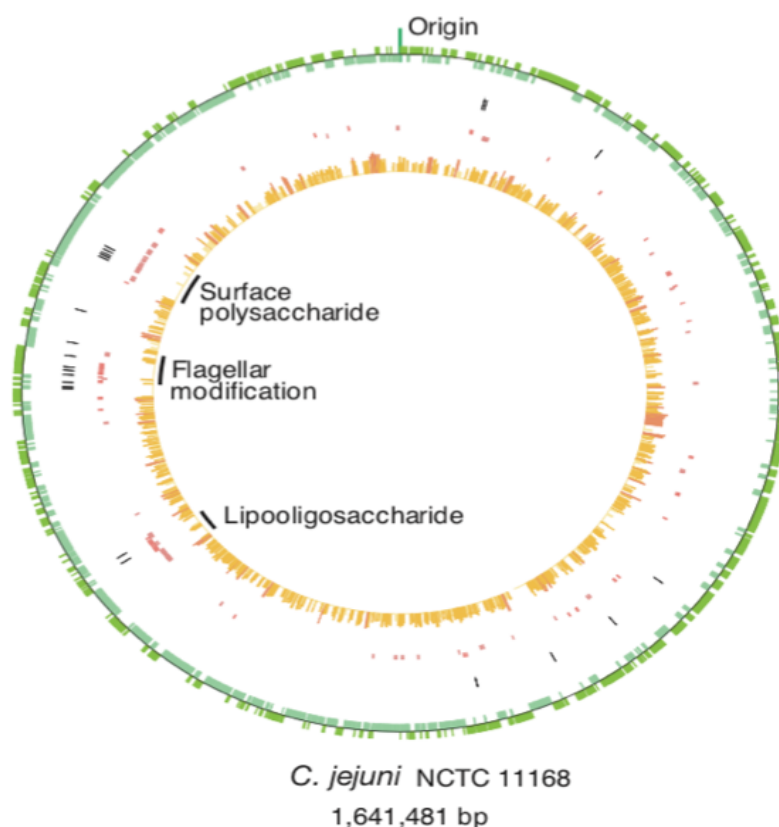


Figure 1.2: *C. jejuni* NCTC11168 genome in circular representation. The first circle in dark green shows coding sequences transcribed in the clockwise direction, the second light green circle shows coding sequences in the anticlockwise direction, the third circle shows the positions of hypervariable sequences in black, the fourth and fifth circles show genes involved in the production of surface structures (clockwise, dark red; anticlockwise, pale red). The similarity of each gene to its *H. pylori* orthologue is shown by the innermost histogram; colour intensity and bar height reflect the degree of similarity. The genes responsible for lipooligosaccharide, flagella and surface polysaccharide are indicated (Parkhill *et al.*, 2000).

1.4: *Campylobacter* metabolism

C. jejuni is microaerophilic, and thus requires oxygen at sub-atmospheric levels to live and grow. In general, strains of *C. jejuni* grow in an atmosphere with between 2 and 13 % oxygen (Neill *et al.*, 1985). *C. jejuni* cannot persist in the high oxygen concentrations of the atmosphere but is also unable to grow without at least some oxygen for respiration and synthesis of nucleic acids. (Krieg and Hoffman, 1986; Kelly *et al.*, 2001)

The microaerophilic property is a distinct difference from other food-borne pathogens such as *Salmonella*, *E. coli* and *Shigella* (Krieg and Hoffman, 1986; Kendall *et al.*, 2014; Lee and Newell, 2006). However, *C. jejuni* is able to resist the reactive oxygen species (ROS) that result from oxygen exposure, such as the toxic molecules hydrogen peroxide (H₂O₂) and superoxide (O₂⁻). *C. jejuni* can eliminate these ROS species through the activity of catalase, peroxidase and superoxide dismutase (SOD) enzymes (Krieg and Hoffman, 1986; Parkhill *et al.*, 2000; Gundogdu *et al.*, 2014). (See 1.10 below for further details)

The metabolic processes of *C. jejuni* are still not fully understood. It has the ability to utilize the nutrients available in the intestine of a range of animals (Stahl *et al.*, 2012), permitting colonisation of the intestine. Unlike many other gut bacteria, *C. jejuni* generally lacks the ability to utilise carbohydrates as energy sources because they lack 6-phosphofructokinase (PFK), a key enzyme in the energy metabolism process of externally supplied sugars. However, genes for the other glycolytic enzymes are present allowing synthesis of glucose via the glycolysis pathway operating in reverse (gluconeogenesis rather than glycolysis) (Parkhill *et al.*, 2000; Velayudhan and Kelly, 2002). Catabolism of L-fucose has been observed in some *C. jejuni* isolates (Muraoka and Zhang, 2011; Stahl *et al.*, 2011). Interestingly, L-fucose is present in the mucosal layer of intestinal epithelial cells, originating from fucosylated mucin glycoproteins, and is taken up via the fucose permease FucP (Stahl *et al.*, 2011). The *fucP* gene is present in a high proportion of *C. jejuni* isolates (de Haan *et al.*,

2012; Zautner *et al.*, 2012) indicative of the ability to utilize L-fucose, and the same genes have been identified in *C. coli* (Sheppard *et al.*, 2013).

C. jejuni obtains its major carbon requirement from amino acids and products of the Krebs cycle. *C. jejuni* NCTC 11168 is able to utilise L-serine, L-aspartic acid, L-proline, L-asparagine and L-glutamic acid (Kelly, 2005; Velayudhan *et al.*, 2004; Line *et al.*, 2010). Also, formate, D-lactate, pyruvate and TCA cycle intermediates such as succinate and malate can provide energy sources during growth and host colonisation (Kelly, 2002; Vegge *et al.*, 2009). In addition, *C. jejuni* has transaldolase, transketolase, ribulose-3-phosphate epimerase and ribose-5-phosphate isomerase enzymes which make up the non-oxidative portion of the pentose phosphate pathway, but it completely lacks the oxidative portion of the pathway (Velayudhan and Kelly, 2002; Line *et al.*, 2010). These enzymes enable *C. jejuni* to utilize pentose through the pentose phosphate pathway (PP). A small number of strains also possess a locus encoding genes enabling glucose uptake and catabolism via the Entner-Doudoroff (ED) pathway (Vegge *et al.*, 2009).

The ED pathway is an important sugar catabolism pathway and has been identified in some *C. jejuni* and *C. coli* strains where it provides several benefits, in addition to glucose utilisation, including survival in the stationary phase and enhanced biofilm formation (Vegge *et al.*, 2016). The ED pathway genes were first observed in the sequence of *C. jejuni* subsp. *doylei* 269.97 which indicated a theoretical way for glucose utilization by this isolate (Miller, 2008; Line *et al.*, 2010). The ED pathway produces 1 mole each of ATP, NADH, and NADPH per mole glucose (Flamholz *et al.*, 2013). Database searches showed that only 1.7% of >6,000 *Campylobacter* genomes analysed, including *C. jejuni* and *C. coli* strains from diverse clinical, environmental and animal sources, encode a complete ED pathway (Vegge *et al.*, 2016). Possession of the pathway was restricted primarily to isolates from wild birds and Norway rats and aside from several *C. jejuni* subsp. *doylei* strains was absent from clinical

isolates. As indicated above, the preferred carbon sources used by *Campylobacter* spp. for growth, particularly *in vivo* are amino acids such as aspartate, glutamate, serine and proline (Velayudhan *et al.*, 2004; Guccione *et al.*, 2008; Hofreuter, 2014), and these are the most common amino acids found in chick excreta which perhaps explains the commensalism of *C. jejuni* in the chicken gut as a major natural reservoir (Wright *et al.*, 2009; Thomas *et al.*, 2011; Hofreuter, 2014; Parsons, 1984).

1.5.1: Motility and chemotaxis

Motility of *C. jejuni* is necessary for colonisation and infection of the host, as this requirement has been recorded in the rabbit, mouse and hamster, as well as chickens (Aguero-Rosenfeld *et al.*, 1990; Pavlovskis *et al.*, 1991; Wassenaar *et al.*, 1993). Inactivation of the gene encoding the major flagellin subunit FlaA in *C. jejuni* 81116 resulted in decreased colonisation of the mutant strain in chicken caecum by 100-1000-fold (Wassenaar *et al.*, 1993). Motility is essential for responding to the different chemotactic conditions and survival in the host gastrointestinal tract (Guerry, 2007; Jagannathan and Penn, 2005). *C. jejuni* has unusual motility, in particular in viscous substances. This is because of the presence of one or two polar flagella and the helical cell shape (Ferrero and Lee, 1988). This aids penetration of the viscous intestinal mucus layer and hence colonisation of the intestine and in some cases induction of disease. In addition, the flagellum filament acts in adhesion assisting in binding to the host epithelium (Nuijten *et al.*, 1990; Guerry *et al.*, 1992; Yao *et al.*, 1994) and hence motility is necessary for the pathogen to initially contact the host cell surface and helps maintain adhesion to the cell surface. In addition to the role of flagella in motility, flagella have been shown to function in the secretion of the non-flagellar proteins, including *Campylobacter* invasion antigens (CiaB and C) (Guerry, 2007; Larson *et al.*, 2008). In this respect, *C. jejuni* flagella have been considered to also function as a Type III Secretion System (T3SS) (Konkel *et al.*, 2004; Malik-Kale *et al.*, 2008; Christensen *et al.*, 2009).

The flagellum consists of three parts: the basal body which acts as a motor and exists inside the cell envelope, the hook and the extracellular filament which extends outside of the cell (Kojima and Blair, 2004). The hook-basal body includes a base embedded in the cytoplasm and inner membrane of the bacterial cell, the periplasmic rod and associated ring structures with the surface localized hook (Sommerlad and Hendrixson, 2007; Lertsethtakarn *et al.*, 2011). Flagellin (the major flagellum subunit that forms the ‘filament’) is encoded by the *flaA* and *flaB* genes. However, the presence of *flaA* alone is sufficient to allow formation of the filament (Nuijten *et al.*, 1990; Nashamkin *et al.*, 1993).

In *C. jejuni*, FlaA and FlaB filaments are immunogenic, but they are not recognized by the innate immune system (Ramos *et al.*, 2004). Filaments in *C. jejuni* are highly glycosylated, via O-linked glycosylated (Szymanski and Wren, 2005). Glycosylation is essential for flagella assembly and is assumed to contribute to immune evasion. Motility of *C. jejuni* is phase variable (Hendrixson, 2006). There are several genes involved in flagellar synthesis that are subject to phase variation via slipped-strand mispairing of homopolymeric nucleotide tracts within the ORF or regulatory region. The master regulator of flagella biosynthesis, *flgR*, is subject to phase variation via loss or gain of nucleotides within a homopolymeric adenine tract in *flgR* (Hendrixson, 2006). Motility accessory factor family (*maf*) genes (especially *maf1* and *maf4*), which encode proteins involved in flagella glycosylation are also subject to phase variation (Karlyshev *et al.*, 2002). Phase variation leads to rapid phenotypic changes which helps the bacteria to adapt appropriately to changes in conditions within the host. In *C. jejuni* phase variation of flagellar genes is necessary for survival within the host (Hendrixson, 2006).

Bacteria can recognize changes in the composition of the surrounding environment using chemoreceptors which are located in a cluster at the pole of the cell. Chemoreceptors give the bacteria sensitivity and accurate motility responses to environmental signals. This

chemotactic motility along a chemical gradient is called chemotaxis. It is an effective type of motility enabling colonisation and infection of the host by *C. jejuni* (Takata *et al.*, 1992; Briegel *et al.*, 2009). *C. jejuni* uses this mechanism to move toward more suitable conditions, in particular, towards chemoattractants within mucus in the crypts of the caecum, which are recognised colonisation sites for *C. jejuni* in the avian gut (Chang and Miller, 2006). Loss of chemotaxis ability results in reduced colonisation capacity (Takata *et al.*, 1992; Yao *et al.*, 1997; Reuter *et al.*, 2018). The mucus mainly consists of mucin and glycoproteins which act as initial chemoattractants (Hermans *et al.*, 2012) enhancing *C. jejuni* colonisation of the chicken caecum, after about 24 h post-ingestion. (Coward *et al.*, 2008; Smith *et al.*, 2008; Jeon *et al.*, 2003). *C. jejuni* chemotaxis involves sensing of the environmental stimuli via methyl accepting chemotaxis proteins (MCPs), also called transducer-like proteins (Tlps), and transduction of the signal via CheW and phospho-relay between the histidine kinase, CheA and the response regulator, CheY. Phosphorylated CheY then stimulates motility via interaction with the flagellar motor (Hendrixson and DiRita, 2004; Reuter *et al.*, 2018). Chemoattractants recognised by *C. jejuni* Tlps include the nutrients L-aspartate, L-asparagine, L-cysteine, L-glutamate, pyruvate and L-serine. (Mohammed *et al.*, 2004; Velayudhan *et al.*, 2004; Guccione *et al.*, 2008). Studies with *C. jejuni* strains carrying mutations in chemotaxis genes have confirmed involvement of chemotaxis in many processes including biofilm formation, cell invasion and host colonisation (Hendrixson and DiRita, 2004; Reuter *et al.*, 2018; Korolik, 2019).

1.5.2: Adhesion and invasion

In humans, there is a strong relationship between severity of infection, and the ability of the pathogen to adhere to and invade the target site in the host. The intestinal mucosa is the specific site of colonisation for *C. jejuni*, involving adhesion to and invasion of the epithelial cells. This results in inflammatory damage resulting in diarrhoea (Fauchere *et al.*, 1986;

Wooldridge and Ketley, 1997). The ability of *C. jejuni* to adhere differs between species and strains and is also influenced by the host epithelial cell. For example, epithelial cells of the human colon and chicken caecum are highly susceptible to adhesion by *C. jejuni* and *C. coli* (Everest *et al.*, 1992; Knokel *et al.*, 1997; Sylte *et al.*, 2019). Since adhesion and invasion are key for *C. jejuni* infection, there has been interest in identifying *C. jejuni* virulence factors involved in both of these processes (Casabonne *et al.*, 2016; Konkel *et al.*, 2005; Konkel *et al.*, 1999). These are discussed below and see Fig. 1.3 for a summary of factors involved in *C. jejuni* infection.

CadF and FlpA. When *C. jejuni* binds to the specific ligand, fibronectin, on the host cell epithelium, bacterial invasion is more efficient (Chen *et al.*, 2006; Monteville and Konkel, 2002). CadF is a 37-kDa fibronectin-binding outer-membrane protein. It has been shown to be an important adhesion-associated protein that promotes adhesion of *C. jejuni* to the epithelial cell fibronectin in the gut (Konkel *et al.*, 1997; Konkel *et al.*, 2005; Cróinín *et al.*, 2012). There is a major decrease in the capacity of *cadF* mutants of *C. jejuni* to adhere to human intestinal epithelial cells (Ziprin *et al.*, 1999; Monteville *et al.*, 2003). FlpA is another fibronectin-binding protein and has a role along with CadF in effective invasion of the host (Flanagan *et al.*, 2009). Fibronectin is an important high molecular weight glycoprotein of the extracellular matrix of gastrointestinal epithelial cells. Binding of *C. jejuni* to fibronectin has the potential to trigger a signalling process, via integrin, that leads to activation of the host GTPases Rac1 and Cdc42 (molecular switches controlling many cellular processes) and thus contributing to internalization of *C. jejuni* into host cells.

Cia proteins. Maximum invasion of host epithelial cells requires production of the virulence factors called *Campylobacter* invasion antigens (Cia) which are secreted through the flagellar apparatus, (Konkel *et al.*, 2004; Malik-Kale *et al.*, 2008; Christensen *et al.*, 2009). Invasion antigen, CiaB, was the first secreted factor characterised in *C. jejuni* and has an important

role in invasion. Mutants of *ciaB* have reduced host adherence and significantly reduced invasion (Konkel *et al.*, 1999; Ó Cróinín and Backert, 2012). CiaI has been reported to have a role in intracellular survival of *Campylobacter* within the host (Buelow *et al.*, 2011; Eucker and Konkel, 2012). Interestingly, synthesis of the Cia proteins by *C. jejuni* is induced as a response to bile salts and other host factors, and their secretion occurs after adhesion of *C. jejuni* to the host intestinal mucosa (Rivera-Amill *et al.*, 2001).

CapA. *Campylobacter* adhesion protein A (CapA) is an autotransporter lipoprotein (Jin *et al.*, 2001) required for adhesion and invasion of human epithelial cells (Ashgar *et al.*, 2007). Interestingly, Flanagan (2009) found no effect of a *capA* mutation on chicken colonisation, possibly because there are other genes enabling *C. jejuni* adhesion in the chicken that can compensate for absence of CapA (Pei and Blaser, 1993).

Peb proteins. Peb proteins 1-4 were initially identified by Pei, Ellison and Blaser (1991) as major antigenic proteins of *C. jejuni*. Peb1 (Cj0921c) is the 28 kDa periplasmic binding protein component of the ABC transport system for aspartate and glutamate (Leon-Kempis *et al.* 2006) and was identified as also being important for cell adherence in *C. jejuni* (Pei and Blaser, 1993). Peb3 is described as a glycoprotein involved in adhesion and Peb4 is an antigenic virulence factor important for colonisation. It shares homology with SurA chaperone of *E. coli* and thus contributes to *C. jejuni* adhesion process through its role in export of outer membrane proteins including CadF (Min *et al.*, 2009; Kale *et al.*, 2011).

LOS. Lipooligosaccharide (LOS) is a major component of the outer leaflet of the outer membrane bilayer and is comprised of LipidA plus core oligosaccharides. In *C. jejuni* the outer sugars of the core are variable between strains and are often additionally glycosylated (Karlyshev *et al.* 2005). Sialylation of the outer core of LOS has been shown to enhance the invasive ability of *C. jejuni* and is thought to have a role in development of Guillain-Barré

Syndrome (Louwen *et al.*, 2008). Inactivation of a gene required for LOS sialylation resulted in significant inhibition of invasion.

pVir. There is evidence that the *C. jejuni* virulence plasmid (pVir) can contribute to adhesion and invasion, and that mutations in some genes can significantly reduce adherence and invasion ability (Bacon *et al.*, 2000). The highly virulent strain *C. jejuni* 81-176 carries the pVir plasmid. However, one survey of clinical isolates did not support a requirement of the pVir plasmid for development of gastroenteritis or bloody diarrhoea in humans (Louwen *et al.*, 2006). pVir was detected in only a very small proportion of clinical isolates.

JlpA. JlpA is a surface exposed lipoprotein of 372 amino acids in *C. jejuni*. Studies with knock out mutants have shown that possession of *jlpA* enhances adhesion to host epithelial (Jin *et al.*, 2001).

1.5.3: Bacterial Toxins

The watery, often bloody diarrhoea symptoms of enteritis caused by *C. jejuni*, indicates the presence of bacterial toxins. Cytotoxic distending toxin (CDT) is a dangerous toxin that is secreted by *C. jejuni* and other species such as *C. lari*, *C. coli*, *C. fetus* and *C. upsaliensis*. Some other Gram-negative bacteria also produce this toxin (Johnson and Lior, 1988; Ge *et al.*, 2008; Gargi *et al.*, 2012). *C. jejuni* NCTC 11168 carries the CDT genes and two genes for haemolysin as well as a phospholipase which are responsible for the haemolytic effect in some cases of *C. jejuni* infection (Wassenaar, 1997; Grant *et al.*, 1997; Parkhill *et al.*, 2000). Both *C. jejuni* 11168 and 81-176 secrete high amounts of the CDT toxin, more than some other less pathogenic strains. *C. jejuni* mutants lacking CDT toxin still have the ability to adhere and invade but do not cause enteritis (Fox *et al.*, 2004). CDT toxin affects the epithelial cells of the intestinal villi of the host, induces inflammation of the intestine and causes rupture of cells leading to lack of absorption in the intestine and in watery diarrhoea

(Whitehouse *et al.*, 1998; Purdy *et al.*, 2000; Lai *et al.*, 2016). In tissue culture, it causes cell swelling, elongation, distention, damage to the DNA and death of mammalian cells such as HeLa cells and Chinese hamster ovary (CHO) cells (White house *et al.*, 1998; Pickett *et al.*, 1996; He *et al.*, 2018), although several types of cells resist CDT toxicity, for example mouse Y-1 adrenal (Johnson and Lior, 1988).

CDT is encoded by the three-gene *cdtABC* operon. CdtA and CdtC combine with CdtB, the enzymatic subunit, to form CDT holotoxin which is required for secretion of the enzymatically active form of CDT (Lara-Tejero and Galan, 2001). CdtA and CdtC remain on the cell membrane of the host whereas the CdtB protein enters into the cytoplasm then moves via the endoplasmic reticulum to the nucleus (Heywood *et al.*, 2005; Lai *et al.*, 2016). Entrance of CdtB to the nucleus is necessary to produce the cytotoxic effects inside the host cell (McSweeney and Dreyfus, 2004). The cytotoxic effect of CDT is due to DNaseI activity of CtdB and arrest in the cell growth cycle at the G2 phase (the second sub phase of the interphase in the cell cycle) during mitosis (Whitehouse *et al.*, 1998; Pickett and Whitehouse, 1999). In humans, CDT action induces interleukin 8 (IL 8) production which causes accumulation of macrophages and neutrophils at the site of infection leading to intestinal inflammation (Hickey *et al.*, 1999). Interestingly, this is not the case in chickens infected with *C. jejuni* where there is no inflammation reaction consistent with the specificity of the CDT effect according the type of host cells (Young *et al.*, 2007). In addition, there has recently been a report that CDT produced by *C. jejuni* 81-176 promotes colorectal cancer and changes the normal microbiota in the host (He *et al.*, 2019).

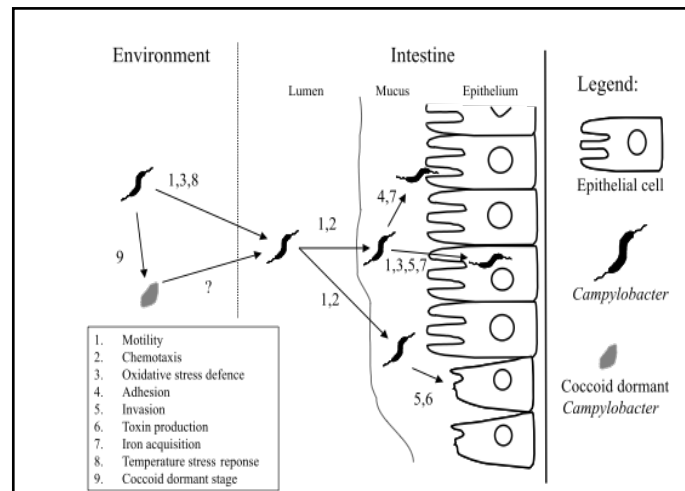


Figure 1.3: Overview of *Campylobacter* colonisation stages in human intestines. During disease in humans *C. jejuni* invade the epithelial cells resulting in a pro-inflammatory response, an increase in cytokine production, inflammation and diarrhoea. 1-Motility, 2- Chemotaxis, 3- Oxidative stress defence, 4- Adhesion, 5- Invasion, 6- Toxin production, 7- Iron acquisition, 8- Temperature stress response, 9- Coccoid dormant stage (van Vliet and Ketley, 2001).

1.6: Niche and epidemiology of *Campylobacter*

C. jejuni is documented as the most common cause of bacterial gastroenteritis in both industrialized countries and worldwide. In addition, autoimmune-mediated demyelinating neuropathy (GBS) occurs as a sequela to this infection in a small number of cases (Nachamkin *et al.*, 1998; Friedman *et al.*, 2000; Butzler *et al.*, 2018). Campylobacteriosis has become widespread in the developed and developing countries due to consumption of contaminated meat or incomplete cooking. There are about 2.5 million cases annually in the UK (Friedman *et al.*, 2000; Kaakoush *et al.*, 2018). Eating contaminated meat from chicken or cattle is considered as the source of 97% of sporadic infection cases in man, and infection from wild animals and the environment accounting for the remaining 3% of infections (Wilson *et al.*, 2008). Occasionally, other routes of *C. jejuni* infection occur such as consumption of contaminated raw milk or water. Also, infection may be transferred from man to man directly (Friedman *et al.*, 2000; Kaakoush *et al.*, 2018).

In the European Union, cases of Campylobacteriosis are higher than those of Salmonellosis. Infection includes people of various ages, but mostly children below four years old and adults between 15-24 years (Nielsen *et al.*, 2013). Also, the rates of infection increase in the summer which indicates that high temperature may be relevant for *Campylobacter* replication and that infection may be associated with summer activities such as barbeques and water-sports (Garcia Rodriguez *et al.*, 2006; Nielsen *et al.*, 2013; Rao *et al.*, 2001). In humans, *C. jejuni* causes gastroenteritis, pain in the abdominal region, vomiting and watery or bloody diarrhoea after 3-7 days infection. Infection requires only a relatively low dose of bacteria of between 500-800 cells in humans. The dose may affect the severity of the infection but does not affect progression of the disease following infection (Black *et al.*, 1988). Sensitivity to colonisation by *C. jejuni* is different in chickens and colonisation requires a higher challenge dose (between 3×10^4 to 6.6×10^5 CFU per chicken). *C. jejuni* efficiently colonises that caecum of chickens and is often observed close to the villi and crypts, but without significant damage of the epithelial cells. Chickens are considered as a natural reservoir for *C. jejuni* because the chicken gut is biologically suitable for its survival. Chickens are colonised by *C. jejuni* approximately 6 days after hatching (Nachamkin *et al.*, 1993; Dasti *et al.*, 2010).

Strains of *C. jejuni* recovered from cases of gastroenteritis in urban regions, particularly from children, are similar to those collected from chickens linking contaminated food as the likely source of infection (Strachan *et al.*, 2009). Multilocus sequence typing (MLST) data has suggested that flocks of chickens and retail chicken are a common source of infection with *C. jejuni* (Allen *et al.*, 2007; Wirz *et al.*, 2010). However, some strains of *C. jejuni* from cattle stocks have been recovered from patients with campylobacteriosis which also indicates a role of cattle and the cattle industry as a source of infection with this pathogen (Sanad *et al.*, 2011).

As indicated above, there is substantial within-species genetic diversity for the *Campylobacter* genus. For instance, *C. coli* isolates collected from humans, suffering from campylobacteriosis, poultry and pigs in Denmark revealed about 84 sequence types (STs) of which 57 were novel (Litrup *et al.*, 2007). A remarkably large number of different genotypes (sequence types) of *C. jejuni* have been catalogued by MLST, many of which are isolates from within the UK (Litrup *et al.*, 2007; Dingle *et al.*, 2008; Cody *et al.*, 2012). Most *C. jejuni* infections are assumed to occur due to food contamination, with a rise in infection rate in the summer. Some infections occur due to travel abroad (Cody *et al.*, 2012; Bessell *et al.*, 2012; McCarthy *et al.*, 2012). Detection and analysis of *Campylobacter* outbreaks relies upon various methods to diagnose the diverse genetic types. Household outbreaks are not common but about 89% of these outbreaks are caused by single strain (Rotariu *et al.*, 2010; Clark *et al.*, 2012).

Stress hormones (norepinephrine) have been shown to increase *C. jejuni* pathogenesis through its effect on colonisation in both humans and chickens (Aroori *et al.*, 2014). Also, *C. jejuni* grows better in iron-restricted media with norepinephrine, its motility and invasive ability are raised (Cogan *et al.*, 2006). This indicates it may be possible to reduce infection by controlling stress hormone levels and improving welfare in both humans and chicken. Various factors, such as the feeding system employed and level of hygiene, can reduce *C. jejuni* incidence in chickens. Indeed, contamination and stress are considered to be major factors in promoting infection and pathogenicity of many zoonotic pathogens, including *C. jejuni* (Humphrey, 2006).

1.7: Iron uptake in *Campylobacter*

1.7.1: Iron

Iron is an essential micronutrient used by nearly all living organisms including bacteria as a vital mineral. It plays an important role in respiration, protein stability and catalysis by enzymes (Wooldridge and William, 1993; Aguado-Santacruz *et al.*, 2012; Zhao *et al.*, 2014; Loreal *et al.*, 2014). Despite being the fourth most common element in the Earth's crust, its availability is poor due to the weak solubility of the predominant ferric at pH 7. At neutral pH under aerobic conditions, iron exists mainly in the ferric (Fe^{3+}) form which is poorly soluble. Inside mammals most of the iron is found in a bound form being associated with iron-binding proteins like transferrin, lactoferrin and ferritin, or the haem-containing protein haemoglobin and thus is not readily available to pathogens (Ratledge and Dover, 2000; Aguado-Santacruz *et al.*, 2012).

Iron acquisition is a critical requirement for bacteria that invade the host, since iron restriction in the host is used as a defence mechanism against microbes (Litwin and Calderwood, 1993; Ratledge and Dover, 2000; Ganz and Nemeth *et al.*, 2015; Ganz, 2018). Indeed, nearly all bacteria have an absolute need for iron, with *Lactobacillus* spp. being one of very few exceptions to this general rule (Archibald, 1983; Weinberg, 1997). Therefore, many strategies are used by pathogenic bacteria for uptake of the iron, such as direct utilisation of the iron compounds from the host and production of siderophores complexes. Furthermore, iron homeostasis is a crucial to most living organisms, including bacteria, to avoid any toxicity that may result from iron excess or growth restriction caused by iron insufficiency (Ratledge and Dover, 2000; Gozzelino and Arosio, 2016). Iron has a strong catalytic capacity to drive the generation of highly reactive hydroxyl radicals (OH^\cdot) (Fenton, 1894). This results in iron toxicity due to combination of iron with oxygen leading to toxic compounds like peroxides and the hydroxyl radical, which in turn cause protein, lipid and

DNA damage. Thus, iron uptake has to be controlled to avoid oxidative stress or cell damage (Ratledge and Dover, 2000; Ishikawa *et al.*, 2003; Zhang, 2014; Paul and Lill, 2015).

1.7.2: The ferrous (Feo) iron uptake system

1.7.2.1: General overview. The Feo system is one of the most important iron transporters in bacteria. It takes up ferrous iron across the cytoplasmic membrane under anaerobic conditions. Ferrous iron is highly soluble (unlike ferric iron) at neutral pH and remains stable anaerobically. Ferrous iron is able to diffuse through the outer membranes of Gram-negative bacteria into the periplasm without energy or active transport. Feo systems of the enteric bacteria consists of three main proteins: FeoA, FeoB and FeoC (Kammler *et al.*, 1993; Carton *et al.*, 2006; Sestok *et al.*, 2018) encoded by a three gene operon. FeoA is a small, cytosolic SH3-like domain protein, similar to the SH3 domain of DtxR (diphtheria toxin regulator protein). Its purpose is unclear, but it is essential for Feo function (Carton *et al.*, 2006; Lau *et al.*, 2013). FeoB is a large (~84.5 kDa) membrane-associated protein acting as the ferrous permease (Carton *et al.*, 2006). The N-terminal domain is a G-protein domain located in the cytosol, which is able to hydrolyse GTP, and may provide energy for active uptake of ferrous iron (Marlovitis *et al.*, 2002). The C-terminal region consists of an integral inner-membrane domain acting as the ferrous permease. This domain is homologous with nucleoside transporters and possesses the two Gate motifs, as found in the nucleoside transport proteins (Carton *et al.*, 2006). The *feoB* genes are found in over 4000 Bacteria and Archaea species from a wide taxonomic range, and they are usually associated with a *feoA* gene, which indicates that the respective products form a conserved functional unit (Carton *et al.*, 2006; Kim *et al.*, 2015a). FeoC is also a small, cytoplasmic protein with a regulatory role – but is largely restricted to the Proteobacteria and is thus most Feo systems lack a FeoC protein. FeoC can form an Fe-S cluster and possess a winged helix-turn-helix motif as found in bacterial gene regulators (Lau *et al.*, 2016; Carton *et al.*, 2006). In *Salmonella*, FeoC

regulates FeoB degradation in response to oxygen, deploying its Fe-S centre to monitor O₂ status (Kim *et al.*, 2015a).

The Feo system of *E. coli* K-12 was the first ferrous iron transporter identified, then later this system was also discovered in *Helicobacter pylori* and *Porphyromonas gingivalis* (Hantke, 1987; Hantke 2003; Velayudhan *et al.*, 2000; Dashper *et al.*, 2005). It is now known to be widespread in pathogenic bacteria and is often required for their colonisation and survival inside the host (Cartron *et al.*, 2006; Stojiljkovic *et al.*, 1993; Tsolis *et al.*, 1996; Cowart, 2002; Lau *et al.*, 2016; Sestok *et al.*, 2018). The *feoABC* expression in *E. coli* is subject to iron repression, which is mediated by the Fur regulator. Indeed, Fur mediates the repression of all dedicated iron transporters in *E. coli*, and such Fur-dependent control is seen in many Gram-negative bacteria as well as some Gram-positive bacteria (van Vliet *et al.*, 1998b). The anaerobic induction of the *feo* operon is controlled by FNR (Kammler *et al.*, 1993; Escolar *et al.*, 1999; Lau *et al.*, 2016). Thus, Feo system of *E. coli* is induced under low-iron and anaerobic-microaerophilic conditions, such as those found inside the digestive tract.

1.7.2.2 FeoAB of *C. jejuni*. In *C. jejunii*, Feo is encoded by *feoA* (cj1397) and *feoB* (cj1398), but no *feoC* gene is apparent in the genome sequence of *C. jejuni* NCTC 11168 (see Fig. 1.4) (Parkhill *et al.*, 2000; Naikare *et al.*, 2006). FeoB of *C. jejuni* has only ~50% and 29% amino acid sequence identity with the *H. pylori* and *E. coli* FeoB proteins, respectively. While for FeoA, the identity is less at just 16% for the *E. coli* protein. Unlike for other FeoB proteins studied, the *C. jejuni* FeoB is not necessary for ferrous iron uptake as *feoB* mutants of *C. jejuni* M129 and F38011 retained ferrous iron uptake. This could be because there is another ferrous iron transporter in the genome sequences of these strains (Raphael and Jones, 2003). However, in another study it was shown that *feo* mutation in three different *C. jejuni* strains (NCTC 11168, 81-176, and ATCC 43431) resulted in colonisation inhibition and decreased *in vivo* survival in the rabbit ileum, chicken caecum and piglet intestine, with a significant

defect in iron acquisition ability (Naikare *et al.*, 2006). This demonstrated that FeoB is functional ferrous iron transporter in these strains of *C. jejuni* and has a critical role for complete colonisation in the host. Other studies demonstrated that *feoB* is functional in the NCTC 11168 and 81116 strains (Parkhill *et al.*, 2000; Pearson *et al.*, 2007), but not in strains 81-176 and RM1221 (Fouts *et al.*, 2005; Hofreuter *et al.*, 2006).

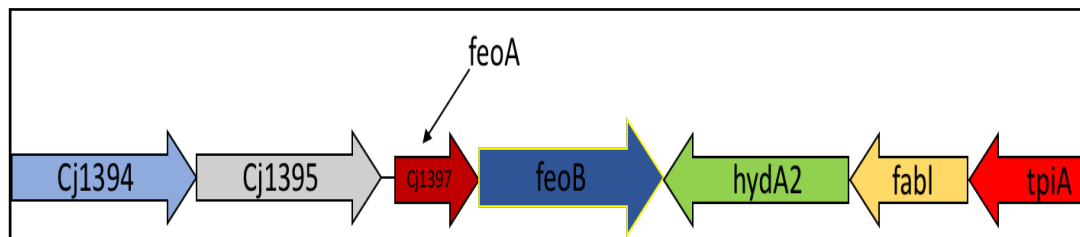


Figure 1.4: Organisation of the *feoAB* operon of *C. jejuni* NCTC 11168. This figure is from the Gene Context Tool III and it shows that the *C. jejuni* Feo system lacks the FeoC component.

1.7.3: Siderophore-dependent iron uptake

1.7.3.1: General overview. Siderophores are small, low molecular weight and high affinity microbial ferric-iron chelators, and they play an important role in acquiring iron from the environment by bacteria. They are secreted by bacteria as a response to the iron starvation (Schroder *et al.*, 2003; Adler *et al.*, 2012). There are different types of siderophores according to their chemical structure with three major families: catecholates (e.g. enterobactin and salmochelin), carboxylates (e.g. staphyloferrin A) and hydroxamates (e.g. desferrioxamine B). In addition, there are mixed type siderophores such as yersiniabactin, pyochelin and aerobactin that share a mixture of features with the siderophores families mentioned above (Hider and Kong, 2010; Crumbliss and Harrington, 2009; Sandy and Butler, 2009). Siderophores can bind to other metals in addition to their ability to bind to the iron, like Mo, Mn, Co and Ni (Schwyn and Neilands, 1987; Bellenger *et al.*, 2008). Thus, some siderophores have functions other than as iron chelators, like control of oxidative stress, antibiotic activity, heavy metal detoxification and transport of other metals as zinc or copper

(Rajkumar *et al.*, 2010; Lemire *et al.*, 2013; Saha *et al.*, 2016). Also, siderophores can also act as important virulence factors in pathogenic bacteria (Johnstone and Nolan, 2015; Holden and Bachman, 2015).

Both Gram-negative and -positive bacteria have the ability to uptake iron from transferrin, lactoferrin, haemoglobin and haem, as well as via siderophores. In Gram-negative bacteria, transport of iron in complex form happens through a system consisting of an outer-membrane (OM) receptor, a periplasmic-binding protein (PBP) and a cytoplasmic-membrane (CM) ATP-binding cassette (ABC) dependent permease (Krewulak and Vogel, 2008). The OM acts as a permeability barrier excluding toxins, detergents and the degradative enzymes. However, porins (trimeric β -barrel proteins) enable diffusion of low molecular weight solutes (<600 Da) through the OM, passively (Nikaido, 2003). Iron-containing molecules of higher MW (like transferrin, lactoferrin, haemoglobin, and ferric-siderophore complexes) need specific OM receptors because they cannot pass via the porins across the OM. Such transport requires energy. In the case of iron-complexes, this energy is obtained from the proton motive force (pmf) of the CM which is transduced to the relevant OM receptor through three proteins: TonB, ExbB and ExbD (Krewulak and Vogel, 2008). Thus, the OM receptors are designated as 'TonB-dependent transporters' (TBDTs). The TBDTs allow ferri-siderophores to pass through the OM to the periplasm in a pmf-dependent fashion (Noinaj *et al.*, 2010). They consist of large, 22-stranded β -barrels with a cork/plug domain located in the central pore to control access to the periplasm (Noinaj *et al.*, 2010). The corresponding PBP then delivers the ferric-siderophore to the ABC permease for ATP-dependent translocation across the CM. The siderophore complex is then either subject to degradation or reduction to enable release of the iron (Schalk and Guillon, 2013). In Gram-positive bacteria, the process is similar except for the lack of the OM receptor (TBDT) and TonB-ExBD systems which are not required in the absence of an OM (Noinaj *et al.*, 2010).

1.7.3.2: Utilisation of ferri-siderophores by *C. jejuni*. *Campylobacter* spp. require iron for invasion and colonisation of the host (Palyada *et al.*, 2004; Naikare *et al.*, 2006; Zeng *et al.*, 2013). There are multiple mechanisms that enable this bacterium to acquire the iron that needs for proliferation and survival (Miller *et al.*, 2009). In addition to the ferrous-iron specific Feo system mentioned above, there are other systems involved in iron utilization in *C. jejuni* that enable uptake of ferric iron. These include systems that allow *C. jejuni* to use enterochelin and ferrichrome as a source of iron if provided exogenously. It should be noted that *C. jejuni* is unable to synthesis siderophores, but it possesses multiple TBDTs (Parkhill *et al.*, 2000; Naikare *et al.*, 2013; Richardson and Park, 1995) and siderophores are produced by other members of the gut microflora so are expected to be available to *C. jejuni*.

Ferri-enterochelin utilisation depends upon the *ceuBCDE* genes which encode a binding-protein-dependent ABC transporter system enabling *C. jejuni* to translocate this ferri-siderophore across the CM (Parkhill *et al.*, 2000). The CfrA protein acts as the corresponding TBDR (Palyada *et al.*, 2004) (or CfrB in some strains' such as JL11) and is necessary for gut colonisation (Palyada *et al.*, 2004; Xu *et al.*, 2010; Zeng *et al.*, 2013). Thus, the *cfrA* gene and *ceuBCDE* operon have an important role in ferri-enterochelin utilisation and mutation in any of these genes leads to decreased colonisation of *C. jejuni* and *C. coli* in the avian intestine (Palyada *et al.*, 2004).

In addition, the *cfhuABD* operon was identified in some *C. jejuni* strains, although is absent in the genome of others. It encodes a system related to ferri-ferrichrome transporters found in other bacteria and is similar to the *fhu* locus of *E. coli*, and thus is predicted to provide the ferrichrome utilisation capacity of *C. jejuni* (Galindo *et al.* 2001). This operon has a higher G+C content ($\geq 35\%$) than that of the *C. jejuni* genome indicating horizontal acquisition (Parkhill *et al.*, 2000; Fouts *et al.*, 2005; Hofreuter *et al.*, 2006; Pearson *et al.*, 2007). The CFhuA protein acts as the TBDR while, CFhuA and CFhuD are similar to the permease

CFhuB and periplasmic binding CFhuD proteins of ferrichrome system in the *E. coli* with identity about 25% (Galino *et al.*, 2001). Interestingly, *C. jejuni* NCTC 11168 has three different TonB–ExbB–ExbD systems, designated as TonB1, TonB2, and TonB3 (Naikare *et al.*, 2013; Gundogdu *et al.*, 2007; Palyada *et al.*, 2004); see (Fig. 1.5).

1.7.4. Haem utilisation. Haem can be used by *C. jejuni* as a source of iron (Pickett *et al.* 1992). *C. jejuni* is able to utilize iron from haemin, haemoglobin, haemoglobin-haptoglobin and haemin-haemopexin (Pickett *et al.* 1992; Palyada *et al.*, 2004; Zeng *et al.*, 2009). The capacity to utilise haem and haemoglobin is dependent on the *chuABCD* operon (van Vliet *et al.*, 1998; Pickett *et al.*, 1992; Parkhill *et al.*, 2000; Ridley *et al.*, 2006). ChuA is the TBDR for haem, ChuBCD forms the ABC-permease, and the adjacent *cj1613* gene specifies a putative haem oxygenase for release of iron from haem. It should be noted that loss of *chuA* or *cj1613c* prevented haem utilisation, but mutation in the other genes of the operon had no effect on haem utilization which indicates either no role of these genes as the inner-membrane haem transporters or the presence of a second IM haem uptake pathway (Ridley *et al.*, 2006).

1.7.5. Transferrin and lactoferrin utilisation. *C. jejuni* NCTC 11168 is also able to take up iron from human-transferrin (Tf) and human-lactoferrin (Lf) via a *cj0173c–cj0178* encoded system (Miller *et al.*, 2008). The gene cluster is organised as two parts with distinct promoters: *cj0176c–cj0173c* and *cj0177–cj0178* (Parkhill *et al.*, 2000). The products resemble the Tf/Lf iron-uptake systems in *Y. pestis* and *Haemophilus influenza* (vanVliet *et al.*, 2002). CfbpA (*cj0175c*) was identified as a periplasmic-binding protein and its crystal structure has been solved, CfbpB (*cj0174c*) is a permease, and CfbpC (*cj0173*) is an ABC protein (Tom-Yew *et al.*, 2005). Mutation of *cj0178* encoding the TBDR for Tf and Lf resulted in inhibition in iron acquisition from Tf and Lf, but not haem. Also, mutation of the

genes specifying the ABC transporter (*cj0173c-cj0175c*) affected growth in the presence of Lf as sole iron source (Chan *et al.*, 2006; Miller *et al.*, 2008) (see Fig. 1.5). Cj0176 is a very small predicted lipoprotein of unknown role, and Cj0177 is also an anticipated lipoprotein that binds haem, but its role is unclear (Miller *et al.*, 2008). The *cfbp* locus is adjacent to the *tonB1* locus (Fig. 1.5) indicated TonB1-dependence for Lf/Tf uptake.

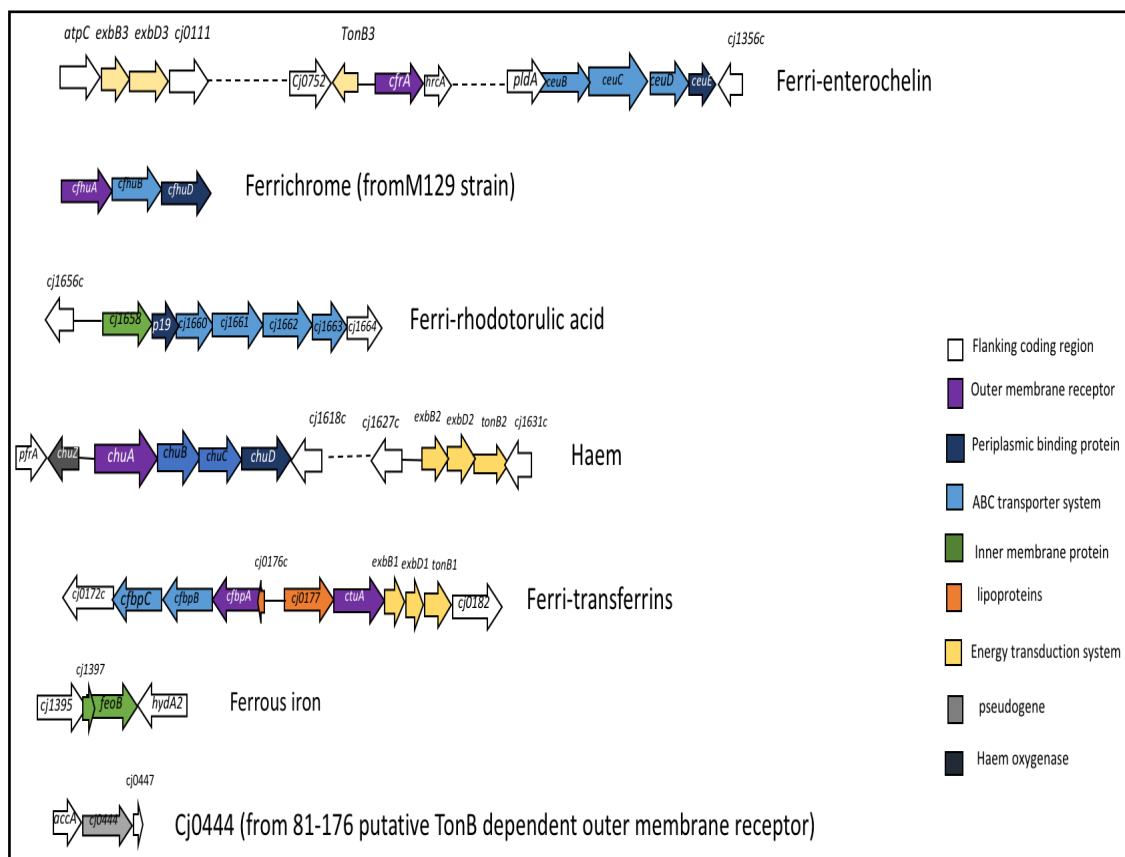


Figure 1.5: Iron-uptake systems of *C. jejuni*. The figure shows the genomic organization of the genes in each system. Based on NCTC 11168 strain, adapter from (Miller *et al.*, 2009).

1.7.6: Ftr-P19 (FetM-FetP) iron uptake system of *C. jejuni*, and related systems

In addition to the systems discussed above, a further iron transport system (Ftr1-P19) has been identified in *C. jejuni*. Initially, P19 was identified as a 19 kDa periplasmic protein induced by *C. jejuni* under iron restriction. It is encoded by *cj1659* (in strain 81176) and is acidic (4.8 isoelectric point) and was suspected to act as an iron-transport component (Janvier *et al.*, 1998). Later, studies of a related protein in *Yersinia pestis* indicated that P19 forms a

functional unit with an Ftr1-like protein (ferric permease) encoded by an adjacent gene. The adjacent gene (*cj1658*) in *C. jejuni* also encodes an Ftr1-like protein, indicating the P19 and Ftr1 of *C. jejuni* likewise form a function unit involved in iron uptake (Carniel, 2001). The *C. jejuni* P19 protein was initially shown to act as part of an iron transporter required for use of rhodotorulic acid as a ferri-siderophore (Stintzi *et al.*, 2008). A more recent study characterised P19 as a homodimeric periplasmic iron-binding protein that is part of a two component, high-affinity iron transporter.

The P19 crystal structure indicates that the P19 macromolecule is a globular homodimer of 70 x 35 x 20 Å, resembling a ‘deflated rugby ball’ in overall shape, with a β sandwich fold as the primary structural motif. It has two distinct metal-binding sites per monomer, one for iron (with Mn^{2+} bound) and another for copper. The copper-binding site employs three His ligands (His42, His95 and His132) along with Met88, while the Mn^{2+} is located just 7.7 Å from the Cu atom in a solvent channel and is bound via Asp92 and Glu44, with the more distantly located Glu3 possibly interacting electrostatically. The Glu44 residue is located between the two metal-binding sites and is proposed to enable interaction between the metals (Fig. 1. 6) (Chan *et al.*, 2010).

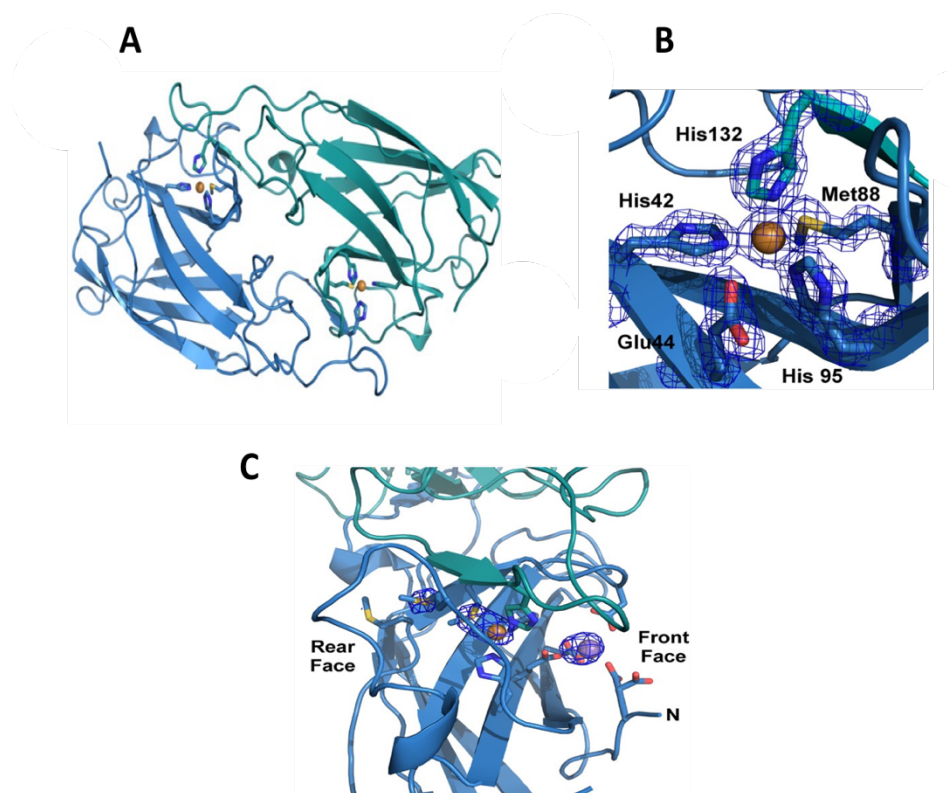


Figure 1.6: Structure of P19 from *C. jejuni*. **A.** The three-dimensional structure of the P19 homodimer with the two subunits distinguished by colour, and the bound Cu shown as a brown sphere. **B.** The Cu-binding site with the corresponding amino acid ligands labelled, along with Glu44. **C.** The Mn-binding site (Mn in purple) was generated through soaking crystals in a Mn^{2+} solution, acidic residues acting as ligands are indicated (Chan *et al.*, 2010).

The P19 protein of *C. jejuni* is encoded by a gene located in a cluster of eight conserved genes (*cj1658-cj1665*) (see Fig. 1.7). Located directly upstream of the *p19* encoding gene is the apparently co-operonic gene, *cj1658*, which specifies an integral inner-membrane protein, similar to Ftr1p of yeast and EfeU of *E. coli* (Große *et al.*, 2006; Larrondo *et al.*, 2007), and thus is anticipated to act as a ferric iron permease (although it should be noted that the Fet3p-Ftr1p and EfeUOB systems utilise ferrous iron in preference to ferric iron as primary substrates). Downstream of the *p19* gene (*cj1659*) is a set of conserved genes (*cj1661-cj1665*) encoding proteins similar to macrolide-exporting ABC transporters in the inner membrane (Parkhill *et al.*, 2000) and two periplasmic thioredoxin proteins (Miller *et al.*, 2009). The FetMP iron transporter of *E. coli* F11 (Koch *et al.*, 2011) resembles that of *C.*

jejuni. FetP was suggested to act as a ferric reductase and results suggested that the system supports uptake of both ferric and ferrous iron without any major impact of pH or anaerobiosis.

Ftr1 systems exist in a range of organisms. In *Saccharomyces cerevisiae*, Ftr1p is also induced by low iron. Its iron uptake activity requires ferrous iron as substrate and its activity is strongly supported by the extracellular ferric iron reductases, Fre1p and Fre2p. Its ferrous iron uptake activity also requires the membrane-tethered multicopper oxidase (Fet3p) which re-oxidises iron prior to transport by Ftr1p into the cytoplasm, using oxygen as the oxidant (Philpott, 2006). There are no homologues of Fet3p and Fre1/2p known to be associated with the P19 transporter system of *C. jejuni*. Also, the ferrous-transporting EfeUOB system of *E. coli* includes a homologue to Ftr1p (EfeU) that contains the two conserved REXxE motifs demonstrated to be needed for ferrous iron transport function in Ftr1 proteins. This transport system is expressed at low pH and in low iron conditions (Cao *et al.*, 2007; Große *et al.*, 2006). EfeO and EfeB are periplasmic proteins with probable roles in periplasmic ferrous-binding and ferrous-oxidation using hydrogen peroxide as oxidant (Große *et al.*, 2006; Cao *et al.*, 2007; Rajasekaran *et al.*, 2010). In *Bacillus subtilis*, the equivalent EfeUOB system is both a ferrous and ferric iron transporter (Miethke *et al.*, 2013). The *ftr_{Bcc}ABCD* locus of *Burkholderia cenocepacia* also encodes an iron transport system with an Ftr1 as well as P19 homologue; this system is conserved in all species of this genus and additionally includes a periplasmic cupredoxin and an integral membrane polyferredoxin. It is able to compensate for defective siderophore utilisation in *Burkholderia* and enhance growth of an *E. coli* strain lacking iron transport systems under iron limitation (Mathew *et al.*, 2014). Similar systems have been studied in *Bordetella pertussis* (Brickman and Armstrong, 2012) and *Brucella abortus* (Elhassanny *et al.*, 2013), where a similar function has been assigned.

In early studies there was no clear phenotype resulting from deleting the *p19* gene in *C. jejuni* (Janvier *et al.*, 1998; van Vliet *et al.*, 2002). However, later studies showed a decreased growth under iron-limiting conditions induced by the presence of the siderophore desferrioxamine as a ferric chelator (Chan *et al.*, 2010). The form of iron utilized by the Ftr1-P19 system was initially suggested to be ferric iron (as provided by rhodotorulic acid, a fungal siderophore) (Stintzi *et al.*, 2008). However, the results of Chan *et al.* (2010) suggest that the Ftr1-P19 system is able to transport iron in the absence of rhodotorulic acid and that the need of Ftr1-P19 for growth with rhodotorulic acid is probably related to its ability to effectively compete for iron in the presence of a strong ferric chelator (Chan *et al.*, 2010). A more recent study on *C. jejuni* strain 81-176, published during the course of this PhD by Liu *et al.* (2018) found that deletion of the six downstream genes (*cj1660-1665*) gives a reduced growth under iron restriction at low pH. The *cj1660-65* genes had been previously shown to be Fur and iron regulated, supporting a role in iron uptake (Holmes *et al.*, 2005), with *cj1660-3* considered to encode an ABC transporter. In addition, Fur was shown to bind upstream of the *p19* gene confirming the Fur regulation of the *p19* gene (Holmes *et al.*, 2005). The *cj1664-5* genes were inactivated by Liu and Kelly (2015) to test their role as a CcsX-like proteins (thioredoxins) in c-type cytochrome biogenesis, but no role was identified although a slight reduction in microaerobic growth was discovered for the *cj1664-5* double mutant.

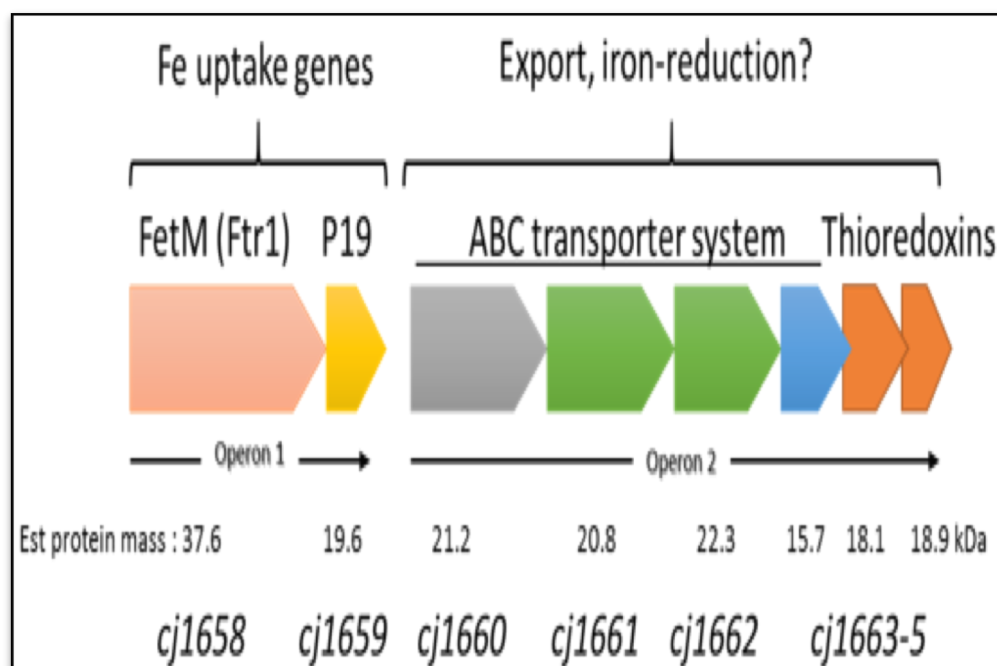


Figure 1.7: The *p19* gene cluster in *C. jejuni* subsp. *jejuni* serotype O:2 (strain ATCC 700819/ NCTC 11168). The predicted mass of each encoded protein (primary product) is indicated. Adapted from (Miller *et al.*, 2009).

1.8: Iron storage in *Campylobacter*

In order to protect the bacterial cell against iron-induced toxicity during excessive iron availability and also to supply iron when external supplies are limiting, additional amounts of iron are stored intracellularly in inert form by related proteins, ferritins and bacterioferritins. These related proteins are hollow and spherical and are composed of 24 (usually identical) subunits. The ferritins do not contain haem in their structure, whereas the bacterioferritins are haem-containing proteins (Andrews, 1998). Ferritins are highly conserved in nature and can carry up to 4500 ferric iron atoms (Chiancone *et al.*, 2004). The ferritin subunit structure is four-helix bundle with a ferroxidase site located within the four-helix bundle of each subunit and micelle nucleation sites facing the internal cavity. These subunits are assembled with 432 symmetry such that small hydrophobic 4-fold and hydrophilic 3-fold channels are formed as symmetry axes, through which iron and other ions pass. The iron passes through the 3-fold channels by a negative electrostatic gradient, then to the ferroxidase sites (Douglas and

Ripoli, 1998). Iron is stored in the ferric form, but at first Fe (II) binds and oxidized at the ferroxidase site, then it moves to the internal cavity of the apoferritin shell which is rich in carboxylate residues that provide the nucleation sites of the ferric oxy-hydroxide core. Ferritin iron can be mobilised by reduction when the iron is required. Ascorbate and flavins can act as ferritin iron mobilizing agents *in vitro* (Jones *et al.*, 1978; Takagi *et al.*, 1998). *C. jejuni* carries a single iron-storage protein gene, *cft* (*Campylobacter* ferritin), mutation of which causes decreased bacterial growth in iron-limited conditions and raised sensitivity to H₂O₂ (Wai *et al.*, 1996). The Dps proteins (DNA binding proteins from starved cells) are ferritin-like proteins also found in bacteria. They are smaller types of iron-storage protein consisting of only 12 identical subunits and are considered as a distinct group in the ferritin superfamily. *C. jejuni* carries a single *dps* gene (*cj1534c*) which, as in other bacteria, protects DNA and stores iron, and enhances survival in response to hydrogen peroxide which is important in colonisation of the chicken caecum (Sanchuki *et al.*, 2015). A role of CjDps *in vivo* was identified in colonisation of the chicken gut and biofilm formation (Theoret *et al.*, 2012). Dps in *H. pylori* (NAP; the neutrophil-activating protein) is similar to that in *C. jejuni* (CjDps) and it has the ability to bind DNA to protect this bacterium under oxidative conditions (Tonello *et al.*, 1999; Cooksley *et al.*, 2003). In some bacteria, the Dps protein plays a ferritin-like iron storage role as in *Listeria innocua* (Chiancone *et al.*, 2004).

1.9: Iron regulation in *Campylobacter*

1.9.1. General overview. Due to the ability of iron to form radical compounds in the presence of oxygen, free iron is toxic in high concentrations aerobically. Thus, cellular iron homeostasis mechanisms are required to avoid harm. For this reason, bacteria regulate iron uptake and metabolism carefully (Andrews *et al.*, 2003; Imlay, 2008; Barker *et al.*, 2015). In many Gram-negative and some Gram-positive bacteria, iron regulation is controlled by the Fur (ferric uptake regulation) protein (van Vliet *et al.*, 1998b; Coy and Neilands, 1991;

Stojiljkovic *et al.*, 1994). Fur is an iron-binding repressor and in *E. coli* it recognises a 19-bp binding site-specific sequence: 5'-GATAATGATAATCATTATC-3'. This 19 bp site is organised as three 5'-GATAAT-3 hexamers (Lavrrar and McIntosh, 2003). The Fur protein is a homodimer of 17 kDa subunits which possess two domains: The N-terminal DNA-binding domain forming a winged helix motif; and the C-terminal dimerization domain. There are two metal-binding sites per subunit, one regulatory site for Fe²⁺ at the interface between domains and another structural Zn²⁺ site within the dimerization domain (Gonzalez *et al.*, 2001).

In response to the intracellular iron levels, Fur regulates the expression of iron homeostasis genes and often does so by collaboration with a small regulatory RNA molecule (RyhB in *E. coli*) (Masse *et al.*, 2007). Under iron depletion, Fur inhibits expression of the genes involved in iron acquisition, the response to the oxidative stress and different virulence factors in *E. coli* (Fillat, 2014; Hanke, 2001; Hassan and Troxell, 2013; Embree *et al.*, 2014). For instance, in *E. coli*, iron acquisition and storage are regulated by Fur together with the sRNA species, RyhB. RyhB functions to down-regulate iron-assimilation proteins when iron is limited, it is negatively regulated by Fur (Masse *et al.*, 2007). When intracellular iron availability is high, Fur binds to ferrous iron and then acts as a negative regulator of *ryhB* and iron-uptake genes by binding to a conserved 'Fur box' DNA sequence located in the promoter region of target genes thus preventing their expression (Escolar *et al.*, 1999; Baichoo and Helmann, 2002) (see Fig. 1.8). Thus, when the external iron sources are less than 5–10 µM (Andrews *et al.*, 2003), Fur becomes inactive and subsequently the production of RyhB and iron acquisition systems is initiated in order to allow transcription of iron-uptake genes to maintain iron homeostasis (Massé and Gottesman, 2002; Masse *et al.*, 2007; Porcheron and Dozois, 2015).

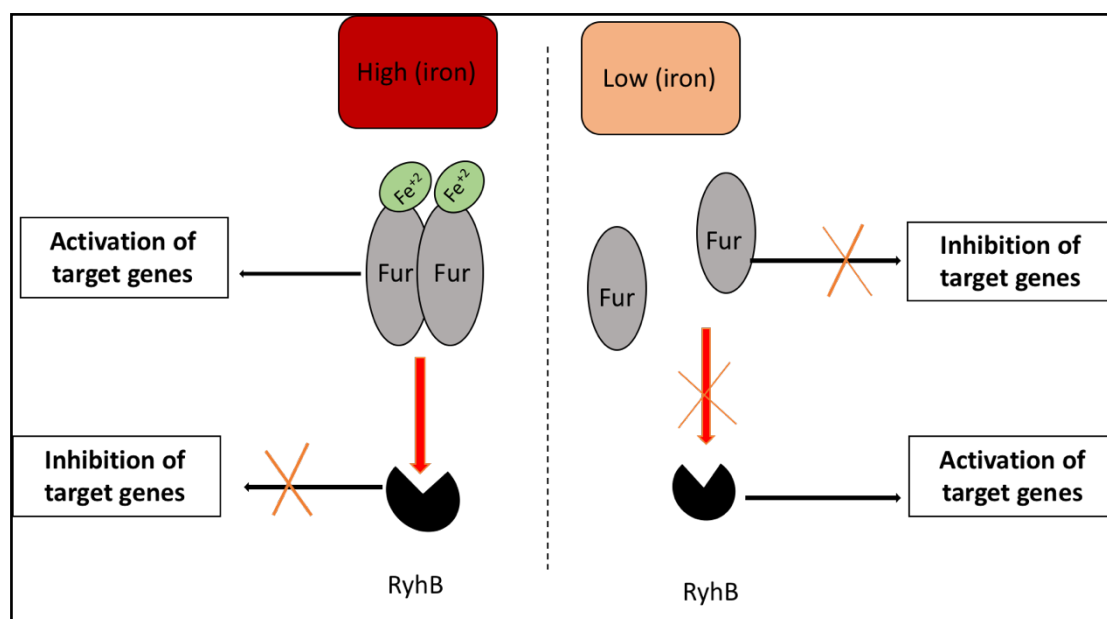


Figure 1.8: Schematic description of Fur and RyhB regulation in *E. coli*. Under high iron conditions, Fur acts as repressor for *ryhB* and other genes (e.g. involved in iron uptake and genes encoding non-iron-dependent isoenzymes of iron dependent proteins), and thus prevents RyhB from repressing the expression of RyhB-target genes. Under iron minimal conditions, *ryhB* is activated as Fur repression is relieved such that iron-protein genes are repressed as part of an iron rationing response (Porcheron and Dozois, 2015).

1.9.2. Fur in *C. jejuni*. In *C. jejuni*, Fur has different properties to that of other Gram-negative bacteria. It is upstream to the *lysS* and *glyA* genes (housekeeping genes) and it has low sequence identity with the Fur protein of other Proteobacteria, about 36.3% identity with *Y. pestis* and 31.8% identity with *Legionella pneumoniae* Fur protein. Fur in *C. jejuni* regulates several iron-uptake systems: Ceu, CfrA, ChuA and P19 (Chan *et al.*, 1995; vanVliet *et al.*, 1998b; Butcher *et al.*, 2015). As compared with the wild type strain, a *C. jejuni fur* mutant strain showed low growth in iron sufficient and limited media, but this was possibly due to an effect on *glyA* and *lysS* caused by the *fur* gene mutation. In addition, PerR (a Fur homologue responding to peroxide stress) has an important role in control and defence against oxidative stress (vanVliet *et al.*, 1999; Hantke, 2001). It was found that *C. jejuni* responds to the changes in iron status by changing uptake and metabolism of iron using both Fur and PerR transcription factors (vanVliet *et al.*, 1998b; vanVliet *et al.*, 1999); transcription analysis of the

C. jejuni genome revealed that PerR has a role in regulating iron homeostasis as well as oxidative stress resistance.

Deletion of *perR* led to expression of a set of genes induced in iron-restricted conditions as in the *fur* mutant. Also, mutation of both *fur* and *perR* showed that each regulator can compensate for the other which reveals the possibility of competition between these two regulators for binding to the same promoters and a strong regulatory linkage between iron homeostasis and redox stress (Butcher *et al.*, 2015). CjFur controls about 60 genes (inducing or repressing), these genes are related to iron uptake, oxidative defence, metabolism and flagellum formation (Palyada *et al.*, 2004; Holmes *et al.*, 2005). Also, there are more than 95 Fur binding sites were identified for CjFur in the *C. jejuni* genome, indicating the global nature of its regulatory control (Butcher *et al.*, 2012). The binding site sequence of CjFur is as follows: TGATAATxATTATCA for Fe-CjFur repression sequences; and TTTGGAxCAxTTTTTGxT for Fe-CjFur activation sequences (Palyada *et al.*, 2004; Butcher *et al.*, 2012).

1.10: Redox stress and oxygen tolerance in *Campylobacter*

C. jejuni is a microaerophilic organism and it is sensitive to atmospheric oxygen, but it is able to survive oxygen concentrations found inside the host intestine and during food processing (Hwang *et al.*, 2011; Sulaeman *et al.*, 2012). The fully aerobic condition causes damage of important oxygen-labile enzymes such as pyruvate: acceptor oxidoreductase (Por) and 2-oxoglutarate: acceptor oxidoreductase (Oor) (Kendall *et al.*, 2014). When *C. jejuni* is exposed to reactive oxygen species (ROS), for instance in cases of high O₂ levels, it responds by increasing its antioxidant defence activity through expression of genes encoding various components, including superoxide dismutase (SodB), alkyl hydroperoxide reductase (AhpC) and catalase (KatA) which are the major contributors to redox stress resistance (Baillon *et al.*, 1999; Grant and Park, 1995; Elvers and Park, 2002). In addition, the peroxiredoxin-like

putative peroxidases thiol peroxidase (Tpx) and bacterioferritin comigratory protein (Bcp) are also expected to provide oxidative stress resistance (Parkhill *et al.*, 2000). Further, *C. jejuni* possesses two cytochrome c peroxidases (CCP), encoded by *docA* and Cj0382. These are periplasmic proteins that reduce peroxide to water, although they may not contribute to peroxide resistance in all strains (Hendrixson and DiRita, 2004; Bingham-Ramos and Hendrixson, 2008; Flint *et al.*, 2014). *C. jejuni* also carries a redox-resistance system associated with anaerobes – a rubredoxin oxidoreductase/rubrerhythrin chimeric Rrc protein acting as an expected peroxide reductase (Yamasaki *et al.*, 2004; Flint *et al.*, 2014). Dps (described above), MsrAB (methionine sulphoxide reductase) and CmeG (efflux pump) also have roles in redox stress resistance (Atack and Kelly, 2008; Jeon *et al.*, 2010).

Superoxide dismutase (SOD) is the primary enzyme responsible for the detoxification of superoxide (Winterbourn *et al.*, 1975). *E. coli* has three *sod* genes (*sodA*, *sodB*, and *sodC*) which encode Mn, Fe and Cu-Zn cofactor-containing SOD, respectively (Imlay, 2008). *C. jejuni*, however, carries just one *sod* gene (*sodB*), encoding an Fe-Sod. Mutation of *sodB* causes increased susceptibility to superoxide and peroxide stress (Pesci *et al.*, 1994; Palyada *et al.*, 2009; Flint *et al.*, 2014). SodB provides resistance to both peroxide and superoxide, AhpC protects against hydroperoxides and KatA is involved in defence from H₂O₂ (Hwang *et al.*, 2011). SodB in *C. jejuni* is the most important enzyme in the detoxification of superoxide and has a role in chicken colonisation and intracellular survival of *C. jejuni* (Pesci *et al.*, 1994; Palyada *et al.*, 2009).

Interestingly, the SoxRS and OxyR regulators that control the redox stress response in *E. coli* are absent in *C. jejuni* (Garénaux *et al.*, 2009). Instead, *C. jejuni* utilises PerR (discussed above) as a regulator of resistance to oxidative stress (Kim *et al.*, 2015b). *perR* inactivation in strain NCTC 11168 causes increased expression of peroxidases, catalase and alkyl hydroperoxide reductase enzymes (Palyada *et al.*, 2009; van Vliet *et al.*, 1999) and had little

impact on normal growth but increased survival with atmospheric oxygen and H₂O₂ challenge (Handley *et al.*, 2015). However, this result is not consistent with the data of Palyada *et al.* (2009) where inactivation of *perR* gene in strain NCTC 11168 led to inhibition of *C. jejuni* colonisation in the chicken gut and decrease of motility. *perR* inactivation causes depression of many genes involved in iron metabolism indicating a role in control of iron uptake in response to redox stress (Butcher *et al.*, 2015) (see Fig. 1.9).

In addition, in *Campylobacter* spp., CosR (*Campylobacter* oxidative stress regulator; *Cj0355c*) is another regulator responsible for control of about 32 proteins involved in various cellular processes including a few proteins that are involved in oxidative resistance: SodB, Dps, Rrc and LuxS are negatively regulated; and AhpC is positively controlled. *cosR* knockdown raises sensitivity to oxidative stress (Hwang *et al.*, 2011).

Oxidative stress in *C. jejuni* arises due to the temperature change as catalase activity increases in *C. jejuni* as temperature rises, and *C. jejuni* is more susceptible to oxidative stress at high temperature (Hazeleger *et al.*, 1998; Garénaux *et al.*, 2008b). Exposure to cold-shock increases the expression of *sodB* and *Cj0358* (cytochrome c551 peroxidase) in *C. jejuni* NCTC 11168 (Stintzi and Whitworth, 2003) and a *sodB* mutation makes *C. jejuni* and *C. coli* more susceptible to freeze-thaw stress (Stead and Park, 2000; Garénaux *et al.*, 2009) indicating that oxidative stress influences the ability of *C. jejuni* to survive under freeze-thaw conditions. In addition, under acidic conditions (HCl or acetic acid), *C. jejuni* induces expression of oxidative stress defence genes (*dps*, *sodB*, *trxB* and *ahpC*; Birk *et al.*, 2012). Indeed, pre-exposure of *C. jejuni* to aerobic conditions increase its resistance to acid stress suggesting that oxidative stress is linked to the acid stress response (Murphy *et al.*, 2003). Furthermore, under high osmotic pressure (e.g. 1% NaCl) the oxidative stress genes, *katA* and *sodB*, are induced allowing *C. jejuni* increased oxidative stress resistance and indicating that oxidative stress defence is involved in the osmotic stress response (Cameron *et al.*, 2012).

The oxidative stress genes (*perR*, *ahpC*, *sodB* and *tpx*) are also induced by starvation (Wright *et al.*, 2009).

The oxidative stress defence systems of *C. jejuni* might also be important in formation of biofilm and stimulation of a viable-but-non-culturable (VBNC) state (Parsek and Singh, 2003). In foodborne bacteria oxidative stress is connected to the biofilm formation. For example, in *E. coli* O157:H7 expression of *tpx* and *sodC* increase in biofilms and mutation in these genes leads to disturbance in biofilm formation (Kim *et al.*, 2006). A similar effect is seen for *C. jejuni*, as during biofilm formation the levels of the oxidative stress proteins (e.g. AhpC and Tpx) are increased (Kalmokoff *et al.*, 2006). In addition, oxidative stress also affects entry of *C. jejuni* into a VBNC state. When the bacteria are in this state, they are alive but not culturable by normal microbiological means, and they appear smaller with a coccoid shape (Oliver, 2010). *C. jejuni* cell length decreases from 6 to 1.19 μm during entry into this state (Thomas *et al.*, 2002). Furthermore, virulence factors of *C. jejuni* may also be induced upon exposure to oxidative stress (Garénaux *et al.*, 2008a, Gundogdu *et al.*, 2011).

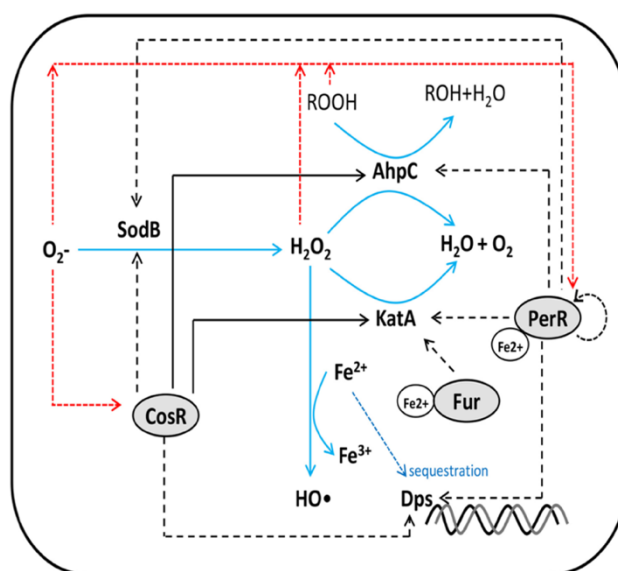


Figure 1.9: Schematic figure of CosR (the oxidative stress regulator), Fur (the ferric uptake regulator) and PerR (the peroxide resistance regulator) control in *C. jejuni*. The black solid and dotted lines indicate positive and negative regulation, respectively, and transcriptional or translational down regulation by reactive oxygen species is indicated by red dotted lines (Kim *et al.*, 2015b).

1.11: Aims and objectives of this study

The aim of this work was to determine the precise function of the Ftr1-P19/Cj1660-65 system and its components (in particular, *cj1660-65* genes) in *C. jejuni*.

The specific objectives of this study were:

- 1- To perform a bioinformatics survey of the conservation and species distribution of the Ftr1-P19 system and operon organisation, with generation a phylogenetic analysis for each encoded protein.
- 2- To determine whether the Ftr1-P19 system can enhance iron-restricted growth in an *E. coli* strain lacking iron transport systems (JC32), either as independent *ftr1-p19* and *cj1660-65* encoded system, or when combined as a complete eight gene system. Also, an objective was to identify the environmental conditions required for maximal low-iron growth enhancement (e.g. oxygen regime, type of chelator, pH, and reductant/oxidant) by the Ftr2-P19 system.
- 3- To generate targeted mutations in the *cj1660-5* and *ftr1-p19* genes (*ftr1*, *cj1660* and *cj1663* were chosen) in *C. jejuni* NCTC 11168 strain and determine whether the mutant strains exhibit reduced growth under iron restriction under different pH conditions.
- 4- To determine whether chicken colonisation is affected by the above mutations.
- 5- To confirm that the *ftr1-p19/cj1660-65* genes are iron, and Fur controlled.

Chapter 2: Materials and Methods

2.1. Chemicals

All chemicals were of analytical grade or higher and were purchased from Bio-Rad, Fisher, Melford or Sigma. Ultra-pure water (qH₂O) was obtained from a NANOpure Diamond (Barnstead)TM system (conductivity of 18.2 μ S/m at 25 °C).

2.2. Enzymes

All restriction enzymes were purchased from Promega, New England Biolabs or Fisher Scientific). DNA polymerase was from Bioline, Fisher Scientific or and CloneTech. All enzymes were used according to the manufacturer's instructions.

2.3. DNA marker

GeneRulerTM 1 kb DNA Ladder from Fermentas was used to determine the size of the DNA of interest and its quantity by gel electrophoresis (Fig. 2.1).

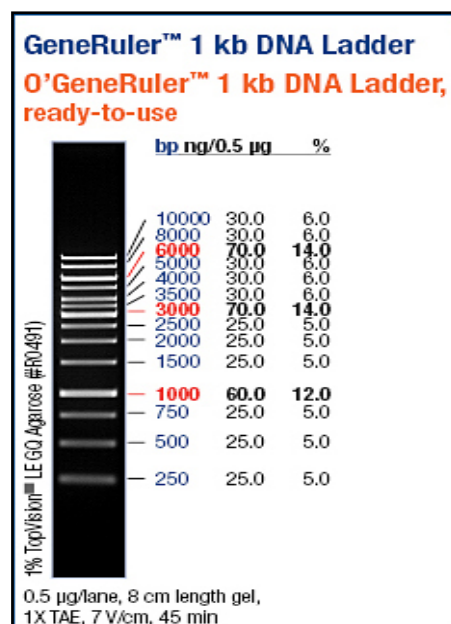


Figure 2.1. GeneRuler 1 kb DNA ladder.

2.4. Antibiotics

Antibiotics were prepared as stocks. Those dissolved in water or (ethanol/suitable dissolvent) were filtered using a sterile 0.22 μm membrane (Whatman) and stored at $-20\text{ }^{\circ}\text{C}$ for future use (Table 2.1).

Table 2.1: Antibiotics used in this work

Antibiotic	Uses	Working Strength
Ampicillin (100 mg/ml) dissolved in qH ₂ O.	Used in Luria Agar (LA) and minimal medium (M9) agar plates to select <i>E. coli</i> strains with pBAD _{ara} /pBAD _{ara} constructs.	100 $\mu\text{g/ml}$
Chloramphenicol (50 mg/ml) dissolved in ethanol.	Used in LA and M9 plates to select <i>E. coli</i> strains with pBAD _{rha} /pBAD _{rha} constructs.	50 $\mu\text{g/ml}$
Kanamycin (50 mg/ml) dissolved in qH ₂ O.	Used in blood agar plates to select <i>C. jejuni</i> strain with PMA1 constructs.	25 $\mu\text{g/ml}$
Trimethoprim (10 mg/ml) dissolved in DMSO	Used in BHI- blood agar to prevent any contamination during electroporation.	5 $\mu\text{g/ml}$
CCDA Selective Supplement SR0155E, one vial for 500 ml medium, dissolved in	Used together in blood agar and M-H agar plates to prevent growth of <i>E. coli</i> following biparental conjugation.	Cefoperazone (32 $\mu\text{g/ml}$) and amphotericin B (10 $\mu\text{g/ml}$)

DMSO		
------	--	--

2.5. Microbiological media

Media components were purchased from Oxoid, Fisher Scientific or Sigma, and were solidified by adding agar as necessary. Media were sterilised by autoclaving at 121 °C and 20 lbs/in² for 20 min, and were then cooled to 55 °C, mixed and poured in sterile Petri dishes. All glassware used in microbiological procedures was dry-heat sterilised (150 °C for 2.25 h). The glassware that used for iron-restricted growth was soaked in 0.1 M HCl for 20 min and then rinsed in qH₂O (before sterilisation).

2.5.1. Lysogeny broth medium (LB)

LB agar was prepared by adding 5 g NaCl, 5 g tryptone and 2.5 g yeast extract to 500 ml qH₂O, then autoclaved with 1.5% agar. Antibiotic and inducer were added after cooling, as required. This medium was used for *E. coli* growth.

2.5.2. M9 minimal medium

M9 minimal medium was prepared by adding 5 g M9 salts (Sigma) to ~400 ml of qH₂O in a 500 ml acid-washed Duran, which was then autoclaved and allowed to cool. The following sterile solutions were then added to the medium: 0.5 ml 1 M MgSO₄ (1 mM final concentration), 0.5 ml 0.1 M CaCl₂ (0.1 mM final concentration), 0.5 ml 20% w/v glucose (0.2% final concentration) and 0.25 ml of 1% w/v thiamine (5 µg/ml). The final volume was then adjusted to 500 ml with sterile qH₂O. This medium was used for *E. coli* growth under iron restriction.

2.5.3. Blood agar

Blood agar (BA) was prepared by adding 40 g of blood agar base to 1 L of qH₂O with 1.5% w/v agar. After sterilisation and cooling to 55 °C, sterile defibrinated horse blood (final concentration of 5% v/v) was aseptically added and mixed. Antibiotics were also added, as required. This solid medium was used for the preparation of *C. jejuni* inoculant and for routine culturing. Agar levels were raised to 2% for colony isolation and colony counting.

2.5.4. Brain Heart Infusion medium

Brain heart infusion (BHI) was prepared by adding 37 g BHI broth to 1000 ml of qH₂O in a 1000 ml acid-washed Duran, which was then autoclaved. Agar was added as required. In some cases, defibrinated horse blood was added at 5% final concentration (after cooling the medium to 50 °C). This medium was used for *C. jejuni* growth.

2.5.5. Muller-Hinton medium

Muller-Hinton (M-H) medium was prepared by adding 21 g M-H broth (Fisher Scientific) to ~950 ml of qH₂O in a 1000 ml acid washed Duran. Agar (if needed) was added at 1.5% for preparation of inocula and routine culture of *C. jejuni*, but at 0.4% for monitoring *C. jejuni* motility. The medium was autoclaved before use and antibiotic was added, as required, once cooled to 50 °C.

2.5.6. Dulbecco's Modified Eagle Medium

Dulbecco's Modified Eagle Medium (DMEM) (low glucose), sterile and ready to use from Thermo-Fisher, used for *C. jejuni* growth in a minimal medium under iron limitation.

2.5.7. SOC media

S.O.C. Medium is used in the final step of bacterial cell transformation to obtain maximal transformation efficiency of *E. coli*. The composition: 2% tryptone, 0.5% yeast extract, 10

mM NaCl, 2.5 mM KCl, 10 mM MgCl₂, 10 mM MgSO₄, and 20 mM glucose. Used ready from ThermoFisher.

2.6. Centrifugation

A Biofuge bench top Micro Centrifuge (MSE) or Eppendorf centrifuge 5424 was used to centrifuge volumes smaller than 1.5 ml. A Biofuge bench top centrifuge (Centaur) was used for centrifugation of large samples. A benchtop BR401 refrigerated centrifuge (Denley) or refrigerated Eppendorf centrifuge 5804 R was used for centrifugation of large samples at 4 °C.

2.7. Bacterial strains

All bacterial strains of *E. coli* and *C. jejuni* used in this research are listed in Table 2.2. These strains were stored at -80 °C in 15% (v/v) glycerol in L-broth or BHI broth using sterile Eppendorf or cryogenic tubes.

Table 2.2. Bacterial strain used in this study

<i>C. jejuni</i> strains	Genotype	Source/ Reference
<i>C. jejuni</i> NCTC 11168	Wild type	From human stool, 1977, UK (Parkhill <i>et al.</i> , 2000)
<i>C. jejuni</i> NCTC 11168	<i>C. jejuni</i> NCTC 11168 (Δ <i>ftrI</i>)::Cm ^R	This study
<i>C. jejuni</i> NCTC 11168	<i>C. jejuni</i> NCTC 11168 (Δ <i>cj1660</i>)::Cm ^R	This study
<i>C. jejuni</i> NCTC 11168	<i>C. jejuni</i> NCTC 11168 (Δ <i>cj1663</i>)::Cm ^R	This study
<i>C. jejuni</i>	<i>C. jejuni</i> NCTC 11168 (Δ <i>ftrI</i>)::Cm ^R carrying pMA1- <i>fetMP</i>	This study

NCTC 11168		
<i>C. jejuni</i> NCTC 11168	<i>C. jejuni</i> NCTC 11168 ($\Delta cj1660$)::Cm ^R Carrying pMA1- <i>fetA-F</i>	This study
<i>C. jejuni</i> NCTC 11168	<i>C. jejuni</i> NCTC 11168 ($\Delta cj1663$)::Cm ^R Carrying pMA1- <i>fetA-F</i>	This study
<i>C. jejuni</i> NCTC 11168	Wild type carrying pMA1 empty vector	This study
<i>C. jejuni</i> NCTC 11168	Wild type carrying pMA1- <i>fetMP</i>	This study
<i>C. jejuni</i> NCTC 11168	Wild type carrying pMA1- <i>fetA-F</i>	This study
<i>C. jejuni</i> NCTC 11168 H	Wild type	High motile variant of the reference isolate. 11168, provided by Andrey Karlyshev (Karlyshev <i>et al.</i> , 2002)
<i>C. jejuni</i> PT 14 strain	Wild type	Highly motile isolate provided by Ian Connerton (Nottingham University)
<i>C. jejuni</i> PT 14 strain	<i>C. jejuni</i> PT14 ($\Delta ftr1$)::Cm ^R	This study
<i>C. jejuni</i> PT 14 strain	<i>C. jejuni</i> PT14 ($\Delta cj1660$)::Cm ^R	This study
<i>C. jejuni</i> PT 14 strain	<i>C. jejuni</i> PT14 ($\Delta cj1663$)::Cm ^R	This study
<i>C. jejuni</i> NCTC 11168 (AS144)	Wild type	Provided by Alain Stintzi (Ottawa university)

<i>C. jejuni</i> NCTC 11168 (AS230)	<i>C. jejuni</i> NCTC 11168 (Δfur)::Cm ^R	Provided by Alain Stintzi (Ottawa University)
--	---	---

<i>E. coli</i> strains	Genotype	Source/ Reference
Top10 <i>E. coli</i>	<i>E. coli</i> F ⁻ , <i>mcrA</i> , $\Delta(mrr$ - <i>hsdRMS-mcrBC)</i> , $\phi 80lacZ\Delta M15$, $\Delta lacX74$, <i>nupG</i> , <i>recA1</i> , <i>araD139</i> , $\Delta(ara-leu)7697$, <i>galE15</i> , <i>galK16</i> , <i>rpsL</i> (Str ^R), <i>endA1</i> , λ^-	(Sambrook <i>et al.</i> , 2001) Lab stock
<i>E. coli</i> W3110	Wild type	Lab stock
<i>E. coli</i> JC28	W3110, $\Delta feoABCD$, $\Delta zupT$, $\Delta mntH$, $\Delta entC$, $\Delta feoABC$	(Cao <i>et al.</i> , 2007)
<i>E. coli</i> JC32#1	W3110, $\Delta feoABCD$, $\Delta zupT$, $\Delta mntH$, $\Delta entC$, $\Delta feoABC$, $\Delta efeu$	(Cao <i>et al.</i> , 2007)
<i>E. coli</i> JC32 pBAD_{rha}- <i>fetMP</i>	W3110, $\Delta feoABCD$, $\Delta zupT$, $\Delta mntH$, $\Delta entC$, $\Delta feoABC$, $\Delta efeu$ carrying pBAD _{rha} - <i>fetMP</i>	This study
<i>E. coli</i> JC32 pBAD_{rha}-<i>fetA</i>- <i>F</i>	W3110, $\Delta feoABCD$, $\Delta zupT$, $\Delta mntH$, $\Delta entC$, $\Delta feoABC$, $\Delta efeu$ carrying pBAD _{rha} - <i>fetA-F</i>	This study
<i>E. coli</i> JC32 pBAD_{ara}- <i>fetMP</i>	W3110, $\Delta feoABCD$, $\Delta zupT$, $\Delta mntH$, $\Delta entC$, $\Delta feoABC$,	This study

	Δ <i>efeu</i> carrying pBAD _{ara} - <i>fetMP</i>	
<i>E. coli</i> JC32 pBAD _{ara} - <i>fetA-F</i>	W3110, Δ <i>feoABCD</i> , Δ <i>zupT</i> , Δ <i>mntH</i> , Δ <i>entC</i> , Δ <i>feoABC</i> , Δ <i>efeu</i> carrying pBAD _{ara} - <i>fetA-F</i>	This study
<i>E. coli</i> JC32 pBAD _{ara} - <i>fetMPABCDEF</i>	W3110, Δ <i>feoABCD</i> , Δ <i>zupT</i> , Δ <i>mntH</i> , Δ <i>entC</i> , Δ <i>feoABC</i> , Δ <i>efeu</i> carrying pBAD _{rha} - <i>fetMP</i> and pBAD _{ara} - <i>fetA-F</i>	This study
<i>E. coli</i> JC32 pBAD _{rha} - <i>fetMPABCDEF</i>	W3110, Δ <i>feoABCD</i> , Δ <i>zupT</i> , Δ <i>mntH</i> , Δ <i>entC</i> , Δ <i>feoABC</i> , Δ <i>efeu</i> carrying pBAD _{ara} - <i>fetMP</i> and pBAD _{rha} - <i>fetA-F</i>	This study
<i>E. coli</i> S17	<i>recA pro hsdR</i> RP4-2-Tc: Mu-Km: Tn7 (T _{mp} ^r Str ^r); used for conjugation	(Parke, 1990)
<i>E. coli</i> S17 pMA1- <i>fetMP</i>	<i>recA pro hsdR</i> RP4-2-Tc: Mu-Km: Tn7 (T _{mp} ^r Str ^r) carrying pMA1- <i>fetMP</i>	This study
<i>E. coli</i> S17 pMA1- <i>fetA-F</i>	<i>recA, pro, hsdR</i> RP4-2-Tc: Mu-Km ^r : Tn7 (T _{mp} ^r Str ^r) carrying pMA1- <i>fetA-F</i>	This study

Stellar competent <i>E. coli</i>	<i>E. coli</i> HST08 strain, F ⁻ , <i>endA1</i> , <i>supE44</i> , <i>thi-1</i> , <i>recA1</i> , <i>gyrA96</i> , <i>phoA</i> , Φ80d <i>lacZ</i> Δ M15, Δ(<i>lacZYA-argF</i>)U169, Δ(<i>mrr-hsdRMS-mcrBC</i>), Δ <i>mcrA</i> , λ ⁻	Clontech
---	---	----------

2.8. Plasmids

All plasmid stocks were maintained at -20 °C in ultra-pure water. Plasmid details are listed in Table 2.3.

Table 2.3. Plasmids used in this study

Plasmid name	Genotype	Antibiotic resistance	Source/ Reference
pBAD_{rha}	Cloning vector with rhamnose inducible promoter (P _{rha})	Cm ^R	(Ford <i>et al.</i> , 2014)
pBAD_{ara}	Cloning vector with arabinose inducible promoter (P _{ara})	Amp ^R	(Guzman <i>et al.</i> , 1995)
pBAD_{rha}-<i>fetMP</i>	pBAD _{rha} plus <i>ftrI</i> - <i>p19</i> genes from <i>C. jejuni</i> NCTC 11168	Cm ^R	This study

pBAD_{rha}-<i>fetA-F</i>	pBAD _{rha} plus <i>fetA-F</i> genes from <i>C. jejuni</i> NCTC 11168	Cm ^R	This study
pBAD_{ara}-<i>fetMP</i>	pBAD _{ara} plus <i>ptr1-p19</i> genes from <i>C. jejuni</i> NCTC 11168	Amp ^R	This study
pBAD_{ara}-<i>fetA-F</i>	pBAD _{ara} plus <i>fetA-F</i> genes from <i>C. jejuni</i> NCTC 11168	Amp ^R	This study
pJET1.2	Cloning vector	Amp ^R	Fermentas
pJET-<i>Δptr1::cat</i>	pJET plus <i>Δptr1</i> gene from <i>C. jejuni</i> NCTC 11168 with <i>cat</i> cassette gene from pVA35 vector	Amp ^R , Cm ^R	This study
pJET-<i>Δcj1660::cat</i>	pJET plus <i>Δcj1660</i> gene from <i>C. jejuni</i> NCTC 11168 with <i>cat</i> cassette from plasmid pVA35	Amp ^R , Cm ^R	This study
pJET-<i>Δcj1663::cat</i>	pJET plus <i>Δcj1663</i> gene from <i>C. jejuni</i>	Amp ^R , Cm ^R	This study

	NCTC 11168 with <i>cat</i> cassette gene from pVA35 vector		
pMA1	10 kb; <i>E. coli</i> / <i>C. jejuni</i> shuttle vector	Km ^R	(van Mourik <i>et al.</i> , 2008)
pMA1-<i>ftr1-p19</i>	PMA plus <i>ftr1-p19</i> genes from <i>C. jejuni</i> NCTC 11168	Km ^R	This study
pMA1-<i>fetA-F</i>	pMA1 plus <i>fetA-F</i> genes from <i>C. jejuni</i> NCTC 11168	Km ^R	This study
pVA35	pBluescript II SK containing <i>C. coli</i> Cm ^R cassette	Cm ^R	(van Vliet <i>et al.</i> , 1998b)

2.9. Primers used in this study for PCR amplification and sequencing

Oligonucleotides primers used in this work are listed in Table 2.4. All primers were from Eurofins or Sigma-Aldrich.

Table 2.4. Primers used for amplification and cloning of wildtype genes into pBAD_{rha} and pBAD_{ara} plasmids, and for sequencing. The underlined sequences represent the restriction enzyme sites.

Name	Sequence 5' -3'	Restriction enzyme	T _m (°C)	Length (bp)
pBAD _{rha} - <i>fetM</i> -P F	TCAGCAGGATCACATATGAAAATTTT TAAAATTATATTTTAAATTATAAGTAT TTTTTTATCAAGC	<i>NdeI</i>	62.2	66
pBAD _{rha} - <i>fetM</i> -P R	TTCAAACACTCGGAAAATCCGAGCGT AAAA	<i>BamHI</i>	58.9	30
pBAD _{rha} - <i>fetA</i> -F F	CAGCAGGATCACATATGAGTATATAT TTTGTGCATTTTCTTATCAGTGTTTAA CC	<i>NdeI</i>	66.1	55
pBAD _{rha} - <i>fetA</i> -F R	GACTCTAGAGGATCCTTAGCTTTTTA CTTTTTTGATTTCTTTTTCAAGTATGC TATAAGG	<i>BamHI</i>	66.7	60
pBAD _{ara} - <i>fetM</i> -P F	GAGGAATTAACCATGAAAATTTTAA AATTATATTTTAAATTATAAGTATTTT TTTATCAAGC	<i>NcoI</i>	60.7	63
pBAD _{ara} - <i>fetM</i> -P R	CCAAAACAGCCAAGCTTAAACACTCG GAAAATCCGAGCGTAAAATTA	<i>HindIII</i>	67.2	47
pBAD _{ara} - <i>fetA</i> -F F	GAGGAATTAACCATGGTATATATTTT GTGCATTTTCTTATCAGTGTTTACC	<i>NcoI</i>	64.6	52
pBAD _{ara} - <i>fetA</i> -F R	CCAAAACAGCCAAGCTTTTAGCTTTT TACTTTTTTGATTTCTTTTTCAAGTAT GCTATAAGG	<i>HindIII</i>	66.6	62
pBAD _{rha} -p19 F1	CTTCCCTGGTTGCCAATG	-	51.1	19
pBAD _{rha} -p19 R1	AAGCTTGCATGCCTGCAGGT	-	53.8	20

pBADara-p19 F1	ATGCCATAGCATTTTTATCC	-	45.6	20
pBADara-p19 R1	TCTGATTTAATCTGTATCAGG	-	46.5	21
Ftr1-rha F2	TTT AGT GAT TAT CGC AAT ACC AAA GT	-	51.7	26
Ftr1-rha F3	TCAAACAATAGTGCAAAAACCCTT	-	50.6	24
Ftr1-rha F4	ATCCAAATGGTTTTCCAGAAGG	-	51.1	22
Ftr1-rha R2	CGCCTGCAAATAAATTTGTACTAATA ACC	-	55.9	29
Fr1-rha R3	GTA CTTGCTTTGATAAGAGCTAC	-	51.7	23
Ftr1-rha R4	TGTGTCAAAGGAGTTCATCTTA	-	49.9	23
Cj-rha F2	AGC CTT TAA CCA TAG ATG AGC C	-	53	22
Cj-rha F3	AGC AGT GCA AGG AGA ATG GGC A	-	56.7	22
Cj-rha F4	CCT CAA TGA GCT TTT TAA AAG C	-	49.2	22
Cj-rha F5	TGC TAG TTT AAT CGG AGC TT	-	47.7	20
Cj-rha F6	AGC TGT AAA ACT TGC TGATGA	-	48.5	21

Cj-rha F7	ACG ATG CAA AAG CTT GGG CTG AT	-	55.3	23
Cj-rha R2	CTCCACTATCACAAGCTACAAA	-	51.1	22
Cj-rha R3	AGTGAGTCTATGCGAAAGTCCTACT	-	56	25
Cj-rha R4	TGAAGTTCATTGCCTGCTTTTAG	-	51.7	23
Cj-rha R5	GCCCATTAAGGATTGGATCTT	-	50.5	21
Cj-rha R6	TTTAGCCAACATCATTCTCCT	-	49.9	23
Cj-rha R7	TCAAATACAAACAAGCAAGGCT	-	49.9	23

Table 2.5. Primers used for generation of knockout constructs

Name	Sequence 5' -3'	Restriction enzyme	T _m (°C)	Length (bp)
pJET- ftr1 F	CACCTTCCATACCTTCGATGAGTTCAT TCATCAATGCCTCGTTTGTGTCC	-	70.3	50
pJET- ftr1 R	CCTAAAGAACTTATACCTTCGCTATCG ATTAAAGAGCTAGTAAAAATAGGGA	-	66.2	52
Ftr1 Inverse <u>F</u>	CAT <u>GCGATCGCGCTTATAGCCGTATTA</u> CTACTC	<i>Asi</i> SI	64.4	33

Ftr1 Inverse R	AGGGCGATCGCAGCTTGGGTGGTTAA AGAGCT	<i>AsiSI</i>	67	32
Δ ftr1- cat- infusion F	CCAAGCTGCGATCGCCGAATTCCTGCA GCCCCGGGGGATCC	<i>AsiSI</i>	75.8	40
Δ ftr1- cat- infusion R	TATAAGCGCGATCGCGGGCGCCGCTCT AGAAGTAGTGGAT	<i>AsiSI</i>	71.7	40
pJET F	CGACTCACTATAGGGAGAGCGGC	-	60.6	23
pJET R	AGAACATCGATTTTCCATGGCA	-	51.1	22
Δ ftr1- F1	CTCAGCTTTTGCTAGGGTAGATG	-	55.3	23
Δ ftr1-R 1	ACCGCAGCTGCAGCAACTACTGAT	-	59.1	24
Δ ftr1- F2	CATGCTTATAGCCGTATTACTAC	-	51.7	23
Δ ftr1-R 2	TGCGATTAAAGCTTCTGCATCA	-	51.1	22
Δ ftr1- F3	GGCGTAGGAAATTATGAACTTAC	-	51.7	23
Δ ftr1-R 3	ATTTGCTTCTTCTTCTCAGCC	-	51.1	22
pJET- cj1660	TCAAGCCTTGCTTTTTGATGCTAAAAC AAGCACTGATTTTGGTGCTGT	-	67.1	48
pJET- cj1660	TTGAAATCGCAATACTTGCAACAATAA GACAAATAATGCAAGTAATGCC	-	65.4	50

Cj1660 Inverse F	CAAGCGAT <u>CGC</u> AGGTTATAAACACCC AAGCTCC	<i>Asi</i> SI	53 / 65.6	22/33
Cj1660 Inverse R	ATTGCGAT <u>CGC</u> AGGAGTGATAAAGGC CATTAAA	<i>Asi</i> SI	49.2/ 61.9	22/33
Δ cj1660- <i>cat</i> infusion R	TCCT <u>GCG</u> ATCGCAATCGAATTCCTGCA GCCCGGGGGATCC	<i>Asi</i> SI	73.7	40
Δ cj1660- <i>cat</i> infusion R	ACCT <u>GCG</u> ATCGCTTGGCGATCGCGGCG GCCGCTCTAGAAC	<i>Asi</i> SI	75.8	40
<i>cat</i> - Δ 1660 F1	TCACCTAGAAGCTGACATTCACG	-	55.3	23
<i>cat</i> - Δ 1660 R1	CTCCTTGCACTGCTAAATAAGGAT	-	54	24
Δ 1660 F2	CGAGTATTTGGACTGAGTTTACAGC	-	56	25
Δ 1660 F3	AGGAGATACTATCAAATTCATAGGAG	-	53.2	26
Δ 1660 R2	TCGCGGCGGCCGCTCTAGAACTA	-	62.4	23
Δ 1660 R3	ACCCGGGATCCCCCGGGCTGCAG	-	67.8	23
pJET- cj1663 F	AAGTCCCAAGCAGGATGAAAATTTTAT CTCCAATACTGAGT	-	63.5	41

pJET-cj1663 R	TGAAAAAACTAAGCACAGGTACTCCA TATATTTCCCC	-	62.2	37
Cj1663 Inverse F	TCGGCGATCGCCAGATCGAACCTTAT CTTACAAC	<i>AsiSI</i>	54/ 66.8	24/ 35
Cj1663 Inverse R	CATGCGATCGCAGACGCTTAAGTTGAT ATTGTTTAAGGC	<i>AsiSI</i>	55.5/ 65.5	28/39
Δ cj1663- <i>cat</i> Infusion F	GTCTGCGATCGCATGCGAATTCCTGCA GCCCCGGGGATCC	<i>AsiSI</i>	74.7	40
Δ cj1663- <i>cat</i> infusion R	TCTGGCGATCGCCGAGCGATCGCGGCG GCCGCTCTAGAAC	<i>AsiSI</i>	76.8	40
<i>cat</i> -1663 F1	ATCGATGCAAAACCTATATCTTCAG	-	52.8	25
<i>cat</i> -1663 R1	TCTATCTTTTATCATCCCATCTTTAAT	-	50.6	27
Δ 1663 F2	ATGGAGTTACAACGATCATCAATCG	-	54.4	25
Δ 1663 F3	TGTAGCTTGTGATAGTGGAGAA	-	51.1	22
Δ 1663 R2	ATCCCGGGTACCTGCAGAATTCA	-	57.1	23
Δ 1663 R3	GCAGACGCTTAAGTTGATATTG	-	51.1	22

Table 2.6. Primers used for generation of complementation constructs

Name	Sequence 5' -3'	T _m (°C)	Length (bp)
Ftr- pMA1 F	TTATGCATCGCGAGCGAAACATCTGAA ACCATACATCCTC	66.5	40
Ftr- pMA1 R	ATTGATCCTCTAGAGCACAAAATATATA CTCATAATTTACTCTTTAAAC	62.1	49
Cj1660- pMA1 F	TTATGCATCGCGAGCTGCAAATATTGCT ATGGAAAAAGATAAAAAAGGTGGC	67.7	52
Cj1660- pMA1 R	ATTGATCCTCTAGAGAGGTTATAGTGAA AAATATCCTGTAATTTTGATG	63.7	49

Table 2.7. Primers used to confirm *C. jejuni* AS230 Δfur

Name	Sequence 5' -3'	Restriction enzyme	T _m (°C)	Length (bp)
<i>fur-F</i>	GGAAGATCTGGCTTAAGGGTATTATCAATG	<i>Bgl</i> III	58.9	30
<i>fur-R</i>	GGAAGATCTCATATCAACATAACGTTTACG	<i>Bgl</i> III	57.5	30

*Match to published primer sequences (Palyada *et al.*, 2004).

2.10. Harvesting and stocking of *C. jejuni* strains

Harvesting of *C. jejuni* strains from plates involved taking a loop full of colonies from a plate after 40-48 h of incubation at 37 °C under microaerophilic conditions. Microaerophilic conditions were generated either using a Campy gas pack (CampyGen™) or a Whitley M35 HEPA atmosphere workstation (5% O₂, 10% CO₂, 83% N₂, 2% H₂). A single colony was streaked on two BA plates; one was used primarily for genomic or plasmid isolation and the other plate was used for stocking at -80 °C in BHI (15% v/v glycerol). All stocks were prepared in a class 2 Biological Safety Cabinet to avoid contamination.

2.11. DNA manipulation and analysis methods

2.11.1. Extraction of genomic DNA

Extraction of *C. jejuni* chromosomal DNA was achieved by plating out the strain from the laboratory stocks followed by incubation for 40-48 h at 37 °C, microaerobically. Then genomic DNA was isolated using the GeneJET™ Genomic DNA (ThermoScientific) purification kit according to the manufacturer's instructions.

2.11.2. Polymerase chain reaction

Amplification of DNA fragments of interest from genomic DNA was performed using the polymerase chain reaction (PCR) in a Bio-Rad MJ mini thermocycler with 0.2 ml thin wall PCR tubes. The reaction volume was 25 µl which included 12.5 µl HiFi PCR premix (Clontech), 0.5 µl of 0.5 µM forward primer, 0.5 µl of 0.5 µM reverse primer, 1.5 µl (50-200 ng/µl) template DNA and qH₂O to give 25 µl final volume. The reaction was performed with an initial denaturation step at 95 °C for 5 min, followed by 30 cycles of 98 °C for 10 s (denaturation), 60-68 °C for 90 s (annealing) and 72 °C for 2 min (extension), with a final polymerisation step at 72 °C for 10 min to ensure all amplification reactions had reached completion.

2.11.3. Purification of PCR products

PCR products were purified using the GeneJET™ PCR Purification Kit (Fermentas), according to the manufacturer's instructions. One volume of binding buffer was added to the PCR product, the re-suspension solution was then transferred to the GeneJET™ purification column which was then micro-centrifuged for 60 s. A 700 µl volume of wash buffer was added and the column was then micro-centrifuged again for 60 s. The column was micro-centrifuged for 1 min, then 30-50 µl of elution buffer or autoclaved qH₂O were added and the column was centrifuged for 3 min. The eluting solution was then stored at -20 °C. All micro-centrifugation was at 13,000 rpm.

2.11.4. Isolation of plasmid DNA (minipreps)

A 3-5 ml overnight culture of *E. coli* was prepared from the colony harbouring the desired plasmid. Growth was in LB containing the selective antibiotic at 37 °C and 250 rpm. The culture was harvested, and the plasmid DNA was then purified using a GeneJET plasmid Miniprep Kit according to the manufacturer's instructions. For *C. jejuni* plasmid extraction, a the desired transformant was grown on a blood agar plate under microaerobic conditions at 37 °C for 40-48 h, and then a loop-full of cells were harvested and resuspended into 250 µl of suspension buffer. The plasmid was then extracted using the GenJET plasmid Miniprep Kit according to the manufacturer's instructions.

2.11.5. Restriction digestion

Plasmid DNA was digested in 20 µl volumes containing 60-100 ng/µl DNA, 2 µl of 10x fast digestion buffer and 0.5 µl of each appropriate restriction enzyme, with remaining volume contributed by qH₂O. The mixture was incubated at 37 °C for about 10-15 min without shaking. The digested DNA was purified using a PCR product purification kit (Fermentas) or were purified, after electrophoresis, using a GeneJET™ Gel Extraction kit (Fermentas),

according to the manufacturer's instructions and was then either held on ice or stored at -20 °C.

2.11.6. Estimation of DNA concentration

Prior to ligation and sequencing reactions, the concentration of DNA was estimated using the Nanodrop spectrophotometer. Plasmid DNA (2 µl) was placed on to the spectrophotometer's pedestal and the absorbance of the sample at 260 nm was determined, with a read out of DNA concentration in ng/µl given. Consideration of the purity of the DNA was provided though the ratio of absorbance at 260 and 280 nm.

2.11.7. In-Fusion cloning

The In-Fusion reaction fuses PCR products into a vector with ends that match those of the insert. PCR primers must be designed to have at least 15 nucleotides of identity with the ends of the linearized vector. Thus, the PCR primer consists of 15 nucleotides of identity to one flank of the vector at the 5'-end, an optional restriction site in the middle, and the gene-specific sequence at the 3'-end. The digested, purified vector and purified PCR product were combined in a 10 µl volume containing 50-100 ng of the purified PCR product and 100-200 ng of the digested plasmid, 2µl of 2x reaction buffer (In-Fusion) and 1 µl of In-Fusion enzyme mix (Gibson cloning). The cloning reaction was incubated at 37 °C for 15 min and then at 50 °C for 15 min. The reaction mixture was then transformed into Stellar competent cells (10 or 5 µl of the cloning reaction combined with 100 or 50 µl of Stellar competent cells, respectively). Plasmid DNA was then isolated from resulting transformants and analysed by restriction mapping, PCR and/or nucleotide sequencing.

2.11.8. Cloning using the CloneJET PCR Cloning Kit

The CloneJET (Fermentas) was used for routine cloning of PCR products. This kit contains a pJET1.2/blunt vector that has the *eco47IR* lethal gene, which is disrupted by ligation of a

DNA insert into the cloning site. As a result, only cells with recombinant plasmids are able to propagate. Initially, PCR products were incubated with a thermostable DNA blunting enzyme at 70 °C for 5 min. This was necessary to remove 3'-overhangs and fill-in 5' overhangs. The mixture was then incubated with the pJET1.2/blunt cloning vector and T4 DNA ligase at 22 °C for 5 min for ligation of PCR fragments into the vector. The ligation reaction was then used to transform chemically competent *E. coli* TOP10. Obtained transformants were then grown overnight in ampicillin-containing LB prior to plasmid DNA isolation.

2.11.9. Blunting reaction

To blunt the sticky ends of a digestion reaction (for use in a blunt-end ligation reactions), the Fermentas blunting enzyme was used (enzyme removes 3'-overhangs and fills in 5'-overhangs). Following the digestion of the plasmid, a 20 µl final volume reaction mixture comprising 10 µl of reaction buffer, 0.15 pmols of sticky-end DNA fragment and 1 µl DNA-blunting enzyme was briefly vortexed and centrifuged. The reaction mixture was incubated at 70 °C for 5 min and used directly in the ligation reaction.

2.11.10. Ligation reaction

All ligation reactions were conducted with the T4 ligase (New England BioLabs), in a final volume of 10 µl comprising 2 µl T4 ligase buffer (Fermentas), 1:3 vector: insert DNA ratio (50-100 ng of vector DNA) and 1 µl of T4 ligase. Sticky end ligations were incubated at room temperature for 10 min whereas blunt end ligations were incubated at room temperature for 1 h. In both cases, the entire 10 µl reaction was used for transformation into 100 µl of chemically competent cells.

2.12. Agarose gel electrophoresis

For analysing plasmid or genomic DNA, or PCR products, agarose gel electrophoresis was performed. Gels were generally 0.7% (w/v) agarose in 1X TBE buffer (0.4 M Tris-base, 0.4

M boric acid and 1 mM EDTA pH 8.0). Gel staining was performed with Biotium Nucleic Acid Stain GelRed™ (dilution of GelRed™ 10,000X stock reagent into the agarose gel solution at 1:50; e.g., 1 µl of the GelRed™ 10,000X stock reagent added to 50 ml of the gel solution). DNA samples (2 µl) were loaded with 2 µl of DNA loading dye (10 mM Tris-HCl pH 7.6, 0.03% bromophenol blue, 0.03 xylene cyanol FF, 60% glycerol 60 mM EDTA) and 6 µl sterile ultrapure water (sterile distilled H₂O). GeneRuler™ 1 kb DNA ladder (Fermentas) was used as the DNA size marker (1 µl GeneRuler™, 2 µl of DNA loading dye, 7 µl sterile distilled H₂O). Samples were electrophoresed for around 60 min in a BioRad horizontal gel tank containing 0.5X TBE buffer. Agarose gels were then visualised and recorded under UV illumination provided by a short wavelength UVP GelDoc-it ultraviolet transilluminator Bio Imaging system.

2.13. RNA extraction

2.13.1. Extraction of total RNA from *C. jejuni*

C. jejuni cultures were grown in M-H broth, with and without 20 µM ferric citrate, microaerobically at 37 °C and the cells were harvested after 24 h (OD₆₀₀ ~0.5-0.6) of incubation. A RNeasy mini-kit (Qiagen, Manchester, England, 74106) was used to isolate total RNA from *C. jejuni* isolates according to the method outlined by Davis *et al.* (2008). Briefly, 15 ml aliquots of the culture were added to 30 ml aliquots of RNA later Reagent (Qiagen), vortexed for 15 s and incubated at room temperature for 5 min. Multiple RNA extractions were performed for each strain (triplicate of *C. jejuni*, wild type and *fur* mutant). The cultures were then centrifuged for 10 min at 2655 ×g at 4 °C before the supernatant was removed. The cell pellets were resuspended with 400 µl TE buffer, pH 8.0 with 1 mg/ml lysozyme (Sigma-Aldrich) and incubated for 10 min at room temperature, vertexing every 2 min. A volume of 1200 µl of Buffer RLT and 12 µl of 2-mercaptoethanol (Sigma-Aldrich)

was added to each tube and vortexed vigorously before 700 μ l of 100% ethanol was added to each tube. A 700 μ l volume of the mixture was transferred to a RNeasy Mini spin column and centrifuged for 15 s at 2655 \times g and the flow-through discarded. This was repeated until all of the mixture had passed through the spin column. The column was then washed twice with 350 μ l Buffer RW1, centrifuged for 15 s at 2655 \times g and the flow-through discarded before 500 μ l Buffer RPE was added to the column and centrifuged at 3504 \times g for 2 min. The flow-through was discarded and the column was placed into a fresh 2 ml collection tube and centrifuged for 1 min at 3186 \times g to eliminate any remaining buffer. The column was transferred to a 1.5 ml microcentrifuge tube and 30 μ l RNase-free water was added to the column membrane and centrifuged for 1 min at 3504 \times g. The flow-through was collected and contaminating genomic DNA was removed using a TURBO DNA-free kit (Ambion) according to manufacturer's instructions: a 0.1 volume of 10x TURBO DNase buffer and 2 μ l TURBO DNase were added to the RNA and mixed gently followed by incubation at 37 $^{\circ}$ C for 20-30 min. Then, 0.2 volumes of resuspended DNase Inactivation Reagent were added and mixed well, and the reaction was then allowed to incubate for 5 min at room temperature, with occasional mixing by flicking tube. The reaction was then centrifuged at 10000 \times g for 1.5 min and the supernatant transferred to a new RNase-free tube without disrupting the white pellet. The concentration and purity of the RNA was measured using a Nanodrop ND-1000 and by 0.7% agarose gel electrophoresis. Samples were kept at -80 $^{\circ}$ C.

2.13.2. Synthesis of cDNA

C. jejuni total RNA (1 μ g) was reverse-transcribed in a 20 μ l reaction using a Tetro cDNA Synthesis Kit according to manufacturer's instructions. The thermal cycle conditions were as follows: 10 min at 25 $^{\circ}$ C, 30 min at 45 $^{\circ}$ C, 5 min at 85 $^{\circ}$ C and cooling at 4 $^{\circ}$ C. The cDNA sample was then stored at -20 $^{\circ}$ C or processed immediately for use in PCR.

2.13.3. Quantitative PCR (qPCR)

The qRT-PCR assay was performed in 96-well plates and reactions were carried out in duplicate for each cDNA sample. Sequences of all primers used in this study are listed in Table 2.8. To determine the qRT-PCR efficiencies for each reaction, a dilution series (10^1 – 10^4) was made from the cDNA template for each target gene and standard curves were constructed using the Light cycler 480 system (Roche Applied Science, West Sussex, UK) and SYBR® Green master mix kit. The qRT-PCR efficiency was determined from the standard curve and the corresponding values applied to the Light cycler 480 software to calculate fold changes between control and stressed strains. Each 20 µl reaction consisted of 10 µl SYBR® Green master mix, 0.8 µl of 10 µM forward and reverse primer mix, 1 µl cDNA template and up to 20 µl nuclease-free water. Cycling conditions on the Light cycler 480 system were as follows: 1 cycle at 95 °C for 2 min, 40 amplification cycles at 95 °C for 5 s, 65 °C for 30 s. The comparative threshold method was used in this study to quantify the RNA for the target genes using the total RNA isolated from *C. jejuni* NCTC 11168 wild type and *fur* mutant, the cultures were grown in M-H medium with and without 20 µM ferric citrate. The relative change in the gene transcription ratio (fold change) for each target gene was calculated by normalizing gene expression to the 16S rRNA reference gene (Hwang *et al.*, 2011; Koolman *et al.*, 2016) and/or *rpoA* gene (Ritz *et al.*, 2008). In addition, positive control genes (Fur regulated) were included: *tonB2* and *tonB3* (Butcher *et al.*, 2015).

Table 2.8. Primers used in qRT-PCR

Name	Sequence 5' -3'	Product size	Length (bp)	T_m (°C)	GC %
Ftr-q F	TGAACCGATTTTATGGCTTGGA	200	22	58.3	40.9
Ftr-q R	GGCACTTCGCCTGCAAATAA	200	20	59.4	50
P19-q F	AGGTTTTGGACGCCATGTTG	95	20	59.3	50
P19-q R	TTGGCGTGCCTGTGTATTTG	95	20	59.4	50
Cj1660-q F	TGTAGAAGAAAACGAAGCCCA	142	21	57.5	42.8
Cj1660-q R	GTAGAGAGCAAAAGCGTGCC	142	20	59.5	55
Cj1661-q F	TTACTTGGTTGCTTACTTCCTATCA	70	25	57.9	36
Cj1661-q R	ATCTACCATAAAGCACTCCTGC	70	22	57.9	45.4
Cj1662-q F	TCAATGTGTGTGAAAATTTGAAAGG	112	25	51.1	32
Cj1662-q R	TAAGGCTTTAACTTTGCCAAATTC	112	24	50.6	33
Cj1663-q F	CCAAATTCGCAGATCGAACCC	134	21	59.9	52.3
Cj1663-q R	CTCCAACTTTTCCAGTATCTTTTGA	134	25	57.4	36

Cj1664- q F	TGATCGTTACGCTGTGTTTGC	108	21	59.8	47.6
Cj1664- q R	AGCTTGGATTTCGAAAAATTCCCA	108	23	59.1	39.1
16S rRNA F	TGC TAG AAG TGG ATT AGT GG	153	20	49.7	45
16S rRNA R	GTA TTA GCA GTC GTT TCC AA	153	20	47.7	40
rpoA F	CGAGCTTGCTTTGATGAGTG	109	20	51.8	50
rpoA R	AGTTCCCACAGGAAAACCTA	109	20	49.7	45
qTonB3 F	GAAACCGACACAACCCACAC	216	20	53.8	55
qTonB3 R	ACGCTTTGGTAAGAGCTGGC	216	20	53.8	55
qTonB2 F	CACCTCCACACCCAATACCA	187	20	53.8	55
qTonB2 R	GCTTGCCTTGGATAAAAATTGTGC	187	23	53.5	43

2.14. Preparation of competent cells

2.14.1. Preparation of chemically competent cells from *E. coli* strains

Chemically competent *E. coli* was prepared as follows. One colony of *E. coli* was inoculated into 5 ml of L broth (LB) on a shaker at 37 °C and 250 rpm. Then, 0.5 ml of the resulting culture was inoculated into a 250 ml sterile glass flask with LB and allowed to grow to an OD of 0.4-0.5 at 650 nm. The culture was then transferred to 50 ml Falcon tubes and centrifuged for 5 min at 5 krpm at 4 °C. Then, the cell pellet was resuspended in 30 ml ice cold 100 mM MgCl₂ and incubated for 10 min on ice. The cells were again centrifuged for 5 min at 5 krpm and 4 °C and were resuspended in 30 ml ice cold 100 mM CaCl₂ with incubation for 30 min on ice. Finally, the cell suspension was re-centrifuged as before and cells were resuspended in 4 ml ice cold 100 mM CaCl₂ with 20% glycerol. The competent cells were then aliquoted into 200 µl samples in 1.5 ml Eppendorf tubes and were kept in -80 °C.

2.14.2. Preparation of electro competent cells from *C. jejuni* strains

To prepare competent cells from *C. jejuni*, the bacteria were cultured from the -80 °C stock on a blood agar plate for 40-48 h at 37 °C under microaerobic conditions. The bacteria were plated again on BHI-TrM (5 µg/ml) blood agar for 40-48 h, then plated again onto a fresh BHI-TrM blood agar plate for 16-18 h. Bacteria were collected (from 2-3 plates) into 5 ml fresh BHI broth to give as high a CFU as possible and cells were then harvested by centrifugation at 2200 rpm, 4 °C for 20 min. The pellets were washed four times in ice-cold wash buffer (272 mM sucrose and 15% v/v glycerol) and finally suspended in 1 ml wash buffer. Cells were aliquoted in 100 µl in sterile Eppendorf tubes and kept at -80 until use (Holt *et al.*, 2012; vanVliet *et al.*, 1998a).

2.15. Using of DNA to transform into the competent cells

2.15.1. Transformation into competent *E. coli* strains

E. coli chemically competent cells (100-200 μ l) were inoculated with 1 μ l plasmid DNA or 5 μ l In-Fusion reaction (Hanahan, 1983; Lederberg and Cohen, 1974; Sambrook, 1989). The cells were incubated on ice for 30 min, heat shocked at 42 °C for 1-2 min, and then immediately returned to ice for further 5 min. Next, 1 ml of LB or SOC broth was added to the cells, and they were incubated at 37 °C for 45-60 min. Following incubation, the tubes were micro-centrifuged at 13,000 rpm for 5 min and 900 μ l of supernatant was then removed. The pellets were re-suspended in the remaining liquid, and then 100 μ l aliquots were plated on to separate LB-agar plates containing the selective antibiotic. Plates were incubated for 14-18 h at 37 °C.

2.15.2. Transformation into *E. coli* Stellar competent cells

The In-Fusion mixture (4 μ l) was transformed into commercial Stellar competent cells (50 μ l). One hundredth to one fifth of each transformation reaction was placed into separate tubes and the volume was brought up to 100 μ l with SOC medium. Each diluted transformation reaction was spread on a separate LB plate containing an antibiotic appropriate for the plasmid. The remainder of each transformation reaction was centrifuged at 6,000 rpm for 5 min. The supernatant was discarded, and each pellet was re-suspended in 100 μ l fresh SOC medium. Each sample was spread on a separate LB plate containing appropriate antibiotic and the plates were then incubated overnight at 37 °C.

2.15.3. Transformation into the *C. jejuni* electro-competent cells by electroporation

To transform plasmids into the *C. jejuni*, 100 μ l of *C. jejuni* electro-competent cells were added to a 0.2 cm pre-chilled electroporation MicroPulser cuvette (Bio-Rad) and then mixed with

plasmid DNA (2-3 μg). Electroporation was performed using a GenePulserXcell system (2.5 Kv, 200 Ω and 25 μF) as described by Holt *et al.* (2012). After a single pulse, 200 μl of pre-warmed SOC medium was added and the suspension was then combined with 2 ml BHI-TrM blood medium in a universal tube (Greiner) without selective antibiotic. After 5 h incubation under microaerophilic conditions at 37 $^{\circ}\text{C}$, 1 ml of pre-warmed BHI medium was added to the bacteria suspension. The bacteria were then centrifuged for 20 min at 8,000 rpm, plated on selective blood agar plates and grown under microaerophilic conditions at 37 $^{\circ}\text{C}$ for 2-3 days.

2.15.4. Transformation into the *C. jejuni* by bi-parental conjugation

The shuttle vector pMA1, and derivatives, were transformed into *C. jejuni* strains using the bi-parental conjugation method (Zeng *et al.*, 2015; Davis *et al.*, 2008). The bacteria were cultured from the -80 $^{\circ}\text{C}$ stock into blood agar and incubated for 40-48 h at 37 $^{\circ}\text{C}$ under microaerobic conditions, then inoculated into the 15 ml fresh M-H broth in a 50 ml flask with microaerobic incubation for 24-30 h at 37 $^{\circ}\text{C}$ and 150 rpm. Then, 100 μl of logarithmic-phase *C. jejuni* culture (after 24-30 h incubation) was spread on M-H plates for overnight microaerophilic incubation at 42 $^{\circ}\text{C}$. In the meanwhile, the *E. coli* donor (S17) strain was inoculated into LB broth supplemented with kanamycin (25 $\mu\text{g}/\text{ml}$) for overnight, aerobic incubation at 37 $^{\circ}\text{C}$ in a rotary shaker (250 rpm). Next day, 500 μl of the *E. coli* donor culture was inoculated into 5 ml of LB broth (supplemented with the same antibiotics) followed by further incubation until the OD at 600 nm (OD_{600}) reached 1.2 (~ 4 h). The recipient *C. jejuni* cells were harvested from M-H plates using 5 ml fresh M-H broth and adjusted to an OD_{600} of about (1.0 to 1.5).

To set up the conjugation, 0.5 ml of log-phase *E. coli* donor cells were pelleted, washed once with 3 ml antibiotic-free M-H broth, and finally suspended in 0.5 ml of fresh M-H broth, which was subsequently mixed with 0.5 ml of the harvested *C. jejuni* recipient cells. These

donor and recipient cell mixtures were pelleted by centrifugation for 10 min at 13,000 rpm and resuspended in 100 µl of fresh M-H broth. The cells were then spotted onto an M-H agar plate and the liquid was allowed to dry (without spreading). The M-H plates containing the cell mixtures were incubated for ~7 h microaerophilically at 42 °C. The mixed *C. jejuni*-*E. coli* cells were then harvested from the M-H agar plates in 500 µl fresh M-H broth, and 100 µl were plated onto M-H plate containing CCDA Selective Supplement SR0155E, plus kanamycin 25µg/ml (for selection of the vector) to recover all *C. jejuni* trans-conjugants that have acquired a pMA1 plasmid from the *E. coli* donor.

2.16. Gene inactivation (knockout)

2.16.1. Gene amplification and ligation

The primers were designed to amplify the genes of interest (*ftr1*, *cj1660* and *cj1663*) of *C. jejuni* NCTC 11168 using HiFi master mix enzyme (CloneTech) to include 1000 up- and down-stream to each gene. The resulting PCR products were ligated into the pJET1.2 vector using the CloneJET PCR Cloning Kit (ThermoFisher) at the *Bgl*III restriction site of the vector. Ligation was performed at 22 °C with T4 DNA ligase (Fermentas) (section, 2.11.8). The ligation reaction was then used to transform chemically competent *E. coli*. The identity of plasmids within transformants obtained was confirmed by plasmid DNA isolation, restriction mapping and DNA sequencing. The resulting plasmids were designated: pJET*ftr1*, pJET*cj1660* and pJET*cj1663*.

2.16.2. Inverse PCR and gene deletion

To disrupt the *ftr1*, *cj1660* and *cj1663* genes, inverse primers (Ftr1 Inverse F and R, Cj1660 Inverse F and R, Cj1663 Inverse F and R) were designed to delete about 1 kb of the central region of each gene target, replacing the central regions with an *Asi*SI restriction site (GCGATCGC). This site allowed confirmation of successful cloning

by digestion using *AsiSI*, and also allowed insertion of an antibiotic cassette. The primers were used with the pJET Δ *ftr1*, pJET Δ *cj1660* and pJET Δ *cj1663* plasmids as templates in the inverse PCR reaction. The resulting PCR products were used directly in the cloning reactions described below (2.16.14).

2.16.3. The PCR amplification of *cat* cassette

The 627 bp *cat* cassette of plasmid pVA35 (3.8 kb; van der Stel, *et al.*, 2015) was PCR amplified using primers *cat*-F and -R (Table 2.5.). The primers were designed to include the *cat* gene promoter and ribosome-binding site within the PCR product giving an expected size of 896 bp. The primers were also designed to provide overlapping flanking sequence identity with the PCR products generated above (2.16.2) to enable ‘In-Fusion cloning’ of the amplified *cat* cassette into the deletion region at the newly introduced *AsiSI* site.

2.16.4. Cloning of the *cat* cassette into the deletion sites

In-Fusion cloning was used to ligate the *cat* cassette (2.16.3) into the PCR products generated above (2.16.2). The reaction products were transformed into competent *E. coli* Stella cells and transformants were selected on ampicillin (100 μ g/ μ l) and chloramphenicol (35 μ g/ μ l). Plasmid DNA was then extracted and analysed by restriction digestion with *AsiSI* to confirm identity. The resulting plasmids were designated pJET- Δ *ftr1::cat*, pJET- Δ *cj1660::cat* and pJET- Δ *cj1663::cat*.

2.17. Phenotypic studies with complemented *E. coli* strains

2.17.1. Serial dilutions tests on M9 agar plates

Overnight cultures of *E. coli* (M9 medium with ferric sulphate and 0.02% v/w inducer; Brook and Wu, 2013) were obtained at 37 °C and 250 rpm, and the pellets were harvested by centrifugation for 10 min at 13000 rpm and washed in pure M9 before being used to generate

fivefold serial dilutions from a starting culture at 0.5 OD_{600nm}. The serial dilutions were then applied to M9 agar plates (containing different levels of iron or DTPA chelator) in 5 µl volumes and plates were incubated for 20 h at 37 °C. The degree of growth achieved was determined on the basis of the lowest dilution where growth was detected.

2.17.2. Growth test for *E. coli* under aerobic conditions

The growth of strains of interest was tested under different iron and pH conditions. A single colony was used to inoculate 5 ml of M9-medium containing antibiotic and inducer (100 µg/µl ampicillin and/or 50µg/µl chloramphenicol, with or without 1 mM rhamnose and/or arabinose), and ferric sulphate (20 µM). Bacteria were grown overnight at 250 rpm, 37 °C in a Sanyo Gallenkamp orbital shaker. After 16-18 h of incubation, the OD₆₀₀ was measured. The cells were then collected by centrifugation (13,000 rpm for 10 min at 4 °C) and were washed twice in 3 ml of fresh M9 medium at 4 °C. The washed cells were then diluted into fresh medium to give a final OD₆₀₀ of 0.01. The diluted cells were then dispensed into a 100-well honeycomb microplate in 250 µl aliquots. The microplates were then incubated in a Bioscreen C at 37 °C for 24 h with shaking and growth was monitored automatically.

2.17.3. Growth test of *E. coli* under low-oxygen conditions

Low-oxygen growths of *E. coli* transformants were monitored in microtiter plates (37 °C, continuous shaking, OD₆₀₀) using a microtiter-plate reader (FLUOstar Omega) fitted with an Atmospheric Control Unit (BMG LABTECH) (located in Food and Nutritional Sciences, lab 3-18 Harry Nursten building). The Atmospheric Control Unit (ACU) independently regulates O₂ and CO₂ within the microplate chamber from 0.1- 20 %. The gas content was set at 13-15% CO₂ and 1% O₂ and was controlled automatically by adjusting the delivery rate of gases (CO₂, O₂, N₂) and monitoring the gas atmosphere (O₂ and CO₂) achieved. The cultures were prepared as described above (2.17.2).

2.18. *Campylobacter* growth assay

2.18.1. Preparation of standardised cultures

Standardised cultures were generally prepared from *C. jejuni* grown on agar plates for use in growth studies, motility tests and chicken trials. To prepare the inoculum, strains were initially sub-cultured on 2% blood agar (w/w), incubated at 37 °C for 40-48 h and then a single colony was subcultured onto BHI or M-H plates, and plates were incubated for 36-40 h. Using a category 2 biological safety cabinet, one loopful (~5 µl) of colony was taken and suspended in 1 ml of fresh M-H broth in an Eppendorf tube. Cells were then centrifuged at 8000 rpm for 4 min at room temperature. The supernatant was removed, and the cells gently re-suspended in 1 ml of fresh medium. A 500 µl volume of suspended cells was used to record the OD₆₀₀ value. The remaining sample was used to prepare a 'standardised culture' of 0.002 OD₆₀₀ by dilution with an appropriate volume medium in Bijou tubes. A loopful of standardised culture was routinely plated on a blood agar and incubated for 48 h aerobically at 37°C to confirm absence of contamination.

2.18.2. Viable cell count (CFU)

The Miles and Misra technique (Miles *et al.*, 1938) was used to enumerate viable *C. jejuni* cells. For growth studies, 10-fold serial dilutions from 10⁻¹ to 10⁻⁷ were prepared in Eppendorf tubes by adding 100 µl sample to 900 µl of PBS diluent. Triplicate serial dilutions were prepared for each sample. Plates of 2% blood agar were pre-dried for ~30 min at 37 °C. Sample dilutions (100 µl) from 10⁻⁴ to 10⁻⁷ were then spread, in triplicate, onto the pre-dried plates using a pipettor with a filter tip. Plates were allowed to dry and were then incubated at 37 °C for 40-48 h before CFU levels were recorded.

2.18.3. *Campylobacter* motility test

A motility test was performed as previously described with slight amendments (Guerry *et al.*, 1991). Strains were prepared, as in section 2.18.1, to a starting OD of 0.2 in sterile M-H broth. Using a sterile pipette filter tip, 5 μ l of standardized culture was inoculated onto the agar at the centre of a 0.4% M-H plate. Plates were incubated inverted under microaerobic conditions at 37 °C for 72 h. The plates were examined and the radius of the bacterial growth area over the plate was recorded; a spread zone diameter of 10-35 mm was used to indicate a high motility strain.

2.18.4. Microtiter plate growth assay

Growth of *C. jejuni* in 96-well plates at 37 °C, under microaerophilic condition, was used to monitor the growth of different strains under a range of conditions. Sterile 96-well polystyrene plates (Corning, 10687551; or Greiner, plates 655161 with lid 656161) were used. Standardised cultures were prepared as described above using the required medium. The microtiter plates were prepared aseptically by addition of 200 μ l of standardised culture per well, in triplicate. Media blanks were included, and each plate was prepared in quadruplicate to allow measurement of four distinct time points (usually at 12, 24, 36 and 48 h). Growth (OD₆₀₀) was measured in a Spectra MAX 340pc spectrophotometer.

2.18.5. Growth in flasks with shaking

Growth of larger volumes was performed under shaking conditions (150 rpm) in 50 ml conical flasks (acid washed) with 15 ml of medium for up to 48 h at 37°C in a sterile microaerobic cabinet. Aliquots were taken at the required time of incubation inside the cabinet. The bacterial cells were removed from the samples by centrifuging at 8,000 rpm for 10 min. The supernatant was then stored at -20 or -80 °C, as required, and the OD₆₀₀ for each time point was measured.

2.19. Preparation of NMR metabolomics samples

Growths were as above (2.18.5) in sterile M-H broth (with or without 20 μ M ferric citrate), with a starting OD₆₀₀ of 0.002. Samples of 1 ml were collected at four time points (12, 24, 36 and 48 h) in Eppendorf tubes on ice. Supernatant was isolated by centrifugation at 4 °C and 8,000 rpm for 15-20 min, and kept in -80 °C. The NMR test was performed in the FMSU lab (3-18 Harry Nursten building) by Dr Anisha Wijeyesekera.

2.20. Preparation of ICP-OES samples

The Inductively Coupled Plasma - Optical Emission Spectroscopy (ICP-OES) analysis was performed to measure a range of elements. *C. jejuni* strains were grown as in 2.19 and 2-ml samples were collected after 48 h of incubation in sterile 15 ml Falcon tubes. The supernatant was isolated by centrifuging at 4 °C and 8,000 rpm for 15-20 min. The supernatant was treated with 735 μ l of nitric acid to give a final concentration of 5%. The samples were then incubated at 80 °C overnight. The next day, qH₂O was added up to a final volume of 10 ml and the samples were filtered using a 0.22 μ m filter (0.22 μ m pore size hydrophilic Polyether sulfone [PES] membrane) and were then kept at 4 or -20 °C pending ICP-OES analysis (performed at the School of Archaeology, Geography and Environment Science, University of Reading with the assistance of Anne Dudley).

2.21. Colonisation of chickens with *C. jejuni*

2.21.1. Chicken trial

The chicken trial was performed at University of Nottingham, Sutton Bonington Campus, School of Biosciences, Division of Food Sciences, in collaboration with Professor Ian Connerton. Prior to starting the trial, chickens were screened for absence of *Salmonella* and *Campylobacter*. The bacterial cells (1 ml volume, $\sim 7 \log_{10}$ CFU, in PBS, cultured in 5% defibrinated horse blood agar medium for 24 h to mid log phase) were delivered into the

stomach of each of the 20-day-old *Campylobacter*-free male 308 Ross broiler chickens (from PD Hook) by oral gavage (four bacterial strains). A bacteria-free control (PBS only) was delivered into the stomach of each of the 14 control chickens for three- and seven-days post infection. The following *C. jejuni* strains were each used to inoculate 14 chickens: PT14 Δ *frt1*, PT14 Δ *cj1660*, PT14 Δ *cj1663* and wild type of *C. jejuni* PT14 strain.

At day 0 (day of hatching), the chickens (64 in total) were cohoused and fed 'starter feed'. At day 8, feed was switched to 'grower feed' and the birds were split into eight groups of eight birds, with birds in each group cohoused in pens. Oral infection was on day 20, and the feed was changed to 'finisher feed'. The average weight of the 16-day old chickens was 528 g. Weight and health was monitored throughout the trial. At day 23, all "a" birds (n=32) were sacrificed and intestinal segments surgically removed. Aliquots of caecal, ileum and jejunum contents were transferred to pre-weighed labelled tubes and stored on ice. Extra-intestinal organs (heart, spleen, kidney, breast, liver) were aseptically removed, placed in individual sterile homogeniser bags and stored on ice. At the same time, samples of caecal content and intestinal tissue were recovered and stored at -80 °C for future metagenomics/cytokine analysis. This was done by following published procedure (Loc Carrillo *et al.*, 2005). At day 27 all "b" birds (n=32) were sacrificed and processed as the same way.

2.21.2. Processing of samples

The Miles-Misra Micro-Plate method was followed to count *C. jejuni* CFU in the caecal, ileal and jejunal contents, essentially as described in section 2.18.2. Intestinal content was suspended in Maximum Recovery Diluent (MRD; Peptone 1gm/L and Sodium chloride 8.5 gm/L) to 1 g/ml giving the first sample at a 10⁻¹ dilution. The contents were then vortexed vigorously for 15-30 s, before a ten-fold serial dilution, in triplicate, was performed to a concentration of 10⁻⁷. Five aliquots (10 μ l) of each triplicate of the 10⁻² to 10⁻⁷ dilutions were dispensed onto a 2% mCCDA plates for selective isolation of *C. jejuni*. The plates were

incubated at 42 °C in a microaerobic atmosphere for 48 h in a Modular Atmospheric Controlled System (MACS) cabinet (Don Whitley Scientific) contained a gas mixture of 88% (v/v) N₂, 5% (v/v) CO₂, 2% (v/v) H₂ and 5% (v/v) O₂ (BOC Limited). After incubation, the colonies were visually inspected for typical shiny, round and grey colonies (Chon *et al.*, 2012) of *C. jejuni*. Confirmed *C. jejuni* colonies were counted to calculate the CFU/g of intestinal contents. Miles and Misra mCCDA plates obtained for the 3- and 7-dpi chicken caecal content analysis were brought back the University of Reading in 3.5 L jars with CampyGen Sachets. Two single colonies from the highest dilution with good growth of each mutant strain were streaked on to 2% blood agar plates, incubated for 40-48 h at 37 °C under microaerobic conditions, and were then used to prepare glycerol stocks for maintenance at -80 °C. Confirmation of strain identity was performed by extraction genomic DNA and testing by PCR for the presence of the *cat* cassette gene inserted at the corresponding locus in each strain. In addition, growth comparisons in M-H broth, with and without iron, were also performed.

2.21.3. Draft genome sequencing

Chromosomal DNA of selected input and recovered isolates from the chicken trial was prepared with a GeneJET™ Genomic DNA purification kit and sequenced with illumina MiSeq technology. A range of volumes, between 50-100 µl of 30 ng/µl, of all genomic DNA samples were submitted to MicrobesNG for Illumina WGS.

2.22. Bioinformatic analysis

2.22.1. Initial analysis of the gene locus of *ftl1-p19* cluster in *C. jejuni* NCTC 11168

The initial analysis of the *ftl1-p19* gene set was generated using the NCBI web site (https://www.ncbi.nlm.nih.gov/NCBI_nucleotide) by using key word searches. Thus, the

nucleotide sequences of the required gene sets were downloaded along with gene location data. The data was then imported into Vector NTI Express to generate genetic maps.

2.22.2. Using Gene Context Tool 3 database

The Gene Context Tool 3 database was the website that used to identify bacteria that have the *ptr1-p19* gene cluster, using COG3470 (P19 protein) as a key word for the search. A total of matches was obtained in the Gene Context among 264 organisms.

2.22.3. Using Geneious prime software

Geneious prime software was used to generate the amino acids alignments and the phylogenetic trees for each protein in P19 system of *C. jejuni* NCTC 11168 after loading the data from Pfam. In addition, membrane organisation (topology), sequence conservation, domain organisation and phylogeny for each gene product, combined with investigation of gene organisation patterns was performed.

2.22.4. Sanger sequencing and analysis of resulting nucleotide-sequence data

To sequence PCR products or cloned inserts in plasmids, pure DNA samples of 15 µl and 50 ng in the sterile Eppendorf tubes were submitted to Eurofins with 15 µl of suitable sequencing primer(s). After receiving the results of nucleotides sequencing from the company (www.ecom.gdna@eurofins), the sequence was analysed using NCBI BLAST compare the sequence with those in the database.

2.23. Statistical analysis

The current version of SPSS 21 program has been used for statistical analysis. Means were compared by using at least three biological replicates. Comparison of two groups was made with Independent (unpaired) Samples T test (two-samples T test) to compare the groups

of interest. Also, standard deviation (error bar) for each sample at each time point was used to detect the consistence of the triplicate reads.

Chapter 3: Bioinformatics analysis of the P19 system of *C. jejuni*

3.1. Introduction

Since iron availability is a crucial factor in *C. jejuni* colonisation and pathogenesis in the host (Palyada *et al.*, 2004; Naikare *et al.*, 2006; Zeng *et al.*, 2013), this study focuses on an important iron transporter in *C. jejuni* (the P19 system) which is apparently encoded by a set of eight genes that are not yet fully studied (Miller *et al.*, 2009). The periplasmic and low-iron-induced 19 kDa protein, named as P19, was purified from *C. jejuni* 81-176 for the first time by Janvier *et al.* (1998). The *p19* gene is under the control of the Fur regulator and is thus induced by low iron, along with about 208 other genes; these Fur-regulated genes have functions related to iron acquisition, oxidative stress and metabolism (Palyada *et al.*, 2004). The periplasmic P19 protein was found to be a homodimer with two distinct metal-binding sites per monomer, one binding copper and another binding manganese (supposedly acting as a ferrous iron binding site). It was also found that inactivation of the *p19* gene caused growth inhibition under iron minimal conditions which indicated its function as an iron transporter induced under iron deficiency (Chan *et al.*, 2010). It had also been shown to be required for utilisation of Fe-rhodotorulic acid as an iron source (Stintzi *et al.*, 2008). Also, multiple-sequence alignment of representative P19 homologues from different genera demonstrated the conservation of the copper and putative iron ligands (Chan *et al.*, 2010).

The *ftr1* gene, (adjacent to *p19*) encoding Ftr1 (homologous to the ferric permease of yeast), is also expressed by iron restriction (Chan *et al.*, 2010). As is directly upstream of, and is apparently co-operonic gene with, the P19-encoding gene (Miller *et al.*, 2009), these two genes are considered to encode proteins that act together in mediating iron uptake. As *ftr1* specifies an integral inner-membrane protein similar to Ftr1p of yeast and EfeU of *E. coli* (Larrondo *et al.*, 2007; Große *et al.*, 2006), it is anticipated to act as a ferric iron permease as is the case for Ftr1p. Because it is now clear that the *ftr1-p19* gene cluster is also associated

with a downstream set genes, *cj1660-cj1665* (Miller *et al.*, 2009), this chapter focusses on providing a further understanding of the full set of eight genes in the P19 system, and in particular the last six genes (*cj1660-65*), through a bioinformatic analysis, as a preliminary study leading to a molecular-genetic examination. The bioinformatic analysis largely involved considering the membrane organisation (topology), sequence conservation, domain organisation and phylogeny for each gene product, combined with investigation of gene organisation patterns. It was envisioned that such an analysis would improve understanding of the roles of the P19 components and thus provide further insight concerning the function and mechanism of action of the system as a whole.

3.2. Initial analysis of the gene locus of the *ftr1-p19* cluster in *C. jejuni*

Initially, the corresponding region of the *C. jejuni* NCTC 11168 genome was imported from the NCBI database and displayed using Geneious Prime (Fig. 3.1). This showed the conserved gene cluster encoding eight co-polar (*cj1658- cj1665*), apparently organised into two clusters possibly corresponding to independent operons: *fetMP* (*ftr1-p19*) of ~2.7 kb; and *fetA-F* (*cj1660-1665*) of ~5.4 kb. These two clusters are separated by an 82 bp intergenic region between, while the remaining adjacent genes are directly abutting or slightly overlapping (Figs. 3.1 and 3.2). Directly upstream (by 877 bp) of the cluster is the divergent (counter-clockwise) Cj1656c gene encoding a hypothetical protein of just 60 amino acids. The following upstream gene is *nhaA1* which is also anticlockwise in orientation. It encodes an Na⁺/H⁺ antiporter 382 amino acids and is 143 bp downstream of Cj1656c. It has no known role in iron transport. Just 10 bp downstream of the *fetA-F* cluster is the anti-polar Cj1666c gene encoding a hypothetical periplasmic protein of 145 amino acids. The following downstream gene is Cj1668c encoding another small (138 amino acids) putative periplasmic protein of unknown function.

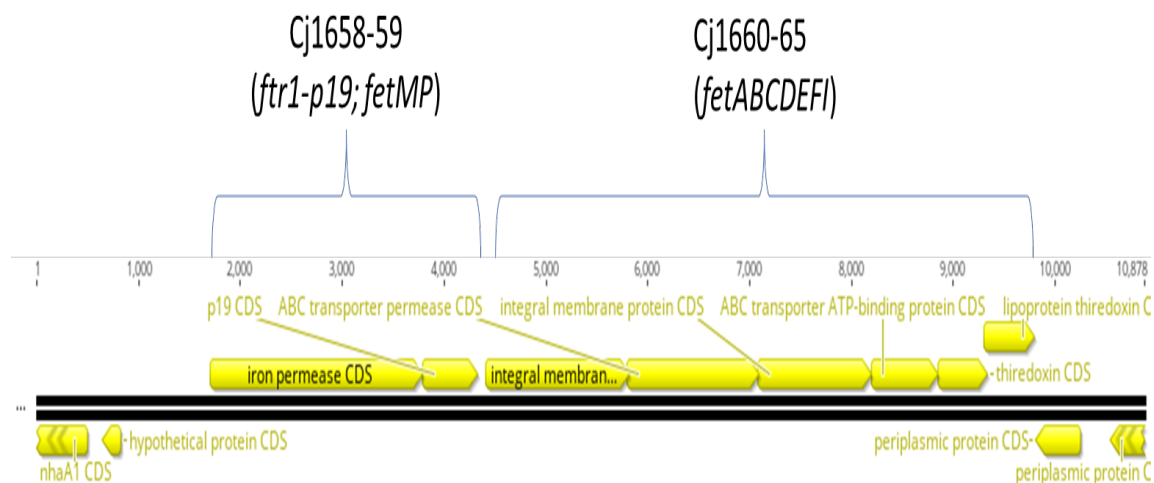


Figure 3.1. Physical map and genetic organisation of the *fetMP-fetABCDEF* region of *Campylobacter jejuni* (subsp. *jejuni* NCTC 11168; ATCC 700819). Regions of interest are indicated. The sequence was obtained from the NCBI database (GenBank flat file) and corresponds to nucleotides 1579-1590 kb (left to right) of the genome sequence. Genes above the two black lines indicate clockwise genes, those below have a counter-clockwise orientation.

It is interesting to note that adjacent genes in the *fetMP* and *fetA-F* cluster overlap by at least 4 bp, the only exception being the *fetP-fetA* genes where there is a spacing of 82 bp (as indicated above). The last two genes (*cj1664-5*) in the cluster are predicted to have an extended region of overlap (40 bp; Fig. 3.2) which is somewhat unusual. The impact that this might have on ribosome recruitment and translation for these two genes is unclear.

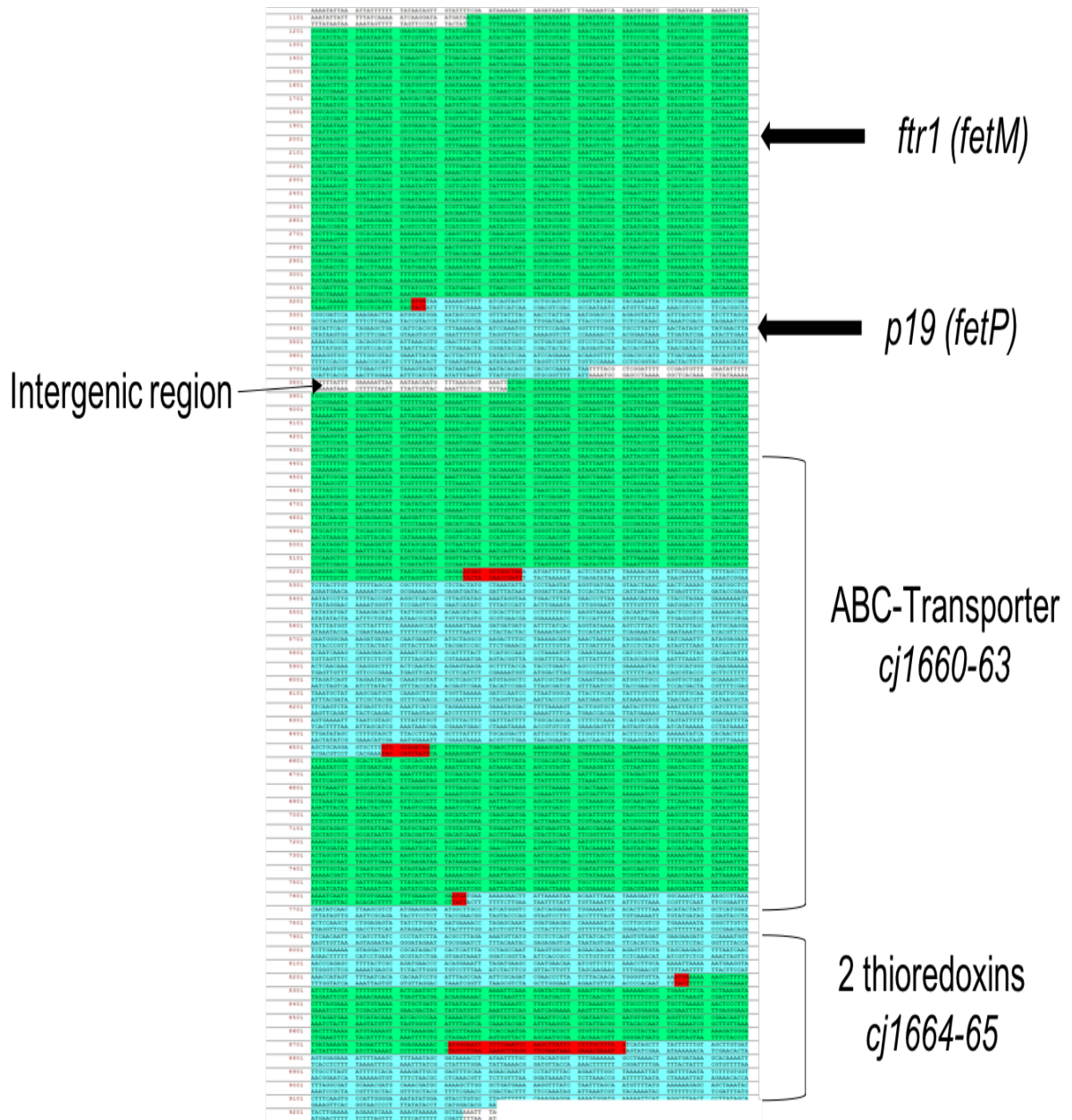


Figure 3.2. Nucleotide sequence of the *fetMP-fetABCDEF* locus of *Campylobacter jejuni* NCTC 11168. The locus (from the first start codon to the final stop codon) is 8099 bp. The 82 bp *fetP-fetA* intergenic region is indicated. Each orf is highlighted in alternating green/blue shading, and regions where orfs overlap are in red. The image is compressed to enable fit onto a single page; the expanded version of the sequence is provided in the Appendix (11). The figure was made using Vector NTI express software.

3.3. *p19* gene cluster distribution and organisation

The Gene Context Tool 3 was used to identify the bacteria that have *ftr1-p19* gene clusters using COG 3470 (P19 protein) as a key word for the search. A total of 264 proteins were thus recovered from 254 Bacteria with just 7 from the Archaea and 3 from the Eukaryotes. In the analysis reported below, only *p19* homologues (189 in total) from the phylum Proteobacteria have been considered, as theirs was the most abundant group and includes the *C. jejuni*. The *p19* loci thus identified could be grouped into three distinct types, on the basis of their genetic organisations (Fig. 3.3) as follows:

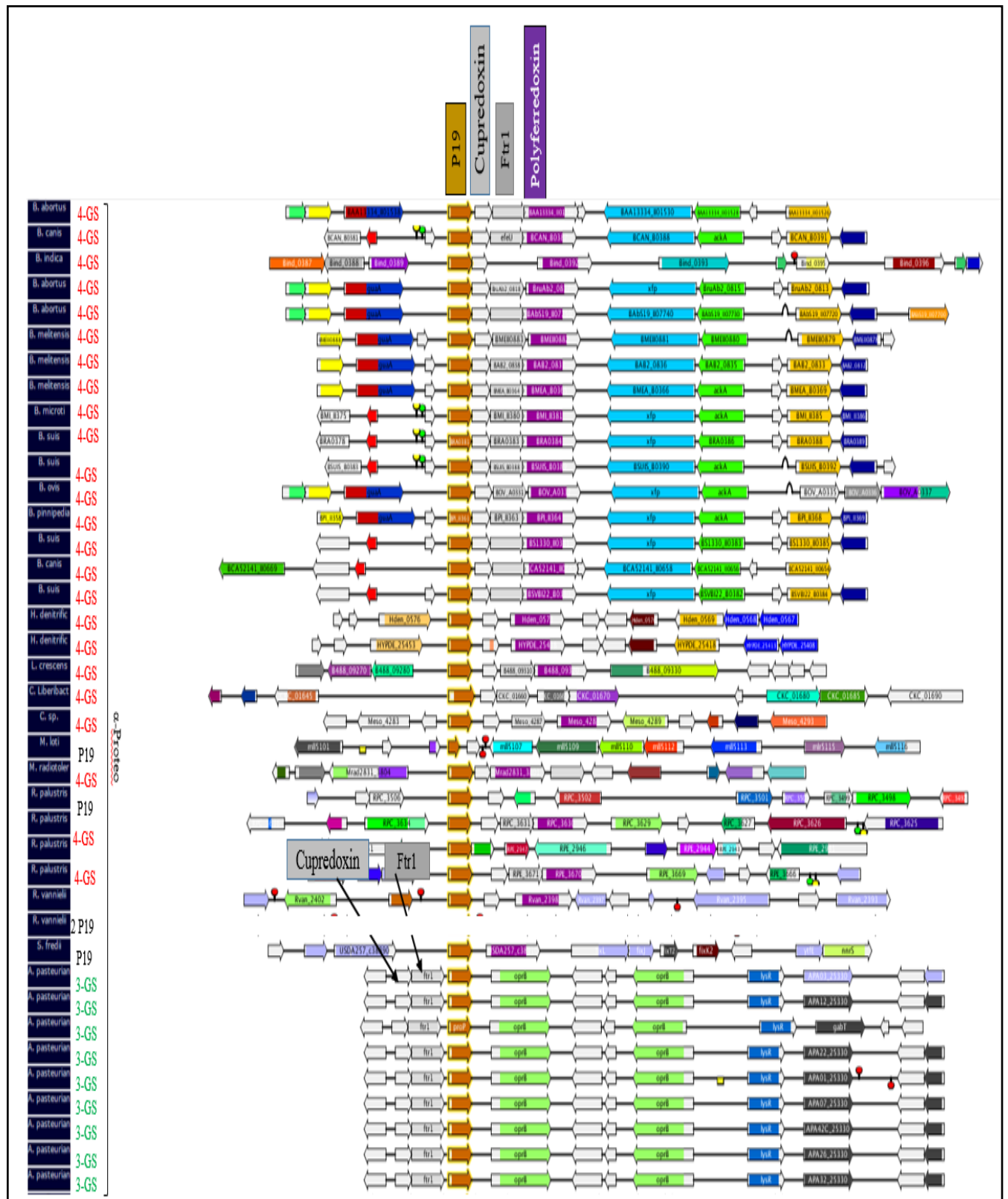
Group 1: The bacteria in this group have a four genes system. Such systems are found in *Brucella*, *Bordetella*, *Pseudomonas*, *Burkholderia*, *Achromobacter* and *Chromobacterium* spp. The first gene encodes a P19 protein, the second specifies a cupredoxin like protein, the third an Ftr1-like protein (ferric permease) and final gene encodes a ‘polyferridoxin’ protein. This is the largest of the P19 groups with 94 members in all. The corresponding system has been characterised in *Brucella ftrABCD*, *Bordetella ftrABCD* and *Burkholderia ftrBccABCD* as a ferrous iron transporter (see section 1.7.4 and the genes designated ‘*fetABCD*’ (Mathew *et al.*, 2014; Brickman and Armstrong, 2012; Elhassanny *et al.*, 2013).

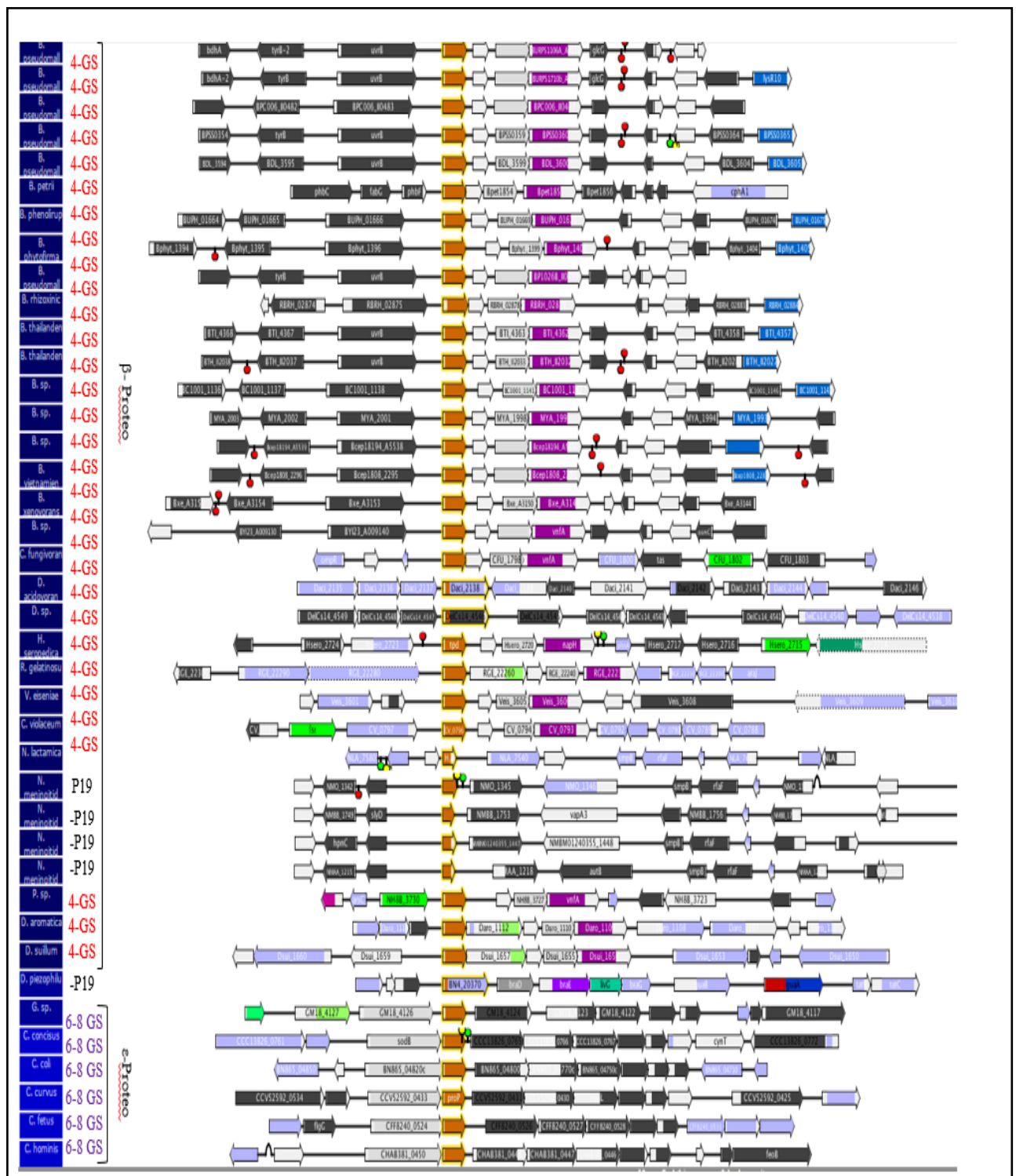
Group 2: The P19 encoding genes in this group are part of an apparent two-gene operon, *fetMP* (*ftr1-p19*), followed by an apparent co-polar operon of up to six conserved genes (*fetABCDEF*) where the first four genes are more highly conserved than the last two. Organisms possessing such systems include *Campylobacter* spp., some strains of *E. coli* (O18: K1:H7, and O17: K52:H18), *Yersinia* spp., *Proteus* spp., *Salmonella* spp., *Pasteurella* spp., *Citrobacter* spp., and *Pectobacterium* spp. in addition to *Bifidobacterium* spp. where this system is conserved in all species (phylum, Actinobacteria; data not shown). The gene order is as follows: *fetM* encodes an Ftr1 protein; *fetP* encodes a P19 protein; *fetABCD* specifies a conserved integral membrane protein and three ABC transport components,

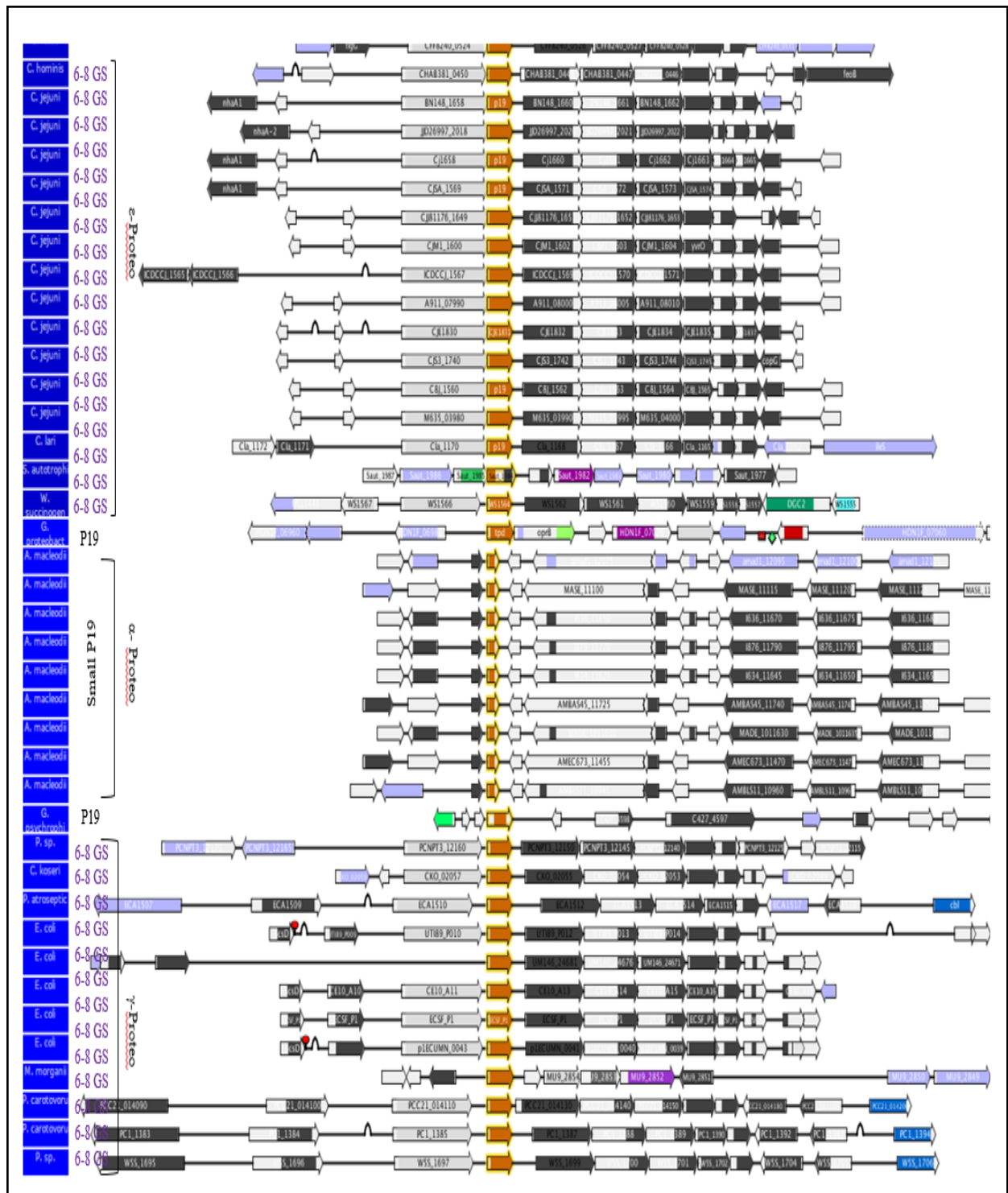
followed by a gene encoding a possibly secreted FMN protein (flavin mononucleotide), although in *Campylobacter* spp. this latter gene protein is replaced one or two genes encoding one or two thioredoxins. This group is the second largest with 73 members.

Group 3: This relatively small group is found in *Acetobacter pasteurianus* strains (9 members) and in *Gluconacibacter diazotrophicus* (2 members) only. The P19 cluster of this group consists of three apparently co-operonic genes encoding: a cupredoxin, an Ftr1 (putative iron permease) protein and a P19 protein, and thus resembles Group 1 apart from the absence of a polyferredoxin.

There are a few other less common organisations also, e.g. the two gene systems (*ftr1* and *p19*) as in *Rhodospirillum rubrum* strains F11 and ATCC 11170. Also, there are some cases where there are two adjacent *p19* genes e.g. *Rhodomicrobium vannielii* and *Magnetospirillum magneticum* associated with other genes related to iron uptake. In addition, there are 9 *Alteromonas* spp. that have a small '*p19*-like' gene apparently matching the N-terminal region only. However, upon closer analysis by BLAST, the gene products appear not to be related to P19 and there is no adjacent iron-uptake-related gene. Thus, the Gene Context Tool reported some genes that are not truly *p19*-like (these cases labelled in Fig. 3.3 as '-P19').







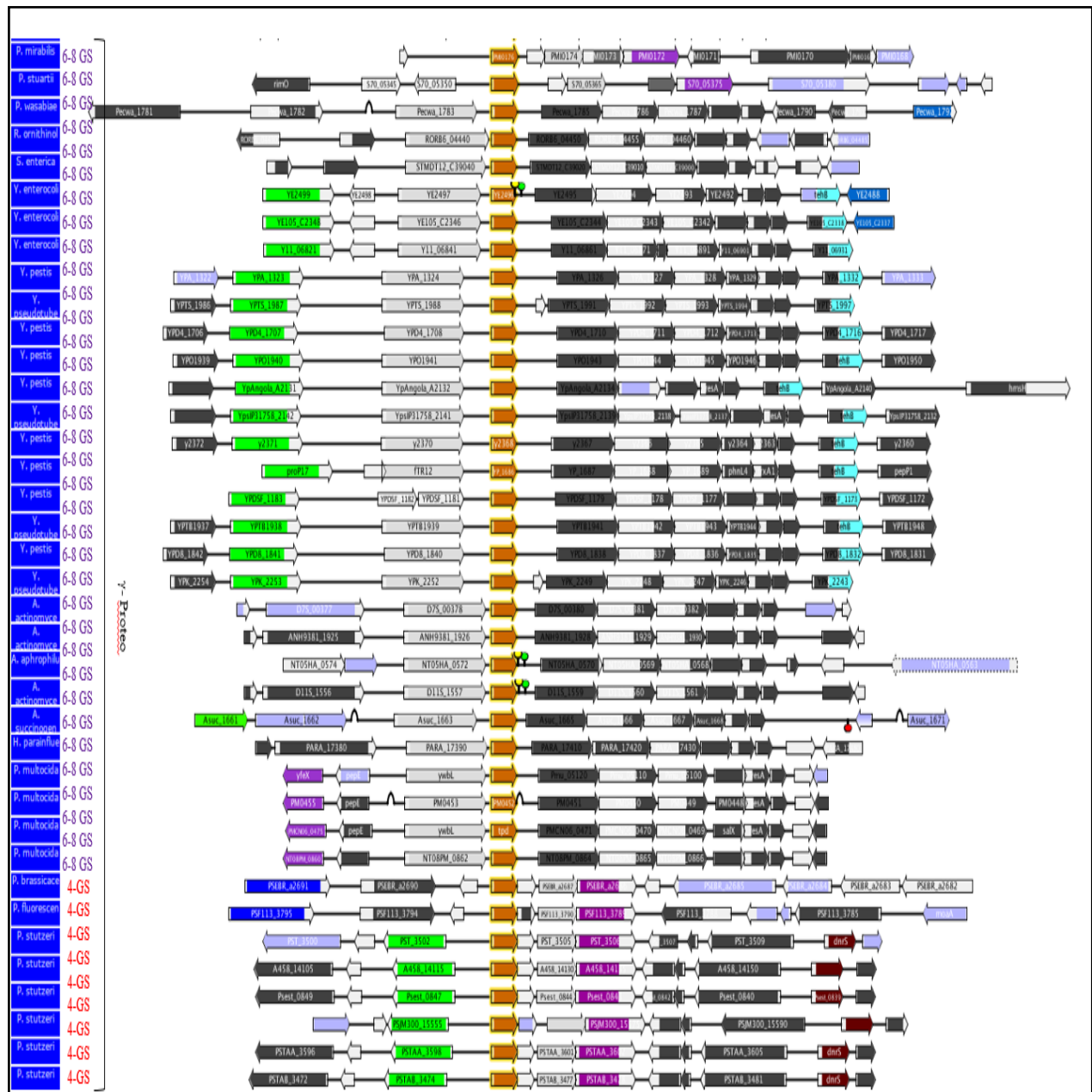


Figure 3.3. Gene Context Tool comparison of selected bacterial genome regions containing *p19* homologues. The figure is split into five segment to cover the 189 organisms from the Gene Context Tool database that have *p19* homologues within the Proteobacteria phylum (189). The figure shows the different groups of bacteria and organisations for the P19 gene cluster. 4-GS, 6-8 GS and 3-GS indicate the three major genetic organisations observed. ‘P19’ indicates the loci where the *p19* gene organisations are distinct from the three major groups; ‘2P19’ indicates the bacteria that have two *p19* genes; and ‘-P19’ indicates those *p19* genes incorrectly reported as *p19*-like. Taxonomical classes are indicated at the Class level. Data are derived from the Gene Context Tool 3, using COG3470 (P19) as a key word and the Proteobacteria was the phylum selected to display the results. A few neighbours upstream were 3 and downstream were 8 genes.

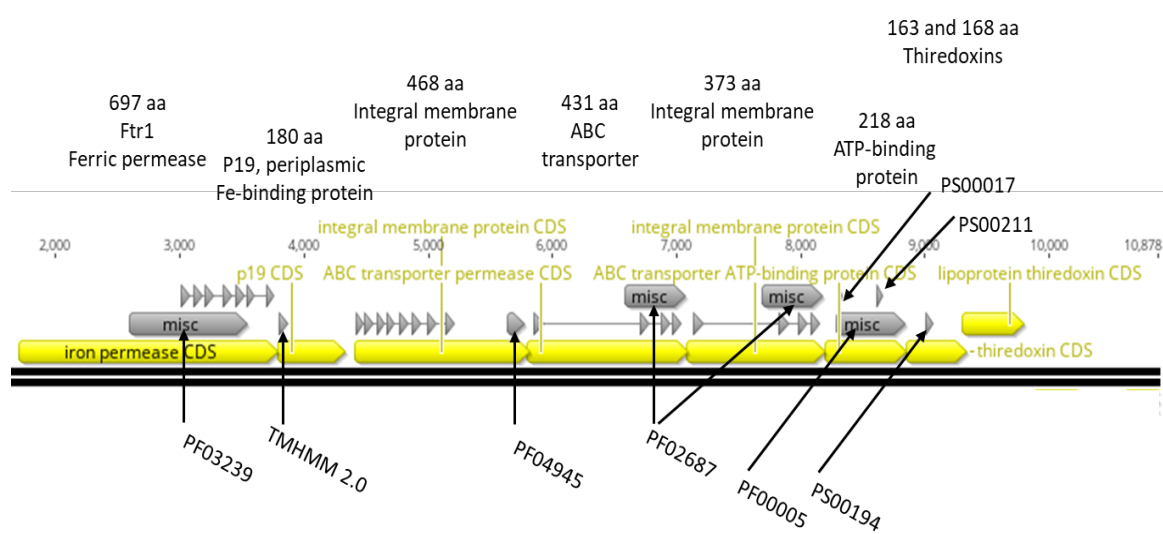


Figure 3.4. A physical map of *ftr1-p19* and *fetA-F* locus of *C. jejuni* NCTC 11168 combined with predicted functional motif data of translation products. The figure shows the predicted size (in amino acid residues) of each gene product and the predicted function annotation of each encoded protein. Image from Geneious Prime (annotate sequence view). Grey arrows indicate motifs: the short, linked grey arrows indicate predicted transmembrane helices; PF03239, Pfam Family ‘Iron permease FTR1’; PF04945, YHS domain ~50 residues; PF02687, FtsX-like permease family; PF00005, ABC transporter; PS00017, Prosite ATP/GTP-binding site motif A (P-loop); PS00211, ABC transporter family signature; PS00194, thioredoxin family active site; TMHMM 2.0, transmembrane helix.

3.4. Ftr1-P19 (FetMP) functional analysis

The *p19* (*fetP*) of *C. jejuni* encodes a periplasmic protein (19.3 kDa) identified as an iron-binding transport component that enhances *C. jejuni* growth under iron restricted conditions (Stintzi *et al.*, 2008; Miller *et al.*, 2009; Chan *et al.*, 2010). The upstream *cjl658* gene specifies an integral membrane-protein similar to Frt1p of yeast, FtrC of *Bordetella* and EfeU of *E. coli* (Larrondo *et al.*, 2007; Brickman and Armstrong, 2012; Große *et al.*, 2006). Genes specifying P19 proteins are usually associated with an Ftr1-encoding gene (99% of cases), as the bioinformatic search results above show. In order to further understand the functional properties and evolution of the Ftr1/P19 system of *C. jejuni*, multiple amino acid sequence

alignment and phylogenetic tree analysis was performed on all components, together with topology prediction where appropriate.

3.4.1. P19 protein

The Pfam database indicates a total of 587 P19 proteins from 560 species. Most (95%) are within three Bacteria phyla and one Archaea phylum: Proteobacteria (64%), Actinobacteria (12%, mostly in the Bifidobacteriales order), Firmicutes (9.2% proteins) and Euryarchaeota (8.5%). Since P19 is only encoded by a subset of *Ftr1* loci with three major genetic organisations (Groups 1-3) and is not known to be associated with any function other than iron uptake, this protein was initially selected to generate an alignment and phylogenetic tree to determine the evolutionary relationship between the P19 systems described above. An alignment was generated using the P19 seed alignment from Pfam (Fig. 3.5). The multiple alignment shows that there are several highly conserved regions. The observation of the conserved DGPHYG and ETGV motifs is consistent with previous work showing the presence of conserved copper and putative iron ligand motifs: DGP (Mn^{2+} ligand), HYG (Cu ligand) and TGV (Cu ligand) (Chan *et al.*, 2010). This motif is also present in the *C. jejuni* P19, supporting its role as a copper-containing and iron-binding protein.

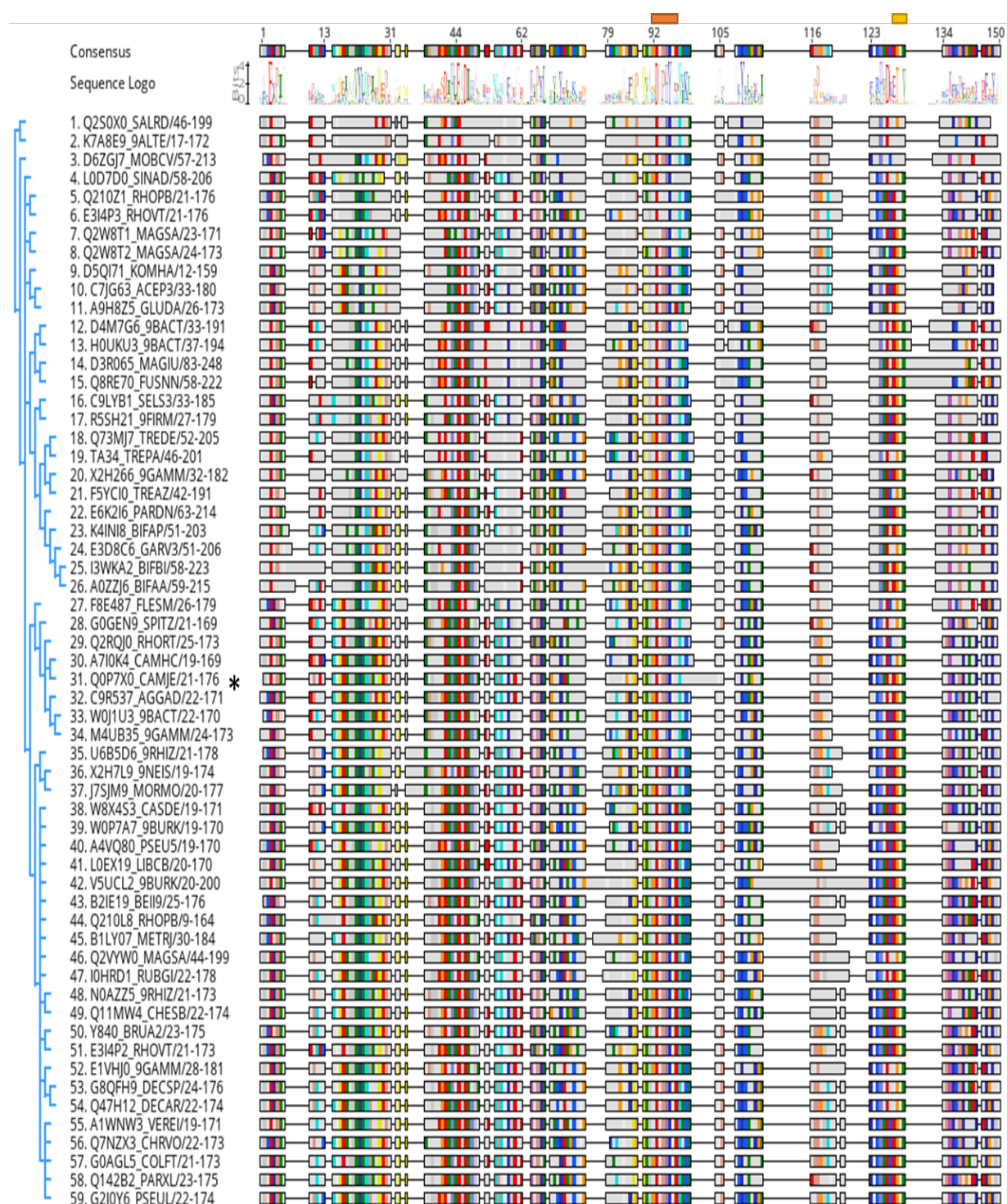


Figure 3.5. Alignment of amino acid sequence of P19 proteins. Multiple alignment of amino acid sequences of 59 P19 proteins obtained from the Pfam Seed alignment. The alignment is displayed using the alignment option of Geneious. The alignment tree is shown on the left-hand side. Consensus is shown in Logo mode above, with the conserved metal-binding motifs indicated by orange and yellow bars. Conserved residues are highlighted in colour. The asterisk indicated the *C. jejuni* sequence.

The derived phylogenetic tree (Fig. 3.6) is clearly divided into two major clads, one corresponding to P19 proteins encoded by gene clusters exemplified by the four-gene system (e.g. *frABCD* of *Bordetella pertussis*) and the other largely comprising P19 proteins encoded by genetic loci of the 6-8 gene type (e.g. *fetMP-fetABCDEF* of *C. jejuni*). This phylogeny thus shows that there are two major types of P19 protein, one associated with the 4-gene system and the other with the 6-8 gene system. It is likely that these two types of P19 are adapted to operate within their respective iron-uptake systems and will thus possess sequence similarities/differences reflecting this diversification and specialisation.

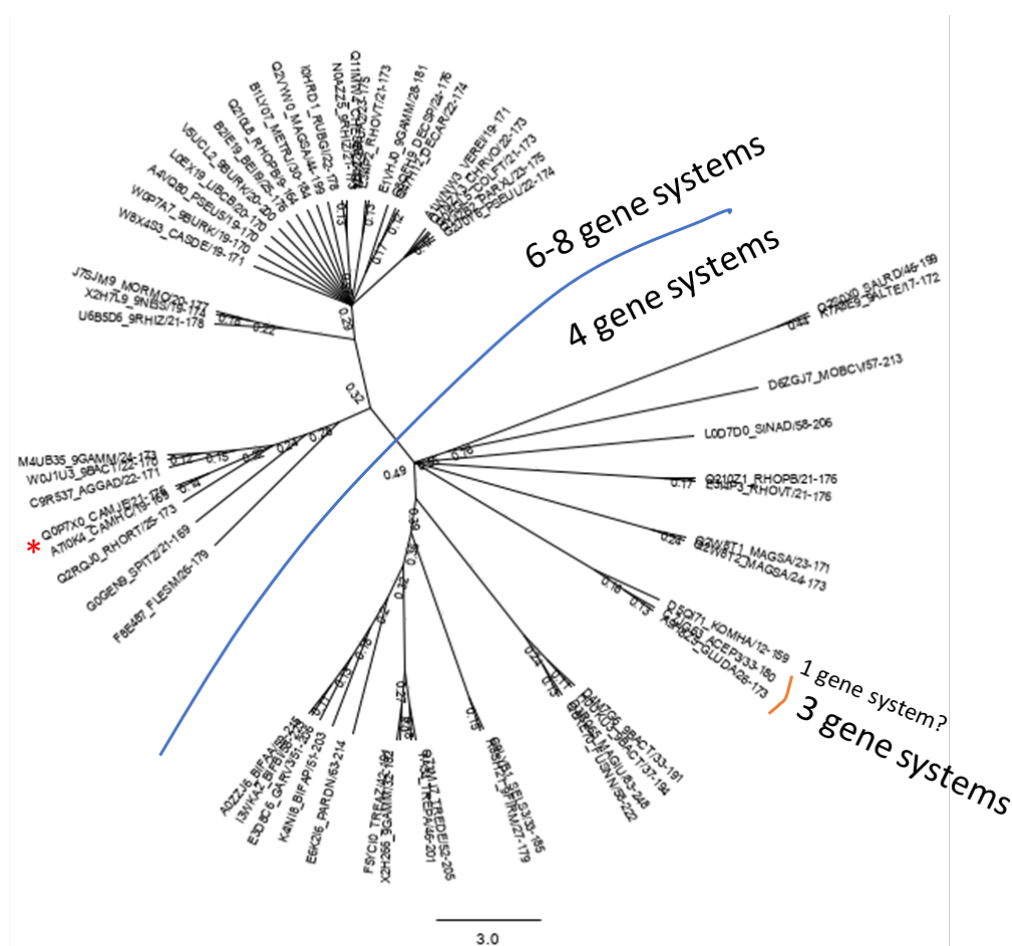


Figure 3.6. Phylogenetic tree of P19 proteins. The tree was composed from the above alignment using the Tree option of Geneious (Jukes-Cantor, UPGMA, Bootstrap 100 and cladogram options were applied). Distance is indicated along with Bootstrap values at nodes. Asterisk indicates *C. jejuni* P19.

3.4.2. Ftr1 (iron permease)

Topological and signal sequence prediction (Fig. 3.7) indicates that the Ftr1 protein of *C. jejuni* has an N-terminal signal peptide of 21 residues that enables export of a large, soluble 417 residue N-terminal domain into the periplasm. This large periplasmic domain is followed by a polytypic transmembrane domain with seven, consecutive transmembrane helices (TMH). The TMHs are separated by short loops, except for TMH3-4, where a larger internal loop of 26 residues is predicted, and for TMH6-7 where a 34-residue external loop is indicated. The FTR1 ferric permease of yeast is in the plasma membrane and also consists of seven TMHs (Severance *et al.*, 2004) organised similarly to those predicted for Ftr1 of *C. jejuni*. Sequence comparisons FTR1 of yeast with related proteins showed the presence two conserved REXLE motifs, one located in TMH1 and the other in TMH4 (Severance *et al.*, 2004), both of which are required for iron uptake activity and are predicted to be iron-binding sites. In addition, the EDLWE and DASE motifs, located in TMH3 and extracellular loop 6 (respectively) of yeast FTR1, were also found to be important for function in FTR1 of yeast (Severance *et al.*, 2004), EfeU also has the same predicted seven-TMH topology, with conserved REXLE motifs in TMHs 1 and 4 required for activity (Große *et al.*, 2006). Such motifs are also apparent for Ftr1 of *C. jejuni*, also located in TMHs 1 and 4, supporting the role of this protein in iron uptake. However, the FTR1 of yeast and EfeU of *E. coli* lack the large, periplasmic N-terminal domain of *C. jejuni* Ftr1. Thus, it is possible that this large N-terminal domain is unique to P19-associated Ftr1-like proteins.

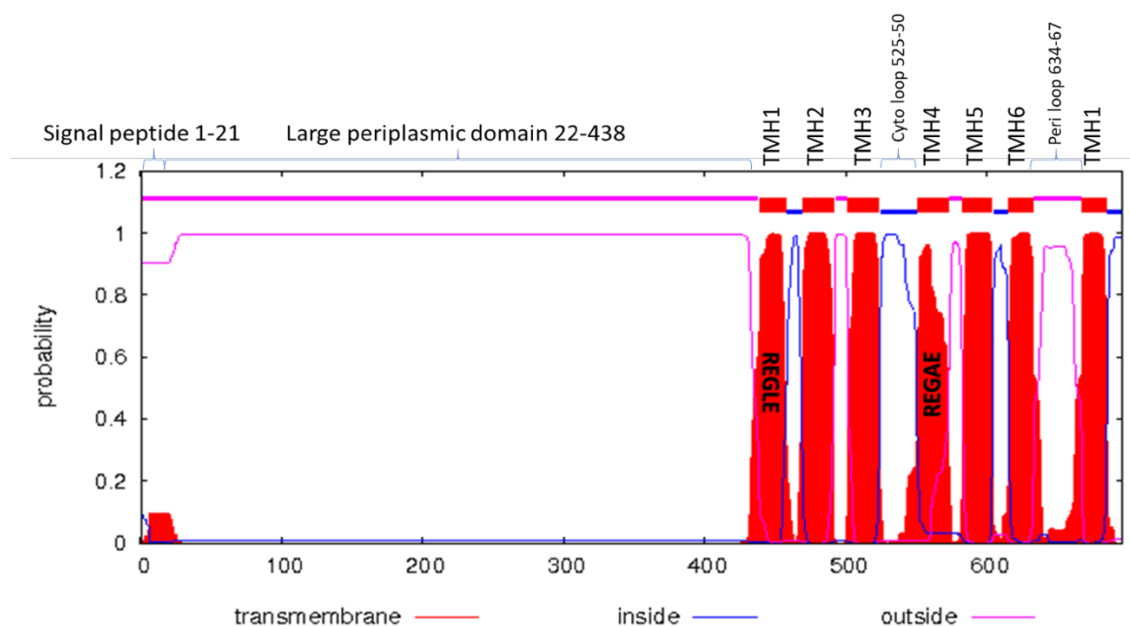


Figure 3.7. Two-dimension plot of the predicted membrane topology of Ftr1 from *C. jejuni* NCTC 11168. A signal peptide (residues 1-21) is predicted at the N-terminus (Phobius). The prediction was generated using the TMHMM Server v. 2.0. Transmembrane helices (TMH) numbered 1-7 (red bars). Amino acids 22-438, extracellular; 439-685, polytopic transmembrane region; 525-550, intracellular loop; 634-667, periplasmic loop; 685-696 intracellular C-terminus. Two conserved REG(A/L)E motifs are indicated in TMH1 and 4.

The Pfam database indicates 4189 FTR1 (PF03239) sequences from 2742 species, associated with 20 domain architectures. The most common domain organisation (DO) is the FTR1-domain-only architecture (DO1, 62%); the next most common is that containing a large, >200 residue N-terminal, extra-cytoplasmic, undefined domain along with the FTR1 domain at the C-terminus (10%, DO2); the third most common organisation (DO3) is that involving a ~300-residue N-terminal, extra-cytoplasmic cytochrome C oxidase (cbb3 type) domain at the N-terminus (8.2%); with the FTR1-EfeO domain organisation (1.6%, DO4) being the fourth most common. All other DOs are rare at less than 0.4%. Ftr1 of *C. jejuni* is within the DO2 group, and most such DO2 group members appear to be associated with a P19 protein (see Fig. 3.3). This supports the earlier suggestion that the N-terminal domain of the Ftr1 of *C.*

jejuni is involved in P19 interaction for P19-systems within the 6-8 gene organisation group (Fig. 3.8).

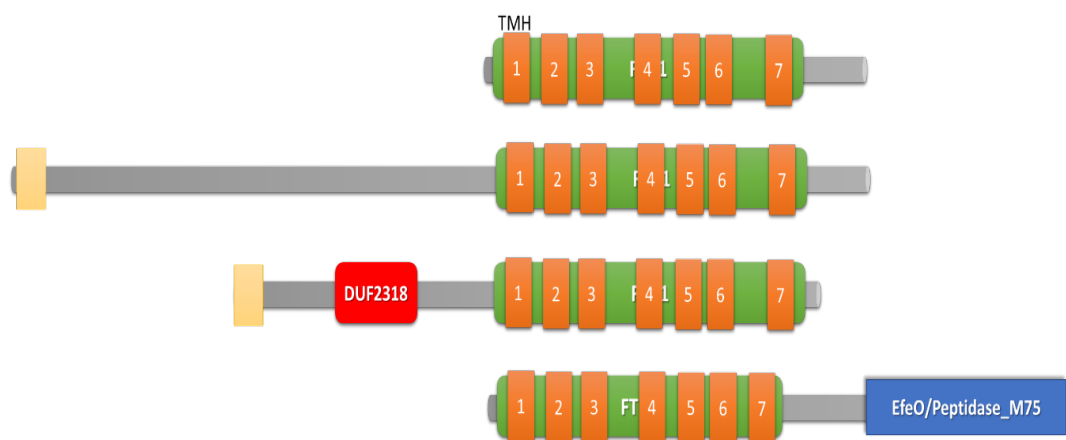


Figure 3.8. Domain organisation of FTR1 domain proteins. Domain architectures for FTR1-domain proteins; only the four most common architectures are shown. The image shows the arrangement of Pfam-predicted domains and is derived from the corresponding Pfam database entries. TMHs and signal sequences are indicated as dark and light orange boxes, respectively. three domains are indicated: red, ‘cytochrome c oxidase, cbb3 type subunit 3’ domain; blue, imelysin like (EfeO) domain; and green, ‘iron-permease FTR1 family.

To generate a multiple sequence alignment and phylogenetic tree, the seed sequence alignment for the FTR1 domain from Pfam was utilised, to which the *C. jejuni* FTR1 domain was aligned (Fig. 3.9). The results show the presence of two highly conserved REGLE motifs associated with the TMH1 and 4 regions of the Ftr1 of *C. jejuni*, which supports the importance of these motifs in the function of the aligned group of FTR1 proteins. The EDLWE motif of yeast FTR1 is well conserved in the other aligned proteins, including *C. jejuni* Ftr1. However, the consensus derived from the alignment is ELxEG (those residues similar/identical to those in the EDLWE motif are underscored), which is slightly different to that reported previously. This thus indicates that this motif is highly conserved in the FTR1 family. The DASE motif of yeast FTR1 is not conserved in the prokaryotic FTR1 proteins (Fig. 3.9).

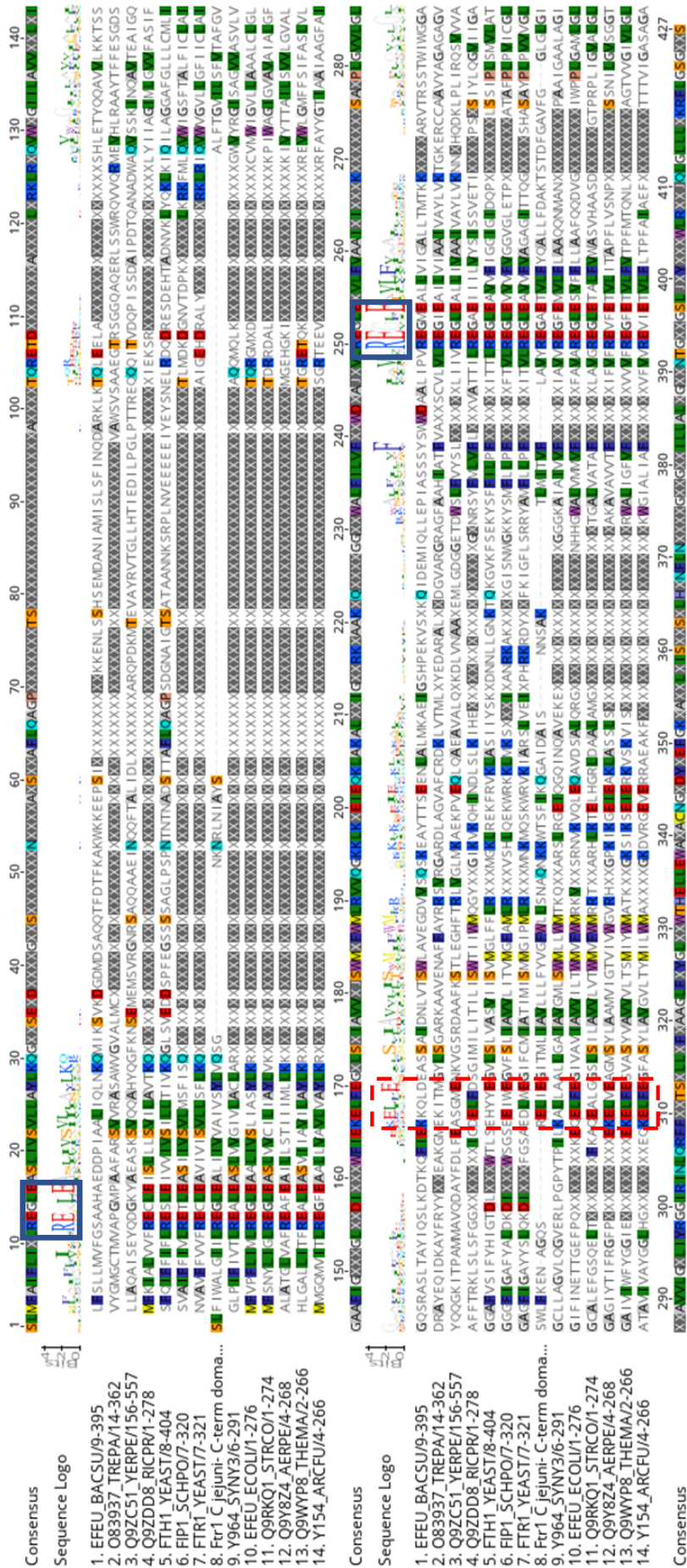


Figure 3.9. Multiple amino acid sequence alignment of Ftr1-like proteins. The alignment is derived from the 13-sequence seed alignment in the Pfam database and is displayed using the multiple sequence alignment option of Geneious (ClustalW) with the N-terminal FTR1 domain of *C. jejuni* Ftr1 included. The two conserved REGLE motifs are indicated by boxes, the conserved EDLWE motif of yeast FTR1 is in a red box (broken line) and the yeast DASE motif is shown in a purple broken box. For other details, see Fig. 3.5.

A phylogenetic tree was generated from the alignment (Fig. 3.10) which shows that the Ftr1-like proteins of yeast form a single clad. All proteins in tree are FTR1-domain only proteins, except for Ftr1 of *C. jejuni* which likely represents the clad associated with all FTR1 proteins in the DO2 group.

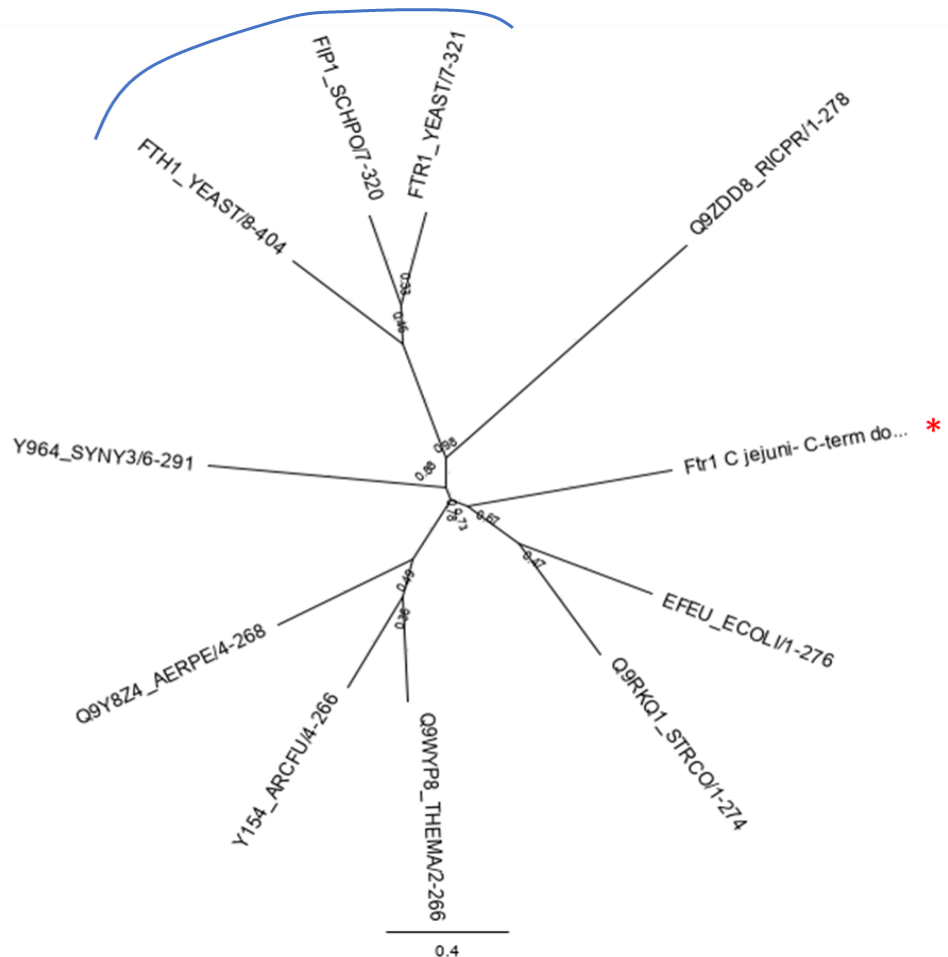


Figure 3.10. Phylogenetic tree of FTR1 domains. The tree was composed using as described for Fig. 3.6 using the sequence alignment of Fig. 3.9. The location of the *C. jejuni* Ftr1 is indicated by an asterisk.



Figure 3.11. Multiple amino acid sequence alignment of the N-terminal domain of *C. jejuni* Ftr1 (residues 1-300) with homologs. The N-terminal domain of Ftr1 (*C. jejuni*) was used to identify homologous proteins using BLASTp. ~1334 hits were obtained from the refseq-protein database. A total of 62 hits were subsequently downloaded (aligned regions only), selected on the basis of distinct taxonomic designation. Sequences were aligned using the multiple sequence alignment option of Geneious Prime (MUSCLE, default options). The alignment tree, alignment logo and consensus are shown, and the *C. jejuni* sequence is indicated by the asterisk. Highly conserved regions are boxed.

Alignment of the ~300 residue N-terminal domain of Ftr1 of *C. jejuni* with 61 homologues (Fig. 3.11) showed that the *Campylobacter* Ftr1 proteins have a larger N-terminal domain than those of the other homologues. A common region ~140 residues (region 1) is shared by all 62 homologues, located at the N-terminal region of the alignment (Fig. 3.11). This is followed by a region of ~80 residues (region 2) shared by a subset of *Campylobacter* species (including *C. jejuni*) and a further region shared by all *Campylobacter* species of ~100 residues (region 3). Highly conserved residues (forming four sequence motifs) are apparent in regions 1 and 3:

Y	at position 45
HFxxFExxE	at position 61-69
ExxF	at positions 85-88
and	
FxxYRNxxxE	at positions 195-204
DxxIQ	at positions 216-220

However, the function and importance of these residues in the GO2 FTR1 proteins remains unclear. The phylogenetic tree derived from the above alignment (Fig. 3.12) shows that the *Campylobacter* sequences form a single clad which includes a sub-group of proteins from ‘mixed taxa’ (namely, Spirochaeles, Chloroflexi, Firmicutes and Gammaproteobacteria). The presence of this cluster within the *Campylobacter* clad is indicative of horizontal gene transfer. The tree is clearly organised according to taxonomy and is almost entirely occupied by proteins from the Proteobacteria phylum. The *Campylobacter* proteins that carry regions 2 and 3 form a distinct group from those that carry region 3 but not region 2 (Fig. 3.12).

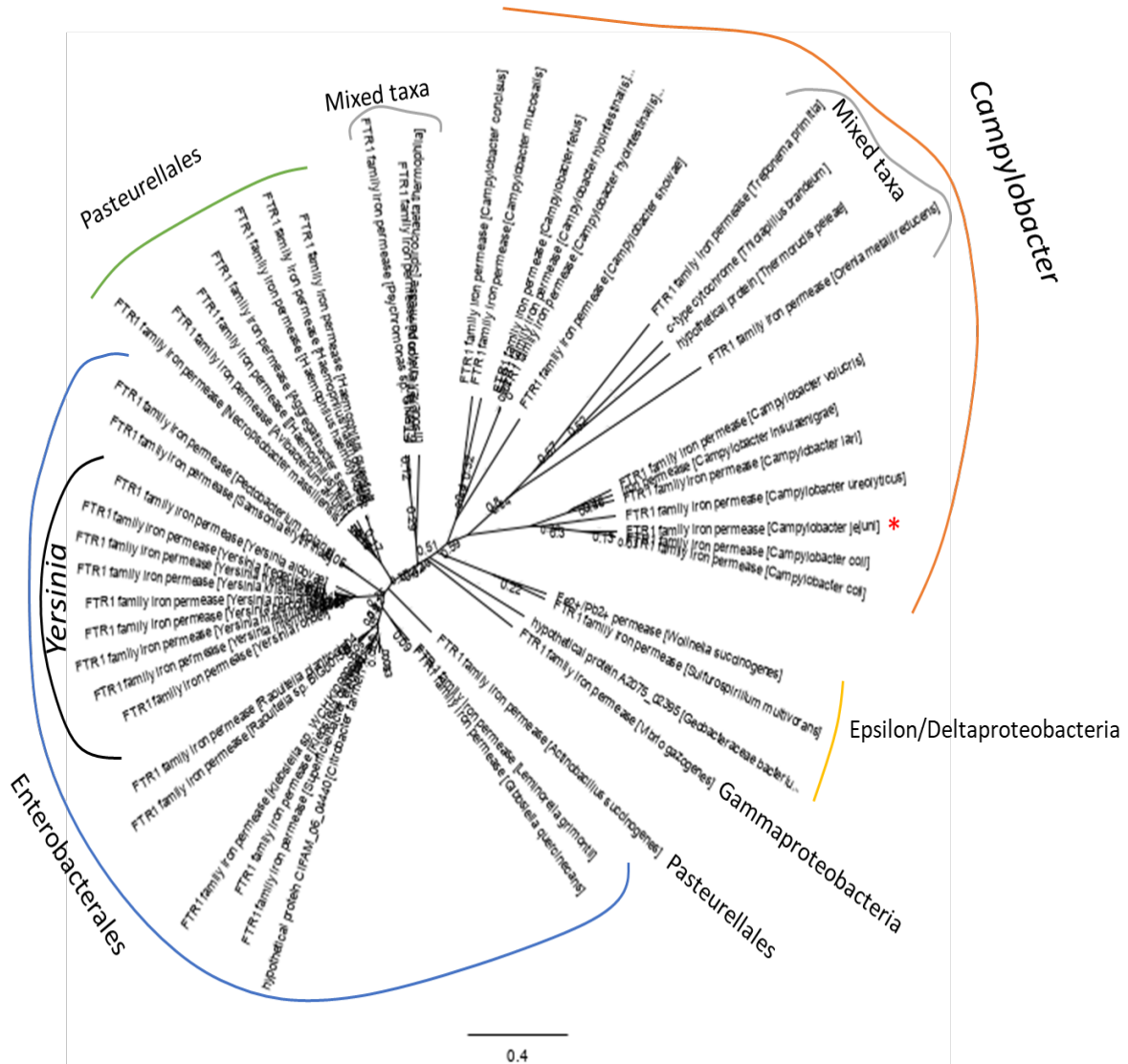


Figure 3.12. Phylogenetic tree of the N-terminal domain of FTR1 proteins in the DO2 group. The tree was composed using Geneious Tree option (UPGMA consensus tree building option, Jukes-Cantor Genetic Distance Model, Bootstrap resampling with 100 reps and a 50% threshold) using the alignment above. Distance and node heights are indicated. The *C. jejuni* sequence is indicated by an asterisk. Taxonomy information is provided for corresponding clades.

3.5. Cj1660-65 and homologues

3.5.1. Cj1660 – an integral membrane protein associated with ABC transporters

The Cj1660 protein of *C. jejuni* NCTC 11168 is predicted to encode a 467 amino acid residue inner-membrane protein. The N-terminal region consists of eight consecutive TMHs generating an integral inner-membrane domain of about 268 amino acids (Fig. 3.13 & 3.14). There is no signal peptide apparent and there is a significant loop of ~30 residues between the 7th and 8th TMH, predicted to be located in the cytoplasm. The C-terminal region is predicted to form a large, ~190 residue periplasmic domain and includes DUF2318- and YHS-domain regions of 103 and 48 residues, respectively (Fig. 3.13). DUF2318 domains are found in bacterial membrane proteins and have no defined function (372 sequences in 347 bacterial species; Pfam). Four major domain architectures are indicated by Pfam (Fig. 3.14B) which includes an FTR1-DUF2318 combination, which further supports the role for Cj1660 (and other DUF2318 domain-containing proteins) in iron transport.

The YHS domains are ~50 residues in size and generally contain two conserved Cys residues considered to be functionally important. There are 3195 YHS-domain sequences in the Pfam database from 2079 species, almost entirely prokaryotic. The YHS domain is associated with Cu-transporting ATPases (where they may be present in duplicate) and some phenol hydroxylases. The domain is presumed to be metal binding and is designed ‘YHS’ on the basis of the corresponding highly conserved residues originally observed. The multiple alignment (Fig. 3.15) of the DUF2318 domain shows that there are three highly conserved Cys-containing motifs. These may act as metal-binding ligands or, more likely, as redox mediators. Indeed, two of the Cys motifs are ‘CxxC’ motifs, which are conserved in Cj1660. The CxxC motif is found in thioredoxins where the two conserved Cys residues enable reduction of Cys residues in other proteins via a cysteine thiol-disulphide exchange reaction (Martin, 1995; Collet *et al.*, 2003), suggesting a possible periplasmic-reduction role for these

motifs in Cj1660. The phylogenetic tree of the DUF2318 domain can be divided into two clads corresponding to the proteins consisting of a DUF2318 domain only (with a short N-terminal TMH or signal peptide) and those containing various additional major domains (YHS, FTR1, integral membrane domain; Fig 3.16). The Cj1660 DUF2318 domain is within the latter clad and thus is appropriately grouped with those proteins likely to be associated with iron uptake.

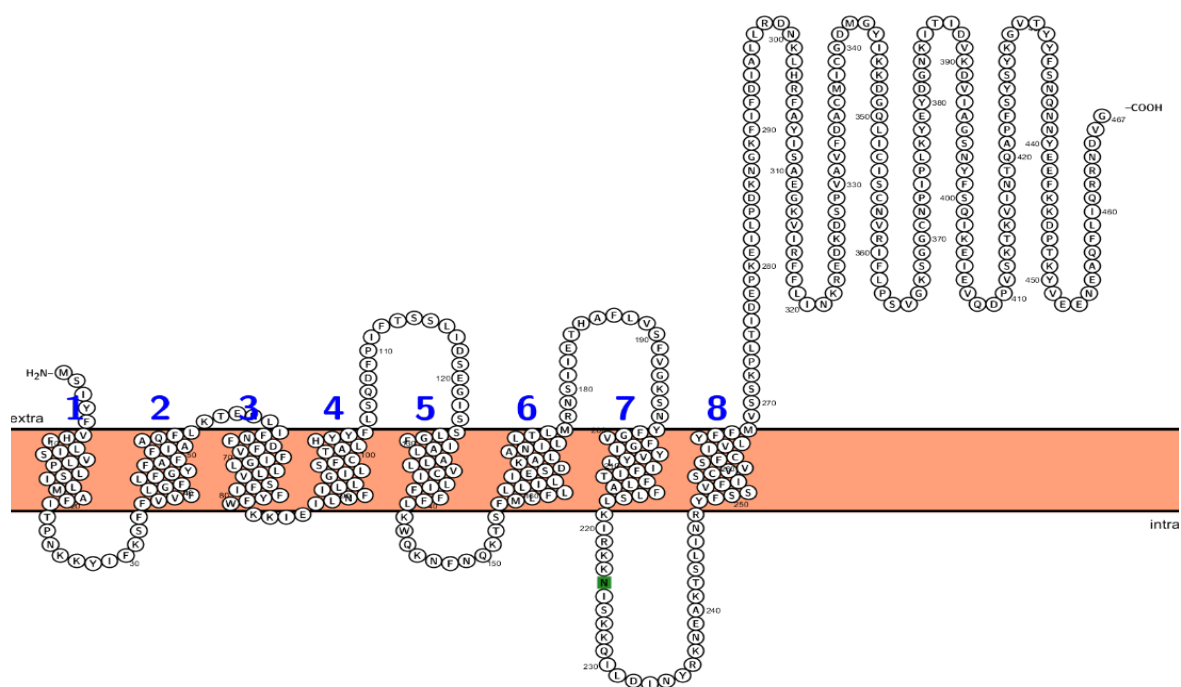


Figure 3.13. Two-dimension plot of *C. jejuni* NCTC 11168 Cj1660 membrane topology. Bacterial membrane (pink), TMH number (blue) determined by Phobius prediction. The predicted N-glycosylation motif (green) is not relevant for bacterial proteins. Using PROTTER-interactive protein feature visualization.

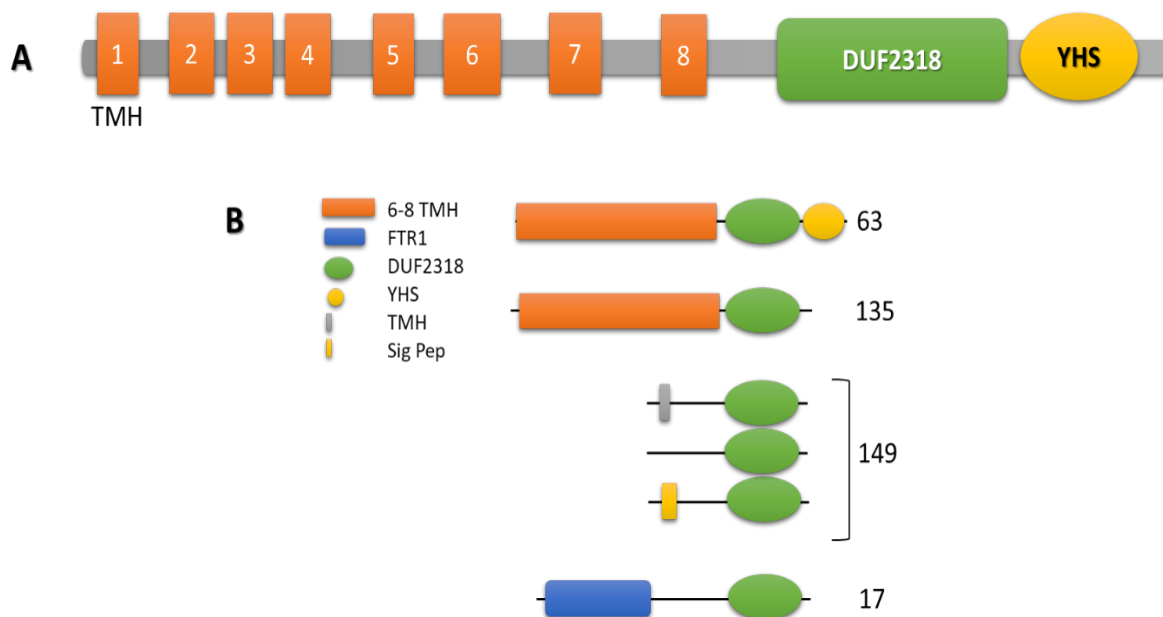


Figure 3.14. Domain organisation of Cj1660. **A.** The image shows the arrangement of Pfam domains and is derived from the Pfam database entry: <http://pfam.xfam.org/protein/Q0P7W9>. TMHs are indicated as orange boxes. The N-terminus is at the far left. **B.** The major domain architectures (and corresponding number of examples) associated with the DUF2318 domain are shown (data derived from Pfam).

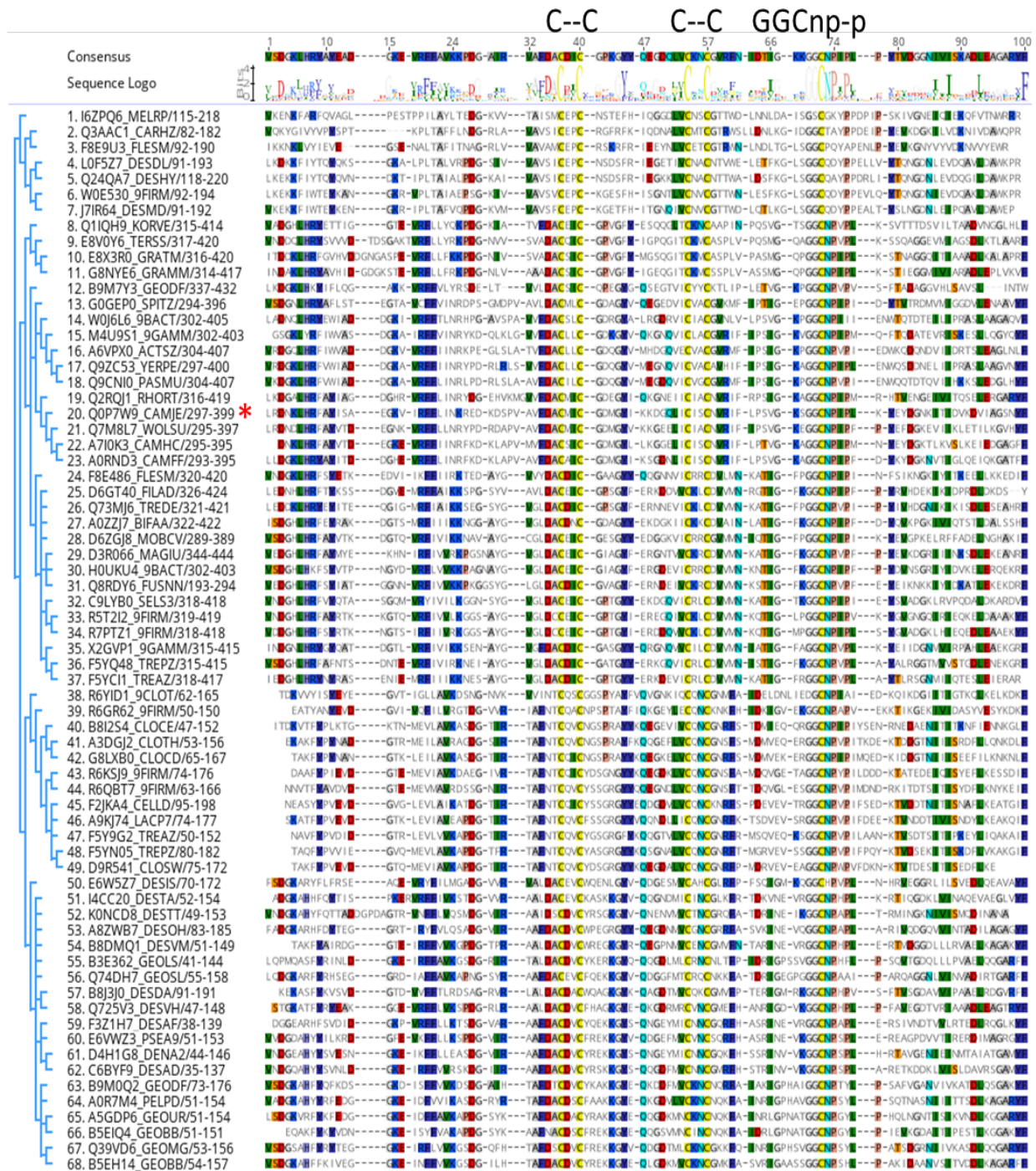


Figure 3.15. Multiple sequence alignment of the DUF2318 domain of Cj1660 and selected homologues. The alignment is from Pfam (68 seed) and is displayed using Geneious. The alignment tree is shown on the left-hand side. Consensus is shown in Logo mode above. Conserved residues are highlighted in colour. Two highly conserved Cys-containing motifs are shown: two CxxC motifs and one GGCNPxP.

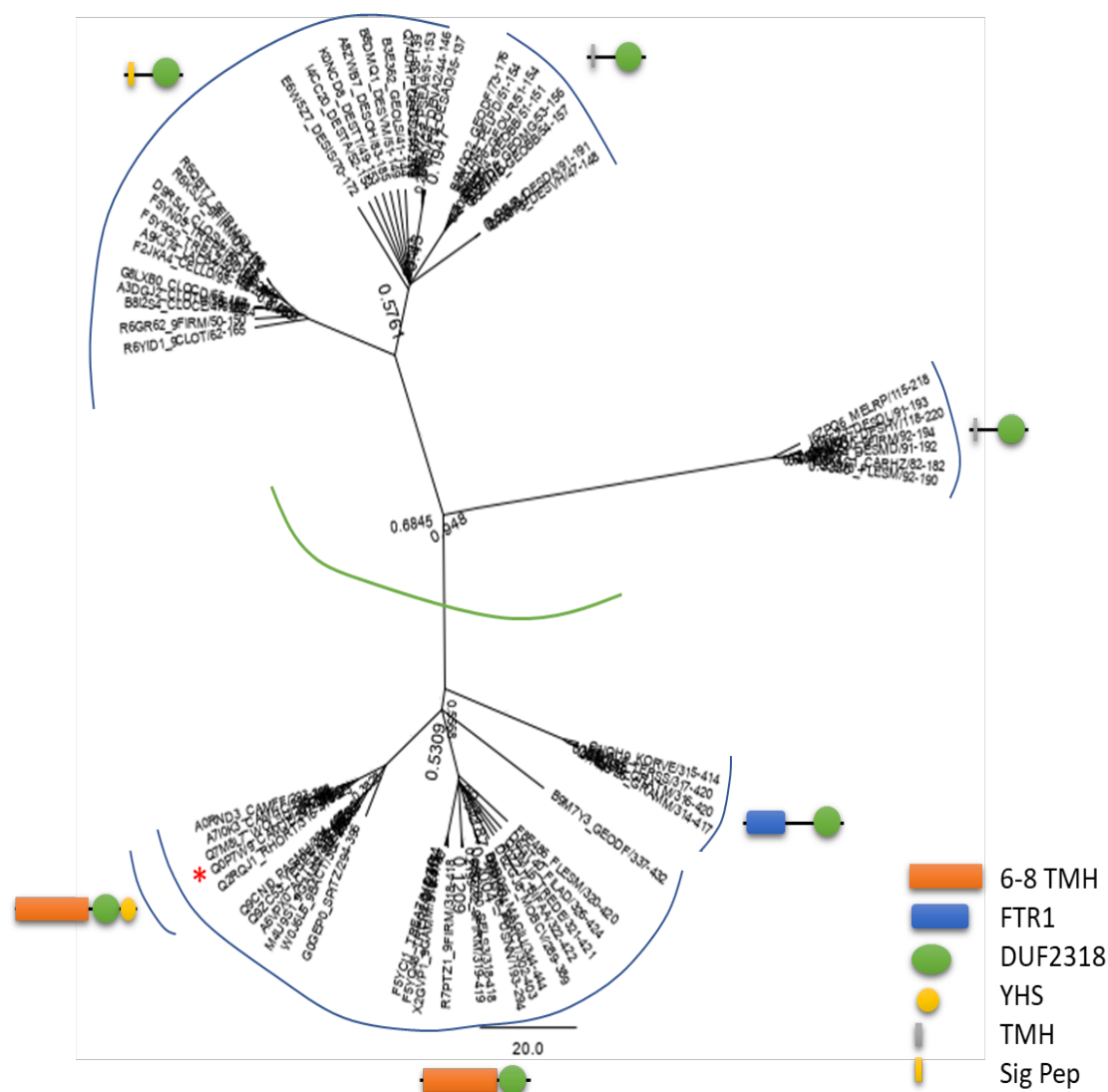


Figure 3.16. Phylogenetic tree of the DUF2318 domain region of Cj1660 and related proteins from a range of taxonomic groups. The tree was composed using Geneious Tree option (UPGMA consensus tree building option, Jukes-Cantor Genetic Distance Model, Jackknife resampling with 100 reps and a 50% threshold). Distance and node confidence values are indicated. *C. jejuni* Cj1660 is indicated by an asterisk. Corresponding domain organisations are indicated and defined in the key. The green line indicates the two major clades (DUF2318 domain only above, and DUF2318 domain combined with other major Fe-transport associated domains).

The YHS domain of Cj1660 was also subjected to multiple sequence alignment and phylogenetic analysis (Fig 3.17). Interestingly, the Cj1660 YHS domain lacks the conserved Cys residues found in other YHS domains and it phylogenetically clusters with other proteins that have a similar domain organisation (DUF2318 associated) and also lack the conserved Cys residues. This suggests that these proteins form a distinct and functionally specialised

evolutionary branch of the YHS-domain family, presumably with a role in iron uptake. Two highly conserved Phe residues are conserved in the Cj1660 protein and its Cj1660-like homologues.

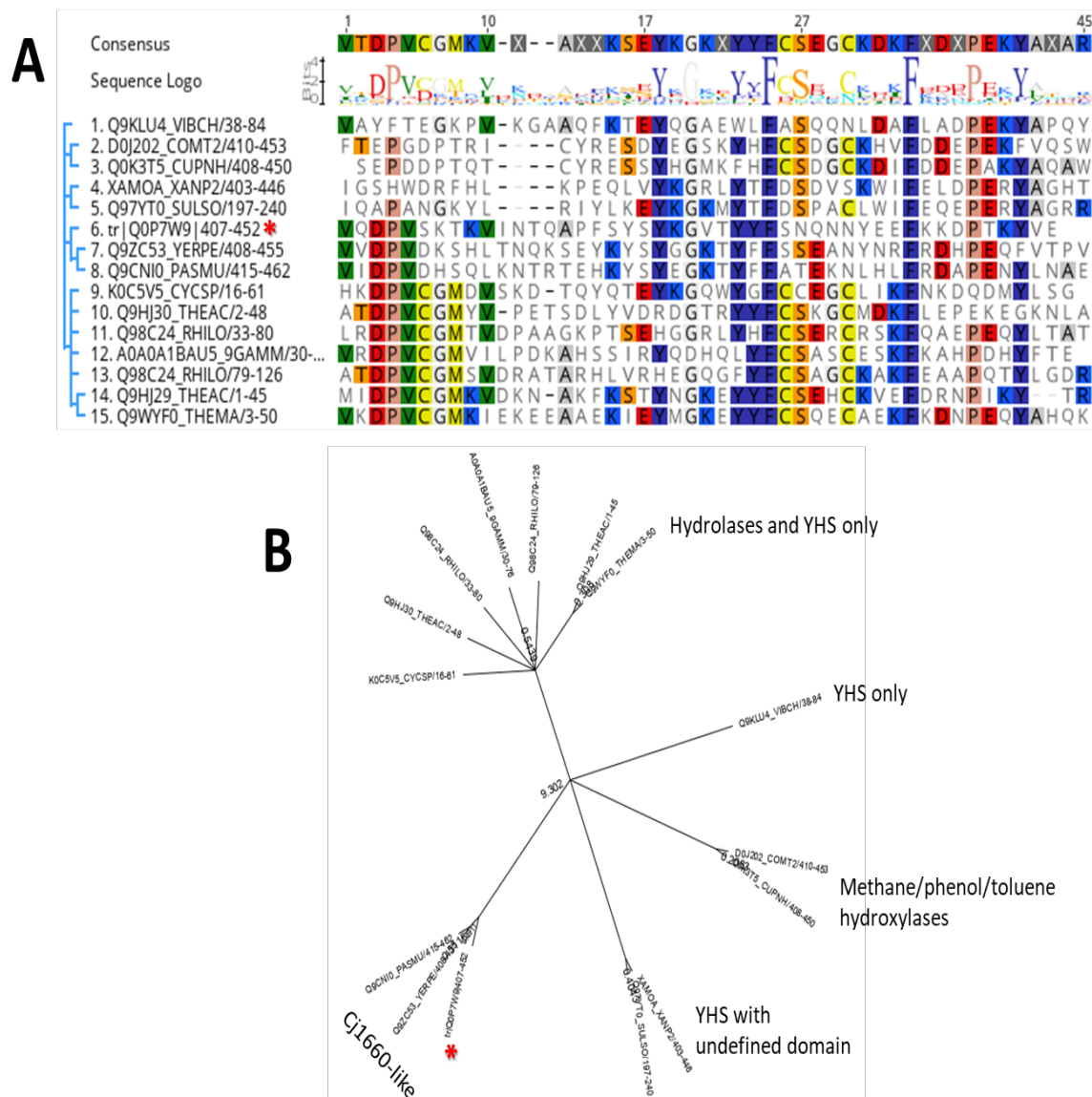


Figure 3.17. Multiple alignment (A) and phylogenetic tree (B) for YHS domain proteins and the YHS domain of Cj1660. A. The alignment is from Pfam (14 seed) and is displayed using Geneious. B. The tree was composed as in Fig. 3.16. *C. jejuni* Cj1660 is indicated by an asterisk. Corresponding domain organisations are indicated in text.

3.5.2. Cj1661 and Cj1662 – noncanonical ABC transport system permease subunits

Cj1661 and Cj1662 are homologous, membrane-associated proteins sharing 26.5% amino acid sequence identity (Fig. 3.18). They are related to the MacB protein, a ‘noncanonical ABC transporter’ component from *E. coli* (also found in other bacteria).



Figure 3.18. Pairwise alignment of Cj1661 and Cj1662. **A.** Pairwise alignment achieved using the pairwise alignment option (default settings of Geneious Prime). Conserved residues are highlighted. **B.** Dot plot (Blosum 62 score matrix) illustrating regions of sequence similarity, with the pairwise alignment path indicated in light blue.

Both *C. jejuni* proteins are predicted to comprise two major domains: a MacB_Periplasmic-Core Domain (PCD) of 210-230 residues located in the periplasm; and an FtsX domain of ~90 residues which includes two TMHs and so is integrated into the inner membrane (Fig. 3.19). The two proteins exhibit identical predicted topologies with an N-terminal TMH which is predicted to anchor the N-terminus to the inner membrane, and three closely spaced TMHs at the C-terminus associated with the FtsX domain. No signal sequences were predicted by SignalP 5.0.

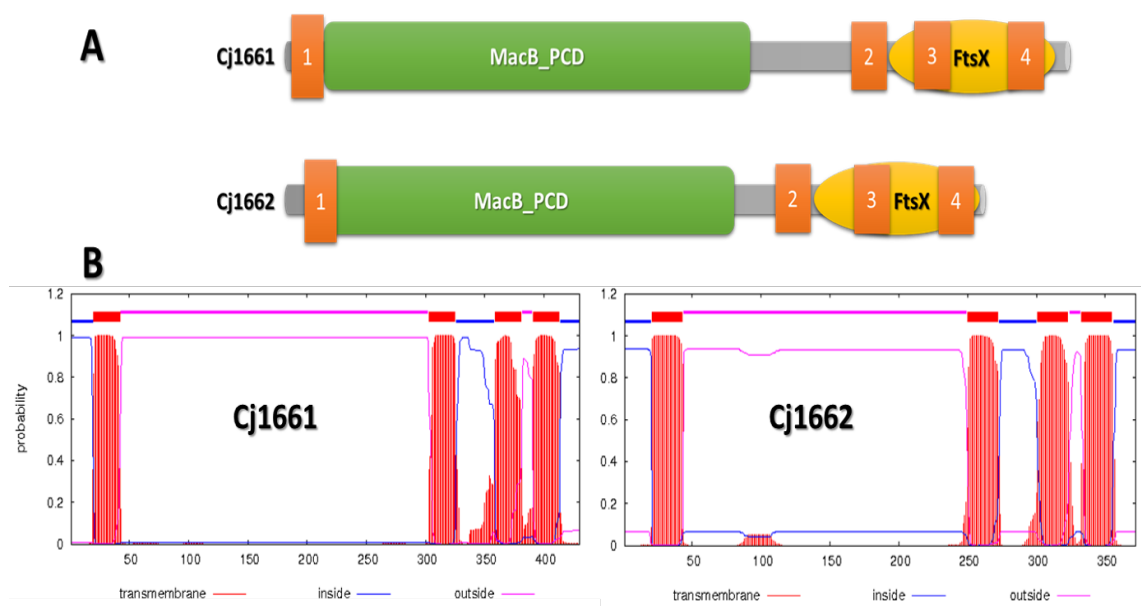


Figure 3.19. Domain organisation and topology plot of Cj1661 and Cj1662. A. Domain organisation of Cj1661 and Cj1662 (430 and 372 amino acid residues). The image shows the arrangement of Pfam-predicted domains and is derived from the corresponding Pfam database entries. TMHs sequences are indicated as dark orange boxes. Two domains are indicated: Mac_PCD and FtsX. B. Membrane topology as predicted by TMHMM.

There are more than >35,000 MacB-like domains (from 7600 prokaryotic species) in the Pfam database and the six most common MacB_PCD domain architectures are shown in Fig. 3.20. As can be seen, the Cj1661 and Cj1662 proteins match the most common domain organisation (row 1, 59% of total number).

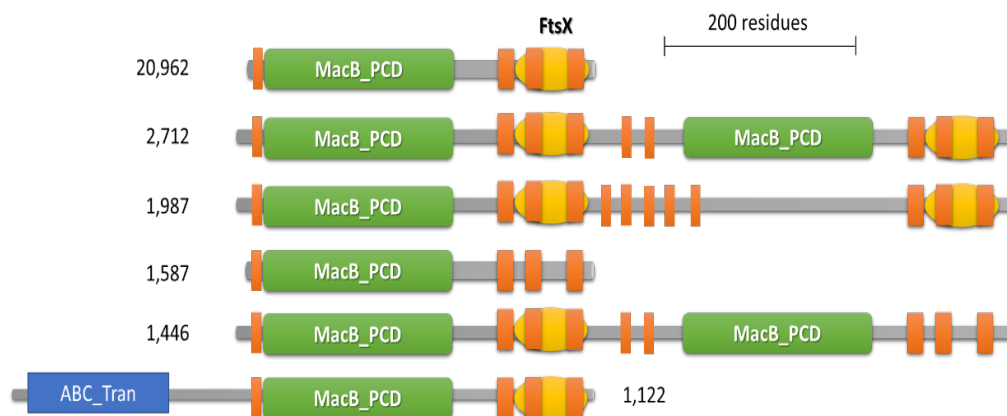


Figure 3.20. The most common MacB_PCD domain architectures. The domain figure is to scale and is derived from the Pfam database (http://pfam.xfam.org/family/macb_pcd). The number of

examples for each architecture is indicated. MacB of *E. coli* matches the domain architecture in the bottom row, whereas Cj1661 and Cj1662 match that in the top. TMHs are indicated as orange bars.

MacB of *E. coli* is the protein after which the domain is designated. It forms part of a tripartite efflux pump (TEP), along with MacA and TolC, that exports macrolides or exotoxins out of the cell (from the periplasm) across the outer membrane (Yamanaka *et al.*, 2008). Other TEP MacAB-TolC systems mediate efflux of agents such as siderophores and protoporphyrin (Imperi *et al.*, 2009). However, many MacB homologues are not part of such tripartite systems (as appears to be the case for Cj1661/2). Examples such ‘TEP-independent’ MacB systems, that are functionally defined, are the LolCDE system (localization of lipoproteins) that removes lipoproteins from the inner membrane to a periplasmic chaperone prior to delivery to the outer membrane, and the FtsEX system that adjusts the activity of periplasmic peptidoglycan hydrolases in cell division (Yakushi *et al.*, 2000; Yang *et al.*, 2011). Thus, like MacB, these systems do not transport substances across the cytoplasmic membrane but instead utilise cytoplasmic ATP to engage in an energy-requiring activity in the periplasm. For this reason, the MacB ‘type VII ABC’ transporters are best described as periplasmic or extra-cytoplasmic mechanotransducers, rather than transporters (Greene *et al.*, 2018).

MacB consists of an N-terminal nucleotide-binding domain (NBD) and thus its DO matches that in row 6 of Fig. 3.20. The N-terminal NBD is absent in the Cj1661 and Cj1662 proteins. However, the associated Cj1663 protein is an NBD protein and would thus likely interact with Cj1661 and Cj1662 in a similar fashion as seen for the NBD of MacB, to generate a tetrameric complex (see Fig. 3.21). Several crystal structures of MacB-like proteins are

known: LolE (Lipoprotein-releasing system transmembrane protein) of *Acinetobacter baumannii*, LolC (Okada *et al.*, 2017) of *E. coli* (Crow *et al.*, 2017), Macrolide export ATP-binding/permease protein (MacB) of *E. coli* (Fitzpatrick *et al.*, 2017), the ABC transporter permease protein of *Porphyromonas gingivalis* (3is6) and an MacB-FtsX efflux protein from *Streptococcus pneumoniae* conferring resistance to antibiotics and antimicrobial peptides (Yang *et al.*, 2018).

The MacAB-TolC structure shows that two MacB subunits combine to provide four TMHs from each subunit. The four TMHs of the MacB_PCD-FtsX unit are shown in Figs. 3.20 and 3.21 and appear well conserved. A schematic representation of the MacB structure is shown in Fig. 3.21. The structure shows a major periplasmic domain which extends well beyond the cytoplasmic membrane due to a stalk structure formed by extended helices 1 and 2; this structure is described as resembling a mushroom. The similarity of Cj1661 and Cj1662 to the MacB proteins, together with the presence of the ABC-like protein Cj1663, strongly suggest that they play an ATP-energy-dependent role in manipulation of substrates in the periplasm. However, it is unclear what the substrate for these proteins would be or what reaction would be performed. LolCDE is similar in organisation to Cj1661-3 since LolC and E are both MacB-like proteins with 4 TMHs each (and no N-terminal NCD), and LolD is an NCD (Narita and Tokuda, 2017). It is thought to extract the lipid moiety of lipoproteins from the outer surface of the cytoplasmic membrane and mediate deliver to the periplasmic LolA for subsequent transfer to the outer membrane via LolB. FtsEX is also similar in organisation to Cj1661-3, with FtsE acting as the NBD and FtsX having the same DO as Cj1661/2. It regulates the activity of extra-cytoplasmic amidases involved in cell wall modification (Crow *et al.*, 2017). HrtAB is another example of a TEP-independent MacB-like system. It is believed to remove haem from the membrane in Gram-positive bacteria (Wakeman *et al.*, 2012; Joubert *et al.*, 2014).

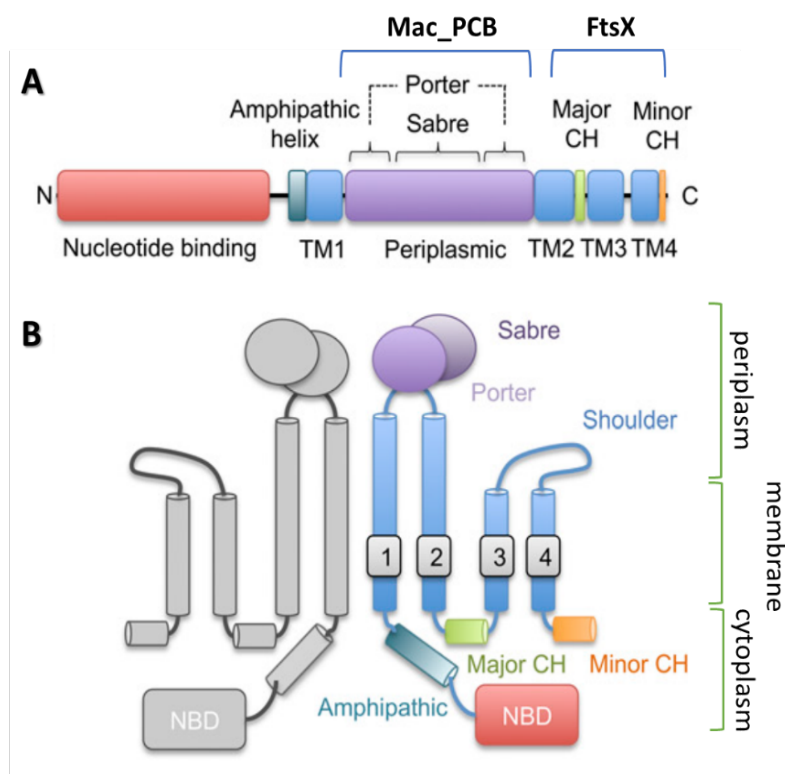


Figure 3.21. Domain organisation and topology of the MacB protein of *Aggregatibacter actinomycetemcomitans*. A. Domain organisation (note that the nucleotide binding domain is not included in the *C. jejuni* proteins). B. Topological organisation. Sabre, small alpha/beta rich extracytoplasmic subdomain; Porter subdomain, comprises two beta-alpha-beta motifs; CH, cytoplasmic helix; shoulder, is a loop that sits at the interface of the membrane periplasmic surface and the periplasm. Figure is from (Crow *et al.*, 2017).

In order to gain an indication of the possible function of Cj1661 and Cj1662, a multiple alignment and phylogenetic tree were constructed to enable the closest homologues of known function to be identified. Only the FtsX domain was considered and only the subset of MacB-like proteins with known functions were included (Fig. 3.22). The results show that the Cj1661/2 proteins are more closely related to non-TEP proteins, particularly the LolCE proteins, than the non-TEP proteins. This would suggest a role in extraction of lipid moieties from the inner membrane rather export from the periplasm and is consistent with the closer organisational similarity of Cj1661/2 system to the non-TEP systems.

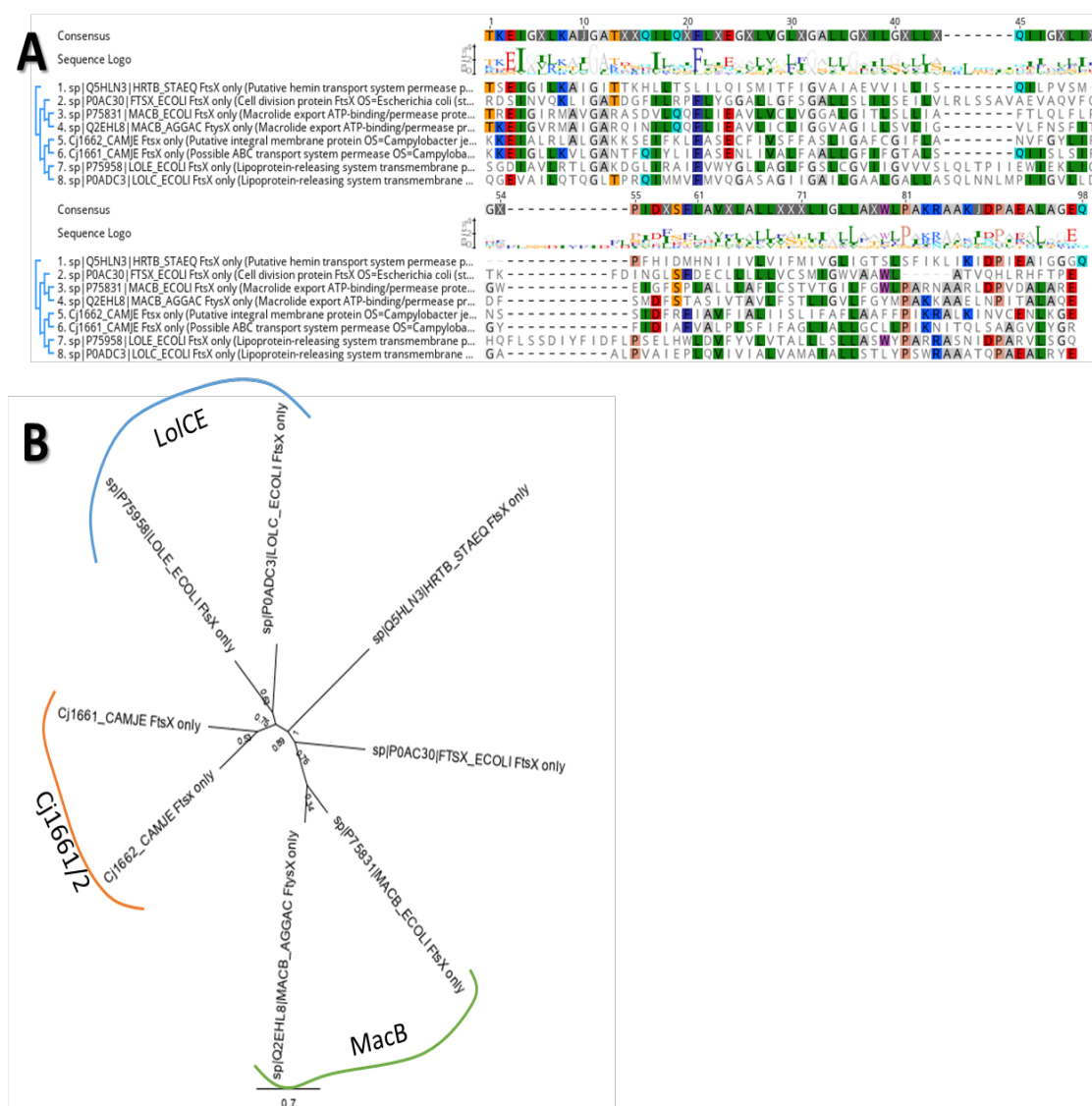


Figure 3.22. Multiple alignment and phylogenetic tree of the FtsX domain of functionally defined MacB-like proteins. The alignment was achieved using the MUSCLE option in Geneious Prime. FtsX domain regions were selected according to regions defined by Pfam. The phylogenetic tree was generated as in Fig. 3.6. Proteins included are Cj1661, Cj1662, MacB of *E. coli*, MacB of *Aggregatibacter actinomycetemcomitans*, LolC of *E. coli*, LolE of *E. coli*, FtsX of *E. coli* and HtrB of *Staphylococcus epidermidis*.

3.5.3. ABC transporter ATP-binding cassette protein (Cj1663)

Cj1663 is an ABC transporter ATP-binding protein of 217 amino acids that would be expected to cytoplasmically located on the inner surface of the cytoplasmic membrane where it would likely form a complex with a heterodimeric complex of membrane-embedded

Cj1661 and Cj1662; this complex would be expected to include two subunits of Cj1663. Cj1663 falls within the ‘ABC_MJ0796_LolCDE_FtsE’ (cd03255) group of ABC proteins (part of the ABC Class 3 group), which includes the MacAB, FtsEX and LolCDE non-canonical ABC systems (NCBI, Conserved Protein Domain Family database). It possesses all of the recognised motifs found in ABC proteins (Walker A, Walker B, Q-loop, D-loop, and H-loop form the nucleotide binding site; InterPro database), and thus would be expected to be a functional ABC protein. No alignment or phylogenetic tree was generated since the function and mechanism of ABC proteins is well understood, and little insight would be expected to be gained by such an analysis.

3.5.4. Thioredoxin proteins

Downstream to the ABC transporter protein genes of the *p19* gene cluster are two thioredoxin encoding genes, *cj1664-65* (*fetEF*). The primary translation products consist of 162 and 167 amino acid residues, respectively. Both Cj1664 and Cj1665 are predicted with high probability (0.9989 and 0.9971, respectively) by SignalP 5.0 (Armenteros *et al.*, 2019) to possess a lipoprotein signal peptide (Sec/SPII) comprising residues 1-16 and 1-21 (LNA-CS and FVA-CD cleavage sites) (Fig. 3.23). It should be noted that the signal peptide (Sec/SPI) prediction was very weak (P value 0.0009 and 0.002, respectively). The indicated cleavage would be expected to give an N-terminal Cys residue in each case that would be lipoylated to give a S-diacylglycerol cysteine, and this residue would subsequently be subject to a second modification of an amide-linked acyl group at the free N-terminus. Thus, both proteins are predicted to be exported into the periplasm and anchored to the inner surface of the cytoplasmic membrane. According to the ‘+2’ rule, since the cleaved Cj1665 protein would have an Asp at position +2, it would be predicted to be strongly retained in the cytoplasmic membrane, whereas Cj1664 carries a Ser at position +2 so would be expected to be

translocated to the outer-membrane by the Lol system (Zückert, 2014; Okuda and Tokuda, 2011).

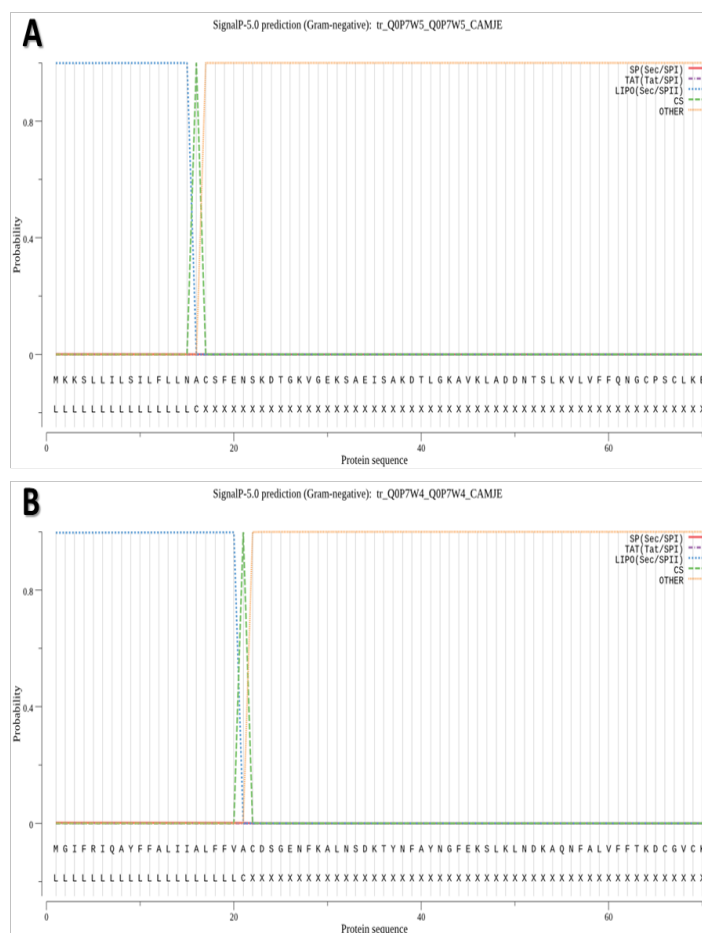


Figure 3.23. Predicted signal cleavage sites for Cj1664 (A) and Cj1665 (B). Cleavage sites were predicted using SignalP 5.0 (Armenteros *et al.*, 2019) using the ‘Gram-negative’ option.

The LolABCDE system of *E. coli* functions to remove lipoproteins from the outer leaflet of the cytoplasmic membrane and transfer them to the inner leaflet of the outer membrane, as discussed above. Such a system would be expected to be required for transfer of Cj1665 into the outer membrane. In *C. jejuni*, there are just two Lol-encoding genes apparent, specifying LolA and LolC/LolE homologues (Fig. 3.24). The *C. jejuni lolA* gene (cj0943) is directly downstream of, and divergent to, the *secA* gene which mediates membrane insertion of preproteins. The *C. jejuni lolC/E* gene (cj0941) is directly downstream of, and co-polar with,

secA. Thus, the *lol* genes are appropriately located adjacent to a key secretion apparatus gene.

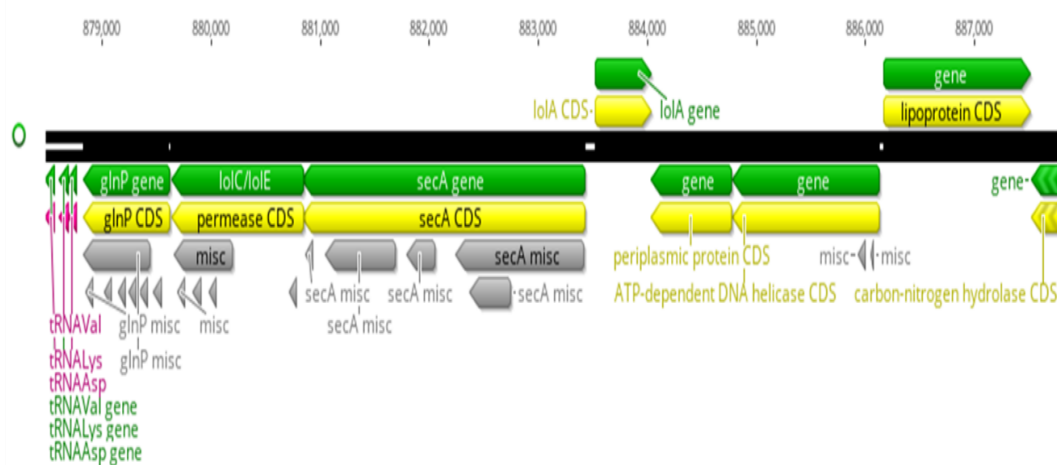


Figure 3.24. Location of the *lolA* and *lolC/E* genes of *C. jejuni* NCTC 11168. Genome at 879-887 kb visualised using Geneious Prime. The gene (*glnP*) downstream of *lolC/E* encodes an ABC-dependent permease subunit.

The lack of a LolB candidate in *C. jejuni* suggests that LolA may perform the roles of both LolA and LolB in inserting lipoproteins into the outer membrane. The presence of a single *lolC/E* candidate suggests that the *C. jejuni* Lol system consists of two Cj0941 subunits. The apparent lack of a LolD equivalent at the *lol-secA* locus suggests that the corresponding ABC encoding gene is located elsewhere in the chromosome. Interestingly, the best match for the *E. coli* LolD gene in *C. jejuni* NCTC 11168 is Cj1663 (FetD) (95% coverage, $5e^{-58}$ E value, 44.2% identity). Thus, Cj1663 may form part of the Lol apparatus of *C. jejuni*. The next closest match is Cj0607, a MacB homologue (93% coverage, $2e^{-56}$ E value, 42.40% identity) that has the same DO as MacB (row 6, Fig. 3.20). The *cj0607* gene is part of a five gene operon (*cj0604-8*) that appears to specify an efflux apparatus. The prediction that Cj1665 is a Lol substrate provides the possibility that the Cj1661-3 components act as a secondary and

highly specific Lol system in mediating the transfer of Cj1665 into the outer membrane, possibly employing LolA as the periplasmic chaperone component.

Thioredoxins are small, ~100 residues proteins found in all domains of life. They take part in a wide range of redox reactions through the reversible oxidation of a disulphide bond at their active site. Those thioredoxins found in the periplasm generally function as disulphide bond isomerase (Dsb), enabling correct disulphide bond formation for periplasmic proteins.

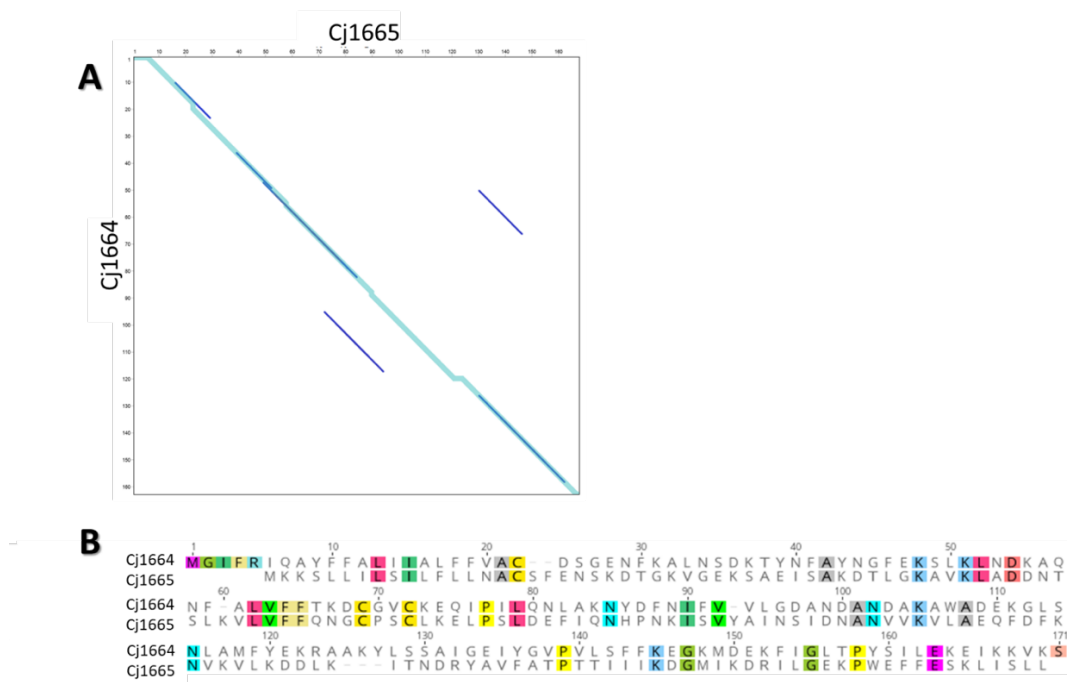


Figure 3.25. Dot plot (A) and pairwise comparison (B) of the Cj1664 and Cj1665 full-length amino acid sequences. Details are as for Fig. 3.18.

Cj1664 and Cj1665 show just 18.8% sequence identity (50.9% similarity; Blosum 90, threshold 0 score matrix) (Fig. 3.25). Thus, they appear distantly related proteins. Three Cys residues are conserved. One corresponds to the N-terminal Cys of the mature proteins. The other two correspond to a CxxC motif that is the distinguishing feature of thioredoxins and provides the active site Cys residues required for redox activity (Martin, 1995; Collet *et al.*, 2003), Therefore, it is predicted that Cj1664 and Cj1665 act as membrane-embedded, extracytoplasmic thioredoxins with roles in iron uptake.

3.6. Discussion and Conclusion

3.6.1. Gene organisation and taxonomic distribution. The bioinformatic analysis performed in this chapter firstly involved identification of *p19* gene clusters in different organisms using the Gene Context Tool 3. Three common genetic organisation groups were observed (Fig. 3.26): Group 1 (94 members) is the largest and consists of 4 co-polar genes, likely giving a single transcript (designated *ftrABCD*). Such systems have been characterised in *Bordetella*, *Burkholderia* and *Brucella* spp. (Brickman and Armstrong, 2012; Mathew *et al.*, 2014; Elhassanny *et al.*, 2013) and are also found in *Salmonella*, *Acetobacter* and *Pseudomonas* spp. The proteins encoded are as follows: P19, cupredoxin, Ftr1 and a polyferredoxin, respectively. Group 2 consists of 6-8 co-polar genes, organised into two apparent transcription units (designated *fetMP* and *fetA-F*).

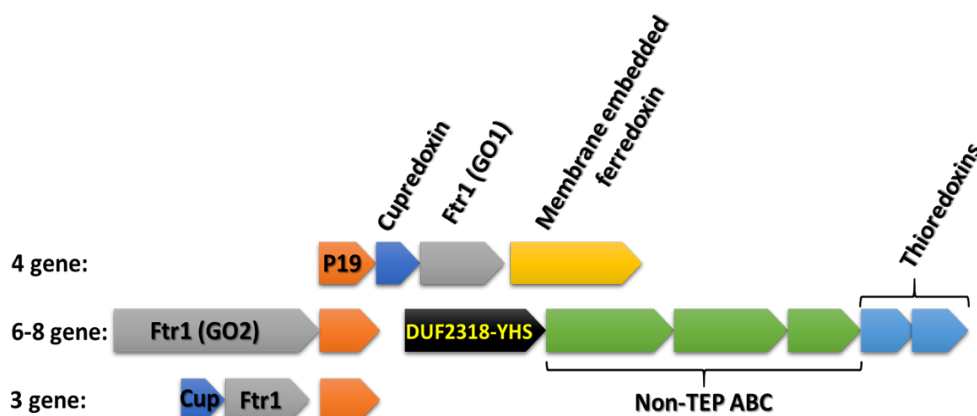


Figure 3.26: Schematic representation of the common gene organisations associated with *p19*.

This group includes the genes of interest from *C. jejuni*, and there was a total of 73 members. The first two genes encode Ftr1 and P19 proteins, whereas genes 3-8 encode an ABC-like transporter (three polypeptide components), an integral membrane protein of unclear function and two thioredoxins or putative FMN-containing protein. Such systems were found in *Campylobacter* spp., *Yersinia* spp., *Fusobacterium* spp., *Actinobacteria* spp., some strains of *E. coli* and also in *Bifidobacterium* spp.. Group 3 (11 members) has relatively few members

being found in only two species of bacteria. These systems consist of three apparently co-operonic genes encoding a cupredoxin, an Ftr1 protein and a P19 protein, and thus resemble Group 1 apart from the absence of a polyferredoxin. Thus, genes specifying P19 proteins are usually associated with an Ftr1-encoding genes (99% of cases) suggesting a clear general role in iron uptake. In addition, nearly all of the Ftr1-P19 clusters also include a gene specifying a redox component (either a cupredoxin, a polyferredoxin, a thioredoxin or an FMN protein). It can therefore be assumed that the P19-dependent transport systems generally require a ferric permease unit and a reduction/oxidation component for their biological function.

3.6.2. P19. The multiple alignment of P19 proteins indicated the highly conserved nature of the DGPHYG and ETGV motifs involved in metal binding (Chan *et al.*, 2010), thus supporting the role of the P19 protein from other species as copper-containing and iron-binding proteins. The derived phylogenetic tree was organised into two major clads corresponding to P19 proteins encoded by the four-gene (e.g. *frABCD* of *Bordetella pertussis*) and 6-8 gene type systems (e.g. *fetMP-fetABCDEFG* of *C. jejuni*). This suggests a functional specialisation of P19 proteins according to their association with the Group 1 or 2 Ftr1-P19 systems.

3.6.3. Ftr1. Ftr1 of *C. jejuni* was predicted to comprise seven TMHs together (as found in other Ftr1-like proteins) with a large N-terminal cytoplasmic domain that is absent in the majority of Ftr1-like proteins and is of unclear purpose. Thus, the *C. jejuni* Ftr1 was classified within the relatively minor 'DO2' domain organisation group of the Ftr1 family. The *C. jejuni* Ftr1 was found to contain the two conserved REG(A/L) E motifs in TMHs 1 and 4, which have been shown to be essential for iron uptake in the Ftr1p of yeast (Severance *et al.*, 2004). These motifs are predicted to act as iron ligands during uptake across the membrane (Severance *et al.*, 2004) and their conservation supports the role for the *C. jejuni*

protein as a ferric permease. Of the two other motifs shown to be important for Ftr1p function in yeast, the DASE motif of loop 6 was not conserved in the *C. jejuni* Ftr1 whereas the EDLWE motif of TMH 3 was conserved, although the derived consensus (ELxEG) was slightly modified. This finding indicated an important role for this motif, but not the DASE motif, in the prokaryotic Ftr1 homologues. Phylogenetic analysis was consistent with the separation of the DO2 type Ftr1 proteins into a distinct clad within the Ftr1 family, although further work is required to confirm this clustering. A multiple alignment of the 300-amino-acid-residue N-terminal domain of the *C. jejuni* Ftr1 protein with the corresponding domain of other Ftr1 proteins revealed a highly conserved region (region 1) of ~140 residues with three novel motifs identified, although no function for these motifs could be predicted. The *Campylobacter* Ftr1 proteins were found to have a more extensive N-terminal domain than that of other Ftr1 proteins in the GO2 group, and to possess a shared region (region 3, ~100 residues) that was conserved only in a subset of GO2 Ftr1 proteins. This region has two apparent motifs, again of unclear purpose. The DO2 Ftr1 proteins were seen to be associated with the 6-8 gene organisation P19 systems (group 2) which suggests a specialised purpose associated with the mechanism of action of the group 2 P19 systems.

3.6.4. The DUF2318-YHS protein. The Cj1660 protein was found to consist of three domains: An N-terminal integral membrane domain of 8 predicted TMHs; a central ~100-residue, extracellular DUF2318 domain; and a C-terminal ~50-residue, extracellular YHS domain. Interestingly, the DUF2318 domain was found to possess three conserved Cys-containing motifs including two 'CxxC' motifs, as in thioredoxins, suggesting that Cj1660 may have a redox function in the periplasm. The DUF2318-domain phylogenetic tree was organised into two major clads according to domain architecture: DUF2318 domains with an N-terminal polytopic integral membrane domain; and DUF2318 domains without any major,

additional domain. There was an apparent association of members of the former clad with iron transport.

Although no purpose for the DUF2318 domain is known, YHS domains are found within proteins with to various functions including the Cu-transporting ATPases. However, the conserved metal-binding Cys residues found in many other YHS domains are not present in the YHS domains of Cj1660 like proteins, suggesting that the Cj1660 YHS domain either does not bind metal or does so using a different set of ligands. Pfam data base showed that there are 23 structures of YHS-domain family. It is 50 amino acids residues with three conserved amino acids; tyrosine, histidine, serine (InterPro IPR007029). Also, it is similar to TRASH domain with cysteine residue as conserved (Ettema *et al.*, 2003).

3.6.5. The ABC-associated extra-cytoplasmic mechanotransducer components. Cj1661 and Cj1662 were found to be homologous (26.5% identity) and are highly likely to be closely associated with the inner membrane. They are related to non-canonical ABC ‘permease’ subunits such as MacB of *E. coli* (involved in export of macrolides out of the periplasm; Yamanaka *et al.*, 2008). Together with Cj1663 (encoding an ATP-binding cassette subunit), they would appear to form a LolCDE-like system (involved in re-localisation of lipoproteins from the cytoplasmic membrane to the outer-membrane; Yakushi *et al.*, 2000; Yang *et al.*, 2011). Such systems utilise energy derived from hydrolysis of cytoplasmic ATP to engage in an energy-requiring process in the periplasm. Thus, they do not mediate translocation of substrates across biological membranes, and cannot be classified as transporters or permeases, but are instead considered as extracytoplasmic mechanotransducers (Greene *et al.*, 2018). Given the similarity of the Cj1661-3 components to their Lol homologues, it is suggested that the Cj1661-3 components might act as a specific Lol system for translocation of the thioredoxins associated with Ftr-P19 system (see below). Interestingly, *C. jejuni* carries close homologues of just two of the five genes found in *E. coli* that are required for Lol

activity (*lolA* and *lolC/E* homologues) – these are adjacent to the *secA* protein-secretion gene supporting their role in lipoprotein translocation.

3.6.6. Membrane-anchored, periplasmic thioredoxins. The Cj1664-65 (FetE-F) proteins are members of the thioredoxin family. Like other thioredoxins, they are small proteins (just 146 predicted residues for the mature polypeptides) with a highly conserved CxxC motif which mediates the characteristic redox activity of this class of proteins (Martin, 1995; Collet *et al.*, 2003). Both are predicted to be exported into the periplasm and to be initially anchored to the periplasmic surface of the cytoplasmic membrane via lipoylation of N-terminal Cys residues that are exposed upon cleavage during export. However, Cj1664 is predicted to be subsequently translocated from the cytoplasmic membrane to the outer-membrane by the Lol system (as discussed above) since it has Ser at position +2 (according to the ‘+2’ rule; Zückert, 2014; Okuda and Tokuda, 2011), whereas Cj1665 is expected to be retained in the cytoplasm due to Asp at position +2 of the mature polypeptide. It would be expected that the LolA protein would act as the periplasmic chaperone protein in mediating delivery of Cj1664 to the outer membrane and it is possible that the Cj1661-3 complex is involved in releasing Cj1664 from the inner membrane for delivery to LolA. However, it is also possible that LolC/E (along with an unidentified ABC component) performs this function.

The likely role of Cj1664 and Cj1665 is to act as redox mediators in the delivery or acceptance of electrons from periplasmic components, in a fashion that supports iron uptake by the Ftr1-P19 system. Since Cj1664 appears to be outer-membrane located, and Cj1661-3 may have a role in lipoprotein localisation, this raises the possibility of shuttling of thioredoxins between membranes in order to drive an extra-cellular ferric reduction reaction. A further possibility is a role in consumption of electrons released from oxidation of ferrous iron upon import by Ftr1-P19; Ftr1p-Fet3p of yeast employs oxygen as oxidant and EfeUOB

likely employs H₂O₂ as oxidant of ferrous iron during uptake, so a similar oxidation of ferrous iron is anticipated for the Ftr1-P19 system.

3.6.7. A model for Cj1660-5 (FetA-F). From the bioinformatics analysis performed in this chapter, it is possible to generate a model that accounts for the features of the Cj1660-5 components (Fig. 3.27). The non-TEP ABC system is depicted as mediating translocation of thioredoxins between the inner and outer membranes. The thioredoxins are potentially reduced by the Cj1660 protein, via the pair of conserved CxxC motifs shown. Potentially, Cj1660 receives electrons from cytosolic thioredoxins or the quinone pool in a manner analogous to the DsbABCD system (Fabianek *et al.*, 2000). The reduced thioredoxins may then drive extra-cytoplasmic reduction of ferric iron to provide ferrous iron for Ftr1-P19 uptake. If the model suggested is correct, then the *cj1660-5* gene cluster may function to assist iron uptake in *C. jejuni* independently of the Ftr1-P19 components by increasing ferrous iron availability for iron uptake by FeoAB, and Ftr1-P19 would be expected to function in ferrous iron uptake independently of the *cj1660-5* cluster. This possibility will be tested in the work presented in subsequent chapters.

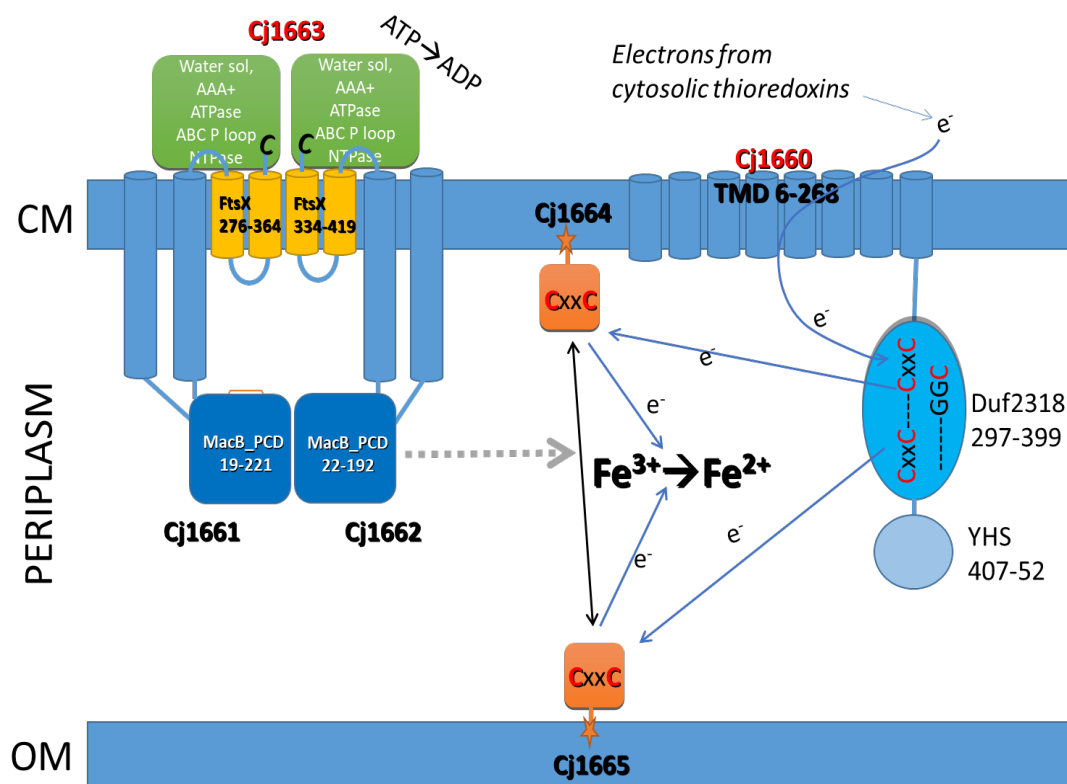


Figure 3.27: Model indicating the potential functions of the Cj1600-5 proteins in assisting Ftr1-P19-mediated iron uptake in *C. jejuni*. In the model, the Cj1661-3 complex mediates relocation of the thioredoxins between membranes, possibly with assistance of LolA (not shown), in an ATP-requiring process. Cj1660 is shown as acting as a conduit for electron delivery to the thioredoxins from cytosolic thioredoxins. The reduced thioredoxins may then function to reduce extracellular ferric iron, making it available for uptake via Ftr1-P19. An alternative possibility is that the thioredoxin/Cj1660 system mediates disposal of electrons released from the oxidation of ferric to ferrous iron during Ftr1-P19 iron uptake (not shown).

Chapter 4: Phenotypic studies of iron-transporter-deficient *E. coli* complemented with the FetMP-FetABCDEF iron transporter from *C. jejuni* NCTC 11168

4.1. Introduction

p19 (fetP) is thought to encode a periplasmic iron-binding protein, with the upstream *cj1658 (fetM)* gene specifying an integral membrane-protein likely acting as a ferric permease that is similar to Frt1p of yeast, FtrC of *Bordetella* and EfeU of *E. coli* (Severance *et al.*, 2004; Brickman and Armstrong, 2012; Große *et al.*, 2006). The well-conserved downstream genes (*cj1660-cj1665*) encode proteins forming a predicted TEP-independent ABC-dependent mechanotransducer system (Cj1661-3, FetBCD) and an apparent extracytoplasmic thiol-dependent redox system (Cj1660 and Cj1664-5, FetAEF; Chapter 3). The *fet* locus is ~8 kb and appears organised as two operons (*fetMP* and *fetA-F*) with an 82 bp as intergenic region separating them (Chapter 3). The function of the 5400 bp *fetA-F* genes had not been determined at the point when this PhD project initiated; although *fetEF* mutants had been generated by Liu and Kelly (2015). The research described in this chapter was conducted in order to understand the precise function of the *fetMP-fetABCDEF* gene cluster in *C. jejuni*. The role of the latter six genes was of particular interest since bioinformatic investigation showed that the eight gene cluster is highly conserved in *Campylobacter* spp. and is also well conserved in other bacterial taxa such as *Yersinia* and *Bifidobacterium* spp. (Chapter 3), although the purpose of the six distal genes was unclear. Bioinformatic analysis enabled a working hypothesis to be generated that described a potential role of FetA-F in extracytoplasmic ferric oxidation or reduction, indicating that these proteins may assist FetMP-mediated ferrous iron uptake.

In this chapter, complementation of an iron-transport mutant of *E. coli* (strain JC32) was achieved using only the *fetMP* or *fetA-F* genes, or a combination of both sets of genes. The *fetMP* and *fetA-F* loci were cloned from *C. jejuni* NCTC 11168 into two distinct, but compatible, inducible plasmids, pBADrha and pBADara. This allowed the combination of both *fetMP* and *fetA-F* in JC32, in two different formats. Initially, PCR was performed with primers designed to generate three adjacent fragments that could be fused together as one fragment allowing expression of all genes from an upstream *Para* or *Prha* promoter. However, no PCR products were obtained (data not reported in this thesis). The primers were therefore redesigned to increase their T_m values which enabled PCR products to be obtained. However, the cloning attempt using the In-Fusion method was unsuccessful (data not reported in this thesis). Finally, primers were designed to allow amplification of the cluster in just two fragments corresponding to *fetMP* and *fetABCDEF*, for independent cloning into the inducible vectors. This strategy was successful, giving four new plasmids for use in functional studies: pBADara-*fetMP*; pBADara-*fetABCDEF*; pBADrha-*fetMP*; and pBADrha-*fetABCDEF* (reported below). In order to determine the effect of these genes on growth under iron restriction, they were used to transform *E. coli* JC32 to give single and double transformants. The results are described below.

4.2. Generation of plasmids carrying iron transport genes from *C. jejuni*

To generate plasmids bearing the genes of interest under control of an inducible promoter, amplification of the *fetM-P* and *fetA-F* genes from the genomic DNA of *C. jejuni* NCTC 11168 strain was performed by PCR. To enable controlled induction of *fetM-P* and *fetA-F*, the genes were cloned into pBADrha and pBADara, such that expression would depend on the vector-borne ribosome-binding sites and promoters. This was achieved by PCR amplification of the two fragments from *C. jejuni* NCTC 11168 genomic DNA using HiFi[®] DNA polymerase and primers pBADrha-*fetMP* (F and R) and pBADara-*fetMP* (F and R), and

pBADrha-*fetA-F* (F and R) and pBADara-*fetA-F* (F and R) (Table 2.4) to give a 2700 bp *fetMP* fragment and a 5400 bp *fetA-F* fragment (Methods 2.11.2; Fig. 4.1-4.3).

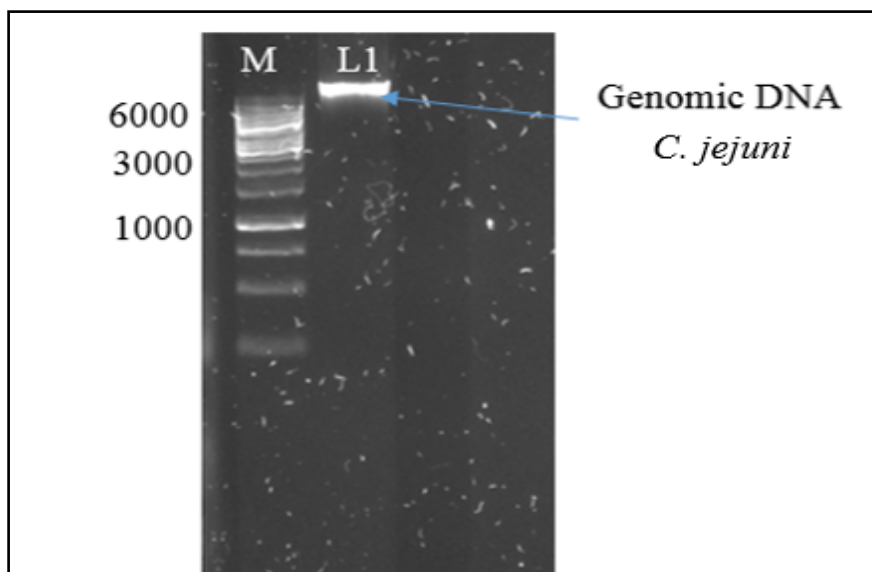


Figure 4.1. Agarose gel (0.7%) electrophoretic analysis of genomic DNA from *C. jejuni* NCTC 11168. Lane 1, genomic DNA. M, 1 kb ladder (Fermentas). Loadings were 1 μ l for ladder and 2 μ l for DNA sample.

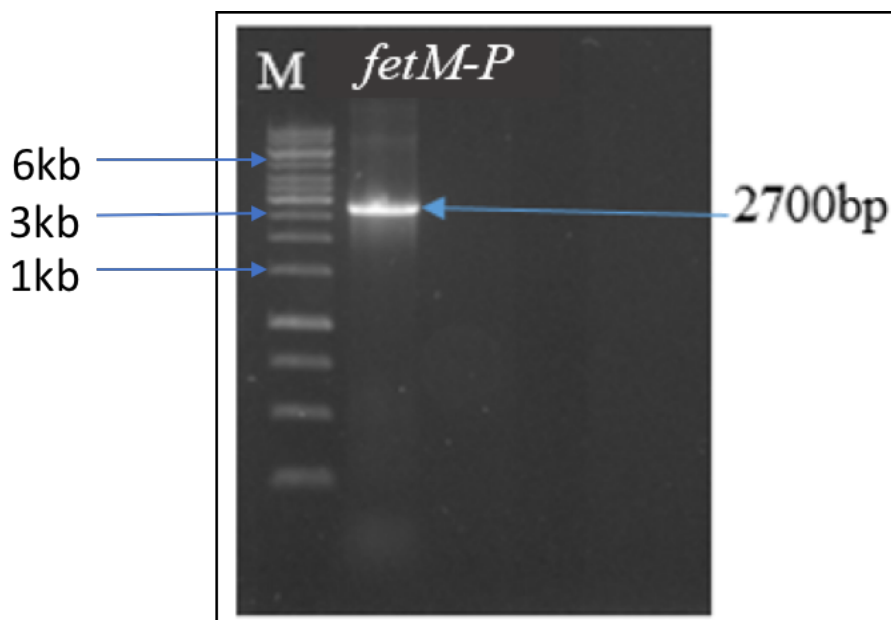


Figure 4.2. Gel electrophoretic analysis of the *fetMP* PCR product. Electrophoresis was performed using a 0.7% agarose TBE gel. Lane M, the GeneRuler 1 kb ladder (Fermentas).

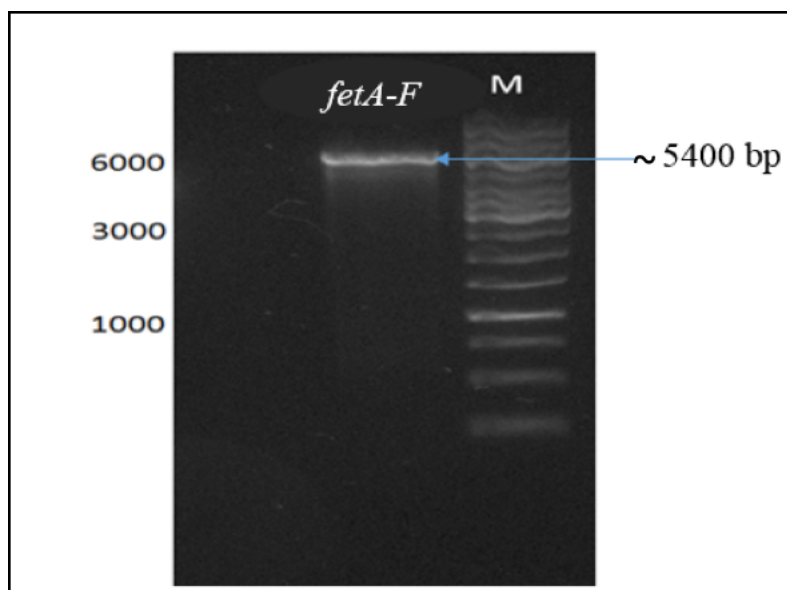


Figure 4.3. Gel electrophoretic analysis of the *fetA-F* PCR product. Electrophoresis was performed using a 0.7% agarose TBE gel. Lane M, the GeneRuler 1 kb ladder (Fermentas).

To generate inducible constructs for testing the roles of *fetMP* and *fetA-F* in *E. coli*, the PCR fragments were to be cloned into the pBADrha vector under control of the rhamnose-inducible *rhaB* promoter, using the *NdeI* and *BamHI* cloning sites in the vector and Gibson cloning methodology (Gibson *et al.*, 2009) using the In-Fusion kit (ClonTech), according to the manufacturer's instructions (Methods 2.11.7). pBADrha plasmid DNA was used to transform *E. coli* TOP10 generating Cm^R transformants that were subjected to plasmid DNA isolation (Methods 2.11.4). The isolated pBADrha plasmid DNA was then treated by double digestion with the restriction enzymes, *NdeI* and *BamHI*, and electrophoretic analysis of the digested DNA indicated the presence of plasmid DNA corresponding to the expected mobility for the uncut and cut plasmid (~4 and 6.1 kb, respectively; Fig. 4.4).

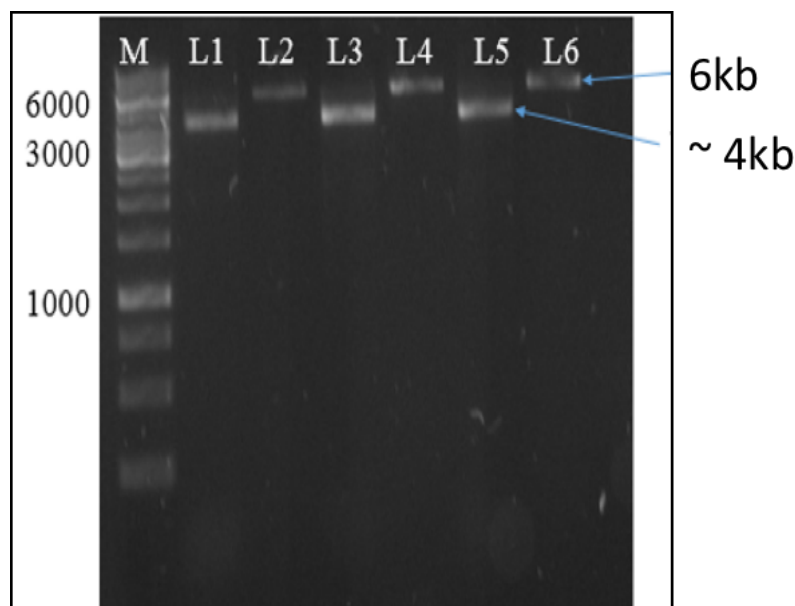


Figure 4.4. Gel electrophoretic analysis of digested and undigested pBADrha. Electrophoresis was performed using a 0.7% agarose TBE gel. Lane 1, 3, and 5 undigested plasmid DNA (#1-3, respectively), while lane 2, 4, and 6 were digested with *Nde*I and *Bam*HI (#1-3, respectively). Lane M, the GeneRuler 1 kb ladder (Fermentas). Three distinct plasmid preparations (#1-3) were analysed.

To allow co-expression of *fetMP* and *fetA-F*, the two fragments were to be cloned into pBADara (as well as pBADrha). Thus, *fetMP* and *fetA-F* were also cloned into pBADara (Table 2.4) under control of the arabinose-induced *ara* promoter, using *Nco*I and *Hind*III cloning sites in the vector and Gibson cloning methodology (Gibson *et al.*, 2009), as indicated above. pBADara DNA was obtained from laboratory stocks. pBADara transformants were then obtained and plasmid DNA was isolated and analysed, as above. Electrophoretic analysis indicated the presence of plasmid DNA of the expected mobility (~3 kb for the uncut plasmid and 4.1 kb for the linearized vector; Figs. 4.5 and 4.6).

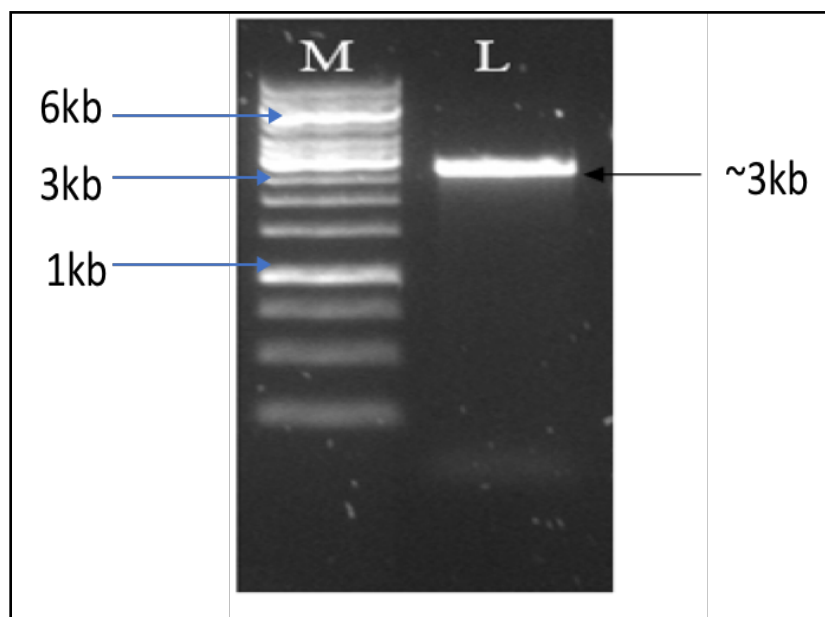


Figure 4.5. Gel electrophoretic analysis of undigested pBADara. Electrophoresis was performed using a 0.7% agarose TBE gel.

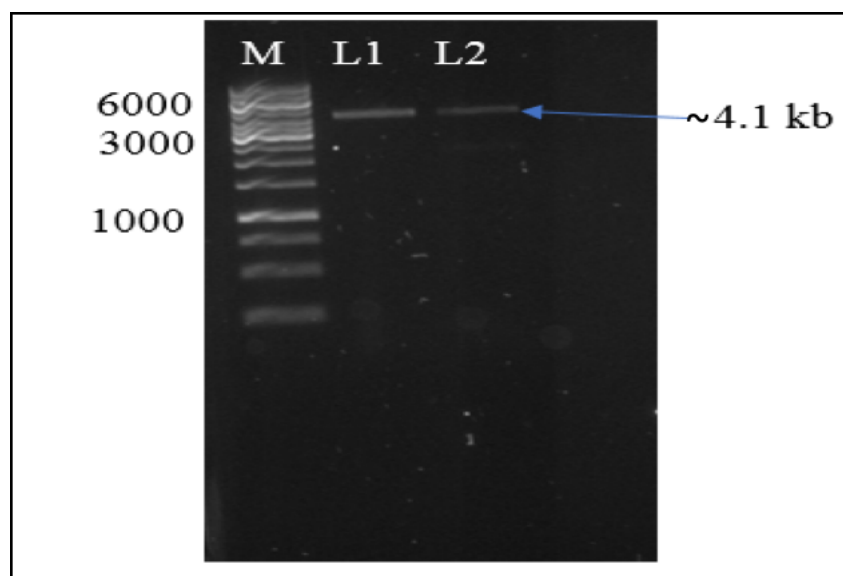


Figure 4.6. Gel electrophoretic analysis of digested pBADara. Electrophoresis was performed using a 0.7% agarose TBE gel. The plasmid digested by *Nco*I and *Hind*III enzymes. Lane M, the GeneRuler 1 kb ladder (Fermentas).

The pBADrha and pBADara double-digested plasmids were purified by gel extraction for use in the cloning (Methods 2.11.5). The In-Fusion Cloning Kit (Clontech) was then used for cloning of the PCR products of *fetMP* and *fetA-F* into pBADrha, individually. The In-Fusion

reactions (PCR products with digested pBADrha) were transformed into chemically competent Stellar competent cells (Clontech). Six colonies for each cloning were selected for plasmid ‘miniprep’ isolation for each of the cloning reactions.

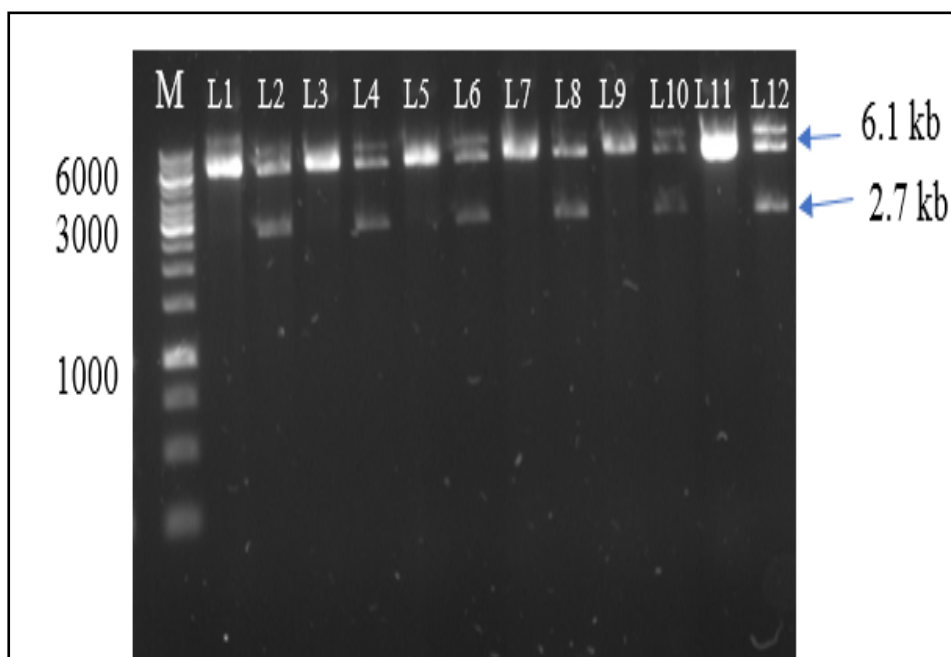


Fig 4.7. Gel electrophoretic analysis of cut and uncut pBADrha plasmid DNA potentially carrying *ftr1-p19* (*fetMP*). Electrophoresis was performed using a 0.7% agarose gel. Potential pBADrha-*fetMP* constructs (#1-6) were loaded in lanes 1, 3, 5, 7, 9 and 11 and after cutting (*NdeI* and *BamHI*) in lanes 2, 4, 6, 8, 10 and 12; the GeneRuler 1 kb ladder was loaded in lane M. (results were similar for all).

The potential pBADrha-*fetMP* plasmid samples were digested by *NdeI* and *BamHI* to release any *fetMP* fragment from the vector and to allow estimation of the size of the recombinant plasmid DNA. The digested samples were expected to give two bands of 6101 bp (pBADrha) and ~2700 bp (the insert), as was observed, supporting the success of the cloning (Fig. 4.7). A higher mass band of ~9 kb was also observed upon digestion which is presumed to correspond to the single cut linearized plasmid.

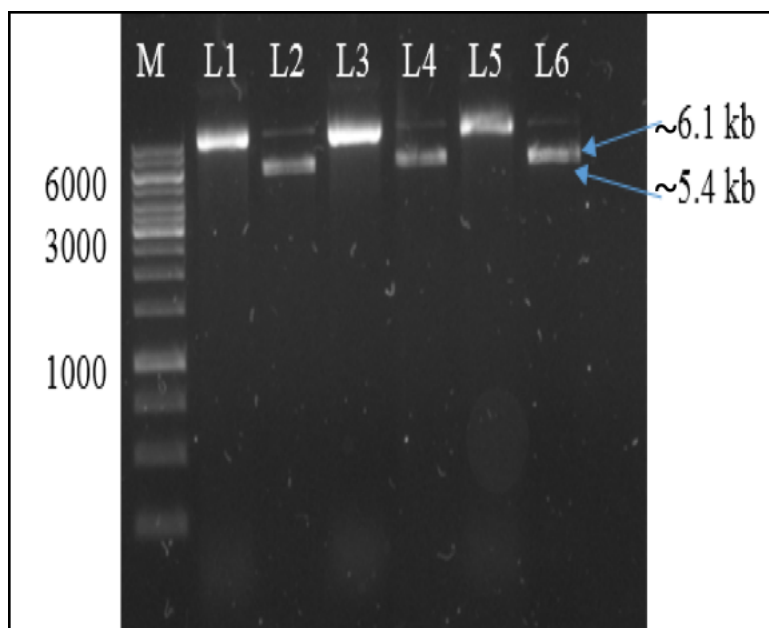


Fig 4.8. Gel electrophoretic analysis of cut and uncut pBADrha plasmid DNA potentially carrying *fetA-F*. Electrophoresis was performed using a 0.7% agarose gel. Potential pBADrha with *fetA-F* constructs (#1-3 shown) were loaded in lanes 1, 3, and 5, and after cutting (*NdeI* and *BamHI*), into lanes 2, 4, 6; the GeneRuler 1 kb ladder was loaded in lane M. Similar results were obtained for all isolates.

Digestion of putative *fetA-F* clones using *NdeI* and *BamHI* also gave the expected fragment sizes of 6101 bp for the pBADrha vector and ~5400 bp for the *fetA-F* insert (very close bands) (Fig. 4.8), suggesting that the cloning had been successful. Two plasmids of each type were selected for analysis by nucleotide sequencing using primers pBADrha-*fetMP* Forward and Reverse (Table 2.8). The sequences obtained were compared with the nucleotide collection (Appendix 11) sequence database using BLAST. The results indicated that the inserts have the expected sequence at their flanks with no errors or gaps, indicating that the cloning was successful.

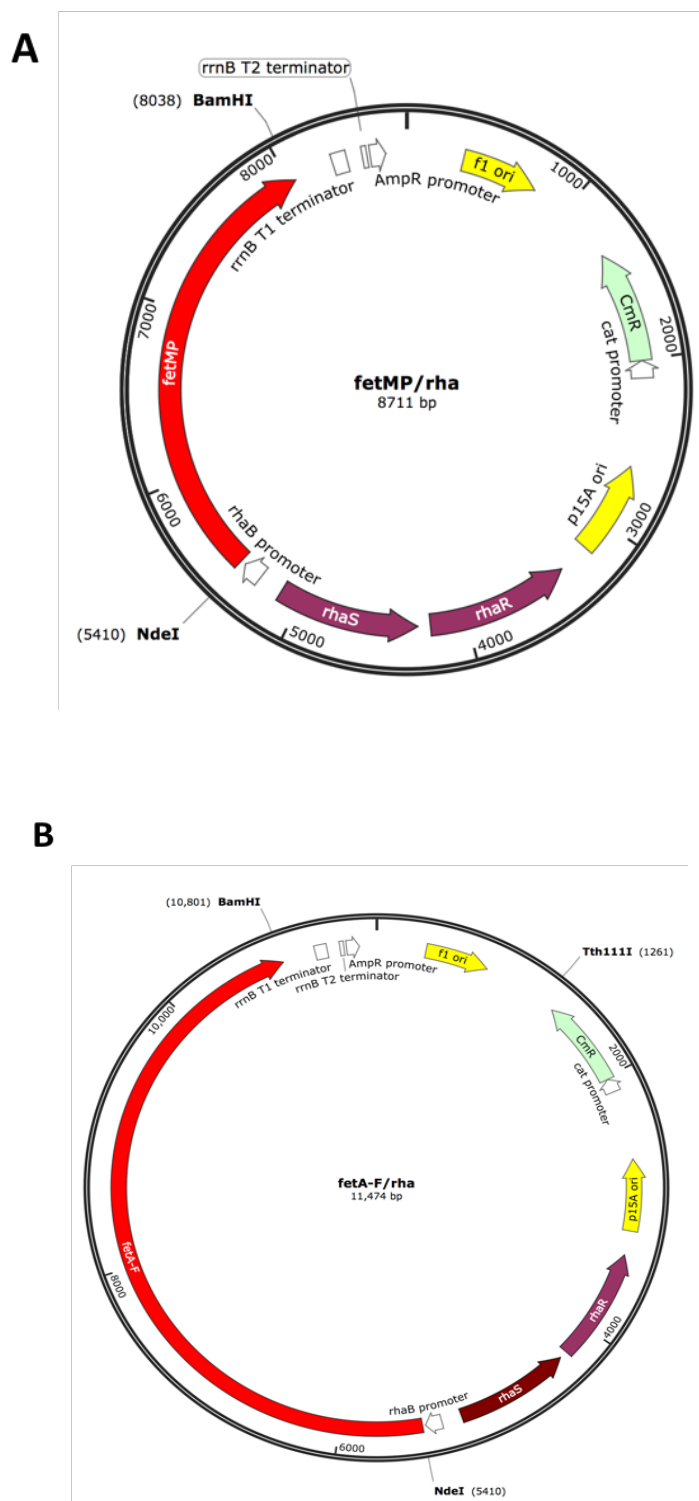


Figure 4.9. Restriction map of **A:** pBADrha-*fetMP* and **B:** pBADrha-*fetA-F*. The plasmids contain *fetMP* or *fetA-F* cloned into the *NdeI* and *BamHI* sites of pBAD_{rha}. The origin (p15Aori), Cm^R locus, and the *rhaS* and *rhaR* genes (Egan and Schleif, 1993) are shown.

The double digested pBADara vector was also used to clone the *fetMP* and *fetA-F* PCR fragments. The In-Fusion kit was also used for cloning of the PCR products into pBADara, as described above. Three resulting transformant colonies for each cloning reaction were subject to plasmid ‘miniprep’ isolation. These plasmids were analysed by gel electrophoresis which showed that all contained DNA fragments of the expected size (Fig. 4.10 and 4.11).

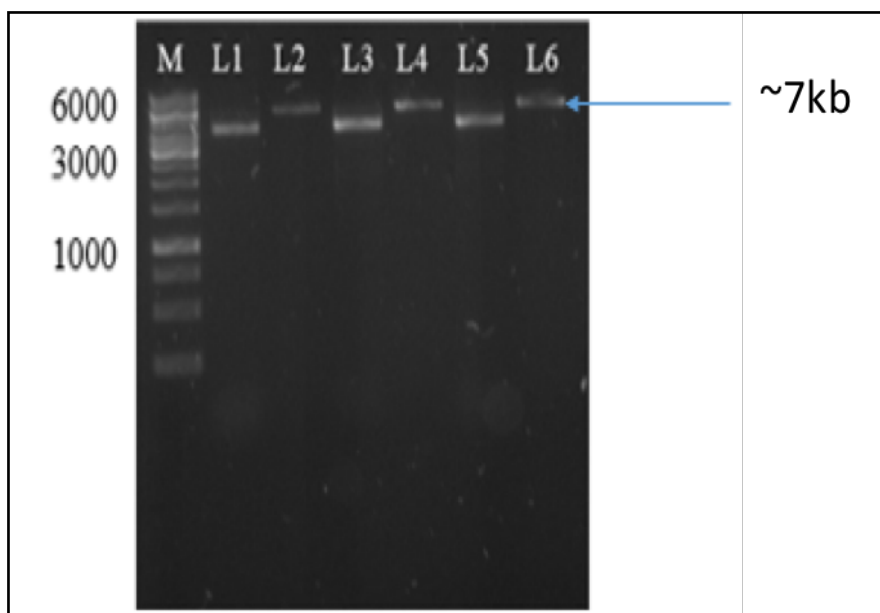


Figure 4.10. Gel electrophoretic analysis of cut and uncut pBADara plasmid DNA potentially carrying *fetMP*. Electrophoresis was performed using a 0.7% agarose gel. Three potential pBADara-*fetMP* constructs were loaded in lanes 1, 3 and 5 and after cutting (with *NcoI*) lanes 2, 4 and 6 (for isolates #1-3, respectively); the GeneRuler 1 kb ladder was loaded in lane M. Results were similar for all isolates.

The *fetMP*-containing plasmids were digested with *NcoI* only, because there are many *HindIII* sites in the *fetMP* fragment. The putative *fetMP* plasmids gave the expected size for the vector-insert combination (4 plus 2.7 kb, giving 6.7 kb) upon linearization with *NcoI*, and a mobility at ~4 kb for the uncut plasmid.

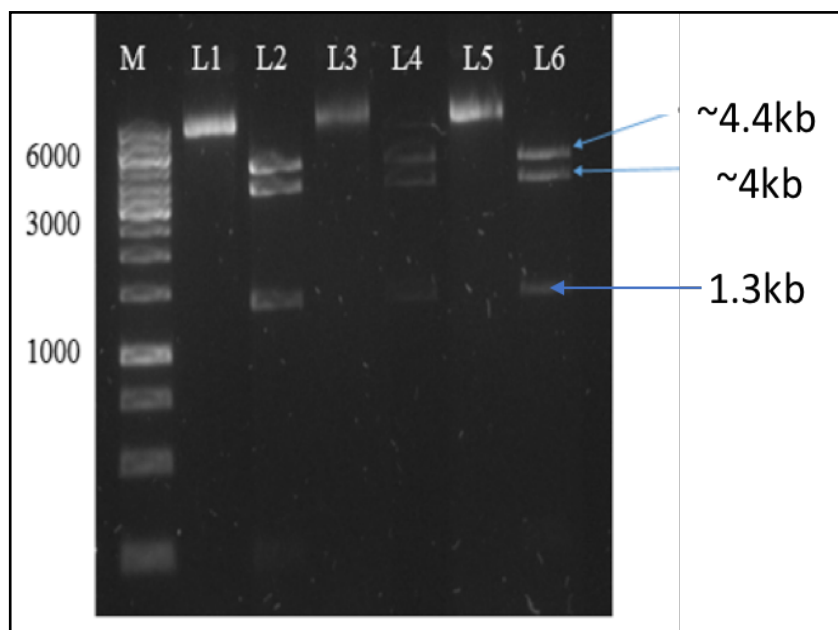


Figure 4.11. Gel electrophoretic analysis of uncut and cut pBADara plasmid DNA potentially carrying *fetA-F*. Electrophoresis was performed using a 0.7% agarose gel. Potential pBADara with *fetA-F* constructs were loaded in lanes 1, 3 and 5 and after cutting (*NcoI* and *HindIII*) lanes 2, 4 and 6 (for isolates #1-3, respectively); the GeneRuler 1 kb ladder was loaded in lane M.

The putative pBADara-*fetA-F* plasmids were digested with *NcoI* and *HindIII*, and the resulting bands were as expected (~4 kb for the plasmid, ~4.4 and 1.3 kb for the insert resulting from the presence of a *NcoI* inside the insert). Two of each of the obtained plasmids were subject to nucleotide sequence analysis (as above) and the resulting sequences were compared with the sequence database using BLAST. The results indicate that the inserts have the expected sequence at their flanks, with no errors or gaps, confirming the identity of the plasmids. The complete sequence of the insert was subsequently obtained and found to match that expected (see Appendix 11).

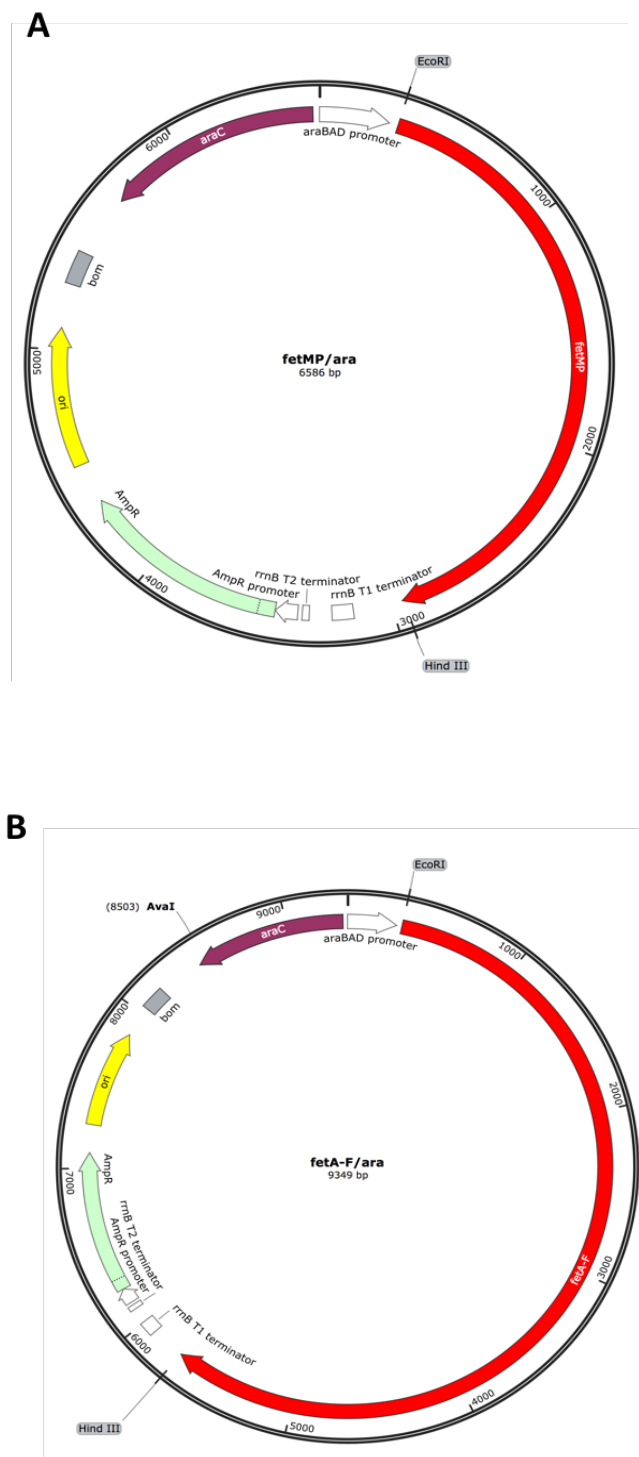


Figure 4.12. Restriction map of **A:** pBADara-*fetMP* and **B:** pBADara-*fetA-F*. The plasmid contains *fetMP* or *fetA-F* cloned into *EcoRI* and *HindIII* sites of pBADara.

4.3. Complementation of iron-uptake mutant *E. coli* JC32 by *fetMP* and *fetA-F* from *C. jejuni* on solid media

4.3.1. Complementation of iron-uptake mutant, *E. coli* JC32, with *fetMP*

E. coli JC32 contains six mutations that eliminate known pathways for iron uptake in un-supplemented minimal medium (Table 2.2). This strain can thus be used to test the ability of the *fet* genes to support iron-restricted growth by provision of enhanced iron-uptake capacity. The complemented strain (*E. coli* JC32 with pBADara-*fetMP*) was tested by growth under three conditions; M9 with 20 μ M ferric citrate, and M9 with 1 and 4 μ M DTPA (ferric iron chelator); antibiotic and the inducer (0.02% w/v arabinose) were included in all cases. Overnight cultures (M9 medium with ferric citrate and 0.02% w/v inducer; Brook and Wu, 2013) were obtained at 37 °C and 250 rpm, and these were harvested by centrifugation and washed in pure M9 before being used to generate fivefold serial dilutions from a starting culture at 0.5 OD₆₀₀ nm. The diluted and washed overnight cultures were then applied to agar plates (containing the medium indicated above) in 5 μ l volumes and plates were incubated for 20 h in 37 °C (Methods 2.17.1). The wild type parent strain was included (W3110) for comparison; this strain gave better growth than JC32 (carrying the vector only) and the pBADara-*fetMP* complemented JC32 strain, particularly when chelator was included at 4 μ M (Fig. 4.13-15). The key comparison here is between the vector control and the *fetMP*-complemented mutant to determine whether *fetMP* has any effect on the growth of the mutant under low iron conditions. The serial dilutions suggest that JC32 growth is slightly diminished by *fetMP* complementation (with respect to the vector control) in both the presence and absence of chelator which indicates that *fetMP* does not assist growth in presence of ferric iron or with the iron chelator in solid medium but may actually provide a slight growth inhibition. This result therefore suggests that *fetMP* does not function to enhance the iron-restricted growth of the JC32 strain in minimal-medium agar plates. The

growth difference between the wildtype and JC32 was relatively modest with added iron (<fivefold) but was much greater (>500 fold) under low iron availability with 4 μM DTPA, which supports the lack of iron transport capacity for JC32.

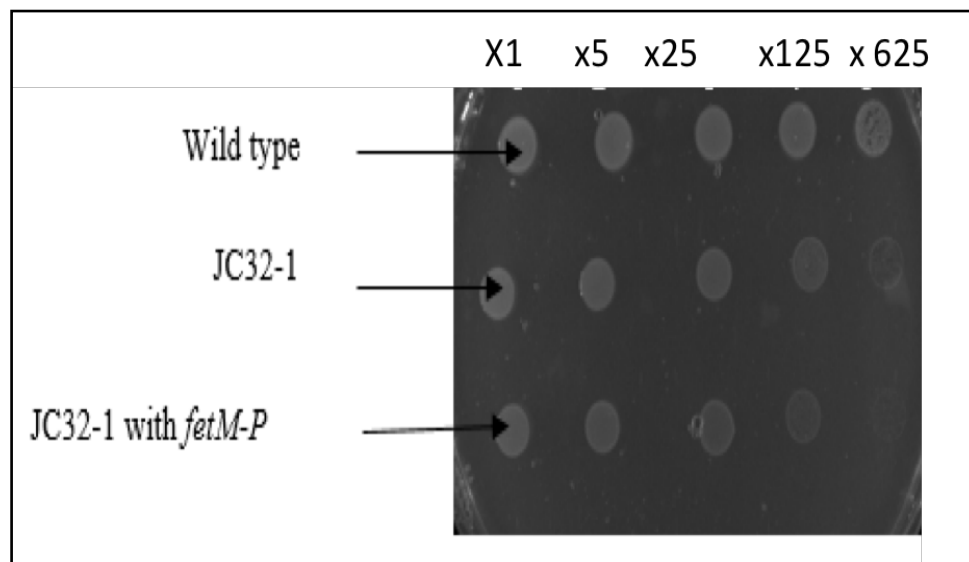


Figure 4.13. Growth of *fetMP*-complemented *E. coli* JC32 on M9 agar plates under high-iron conditions. Growth of washed overnight cultures (5 μl volumes) on 0.4% glucose in M9 salts agar at 37 $^{\circ}\text{C}$, overnight. Cultures were serially diluted: x1, x5, x25, x125 and x625 (1-5). Strains used are as indicated transformed either with the vector (pBADara) or pBADara-*fetMP*. The medium contained 20 μM ferric sulphate, 0.02% arabinose and ampicillin (100 $\mu\text{g}/\text{ml}$). All plate growth tests were performed twice or three times, and representative results are shown.

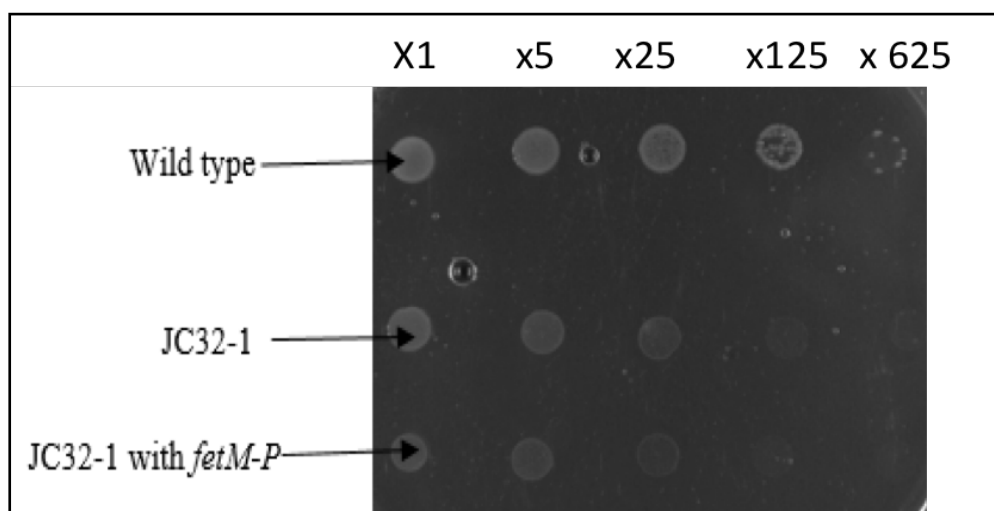


Figure 4.14. Growth of *fetMP*-complemented *E. coli* JC32 on M9 agar plates under low iron conditions (1 μM DTPA). Details are as for Fig. 4.13, except for the use of 1 μM DTPA in place of ferric sulphate.

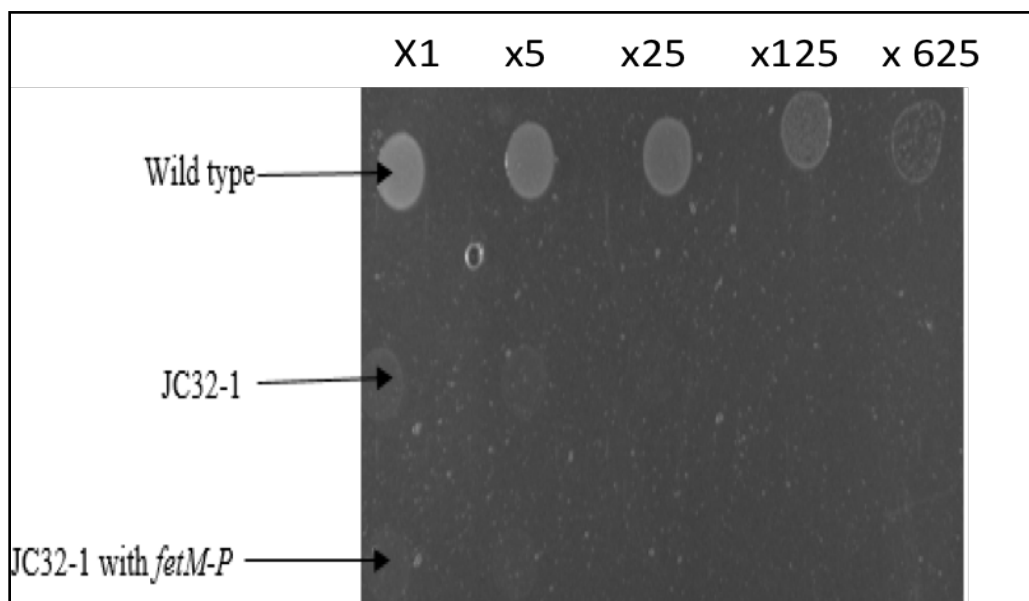


Figure 4.15. Growth of *fetMP*-complemented *E. coli* JC32 on M9 agar plates under low iron conditions (4 μ M DTPA). Details are as for Fig. 4.13, except for the use of 4 μ M DTPA in place of ferric sulphate.

4.3.2. Complementation of iron-uptake mutant *E. coli* JC32 by *fetA-F*

E. coli JC32 carrying pBADara-*fetA-F* was also tested under the three different conditions, as employed above. The results revealed that the JC32 transformants grow less well than the wildtype, particularly under low iron (as above, and as expected). The presence of the *fetA-F* system resulted in diminished growth with respect to the vector control, under both high iron (Fig. 4.16) and under low iron with 1 μ M DTPA (Fig. 4.17). Growth of the JC32 transformants was similarly weak with 4 μ M DTPA (Fig. 4.18). The results thus indicate that the *fetA-F* system does not support low-iron growth in JC32, under the conditions employed here, but instead reduces growth in a manner that appears independent of iron regime. These findings are thus similar to those obtained for *fetMP*, above

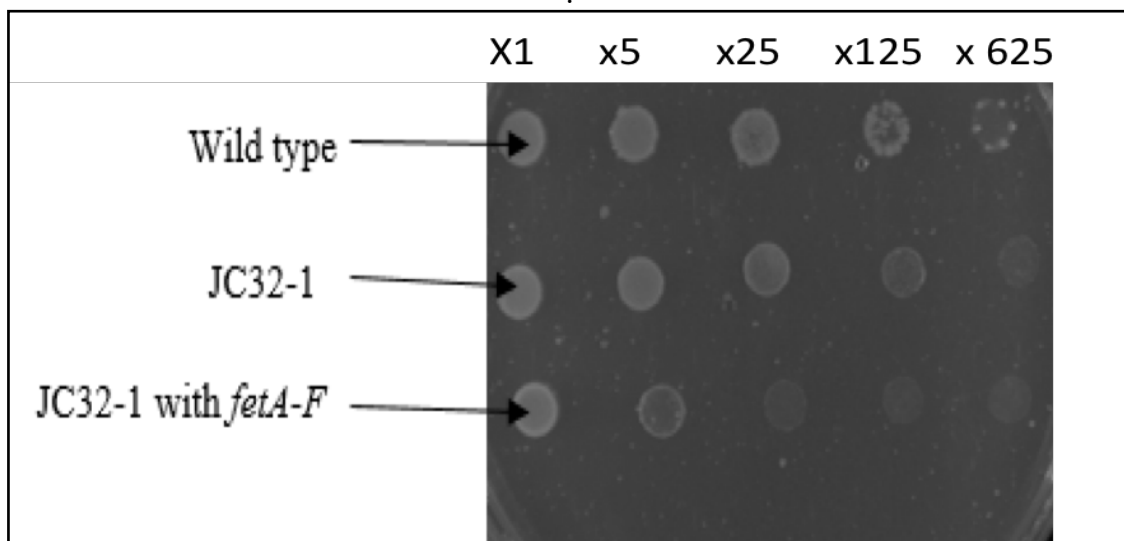


Figure 4.16. Growth of *fetA-F*-complemented *E. coli* JC32 on M9 agar plates under high iron conditions. Details are as for Fig. 4.13, except for the use of pBADara-*fetMP* in place of pBADara-*fetMP*.

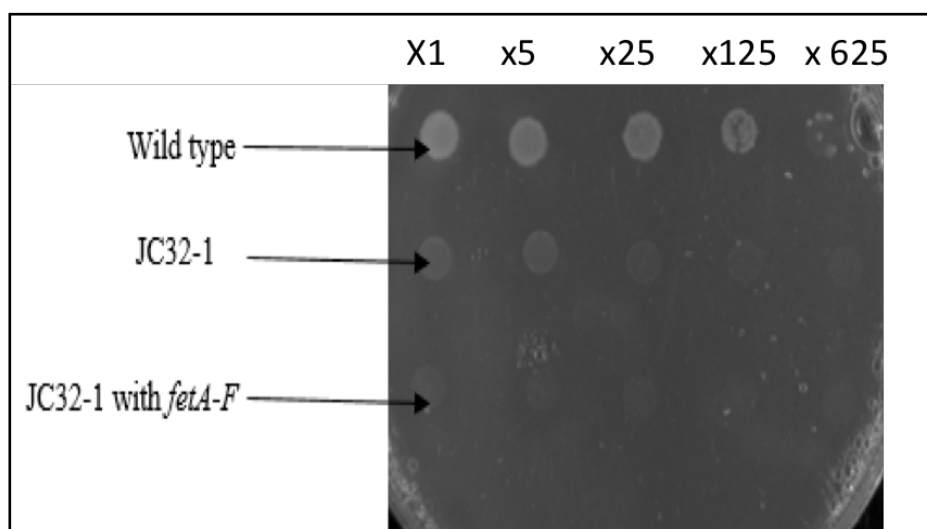


Figure 4.17. Growth of *fetA-F*-complemented *E. coli* JC32 on M9 agar plates under low iron conditions. Details are as for Fig. 4.14, except for the use of 1 μ M DTPA in place of ferric sulphate.

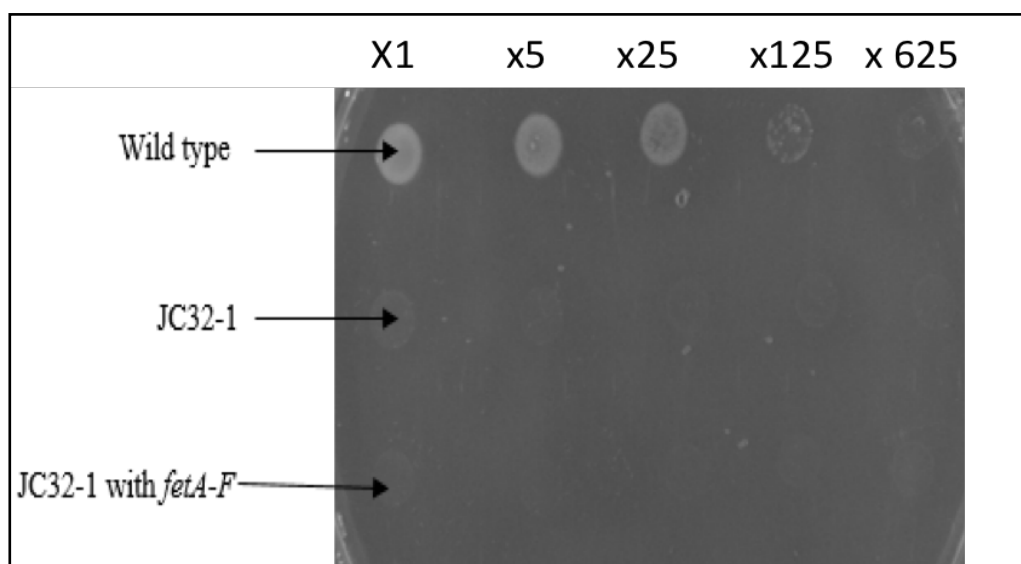


Figure 4.18. Growth of *fetABCDEF*-complemented *E. coli* JC32 on M9 agar plates under low iron conditions. Details are as for Fig. 4.14, except for the use of 4 μ M DTPA in place of ferric sulphate.

4.3.3. Complementation of iron-uptake mutant *E. coli* JC32 by both *fetMP* and *fetA-F*

The above results suggest that neither *fetMP* nor *fetA-F* can support iron-restricted growth of *E. coli* JC32, when expressed from pBADara, in M9 solid medium. Since these two loci exhibit a conserved genetic context indicative of a cooperative function, it was considered possible that the absence of any complementation effect could be due to the need to co-express the two clusters. Thus, JC32 was co-transformed with pBADrha-*fetMP* and pBADara-*fetA-F* (and corresponding vector controls were also generated) and growth comparisons were made as above. Comparing the growth zones of the wild type (transformed with both empty vectors) and the mutant (transformed with both vectors or with the *fetMP* and *fetA-F* plasmids) showed that the presence of both *fetMP* and *fetA-F* caused marked inhibition of growth for JC32 in iron-rich conditions (Fig. 4.19) but had relatively little effect under iron-restricted conditions with 1 μ M DTPA (Fig. 4.20); with 4 μ M DTPA no growth was seen for the JC32 transformants (data not shown).

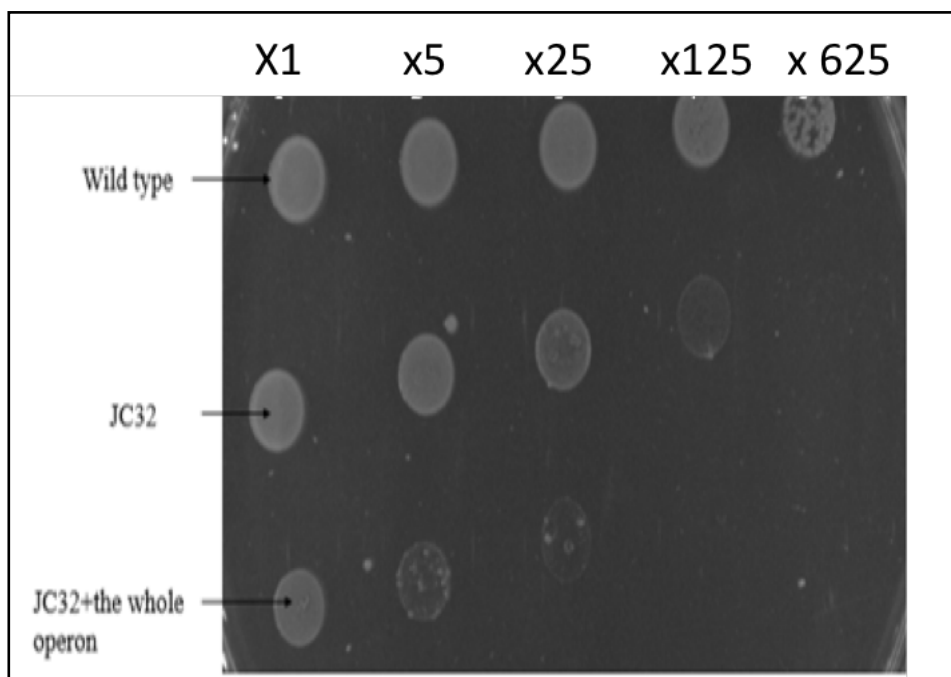


Figure 4.19. Growth of *fetMP/fetABCDE* complemented *E. coli* JC32 on M9 agar plates under high-iron conditions. Details are as for Fig. 4.11, except for the use of strains co-transformed with both pBADrha-*fetMP* and pBADara-*fetA-F* or with both pBADrha and pBADara, and the inclusion of both chloramphenicol (50 $\mu\text{g/ml}$) and ampicillin (100 $\mu\text{g/ml}$), as well as rhamnose (0.02% w/v) and arabinose (0.02% w/v). ‘Wild type’, W3110 with both pBADara and pBADrha; ‘JC32’, JC32 with both pBADara and pBADrha; and JC32+*fetMP/fetA-F*’, JC32 complemented with pBADrha-*fetMP* and pBADara-*fetA-F*

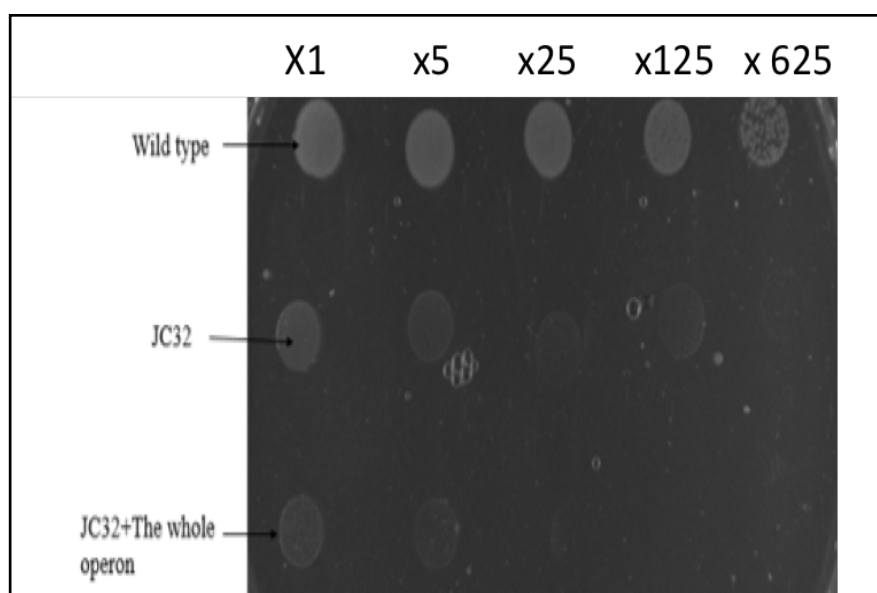


Figure 4.20. Growth of *fetMP/fetA-F* complemented *E. coli* JC32 on M9 agar plates under low iron (1 μM DTPA) conditions. Details are as for Fig. 4.19 except for the use of 1 μM DTPA in place of ferric sulphate.

From these results, it can be concluded that the combined *fetMP-fetABCDEF* system does not support iron restricted growth of JC32 under the conditions employed, although does appear to inhibit growth under iron sufficient (20 μ M ferric sulphate) as well as deficient (1 μ M DTPA) conditions. Thus, the data so far obtained suggests that neither *fetMP* nor *fetA-F*, either alone or in combination, can act to drive iron uptake sufficiently to support growth of an iron-uptake impaired *E. coli* strain when the genes are provided in the format utilised above. Note that all experiments above were performed both with and without inducer (rhamnose) in duplicate (or triplicate), and the presence/absence of inducer did not affect the results obtained (results not shown).

4.4. Complementation of iron-uptake mutant phenotype *E. coli* JC32 by *fetMP* and *fetA-F* from *C. jejuni* in liquid medium

4.4.1. *fetMP* enhances low-iron growth under acidic pH

Koch *et al.* (2011) reported that for the *fetMP* system of the uropathogenic *E. coli* (strain F11) (closely homologous to the equivalent system in *C. jejuni*), the low-iron-enhanced growth effect was much affected by pH. It was shown that in an *E. coli* K-12 strain lacking iron-uptake systems, expression of the *fetMP* system of *E. coli* F11 greatly enhances growth in the absence of iron at pH 5 but had only a modest effect at pH 7. A strong effect was also seen at pH 9. These results suggest that the iron-uptake activity of the FetMP-FetABCDEF system of *C. jejuni* might also have specific pH requirements.

Also, Brickman and Armstrong (2012) showed that the *ftrABCD* promoter of *Bordetella* exhibits maximum activity under low-iron levels when conditions are acidic (this system encodes a FetM and FetP homologue) and that the iron uptake activity driven by this system is strongest under low pH conditions. This provides further evidence of a pH dependence for

FetMP-related iron transporters. The low-iron growth advantage provided by EfeUOB of *E. coli* was also enhanced by low pH (Cao *et al.*, 2007).

To test any role of pH on the ability of the *C. jejuni fetMP* system to support low iron growth, growth experiments were performed in buffered liquid minimal medium; M9 buffered with 25 mM of MES-Tris buffer at a range of pH values (5, 7 and 9). The overnight cultures were prepared in 5 ml of M9 minimal media with 20 μ M ferric citrate at 37 °C and 250 rpm. Cell pellets were washed with fresh M9 medium and then resuspended for use to inoculate cultures to give a starting OD of 0.01 (Methods 2.17.2). The growth curves were generated in 250 μ l of culture in 100-well honeycomb microplate in a Bioscreen C over a 24 h period, with constant shaking at 37 °C. Inducer (rhamnose and/or arabinose) and antibiotics (ampicillin and/or chloramphenicol) were added to the overnight precultures and post cultures in the microplates. The results showed that the *fetMP* genes enhances the growth of *E. coli* JC32 under acidic condition (pH 5), but not at pH 7 nor 9. The enhanced growth effect was seen in both the presence and absence of additional iron in the medium, but effect was much greater in iron-restricted conditions than in iron rich conditions (~two fold increase in OD from 0.08 to 0.17 at 19 h; c.f. ~5% increase with iron; $P < 0.01$), which supports a role of the *fetMP* genes in iron transport during iron deficiency at low pH (Fig. 4.21). At total increase in growth of up to 0.01 OD units was observed for the non-complemented JC32 at pH 5 and low iron (20 h), whereas the complemented strain showed a tenfold greater increase in growth (0.1 OD units) under the same conditions. The enhanced growth caused by *fetMP* did not require inducer which indicates that the *Prha* promoter allows *fetMP* expression even in the absence of inducer and presence of glucose (which is a surprise), $P < 0.01$.

Iron caused an increase in growth for the JC32 transformants, as expected, at all pH levels tested. However, this was not the case for the wildtype where iron caused a modest reduction in growth at pH 5, although at pH 7 and 9, iron stimulated growth as expected (Fig. 4.21).

This result suggests that iron may be somewhat toxic for the wildtype at pH 5 (presumably due to its high iron uptake capacity and the high solubility of iron at acid pH). JC32 showed a lower growth than the wildtype in the absence of iron under all conditions, confirming its iron-restriction phenotype.

The experiment above was repeated using the pBADara constructs at pH 5 and very similar results were obtained (Fig. 4.22), which thus supports the results in Fig. 4.21 showing that *fetMP* enhances growth of JC32 under low iron, low pH conditions.

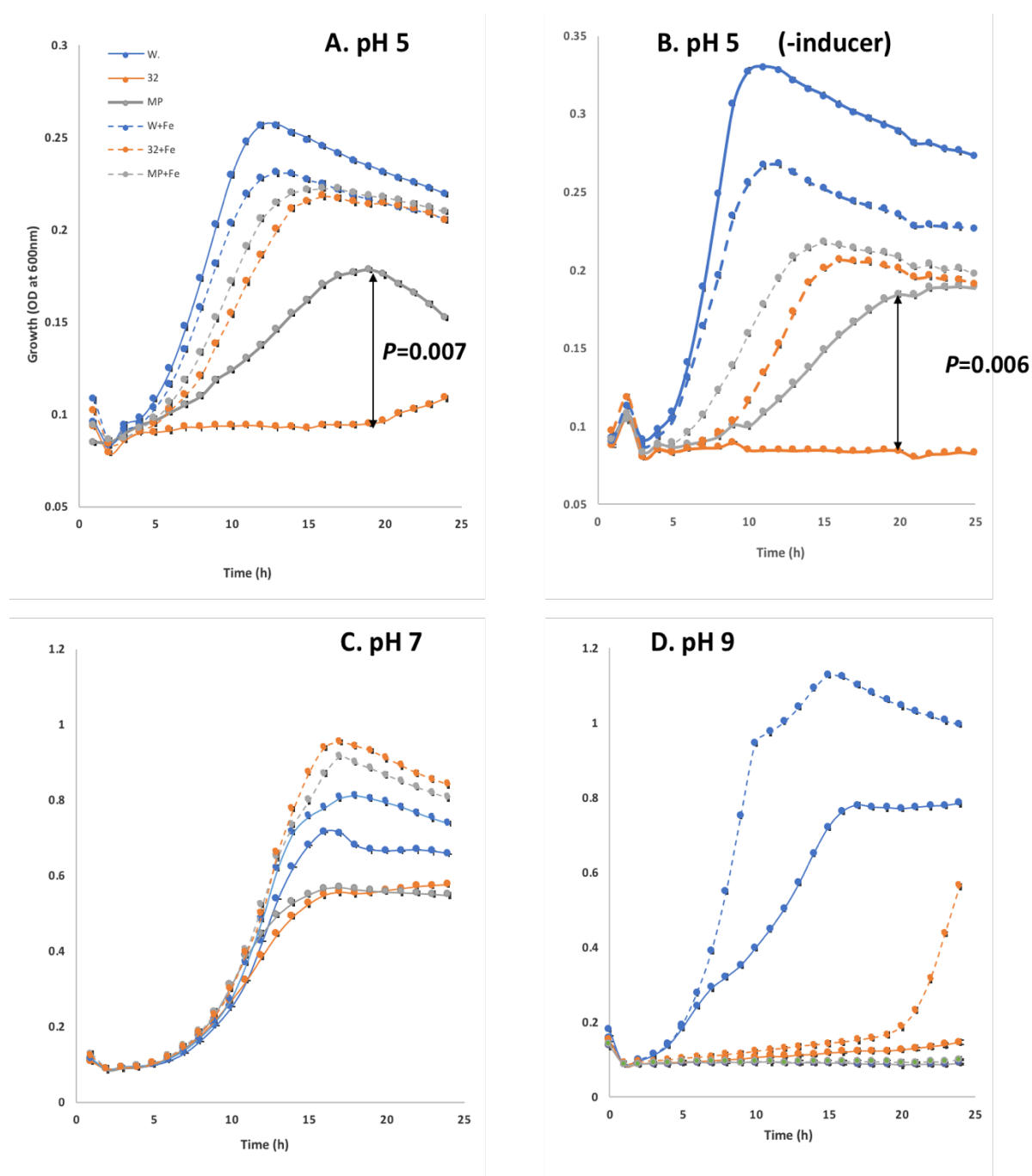


Figure 4.21. Effect of *fetMP* on growth of JC32 under iron restriction at pH 5-9. Growths were performed in a Bioscreen C apparatus (constant shaking, 37 °C) in triplicate. Strains were: W (the wildtype *E. coli* W3110 with pBADrha), JC32 (the mutant strain, with pBADrha), 32+F1 (the mutant strain complemented with pBADrha-*fetMP*). ‘+Fe’ indicates the presence of 20 μM ferric sulphate. The precultures were grown overnight in 0.2% glucose with M9 salts medium, 20 μM ferric sulphate and chloramphenicol at 50 μg/ml, without inducer, and under normal pH (without buffer). For the growth experiment, the same medium as above was used but with inducer (0.02% rhamnose) as well as 25 mM MES-Tris buffer, and without iron. **A.** Medium was at pH 5. **B.** As for A except for the growth was without inducer. **C.** Details are as for A except for use of pH 7, **D.** Details are as for A

except that the growth was at pH 9. A major difference between the growth of the complemented and un-complemented mutant is indicated by the arrows. The above experiment is representative of three independent experiments, and all growths were in triplicate. Statistically significant differences were determined by the Independent Samples t-test.

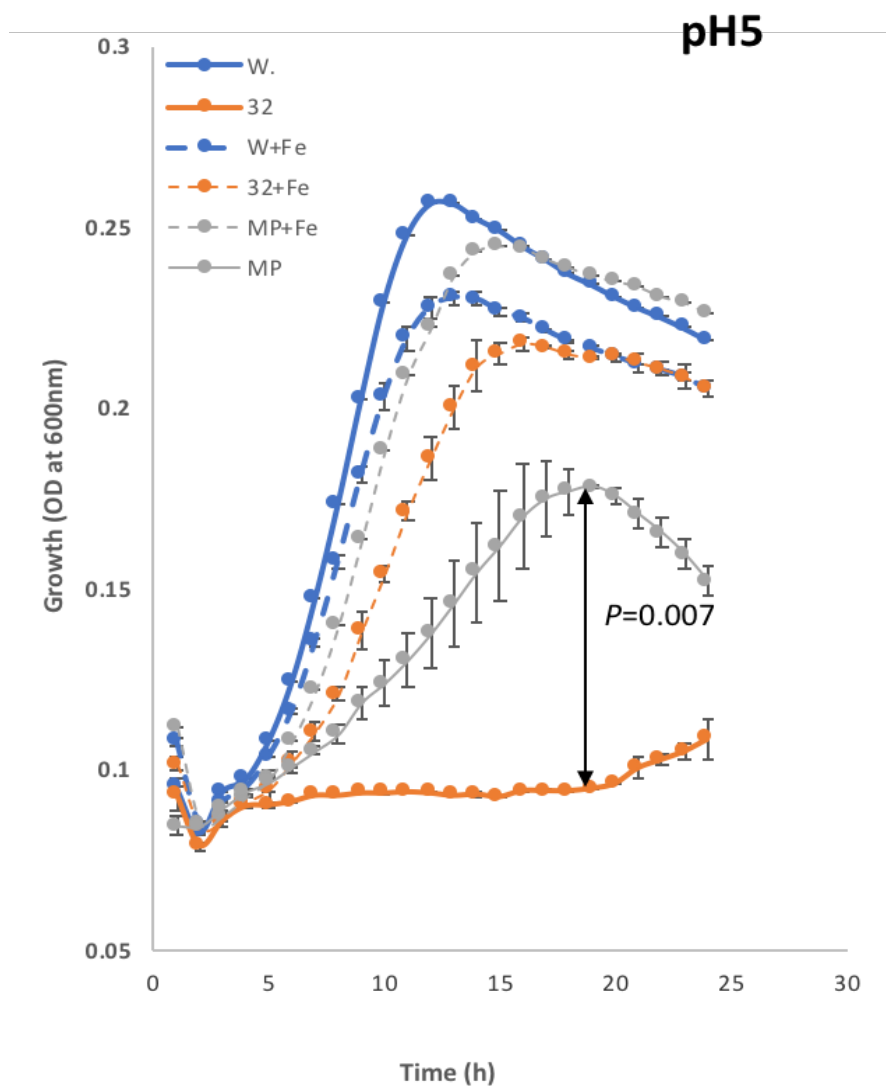


Figure 4.22. Effect of *fetMP* on growth of JC32 under iron restriction at pH 5. Details as in Fig. 4.21 except for alternative plasmid was used (*fetMP* /ara) and acidic pH only, $P < 0.01$ between the JC32 mutant strain and the JC complemented with *fetMP*. The above experiment is representative of two independent experiments, and all growths were in triplicate.

4.4.2. *fetA-F* enhances growth of *E. coli* JC32 under acidic pH

The possibility that the *fetA-F* genes have the capacity to support iron-restricted growth, as seen above for *fetMP*, was also tested in liquid medium at low pH under iron restriction, as in the previous section. The results show that the *fetA-F* genes caused an enhanced growth for JC32 under iron restriction at low pH: at 20 h, there was an increase of growth of 0.01 OD units for vector-complemented JC32 under low iron, but for the *fetA-F* complemented strain the increase in growth was 0.07 OD units (seven fold higher) (Fig. 4.23). However, there was no such growth difference under iron sufficiency. Thus, *fetA-F* (like *fetMP*) supports iron-restricted growth under low pH in liquid medium. In contrast, at neutral and basic pH, *fetA-F* did not notably enhance the growth of JC32. Indeed, at pH 9 the *fetA-F* genes caused a reduction in growth both under high and low conditions. Role of the inducer was clear in this experiment, *fetA-F* could not enhance the growth of the complemented JC32 but in contrast a low growth inhibition was noticed without inducer (Fig. 4.23B).

The above results provide the first strong experimental evidence that the FetA-F systems has a role in iron uptake, and further indicates that it can play a role independent to that of FetMP. The experiment above was repeated using the pBADara constructs with inducer at pH5 and very similar results were obtained (Fig. 4.24), which thus supports the results in Fig. 4.23A showing that *fetA-F* enhances growth of JC32 under low iron, low pH conditions.

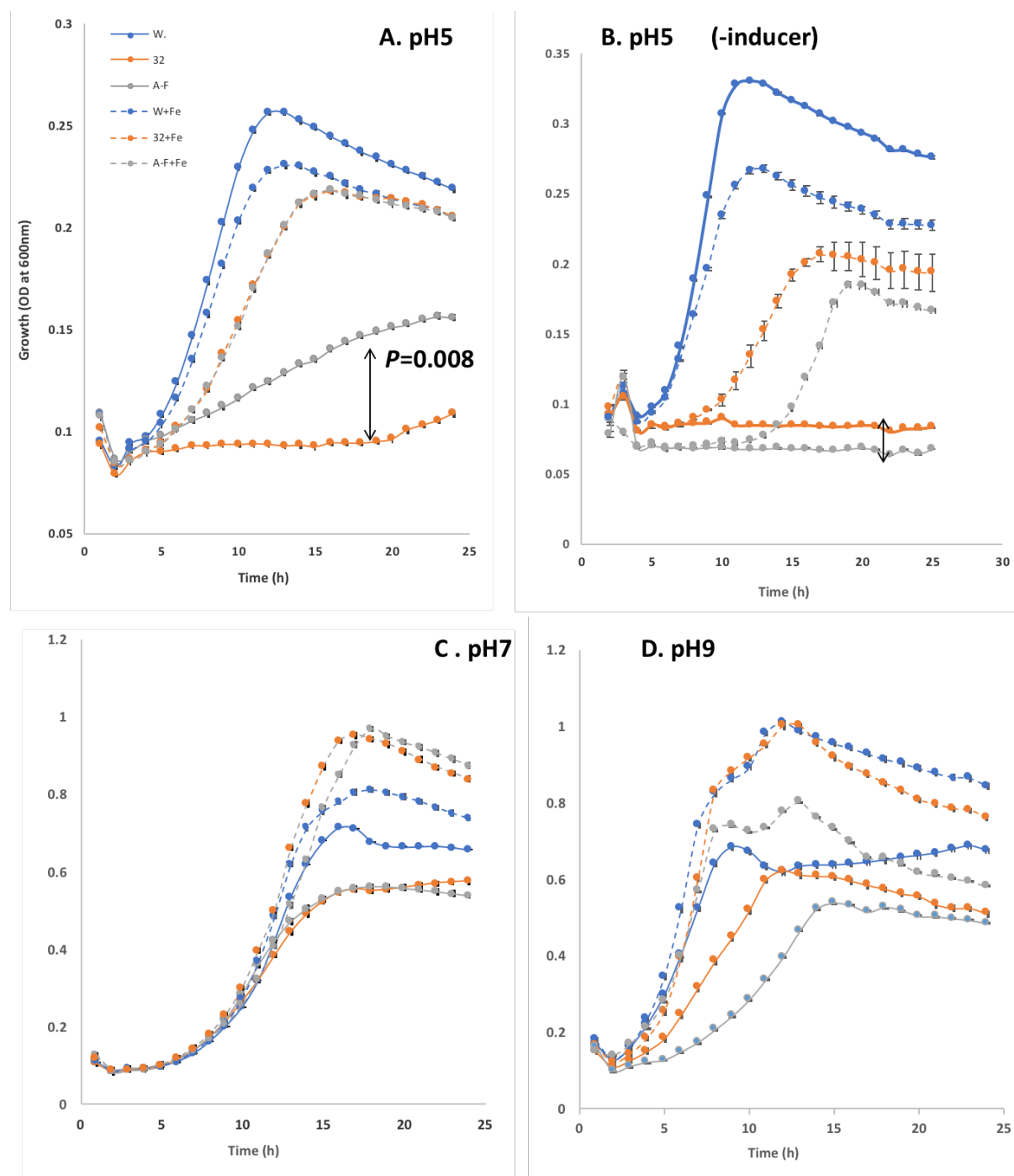


Figure 4.23. Effect of *fetA-F* on growth of JC32 under iron restriction at pH 5-9. Conditions were as in Fig. 4.21, inducer (0.02% rhamnose) was included as indicated. The above experiment is representative of two independent experiments, and all growths were in triplicate.

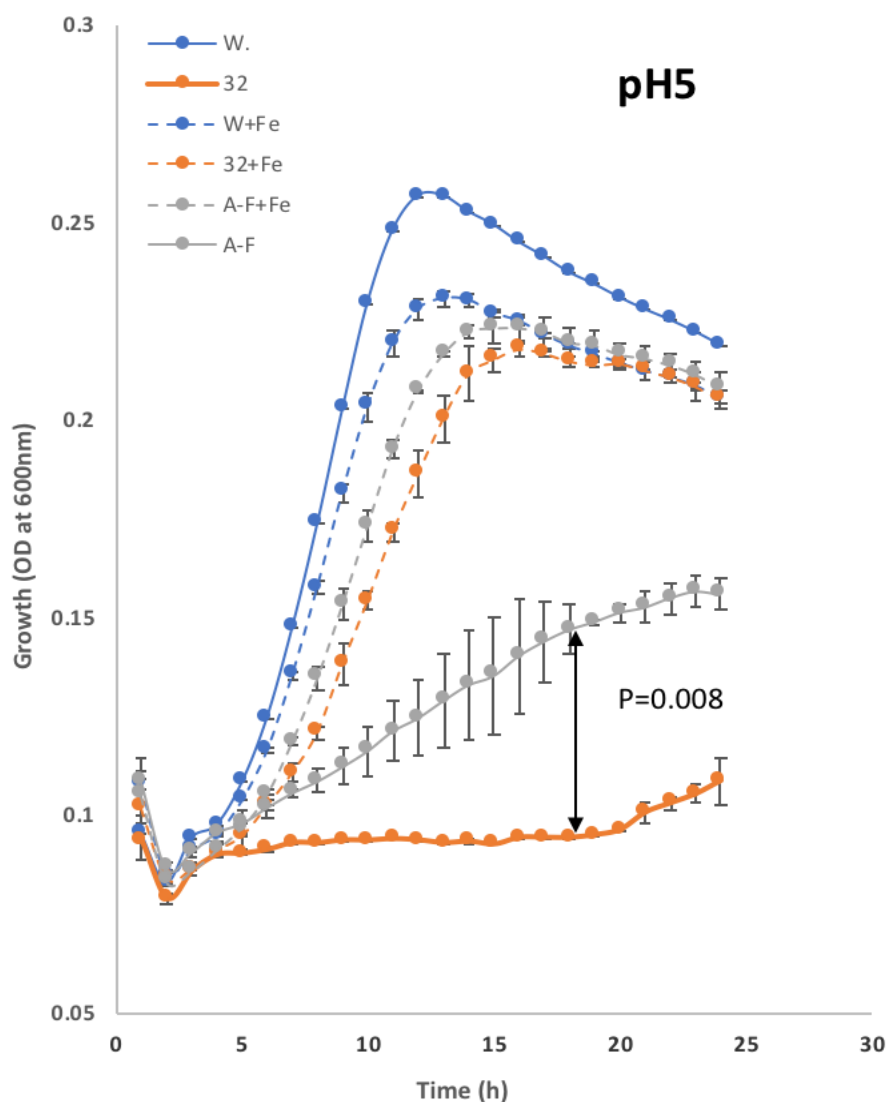


Figure 4.24. Effect of *fetA-F* on growth of JC32 under iron restriction at pH 5. Conditions were as in Fig. 4.21 except for the use of pBADara and BADara-*fetA-F* in place of pBADrha and pBADrha-*fetMP*, respectively, induced (0.02% arabinose was included throughout). The above experiment is representative of two independent experiments, and all growths were in triplicate.

4.4.3. Can *fetMP* and *fetA-F* act together to enhance growth of JC32 under acidic pH?

The next experiment aimed to explore whether the *fetMP* and *fetA-F* genes in combination can provide an enhanced low-iron growth capacity (greater than either of the single sets of genes) due to cooperative behaviour. pBADrha and pBADara vectors expressing *fetMP* and *fetA-F* were used to transform to *E. coli* JC32 (as pBADrha-*fetMP* and pBADara-*fetA-F* or pBADara *fetMP* and pBADrha-*fetA-F*). Also, both empty vectors were transformed in to the

E. coli wild type and JC32 to use as a vector control. Growths were as above except for the use of both inducers (rhamnose and arabinose), both at 0.01%. In the experiments below, pH 8 was used in place of pH 9 as the double transformants grew very poorly at pH 9 (data not shown).

It should be noted that initially experiments were performed with both inducers at 0.02% and this led to a major growth inhibition of all transformants carrying both *fetMP* and *fetA-F* (data not shown). Also, when only one inducer was at 0.02%, and the other was excluded, a major growth inhibition was seen for JC32 carrying both *fetMP* and *fetA-F* (data not shown). Similarly, no consistent and clear growth advantage was seen at pH 5 under low iron conditions (or at pH 7 and 8, or with iron) for JC32 carrying both *fetMP* and *fetA-F* when both inducers were excluded (data not shown).

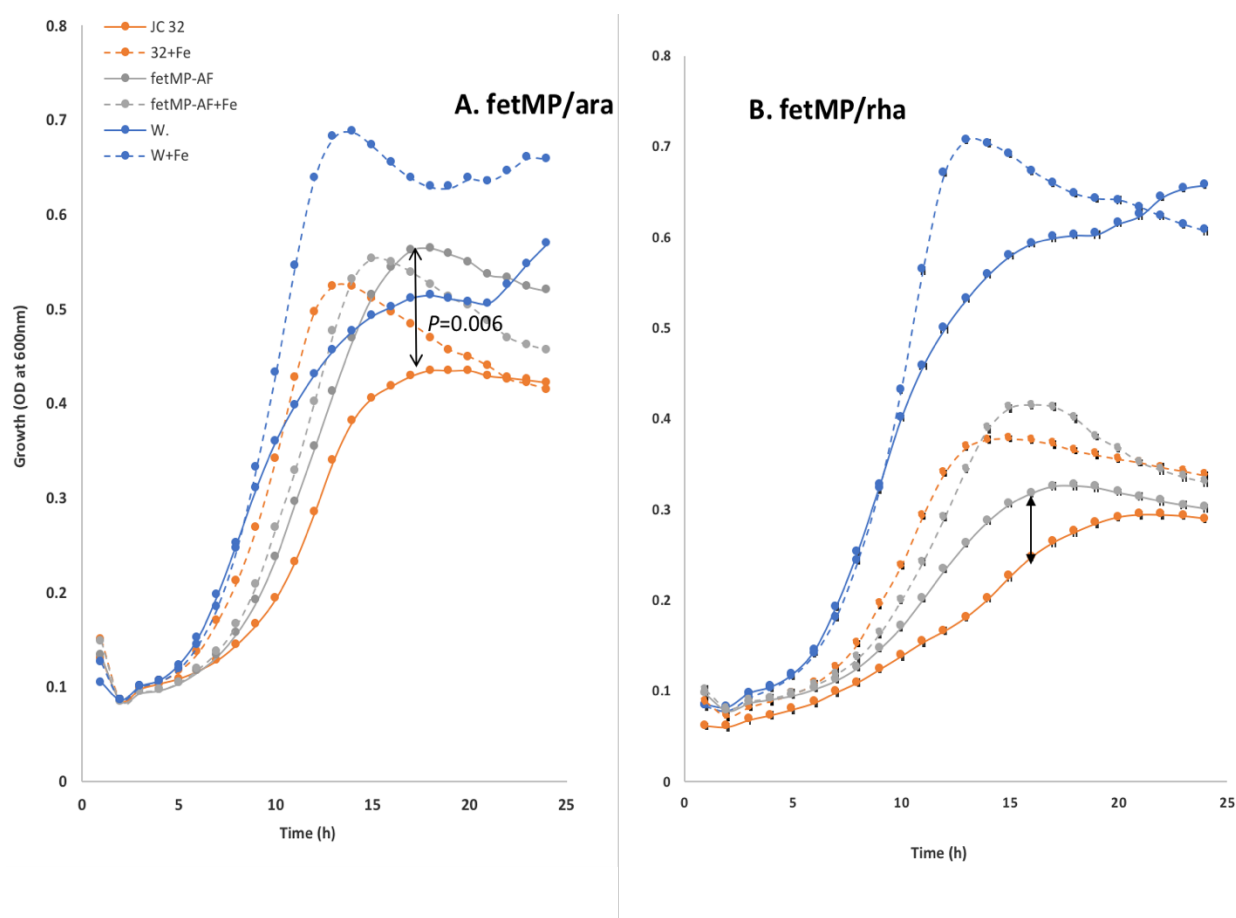


Figure 4.25. Effect of complementation with both *fetMP* and *fetA-F* on growth of JC32 under iron restriction at pH 5. Growths were at pH 5 and as described in Fig. 4.21, except for the use of two inducers (arabinose at 0.01% and rhamnose at 0.01%). **A.** Strains were: W, wildtype *E. coli* W3110 with pBADara and pBADrha; JC32, with pBADara and pBADrha; 32+*fetMP-AF* (JC32 complemented with pBADara-*fetMP* and pBADara-*fetA-F*). '+Fe', indicates with 20 μ M ferric sulphate). Arrow: $P=0.006$ between JC32 and the complemented strain. **B.** Strains were as in A, but JC32 was complemented with pBADrha-*fetMP* and pBADara-*fetA-F*. Arrow between JC32 and the complemented strain. The above experiment is representative of two independent experiments, and all growths were in triplicate.

The results show a significant low-iron growth enhancement for the ara-*fetMP* rha-*fetA-F* complemented JC32 strain with respect to the vector control, with the former giving an OD of 0.56 at 17 h, whereas the latter gave an OD of 0.43 at the same point (Fig. 4.25A) ($P < 0.01$). With addition of iron, a growth advantage was still seen for the double-complemented strain, but this was more than twofold weaker than for seen in the absence of iron and ~ 1 -2 h delayed growth with respect to the control was also observed (Fig. 4.25A), thus indicating an iron-restriction dependence for the growth enhancement. Interestingly, the complemented JC32 strain gave better growth than the wildtype control under iron restriction. This indicates a very strong enhancement of iron uptake was achieved by the *fetMP/fetA-F* complementation. When JC32 was complemented with the rha-*fetMP* and ara-*fetA-F* genes (Fig. 4.25B), an increase (with respect to the vector control) in iron-restricted growth of 0.07 OD units (at 17 h) was obtained, whereas in the presence of iron the growth increase observed was less marked (0.04 OD units). However, these differences were not significant ($P > 0.01$).

The impact of iron on the growth of the JC32 strains was less marked than seen in Fig. 4.21A, which might reflect the presence of two inducers or two plasmids in this case or could result from variability in the amounts of adventitious iron within different batches of M9 medium. Indeed, low iron growths were stronger for the JC32 strains in Fig. 4.25 than 4.20-24, which is suggestive of higher iron availability.

Unlike in the previous growth experiments at pH 5, the wildtype showed raised growth with addition of iron, rather than lower growth. This may also be related to the presence of two plasmids in this case and the difference in the culturing conditions (two antibiotics and two inducers).

4.4.4 Complementation of JC32 with two plasmids - a vector control together with a *fetMP* or *fetA-F*-carrying plasmid

4.4.4.1. Aerobic growth

The initial *fetMP* and *fetA-F* complementation experiments (4.4.1) in liquid culture showed a clear, low-iron growth enhancement at pH 5 for JC32. This suggested that combining the *fetMP* and *fetA-F* plasmids might lead to an even stronger growth advantage than observed for the single-plasmid complementations. However, this was not the case although a growth advantage was observed for the *fetMP fetA-F* double complementations, the growth effect appeared weaker than that obtained when only one plasmid was used for the complementation (4.4.3). This suggests that the presence of both a *fetMP* and *fetA-F* plasmid might be deleterious to JC32 under low-iron conditions. Therefore, in order to be able to directly compare the impact of the double and single complementations, JC32 double transformants were prepared that carry an empty vector (pBADara or pBADrha) together with the compatible pBAD plasmid carrying either *fetMP* or *fetA-F*. The growth of the transformants was then compared as above.

The results in Fig. 4.26 show that with 0.01% of both inducers at pH 5 under low-iron conditions, there is a 4-5 fold growth enhancement for JC32 complemented with both pBADrha-*fetMP* and pBADara, and also for JC32 complemented with both pBADrha-*fetMP* and pBADara-*fetA-F* (growth increase of 0.14 OD units cf. 0.03 OD units for the vector control). A similar, but much more modest growth enhancement (~20%), was also seen under

high-iron conditions, indicating that the growth advantage afforded by *fetMP*, and *fetMP* with *fetA-F*, is largely associated with iron restriction.

In contrast, pBADara-*fetA-F* with pBADrha caused a clear growth inhibition to the complemented strain under low iron at pH 5 (Fig. 4.26). This result indicates that *fetA-F* does not enhance low-iron growth of JC32 at pH 5 in the presence of *fetMP* or in any pBADara/pBADrha double-plasmid format. This finding is contrary to that observed above where *fetA-F* provided in single-plasmid format enhanced low-iron growth at pH 5. This discrepancy likely relates to a negative impact inflicted by the presence of two plasmids in the JC32 strain combined with the presence of the foreign *fetA-F* products resulting in increased stress and lower growth.

Similar growth effects were seen at pH 7, but the low-iron advantage afforded by pBADrha-*fetMP* combined with pBADara, and also by pBADrha-*fetMP* with pBADara-*fetA-F*, were less pronounced (~10% growth increase; data not shown). At pH 8, growth of the double plasmid transformants under low iron was very poor such that no notable growth difference was apparent (data not shown).

In the absence of inducers, or with both inducers present at 0.02%, no low-iron growth enhancement of *E. coli* JC32 complemented with *fetMP*, and/or *fetA-F* in double plasmid format was observed at pH 5, 7 or 8 (data not shown).

In summary, the results above indicate that the low-iron growth enhancement of JC32 observed at pH 5 when *fetMP* and *fetA-F* are both provided in trans, is largely caused by the presence of *fetMP* with little contribution from *fetA-F*.

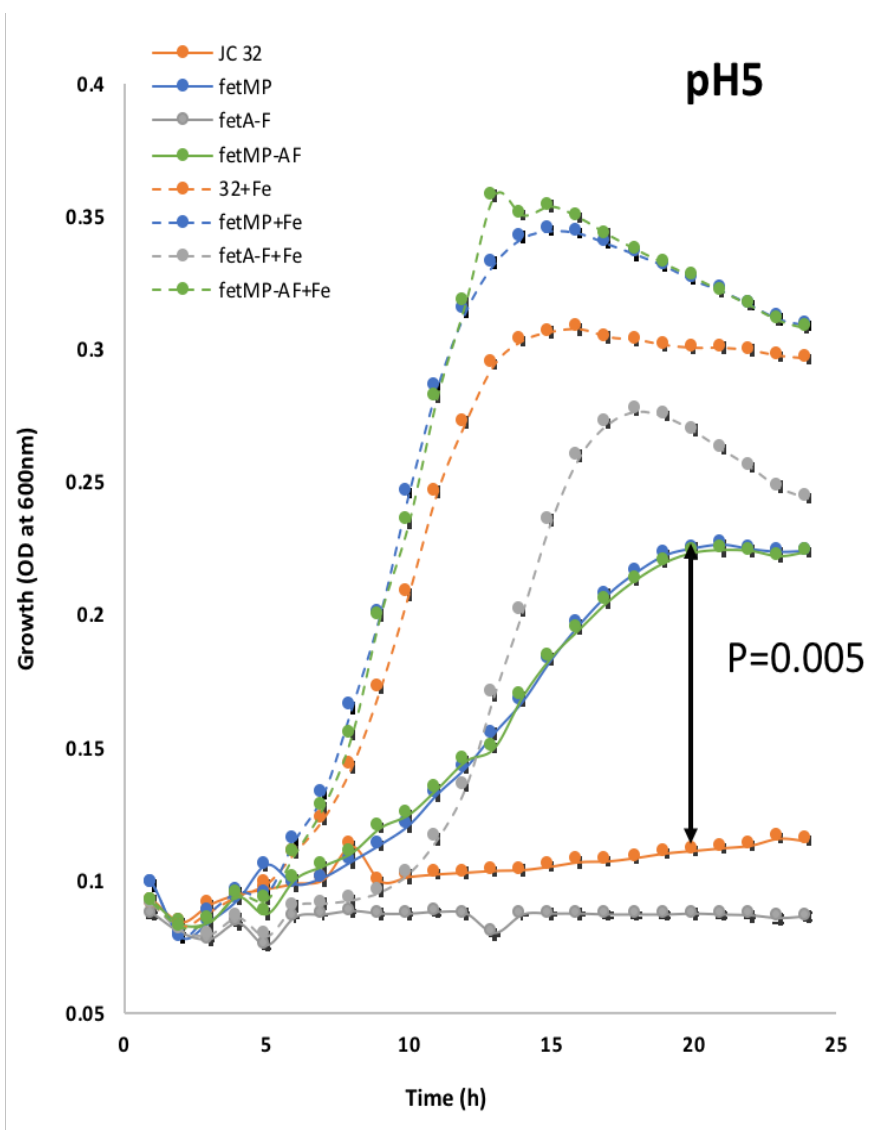


Figure 4.26. Effect of *rha-fetMP* or *ara-fetA-F*, along with a compatible pBAD vector, on the growth of JC32 under iron restriction. Conditions were as in Fig. 4.21 except for the presence of two antibiotics (ampicillin and chloramphenicol), and both inducers at 0.01% concentration. The pH was 5. Strains were as follows: orange, JC32 with pBADara and pBADrha; blue, JC32 with pBADrha-*fetMP* and pBADara; grey, JC32 with pBADara-*fetA-F* and pBADrha; and green, JC32 with pBADrha-*fetMP* and pBADara-*fetA-F*. '+Fe' indicates with 20 μ M ferric citrate. Arrow: $P < 0.01$ between the JC32 and the JC complemented with the whole operon (*fetMP* and *fetA-F*) only *fetMP* at pH 5, inducers were at 0.01%. The above experiment is representative of two independent experiments, and all growths were in triplicate.

4.4.4.2. Low-oxygen growth

The above results clearly show that *fetMP* and *fetA-F* are able to enhance the low-iron growth of *E. coli* JC32 under acidic pH, although for *fetA-F* growth enhancement was only observed in the single-plasmid format. Previous work with Ftr1-dependent iron transporters has demonstrated a need for an oxidant (O_2 for Ftr1 of yeast, H_2O_2 suggested for EfeUOB of *E. coli*; Larrondo *et al.*, 2007; Große *et al.*, 2006) in order to drive the uptake of ferrous iron and its suggested oxidation during the uptake process. So far, the low-iron, low pH growth enhancement provided by the FetMP and FetA-F systems has been achieved under aerobic conditions. However, *C. jejuni* is a microaerophile and thus the conditions employed do not match those associated with the niche occupied by *C. jejuni* and fail to test for the possible requirement for oxygen. Thus, the growth comparisons above were repeated under low-oxygen conditions to determine if there is any O_2 requirement for FetMP-FetA-F mediated iron uptake activity. Growths were as before (section 4.4.1) except that a microtiter-plate reader equipped with an Atmospheric Control Unit (BMG LABTECH) (located in Food and Nutritional Sciences, lab 3-18 Harry Nursten building) was used for propagation of cultures (Methods 2.17.3). This provides a low oxygen atmosphere of 13-15% CO_2 and ~1% O_2 . In this case, the acidic pH used was pH 6, rather than 5, as very weak growth was observed under low oxygen at pH 5 and growth was much better at pH 6 (data not shown). Growth was also tested at pH 8. Strains were employed in the double-plasmid format, as used above (4.4.4.1), with 0.01% rhamnose and arabinose.

At pH 6 under low oxygen and iron regime, *fetMP* slightly inhibited the growth of JC32 (reducing OD at 18 h from 0.32 to 0.30; Fig. 4.27). In contrast, *fetA-F* caused a very slight growth enhancement of ~0.01 OD units at 24 h, but also caused an extended lag phase of ~5 h. For the *fetMP* plus *fetA-F* complementation there was a clear enhancement of growth under low-iron conditions was observed (growth increase of 0.035 OD units at 20 h with

respect to the vector control), although this increase is less than that seen for the *fetMP* plus *fetA-F* aerobically (Fig. 4.26). Further, the double-complemented strain showed much better low-iron growth than the two singly complemented strains (growth increase of 0.06 OD units at 18 h). This result indicates that FetA-F can enhance low-iron growth of JC32 under low-oxygen conditions, at pH 6, when provided in double-plasmid format with FetMP or with vector-only, which is in contrast to the case under fully aerobic conditions.

At pH 8 under low oxygen and low iron regime, the double-plasmid bearing strains exhibited very weak growth, although very similar strong growth was seen upon addition of iron for all transformants (data not shown).

In summary, the use of low-oxygen conditions appears to have little inhibitive impact on the ability of FetMP to promote low-iron growth at acidic pH. For FetA-F, ideally the low-oxygen experiment should be repeated using the single-plasmid format to determine whether the ability of FetA-F to increase low-iron growth of JC32 under acidic conditions (in this format) is affected by low O₂ availability.

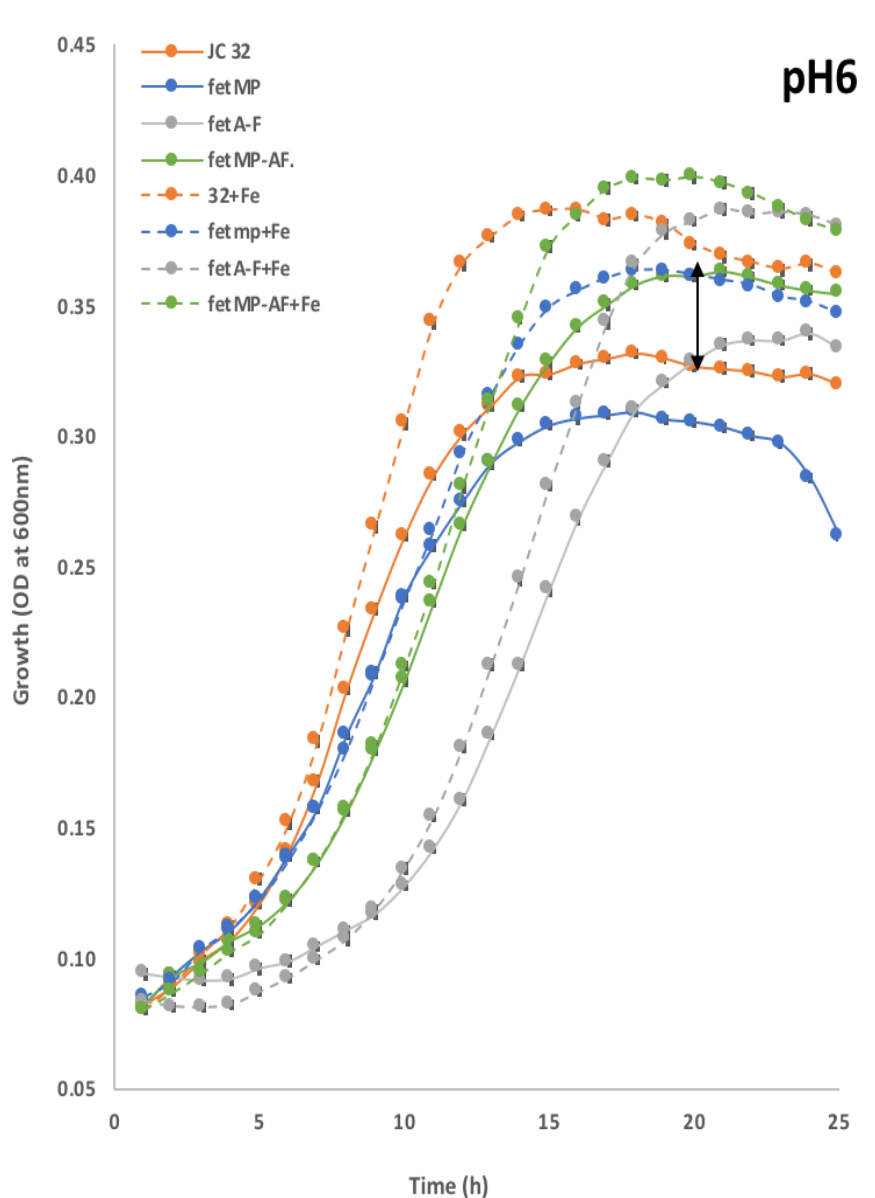


Figure 4.27. Effect of *rha-fetMP* or *ara-fetA-F*, along with the corresponding compatible pBAD vector, on the growth of JC32 under iron restriction and low-oxygen conditions, at pH 6. Details are as for Fig. 4.26 except for the use of low oxygen conditions and pH 6, inducers were at 0.01%. The above experiment is representative of two independent experiments, and all growths were in triplicate. $P > 0.01$ between the JC 32 and the JC complemented with the whole operon (*fetMP* and *fetA-F*).

4.5. Discussion

In this chapter, the role of the *C. jejuni* FetMPA-F system as an iron transporter was explored. In order to enable this, the eight-gene cluster was amplified as two fragments, *fetMP* and *fetA-F*, and cloned into the pBADrha and pBADara inducible vectors separately to allow complementation of an *E. coli* strain (JC32) lacking iron transport capacity and enabling controlled expression within this strain. The phenotypic effect of the complementations under iron-restriction conditions was then tested, using different pH and oxygen regimes. The phenotypic studies indicated that the cloned and inducible versions of the *C. jejuni* *fetMP* and *fetA-F* genes do not support growth of JC32 under iron restriction in solid medium. Indeed, the *fetA-F* genes caused a major growth inhibition of the JC32 strain indicating that their expression is deleterious in *E. coli* (Fig. 4.13-4.20).

On the other hand, in minimal liquid medium, complementation with either *fetMP* or *fetA-F* enhanced the growth of *E. coli* JC32 under iron-poor conditions, but only at acidic pH. This may explain why the growth tests using solid medium failed to provide a phenotype, as the effect of pH was not considered with solid medium. Low pH is known to favour the stability of ferrous iron under aerobic conditions (Widdel *et al.*, 1993). Thus, the low pH effect observed is suggestive of a role for FetMP and FetA-F in ferrous iron uptake. Brickman and Armstrong (2012) also found that the FtrABCD system of *Bordetella* (with FetMP homologues) exhibits maximum iron-uptake activity under low pH conditions, which matches the induction of the corresponding genes under acidity. Similar findings were observed for EfeUOB (Cao *et al.*, 2007).

Koch *et al.* (2011) studied the role of the dipartite *fetMP* system from uropathogenic *E. coli* (UPEC) strain F11 (the corresponding FetM proteins display 56% identity with 100% query coverage), which is closely related to the *C. jejuni* system, and also found a role in iron uptake upon complementation of an iron-uptake deficient *E. coli* strain. However, the effect

observed was not pH dependent, which contrasts to the results obtained here with the *C. jejuni* system. Koch *et al.* (2011) did not consider the impact of the corresponding *fetA-F* system in the F11 strain although sequence analysis shows that the three downstream genes (EcF11_1993-1) in the F11 strain correspond to *fetA-C*; the genes further downstream are unclear as the genome sequence is not fully assembled (locus AAJU02000030). Thus, the F11 FetMP system is likely to be also associated with a FetA-F system and is thus likely to be closely similar to FetMPA-F of *C. jejuni*. Another difference from the studies of Koch *et al.* (2011) was the use of the native promoter from the F11 strain rather than a plasmid borne inducible promoter as employed here. This provided the potential for Fur titration since the F11 system was shown to be Fur regulated. Such a titration effect could stimulate expression of Fur-repressed genes that might promote iron restrict gene expression from the host *E. coli* strain employed which could result in unanticipated phenotypic effects.

The possibility that FetMP and FetA-F might exhibit cooperative behaviour in enhancing low-iron growth was tested by providing *fetMP* and *fetA-F* together within compatible, inducible plasmids in JC32. This resulted in a clear enhancement of iron-restricted growth at acidic pH (Fig. 4.25). However, it was unclear whether this enhancement was greater than seen when *fetMP* or *fetA-F* were provided individually. To obtain an indication of whether any synergistic effect might occur, the *fetMP* and *fetA-F* plasmids were transformed into JC32 along with the corresponding vector controls to generate transformants carrying both pBADara and pBADrha plasmids. The resulting growth experiments confirmed that *fetMP* stimulates JC32 growth under low-iron, low-pH conditions, but this growth enhancement was not further improved by combination with *fetA-F*. Further, when *fetA-F* was provided alongside the corresponding empty vector (i.e. rh*fetA-F* and empty pBADara), *fetA-F* caused a clear inhibition in the growth of JC32 under low pH and low iron. This suggests that the expression of the *fetA-F* genes combined with the presence of a second plasmid results in

sufficient physiological stress to inhibit growth. Indeed, when the levels of both inducers were at 0.02% (rather than 0.01%), a general growth repression was observed for all double transformants under low iron, low pH conditions.

Since *fetMP* and *fetA-F* promoted a clear low-iron growth enhancement for JC32 at acidic pH under the aerobic growth conditions employed, it was decided to test the impact of low-oxygen conditions on this phenotype; the yeast Ftr1p-Fet3p system requires oxygen as an oxidant for ferrous iron transport (Jensen and Culotta, 2002), but the role of microaerobic oxygen is not clear for FetMP/FetA-F of *C. jejuni*. The results obtained were different to those achieved aerobically, for *fetMP* suggesting that FetMP cannot drive iron uptake at low pH under microaerophilic conditions that was used. This finding is not consistent with that of Koch *et al.* (2011) who found that the FetMP system of F11 enhances growth of *E. coli* under both aerobic and anaerobic iron-restriction conditions may be due to different anaerobic conditions that achieved in the two experiments. Koch *et al.* (2011) also showed that the iron uptake activity of FetMP is lost when FetM is excluded, and that FetP only seemed to be required aerobically. This led to the suggestion that FetP may function as a periplasmic ferric reductase (which has not been tested in this thesis) and limited evidence was provided that supported this proposal. Ideally, the impact of full anaerobiosis should be tested for *fetMP* and *fetA-F* in the single plasmid formats.

In summary, the results obtained above are consistent with independent roles of the FetMP and FetA-F systems in promoting iron uptake under iron-restriction, low-pH conditions. This activity would be consistent with roles in ferrous iron uptake (as ferrous iron is stable at low pH; Cao *et al.*, 2007). However, the suggested capacity of FetA-F to promote iron uptake was not exhibited when JC32 was placed under increased pressure through provision of a second plasmid alongside that carrying *fetA-F*. This indicates that expression of the *C. jejuni fetA-F* system in JC32 is deleterious and can result in growth inhibition. However, when low-oxygen

conditions were employed the combination of FetMP with FetA-F appeared to result in an enhanced growth under low iron, suggesting that FetA-F may support FetMP iron uptake activity under low oxygen conditions.

Chapter 5: Targeted mutation on the P19 system

5.1. Introduction

Iron-acquisition systems are crucial for the pathogenesis of bacteria in the host. Thus, bacteria employ a range of mechanisms for iron uptake (Guerinot, 1994; Zeng and Lin, 2017). Like other bacteria, *C. jejuni* needs iron for successful colonisation, survival and proliferate inside the gut (Palyada *et al.*, 2004; Miller *et al.*, 2009; Zeng *et al.*, 2013). *C. jejuni* has specific strategies to obtain iron from many sources to allow it to survive in the host (Palyada *et al.*, 2004; Naikare *et al.*, 2006). Considering the relatively small size of its genome (Parkhill *et al.*, 2000; Hofreuter *et al.*, 2006; Pearson *et al.*, 2007), *C. jejuni* contains a large number of genes (~25) involved in iron-uptake function, although there are some differences between strains (Miller *et al.*, 2009).

The focus of this thesis is the *cj1658–cj1663* encoded system of *C. jejuni* NCTC 11168, associated with Ftr1 and P19 (FetMP). In this chapter, the importance of the P19 system as an iron transporter in *C. jejuni* was tested by inactivation of three of the genes of this eight gene system, to determine whether any growth defect can be obtained. Briefly, three separate genes in P19 system of *C. jejuni* NCTC 11168 wild type were selected for knockout: the *ftr1* (*cj1658*, iron permease) gene specifying the integral membrane-protein similar to Ftr1p of yeast and EfeU of *E. coli* (Kosman, 2003; Große *et al.*, 2006); the *cj1660* gene, encoding an integral-membrane protein with predicted periplasmic DUF2318 and YHS domains; and the *cj1663* gene which encodes an ABC protein associated with a predicted type VII ABC transporter likely acting as an extra-cytoplasmic mechanotransducer (Parkhill *et al.*, 2000; Miller *et al.*, 2009; Butcher *et al.*, 2010). These genes were inactivated by deletion of about 1 kb from the middle of each gene and insertion of a *cat* cassette gene (Cm resistant) from pVA35 plasmid (van Vliet *et al.*, 1998b) in the deletion site following the van der Stel *et al.*

(2015) strategy to generate three single mutant strains. These mutant strains were confirmed genotypically by PCR and tested phenotypically by growth curve comparison along with the wild type.

The growth curve experiments were generated under different conditions in M-H broth with and without 20 μ l ferric citrate, or Desferrioxamine (iron chelator), or 25 mM MES-HEPES buffer at pH 5, 7, and 8. In some cases, growth comparison was in BHI-enriched medium. In addition, complementation tests were performed to reverse the growth defect of the mutants and thus confirm that the growth defects obtained were due to the generated mutations. The strategy followed to generate the complementation plasmids involved use of the pMA1 (Kⁿ^R) shuttle vector carrying either *ptr1-p19* or *cj1660-65* where expression was dependent on the natural promoters upstream of the corresponding genes (Dugar *et al.*, 2013).

5.2. Generation of a $\Delta ptr1$ mutant

5.2.1. Amplification the DNA of interest and cloning into the pJET 1.2 plasmid

The *ptr1* (2091 bp) gene was amplified from the chromosomal DNA of *C. jejuni* NCTC 11168 wild type with about 1 kb of upstream and downstream DNA to give an ~4 kb PCR product (Fig. 5.2). The PCR was performed using HiFi PCR premix and pJET-*ptr1* F and R primers (Table 2.4) as described in (Methods 2.11.2). The resulting PCR product was cleaned and cloned into the pJET1.2 vector using Clone JET PCR Cloning Kit. Several colonies from the transformed colonies on the selected antibiotic LB plates was collected for overnight growth in LB broth with Amp and plasmid DNA was extracted by (Methods 2.11.4) and digested with *Bgl*II (Method 2.11.5) which confirmed the presence of the PCR fragment (expected product sizes of 2.9 and 4 kb).

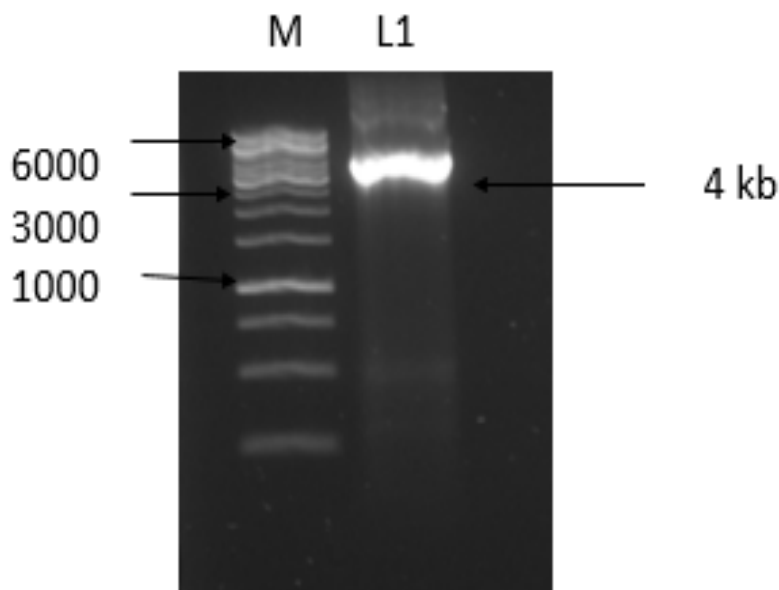


Figure 5.1: Agarose gel (0.7%) electrophoretic analysis of *ftr1* PCR product with 1 kb upstream and 1 kb downstream region of *C. jejuni* NCTC 11168. L1: *ftr1*, M: 1 kb ladder (Fermentas). Loadings were 1 μ l for ladder and 2 μ l for DNA sample.

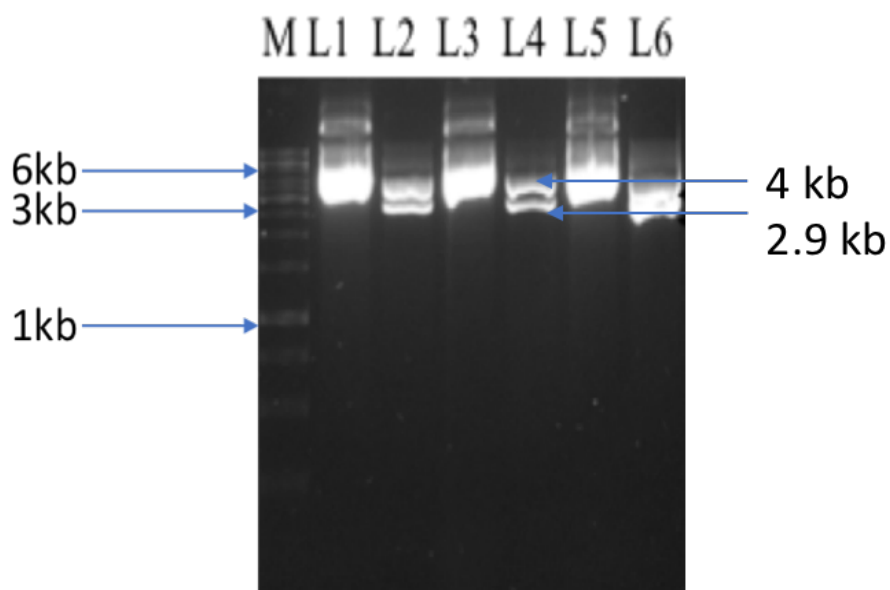


Figure 5.2: Gel electrophoretic analysis of (pJET-*ftr1*) plasmid before and after digestion by *Bgl*III enzyme. L1: the plasmid before digestion, L2: the plasmid after digestion (two sites flanking the insert).

5.2.2. The *ptr1* deletion by inverse PCR

The pJET-*ptr1* plasmid from the cloning above was used for inverse PCR (Methods 2.11.2) with inverse F & R primers (Table 2.4) to generate an $\Delta ptr1$ derivative (5.9 kb; 3 kb *ptr1* region and 2.9 kb for pJET1.2) PCR product which resulted in deletion of ~980 bp from the middle of the *ptr1* gene.

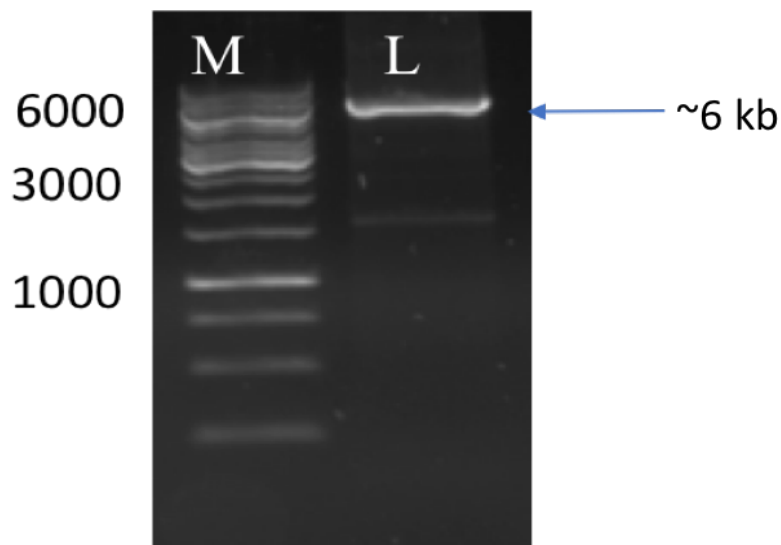


Figure 5.3: Agarose gel (0.7%) electrophoretic analysis of inverse PCR product of pJET- $\Delta ptr1$. M: 1 kb ladder (Fermentas), L1: is $\Delta ptr1$ PCR product obtained using HiFi polymerase.

The *cat* gene was PCR amplified using the *cat* F&R primers and the pVA35 plasmid (Fig. 5.4) as a template (Fig. 5.5). The chloramphenicol-resistant gene, 896 bp, included the expected promoter and terminator region.

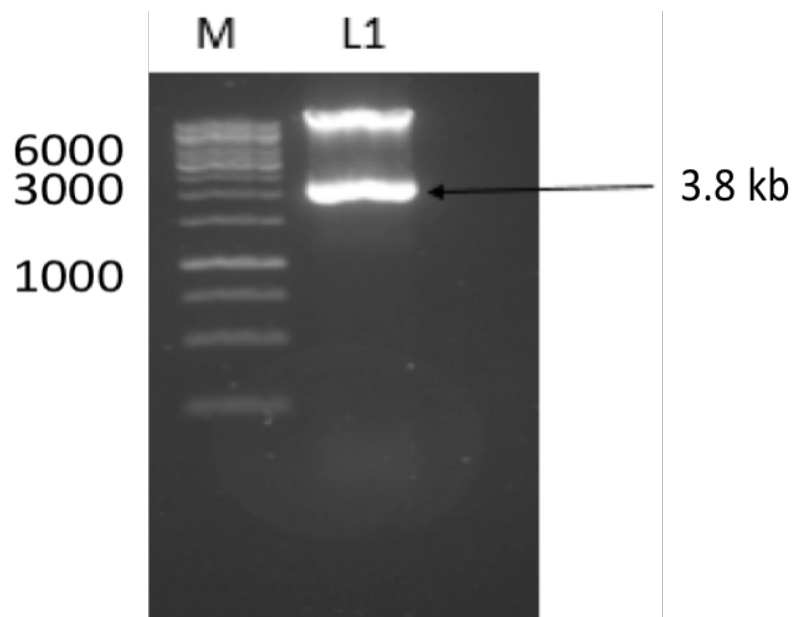


Figure 5.4: Gel electrophoretic analysis of pVA35 vector (3811 bp), Cm^R plasmid extracted from *E. coli* Top10. M, Gene Ruler 1 kb; and L1, pVA35 plasmid.

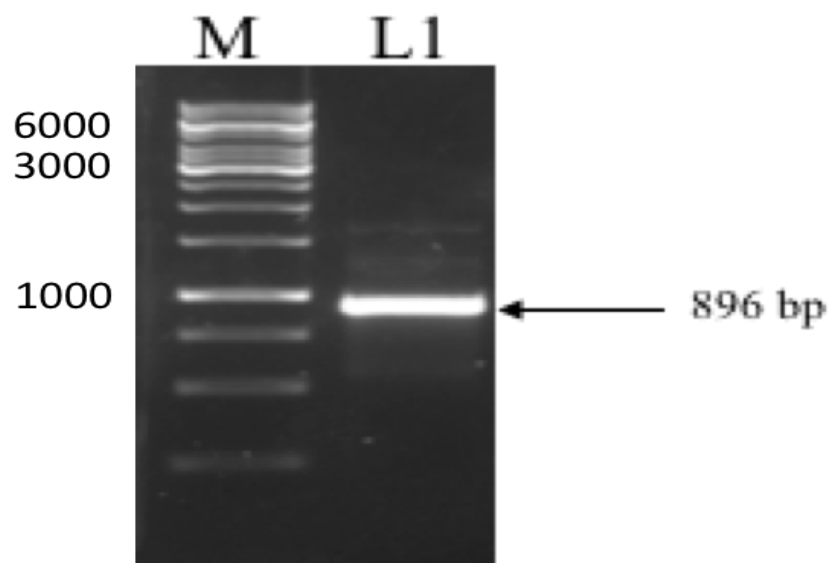


Figure 5.5: Gel electrophoretic analysis of the *cat* gene (896 bp, 40 ng) PCR product. M, Gene Ruler 1 kb; and L1, *cat* gene extracted from the gel.

5.2.3. Cloning of the *cat* cassette into the pJET- Δ *ftr1* deletion site

The resulting PCR products, pJET- Δ *ftr1* and the *cat* gene, were purified by gel extraction (Methods 2.11.5). The two purified PCR products thus obtained were combined in an In-Fusion cloning reaction to enable the *cat* gene to be inserted at the deletion site of the Δ *ftr1* gene; flanking *AsiSI* sites (GCGATCGC) had been engineered at the deletion site through the inverse PCR process (Table 2.5) to enable confirmation of successful cloning by digestion of the resulting plasmid with this enzyme. Following transformation of the In-Fusion cloning products into competent *E. coli*, three of the resulting Cm^R transformant colonies were chosen for plasmid isolation. These were then digested with *AsiSI* (Methods 2.11.4 and 2.11.5) and the expected fragment sizes (pJET- Δ *ftr1*, 5.9 kb; *cat* gene, 896 bp) were obtained which indicated successful cloning (Fig. 5.6). The plasmid was designated pJET- Δ *ftr1*::*cat* (Fig. 5.9).

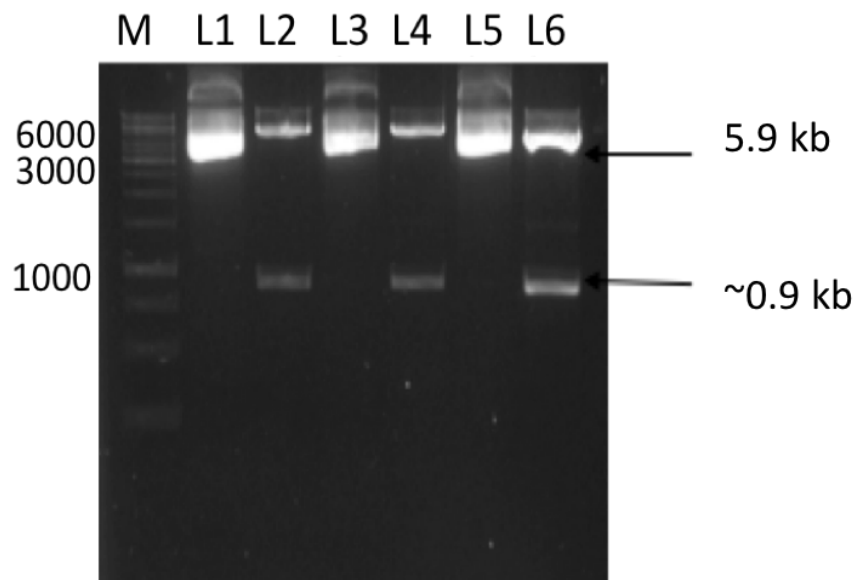


Figure 5.6: Gel electrophoretic analysis of *AsiSI*-digested pJET Δ *ftr1*::*cat* candidates. M: Gene Ruler 1 kb, L1, 3 and 5: undigested plasmids (#1-3), L2, 4, and 6: plasmids #1-3 digested by *AsiSI* restriction enzyme. Plasmids were extracted from *E. coli* Top10.

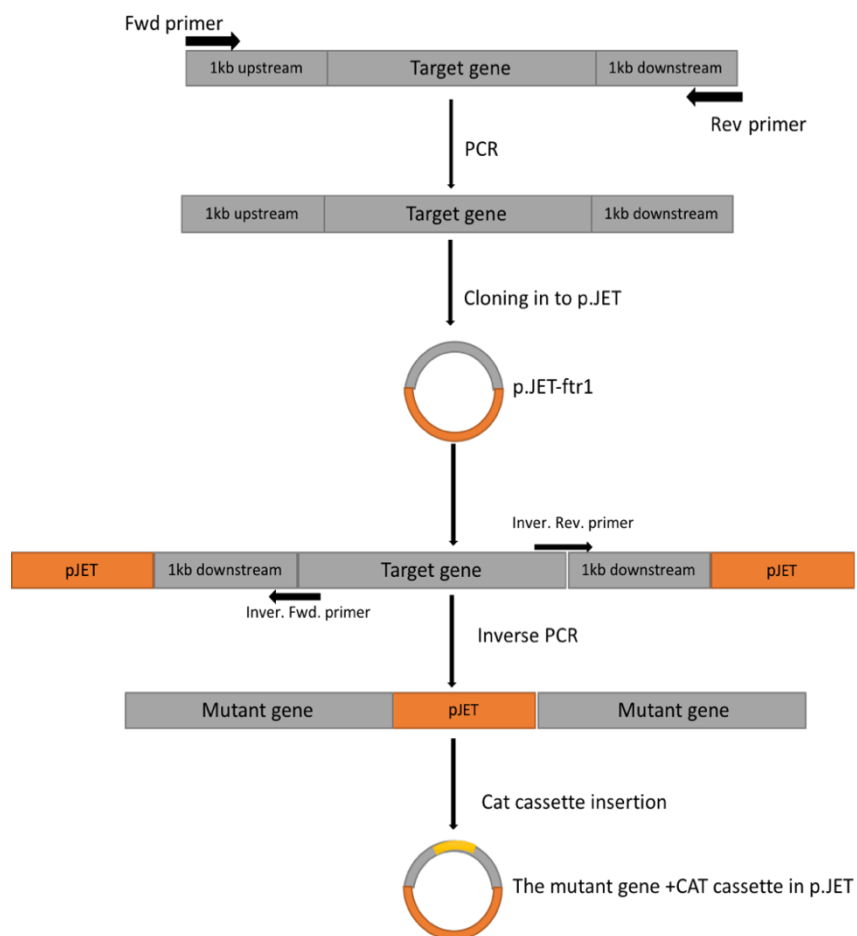


Figure 5.7: Diagram describing the strategy for generation of the gene knockout plasmids.

5.2.4. Transformation of pJET- $\Delta ftr1::cat$ into the *C. jejuni*

To disrupt the *ftr1* gene in the *C. jejuni* NCTC 11168, the pJET- $\Delta ftr1::cat$ plasmid was introduced into this strain by electroporation (Methods 2.15.3). Double cross-over recombination was confirmed by extraction of the genomic DNA from the transformed colonies that were resistant to chloramphenicol at 50 $\mu\text{g/ml}$ and performing PCR using the *cat* gene F primer with the *ftr1R* primer (the expected PCR product size was 2.4 kb). The resulting genotype is ($\Delta ftr1$)::Cm^R.

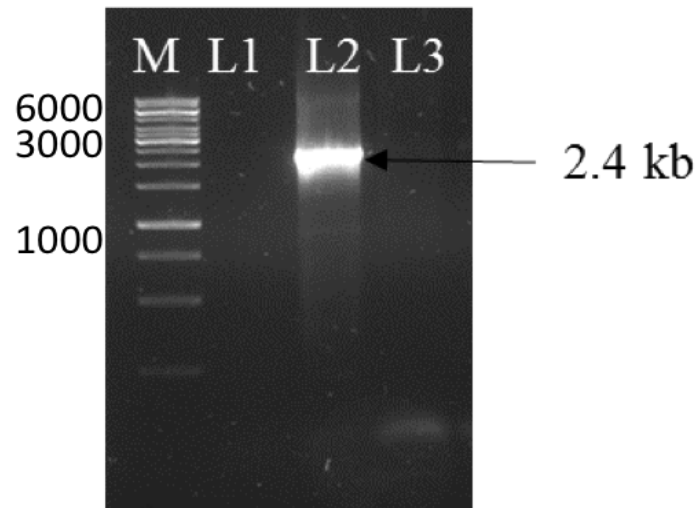


Figure 5.8: Gel electrophoresis analysis of an $\Delta ftr1::Cm^R$ mutant of *C. jejuni* NCTC 11168 using *ftr1* F and *cat* R primers. L1: wild type, L2: mutant, L3: blank. Note, three isolates of the mutant strain were obtained in total, obtained following three different transformations.

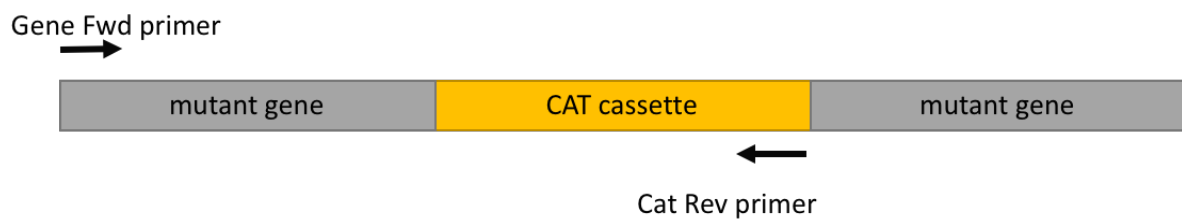


Figure 5.9: Diagram describing the strategy for PCR-confirmation of the mutations in the *C. jejuni* chromosome.

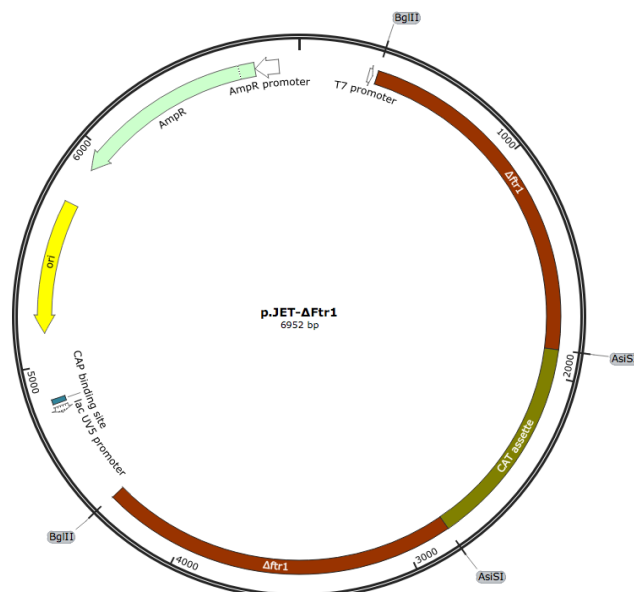


Figure 5.10: pJET1- $\Delta ftr1::cat$ map. Brown bars indicate the $\Delta ftr1$ gene. Dark yellow bar indicates the CAT cassette inside at the deletion point. The two *Bgl*II sites used to linearize the plasmid and the two *Asi*SI restriction sites are shown.

5.3. Generation of a $\Delta cj1660$ mutant

The strategy used to knockout *cj1660* was the same as that used for the *ftr1* knockout. The region of interest (3.3 kb: 1.3 kb *cj1660*, with 1 kb of upstream and downstream DNA) was amplified (Fig. 5.11) and cloned into the pJET1.2 as above (Fig. 5.12). The resulting pJET-*cj1660* plasmid was subject to inverse PCR to give a pJET- $\Delta cj1660$ (5.1 kb PCR product; 2.9 kb vector and 2.2 kb $\Delta cj1660$ region) derivative (Fig. 5.13). Then the *cat* cassette was cloned into the deletion site using In-Fusion cloning and the identity of the resulting constructs was confirmed by digestion with *Asi*SI (Fig. 5.14). Finally, the pJET- $\Delta cj1660::cat$ plasmid (Fig. 5.15) thus generated was transformed into the *C. jejuni* NCTC 11168 wild type strain to produce Cm^R transformants that were screened by PCR with *cat* F and *cj1660* R primers (Table 2.4) for PCR products of the expected size (2.2 kb) (Fig. 5.15) see Fig. 5.7.

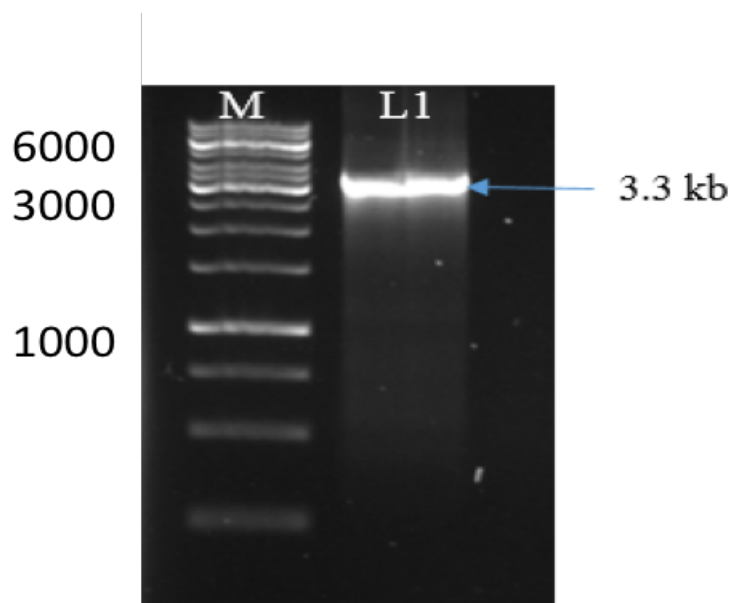


Figure 5.11: Gel electrophoresis analysis of PCR product of *cj1660* with 1 kb upstream and downstream regions. (3.3 kb, 55 ng).

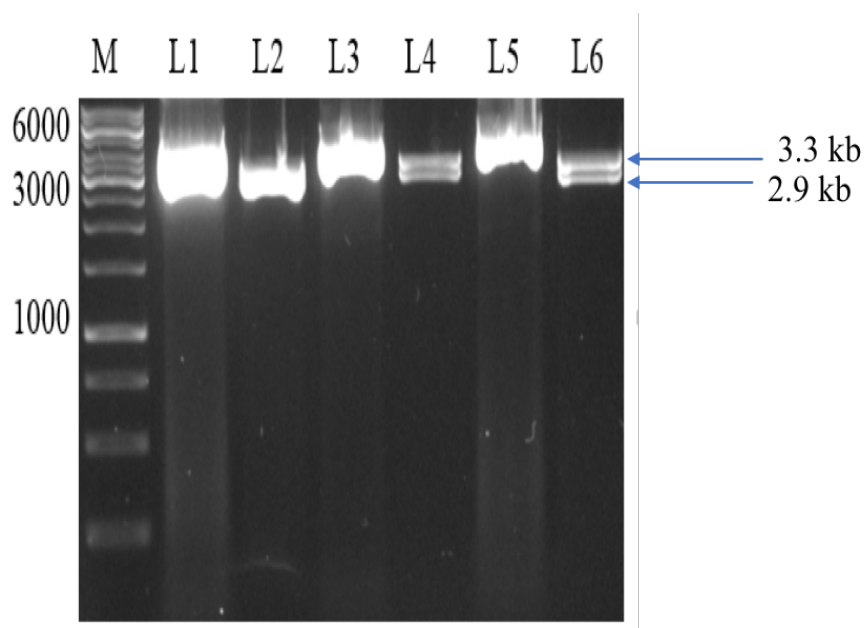


Figure 5.12: Gel electrophoresis analysis of pJET-*cj1660* candidate plasmids digested with *Bgl*II. M: Gene Ruler (1kb), L1,3 and 5: are undigested plasmids, L2, 4 and 6: are the plasmids after digestion by *Bgl*II enzyme to give expected fragment sizes of 2.9 and 3.3 kb.

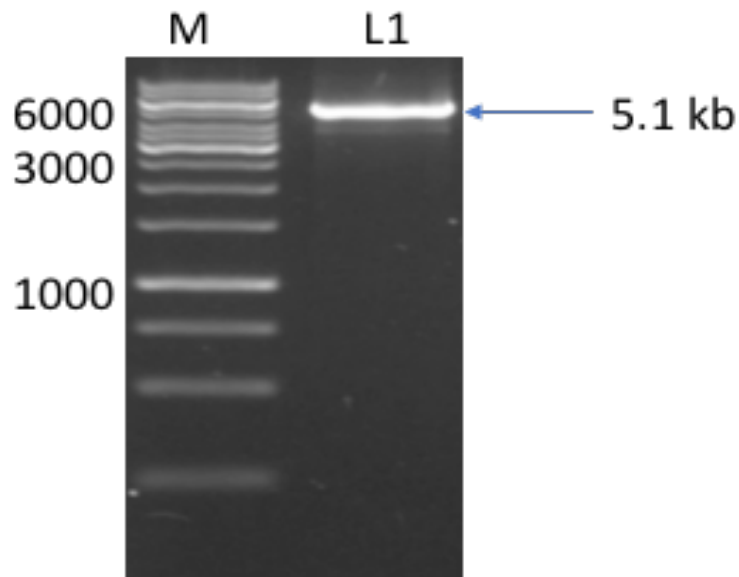


Figure 5.13: Gel electrophoresis analysis of inverse PCR of pJET-*cj1660*. L1, expected PCR product size of 5.1 kbB (2.2 + 2.9 kb).

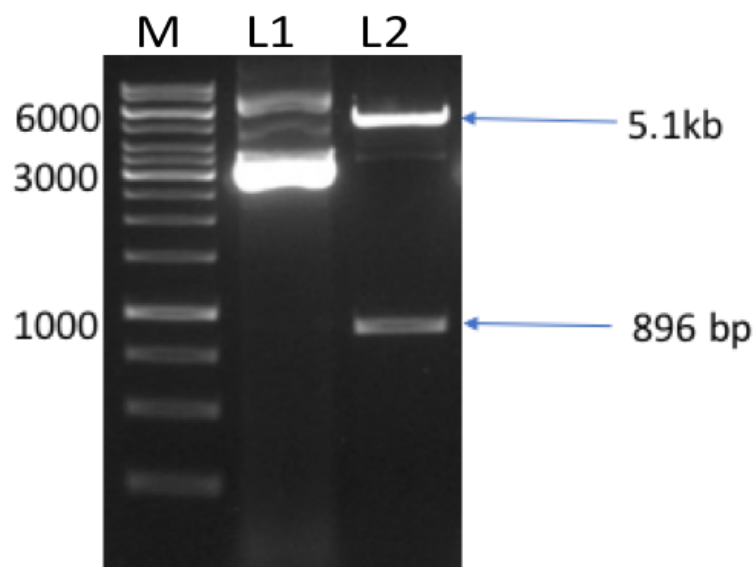


Figure 5.14.: Gel electrophoresis of pJET- Δ *cj1660::cat* candidate digested with *AsiSI*. Plasmid extracted from *E. coli* Top10, L1, the extracted plasmid before digestion; L2, plasmid digested with *AsiSI*.

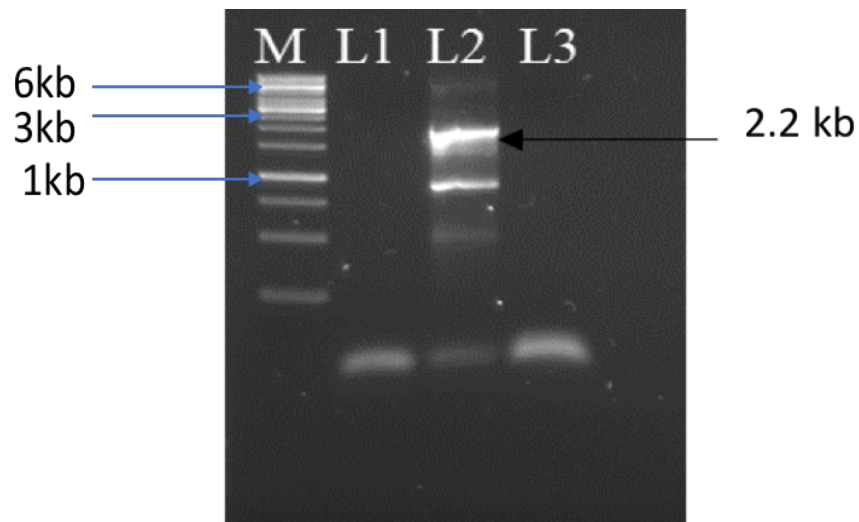


Figure 5.15: Gel electrophoresis analysis of PCR amplified $\Delta cj1660::Cm^R$ in *C. jejuni*. L1, wild type; L2, mutant. 1660 R and *cat* gene F primers were used to give the expected size (2.2 kb). Note: three isolates of the mutant strain were obtained.

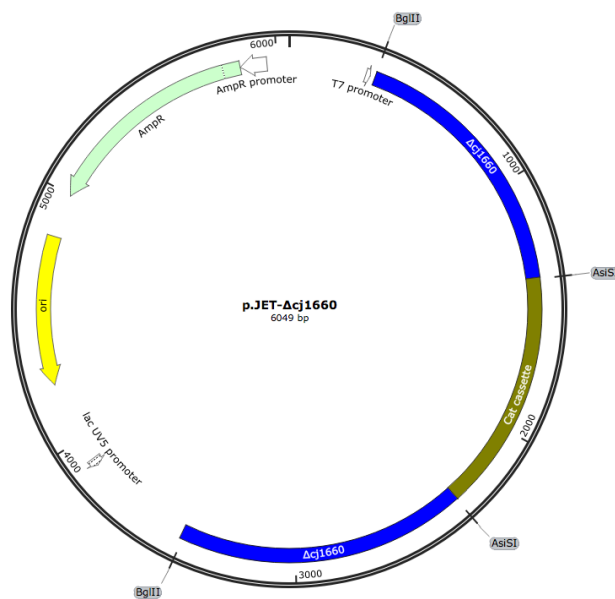


Figure 5.16: pJET- $\Delta cj1660::cat$ plasmid map. Blue bars indicate the $\Delta cj1660$ gene. Other details as Fig. 5.10.

5.4. Generation of a $\Delta cj1663$ mutant

The strategy used to knockout *cj1663* was the same as that used for *ptr1* and *cj1660* genes, above. The region interest (2.4 kb: 0.5 kb *cj1663* with 980 bp of flanking DNA upstream and ~900 bp downstream) was PCR amplified (Fig. 5.17) and cloned in to the pJET1.2 (Fig. 5.18). The resulting pJET-*cj1663* plasmid was used for inverse PCR with inverse F & R primers to generate a pJET- $\Delta cj1663$ fragment (4.8 kb, with 2.9 kb of vector and 1.8 kb of $\Delta cj1663$ DNA) (Fig. 5.18). Then the *cat* cassette was cloned into the *Asi*SI deletion site (Fig. 5.20). Finally, the thus derived pJET- $\Delta cj1663::cat$ (Fig. 5.21) was transformed in to *C. jejuni* NCTC 11168 by electroporation, and Cm^R transformants generated were screened by PCR using *cat* F and *cj1663* R primers (Fig. 5.21).

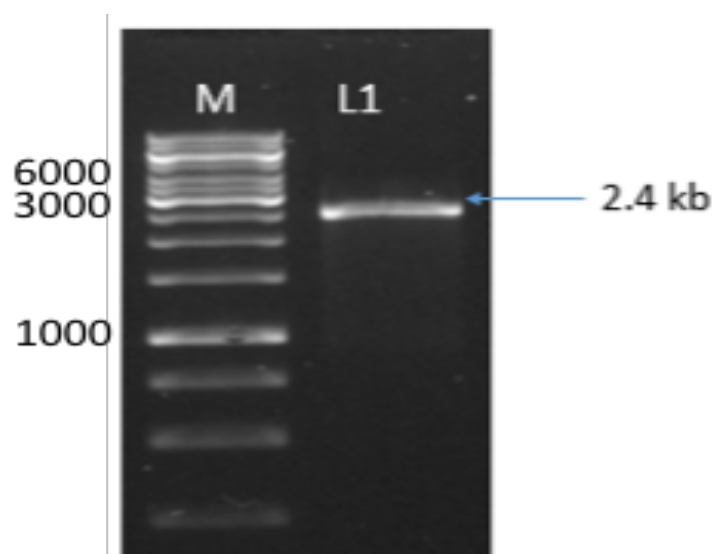


Figure 5.17: Gel electrophoresis analysis of the *cj1663* PCR product with 1 kb flanking DNA. L1, 2.4 kb PCR product extracted from the gel.

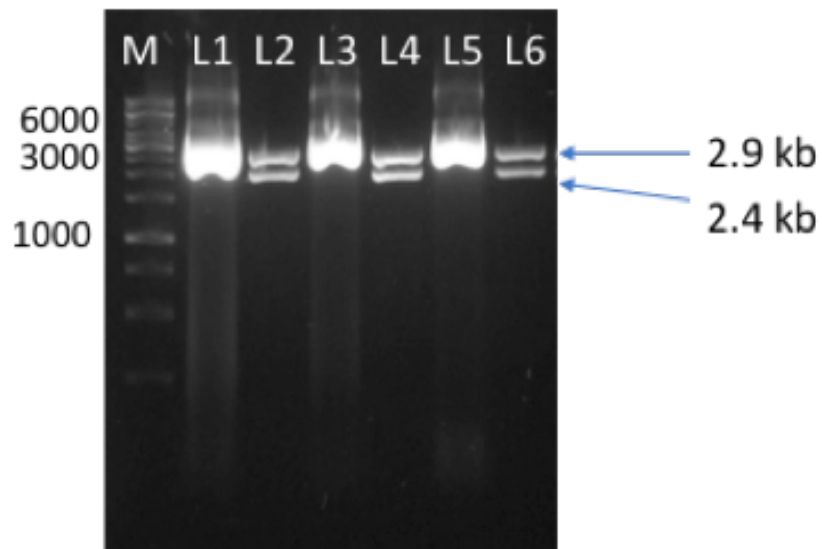


Figure 5.18: Gel electrophoretic analysis pJET-*cj1663* candidates digest with *Bgl*II. M, Gene Ruler (1kb); L1, 3 and 5, are undigested plasmids; L2, 4 and 6, the same plasmids after digestion with *Bgl*II.

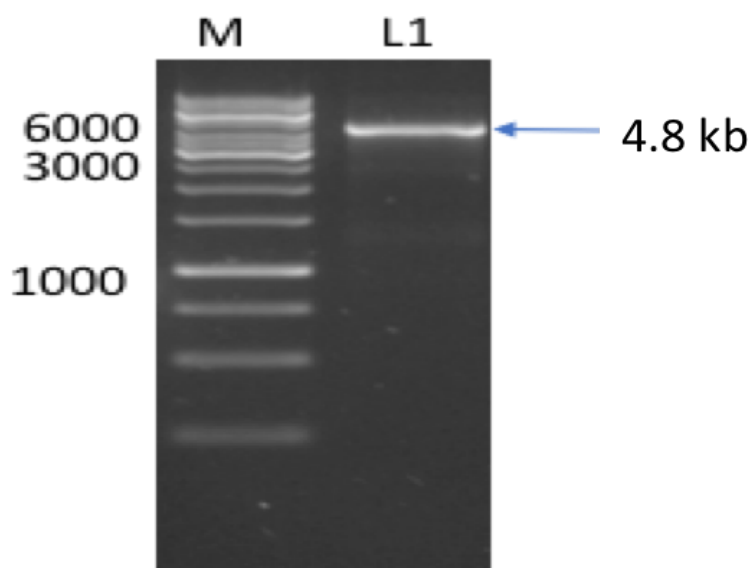


Figure 5.19: Gel electrophoretic analysis of the pJET- Δ 1663 product. M, Gene Ruler (1kb); L1, PCR product (4.8 kb, 1.9 kb for Δ 1663 gene and 2.9 kb for pJET).

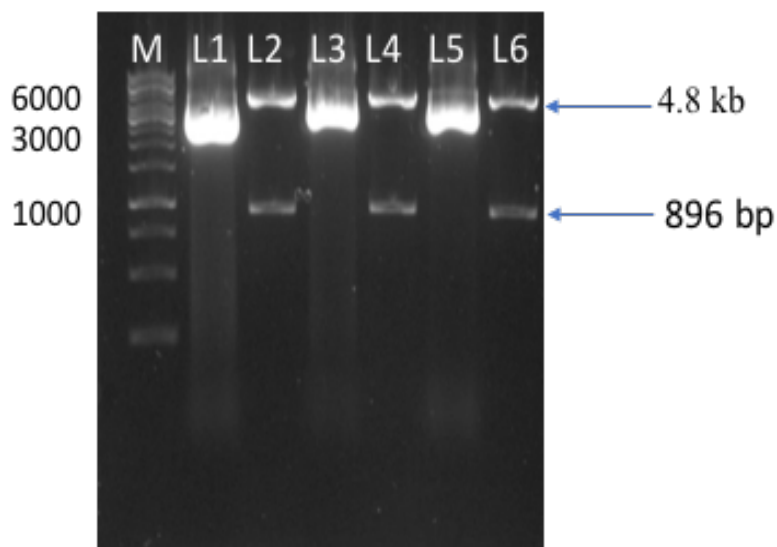


Figure 5.20: Gel electrophoretic analysis of pJET- Δ 1663::cat digested with AsiSI. The plasmids were extracted from *E. coli* Top10. M, Gene Ruler (1kb); L1, 3 and 5, undigested plasmids; L2, 4 and 6, the plasmids after digestion by AsiSI.

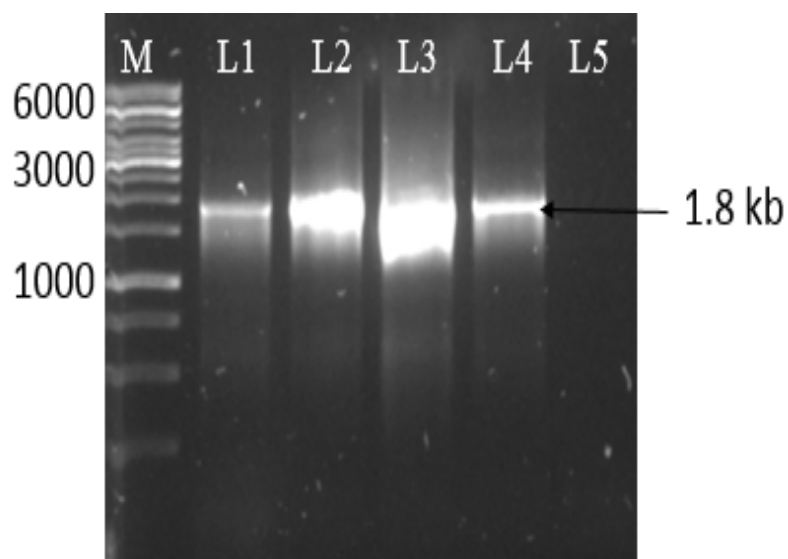


Figure 5.21: Gel electrophoresis analysis of PCR products derived from candidate Δ cj1663::Cm^R mutants. L1, 2, 3 and 4 are confirmed Δ cj1663::Cm^R mutants; L5, wild type. PCR primers were 1663 F and cat gene R. The expected size was 1.8 kb.

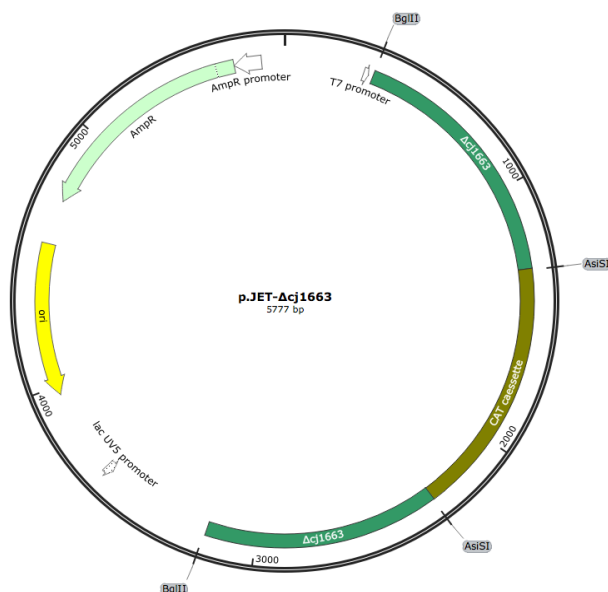


Figure 5.22: pJET- $\Delta cj1663::cat$ plasmid map. Dark green bars indicate the $\Delta cj1663$ gene. Other details as Fig. 5.10.

5.5. Construction of the *ftr1-p19* and *cj1660-65* complementation plasmids

The *ftr1-p19* and *cj1660-65* regions of interest were amplified from the chromosomal DNA of *C. jejuni* NCTC 11168 using HiFi polymerase enzyme and Ftr1KpnI and Ftr1XhoI or (cj1660KpnI and cj1660XhoI) primers (Table 2.6; Methods 2.11.2) (Fig. 5.24- 5.28). 900 and 300 bp of DNA upstream of the first coding region was included, respectively, in an attempt to incorporate the respective promoters. Also, the pMA1 plasmid includes the *C. jejuni metK* promoter for expression purposes, located just upstream of the *KpnI* cloning site. Plasmid pMA1 (Table 2.3) was propagated by transformation into the *E. coli* Top10 and plasmid DNA was extracted following overnight culture in LB containing 35 $\mu\text{g/ml}$ kanamycin. pMA1 (10.7 kb) was double digested by *KpnI* and *XhoI* restriction enzymes and purified by extraction from a gel (Fig. 5.23). The *ftr1-p19* and *cj1660-65* PCR fragments of interest were then ligated into the linearized pMA1 plasmid (van Mourik *et al.*, 2008) by In-Fusion cloning (Methods 2.11.7). Ligation reactions were transformed into Top10 and Kn^{R} transformants were isolated and treated for plasmid DNA purification. The plasmids thus obtained were tested by PCR reaction with ‘pMA1 vector primers F and R’ (Table 2.4) to confirm

success of the cloning (Fig. 5.24 & 5.28). Plasmids with the expected PCR pattern were sent for DNA sequencing (Methods 2.22.4) using primers Ftr1-rha F, R 1-4 and Cj-rha F, R 1-7 to confirm their identity. The resulting complementing plasmids pMA1-*ftr1-p19* (Fig. 5.26) and pMA1-*cj1660-65* (Fig. 5.29) were initially transformed into the *E. coli* S17 (Parke, 1990), then conjugated into the required *C. jejuni* strains by biparental conjugation (Labigne-Roussel *et al.*, 1987).

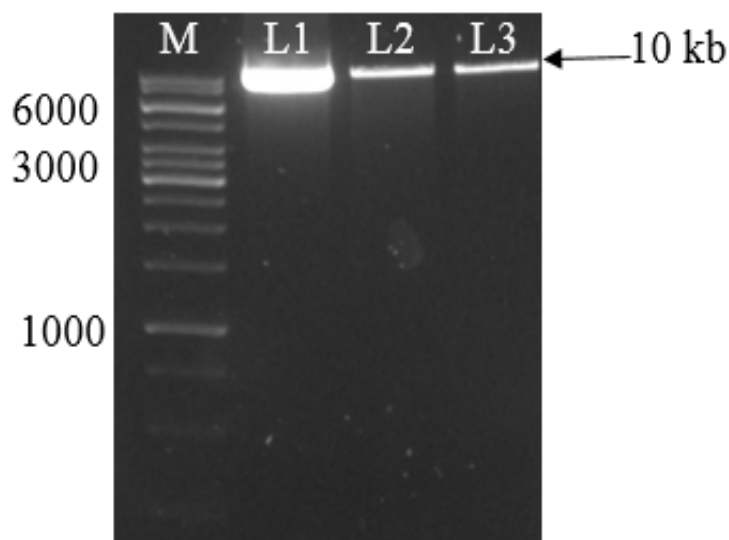


Figure 5.23: Gel electrophoresis analysis of the pMA1 vector. L1, undigested vector; L2, *Kpn*I and *Xho*I double digested vector after PCR purification (25 ng); L3, *Kpn*I and *Xho*I double digested vector extracted from the gel (10 ng).

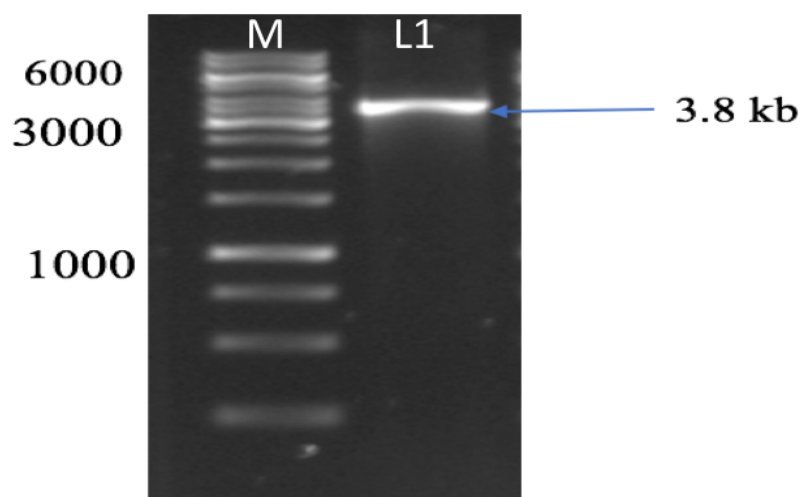


Figure 5.24: Gel electrophoresis analysis of the *ftr1-p19* PCR product with *Kpn*I and *Xho*I restriction sites included for subsequent cloning into the pMA1 shuttle vector.

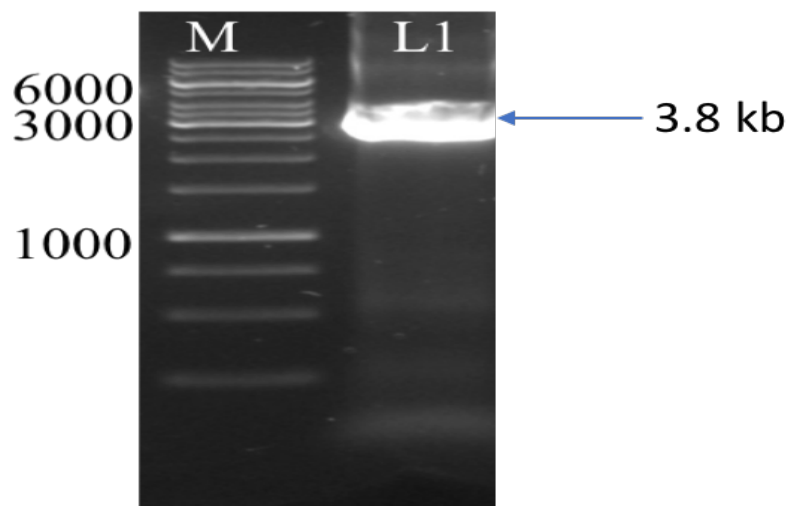


Figure 5.25: Gel electrophoresis analysis of the *ftr1-p19* PCR product pMA1-*ftr1-p19*. M, Gene Ruler (1kb); L1, PCR product. Size of product is about (3.8 kb) as expected.

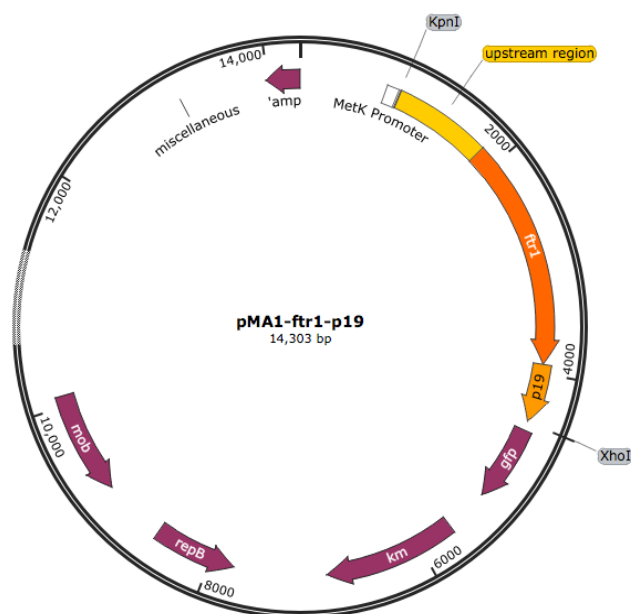


Figure 5.26: pMA1-*ftr1-p19* (*fetMP*) plasmid map. Dark and light arrows indicate the direction of *ftr1* and *p19* genes. Gold bar indicates *ftr1* upstream region. *KpnI* and *XhoI* are the restriction enzymes used to linearize the plasmid for cloning purposes.

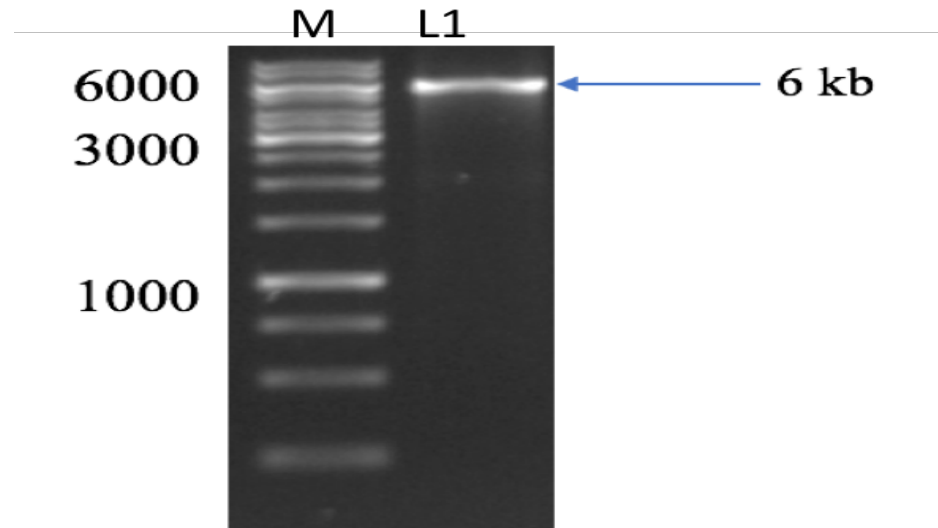


Figure 5.27: Gel electrophoretic analysis of the *cj1660-65* PCR product with *KpnI* and *XhoI* sites included. M, Gene Ruler(1kb); L1, PCR product obtained using *cj1660* F and R primers.

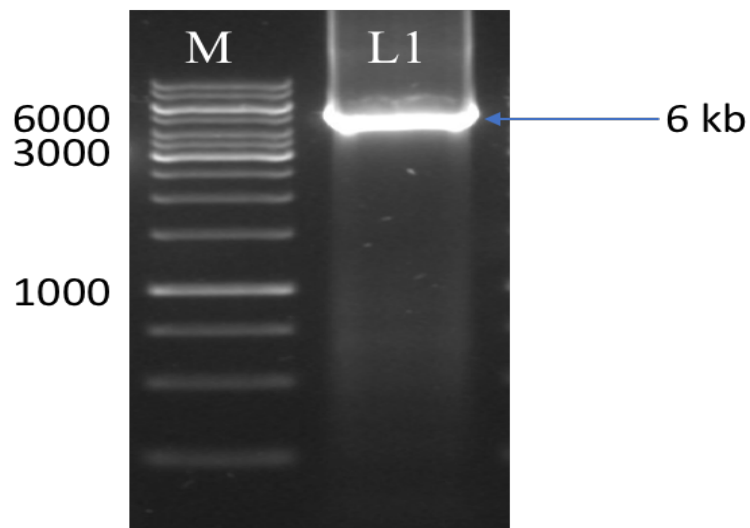


Figure 5.28: Gel electrophoretic analysis of the confirmation of the identity of pMA1-*cj1600-5* candidate by PCR. M, Gene Ruler (1kb); L1, PCR product (6 kb expected size).

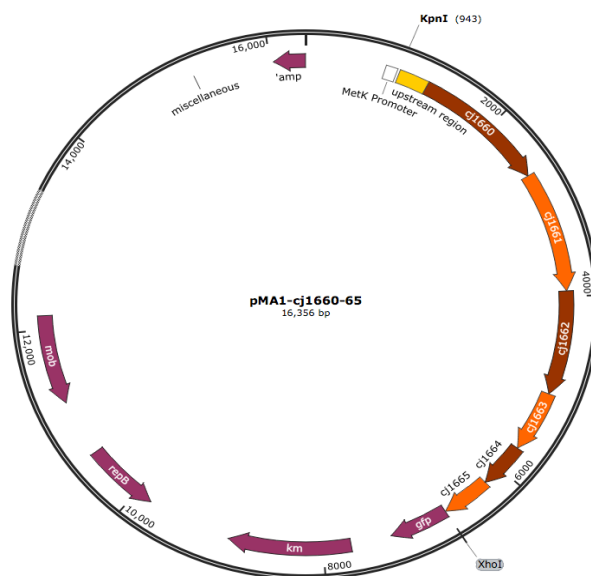


Figure 5.29: pMA1-cj1660-65 (*fetA-F*) plasmid map. Details as in Fig. 5.26.

5.6. Phenotypic studies of the *C. jejuni* NCTC 11168 mutants

5.6.1. Growth of the mutant strains in the minimal media

To test role of the *C. jejuni* P19 system as an iron transporter and to determine any role for the *cj1660-5* encoded proteins, growth curve comparison experiments were performed for all three mutants ($\Delta ftr1$, $\Delta cj1660$ and $\Delta cj1663$) with the wildtype in minimal medium. A *C. jejuni* $\Delta p19$ mutant (strain 81-176) was previously shown by Chan *et al.* (2010) to exhibit growth inhibition in M-H medium with desferrioxamine (DFO), but not in M-H without DFO, indicating that *p19* is involved in an iron acquisition function. A similar iron-dependent phenotype was anticipated for the $\Delta ftr1$ mutant.

Growth was compared under microaerophilic conditions (5% O₂, 10% CO₂, 2% H₂ and 83% N₂) using a Whitley M35 HEPA variable atmosphere workstation at 37 °C. Growth was in 200 μ l volumes in 96-well microtiter plates, without shaking, using M-H or DMEM minimal medium. Cultures were prepared as in Methods (2.18.1; 2.18.4). All media were prepared in acid washed glassware and sterile Falcons or Eppendorfs. Cultures were inoculated to give a starting OD₆₀₀ of 0.002 and incubations was for 48 h. The OD₆₀₀ was measured ever 12 h

using in a Spectra MAX 340pc spectrophotometer. Plates were prepared in quadruplicate and each was used for a single time point measurement (to avoid exposure of the bacterial cultures to the atmospheric conditions).

The media used (BHI, M-H and DMED) were analysed by the Inductively Coupled Plasma Mass Spectrometry (ICP-MS) to measure their iron levels (Methods 2.20). The results showed that M-H broth contains 6.7 μM of iron, while the BHI contains 15.4 μM . DMEM is estimated to contain less than 1 μM Fe, which is extremely iron limited.

The results of the growths in M-H broth show that there is a clear growth reduction for the three mutant strains compared to the wild type, in particular at time points between 24-36 h of incubation (Fig. 5.30A). The degree of growth inhibition was 4-25-fold (at 24 h, the OD_{600} was 0.25 for the wildtype but just 0.06, 0.01 and 0.04 for the Δftr1 , Δcj1660 and Δcj1663 strains, respectively; representing a; 4- ($P=0.001$), 25- ($P=0.001$) and; 6-fold ($P=0.002$), growth reduction with respect to the wildtype) and 1.5-2.5-fold at 36 h (Fig. 5.30A). The Δcj1663 strain displayed the greatest low-iron inhibition with respect to the other mutants with the Δftr1 strain generally showing better low-iron growth than the other two mutants (Fig. 5.30). These findings suggest a role for the product of *ftr1*, as well as those of the downstream *cj1660* and *cj1663* genes (and corresponding genes downstream of the *cat* insertions), under iron deficiency.

Also, in a separate experiment, the number of colonies forming units for each strain was tested under the same conditions at each time point. There was a significant inhibition ($P=0.1$, 0.05 and 0.02 for the *ftr1*, *cj1660* and *cj1663* strains) in the number of the cfu/ml obtained for the mutants compared to the wild type strain at time points 36 and 48 h (8.6 ± 0.6 , 7.3 ± 0.3 , 6.4 ± 0.2 and 6.4 ± 0.15 \log_{10} CFU/ml for the wild type, Δftr1 , Δcj1660 and Δcj1663 strains, respectively at 36 h; Fig. 5.30B).

Growth in M-H broth at 42 °C was higher than at 37 °C in general (by 1.6-fold for the wildtype at 48 h) indicating that *C. jejuni* grow better at this temperature, as shown previously (Wang *et al.*, 1993; Griffiths *et al.*, 1990). The growth inhibition of the mutants was less apparent and was only exhibited at the 24 h time point; the wild type reached an OD₆₀₀ of 1.02 while the mutants achieved 0.54 ($\Delta ftrI$), 0.48 ($\Delta cj1660$) and 0.46 ($\Delta cj1663$) (Fig. 5.30C).

When the cultures were subject to shaking (at 600 rpm) results similar to those without shaking were obtained, although growth progressed more rapidly (Fig. 5.30D). A significant growth inhibition for the mutants with respect to the wild type was seen at the 24 and 36 h time points of 1.7-2.3-fold (24 h; $P > 0.05$) and 2-4-fold (36 h; $P > 0.05$). The $\Delta ftrI$ strain again showed better growth than the $\Delta cj1660$ and $\Delta cj1663$ strains (Fig. 5.30D).

When growth was performed in 50 ml acid-washed flasks with shaking, a significant reduction in growth was again seen for the mutant strains compared to the wild type, which was particularly apparent at 24 (1.7-2 fold; $P < 0.05$) and 36 h (1.5-2 fold; $P < 0.05$) (Fig. 5.30E). The $\Delta ftrI$ strain again showed better growth than the other mutants, with the $\Delta cj1663$ strain again showing the weakest growth.

When growths were attempted in DMEM minimal medium (using conditions otherwise as indicated in Fig. 5.30F), the mutant strains were unable to grow, and the wild type grew weakly to OD₆₀₀ of 0.2 at 36 h (data not show). This effect is presumably related to the very low iron content of DMEM. However, when 20 μ M ferric citrate was added to the medium, good growth of all strains was obtained, and the mutants showed better growth than the wildtype initially (12 h) but weaker growth subsequently (24-48 h). The results showed a clear growth inhibition in the mutants' growth level at time point 36 h $P > 0.05$ (Fig. 5-30F), which was not expected.

In summary, the above results reveal that *ptr1*, *cj1660* and *cj1663* genes have roles in supporting growth in M-H and DMEM medium. This phenotype may relate to the low-iron levels of these media. Addition of iron to DMEM supported growth of all four strains but did not eliminate the growth defect of the mutants, which does not support an iron transport role for the mutated gene products. However, results below (Fig. 5.31) show that provision of iron in M-H medium reverses the growth defect shown in Fig. 5.30A-E, suggesting that the failure of ferric citrate to reverse the growth defect in DMEM is medium-specific.

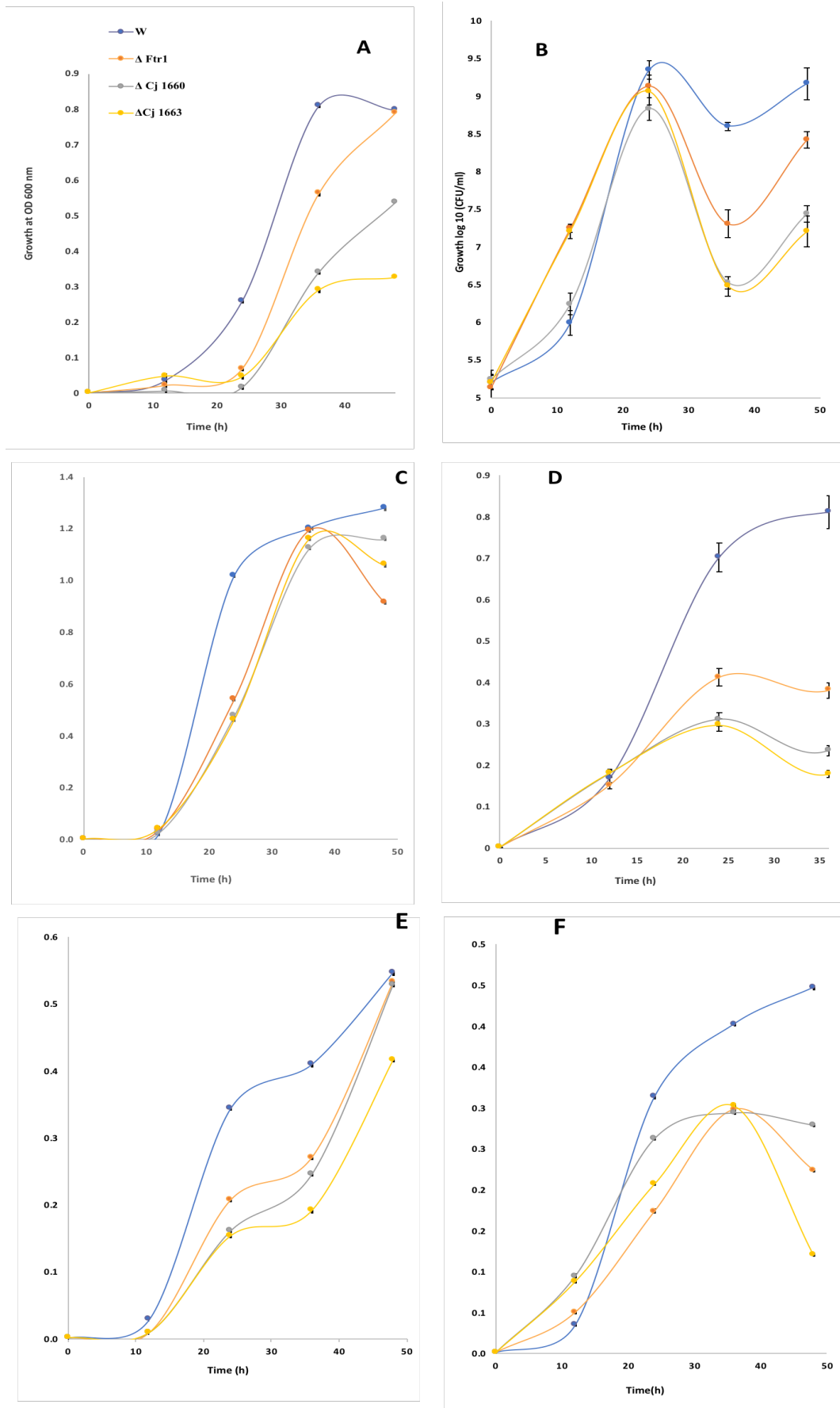


Figure 5.30: Microaerophilic growth comparisons of *C. jejuni* NCTC 11168 mutant and wildtype strains. The strains are wild type, Δ *ftr1*, Δ *cj1660* and Δ *cj1663*. **A.** Growth in microtiter plates without shaking in M-H broth at 37 °C. **B.** As in A, except measurement was in CFU/ml instead of OD. **C.** As in A, except that the incubation was at 42 °C. **D.** As A, except for shaking at 600 rpm. **E.** As in A, except the bacterial cultures were propagated in 50 ml acid washed flasks with 15 ml of M-H broth shaking at 150 rpm. **F.** As in A, except for use of DMEM minimal medium with 20 μ M of ferric citrate instead of M-H broth. Each growth was in triplicate, and the experiment was repeated three times and similar results were obtained. Error bars (very small in some cases) indicate standard deviation.

5.6.2. Growth of the mutant strains in iron-rich media

To determine whether the poor growths of the mutants seen above is reversed by the provision of iron the growth experiments were repeated under iron replete conditions.

When M-H medium was provided with 20 μ M ferric citrate the mutant strains displayed a growth delay with respect to the wildtype but achieved final ODs that were very similar to those of the wildtype (Fig. 5.31A). Also, the CFU levels were very similar at 48 h although significant differences were seen at other time points, with weaker numbers for the wildtype at 12 h (1-1.3 fold) and higher numbers at 36 h (1.1 fold) (Fig. 5.31B). When the growth comparison was performed in shaking 50 ml flasks (with 20 μ M ferric citrate), no notable difference between the mutant strains and wildtype was apparent (Fig. 5.31C), in contrast to the result obtained without iron (Fig. 5.30E). Furthermore, when the iron-rich medium, BHI broth, was used growth comparison the mutant strains grew very similarly to the wild type with similar OD levels being achieved at all time points (Fig. 5.31D).

Overall, these results suggest that high availability of iron in the medium supports the mutant strains to achieve growth levels similar to that of the wild type, and thus reverse the weak growth that obtained in iron-limited minimal medium. This supports the suggested role of the *ftr1-p19* and *cj1660-65* gene products in iron transport. However, growth defects for the mutants were still apparent under some of the high-iron conditions employed (Figs. 5.31A

and 5.31B). This suggests that even under iron-sufficient conditions the FetMPA-F system contributes to iron provision.

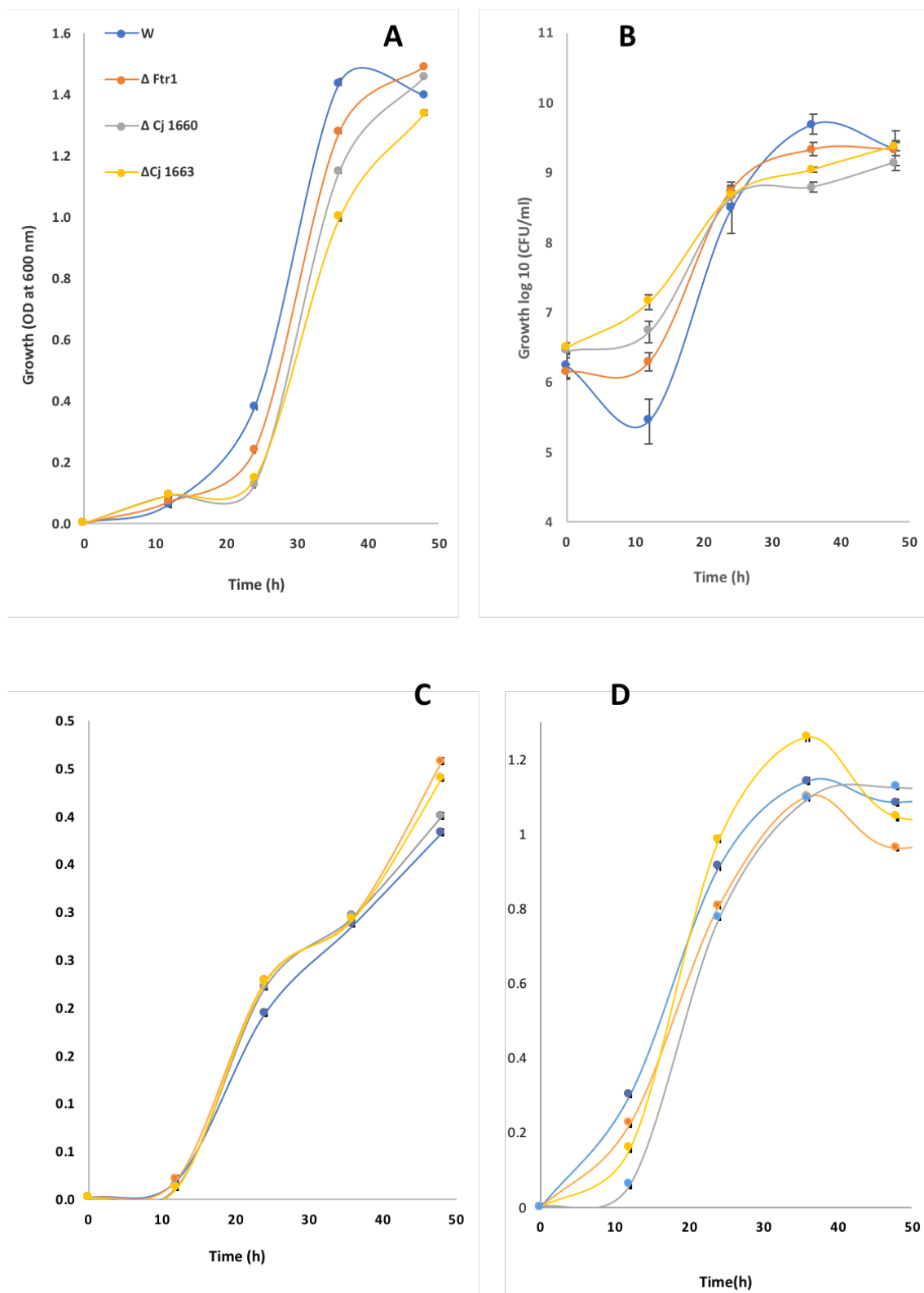


Figure 5.31: Microaerophilic growth of *C. jejuni* NCTC 11168 wild type and mutant strains under iron-rich conditions. The growth was as in Fig. 5.29, unless otherwise indicated. **A.** M-H medium with 20 μ M ferric citrate. **B.** As in A, that CFU/ml was measured. **C.** As in A, except for growth in 15 ml medium in 50 ml acid-washed flasks with continuous shaking at 150 rpm. **D.** As in A, except for growth in BHI broth instead of M-H medium.

5.6.3. Effect of pH on the low-iron growth of the mutant strains

The closely-related *fetMP* system of *E. coli* is reported to display a degree pH dependence in its iron-transport capacity (Koch *et al.*, 2011). Also, the *ftrABCD* system (encoding an Ftr1 homologue) of *Bordetella* shows optimal activity at low pH (Brickman and Armstrong, 2012). The EfeUOB system (also encoding an Ftr1 homologue) of *E. coli* also shows optimal iron-uptake activity at low pH (Cao *et al.*, 2007). Furthermore, experiments with *E. coli* JC32 complemented with the *C. jejuni* P19 system (Chapter 4) showed that the P19 system gives greater low-iron growth at low pH. Thus, the possibility of that $\Delta ftr1$, $\Delta cj1660$ and $\Delta cj1663$ mutants display a stronger low-iron growth phenotype at low pH than at high pH was explored. This was achieved by performing growth comparison experiments in M-H medium as before (Fig. 5.30), but with inclusion of 25 mM MES-HEPES buffer at pH 6, 7 or 8.

Preliminary growth comparisons showed that the mutant strains were unable to grow at pH 5 (data not show) and that the wild type grew very poorly at this pH (no growth at 24 h) (data not shown), so the impact of pH 5 was not further explored. At pH 6, a clear and significant inhibition in the growth of all the three mutants was seen as a compared to the wildtype (Fig. 5.32A). At 24 h the OD₆₀₀ reached of the wildtype was 1.3 whereas the mutant gave OD values of 0.09, 0.06 and 0.05 (for the $\Delta cj1660$, $\Delta ftr1$ and $\Delta cj1663$ strains, respectively), a 14-26-fold difference ($P < 0.05$; Fig. 5.32A). A clear and significant ($P < 0.05$) growth difference was also seen at 36 h with the wildtype reaching an OD of 1.4 but the mutants achieving ODs of just 0.6, 0.4, 0.2 (for the $\Delta cj1660$, $\Delta ftr1$ and $\Delta cj1663$ strains, respectively). Interestingly, the mutants showed an extended growth lag (of ~20 h) at pH 6 with little growth seen before 24 h (Fig. 5.32A).

At pH 7, a significant growth reduction for the mutant strains compared to the wildtype was also seen, but this was less than at pH 6 (Fig. 5.32B). At time point 24 h there was a clear inhibition in the growth of all the mutants: the wildtype reached an OD of 1.3 whilst the

mutants achieved OD values of 0.21, 0.26 and 0.41 (for the $\Delta cj1663$, $\Delta ftr1$ and $\Delta cj1660$ strains, respectively), representing a significant ($P < 0.05$) 3-6 fold growth reduction. At 36 h the $\Delta ftr1$ and $\Delta cj1660$ strains has recovered to achieve growth similar to the wildtype (although the $\Delta cj1663$ mutant still lagged behind) and by 48 h, all four strains displayed very similar OD values (Fig. 5.32B). This observation suggests that the mutants were able to obtain sufficient iron to support growth at pH 7, but did so less efficiently than the wildtype, hence the delayed growth. It should be noted that the mutants still possess other modes of iron uptake, in particular FeoAB, which could support iron uptake under low-iron conditions. The average growth lag seen for the mutants at pH 7 was ~12 h, which is considerably less than that seen at pH 6 (~20 h).

At pH 8, a significant ($P = 0.002, 0.005, 0.002$) growth reduction (1.5-, 3.6- and 5.5-fold for the $\Delta cj1660$, $\Delta ftr1$ and $\Delta cj1663$ mutants, respectively) was still observed for the three mutants at 24 h (Fig. 5.32C). However, the growth of the $\Delta ftr1$ and $\Delta cj1663$ mutants appeared more greatly affected than that of the $\Delta cj1660$ mutant (Fig. 5.32C), with weaker growth also seen at 36 h for the $\Delta ftr1$ and $\Delta cj1663$ mutants, whereas the $\Delta cj1660$ mutant showed similar growth to the wild type for all time points other than 24 h (Fig. 5.32C). The average growth lag at pH 8 for the three mutants (cf. the wildtype) was 10 h, which is shorter than that seen at pH 6 and 7.

In summary, the data above indicate a stronger phenotype for the mutants at pH 6 than at pH 7 or 8, with average growth differences (cf. the wildtype) at 24 h of 26-fold, 4.3-fold and 3-fold at pH 6, 7 and 8, respectively. The main impact of pH on the mutant strains appears to be an extended lag phase. Interestingly, the $cj1660$ mutant showed better growth than in the other two, particularly at pH 8. However, the $cj1663$ mutant continued to give the lowest overall growth. It was noted that the degree of growth achieved with buffer was generally

greater than that achieved without buffer (Fig. 5.30), indicating that the provision of buffer did not negatively impact growth of the *C. jejuni* strains employed.

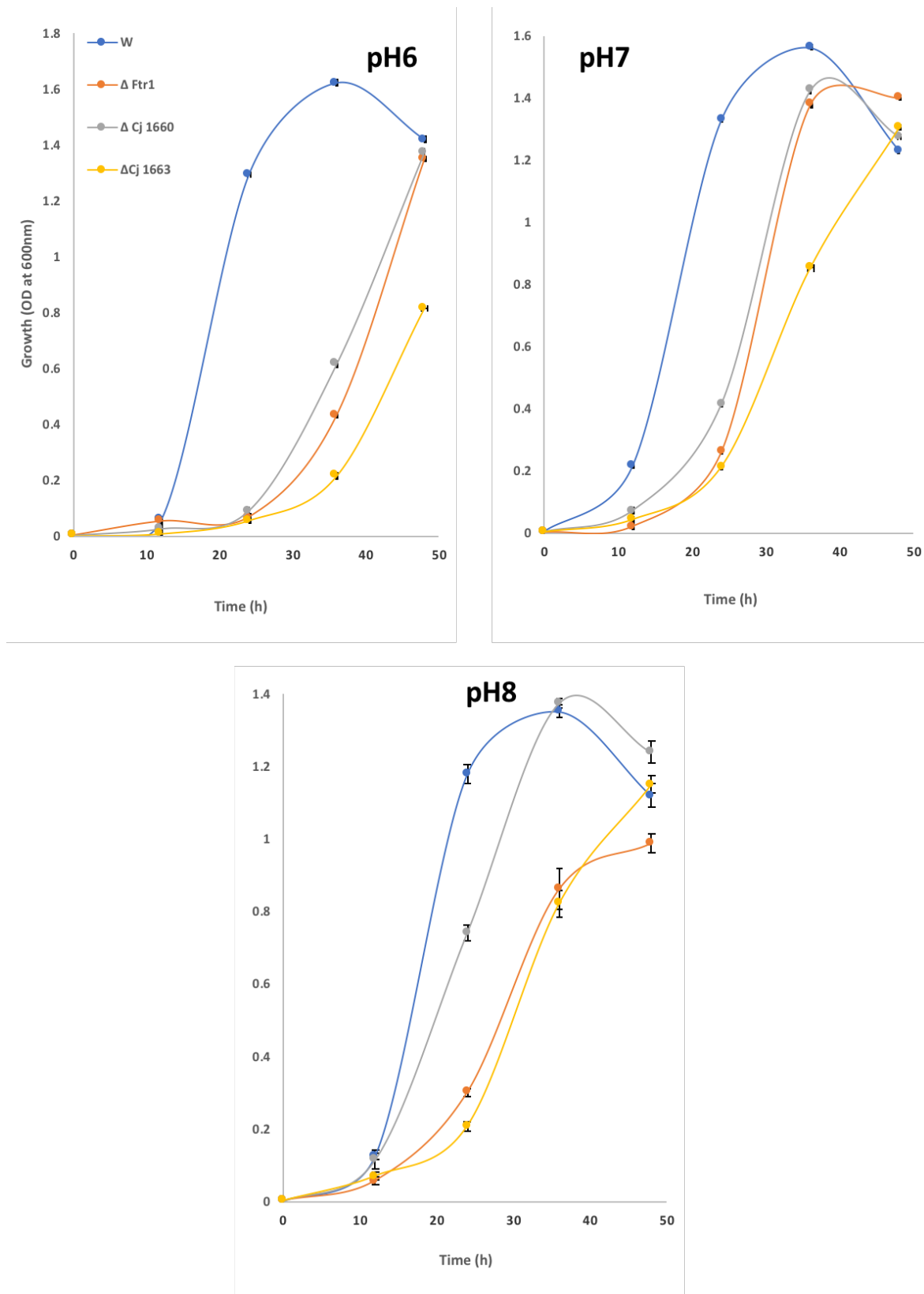


Figure 5.32: Microaerophilic growth curve of the *C. jejuni* NCTC 11168 wildtype and mutant strains in M-H broth medium buffered at pH 6, 7 and 8 with 25 mM MES-HEPES. The strains are wild type, $\Delta ftr1$, $\Delta cj1660$ and $\Delta cj1663$, this curve from growth in microtiter plate 96 wells without

shaking, four plates prepared at the same time, one for each time point. Each growth was in triplicate, the experiment was repeated for three times. Error bars indicate standard deviation and they are very small to be seen in some cases.

5.6.4. Growth of the mutant strains with iron chelator and iron reductant

Previous results showed equivalent growth of the *C. jejuni* mutant and wildtype strains in BHI broth, where iron levels are relatively high (15.4 μM). To determine whether the provision of an iron chelator could induce a growth phenotype for the mutants in BHI by lowering iron availability, the experiment shown in Fig. 5.30D was repeated in the presence of the ferric chelator, desferrioxamine (DFO), at 10 and 20 μM . DFO was used in a previous study as an iron chelator to show a growth defect in a $\Delta p19$ *C. jejuni* mutant strain in M-H medium with DFO at 16 μM (Chan *et al.*, 2010). However, the results in the experiments reported in this thesis showed a growth defect in M-H medium without DFO. When DFO was applied to BHI medium a general three-six fold growth inhibition for all the *C. jejuni* strains (wild type and the mutants) was observed with respect to the DFO-free control (see Fig. 5.31D), with \sim twofold lower growth at 20 than at 10 μM DFO (Fig. 5.33). However, no major difference in growth between the wild type and the mutant strains was observed (Fig. 5.33). This difference in the effect of DFO seen here with respect to that observed previously (Chan *et al.*, 2010) likely reflects the media employed, BHI being more iron rich, and M-H being iron poor (15.4 and 6.7 μM Fe, respectively).

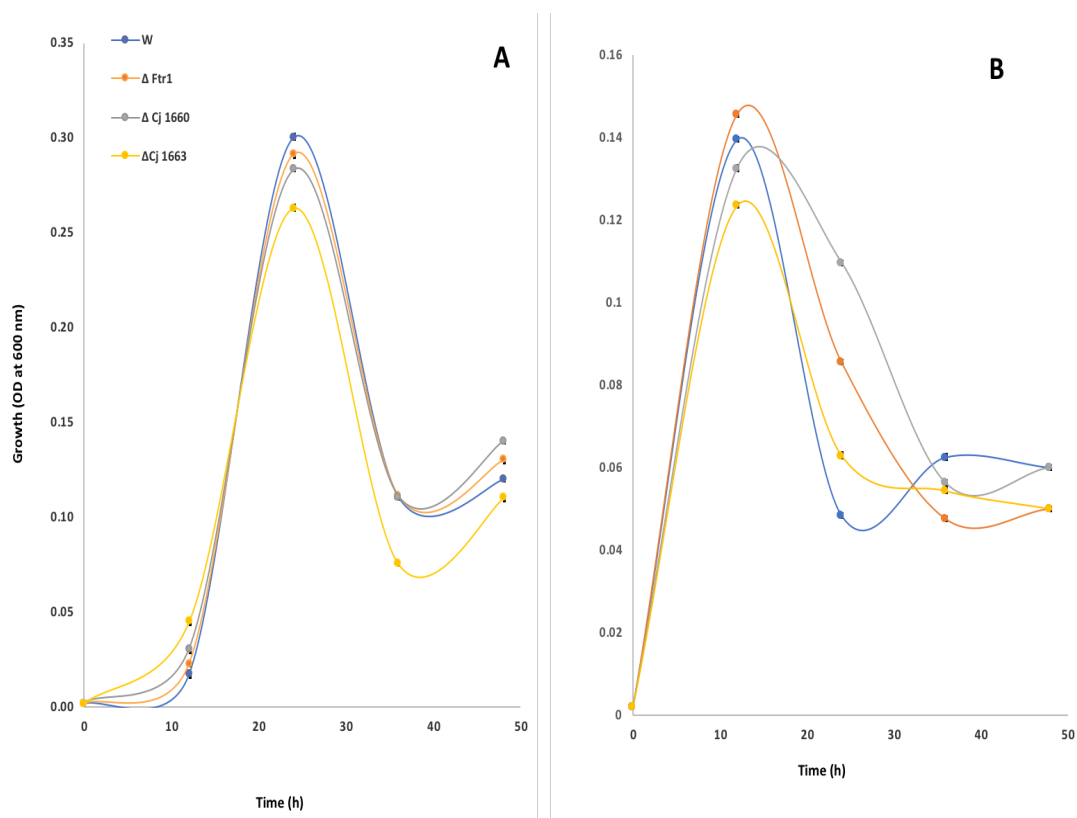


Figure 5.33: Microaerophilic growth of *C. jejuni* in BHI broth medium with desferrioxamine chelator. A. 10 μ M DFO. B. 20 μ M DFO. The strains were wild type, and the $\Delta ftr1$, $\Delta cj1660$, and $\Delta cj1663$ mutants of *C. jejuni* NCTC 11168. Experiment was performed as in Fig. 5.30D except for the inclusion of DFO. Each growth was in triplicate, the experiment was repeated three times and similar results were obtained. Error bars indicate standard deviation.

The possibility that the presence of reductant might impact the growth phenotype of the mutant strains was also investigated. It was hypothesised that provision of ascorbate would promote the production of ferrous over ferric iron, which would support FetMPA-F dependent iron uptake if the system is ferrous-iron specific (as is expected) but would have the opposite effect if the transporter is ferric-iron specific. Thus, growth comparisons were performed, as in Fig. 5.30A, in M-H medium with 5- or 10-mM ascorbate (Fig. 5.34).

The addition of ascorbate caused a clear growth inhibition for all four strains with respect to the no-addition control (Fig. 5.30A) with the degree of inhibition similar at 10- and 20-mM ascorbate (Fig. 5.34). For the wildtype, the degree of growth reduction with ascorbate was

~threefold. No notable growth differences were observed between the wildtype and the $\Delta ftr1$ and $\Delta I660$ mutants, however the $\Delta cj1663$ mutant displayed a clear disadvantage with respect to the wildtype, at both 10 and 20 mM ascorbate, which was particularly apparent at 36 h (Fig. 5.34), where an ~2.5-fold growth difference was seen for the $\Delta cj1663$ strain with respect to the other strains ($P < 0.05$).

The reason for the lack of growth phenotype for the $\Delta ftr1$ and $\Delta I660$ mutants with addition of ascorbate is unclear, but this would be consistent with the use of ferric iron, rather than ferrous iron, as preferred substrate by the FetMPA-F system (although this is unexpected given the known preference of the Ftr1p/Fet3p system for ferrous iron). This effect might also arise as a result of iron-uptake becoming more strongly FeoAB dependent in the presence of reductant, since FeoAB activity would be expected to be supported by reductant-mediated conversion of ferric to ferrous iron. The difference in growth phenotype for the $cj1663$ mutant and the $ftr1$ and $cj1660$ mutants was also unexpected. The $cj1663$ specifies a component of a putative extra-cytoplasmic mechanotransducer with a speculated role in membrane insertion/release for the periplasmic thioredoxin proteins, Cj1664/5 (Chapter 3). Thus, it has a possible role in supporting periplasmic redox reactions. One possibility explanation for the weak growth of the $cj1663$ mutant, is that this is caused by aberrant iron-uptake activity of the FetMP system (under reducing conditions) as a result of lack of Cj1663 activity. Such an effect might arise if the Cj1663 protein is required to assist in the disposal of electrons during the proposed ferrous-oxidation-driven iron-uptake process mediated by Ftr1-P19, particularly under the conditions used where reduction by ascorbate might limit the availability of alternative electron acceptors for electron disposal.

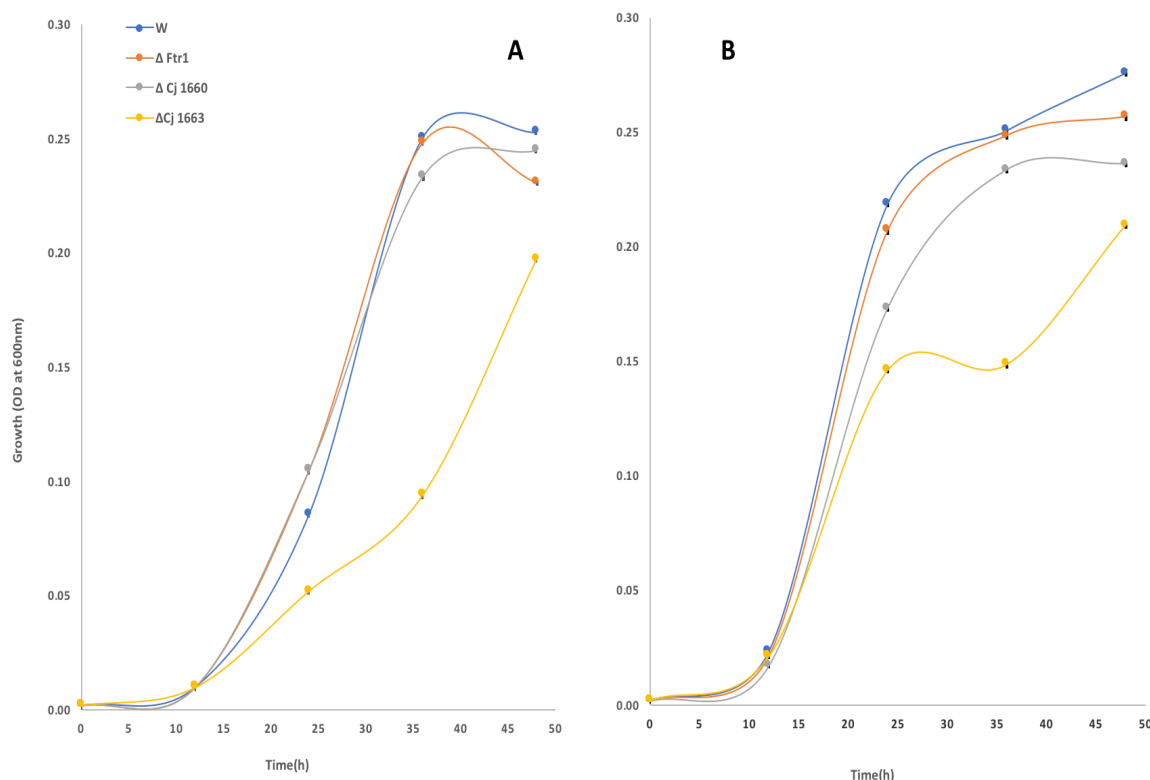


Figure 5.34: Microaerophilic growth of *C. jejuni* in M-H broth medium with ascorbate. A. 5 mM ascorbate B. 10 mM ascorbate. Conditions were as in Fig. 5.29A except for the presence of ascorbate as indicated. Each growth was in triplicate, the experiment was repeated two times and similar results were obtained. Error bars indicate standard deviation and $P < 0.05$ between the wild type and $\Delta cj1663$ at time point 36 h.

5.7. Genetic complementation

In order to confirm that the mutant phenotypes observed above are indeed caused by the specified $\Delta ftr1$, $\Delta cj1660$ and $\Delta cj1663$ mutations, the mutant strains (and wildtype) were complemented with pMA1-*ftr1-p19* or pMA1-*cj1660-65*. In addition, the mutants and wildtype were transformed with the vector, pMA1, to provide suitable non-complemented controls for comparison purposes.

The growth comparison was performed in M-H medium using static, 96 well microtiter plates under microaerobic conditions at 37 °C, as in Fig. 5.30A, but antibiotic was included in all cases (25 μ g/ml Kanamycin). The complementing plasmids (pMA1-*ftr1-p19* or pMA1-

cj1660-65) considerably improved the growth of all four strains (including wildtype) in M-H medium (Fig. 5.35), such that growth of the complemented wildtype and mutants was similar. However, the pMA1 vector control appeared to have little impact on growth of the wildtype and mutant strains (Fig. 5.35). This effect is illustrated by comparing the OD values of the wildtype with pMA1-*cj1660-5* (1.3) or with pMA1 (0.22) where a ~six-fold difference is apparent (Fig. 5.35C). The reason for this effect is unclear, but it suggests that raising the copy number of the *ftr1-p19* or *cj1660-5* genes supports growth in low iron M-H medium. The *ftr1* mutant showed a twofold lower growth than the wildtype at 36 h (Fig. 5.35A), but upon complementation with pMA1-*ftr1-p19* this was reduced to just 1.15-fold. The *cj1660* and *cj1663* mutants showed a 2.3 and 2-fold lower growth than the wildtype at 36 h (Fig. 5.35BC), but this was reduced upon complementation with pMA1-*cj1660-5* to no difference or a 1.2-fold lower growth. The results therefore suggest that complementation was achieved.

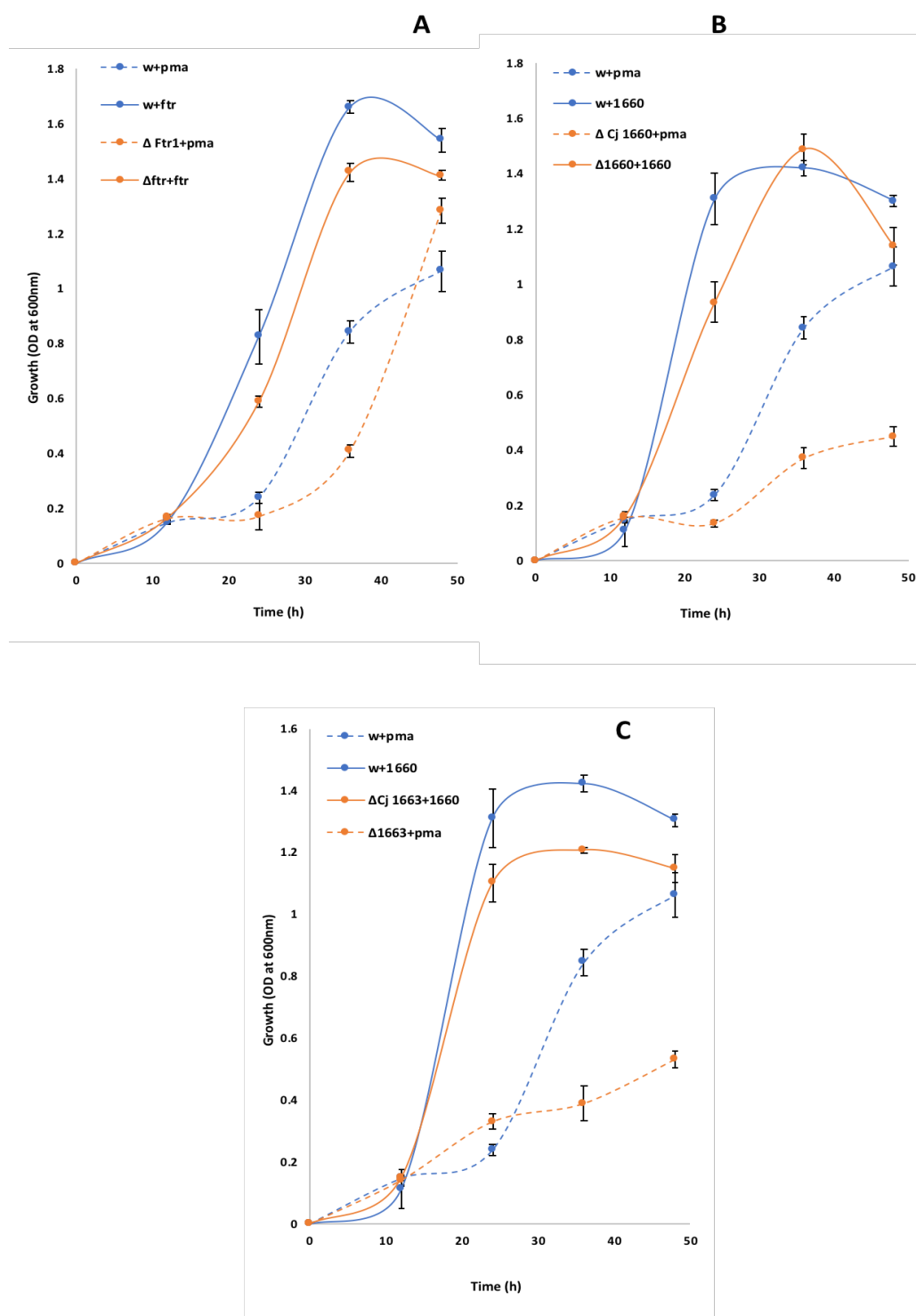


Figure 5.35: Complementation of the *C. jejuni* NCTC 11168 mutants with plasmid-borne *ftr1-p19* or *cj1600-5*. Each growth was in triplicate, and the experiment was repeated for three times with similar results. Error bars indicate standard deviation. Conditions were as in Fig. 5.29A (37 °C, microaerobic, M-H medium, 96 well plates, static) except for the strains employed. **A.** $\Delta ftr1$ mutant or wildtype with pMA1 or pMA1-*ftr1-p19*. **B.** $\Delta cj1660$ mutant or wildtype with pMA1 or pMA1-*cj1660-65*. **C.** The $\Delta cj1663$ mutant or wildtype with pMA1 or pMA1-*cj1660-65*. $P < 0.05$ between each mutant and its complemented strain.

5.8. Discussion

In this chapter, mutations in three (*ftr1*, *cj1660* and *cj1663*) of the eight genes of the *ftr1-p19/cj1660-5* cluster were generated in the genome of *C. jejuni* NCTC 11168 by replacement of central fragments with an antibiotic resistance cassette. These mutations are likely to cause polarity effects on co-transcribed downstream genes, and thus the phenotypes observed could partly be the result of loss of expression of downstream genes within the cluster. Growth studies in iron-deficient M-H medium showed a clear and significant reduction in the growth of the mutants with respect to the wildtype in M-H medium, particularly between 24 and 36 h, suggesting role of the Ftr1-p19 and associated FetA-F system as an iron transporter supporting growth under iron-limited conditions. Addition of ferric citrate largely reversed the growth phenotypes in M-H medium, supporting the designation of the Ftr1-p19/FetA-F system as an iron transporter. The results here support findings of previous work showing that inactivation of the *p19* gene in *C. jejuni* 81-176 results in growth reduction in M-H medium with DFO as iron chelator (Chan *et al.*, 2010). In iron-rich media (BHI and M-H with ferric citrate) no notable growth phenotype was observed for the three mutants with respect to the wildtype. This is consistent with results of the previous chapter which showed that the Ftr1-p19/FetA-F system supported growth of *E. coli* JC32 under low-, but not high-iron conditions.

The impact of pH (6-8) on the growth phenotype of the mutants was assessed using M-H broth buffered with 25 mM MES-HEPES. This showed that the low-iron growth defect of the mutants was more pronounced at pH 6, than at pH 7 or 8; unfortunately the mutants failed to grow at pH 5 and the wildtype grew poorly at this pH, so it was not possible to compare low-iron growth at pH 5. The main impact of low-iron growth at pH 6, cf. pH 7-8, was an extended lag phase for the mutants. This suggests that the Ftr1-p19/FetA-F system provides a more important function in iron uptake under acidic than neutral or basic conditions. This is

of relevance to the environment of the chicken cecum where *C. jejuni* resides as the pH is considered acidic (pH 5.5-6; van der Wielen *et al.*, 2000) as well as microaerophilic. A role for *p19* and its associated components in the acid tolerance in *C. jejuni* has been suggested as the *p19* gene was shown to be induced ~fourfold by acidity (pH 5.2/5.7) in one study (Birk *et al.*, 2012), and the *p19*, *cj1660* and *cj1662-3* genes were shown to be 4-6 fold up regulated by exposure to pH 5.5 in another study (Varsaki *et al.*, 2015). The CfbpABC iron-transport system was also found to be acid induced, suggesting a Fur-dependent low-pH induction mechanism (Varsaki *et al.*, 2015). Since acidic pH allows stability of ferrous iron against oxidation in the presence oxygen (Widdel *et al.*, 1993), the low pH preference of the *p19* system supports its presumed role as a ferrous-iron transporter, and its reported induction by low pH resembles the low pH induction reported for related EfeUOB system of *E. coli* (Cao *et al.*, 2007).

DFO (ferric chelator) addition to BHI broth failed to reveal a phenotype for the mutant strains, although a major growth reduction was obtained for all strains suggestive of an iron restriction effect induced by DFO. This indicates that the Ftr1-*p19*/FetA-F system is not required for low-iron growth under the conditions employed, although the reason for this is unclear and so requires further investigation. Addition of ascorbate to M-H medium reversed the growth phenotype of the *ftr1* and *cj1660* mutants. This was considered to be potentially due to raised provision of ferrous iron which might support FeoAB activity and thus diminish the need for Ftr1-*p19*/FetA-F. Interestingly, the *cj1663* mutant phenotype was retained under low-iron with ascorbate, revealing a distinct phenotype difference with respect to the *ftr1* and *cj1660* mutants. The reason for this difference is unclear but it is speculated that it may relate to aberrant and deleterious Ftr1-P19 iron-uptake function caused by the absence of Cj1663.

Complementation of the mutant strains was achieved using the pMA1 plasmid. The growth comparison results in M-H broth showed that the complemented $\Delta ftr1$, $\Delta cj1660$ and $\Delta cj1663$

strains grew more similarly to the complemented wildtype than did the mutants and wildtype treated with vector control, indicating that complementation had been achieved. There was an unexpected enhanced growth for the mutants and wildtype carrying the *ftr1-p19* or *cj1660-5* genes in multicopy. This suggests that raised *ftr1-p19* or *cj1660-5* gene copy number supports low-iron growth in M-H medium through raising iron-transport capacity.

In summary, the results provided in this chapter indicate that the Ftr1-p19 system functions as an iron transporter and that the associated Cj1660-1665 components are also required for this function. The *cj1663* mutant generally gave a more extreme low-iron growth phenotype than the other mutations, further suggesting that the eight genes of the cluster contribute to a single iron-uptake pathway for *C. jejuni* in which Ftr1, P19, Cj1660 and Cj1663 all play essential roles.

Chapter 6: Gut colonisation with *C. jejuni* in chicken

6.1. Introduction

Studies on *C. jejuni* pathogenicity were restricted due to the difficulty in identifying the suitable animal models that can easy use and be representative of infection in the humans (Newell, 2001). An early attempt to study the virulence of *C. jejuni* and *C. coli* was with 11-day old chicken embryos by inoculation into the chorioallantoic membrane, using 50% lethal doses, with infection calculated after 72 h (Field *et al.*, 1986). Also, inoculation of one day old chicks with 5×10^8 *C. jejuni* in PBS was another early study on colonisation and showed colonisation of the cecum after seven days post infection (10^{4-7} CFU/g) (Beery *et al.*, 1988). The chicken model is used to study risk factors associated with infection of *C. jejuni* in humans because the chicken is considered the main and natural source of human infection (Wingstrand *et al.*, 2006; EFSA, 2010) with ~80% of human infections deriving from chicken as the reservoir source (Hermans *et al.*, 2011). Consumption and handling of contaminated chicken meat during slaughter and processing is considered as a main cause of transmission of this pathogen to humans (Berrang *et al.*, 2001; EFSA, 2010). Initially, *C. jejuni* colonises the caeca and large intestine. However, it can colonise the small intestine or extra-intestinal organs like the liver, but this varies between different isolates of *C. jejuni* (Beery *et al.*, 1988; Humphrey *et al.*, 2015).

Newly hatched chickens are usually *C. jejuni* free which enables assessment of the colonisation ability of *C. jejuni*. The chicken model is thus used to understand the factors that affect *C. jejuni* colonisation and host infection, and has been used to estimate the importance of ferrous iron acquisition in *C. jejuni* pathogenesis and colonisation in NCTC 11168, 81-176 and ATCC 43431 strains (Naikare *et al.*, 2006; Gaynor *et al.*, 2004; Jones *et al.*, 2004; Byrne *et al.*, 2007).

Therefore, the chicken was chosen to study the role of the P19 system in *C. jejuni* colonisation *in vivo* as a model for humans to test the capacity of the mutant strains generated here to colonise the caecum. The *C. jejuni* PT14 mutants were made at Reading, while, the colonisation and sample collection were performed by Prof Ian Connerton group (Food Sciences, University of Nottingham), with assistance from myself during the sample collection days (days 3 and 7 post infection). Since these mutants were generated originally in *C. jejuni* NCTC 11168, a strain which is a poor coloniser in chickens compared to other *C. jejuni* strains (Gaynor *et al.*, 2004), another strain of *C. jejuni* with high colonisation capacity in the chicken cecum was used for the gut colonisation trial. The strain (*C. jejuni* PT14) was obtained from Prof Ian Connerton (Food Sciences, University of Nottingham) and was originally isolated from infected chicken gut and is noted for its high motility. The three plasmids that carry the inactivated genes (pJET- Δ *ptr1*, pJET- Δ *cj1660* and pJET- Δ *cj1663*) were introduced into highly-motile, wild type isolates of *C. jejuni* PT14 by electroporation and their identity was confirmed genotypically by PCR and phenotypically by growth curve comparison in M-H broth. The high motility of the mutants thus generated was then confirmed on soft agar plates (Methods 2.18.3). The chicken gut colonisation experiment was as described in Methods 2.21 and was performed University of Nottingham (Sutton Bonington Campus, Division of Food Sciences) in collaboration with Professor Ian Connerton. The chickens were screened for absence of *Salmonella* and *Campylobacter* before starting the experiment.

6.2. Generation of the mutations in *C. jejuni* PT14

The motility of *C. jejuni* NCTC and PT14 strains was tested to ensure that the PT14 strain used for mutation was suitably motile, as low motility strains are considered to be poor colonisers (personal communication, Ian Connerton). The strains were subcultured (Method 2.18.3) in fresh M-H broth until an OD₆₀₀ of 0.2 was achieved. The bacteria were then

harvested and resuspended in fresh medium to give an OD of 1.0. The centres of duplicate M-H 0.4% agar plates were stabbed with 5 μ l of each culture and after 48–72 h of microaerobic incubation at 37 °C, the radius of the growth zone from the centre to the edge was measured with a ruler (Kalmokoff *et al.*, 2006). The results showed that a clear difference between the two strains. While the radius of growth zone was about 5 mm for *C. jejuni* NCTC 11168 strain, it was about 30 mm for PT14 strain (Fig. 6.1). Thus, the PT14 strain was used to regenerate the mutations to provide mutant strains suitable for chicken colonisation.

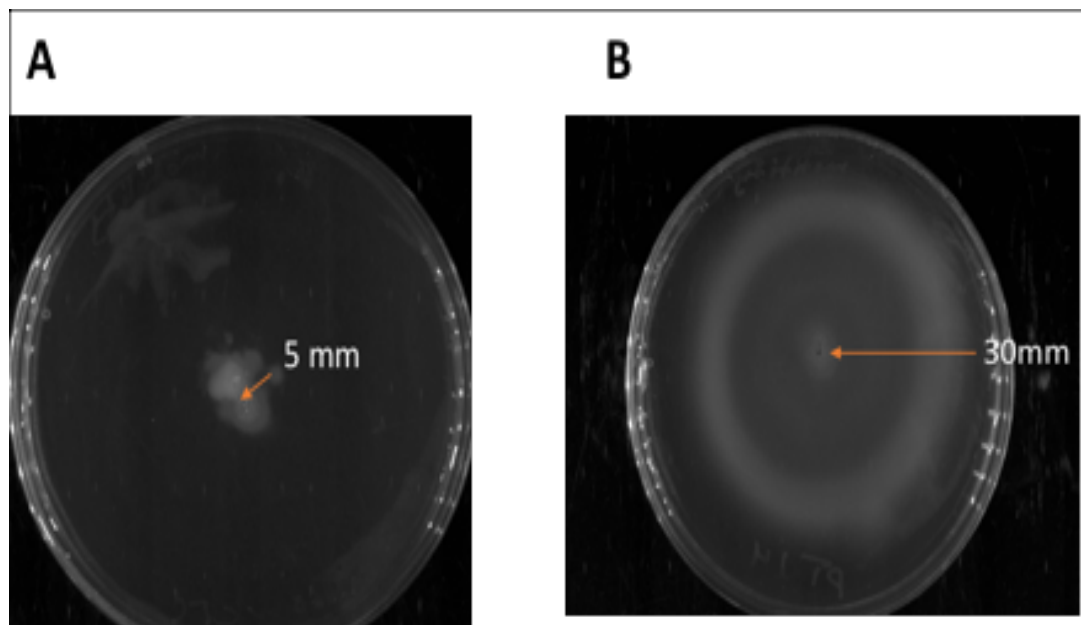


Figure 6.1.: Zones of growth for *C. jejuni* NCTC 11168 on 0.4% agar M-H plates. A. NCTC 11168 strain, the radius of the zone is about 5 mm. **B.** PT14 strain, the radius of the zone about 30 mm.

The process for mutant construction was exactly as described in the preceding chapter, and the PCR confirmations of the mutations in PT14 are shown below (Fig. 6.2-6.4).

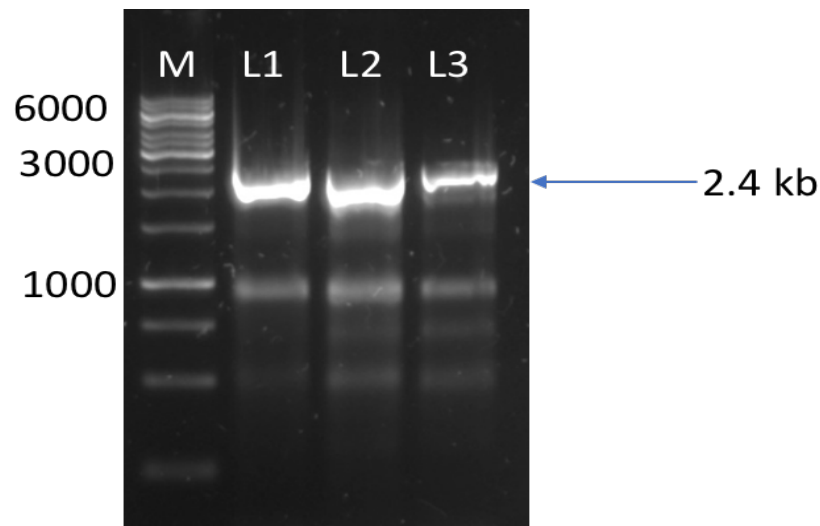


Figure 6.2: Gel electrophoresis of the PCR amplification product of the $\Delta fir1::cat$ mutation in *C. jejuni* PT14. L1, L2 and L3, PCR products of three $\Delta fir1$ isolates. PCR employed the *fir1* F primer and the *cat* gene R primer; the expected fragment size (2.4 kb) was obtained.

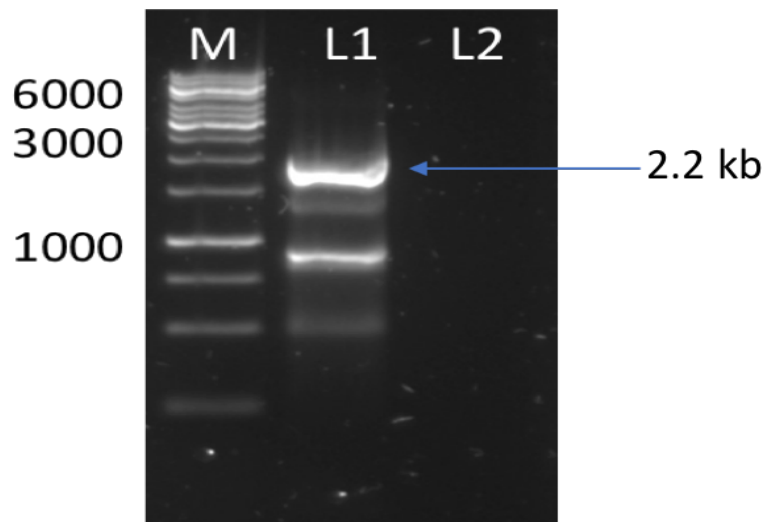


Figure 6.3: Gel electrophoresis of the PCR amplification product of the $\Delta cj1660::cat$ mutation in *C. jejuni* PT14. L1, PCR product of a $\Delta cj1660$ isolate; L2, wild type. PCR employed the *cj1660* F and *cat* gene R primers, the expected size (2.2 kb) was obtained. Several other isolates were also identified (data not shown).

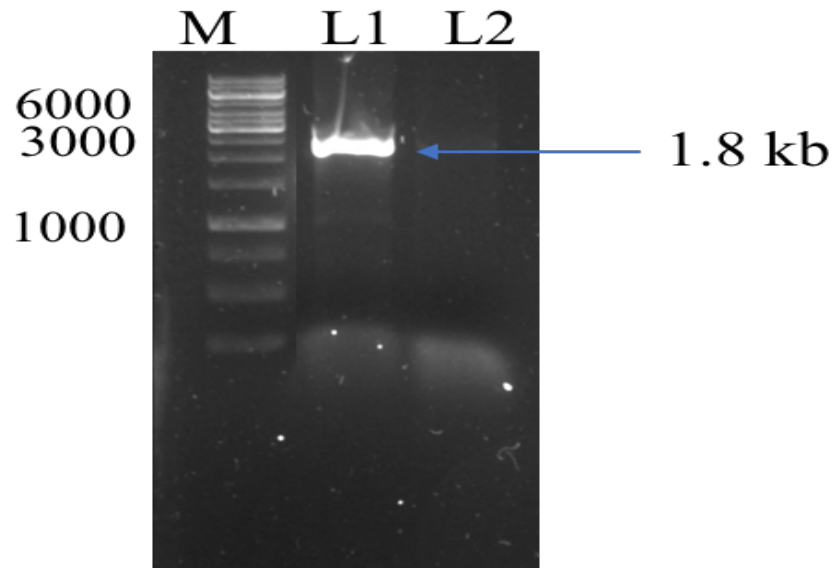


Figure 6.4: Gel electrophoresis of the PCR amplification product of the $\Delta cj1663::cat$ mutation in *C. jejuni* PT14. L1, PCR product of a $\Delta cj1663$ isolate; L2, wild type. PCR employed the *cj1663* F and *cat* gene R primers, the expected size (1.8 kb) was obtained. Several other isolates were also identified (data not shown).

The motility test was also performed for the mutant strains obtained above which showed that the mutants (PT14 $\Delta ftr1$, $\Delta cj1660$ and $\Delta cj1663$) had retained their high-motility status with growth zones on soft agar of between 25-30 mm (Fig. 6.5).

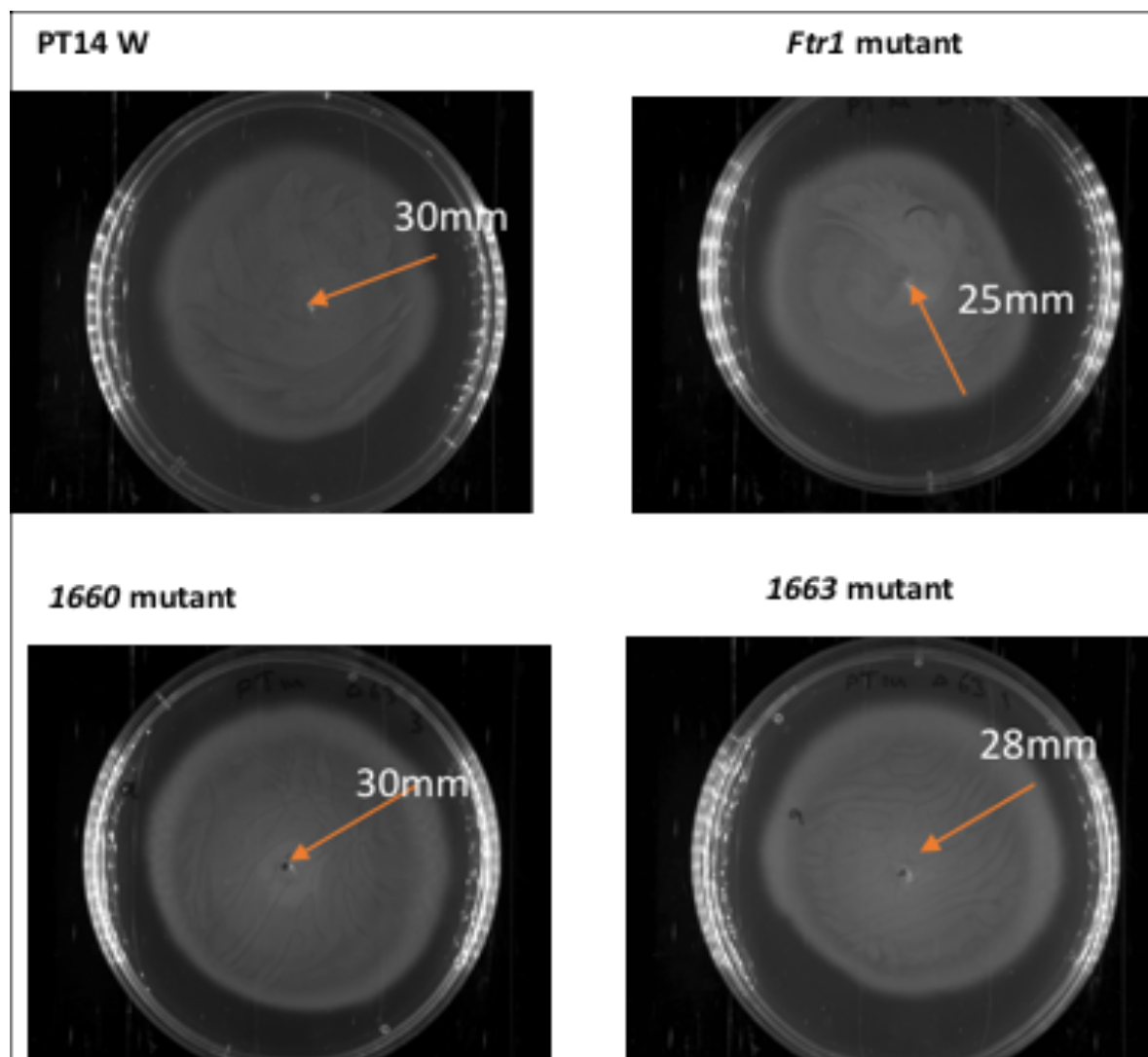


Figure 6.5: Zones of growth for *C. jejuni* PT14 mutant strains on 0.4% agar M-H plates. *C. jejuni* PT14 wild type, and PT14 $\Delta ftr1$, $\Delta cj1660$ and $\Delta cj1663$ strains showing radius of growth zones.

6.3. PT14 mutant phenotypes

In order to confirm that the PT14 $\Delta ftr1$, $\Delta cj1660$ and $\Delta cj1663$ mutant strains exhibit the low-iron growth phenotype observed in the NCTC 11168 mutant strains, a growth comparison was performed under the same conditions used previously. Growths were in M-H broth at 37 °C, under microaerobic conditions, and a starting OD₆₀₀ of 0.002, in 96-well static microtitre plates (Method 2.18.4). The results showed that there is a significant reduction in the growth of the three mutant strains compared to the wildtype, particularly at the 24 h time point (Fig. 6.6). At 24 h, the wildtype achieved an OD of 0.75 while the $\Delta ftr1$, $\Delta cj1660$ and

$\Delta cj1663$ mutants achieved ODs of just 0.04, 0.04 and 0.16, respectively. These differences are significant (P values of 0.05, 0.05 and 0.09). At 36 h the OD₆₀₀ of the $\Delta ftr1$ and $\Delta cj1660$ mutants (0.85 and 0.86) remained significantly lower (P 0.06 and 0.05) than that of the wildtype (1.4) although the $\Delta cj1663$ mutant had an OD (1.3) similar to that of the wildtype at this time point (Fig. 6.6). By 48 h, the mutants had all achieved OD levels similar to that of the wildtype indicating that the growth differences seen represent a delay in growth (extended lag), as was observed for the NCTC 11168 mutants in Chapter 5. Thus, the growth phenotype for the PT14 mutants in M-H medium is similar to that seen for the NCTC 11168 mutants.

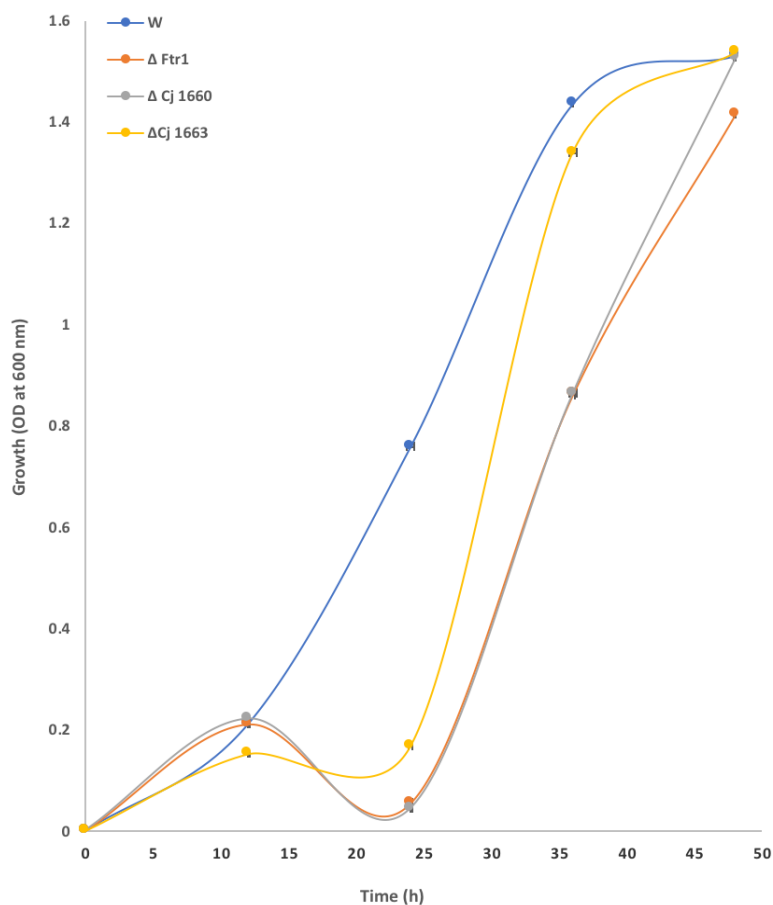


Figure 6.6: Microaerophilic growth of *C. jejuni* PT14 mutants in M-H medium at 37 °C. The strains are *C. jejuni* PT14 strains: wildtype and $\Delta ftr1$, $\Delta cj1660$, and $\Delta cj1663$ mutants. Each growth was in triplicate, the experiment was repeated two times and similar results were obtained. Error bars indicate standard deviation.

6.4. The chicken trials

A total of 64 male 308 Ross broiler chickens were obtained as one-day-old chicks from a commercial hatchery (PD Hook; UK) and reared under bio-secure conditions. Chicks were co-housed in pens with a bedding of wood shavings. A 12-h light-dark cycle was followed for the duration of rearing. Temperatures were as outlined in the Code of Practice for the Housing and Care of Animals Bred, Supplied or Used for Scientific Purposes, with minor adjustments made as guided by bird thermoregulatory behaviour. Standard commercial broiler diets (starter, grower, and finisher) were used. Cloacal swabs were taken at day 13 and tested for *Campylobacter* by direct plating on CCDA and *Salmonella* by enrichment; all were found to be *Campylobacter*- and *Salmonella*-free.

At day 8, the chickens were split into four groups (1-4) of 16 (one per test strain); which were further split into two groups (i and ii, corresponding three- and seven-day infection groups) of eight for co-housing in pens. Before inoculation, one of the eight chickens in each group was separated and housed individually to act as an infection-free control. It should be noted that chickens are ‘coprophagic’ (faeces-eating) and so co-housing supports a shared microbiota and cross infection (Newell & Fearnley, 2003). At day 20, the chickens were infected with $\sim 7 \log_{10}$ CFU of one of the four test strains by the oral gavage method. Groups (a) and (b) were sacrificed at 3- and 7-days post-infection (dpi), respectively, and caecal, ileum and jejunum contents individually removed for quantitation of viable *C. jejuni* on mCCDA agar. Caecal contents and intestinal tissue were also stored at -80°C for future metagenomics/cytokine analysis (not as yet completed). See Methods 2.21 for further detail.

6.4.1. Variation in the efficiency of chicken colonisation by the *C. jejuni* strains

6.4.1.1. 3 dpi. The CFU count of the recovered for the collected caecal contents of the infected chicken after 3 dpi showed a low level of colonisation in group 2 ($\Delta ftr1$), group 3

($\Delta cj1660$) and group 4 ($\Delta cj1663$) in general, in comparison to group 1 (the wildtype) after three-day post infection (Fig. 6.7A). For group 2 ($\Delta ftr1$), one inoculated chicken (no. 7) showed no *C. jejuni* recovery from the chicken caecum at 3 dpi. All but one of other $\Delta ftr1$ -inoculated chickens showed very low colonisation levels with values below $5.0 \log_{10}$ CFU/g whereas only one wildtype-inoculated chicken gave colonisation values above 5.0. The mean colonisation level with the $\Delta ftr1$ mutant was $4.62 \log_{10}$ CFU/g which is significantly ($P=0.02$) lower than that (6.95) obtained for the wildtype. It should be noted that one $\Delta ftr1$ -inoculated chicken (no. 6) showed a high colonisation level, compared to the wild type, of $9.39 \log_{10}$ CFU/g.

For group 3 ($\Delta cj1660$), three inoculated chickens showed no *C. jejuni* colonisation and all but one of the other chickens showed relatively low *C. jejuni* colonisation with colonisation levels below $5.0 \log_{10}$ CFU/g. The average colonisation level was $4.13 \log_{10}$ CFU/g which was significantly lower than that ($6.92/6.95$) of the wildtype ($P=0.01$).

For group 4 ($\Delta cj1663$), one chicken showed no sign of *C. jejuni* colonisation and four out of seven had colonisation levels below $5.0 \log_{10}$ CFU/g. The mean colonisation level was $4.86 \log_{10}$ CFU/g which again is significantly ($P=0.01$) lower than that of the wildtype ($3-4 \log_{10}$ CFU/g). Thus, it can be concluded that the three mutant strains ($\Delta ftr1$, $\Delta cj1660$ and $\Delta cj1663$) poorly colonised the gut of chickens with respect to the wildtype within the short period of infection corresponding to 3 dpi. The average fold differences (cf. the wildtype) in colonisation levels observed at 3 dpi were: 2.32 , 2.79 and $2.06 \log_{10}$ for the $\Delta ftr1$, $\Delta cj1660$, and $\Delta cj1663$ mutants, respectively.

6.4.1.2. 7 dpi. The results obtained at 7 days post inoculation (Fig. 6.7B) did not well reflect those obtained at 3 dpi. Chickens in group 3 ($\Delta cj1660$) and group 4 ($\Delta cj1663$) showed good mean levels of *C. jejuni* colonisation (6.1 and $6.69 \log_{10}$ CFU/g, respectively) that were similar to that of the wildtype ($6.45 \log_{10}$ CFU/g). However, group 2 ($\Delta ftr1$) showed a wide

range of colonisation levels with four infected chickens showing a poor *C. jejuni* colonisation (below 5.0 log₁₀ CFU/g) and the three other infected chickens showing a good degree of colonisation at >6.0 log₁₀ CFU/g (Fig. 6.7.B), giving a mean colonisation level of 3.27 log₁₀ CFU/g, some 2 fold lower than that of the wildtype ($P= 0.005$).

6.4.1.3. Conclusion. The mutant strains showed a significantly reduced (by 2.1-2.9 log₁₀ fold) chicken-caecum colonisation ability at 3 dpi. However, the colonisation level of these strains was largely similar to that of the wildtype after 7 dpi. This indicates that the mutant strains were able to adapt to the conditions of the chicken caecum in order to colonise the chicken gut and overcome their poor initial colonisation as caused by inactivation of the *cj1660* and *cj1663* genes. Thus, although the corresponding mutant strains showed a significantly low-level of chicken caecum colonisation at 3 dpi, two of the three were able to reach a normal level of colonisation by day 7. This indicates that the low-iron growth phenotype associated with the mutants (as discerned in Chapter 5) slows the rate at which gut colonisation occurs such that at 3 dpi a low colonisation level is observed. However, by day 7 the mutants have had sufficient time to achieve a colonisation level similar to that of the wildtype. Indeed, this colonisation phenotype reflects the low-iron extended lag-phase phenotype seen *in vitro*. Thus, the mutations appear to slow rather than prevent colonisation. However, it should be emphasised that the colonisation experiments were performed in birds that were otherwise *C. jejuni*-free and it is thus likely that the mutants used here would be non-competitive if co-colonised with the wildtype.

It is interesting to note that the Δ *ftr1* mutant continued to show poor colonisation at 7 dpi. Although it is apparent that the degree of colonisation achieved was highly variable. This suggests that this mutation may have a greater impact on gut colonisation than the other two mutations and possibly suggests that the Ftr1-p19 components are more critical than the

Cj1660-5 components for gut colonisation. This is in contrast to the *in vitro* phenotype analysis (Chapter 5) which indicated that the *ftr1* mutations gives the weakest phenotype.

In summary, it can be concluded that the entire P19 system (including the Cj1660 and Cj1663 components) is required for optimal colonisation ability of *C. jejuni* in the chicken gut, but that *C. jejuni* mutant strains lacking Ftr1-p19/Cj1660-5 function can adapt to survive in the chicken gut given sufficient time such that 'normal' colonisation levels can be achieved, at least in the absence of a wildtype competitor.

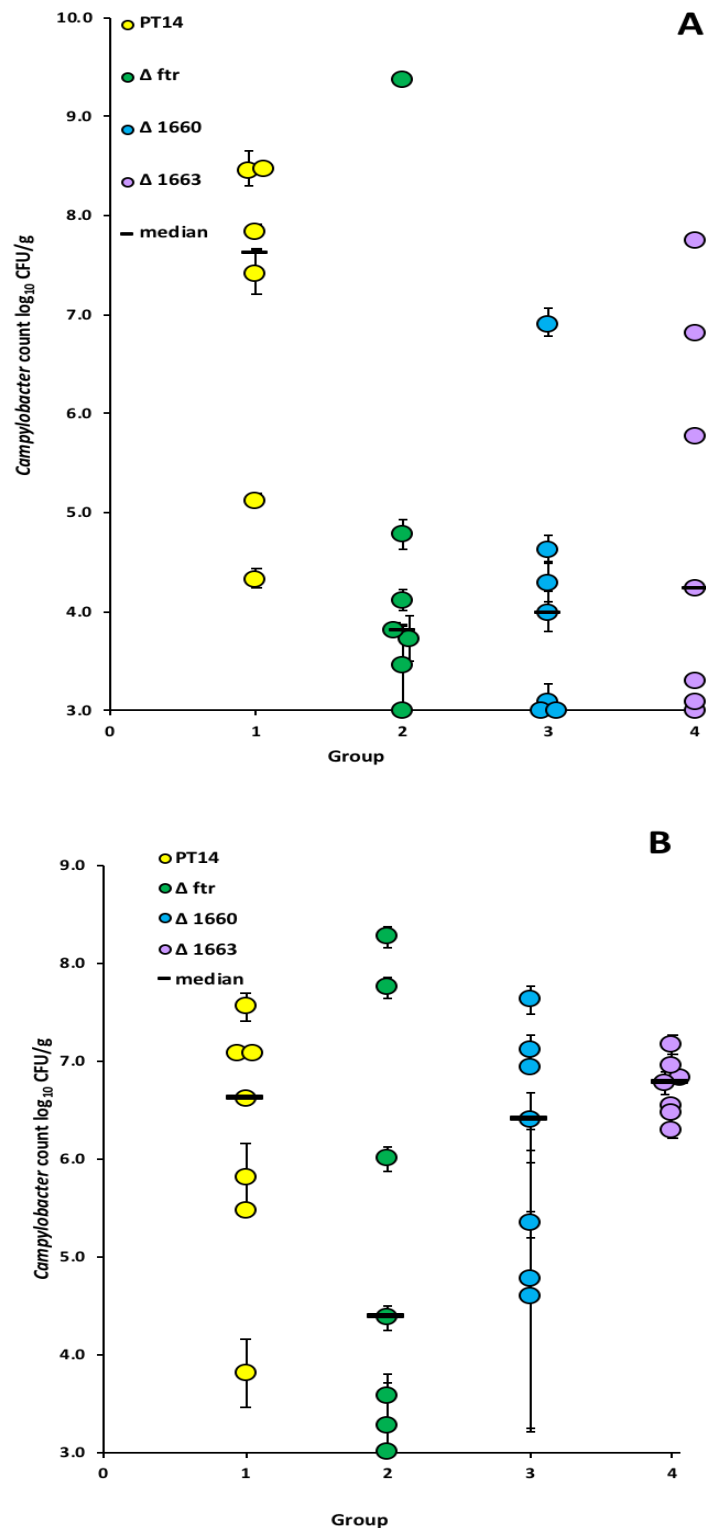


Figure 6.7: Recovery of *C. jejuni* strains from the caecum of chickens at 3- and 7-days post challenge. The 20-day-old chickens were administered with ~ 7 -log₁₀ CFU of the bacterial strains by the oral gavage technique as described. (A) At 3 dpi (23 days-old) and (B) 7 dpi (27 day-old) the chickens were sacrificed, and colonisation of the caecum assessed by the Miles and Misra viable

count method on mCCDA. All strains were confirmed by colony morphology. The minimum detectable level of *C. jejuni* in the faecal samples was $2.3 \log_{10}$ CFU/g. Standard deviations for *Campylobacter* counts for individual birds using triplicate technical replicates were all below $0.5 \log_{10}$ CFU/g except for two chicken (were 1.5 and 1.3 in group 3 at 7 dpi).

6.4.2. Variation in the body weights of chickens following colonisation by the *C. jejuni* strains

Body weights of the chickens were recorded over the course of the experiment (Fig. 6.8). The results show that there was a significant reduction in body weight of the chickens following infection with the *C. jejuni* PT14 wildtype (Group 1), compared to the control (non-infected) group ($P=0.04$). Interestingly, the chickens infected with the mutant strains (Groups 2, 3 and 4) showed no significant inhibition in body weight when compared to the control group. This suggests that the mutant strains did not have the same impact on the growth of the chickens as seen for the wildtype. This is likely due to the low level of *C. jejuni* colonisation in the early stages of infection, and this effect further supports the poor colonisation of the chicken by the mutant strains in the first few days post-infection. This in turn supports the suggested role of the P19 system in the normal colonisation ability of *C. jejuni* and the importance of its proposed iron-uptake role for optimal gut survival (Fig. 6.8).

Previous work has shown that PT14 colonisation of chicken has a negative impact on body weight compared with a control group of chickens (Awad *et al.*, 2014; 2015). Colonisation of *C. jejuni* in the chicken gut was shown to cause a change in the gut microbiota as well as preventing the normal weight gain. Potentially, the alteration in the gut microbiota is responsible for the weight-gain reduction. Other previous results also show that inoculation with *C. jejuni* changes the normal balance of the commensal and opportunistic bacteria (Wigley, 2015) and slows weight gains (Bull *et al.*, 2008; Williams *et al.*, 2013). However, other data indicate there is no clear lesion in the gut of *C. jejuni* infected chickens and show no effect on weight gain (Dhillon *et al.*, 2006; Pielsticker *et al.*, 2012).

In summary, it can be concluded from the results above that the P19 system has a role in the colonisation ability of *C. jejuni* in the chicken host such that lack of this system limits *C. jejuni* colonisation to a degree that positively effects chicken weight gain.

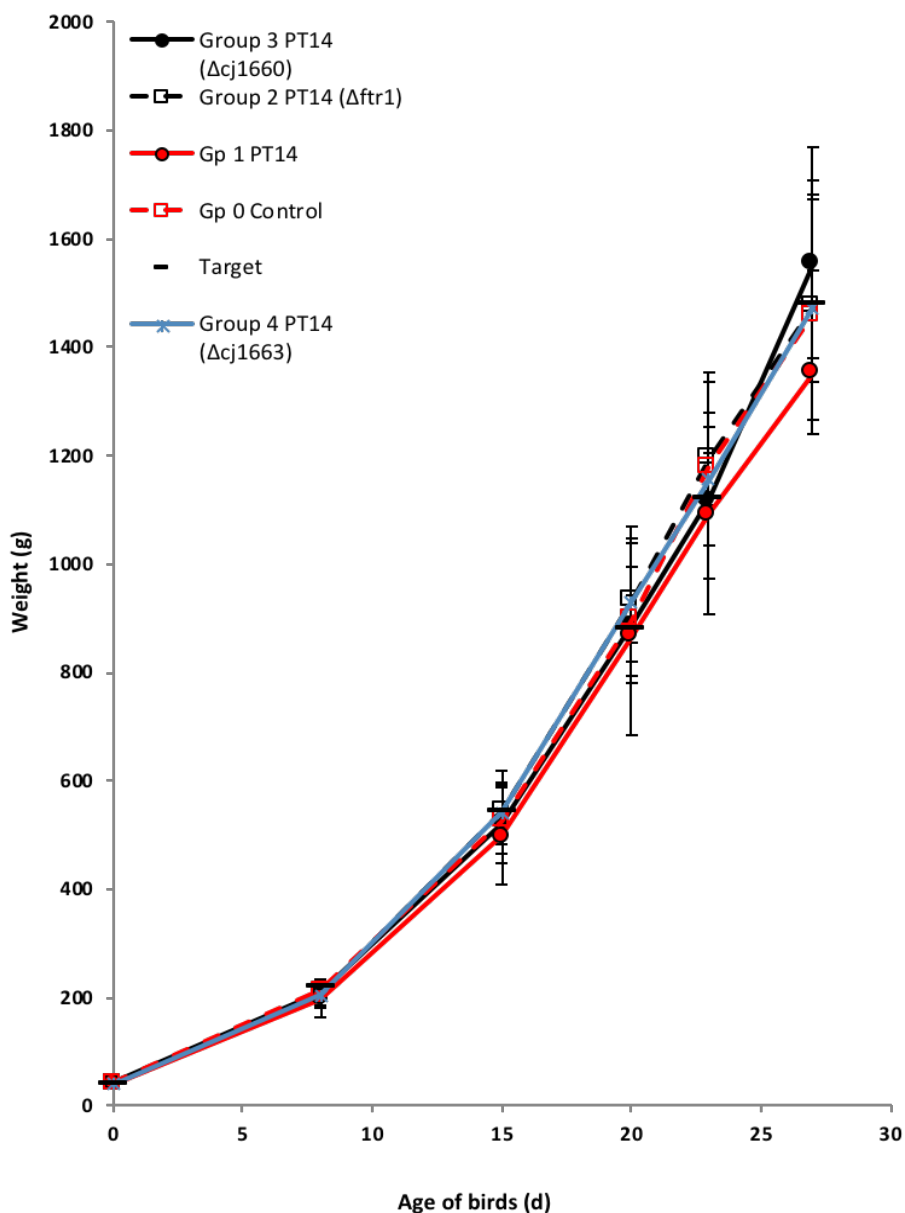


Figure 6.8: Body weight of the infected and control chickens over 27 days. These data were provided by veterinarians working in the animal house.

6.4.3. Confirmation of the presence of the mutant genes in the recovered strains

To confirm that the mutations are still present in the *C. jejuni* strains recovered from the cecum contents of the chickens infected by *C. jejuni* PT14 strains, two colonies of each strain isolated from the cecum either after 3 dpi or 7 dpi, were selected for investigation. All those selected were from birds where a high level of colonisation was observed. The strains of interest were transferred to Reading from University of Nottingham on mCCDA plates. The selected colonies were recovered on 2% blood agar for 40-48 h incubation, stocked and genomic DNA was extracted as template for PCR. Three pairs of primers were used to check the presence of the three mutations of interest. The results of the PCR showed that the mutations are present in the tested strains recovered at 3 and 7 dpi (Figs. 6.9 and 6.10). Thus, the high levels of colonisation observed for the mutant strains, particularly at 7 dpi, were not due to loss of the corresponding mutations.

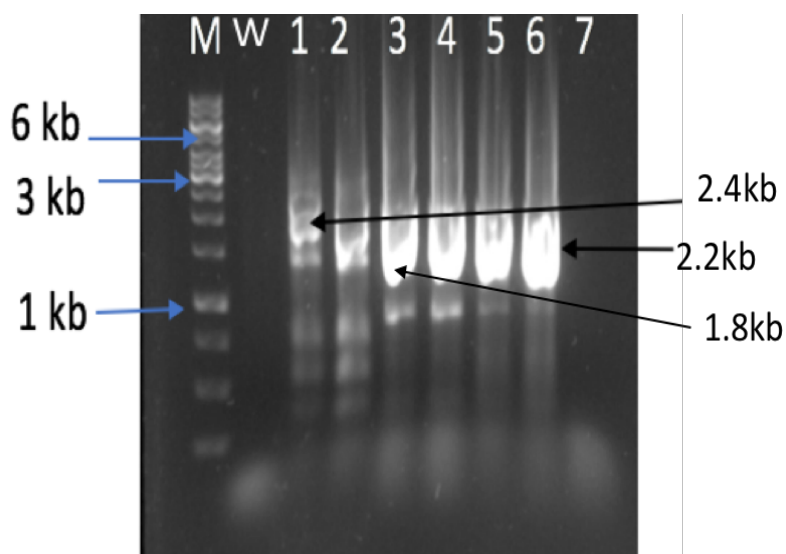


Figure 6.9: Gel electrophoretic analysis of the PCR products confirming the identity of the mutants in the strains recovered from the chicken cecum contents at 3 dpi. Genomic DNA was used as a template and forward primers of each corresponding gene with the reverse primer for the *cat* cassette were used. M, Gene Ruler 1kb; 1 and 2, confirmation of Δ *ftrI*; 3 and 4, confirmation of Δ *cj1660*; 5 and 6; confirmation of Δ *cj1663*; 7, blank; W, the wild type. The samples were from the chicken after 3 dpi.

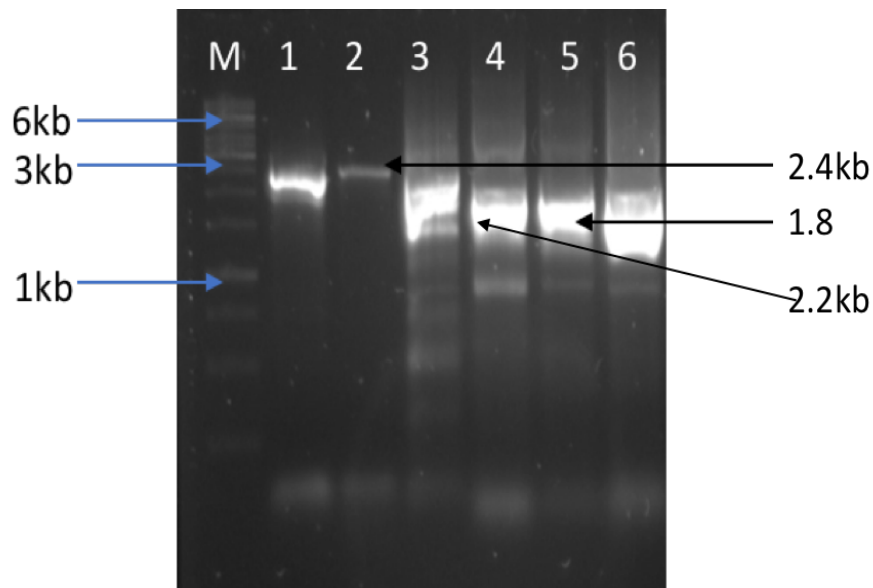


Figure 6.10: Gel electrophoretic analysis of the PCR products confirming the identity of the mutants in the strains recovered from the chicken cecum contents at 7 dpi. M, Gene Ruler 1kb; 1 and 2, confirmation of $\Delta ftr1$; 3 and 4, confirmation of $\Delta cj1660$; 5 and 6, confirmation of $\Delta cj1663$. The samples from the chicken at 7 dpi. Other details are as in Fig. 6.9.

It should also note that the whole-genome sequences of the PT14 (and a subset of recovered strains) and NCTC 11168 mutants were determined (MicrobeNG) and the mutations thus confirmed (Fig. 6.11).

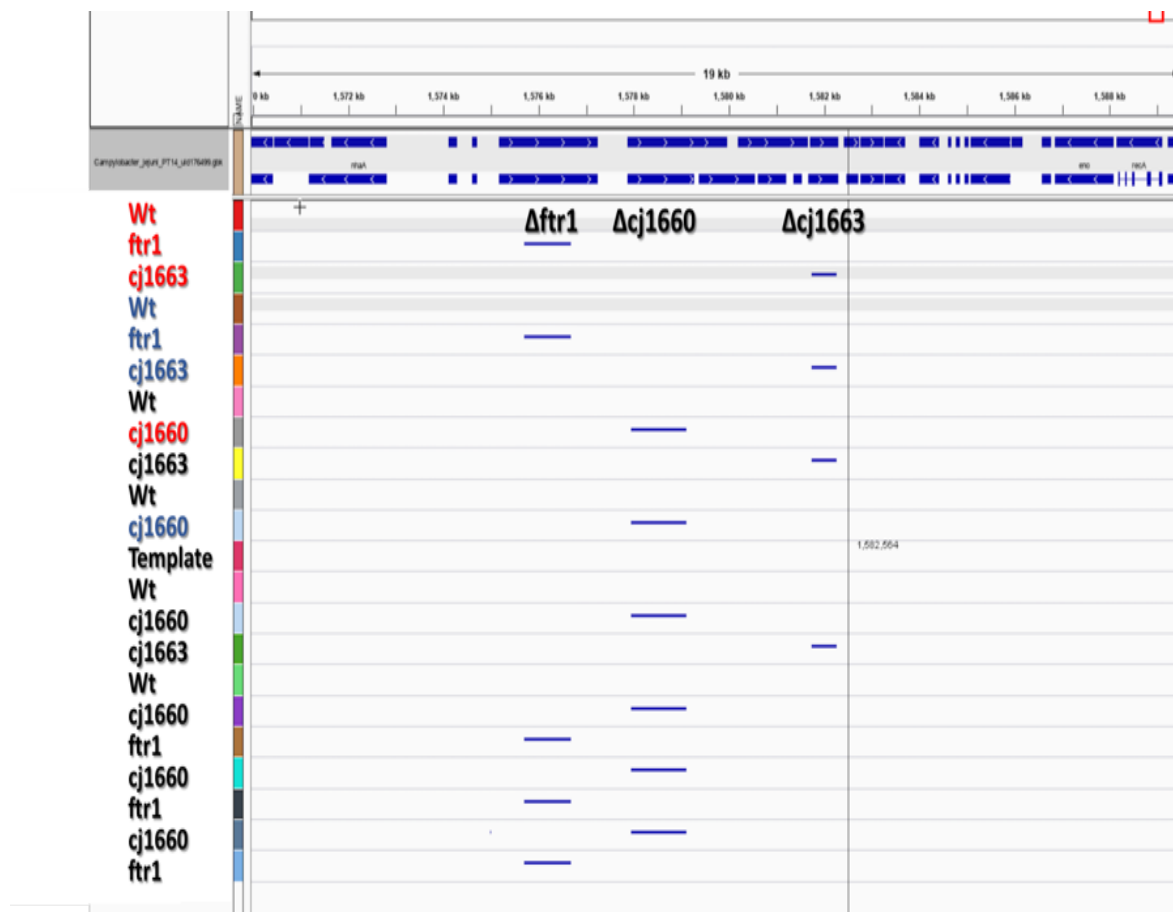


Figure 6.11: The figure from IGV (Integrative Genomics Viewer) shows the deletion regions in the *C. jejuni* genomes of the mutant strains. The Illumina whole-genome sequencing for 18 samples of *C. jejuni* NCTC 11168 and PT14 strains (wild type and $\Delta ftr1$, $\Delta cj1660$ and $\Delta cj1663$ strains). The PT14 strains include those recovered from chickens after infection at 7 dpi. In red font are the NCTC 11168 strains, in blue font are the original PT14 strains, in black font are the strains recovered from the chicken trial. Template was the PT14 genome sequence, used for alignment. Blue bars indicate missing DNA with respect to the template. A map of the relevant region of the PT14 genome can be seen above with coordinates and open-reading frames (with polarities) indicated.

6.5. Discussion

Data obtained in this chapter has shown that chickens infected with the $\Delta ftr1$, $\Delta cj1660$ and $\Delta cj1663$ mutants of *C. jejuni* PT14 are poorly colonised compared to chickens infected with the wildtype at the 3-day post infection stage. This suggests a role for the Ftr1-p19 and FetA-F system in *C. jejuni* colonisation of the chicken gut. In contrast, at 7-days post infection the $\Delta cj1660$ and $\Delta cj1663$ mutants showed a high colonisation level that was similar to that of the wildtype strain. Also, although the $\Delta ftr1$ strain showed a reduced degree of colonisation at 7 dpi, the level of colonisation had improved with respect to that seen at 3 dpi (by twofold, $P=0.03$), although not sufficiently to match the other strains. Possibly, this mutant might achieve the same colonisation levels as the wildtype over a longer post-infection time period. The results suggest that the $\Delta cj1660$ and $\Delta cj1663$ mutants had adapted to enable colonisation of the chicken gut by day 7 and were able to thus overcome the growth/colonisation defect that limited their colonisation capacity at 3 dpi. For the $\Delta ftr1$ mutant, the results indicate that its colonisation capacity is weaker than that of the other two mutants and this suggests that the Ftr1-p19 component plays a more important role in iron uptake in the caecum than does the FetA-F system. The delayed colonisation response of the mutants is likely related to their extended lag phase under iron-limited growth conditions as seen in Chapter 5. Thus, the mutants are still able to colonise the chicken well, if given sufficient time. It would be interesting to consider the colonisation of the mutant strains when in direct competition with the wildtype in co-infection studies, since the slow colonisation behaviour of the mutants would be expected to result in a significant reduction in their competitive fitness.

The body weights of the chickens infected with wildtype PT14 was significantly lower than that of the control group (chickens not infected) following infection. However, the chickens infected with the mutant strains did not show a notable reduction in body weight gain compared to the control group. This finding is consistent with the observed reduced

colonisation levels of the mutants at 3 dpi, and thus supports a role for the Frt1-p19/FetA-F system in the successful colonisation, and pathogenesis progression, in the chicken gut.

C. jejuni clearly needs access to iron for successful colonisation of the host (Palyada *et al.*, 2004; Naikare *et al.*, 2006; Zeng *et al.*, 2013). Ferrichrome has been shown to support growth of *C. jejuni* and the presence of homologues of *E. coli fhuABD* genes are required for this function. Since *p19* genes appears to be involved in the uptake of ferri-rhodotorulic acid (Miller *et al.*, 2009), one reason for the poor colonisation of the chicken gut by the mutants investigated here could be an impaired ability to obtain iron from siderophores. In a previous study, the role of the enterobactin-mediated iron acquisition system of *C. jejuni* NCTC 11168 in colonisation of the chicken cecum was tested (Palyada *et al.*, 2004). The *cfrA*, *ceuE* and *cj0178* mutants showed a notably reduced colonisation with respect to the wildtype (<500 CFU/g of cecum) which suggested a role of these genes in colonisation of the gut. The chickens were 3-4 days old, inoculated with 1×10^5 and 3×10^5 for 4 days. This indicates that iron is required for optimal colonisation of the chicken gut (Palyada *et al.*, 2004).

In addition, the role of *feoB* in gut colonisation of 4-day-old chicken was tested in three *C. jejuni* strains (ATCC 43431, NCTC 11168 and 81-176) and it was shown that *feoB* mutants display a lower colonisation ability than the wildtypes, by 5×10^4 , 2×10^4 and 31-fold (respectively) indicating a role for the FeoB ferrous-iron transporter in successful colonisation of the chicken cecum. The chickens were infected with 10^4 to 10^5 cfu of bacteria and samples were collected at 4 dpi (Naikare *et al.*, 2006). These results are consistent with the results obtained in this chapter indicating the importance of iron-uptake systems for chicken gut colonisation. However, the above previously published results used very young chickens that would be more susceptible to colonisation than the older (20 day) chickens used here. Also, the work presented in this thesis shows that iron-uptake mutants can fully colonise the chicken gut if given sufficient time, and the previous published work

only considered colonisation at an early time point such that any subsequent recovery would not be apparent. Thus ideally, such experiments should be performed in parallel with colonisation considered at shorter and longer time points in order to directly compare impact on colonisation of the different iron-uptake mutations with and without a competing wildtype.

In summary, it can be concluded that *ptr1*, *cj1660* and *cj1665* mutations in *C. jejuni* PT14 decrease the early colonisation capacity of *C. jejuni*, as seen for other iron-uptake mutations in *C. jejuni*, which suggests a role for the iron-uptake function of the FetMPA-F system in *C. jejuni* host colonisation.

Chapter 7: Iron- and Fur-regulation of *ptr1-p19/fetA-F* expression

7.1. Introduction

Fur is a most common regulator of iron-uptake genes in Gram-negative bacteria, also being found in some Gram-positive bacteria (van Vliet *et al.*, 1998b; Fleischhacker and Kiley, 2011; Hassan and Troxell, 2013). Fur functions to regulate iron levels in the cytoplasm and helps to ensure that the iron uptake, iron storage and iron assimilation processes are under homeostatic control (Helman, 2014). In general, Fur acts as transcriptional repressor for iron-uptake genes through Fe⁺²-Fur binding to the promoter region (vanVliet *et al.*, 1998b). However, there are now many examples showing its role as a transcriptional activator for groups of genes related to metabolism, motility and chemotaxis (Seo *et al.*, 2014; Yu and Genco, 2012; Delany *et al.*, 2004; Nandal *et al.*, 2010) as in *Neisseria gonorrhoeae* (Yu and Genco, 2012), *H. pylori* (Danielli *et al.*, 2006) and *Caulobacter crescentus* (da Silva *et al.*, 2009). Thus, Fur is able to repress and activate genes with a range of functions, that are either iron-dependent or independent (Carpenter *et al.*, 2009; Carpenter *et al.*, 2013; Deng *et al.*, 2012).

Fur in *C. jejuni* responsible for regulation of many iron transporters, e.g. Ceu, CfrA, ChuA and P19, as shown by van Vliet *et al.* (1998b). Also, *C. jejuni* Fur was identified as a regulator for more than 200 genes under both iron restricted and sufficient conditions, acting as both a repressor and activator depending on the target. The Fur-regulated genes of *C. jejuni* are mainly related to iron acquisition or storage, oxidative resistance, metabolism and flagellar synthesis (Palyada *et al.*, 2004; Holmes *et al.*, 2005). The expression of iron-transport systems is activated under low-iron conditions (e.g. *p19*, *cj1658*, *cfrA*, *cj1660–cj1665*; Holmes *et al.*, 2005). However, a more recent study by Butcher and Stintzi (2013) showed 77 genes as iron stimulated and 50 genes are iron depressed (involved in iron uptake and oxidative stress), but many iron-regulated genes are not under Fur control which indicates that there could be another regulator involved.

A further transcriptomic study by Butcher *et al.* (2015) showed that Fur and PerR co-regulate the expression of more than 200 different genes related to iron transport and storage, and oxidative stress including the *p19* gene cluster in *C. jejuni*. PerR (Fur related peroxide stress regulator) was also found to control the expression level of many genes under iron limitation which indicates that PerR function similarly to Fur in controlling iron-related genes (Butcher *et al.*, 2015).

A high-resolution RNAseq-based transcriptional study on four different *C. jejuni* strains (NCTC 11168, 81116, 81-176 and RM1221) indicates three promoters are associated with (and co-polar with) the *ftr1* operon (*cj1658-65*) (Dugar *et al.* 2013), designated here P1-P3. P1 appears sigma 70 dependent and is located 52 bp upstream of the *ftr1* gene; P2 is also apparently sigma 70 dependent and is located within the *cj1660* gene; and P3 is apparently sigma 28 dependent and is inside the *cj1664* gene, suggesting a stress resistance role for *cj1665* (Fig. 7.1). An excellent holo-Fur-binding site sequence is also located upstream of the *ftr1* gene, just downstream of the P1 promoter. This site presumably explains the reported iron and Fur regulation of the *ftr1* locus, which will be further explored in this chapter.

qRT-PCR analysis was used in this chapter to determine the transcription profile of the *ftr1-p19/fetA-F* genes in the *C. jejuni* NCTC 11168 wild type and Δfur mutant strains of the entire P19 system in response to Fur and iron. The strains used were *C. jejuni* NCTC 11168 wild type (AS144) and AS230 Δfur strains from the University of Ottawa (Department of Biochemistry and Molecular Biology, Canada). Total RNA was extracted from the bacterial cultures after the growth under iron sufficient and iron restriction conditions. Growth was in 15 ml of M-H broth, with and without 20 μ M ferric citrate, using 50 ml acid-washed flasks. Incubation was under microaerobic condition, at 37 °C and 150 rpm, with a starting OD₆₀₀ of 0.005. Samples were harvested at 24 h (mid log-phase with OD₆₀₀ of 0.5-0.6).

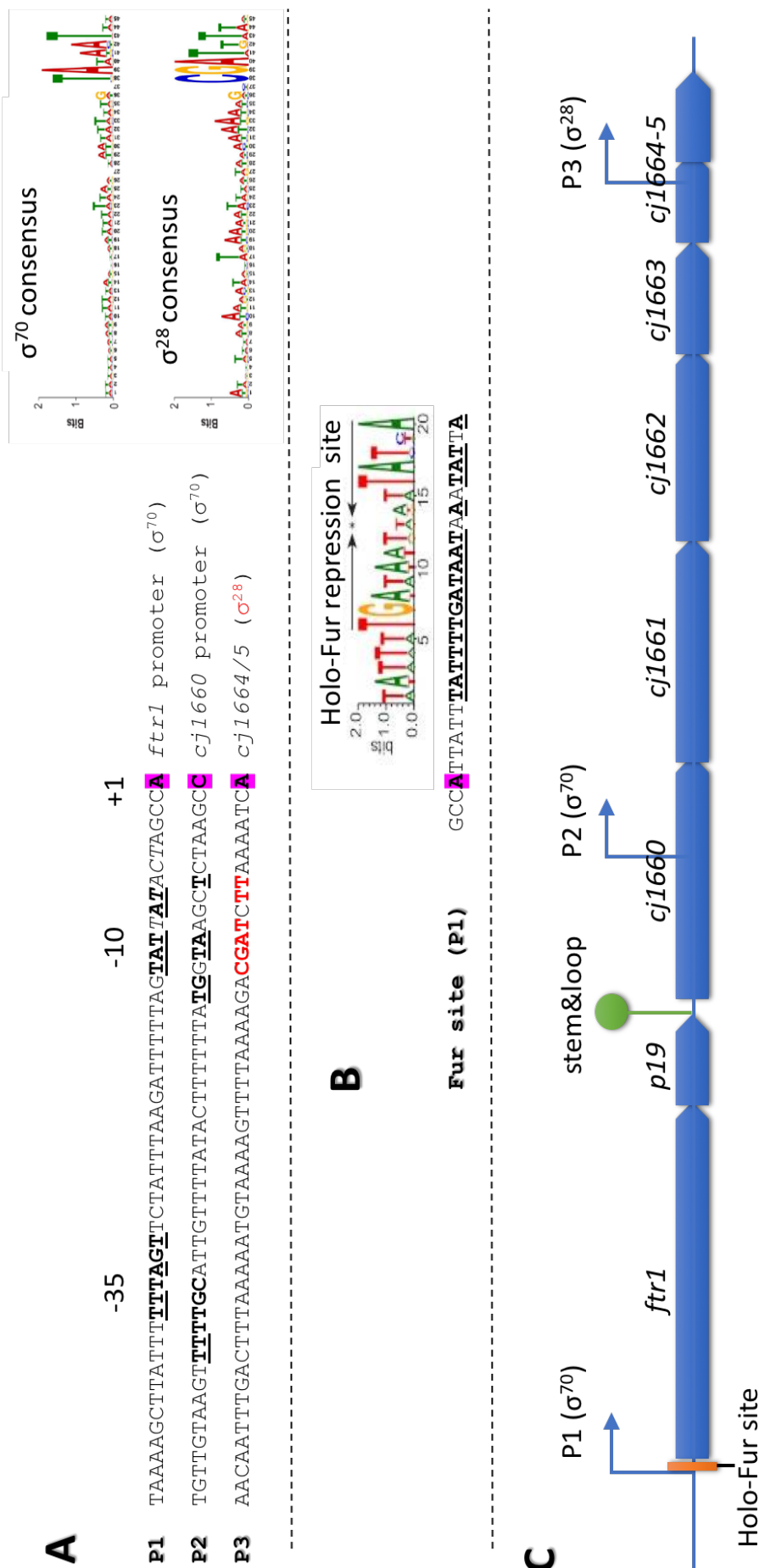


Fig. 7.1. Transcriptional organisation of the *ftr1-p19/fetA-F* locus. A. The three defined promoter sequences associated with the locus together with the corresponding consensus sequences. Matches to the sigma 70 -10 and -35 consensus are indicated with bold/under-scored text, or with italics (to distinguish two potential and overlapping -10 site for P1). Matches to the sigma 28 consensus are in red. The +1 site is highlighted in purple. B. The Fur site (and consensus sequence) downstream of P1, with matching residues in bold underscore. C. Genetic map of the *ftr1* locus showing the three mapped promoters, the Fur-binding site, and an intergenic stem & loop element. Data from Dugar *et al.* (2013) and Butcher *et al.* (2015).

7.2. Quantitative RT-PCR (qRT-PCR) analysis

Quantitative RT-PCR was used to study the expression profile of the *ftr1-p19* and *cj1660-65* gene set in *C. jejuni* wildtype and Δfur strain to detect any differences that can be obtained under low and high iron conditions for these two strains, as well as any strain differences caused by *fur* status. *C. jejuni* cultures were grown as indicated above and RNA was extracted using a RNeasy Plus Mini kit (Qiagen) (Methods 2.13.1). The qRT-PCR was performed due to the accuracy of detection offered by qPCR through multi cycle PCR amplification of cDNA. The crucial phase in this reaction is the first phase (exponential phase) where the amount of the PCR product double at each cycle (about 100% reaction efficiency) which enables the accurate detection of less than two-fold differences (vanGuilder *et al.*, 2008).

There are two techniques to quantify PCR product by qRT-PCR, the TaqMan technique and the SYBR green 1 dye technique. The TaqMan method is characterised as a highly accurate and sensitive method used in specific gene expression analysis incorporating fluorescently-labelled oligonucleotide probes that are subject to hydrolysis during the PCR reaction releasing the fluorescent fluorophore from the quencher generating an quantitative amplification signal (Mocellin *et al.*, 2003; Godfrey *et al.*, 2000; Cohen *et al.*, 2002). The SYBR green 1 dye is used to detect PCR product accumulation by binding the SYBR green 1 dye to the double strand DNA which is then detected by fluorescence. The dye can bind to any double strand DNA even it is just primer dimer or non-specific PCR product (which can result in non-specificity), but it is useful as it can be used to detect multiple gene expression (Zipper *et al.*, 2004). This was the approach used in this chapter. In addition, determination of the amount of the target mRNA can be measured by two methods - either absolute quantification to the whole amount of the expressed mRNA from the target gene or by relative quantification through determination of the ratio between the amount of the target

and a reference gene transcript (Wilkening and Bader, 2004; Livak and Schmittgen, 2001).

The ratio method was used in this chapter.

The region between gene pairs in the *p19* cluster was targeted for amplification (Fig. 7.2).

The primers were designed to anneal within the last 50-100 bp within the 3'-end of the upstream gene and within the first 50-100 bp at the beginning of following downstream gene.

This allowed the determination of transcriptional organisation – in particular whether there is

a *p19-cj1660* co-transcript (see Table 2.8). The length of the primers was between 20-25

nucleotides and the amplified products were ~100-200 bp. All primer pair were first tested in

a normal PCR reaction with genomic DNA of *C. jejuni* and they showed the expected product

sizes (Fig. 7.3). Also, the amount (by Nanodrop) and quality of total RNA isolated from the

C. jejuni cultures for use in this experiment were determined (Fig. 7.4). The isolated total

RNA was tested for DNA contamination by PCR (Fig. 7.5).

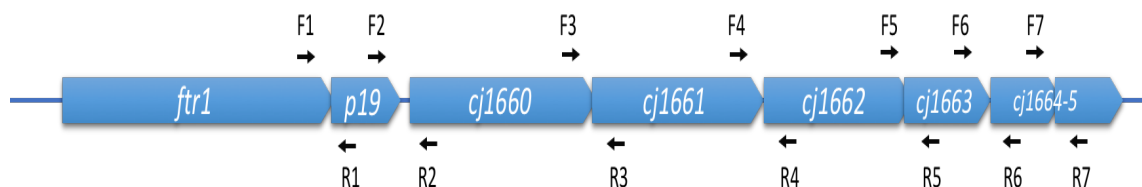


Figure 7.2: Genetic map of *ftr1* cluster showing the amplified intergenic regions between neighbouring genes. The arrows indicate the sites of the primers that were used.

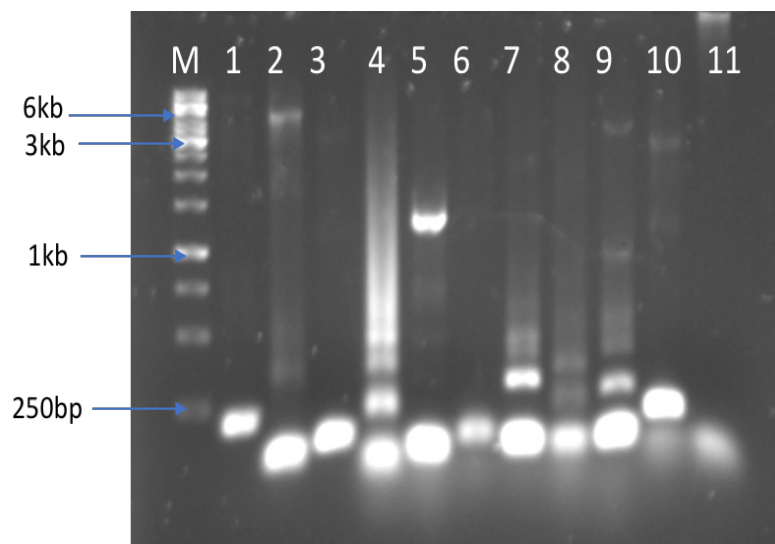


Figure 7.3: Gel electrophoresis of PCR products generated in order to test the qPCR primers with the genomic DNA of *C. jejuni* NCTC 11168 as template. Lane 1-7 the genes *fir1-p19*, *p19-cj1660*, *cj1660-1*, *cj1661-2*, *cj1662-3*, *cj1663-4*, and *cj1664-5*, respectively. Lanes 8-10 are PCR products from the 16S rRNA, *rpoA* and *tonB2* genes, respectively. Lane 11, blank.

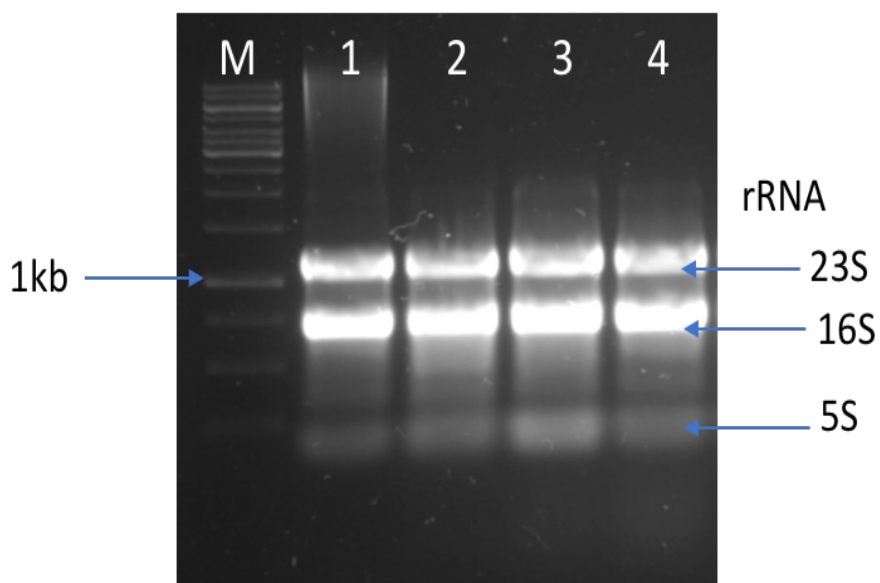


Figure 7.4: Gel electrophoresis of RNA samples extracted from *C. jejuni* NCTC 11168 grown in M-H medium. Lanes 1 and 2, from the growth in M-H wild type and *fur* mutant respectively; 3 and 4, growth in M-H broth with 20 μ M ferric citrate, wild type and *fur* mutant respectively.

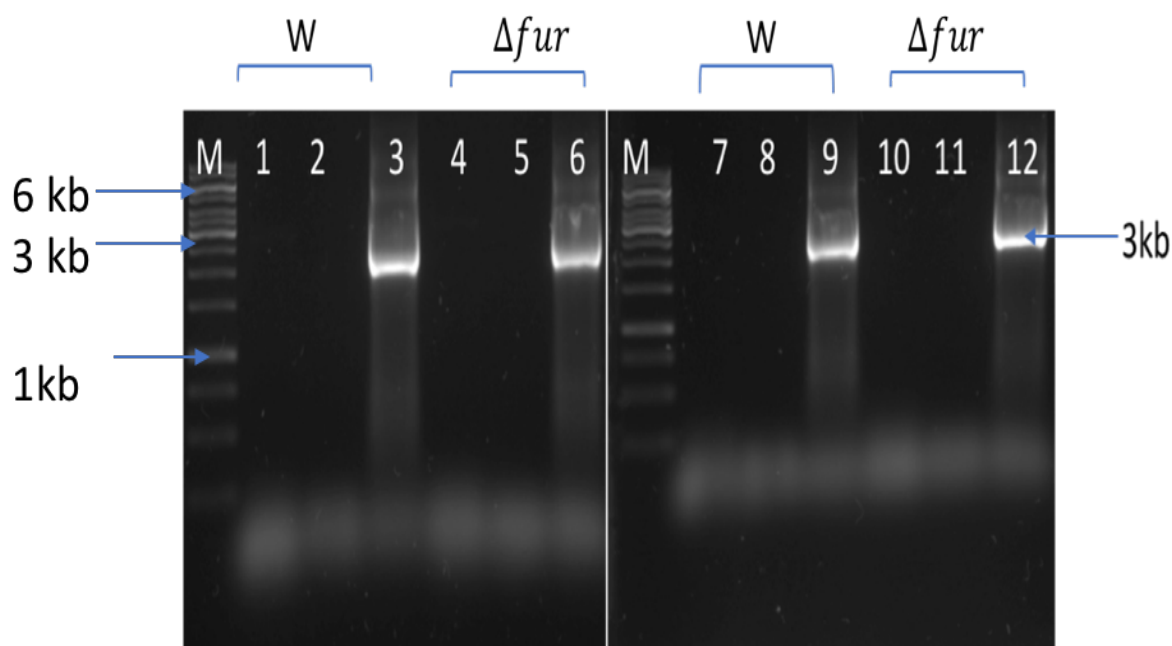


Figure 7.5: Gel electrophoresis of PCR products obtained using isolated total RNA as template to demonstrate lack of DNA contamination. Lanes 1, 4, 7 and 10, the PCR reaction with the RNA isolated from the indicate strains; lanes 2, 5, 8 and 11, the PCR reaction with water as control; Lane 3, 6, 9 and 12 the PCR reaction with the genomic DNA using primers to amplify about 3 kb from *C. jejuni* NCTC 11168 (cj1660 F and R primers, used to confirm DNA-free status).

7.3. Control transcripts

The genes encoding 16S ribosomal RNA (16S rRNA or *cjr01*) was used as a negative control since its expression is considered stable under different growth conditions as it has crucial housekeeping function (Hwang *et al.*, 2011). The *tonB2* and *tonB3* genes were used as a positive control since they are induced by iron starvation and are under Fur control (Butcher *et al.*, 2015). The *tonB2* and *tonB3* genes encode as energy-transduction systems for translocation of iron-complexes across the OM (Introduction 7.1). The experiment performed allowed determination of iron dependence in the wildtype and the *fur* mutant which would reveal the degree of dependence on iron for expression, and whether this dependence is Fur mediated. Thus, comparison was made between the wildtype and the *fur* mutant, and between

the transcription profile under iron sufficient and deficient conditions. The concentrations of the total RNA used in each reaction were equal.

7.4. Generation of standard curve

To analyse the results obtained from qPCR reactions, a standard curve is considered as essential for absolute quantification and also assists relative quantification. It allows the direct comparison of the results for each transcript from all reactions. However, a group of standards are necessary before such results can be obtained. In order to detect the actual level of *p19* gene expression and generate a comparison between the wildtype and the mutant strain, levels of the gene expression should be compared to the expression level of a standard gene, used as an internal control that is not affected by iron availability or *fur* status. To enable this, the efficiency of all primers should be equal or similar during amplification.

Thus, the efficiency of the qPCR primers was tested in triplicate for each cDNA sample, by using a dilution series (10^1 - 10^5) from the template cDNA of the wildtype strain (grown in M-H medium) for each target gene (Fig. 7.6). The standard curves were constructed using an iCycler iQ™ system and qPCRBIO SyGreen Mix with a Fluorescein kit. Fold changes between control and target genes were calculated after normalizing the gene expression level of each gene to the internal standard housekeeping gene (16S rRNA).

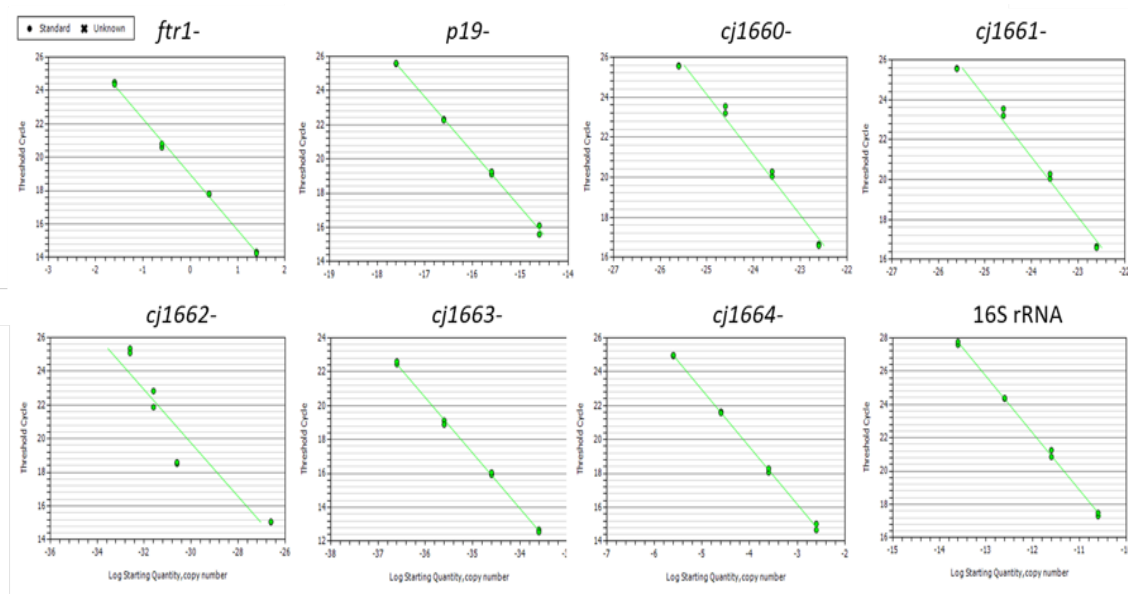


Figure 7.6: Standard curve charts of the efficiency of the qPCR for each pair of primers. The primers efficiency was tested in triplicate for each cDNA sample, by using a dilution series (10^1 - 10^5) from the template cDNA of the wildtype strain (grown in M-H medium) for each target gene.

7.5. Results

The relative levels of the PCR signals obtained for the target-gene transcripts were normalised with respect to that of the internal control gene (16S rRNA). The ΔC_t values thus obtained from one condition were compared to those of the same genes under a second condition (relative quantitative RT-PCR) in order to fully normalise the data and to give $\Delta\Delta C_t$ values. The calculation was as in the $2^{-\Delta\Delta C_t}$ method (Winer *et al.*, 1999; Schmittgen *et al.*, 2000; Livak and Schmittgen, 2001). Thus, the expression ratios of the target genes were calculated depending on 16S rRNA transcript levels; this transcript appeared to show an equal transcriptional level under all the conditions used indicating that it is suitable as an internal control for standardisation of the data. The transcript levels of *tonB2* and *tonB3* were used as positive controls (known to be Fur and iron repressed; Naikare *et al.*, 2006; Butcher *et al.*, 2015) and the results showed that their transcriptional levels are similar, and that they are induced under low-iron conditions in the wildtype strain in a fashion similar to that observed for the *ftr1-p19/fetA-F* genes (Fig. 7.7). This finding indicates that appropriate iron-

dependent expression was achieved. However, the negative control (16S rRNA) showed no iron or Fur dependent change in expression, thus confirming the specificity of the iron/Fur expression effects observed.

The expression profile of the *ftr1-p19/fetA-F* genes in the *C. jejuni* NCTC 11168 wildtype following growth in M-H medium showed a substantive upregulation in all cases compared to that achieved in M-H with ferric citrate (Fig. 7.7). This is consistent their induction under iron restriction and their suggested role in iron acquisition. The *ftr1-p19*, *p19-cj1600* and *cj1660-1* genes were particularly heavily induced by low iron, with expression increases of between 112-2165-fold observed (Fig. 7.7). The *cj1661-2*, *cj1662-3*, *cj1663-4* and *cj1664-5* genes were also highly induced in the wildtype by lack of iron, but the degree of induction was less marked, at 111, 116, 108 and 100-fold respectively (Fig. 7.7). The *tonB2* and *tonB3* genes were also highly induced by lack of iron in the wildtype, at 304 and 876-fold. The 16S rRNA gene showed a less than twofold expression response to iron in the wildtype. However, the expression response of the *ftr1-cj1665* locus and *tonB* genes to iron was very different in the Δfur strain with very little change exhibited in most cases, ranging between 0.36 to 2.32-fold changes in response to lack of iron. The exception was the *cj1664-5* transcript which showed a major 0.08-fold reduction in expression in the *fur* mutant in the absence of iron (i.e. a 12.5-fold Fur-independent iron induction). This effect might well reflect P3 promoter activity (Fig. 7.1) since this promoter is in position for transcription control of the *cj1664-5* transcript, but none of the other transcripts considered here, and it is σ^{28} (FliA) dependent suggesting a link to motility. Indeed, a number of flagella genes are known to be subject to Fur and PerR control indicating a link between iron availability or redox-stress and motility. Only 1.8% of transcription start sites are predicted to be σ^{28} associated (Dugar *et al.*, 2013) so this apparent regulatory control for the *cj1665* gene is indicative of a specialised function for the Cj1665 thioredoxin with respect to the other genes in the *ftr1-cj1665* cluster.

Interestingly, a few other iron-related genes were found to possess sigma 28 promoters (*cj0045c*, encoding a hemerythrin; *ceuB* and *ceuC*, encoding enterobactin uptake permease subunits; Dugar *et al.*, 2013) which is indicative of a broader link between motility and iron homeostasis. Reassuringly, the negative control (16S rRNA) also showed a weak response (less than twofold) to iron in the absence of Fur.

Comparison of the wildtype and *fur* mutant expression data indicates that the *ftr1-cj1665* and *tonB* genes are regulated by iron in a Fur-dependent manner, since no substantial iron-dependent change is seen in the *fur* mutant background. However, Fur normally acts as a repressor of iron uptake genes in Gram-negative bacteria. In the expression data generated here, the *C. jejuni fur* mutant showed weaker (by a factor of up to ~2000) expression of the Fe and Fur-dependent genes under study with respect to the wildtype under high-iron (data not shown). Although previous researcher has shown that the *tonB* and *ftr1-cj1665* genes are iron repressed and Fur dependent, this control is exerted through Fur repression, not activation (van Vliet *et al.*, 1998b; Butcher *et al.*, 2015). The pattern of expression generated here indicates that, under the conditions used here, apo-Fur acts as an activator of expression for all nine iron-controlled genes examined. It is unclear why this mode of Fur control is seen here, but not in previous work. This discrepancy is considered further in the discussion below.

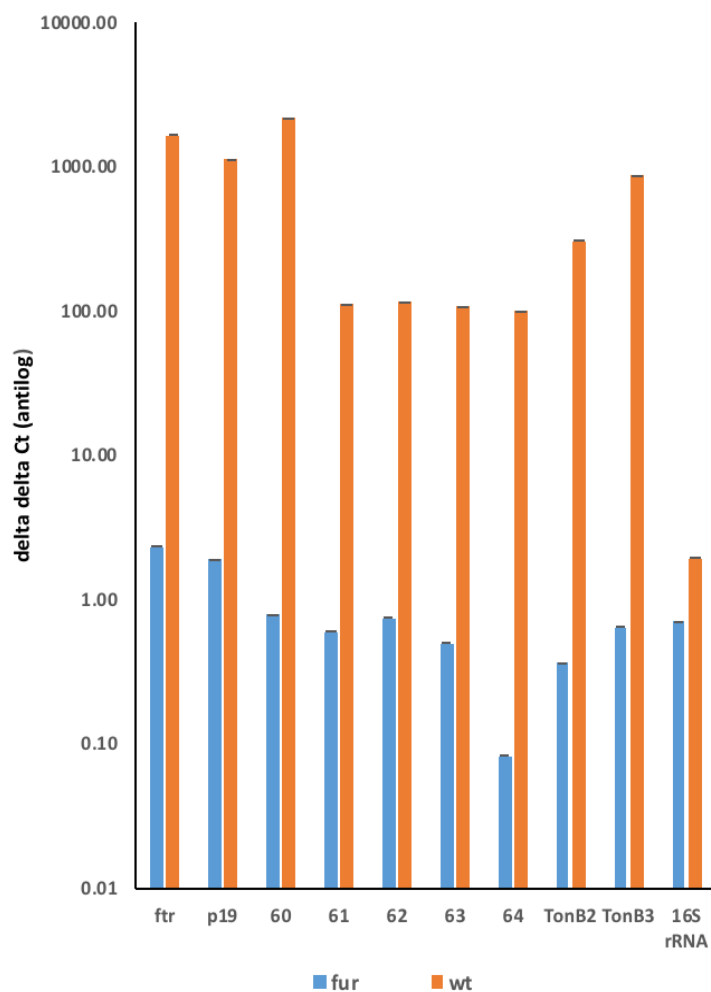


Figure 7.7: Effect of +/- Fe on relative expression in a wildtype and Δfur background. Gene expression was estimated using qRT-PCR with the comparative critical threshold ($\Delta\Delta Ct$) method. The wildtype strain and *fur* mutant in M-H medium, with/without 20 μM ferric citrate, are compared. The 16S rRNA gene was used as a negative control, *tonB2* and *3* as positive controls, and *rpoA* was used as the housekeeping comparator for ΔCt calculation purposes. In this case, the ΔCt data obtained with iron were normalised against the data obtained without iron, and thus bar heights indicate levels of repression in response to iron (or activation in response to absence of iron). Error bars represent +/- values obtained from technical duplicates.

Table 7.1: Fold differences and *P* values for expression levels of each *p19* target between the wildtype and Δfur in the absence of iron

Gene	Fold difference	<i>P</i> value
<i>ptr1-p19</i>	723	<i>P</i> <0.001
<i>p19-cj1660</i>	600	<i>P</i> <0.001
<i>cj1660-61</i>	2774	<i>P</i> <0.001
<i>cj1661-62</i>	185	<i>P</i> <0.001
<i>cj1662-63</i>	165	<i>P</i> <0.001
<i>cj1663-64</i>	216	<i>P</i> <0.001
<i>cj1664-65</i>	1250	<i>P</i> <0.001
<i>tonB2</i>	844	<i>P</i> <0.001
<i>tonB3</i>	1368	<i>P</i> <0.001
16S rRNA	2.7	<i>P</i> >0.05

7.6. Discussion

In this chapter, the major aim was to determine the response of the *C. jejuni ftr1-cj1665* genes to the level of iron available in the medium and their control by the Fur transcription factor. qRT-PCR analysis was used to study the expression profile of the *ftr1-cj1665* genes in the *C. jejuni* NCTC 11168 wildtype and *fur* mutant. PCR primers were designed to amplify the regions flanking adjacent genes. This allowed the determination of whether adjacent genes form co-transcripts. Since all seven pairs of primers for adjacent genes gave similar levels of amplified PCR product, it can be assumed that *ftr1-cj1665* genes cluster forms a cotranscript with the Fur-box associated P1 promoter acting as the primary promoter that drives iron/Fur dependent control.

The qRT-PCR analysis showed that the relative expression level of the *ftr1-cj1665* genes in *C. jejuni* NCTC 11168 wildtype was much higher in iron limited M-H medium than in iron-supplemented M-H medium, which demonstrates that low iron induces expression of the *ftr1-cj1665* locus. This is consistent with the previous transcriptional studies showing that *ftr1-p19* associated genes (*cj1660-65*) are iron-repressed such that their expression increases under iron deficiency in wildtype *C. jejuni* (van Vliet *et al.*, 1998b; Holmes *et al.*, 2005; Palyada *et al.*, 2004; Butcher *et al.*, 2015; Butcher and Stintzi, 2013). Also, this regulatory control is consistent with the expected role of the Ftr1-p19/FetA-F system as an iron transporter required for good growth under iron restriction, as shown here (Chapter 5) and elsewhere (Chan *et al.*, 2010).

Unexpectedly, the expression profile of the Δfur strain showed a clear repression for the *ftr1-cj1665* and *tonB2/3* genes in both low and high-iron conditions. This suggests a role of Fur in iron-dependent control of these genes by acting as an activator in the absence of iron. Much previous work has shown that Fur of *C. jejuni* largely acts as an Fe-dependent repressor of iron transporter genes (van Vliet *et al.*, 1998b; Holmes *et al.*, 2005; Palyada *et al.*, 2004) and

so the apparent activation of expression by apoFur, as indicated here, contrasts with such previous work. However, Fur is known to work as an activator for some groups of genes, such as those related to oxidative resistance, motility and iron storage (Palyada *et al.*, 2004; Holmes *et al.*, 2005; Butcher *et al.*, 2015). Thus, the apparent activation of expression by Fur, as observed here, is not without precedent.

Importantly, there are some differences between this work and the previous expression studies of relevance, such as the type of medium used, the incubation conditions and the manner in which iron restriction/sufficiency was achieved for cultures prior to the RNA extraction. For example, van Vliet *et al.* (1998b) found that P19 protein levels were raised in the periplasm under iron restriction and in a *fur* mutant of *C. jejuni* NCTC 11168 strain (same strain as used here), but induction by iron restriction was compared following growth in M-H medium with or without 20 μ M deferoxamine mesylate as chelator. In addition, expression was compared in MEM with and without 40 μ M ferric sulphate. These conditions vary to those used here (M-H medium with/without ferric citrate) and this might explain the differences observed. The microaerobic conditions (37 °C; 10% CO₂, and 5% O₂) were similar to those used here (37 °C; 10% CO₂, and 5% O₂).

In Palyada *et al.* (2004), DNA microarrays and qRT-PCR analyses were used to determine global iron-dependent expression in early log-phase for *C. jejuni* NCTC 11168 upon growth in MEM medium with/without 40 μ M ferrous sulphate (1-15 min induction period), under microaerobic condition (37 °C; 4% H₂, 8% O₂, 5% CO₂). A 4-256-fold reduction in mRNA levels for *ptr1-p19* and *cj1661-3* was observed upon iron addition and all were Fe-Fur repressed. The use of MEM (not M-H) represents a clear difference with respect to the conditions used in this thesis.

In Holmes *et al.* (2005), *C. jejuni* NCTC 11168 was again used, but incubation was at 42 °C (10% CO₂, 5% O₂), and expression was tested by qRT-PCR and DNA microarrays at mid-

late log (7.5 h) using high/low iron medium, as in van Vliet *et al.* (1998b), i.e. M-H medium with either 20 μ M DFO or 40 μ M ferrous sulphate. The *p19* gene cluster was iron and Fur repressed. In Butcher *et al.* (2015), *C. jejuni* NCTC 11168 was again used with growth but in MEM α medium (with 10 mM pyruvate) +/- 40 μ M ferrous sulphate at 37 °C (4% H₂, 8% O₂, 5% CO₂). Again, the *p19* genes were found to be iron and Fe-Fur repressed.

The major difference between the conditions used above and those used here of M-H medium with/without ferric citrate. The conditions of Holmes *et al.* (2005) are the closest match to those used here, but the form of iron used (ferrous, not ferric) is a clear difference. Further work should explore the nature of the *fur* mutant used in this work and compare expression effects under conditions that match those used by others as closely as possible. In addition, the effect of Fur complementation should be determined to demonstrate that the aberrant expression pattern can be restored to that of the wildtype.

Chapter 8: General discussion

8.1. Introduction

C. jejuni is a microaerophilic gut-dwelling bacterium that colonises the caecum of birds and other animals. In man, *C. jejuni* is pathogenic and is the major cause of gastroenteritis (Adak *et al.*, 2005; Coker *et al.*, 2002; Mead *et al.*, 1999). Infection of man by *C. jejuni* occurs mainly through the consumption of contaminated water or food (Blaser, 1997). Poultry are considered to be the main source for human infection (Skarp *et al.*, 2016). Iron is required for many functions in cell metabolism and for many micro-organisms, acquisition of iron is considered as a crucial factor for colonisation and infection of the host (Miethke & Marahiel, 2007). *C. jejuni* requires mechanism for uptake of iron from its environment for successful colonisation in the host (Naikare *et al.*, 2006; Naikare *et al.*, 2013). Previous studies have shown that *C. jejuni* has several types of iron-uptake system (Miller *et al.*, 2009). These include a ferri-enterochelin uptake system (CrfA & CeuBCDE; Palyada *et al.*, 2004), a ferrichrome-uptake system (CFhuABD; Galindo *et al.*, 2001), a ferri-rhodotorullic acid uptake system (Cj1658-59/Ftr1-p19; Janvier *et al.*, 1998), a haemin-uptake system (ChABCDZ; Ridley *et al.*, 2006), a putative transferrin-bound iron utilisation system (cj0173c-78; Miller *et al.*, 2008), a TonB-dependent OM receptor of unknown purpose (cj0444; Miller *et al.*, 2009) and a putative ferrous iron-transport protein (FeoAB; Naikare *et al.*, 2006). Also, *C. jejuni* has three TonB-ExbBD systems (designated 1-3), associated with the ferri-transferrin uptake (1), the haem uptake (2) and ferri-enterobactin uptake gene clusters (3) (Miller *et al.*, 2009). Of these, the FeoAB, TonB1, TonB3 and enterobactin systems have been shown to be required for chicken gut colonisation (Naikare *et al.*, 2006; Naikare *et al.*, 2013; Palyada *et al.*, 2004).

The Ftr1-p19 system is the subject of this thesis. It was initially discovered on the basis of accumulation of the P19 protein in the periplasm during iron restriction and upon *fur*

mutation (Janvier *et al.*, 1998). Subsequently, the association of the *p19* gene with the upstream *Ftr1*-encoding (a putative ferric permease) gene was revealed and mutation of the *ftr1* or *p19* gene was shown to reduce capacity to utilise ferri-rhodotoulic acid as an iron source (Stintzi *et al.*, 2008). However, the *Ftr1*-*p19* iron transporter was suggested to be more complex than originally thought when it was noted that it is associated with a set of additional, adjacent downstream genes (*cj1658-1665*) potentially encoding an ABC transporter (Miller *et al.*, 2009). The *ftr1-p19* and most of the *cj1660-5* were found to be induced by low iron, and to be under Fe-Fur repression (Chan *et al.*, 2010; Palyada *et al.*, 2004; Holmes *et al.*, 2005), further supporting a role in iron uptake. Chan *et al.* (2010) showed that the *p19* gene supports iron-restricted growth in the presence of an iron chelator (DFO), indicating a role for *Ftr1*-*p19* as an elemental iron transporter. The structure of P19 was also solved showing that it is a homodimer with two-metal binding sites, one for copper and the other considered to accommodate ferrous iron (Chan *et al.*, 2010).

The main aim in this study was to investigate whether the *cj1660-65* genes play a role in iron transport. This aim was pursued by:

- performing a bioinformatic analysis of the likely functions of the encoded proteins,
- determining whether the *C. jejuni ftr1-p19* and *cj1660-5* genes could complement iron-uptake deficiency in an *E. coli* mutant strain,
- inactivating the corresponding genes in *C. jejuni* and identifying a growth phenotype under iron restriction,
- determining whether such mutations affect chicken gut colonisation, and
- determining the degree of regulatory control exerted by iron and Fur, and the potential for a *ftr1-cj1665* co-transcript.

8.2. Gene organisation of p19 system

As indicated, *Campylobacter* species have a conserved gene cluster encoding an incompletely characterised type of iron transport system; this cluster consists of eight co-polar genes in *C. jejuni* NCTC 11168 (*cj1658-cj1665*; Miller *et al.*, 2009) (Fig. 3.1). However, P19 homologues in some bacteria (*Bordetella*, *Burkholderia* and *Brucella* spp.) are encoded as part of a four gene system (Brickman and Armstrong, 2012). A survey was performed using the Gene Context Tool to detect *p19*-encoding genes in different organisms and determine their genetic context. The results showed that genes encoding p19 are found in three major genetic context types, all of which include an Ftr1 component and a small, extracytoplasmic redox component (a cupredoxin or a thioredoxin). The co-association of *p19* with *ftr1* strongly suggests a role in iron uptake in all such cases, and the presence of the cupredoxin/thioredoxin components indicates an electron-transfer function. This is consistent with the mechanism of Ftr1p-Fet3p of yeast in which ferrous iron is oxidised by Fet3p during uptake via Ftr1p using O₂ as the electron acceptor and suggests that the Ftr1-p19 systems of bacteria engage in a related ferrous-iron oxidation process. Homologues of the *ftr1-p19/cj1660-5* cluster were found to be common and well-conserved in the *Campylobacter*, *Yersinia* and *Bifidobacterium* genera, indicating that the system is quite widespread and likely to be of importance in a range of organisms (Fig. 3.3).

8.3. Bioinformatic analysis of the Ftr1-P19 and Cj1660-5 components

Bioinformatic analysis showed that Ftr1 of *C. jejuni* has a substantial N-terminal domain of ~400 residues located in the periplasm, that is not found in the Ftr1p of yeast or related EfeU of *E. coli*. This type of domain organisation ('DO2') was found for 10% of Ftr1 proteins in the Pfam database (Fig. 3.8) and was seen to be associated Ftr1 proteins within the 6-8 gene organisation P19 systems, which suggests a specialised purpose for this domain associated with the mechanism of action of these systems. However, it is unclear what the purpose of

this domain might be possibly interaction with p19. This domain was found to contain five conserved motifs, but no role for these was apparent. The *C. jejuni* Ftr1 C-terminal integral-membrane domain possesses the well-conserved REG(A/L) E motifs for TMHs 1 and 4, and EDLWE-like motif, which have been shown to be essential for iron uptake in the Ftr1p of yeast (Severance *et al.*, 2004). This suggests that the *C. jejuni* Ftr1 is likely to be a functional ferric permease.

Bioinformatics indicates that the Cj1664 and Cj1665 proteins are both secreted lipoylated thioredoxins and are quite distantly related (just 19% amino acid sequence identity). They are predicted to be anchored to the periplasmic faces of the outer and inner membranes, respectively. The bioinformatic analysis suggested that the Cj1661-3 proteins specify a membrane-associated MacB-like tripartite ‘type VII’ ATP-Binding Cassette complex. However, as no MacA-like component is provided by the Cj1660-5 components, it suggested that this complex is not a transporter, but is instead an extra-cytoplasmic mechanotransducer (Greene *et al.*, 2018) that uses cytoplasmic ATP hydrolysis to drive an energy-requiring mechanism in the periplasm, as seen for the related LolCDE system of *E. coli*. The LolCDE (localization of lipoproteins) system excises lipoproteins from the outer surface of the inner membrane and delivers them to a periplasmic chaperone protein that subsequently mediates their insertion into the outer membrane (Yakushi *et al.*, 2000; Yang *et al.*, 2011). It is suggested that the predicted Cj1660-3 complex acts similarly to the Lol system of *E. coli* but is specific for the Cj1664/5 thioredoxins and thus acts to enable their insertion and/or removal from the membrane surfaces enclosing the periplasm.

The cj1660 protein is predicted to be embedded in the inner membrane though a large polytopic N-terminal domain and to possess a second large domain at the C-terminus that is located in the periplasm. This soluble domain consists of two sub-domains, DUF2318 and YHS. It is of interest to note that the DUF2318 domain possess three well-conserved motifs

each containing highly-conserved Cys residues (five in total), four of which form two CXXC motifs. Such motifs are found in thioredoxins where they provide the Cys residues involved in the thiol-disulphide exchange reaction. This indicates that these DUIF2318 motifs could act in thiol-disulphide exchange reactions with the two periplasmic thioredoxins. The YHS domain is known to be associated with heavy metal ATPase transporters and may provide metal sensing capacity.

From the above, a predictive model was generated for Cj1660-5 function (Fig. 3.27). This suggests that the two thioredoxins have a redox role in either accepting electrons from Ftr1/p19 for disposal via *C. jejuni* metabolic processes or that the thioredoxins have a ferric reduction role and thus support Ftr1/p19 by providing ferrous iron for uptake. The suggested role of Cj1660 is to mediate removal/delivery of electrons from/to the thioredoxins, whilst the Cj1661-3 complex is thought to allow the thioredoxins to move between membranes to enhance their interaction with redox exchange partners.

8.4. Complementation of an iron-uptake deficient *E. coli* strain

To demonstrate a role for the *C. jejuni* Ftr1-P19 system in iron uptake and test any role for the Cj1660-5 components, the *ftr1-p19* and *cj1660-5* genes were used to complement the low-iron growth defect of *E. coli* JC32 (mutant lacking iron transport systems). For this purpose, the *ftr1-p19* and *cj1660-5* genes were cloned into two compatible and inducible plasmids, pBADrha and pBADara, to allow their controlled expression in *E. coli*. This experiment demonstrated that *ftr1-p19* genes provide a growth advantage at low pH in iron-restricted medium, aerobically (Fig. 4.21 and 4.22). However, no advantage was seen at neutral or alkaline pH. This finding matches that of Koch *et al.* (2011) using an Ftr1-p19 system from a uropathogenic *E. coli* strain where a clear low-iron growth advantage was imposed when it was transferred to an *E. coli* mutant lacking iron-uptake capacity, although the effect was seen at a range of pH values. It is suggested that the low-iron growth advantage

at acidic pH provided by the *C. jejuni* Ftr1-p19 system, as observed here, is a result of raised stability for ferrous iron under aerobic conditions (Ratledge and Dover, 2000; Andrews *et al.*, 2003).

For Cj1660-5, the results showed that they also enhance growth of the mutant strain under low-iron, low pH conditions, but not at neutral or alkaline pH (Fig. 4.23 and 4.24). This is strongly suggestive of a role for this system in iron uptake that is independent of that of the Ftr1-p19 system. This would support a potential role for Cj1660-5 in ferric reduction, rather than disposal of electrons from Ftr1-p19 mediated ferrous oxidation.

When the *cj1660-65* and *ftr1-p19* plasmids were provided together, a slight low-iron growth enhancement was achieved under acidic pH conditions, both aerobically and anaerobically. Interestingly, when the two systems were provided in isolation, there was no clear low-iron growth enhancement anaerobically which indicates a collaborative activity for Ftr1-p19 and Cj1660-5 in iron uptake under low oxygen conditions. Ideally, these experiments would be repeated under a range of oxygen regimes with the single and double complemented strains in order to determine any enhanced Ftr1-p19/Cj1660-5 iron uptake activity under microaerobic conditions

8.5. The Ftr1-p19 and Cj1660-5 systems enhanced *in vitro* growth of *C. jejuni* under iron restriction

Mutations were generated using the well-characterised NCTC 11168 strain in three of the eight genes of interest, giving $\Delta ftr1::cat$, $\Delta cj1660::cat$ and $\Delta cj1663::cat$ mutants. These were confirmed by genome sequencing. Growth under the iron restriction showed a clear and significant growth inhibition for all three mutants which was enhanced under acidic pH. This suggests role of the Ftr1-p19 and Cj1660-5 system in iron uptake in *C. jejuni*. The phenotypes observed were similar for the three mutants, although were slightly weaker for the *ftr1* mutant and slightly stronger for the *cj1663* mutant. Iron sufficient conditions allowed

similar growth for the mutants and wildtype, further suggesting an iron uptake role for the Ftr1-Cj1665 systems. The enhanced phenotype at low pH is consistent with the reported low-pH induction of the *ftr1-cj1665* genes (Birk *et al.*, 2012; Varsaki *et al.*, 2015).

The mutants were complemented with a pMA1 plasmid carrying either *ftr1-p19* or *cj1660-5*. This resulted in enhanced growth with respect to the vector controls suggesting that multicopy versions of the *ftr1-p19* or *cj1660-5* genes provides an advantage for growth in low iron M-H medium. Growth was also very similar with that seen by the wildtype control indicating that complementation had been achieved.

8.6 Inactivation of *ftr1*, *cj1660* or *cj1665* results in weak chicken gut colonisation

The role of Ftr1-p19/Cj1660-5 system in the successful colonisation of *C. jejuni* in the chicken gut was tested using 64 chickens infected at day 20 with 10^7 cfu of *C. jejuni* (strain PT14, wildtype and mutants) and tested for colonisation at 3- and 7-days post infection. The results showed that the $\Delta ftr1$, $\Delta cj1660$ and $\Delta cj1663$ mutants cause a significant reduction in *C. jejuni* colonisation of the chicken cecum at 3-day post infection (Fig. 6.7A) which suggest a role for the Ftr1-p19/Cj1660-5 system in *C. jejuni* of the host. However, at 7 days post infection the $\Delta cj1660$ and $\Delta cj1663$ mutants showed higher colonisation levels and these were similar those of the wild type strain. The $\Delta ftr1$ mutant also showed higher colonisation at 7 than at 3 dpi but it did not achieve the levels seen for the wildtype (Fig. 6.7B). In addition, the chicken body weight gain through the experiment showed a significant decrease in the chicken group infected with the wild type but not those infected with the mutants (Fig. 6.8). These findings are consistent with a role for the iron-uptake activity of the Ftr1-p19/Cj1660-5 system in supporting gut colonisation. They also suggest that the mutations do not prevent colonisation, but instead reduce the time taken to achieve full colonisations. This would match the in vitro growth phenotype for the mutants whereby the major impact on growth

seen at low iron was an extended lag phase. The recovered strains at 7 dpi were found to still carry the expected mutations despite their normal (or near normal) colonisation levels.

8.7. The *ftr1-cj1665* genes are highly induced by iron restriction in a Fur-dependent manner and form a co-transcript

Quantitative RT-PCR analysis was used to measure the expression of the *ftr1-cj1665* genes under iron sufficient and deficient conditions using M-H medium. The PCR primers employed were designed to amplify regions encompassing the downstream-upstream regions of adjacent genes. This allowed the potential for co-transcript formation to be determined. All seven pairs of primers gave PCR products and indicated similar expression response to iron and *fur* status. This strongly suggests that a *ftr1-cj1665* co-transcript is generated from the 'P1' promoter upstream of *ftr1*.

Previous work of Fetherstone *et al.* (2012) in *Y. pestis* showed that *ftr1-p19 (fetMP)* mutation caused impaired low-iron growth that could only be restored when the entire locus (including downstream genes *y2367-2*) was included along with *fetMP* in for complementation, which provides strong circumstantial evidence for organisation of these genes as a single operon.

The cluster was highly induced by lack of iron, with an induction of between 112-2165-fold observed. This consistent with previous studies showed that *C. jejuni ftr1, p19* and *cj1660-63* are iron repressed genes (van Vliet *et al.*, 1998b; Holmes *et al.*, 2005; Palyada *et al.*, 2004; Butcher *et al.*, 2015; Butcher and Stintzi, 2013). The iron regulation was largely abolished in the *fur* mutant, indicating that the control by iron observed is Fur dependent, as observed previously. However, the regulatory response seen is indicative of apoFur induction, rather than Fe-Fur repression, with is contradictory to results published by other for the genes investigated (van Vliet *et al.*, 1998b; Holmes *et al.*, 2005; Palyada *et al.*, 2004). Indeed, Fur is generally considered to act as a repressor with ferrous iron as co-repressor, although there are reports of Fur-mediated transcriptional activation in some bacteria, including *C. jejuni*

(Palyada *et al.*, 2004; Holmes *et al.*, 2005; Butcher *et al.*, 2015). This could suggest that Fur may work as activator of iron transports in some conditions related to the growth phase, incubation condition and type of media that used. Without further investigation, it is difficult to understand how the Fur control response found here with respect to that previously reported can be accounted for.

An interesting observation is that the *ftr1-cj1665* operon contains two internal promoters (Dugar *et al.*, 2013). P2 is upstream of *cj1661* and could thus control expression of the putative *cj1661-3* MacB-like complex genes. This σ^{70} promoter might enable production of the Cj1661-3 complex in response to requirement for Lol activity. The P3 promoter is predicted to be σ^{28} dependent and is upstream of *cj1665* indicating that the Cj1665 thioredoxin might be involved in processes beyond iron uptake potentially related to motility.

8.8. Recent work by others on the Ftr1 system of *C. jejuni* strain 81-176

The paper of Liu *et al.* (2018) published during the course of this study was aimed at investigating the transcriptional response (by RNA sequencing) of the *C. jejuni* 81-176 strain to intestinal extracts of humans and chickens. They found that human faecal or chicken cecal extracts increased expression of 40 genes involved in iron transport, chemotaxis, metabolism and the response to osmotic pressure. These genes included *CJJ81176_1649-1655* (*cj1658-1664* in NCTC 11168) with induction levels of up to 4.2-fold. This finding is consistent with that of Croft *et al.* (2018) showing 6 of the 8 *1649-1656* genes are induced in human faeces upon *C. jejuni* colonisation. They found that the Ftr1-Cj1665 system is conserved in 33 bacterial species (6 phyla) and thus considered it likely to be of importance in *C. jejuni*, as suggested here. They subsequently generated a $\Delta 1651-1656$ (*cj1660-5*) mutant and showed that it exhibits reduced growth under low iron (as for a $\Delta p19$ mutant) in M-H medium that was enhanced by DFO and reversed by iron citrate. The mutants (*p19* and *1651-6*) also showed inhibited growth at pH 5 that was partially reversed by iron addition. The mutants

were more sensitive to streptomycin under low (but not other antibiotics tested) but not under high iron conditions and were more H₂O₂ sensitive (the reason for this is unclear). These effects were fully reversed by complementation. Although no *in vivo* experiments were performed, the effect of growth in media containing human fecal and chicken cecal extracts was examined, and reduced growth of both mutants was observed, indicating the 1649-1656 system is needed for maximum growth (and iron uptake) in the human faecal and chicken cecal extracts. Liu *et al.* (2018) suggest that the DUF2318 domain carries Fe-S clusters, but this is unlikely given its periplasmic location. They also considered that the Cj1661-3 components form a transporter, which also seems unlikely (as discussed above).

The findings of Liu *et al.* (2018) are consistent with those obtained here in that a low-iron growth defect was found in both cases for mutations in *cj1660-5* genes and a low pH phenotype was observed. In addition, the results here indicate an *in vivo* phenotype for the mutants, poor colonisation of the chicken cecum, which is consistent with the finds of Liu *et al.* (2018) showing poor growth with cecal extracts. The complementation strategy of Liu *et al.* (2018) involved incorporating a single copy of the complementary wildtype gene(s) into the chromosome at the 16S rRNA locus, which restored growth to that of the wildtype, which appears to be a more effective approach than that employed here with pMA1.

8.9. Future work

Currently, the mechanism of action of the Ftr1-p19 and Cj1660-5 systems is unclear. To further understand their role the location of the thioredoxins in the *C. jejuni* membrane should be determined in strains with and without Lol activity and in which the Cj1661-3 system is inactivated. In addition, the potential role of the Cj1660-5 components as an extracellular ferric reductase should be tested using $\Delta ftr1$, $\Delta cj1660$ and $\Delta cj1663$ mutants under high/low iron regime and at different pH. To determine whether the Ftr1-p19 and Cj1660-5 systems do indeed have independent iron-uptake activities, mutations that inactivate both systems

together should be introduced, and the effect on low-iron growth and gut colonisation should then be determined. It would also be of interest to examine the redox stress phenotype identified by Liu *et al.* (2018) to determine if this applied in the NCTC 11168 strain, and to include DFO in M-H growth experiments to attempt to enhance the low-iron growth phenotype. In future, complementation should involve insertion into the chromosome. In addition, it would be interesting to perform radioactive iron uptake experiments with Fe^{2+} and Fe^{3+} to determine the preferred substrate for the Ftr1-p19 system with/without Cj1660-5. Such work should ideally be performed in the *feoAB* mutant background and should compare uptake for FeoAB and Ftr1-p19. It would be particularly interesting to test the effect of pH and O_2 levels on the rate of uptake, to determine whether FeoAB function is enhanced in absence of O_2 and whether Ftr1-p19 activity is at all influenced by O_2 (as is the case of Ftr1-fet3p of yeast).

To understand the relative contributions of FeoAB and the Ftr1-p19/Cj1660-5 systems to ferrous iron uptake, *feoAB ftr1-p19*, *feoAB cj1660-5* and *feoAB ftr1-cj1665* double mutants should be generated and tested for their low-iron growth properties and chicken colonisation capacity, alongside the corresponding single mutants and wildtype. It would also be desirable to include complemented mutants (through chromosome insertion) in the chicken gut colonisation experiments, and competition experiments, to further strengthen the evidence for a colonisation impact. In addition, the effect of *fur* mutation on *ftr1-cj1665* expression should be reconsidered using an alternative *fur* mutant.

References

- Adak, G. K., Meakins, S. M., Yip, H., Lopman, B. A., & O'Brien, S. J. (2005). Disease risks from foods, England and Wales, 1996–2000. *Emerging Infectious Diseases*, 11(3), 365.
- Adler, C., Corbalán, N. S., Seyedsayamdost, M. R., Pomares, M. F., de Cristóbal, R. E., Clardy, J., ... & Vincent, P. A. (2012). Catecholate siderophores protect bacteria from pyochelin toxicity. *PloS One*, 7(10), e46754.
- Aguado-Santacruz, G. A., Moreno-Gomez, B., Jimenez-Francisco, B., Garcia-Moya, E., & Preciado-Ortiz, R. E. (2012). Impact of the microbial siderophores and phytosiderophores on the iron assimilation by plants: a synthesis. *Revista Fitotecnia Mexicana*, 35(1), 9-21.
- Aguero-Rosenfeld, M. E., Yang, X. H., & Nachamkin, I. R. V. I. N. G. (1990). Infection of adult Syrian hamsters with flagellar variants of *Campylobacter jejuni*. *Infection and Immunity*, 58(7), 2214-2219.
- Agunos, A., Waddell, L., Léger, D., & Taboada, E. (2014). A systematic review characterizing on-farm sources of *Campylobacter* spp. for broiler chickens. *PLoS One*, 9(8), e104905.
- Allen, K. J., & Griffiths, M. W. (2001). Use of luminescent *Campylobacter jejuni* ATCC 33291 to assess eggshell colonization and penetration in fresh and retail eggs. *Journal of Food Protection*, 64(12), 2058-2062.
- Allen, V. M., Bull, S. a., Corry, J. E. L., Domingue, G., Jørgensen, F., Frost, J. a., ... Humphrey, T. J. (2007). *Campylobacter* spp. contamination of chicken carcasses during processing in relation to flock colonisation. *International Journal of Food Microbiology*, 113, 54–61.
- Ames, G. F. L., Mimura, C. S., & Shyamala, V. (1990). Bacterial periplasmic permeases belong to a family of transport proteins operating from *Escherichia coli* to human: traffic ATPases. *FEMS Microbiology Letters*, 75(4), 429-446.
- Andrews, S. C. (1998). Iron storage in bacteria. *Advances in Microbial Physiology*, 40, 281-351.
- Andrews, S. C., Robinson, A. K., & Rodríguez-Quñones, F. (2003). Bacterial iron homeostasis. *FEMS Microbiology Reviews*, 27(2-3), 215-237.
- Archibald, F. (1983). *Lactobacillus plantarum*, an organism not requiring iron. *FEMS Microbiology Letters*, 19(1), 29-32.
- Armenteros, J. J. A., Tsirigos, K. D., Sønderby, C. K., Petersen, T. N., Winther, O., Brunak, S., ... & Nielsen, H. (2019). SignalP 5.0 improves signal peptide predictions using deep neural networks. *Nature Biotechnology*, 1.

References

- Aroori, S. V., Cogan, T. A., & Humphrey, T. J. (2014).** Effect of noradrenaline on the virulence properties of *Campylobacter* species. *International Journal of Microbiology*, 2014.
- Ashgar, S. S., Oldfield, N. J., Wooldridge, K. G., Jones, M. A., Irving, G. J., Turner, D. P., & Ala'Aldeen, D. A. (2007).** CapA, an autotransporter protein of *Campylobacter jejuni*, mediates association with human epithelial cells and colonization of the chicken gut. *Journal of Bacteriology*, 189(5), 1856-1865.
- Atack, J. M., & Kelly, D. J. (2008).** Contribution of the stereospecific methionine sulphoxide reductases MsrA and MsrB to oxidative and nitrosative stress resistance in the food-borne pathogen *Campylobacter jejuni*. *Microbiology*, 154(8), 2219-2230.
- Awad, W. A., Aschenbach, J. R., Ghareeb, K., Khayal, B., Hess, C., & Hess, M. (2014).** *Campylobacter jejuni* influences the expression of nutrient transporter genes in the intestine of chickens. *Veterinary Microbiology*, 172(1-2), 195-201.
- Awad, W. A., Molnár, A., Aschenbach, J. R., Ghareeb, K., Khayal, B., Hess, C., ... & Hess, M. (2015).** *Campylobacter* infection in chickens modulates the intestinal epithelial barrier function. *Innate Immunity*, 21(2), 151-160.
- Bacon, D. J., Alm, R. A., Burr, D. H., Hu, L., Kopecko, D. J., Ewing, C. P., & Guerry, P. (2000).** Involvement of a plasmid in virulence of *Campylobacter jejuni* 81-176. *Infection and Immunity*, 68(8), 4384-4390.
- Bae, J., Oh, E., & Jeon, B. (2014).** Enhanced transmission of antibiotic resistance in *Campylobacter jejuni* biofilms by natural transformation. *Antimicrobial Agents and Chemotherapy*, 58(12), 7573-7575.
- Bagg, A., & Neilands, J. B. (1987).** Ferric uptake regulation protein acts as a repressor, employing iron (II) as a cofactor to bind the operator of an iron transport operon in *Escherichia coli*. *Biochemistry*, 26(17), 5471-5477.
- Baichoo, N., & Helmann, J. D. (2002).** Recognition of DNA by Fur: a reinterpretation of the Fur box consensus sequence. *Journal of Bacteriology*, 184(21), 5826-5832.
- Baillon, M. L. A., Van Vliet, A. H., Ketley, J. M., Constantinidou, C., & Penn, C. W. (1999).** An iron-regulated alkyl hydroperoxide reductase (AhpC) confers aerotolerance and oxidative stress resistance to the microaerophilic pathogen *Campylobacter jejuni*. *Journal of Bacteriology*, 181(16), 4798-4804.
- Barker, R. A., Tisnado, J., Lambert, L. A., Gärdes, A., Carrano, M. W., Carrano, P. N., ... & Carrano, C. J. (2015).** Molecular characterization of a homolog of the ferric-uptake regulator, Fur, from the marine bacterium *Marinobacter algicola* DG893. *Biomaterials*, 28(1), 197-206.
- Beauchamp, J. M., Leveque, R. M., Dawid, S., & DiRita, V. J. (2017).** Methylation-dependent DNA discrimination in natural transformation of *Campylobacter jejuni*. *Proceedings of the National Academy of Sciences*, 114(38), E8053-E8061.

References

- Beery, J. T., Hugdahl, M. B., & Doyle, M. P. (1988).** Colonization of gastrointestinal tracts of chicks by *Campylobacter jejuni*. *Applied and Environmental Microbiology*, *54*(10), 2365-2370.
- Bellenger, J. P., Wichard, T., Kustka, A. B., & Kraepiel, A. M. L. (2008).** Uptake of molybdenum and vanadium by a nitrogen-fixing soil bacterium using siderophores. *Nature Geoscience*, *1*(4), 243.
- Berrang, M. E., Buhr, R. J., Cason, J. A., & Dickens, J. A. (2001).** Broiler carcass contamination with *Campylobacter* from feces during defeathering. *Journal of Food Protection*, *64*(12), 2063-2066.
- Bersudsky, M., Rosenberg, P., Rudensky, B., & Wirguin, I. (2000).** Lipopolysaccharides of a *Campylobacter coli* isolate from a patient with Guillain-Barré syndrome display ganglioside mimicry. *Journal of the Peripheral Nervous System*, *5*(4), 240-240.
- Bessell, P. R., Rotariu, O., Innocent, G. T., Smith-Palmer, A., Strachan, N. J., Forbes, K. J., ... & Matthews, L. (2012).** Using sequence data to identify alternative routes and risk of infection: a case-study of campylobacter in Scotland. *BMC Infectious Diseases*, *12*(1), 80.
- Bevilacqua, D. (2010).** L'Autorità Europea per la Sicurezza Alimentare: Genesi, Aspetti Problematici e Prospettive di Riforma, edited by Simone Gabbi. Milan/Italy: Giuffrè, 2009, 375 pp., € 40.00, Paperback. *European Journal of Risk Regulation*, *1*(3), 330-332.
- Bingham-Ramos, L. K., & Hendrixson, D. R. (2008).** Characterization of two putative cytochrome c peroxidases of *Campylobacter jejuni* involved in promoting commensal colonization of poultry. *Infection and Immunity*, *76*(3), 1105-1114.
- Birk, T., Wik, M. T., Lametsch, R., & Knöchel, S. (2012).** Acid stress response and protein induction in *Campylobacter jejuni* isolates with different acid tolerance. *BMC Microbiology*, *12*(1), 174.
- Black, R. E., Levine, M. M., Clements, M. L., Hughes, T. P., & Blaser, M. J. (1988).** Experimental *Campylobacter jejuni* infection in humans. *Journal of Infectious Diseases*, *157*(3), 472-479.
- Blaser, M. J. (1997).** Epidemiologic and clinical features of *Campylobacter jejuni* infections. *Journal of Infectious Diseases*, *176*(Supplement_2), S103-S105.
- Bolton, F. J., Coates, D., & Hutchinson, D. N. (1984).** The ability of *Campylobacter* media supplements to neutralize photochemically induced toxicity and hydrogen peroxide. *Journal of Applied Bacteriology*, *56*(1), 151-157.
- Bolton, F. J., Hutchinson, D. N., & Parker, G. (1988).** Reassessment of selective agars and filtration techniques for isolation of *Campylobacter* species from faeces. *European Journal of Clinical Microbiology and Infectious Diseases*, *7*(2), 155-160.

References

- Borrmann, E., Berndt, A., Hänel, I., & Köhler, H. (2007).** Campylobacter-induced interleukin-8 responses in human intestinal epithelial cells and primary intestinal chick cells. *Veterinary Microbiology*, *124*(1-2), 115-124.
- Brickman, T. J., & Armstrong, S. K. (2012).** Iron and pH-responsive FtrABCD ferrous iron utilization system of *Bordetella* species. *Molecular Microbiology*, *86*(3), 580-593.
- Briegel, A., Ortega, D. R., Tocheva, E. I., Wuichet, K., Li, Z., Chen, S., ... & Zhulin, I. B. (2009).** Universal architecture of bacterial chemoreceptor arrays. *Proceedings of the National Academy of Sciences*, *106*(40), 17181-17186.
- Brook, B., & Wu, A. (2013).** Induction of pBAD-ompA Fails to Enhance Conjugation in ompA-Deletion Mutant *Escherichia coli* Strains Containing the Plasmid. *Journal of Experimental Microbiology and Immunology (JEMI) Vol,17*, 88-92.
- Brown, S. A., Palmer, K. L., & Whiteley, M. (2008).** Revisiting the host as a growth medium. *Nature Reviews Microbiology*, *6*(9), 657-666.
- Buelow, D. R., Christensen, J. E., Neal-McKinney, J. M., & Konkel, M. E. (2011).** Campylobacter jejuni survival within human epithelial cells is enhanced by the secreted protein CiaI. *Molecular Microbiology*, *80*(5), 1296-1312.
- Buhr, R. J., Cox, N. A., Stern, N. J., Musgrove, M. T., Wilson, J. L., & Hiett, K. L. (2002).** Recovery of Campylobacter from segments of the reproductive tract of broiler breeder hens. *Avian diseases*, *46*(4), 919-924.
- Bull, S. A., Thomas, A., Humphrey, T., Ellis-Iversen, J., Cook, A. J., Lovell, R., & Jorgensen, F. (2008).** Flock health indicators and Campylobacter spp. in commercial housed broilers reared in Great Britain. *Applied and Environmental Microbiology*, *74*(17), 5408-5413.
- Bunting, K. D. (2002).** ABC transporters as phenotypic markers and functional regulators of stem cells. *Stem Cells*, *20*(1), 11-20.
- Buswell, C. M., Herlihy, Y. M., Lawrence, L. M., McGuiggan, J. T., Marsh, P. D., Keevil, C. W., & Leach, S. A. (1998).** Extended survival and persistence of Campylobacter spp. in water and aquatic biofilms and their detection by immunofluorescent-antibody and-rRNA staining. *Appl. Environ. Microbiol.*, *64*(2), 733-741.
- Butcher, J., Handley, R. A., van Vliet, A. H., & Stintzi, A. (2015).** Refined analysis of the Campylobacter jejuni iron-dependent/independent Fur-and PerR-transcriptomes. *BMC Genomics*, *16*(1), 1.
- Butcher, J., Flint, A., Stahl, M., & Stintzi, A. (2010).** Campylobacter Fur and PerR regulons. *Iron Uptake and Homeostasis in Microorganisms*, 168-202.
- Butcher, J., & Stintzi, A. (2013).** The transcriptional landscape of Campylobacter jejuni under iron replete and iron limited growth conditions. *PloS One*, *8*(11), e79475.

References

- Butzler, J.-P. (2004).** Campylobacter, from obscurity to celebrity. *Clinical Microbiology and Infection: The Official Publication of the European Society of Clinical Microbiology and Infectious Diseases*, 10(10), 868–76.
- Butzler, J. P., De Mol, P., & Mandal, B. K. (2018).** Clinical Aspects of Campylobacter Infections in Humans. In *Campylobacter Infection in Man and Animals* (pp. 21-32). CRC Press.
- Byrne, C. M., Clyne, M., & Bourke, B. (2007).** Campylobacter jejuni adhere to and invade chicken intestinal epithelial cells in vitro. *Microbiology*, 153(2), 561-569.
- Cameron, A., Fridrich, E., Huynh, S., Parker, C. T., & Gaynor, E. C. (2012).** Hyperosmotic stress response of Campylobacter jejuni. *Journal of Bacteriology*, 194(22), 6116-6130.
- Cao, J., M. R. Woodhall, J. Alvarez, M. L. Cartron and S. C. Andrews (2007).** "EfeUOB (YcdNOB) is a tripartite, acid-induced and CpxAR-regulated, low-pH Fe²⁺ transporter that is cryptic in *Escherichia coli* K-12 but functional in *E. coli* O157:H7." *Mol Microbiol* 65(4): 857-875.
- Carniel, E. (2001).** The Yersinia high-pathogenicity island: An iron-uptake island. *Microbes and Infection*, 3, 561–569.
- Carpenter, B. M., Whitmire, J. M., & Merrell, D. S. (2009).** This is not your mother's repressor: the complex role of fur in pathogenesis. *Infection and Immunity*, 77(7), 2590-2601.
- Carpenter, B. M., Gilbreath, J. J., Pich, O. Q., McKelvey, A. M., Maynard, E. L., Li, Z. Z., & Merrell, D. S. (2013).** Identification and characterization of novel Helicobacter pylori apo-Fur-regulated target genes. *Journal of Bacteriology*, 195(24), 5526-5539.
- Cartron, M. L., Maddocks, S., Gillingham, P., Craven, C. J., & Andrews, S. C. (2006).** Feo--transport of ferrous iron into bacteria. *Biometals*, 19(2), 143–57.
- Casabonne, C., Gonzalez, A., Aquili, V., Subils, T., & Balague, C. (2016).** Prevalence of seven virulence genes of Campylobacter jejuni isolated from patients with diarrhea in Rosario, Argentina. *International Journal of Infection*, 3(4).
- Chan, A. C., Doukov, T. I., Scofield, M., Tom-Yew, S. A., Ramin, A. B., MacKichan, J. K., ... & Murphy, M. E. (2010).** Structure and function of P19, a high-affinity iron transporter of the human pathogen Campylobacter jejuni. *Journal of Molecular Biology*, 401(4), 590-604.
- Chan, A. C., Lelj-Garolla, B., Rosell, F. I., Pedersen, K. A., Mauk, A. G., & Murphy, M. E. (2006).** Cofacial heme binding is linked to dimerization by a bacterial heme transport protein. *Journal of Molecular Biology*, 362(5), 1108-1119.

References

- Chan, K. F., Le Tran, H., Kanenaka, R. Y., & Kathariou, S. (2001).** Survival of clinical and poultry-derived isolates of *Campylobacter jejuni* at a low temperature (4 C). *Applied and Environmental Microbiology*, 67(9), 4186-4191.
- Chan, V. L., Louie, H., & Bingham, H. L. (1995).** Cloning and transcription regulation of the ferric uptake regulatory gene of *Campylobacter jejuni* TGH9011. *Gene*, 164(1), 25-31.
- Chang, C., & Miller, J. F. (2006).** *Campylobacter jejuni* colonization of mice with limited enteric flora. *Infection and Immunity*, 74(9), 5261-5271.
- Chang, N., & Taylor, D. E. (1990).** Use of pulsed-field agarose gel electrophoresis to size genomes of *Campylobacter* species and to construct a Sall map of *Campylobacter jejuni* UA580. *J. Bacteriol.*, 172, 5211–5217.
- Chen, M. L., Ge, Z., Fox, J. G., & Schauer, D. B. (2006).** Disruption of tight junctions and induction of proinflammatory cytokine responses in colonic epithelial cells by *Campylobacter jejuni*. *Infection and Immunity*, 74(12), 6581-6589.
- Chiancone, E., Ceci, P., Ilari, A., Ribacchi, F., & Stefanini, S. (2004).** Iron and proteins for iron storage and detoxification. *Biometals*, 17(3), 197-202.
- Chon, J. W., Hyeon, J. Y., Yim, J. H., Kim, J. H., Song, K. Y., & Seo, K. H. (2012).** Improvement of modified charcoal-cefoperazone-deoxycholate agar by supplementation with a high concentration of polymyxin B for detection of *Campylobacter jejuni* and *C. coli* in chicken carcass rinses. *Applied and Environmental Microbiology*, 78(5), 1624-1626.
- Christensen, J. E., Pacheco, S. A., & Konkel, M. E. (2009).** Identification of a *Campylobacter jejuni*-secreted protein required for maximal invasion of host cells. *Molecular Microbiology*, 73(4), 650-662.
- Clark, C. G., Taboada, E., Grant, C. C. R., Blakeston, C., Pollari, F., Marshall, B., Ng, L.-K. (2012).** Comparison of molecular typing methods useful for detecting clusters of *Campylobacter jejuni* and *C. coli* isolates through routine surveillance. *Journal of Clinical Microbiology*, 50(3), 798–809. Clench, M. H., & Mathias, J. R. (1995). The Avian Cecum: A Review. *The Wilson Bulletin*, 107(1), 93–121.
- Cody, A. J., McCarthy, N. M., Wimalarathna, H. L., Colles, F. M., Clark, L., Bowler, I. C., & Dingle, K. E. (2012).** A longitudinal 6-year study of the molecular epidemiology of clinical *Campylobacter* isolates in Oxfordshire, United Kingdom. *Journal of Clinical Microbiology*, 50(10), 3193-3201.
- Cogan, T. A., Thomas, A. O., Rees, L. E., Taylor, A. H., Jepson, M. A., Williams, P. H., ... & Humphrey, T. J. (2007).** Norepinephrine increases the pathogenic potential of *Campylobacter jejuni*. *Gut*, 56(8), 1060-1065.
- Coker, A. O., Isokpehi, R. D., Thomas, B. N., Amisu, K. O., & Obi, C. L. (2002).** Human *Campylobacteriosis* in developing countries. *Emerging Infectious Diseases*, 8(3), 237.

References

- Collet, J. F., D'Souza, J. C., Jakob, U., & Bardwell, J. C. (2003).** Thioredoxin 2, an oxidative stress-induced protein, contains a high affinity zinc binding site. *Journal of Biological Chemistry*, 278(46), 45325-45332.
- Cooksley, C., Jenks, P. J., Green, A., Cockayne, A., Logan, R. P., & Hardie, K. R. (2003).** NapA protects *Helicobacter pylori* from oxidative stress damage, and its production is influenced by the ferric uptake regulator. *Journal of Medical Microbiology*, 52(6), 461-469.
- Costerton, J. W., Lewadowski, Z. M., Caldwell, D. E., Korber, D. R., Lappin-Scott, H. M. (1995).** *Microbial Biofilms. Ann. Rev. Microbiol.*, 49, 711-745.
- Coward, C., van Diemen, P. M., Conlan, A. J., Gog, J. R., Stevens, M. P., Jones, M. A., & Maskell, D. J. (2008).** Competing isogenic *Campylobacter* strains exhibit variable population structures in vivo. *Applied and Environmental Microbiology*, 74(12), 3857-3867.
- Cowart, R. E. (2002).** Reduction of iron by extracellular iron reductases: Implications for microbial iron acquisition. *Archives of Biochemistry and Biophysics*, 400(2), 273-281.
- Cox, N. A., Richardson, L. J., Maurer, J. J., Berrang, M. E., Fedorka-Cray, P. J., Buhr, R. J., ... & Lammerding, A. M. (2012).** Evidence for horizontal and vertical transmission in *Campylobacter* passage from hen to her progeny. *Journal of Food Protection*, 75(10), 1896-1902.
- Cox, N. A., Stern, N. J., Wilson, J. L., Musgrove, M. T., Buhr, R. J., & Hiett, K. L. (2002).** Isolation of *Campylobacter* spp. from semen samples of commercial broiler breeder roosters. *Avian Diseases*, 46(3), 717-720.
- Coy, M., & Neilands, J. B. (1991).** Structural dynamics and functional domains of the Fur protein. *Biochemistry*, 30(33), 8201-8210.
- Crofts, A. A., Poly, F. M., Ewing, C. P., Kuroiwa, J. M., Rimmer, J. E., Harro, C., ... & DeNearing, B. (2018).** *Campylobacter jejuni* transcriptional and genetic adaptation during human infection. *Nature Microbiology*, 3(4), 494.
- Crow, A., Greene, N. P., Kaplan, E., & Koronakis, V. (2017).** Structure and mechanotransmission mechanism of the MacB ABC transporter superfamily. *Proceedings of the National Academy of Sciences*, 114(47), 12572-12577.
- Crumbliss, A. L., & Harrington, J. M. (2009).** Iron sequestration by small molecules: thermodynamic and kinetic studies of natural siderophores and synthetic model compounds. *Advances in Inorganic Chemistry*, 61, 179-250.
- Danielli, A., Roncarati, D., Delany, I., Chiarini, V., Rappuoli, R., & Scarlato, V. (2006).** In vivo dissection of the *Helicobacter pylori* Fur regulatory circuit by genome-wide location analysis. *Journal of Bacteriology*, 188(13), 4654-4662.

References

- Dashper, S. G., Butler, C. a, Lissel, J. P., Paolini, R. a, Hoffmann, B., Veith, P. D., Reynolds, E. C. (2005).** A novel Porphyromonas gingivalis FeoB plays a role in manganese accumulation. *The Journal of Biological Chemistry*, 280(30), 28095–102.
- da Silva Neto, J. F., Braz, V. S., Italiani, V. C., & Marques, M. V. (2009).** Fur controls iron homeostasis and oxidative stress defense in the oligotrophic alpha-proteobacterium *Caulobacter crescentus*. *Nucleic Acids Research*, 37(14), 4812-4825.
- Dasti, J. I., Tareen, A. M., Lugert, R., Zautner, A. E., & Groß, U. (2010).** *Campylobacter jejuni*: a brief overview on pathogenicity-associated factors and disease-mediating mechanisms. *International Journal of Medical Microbiology*, 300(4), 205-211.
- Davis, L., Young, K., DiRita, V., 2008.** Genetic manipulation of *Campylobacter jejuni*. *Curr. Protoc. Microbiol.* 10 (8A.2.1-8A.2.17).
- de Haan, C. P., Llarena, A. K., Revez, J., & Hänninen, M. L. (2012).** Association of *Campylobacter jejuni* metabolic traits with multilocus sequence types. *Applied and Environmental Microbiology*, 78(16), 5550-5554.
- Deka, R. K., Brautigam, C. A., Tomson, F. L., Lumpkins, S. B., Tomchick, D. R., Machius, M., & Norgard, M. V. (2007).** Crystal Structure of the Tp34 (TP0971) Lipoprotein of *Treponema pallidum* implications of its metal-bound state and affinity for human lactoferrin. *Journal of Biological Chemistry*, 282(8), 5944-5958.
- Delany, I., Rappuoli, R., & Scarlato, V. (2004).** Fur functions as an activator and as a repressor of putative virulence genes in *Neisseria meningitidis*. *Molecular Microbiology*, 52(4), 1081-1090.
- Del Rocio Leon-Kempis, M., Guccione, E., Mulholland, F., Williamson, M. P., & Kelly, D. J. (2006).** The *Campylobacter jejuni* PEB1a adhesin is an aspartate/glutamate-binding protein of an ABC transporter essential for microaerobic growth on dicarboxylic amino acids. *Molecular Microbiology*, 60(5), 1262-1275.
- Deng, X., Sun, F., Ji, Q., Liang, H., Missiakas, D., Lan, L., & He, C. (2012).** Expression of multidrug resistance efflux pump gene *norA* is iron responsive in *Staphylococcus aureus*. *Journal of Bacteriology*, 194(7), 1753-1762.
- Denis, M., Tanguy, M., Chidaine, B., Laisney, M. J., Mégraud, F., & Fravallo, P. (2011).** Description and sources of contamination by *Campylobacter* spp. of river water destined for human consumption in Brittany, France. *Pathologie Biologie*, 59(5), 256-263.
- Dhillon, A. S., Shivaprasad, H. L., Schaberg, D., Wier, F., Weber, S., & Bandli, D. (2006).** *Campylobacter jejuni* infection in broiler chickens. *Avian diseases*, 50(1), 55-58.
- Dingle, K. E., McCarthy, N. D., Cody, A. J., Peto, T. E. a, & Maiden, M. C. J. (2008).** Extended sequence typing of *Campylobacter* spp., United Kingdom. *Emerging Infectious Diseases*, 14(10), 1620–1622.
- Dorrell, N., Mangan, J. A., Laing, K. G., Hinds, J., Linton, D., Al-Ghusein, H., ... & Butcher, P. D. (2001).** Whole genome comparison of *Campylobacter jejuni* human

References

- isolates using a low-cost microarray reveals extensive genetic diversity. *Genome Research*, 11(10), 1706-1715.
- Douglas, T., & Ripoll, D. R. (1998).** Calculated electrostatic gradients in recombinant human H-chain ferritin. *Protein Science*, 7(5), 1083-1091.
- Dubbels, B. L., DiSpirito, A. A., Morton, J. D., Semrau, J. D., Neto, J. N. E., & Bazylnski, D. A. (2004).** Evidence for a copper-dependent iron transport system in the marine, magnetotactic bacterium strain MV-1. *Microbiology*, 150(9), 2931-2945.
- Dugar, G., Herbig, A., Förstner, K. U., Heidrich, N., Reinhardt, R., Nieselt, K., & Sharma, C. M. (2013).** High-resolution transcriptome maps reveal strain-specific regulatory features of multiple *Campylobacter jejuni* isolates. *PLoS Genetics*, 9(5), e1003495.
- Duong, T., & Konkel, M. E. (2009).** Comparative studies of *Campylobacter jejuni* genomic diversity reveal the importance of core and dispensable genes in the biology of this enigmatic food-borne pathogen. *Current Opinion in Biotechnology*, 20(2), 158-165.
- EFSA Panel on Biological Hazards (BIOHAZ). (2010).** Scientific opinion on quantification of the risk posed by broiler meat to human campylobacteriosis in the EU. *EFSA Journal*, 8(1), 1437.
- Egan, S. M., and R. F. Schleif. 1993.** A regulatory cascade in the induction of rhaBAD. *Journal of Molecular Biology*. 234: 87-98.
- Elhassanny, A. E., Anderson, E. S., Menscher, E. A., & Roop, R. M. (2013).** The ferrous iron transporter FtrABCD is required for the virulence of *Brucella abortus* 2308 in mice. *Molecular Microbiology*, 88(6), 1070-1082.
- El-Shibiny, A., Connerton, P., & Connerton, I. (2009).** Survival at refrigeration and freezing temperatures of *Campylobacter coli* and *Campylobacter jejuni* on chicken skin applied as axenic and mixed inoculums. *International journal of Food Microbiology*, 131(2-3), 197-202.
- Elvers, K. T., & Park, S. F. (2002).** Quorum sensing in *Campylobacter jejuni*: detection of a luxS encoded signalling molecule. *Microbiology*, 148(5), 1475-1481.
- Embree, M., Qiu, Y., Shieu, W., Nagarajan, H., O'Neil, R., Lovley, D., & Zengler, K. (2014).** The iron stimulon and fur regulon of *Geobacter sulfurreducens* and their role in energy metabolism. *Appl. Environ. Microbiol.*, 80(9), 2918-2927.
- Engberg, J., On, S. L., Harrington, C. S., & Gerner-Smidt, P. (2000).** Prevalence of *Campylobacter*, *Arcobacter*, *Helicobacter*, *Andsutterella* spp. in human fecal samples as estimated by a reevaluation of isolation methods for campylobacters. *Journal of Clinical Microbiology*, 38(1), 286-291.
- Escolar, L., Pérez-Martín, J., & De Lorenzo, V. (1999).** Opening the iron box: Transcriptional metalloregulation by the fur protein. *Journal of Bacteriology*, 181(20), 6223-6229.

References

- Ettema, T. J., Huynen, M. A., de Vos, W. M., & van der Oost, J. (2003).** TRASH: a novel metal-binding domain predicted to be involved in heavy-metal sensing, trafficking and resistance. *Trends in Biochemical Sciences*, 28(4), 170-173.
- Eucker, T. P., & Konkel, M. E. (2012).** The cooperative action of bacterial fibronectin-binding proteins and secreted proteins promote maximal *Campylobacter jejuni* invasion of host cells by stimulating membrane ruffling. *Cellular Microbiology*, 14(2), 226-238.
- Everest, P. H., Goossens, H., Butzler, J. P., Lloyd, D., Knutton, S., Ketley, J. M., & Williams, P. H. (1992).** Differentiated Caco-2 cells as a model for enteric invasion by *Campylobacter jejuni* and *C. coli*. *Journal of Medical Microbiology*, 37(5), 319-325.
- Fabianek, R. A., Hennecke, H., & Thöny-Meyer, L. (2000).** Periplasmic protein thiol: disulfide oxidoreductases of *Escherichia coli*. *FEMS Microbiology Reviews*, 24(3), 303-316.
- Fauchere, J. L., Rosenau, a, Veron, M., Moyon, E. N., Richard, S., & Pfister, a. (1986).** Association with HeLa cells of *Campylobacter jejuni* and *Campylobacter coli* isolated from human feces. *Infection and Immunity*, 54(2), 283–287.
- Fenton, H. J. H. (1894).** LXXIII.—Oxidation of tartaric acid in presence of iron. *Journal of the Chemical Society, Transactions*, 65, 899-910.
- Ferrero, R. L., & Lee, A. (1988).** Motility of *Campylobacter jejuni* in a viscous environment: comparison with conventional rod-shaped bacteria. *Microbiology*, 134(1), 53-59.
- Fetherston, J. D., Mier, I., Truszczynska, H., & Perry, R. D. (2012).** The Yfe and Feo transporters are involved in microaerobic growth and virulence of *Yersinia pestis* in bubonic plague. *Infection and Immunity*, 80(11), 3880-3891.
- Field, L. H., Headley, V. L., Payne, S. M., & Berry, L. J. (1986).** Influence of iron on growth, morphology, outer membrane protein composition, and synthesis of siderophores in *Campylobacter jejuni*. *Infection and Immunity*, 54(1), 126–132
- Fillat, M. F. (2014).** The FUR (ferric uptake regulator) superfamily: diversity and versatility of key transcriptional regulators. *Archives of Biochemistry and Biophysics*, 546, 41-52.
- Fitzpatrick, A. W., Llabrés, S., Neuberger, A., Blaza, J. N., Bai, X. C., Okada, U., ... & Luisi, B. F. (2017).** Structure of the MacAB–TolC ABC-type tripartite multidrug efflux pump. *Nature Microbiology*, 2(7), 17070.
- Flamholz, A., Noor, E., Bar-Even, A., Liebermeister, W., & Milo, R. (2013).** Glycolytic strategy as a tradeoff between energy yield and protein cost. *Proceedings of the National Academy of Sciences*, 110(24), 10039-10044.
- Flanagan, R. C., Neal-McKinney, J. M., Dhillon, A. S., Miller, W. G., & Konkel, M. E. (2009).** Examination of *Campylobacter jejuni* putative adhesins leads to the

References

- identification of a new protein, designated FlpA, required for chicken colonization. *Infection and Immunity*, 77(6), 2399-2407.
- Fleischhacker, A. S., & Kiley, P. J. (2011).** Iron-containing transcription factors and their roles as sensors. *Current Opinion in Chemical Biology*, 15(2), 335-341.
- Flint, A., Sun, Y. Q., Butcher, J., Stahl, M., Huang, H., & Stintzi, A. (2014).** Phenotypic screening of a targeted mutant library reveals *Campylobacter jejuni* defenses against oxidative stress. *Infection and Immunity*, 82(6), 2266-2275.
- Ford, D. C., P. M. Ireland, H. L. Bullifent, R. J. Saint, E. V. McAlister, M. Sarkar-Tyson and P. C. F. Oyston. 2014.** Construction of an inducible system for the analysis of essential genes in *Yersinia pestis*. *Journal of Microbiological Methods*. 100: 1-7.
- Fouts, D. E., Mongodin, E. F., Mandrell, R. E., Miller, W. G., Rasko, D. a, Ravel, J., ... Nelson, K. E. (2005).** Major structural differences and novel potential virulence mechanisms from the genomes of multiple campylobacter species. *PLoS Biology*, 3(1), e15.
- Fox, J. G., Rogers, A. B., Whary, M. T., Ge, Z., Taylor, N. S., Xu, S., ... Erdman, S. E. (2004).** Gastroenteritis in NF-kappaB-deficient mice is produced with wild-type *Campylobacter jejuni* but not with *C. jejuni* lacking cytolethal distending toxin despite persistent colonization with both strains. *Infection and Immunity*, 72(2), 1116–25.
- Friedman, C.R., Neimann, J., Wegener, H.G., Tauxe, R.V. (2000).** Epidemiology of *Campylobacter jejuni* infections in the United States and other industrialized nations. In: Nachamkin, I., Blaser, M.J.(Eds.). *Campylobacter*. ASM Press, Washington, pp.121–139.
- Fux, C. A., Costerton, J. W., Stewart, P. S., & Stoodley, P. (2005).** Survival strategies of infectious biofilms. *Trends in Microbiology*, 13(1), 34-40.
- Galindo, M. A., Day, W. A., Raphael, B. H., & Joens, L. A. (2001).** Cloning and characterization of a *Campylobacter jejuni* iron-uptake operon. *Current Microbiology*, 42(2), 139-143.
- Ganz, T. (2018).** Iron and infection. *International Journal of Hematology*, 107(1), 7-15.
- Ganz, T., & Nemeth, E. (2015).** Iron homeostasis in host defence and inflammation. *Nature Reviews Immunology*, 15(8), 500.
- García Rodríguez, L. A., Ruigómez, A., & Panés, J. (2006).** Acute gastroenteritis is followed by an increased risk of inflammatory bowel disease. *Gastroenterology*, 130(6), 1588–94.
- Garénaux, A., Guillou, S., Ermel, G., Wren, B., Federighi, M., & Ritz, M. (2008a).** Role of the Cj1371 periplasmic protein and the Cj0355c two-component regulator in the *Campylobacter jejuni* NCTC 11168 response to oxidative stress caused by paraquat. *Research in Microbiology*, 159(9-10), 718-726.

References

- Garénaux, A., Jugiau, F., Rama, F., De Jonge, R., Denis, M., Federighi, M., & Ritz, M. (2008b).** Survival of *Campylobacter jejuni* strains from different origins under oxidative stress conditions: effect of temperature. *Current Microbiology*, *56*(4), 293-297.
- Garénaux, A., Ritz, M., Jugiau, F., Rama, F., Federighi, M., & de Jonge, R. (2009).** Role of oxidative stress in *C. jejuni* inactivation during freeze-thaw treatment. *Current Microbiology*, *58*(2), 134-138.
- Gargi, A., Reno, M., & Blanke, S. R. (2012).** Bacterial toxin modulation of the eukaryotic cell cycle: are all cytolethal distending toxins created equally? *Frontiers in cellular and Infection Microbiology*, *2*, 124.
- Gaynor, E. C., Cawthraw, S., Manning, G., MacKichan, J. K., Falkow, S., & Newell, D. G. (2004).** The genome-sequenced variant of *Campylobacter jejuni* NCTC 11168 and the original clonal clinical isolate differ markedly in colonization, gene expression, and virulence-associated phenotypes. *Journal of Bacteriology*, *186*(2), 503-517.
- Ge, B., Wang, F., Sjoelund-Karlsson, M., & McDermott, P. F. (2013).** Antimicrobial resistance in *Campylobacter*: susceptibility testing methods and resistance trends. *Journal of Microbiological Methods*, *95*(1), 57-67.
- Ge, Z., Schauer, D. B., & Fox, J. G. (2008).** In vivo virulence properties of bacterial cytolethal-distending toxin. *Cellular Microbiology*, *10*(8), 1599-1607.
- Genco, C. A., & Dixon, D. W. (2001).** Emerging strategies in microbial haem capture: MicroReview. *Molecular Microbiology*, *39*(1), 1-11.
- Ghigo, J. M., Letoffe, S., & Wandersman, C. (1997).** A new type of hemophore-dependent heme acquisition system of *Serratia marcescens* reconstituted in *Escherichia coli*. *Journal of bacteriology*, *179*(11), 3572-3579.
- Gibreel, A., Sköld, O., & Taylor, D. E. (2004).** Characterization of plasmid-mediated aphA-3 kanamycin resistance in *Campylobacter jejuni*. *Microbial Drug Resistance*, *10*(2), 98-105.
- Gibson, D. G., Young, L., Chuang, R. Y., Venter, J. C., Hutchison III, C. A., & Smith, H. O. (2009).** Enzymatic assembly of DNA molecules up to several hundred kilobases. *Nature Methods*, *6*(5), 343.
- Gillespie, J., De Nardin, E., Radel, S., Kuracina, J., Smutko, J. & Zambon, J. J. (1992).** Production of an extracellular toxin by the oral pathogen *Campylobacter rectus*. *Microbial Pathogenesis* *12*, 69-77.
- Gonzalez de Peredo, A., Saint-Pierre, C., Latour, J.M., MichaudSoret, I. and Forest, E. (2001).** Conformational changes of the ferric uptake regulation protein upon metal activation and DNA binding: first evidence of structural homologies with the diphtheria toxin repressor. *J. Mol. Biol.* *310*, 83-91.
- GOODWIN, C. S., ARMSTRONG, J. A., CHILVERS, T., PETERS, M., COLLINS, M. D., SLY, L., ... & HARPER, W. E. (1989).** Transfer of *Campylobacter pylori* and

References

- Campylobacter mustelae to Helicobacter gen. nov. as Helicobacter pylori comb. nov. and Helicobacter mustelae comb. nov., respectively. *International Journal of Systematic and Evolutionary Microbiology*, 39(4), 397-405.
- Goodwin, C. S., McConnell, W., McCulloch, R. K., McCullough, C., Hill, R., Bronsdon, M. A., & Kasper, G. (1989).** Cellular fatty acid composition of Campylobacter pylori from primates and ferrets compared with those of other campylobacters. *Journal of Clinical Microbiology*, 27(5), 938-943.
- Gozzelino, R., & Arosio, P. (2016).** Iron homeostasis in health and disease. *International Journal of Molecular Sciences*, 17(1), 130.
- Grant, C. C., Konkol, M. E., Cieplak, W., & Tompkins, L. S. (1993).** Role of flagella in adherence, internalization, and translocation of Campylobacter jejuni in nonpolarized and polarized epithelial cell cultures. *Infection and Immunity*, 61(5), 1764–71.
- Grant, K. A., & Park, S. F. (1995).** Molecular characterization of katA from Campylobacter jejuni and generation of a catalase-deficient mutant of Campylobacter coli by interspecific allelic exchange. *Microbiology*, 141(6), 1369-1376.
- Grant, K. A., Belandia, I. U., Dekker, N., Richardson, P. T., & Park, S. F. (1997).** Molecular characterization of pldA, the structural gene for a phospholipase A form Campylobacter coli, and its contribution to cell-associated hemolysis. *Infection and Immunity*, 65(4), 1172–80.
- Greene, N. P., Kaplan, E., Crow, A., & Koronakis, V. (2018).** Antibiotic resistance mediated by the MacB ABC transporter family: A structural and functional perspective. *Frontiers in Microbiology*, 9.
- Große, C., Scherer, J., Koch, D., Otto, M., Taudte, N., & Grass, G. (2006).** A new ferrous iron-uptake transporter, EfeU (YcdN), from Escherichia coli. *Mol Microbiol*, 62(1), 120–131.
- Guccione, E., Del Rocio Leon-Kempis, M., Pearson, B. M., Hitchin, E., Mulholland, F., Van Diemen, P. M., ... & Kelly, D. J. (2008).** Amino acid-dependent growth of Campylobacter jejuni: key roles for aspartase (AspA) under microaerobic and oxygen-limited conditions and identification of AspB (Cj0762), essential for growth on glutamate. *Molecular Microbiology*, 69(1), 77-93.
- Guerinot, M. L. (1994).** Microbial iron transport. *Annual Reviews in Microbiology*, 48(1), 743-772.
- Guerry, P., 2007.** Campylobacter flagella: not just for motility. *Trends Microbiol.* 15, 456e461.
- Guerry, P., Alm, R.A., Power, M.E., Trust, T.J. (1992).** Molecular and structural analysis of Campylobacter flagellin. In: Nachamkin, I., Blaser, M.J., Tompkins, L.S.(Eds.), *Campylobacter jejuni: Current Status and Future Trends*. ASM Press, Washington, pp.267–281.

References

- Guerry, P., Alm, R.A., Power, M.E., Logan, S.M., & Trust, T.J. (1991).** Role of two flagellin genes in *Campylobacter* motility. *J Bacteriol*, 173(15), 4757-4764.
- Gundogdu, O., Bentley, S. D., Holden, M. T., Parkhill, J., Dorrell, N., & Wren, B. W. (2007).** Re-annotation and re-analysis of the *Campylobacter jejuni* NCTC11168 genome sequence. *BMC Genomics*, 8(1), 162.
- Gundogdu, O., Mills, D. C., Elmi, A., Martin, M. J., Wren, B. W., & Dorrell, N. (2011).** The *Campylobacter jejuni* transcriptional regulator Cj1556 plays a role in the oxidative and aerobic stress response and is important for bacterial survival in vivo. *Journal of Bacteriology*, 193(16), 4238-4249.
- Gundogdu, O., Wren, B. W., & Dorrell, N. (2014).** Genetic Mechanisms Involved in *Campylobacter jejuni* Survival Under Oxidative Stress Conditions. *Campylobacter Ecology and Evolution*, 125.
- Guzman, L. M., D. Belin, M. J. Carson and J. Beckwith. 1995.** Tight regulation, modulation, and high-level expression by vectors containing the arabinose PBAD promoter. *Journal of Bacteriology*. 177: 4121-4130.
- Hall-Stoodley, L., & Stoodley, P. (2005).** Biofilm formation and dispersal and the transmission of human pathogens. *Trends in Microbiology*, 13(1), 7-10.
- Hanahan, D. 1983.** Studies on transformation of *Escherichia coli* with plasmids. *Journal of Molecular Biology*. 166: 557-580.
- Handley, R. A., Mulholland, F., Reuter, M., Ramachandran, V. K., Musk, H., Clissold, L., ... & van Vliet, A. H. (2015).** PerR controls oxidative stress defence and aerotolerance but not motility-associated phenotypes of *Campylobacter jejuni*. *Microbiology*, 161(7), 1524-1536.
- Hantke, K. (1981).** Regulation of ferric iron transport in *Escherichia coli* K12: isolation of a constitutive mutant. *Molecular and General Genetics MGG*, 182(2), 288-292.
- Hantke, K. (1987).** Ferrous iron transport mutants in *Escherichia coli* K12. *FEMS Microbiology Letters*, 44(1), 53-57.
- Hantke, K. (2001).** Iron and metal regulation in bacteria. *Current Opinion in Microbiology*, 4(2), 172-177.
- Hantke, K. (2003).** Is the bacterial ferrous iron transporter FeoB a living fossil? *Trends in Microbiology*, 11(5), 192-195.
- Hassan, H. M., & Troxell, B. (2013).** Transcriptional regulation by Ferric Uptake Regulator (Fur) in pathogenic bacteria. *Frontiers in cellular and infection microbiology*, 3, 59.
- Havelaar, A. H., van Pelt, W., Ang, C. W., Wagenaar, J. A., van Putten, J. P., Gross, U., & Newell, D. G. (2009).** Immunity to *Campylobacter*: its role in risk assessment and epidemiology. *Critical Reviews in Microbiology*, 35(1), 1-22.

References

- Hazeleger, W. C., Wouters, J. A., Rombouts, F. M., & Abee, T. (1998).** Physiological activity of *Campylobacter jejuni* far below the minimal growth temperature. *Applied and Environmental Microbiology*, *64*(10), 3917-3922.
- He, Y., & Chen, C. Y. (2010).** Quantitative analysis of viable, stressed and dead cells of *Campylobacter jejuni* strain 81-176. *Food Microbiology*, *27*(4), 439-446.
- He, Z., Gharaibeh, R. Z., Newsome, R. C., Pope, J. L., Dougherty, M. W., Tomkovich, S., ... & Jobin, C. (2019).** *Campylobacter jejuni* promotes colorectal tumorigenesis through the action of cytolethal distending toxin. *Gut*, *68*(2), 289-300.
- Helmann, J. D. (2014).** Specificity of metal sensing: iron and manganese homeostasis in *Bacillus subtilis*. *Journal of Biological Chemistry*, *289*(41), 28112-28120.
- Hendrixson, D. R., & DiRita, V. J. (2004).** Identification of *Campylobacter jejuni* genes involved in commensal colonization of the chick gastrointestinal tract. *Molecular Microbiology*, *52*(2), 471-484.
- Hendrixson, D. R. (2006).** A phase-variable mechanism controlling the *Campylobacter jejuni* FlgR response regulator influences commensalism. *Molecular Microbiology*, *61*(6), 1646-1659.
- Hermans, D., Pasmans, F., Messens, W., Martel, A., Van Immerseel, F., Rasschaert, G., ... & Haesebrouck, F. (2012).** Poultry as a host for the zoonotic pathogen *Campylobacter jejuni*. *Vector-Borne and Zoonotic Diseases*, *12*(2), 89-98.
- Hermans, D., Van Deun, K., Martel, A., Van Immerseel, F., Messens, W., Heyndrickx, M., ... & Pasmans, F. (2011).** Colonization factors of *Campylobacter jejuni* in the chicken gut. *Veterinary Research*, *42*(1), 82.
- Heywood, W., Henderson, B., & Nair, S. P. (2005).** Cytolethal distending toxin: creating a gap in the cell cycle. *Journal of Medical Microbiology*, *54*(3), 207-216.
- Hickey, T., Baqar, S., Bourgeois, L., Ewing, C., & Guerry, P. (1999).** *Campylobacter jejuni*-stimulated secretion of interleukin-8 by INT407 cells. *Infection and Immunity*, *67*(1), 88-93.
- Hider, R. C., & Kong, X. (2010).** Chemistry and biology of siderophores. *Natural Product Reports*, *27*(5), 637-657.
- Hilbert, F., Scherwitzel, M., Paulsen, P., & Szostak, M. P. (2010).** Survival of *Campylobacter jejuni* under Conditions of Atmospheric Oxygen Tension with the Support of *Pseudomonas* spp. *Applied and Environmental Microbiology*, *76*(17), 5911-5917.
- Hoffman, P. S., George, H. A., Krieg, N. R., & Smibert, R. M. (1979).** Studies of the microaerophilic nature of *Campylobacter fetus* subsp. *jejuni*. II. Role of exogenous superoxide anions and hydrogen peroxide. *Canadian Journal of Microbiology*, *25*(1), 8-16.

References

- Hoffman, P. S., & Goodman, T. G. (1982).** Respiratory physiology and energy conservation efficiency of *Campylobacter jejuni*. *Journal of Bacteriology*, *150*(1), 319-326.
- Hofreuter, D. (2014).** Defining the metabolic requirements for the growth and colonization capacity of *Campylobacter jejuni*. *Frontiers in Cellular and Infection Microbiology*, *4*, 137.
- Hofreuter, D., Novik, V., & Galán, J. E. (2008).** Metabolic Diversity in *Campylobacter jejuni* Enhances Specific Tissue Colonization. *Cell Host and Microbe*, *4*(5), 425–433.
- Hofreuter, D., Tsai, J., Watson, R. O., Novik, V., Altman, B., Benitez, M., Galán, J. E. (2006).** Unique features of a highly pathogenic *Campylobacter jejuni* strain. *Infection and Immunity*, *74*(8), 4694–707.
- Holden, V. I., & Bachman, M. A. (2015).** Diverging roles of bacterial siderophores during infection. *Metallomics*, *7*(6), 986-995.
- Holmes, K., Mulholland, F., Pearson, B. M., Pin, C., McNicholl-Kennedy, J., Ketley, J. M., & Wells, J. M. (2005).** *Campylobacter jejuni* gene expression in response to iron limitation and the role of Fur. *Microbiology*, *151*, 243–257.
- Holt, J. P., Grant, A. J., Coward, C., Maskell, D. J., & Quinlan, J. J. (2012).** Cj1051c is a Major Determinant for the Restriction Barrier of *Campylobacter jejuni* Strain NCTC11168. *Applied and Environmental Microbiology*, AEM-01799.
- Hu, L., & Hickey, T. E. (2005).** *Campylobacter jejuni* induces secretion of proinflammatory chemokines from human intestinal epithelial cells. *Infection and Immunity*, *73*(7), 4437-4440.
- Hu, L., Bray, M. D., Osorio, M., & Kopecko, D. J. (2006).** *Campylobacter jejuni* induces maturation and cytokine production in human dendritic cells. *Infection and Immunity*, *74*(5), 2697-2705.
- Humphrey, T. (2006).** Are happy chickens safer chickens? Poultry welfare and disease susceptibility. *British Poultry Science*, *47*(4), 379–391.
- Humphrey, T. J., & Cruickshank, J. G. (1985).** Antibiotic and deoxycholate resistance in *Campylobacter jejuni* following freezing or heating. *Journal of Applied Bacteriology*, *59*(1), 65-71.
- Humphrey, S., Lacharme-Lora, L., Chaloner, G., Gibbs, K., Humphrey, T., Williams, N., & Wigley, P. (2015).** Heterogeneity in the Infection Biology of *Campylobacter jejuni* Isolates in Three Infection Models Reveals an Invasive and Virulent Phenotype in a ST21 Isolate from Poultry. *PLoS One*, *10*(10), e0141182. doi: 10.1371/journal.pone.0141182
- Hwang, S., Kim, M., Ryu, S., & Jeon, B. (2011).** Regulation of oxidative stress response by CosR, an essential response regulator in *Campylobacter jejuni*. *PloS One*, *6*(7), e22300.

References

- Hyde, S. C., Emsley, P., Hartshorn, M. J., Mimmack, M. M., Gileadi, U., Pearce, S. R., ... & Higgins, C. F. (1990). Structural model of ATP-binding proteing associated with cystic fibrosis, multidrug resistance and bacterial transport. *Nature*, 346(6282), 362.
- Imlay, J. A. (2008). Cellular defenses against superoxide and hydrogen peroxide. *Annu. Rev. Biochem.*, 77, 755-776.
- Imperi, F., Tiburzi, F., & Visca, P. (2009). Molecular basis of pyoverdine siderophore recycling in *Pseudomonas aeruginosa*. *Proceedings of the National Academy of Sciences*, 106(48), 20440-20445.
- Ishikawa, T., Mizunoe, Y., Kawabata, S. I., Takade, A., Harada, M., Wai, S. N., & Yoshida, S. I. (2003). The iron-binding protein Dps confers hydrogen peroxide stress resistance to *Campylobacter jejuni*. *Journal of Bacteriology*, 185(3), 1010-1017.
- Jagannathan, A., Penn, C., 2005. In: Ketley, J.M., Konkel, M.E. (Eds.), *Motility in Campylobacter. Molecular and Cellular Biology*. Horizon Bioscience, Norfolk, pp. 331e347.
- Janvier, B., Constantinidou, C., Aucher, P., Marshall, Z. V., Penn, C. W., & Fauchere, J. L. (1998). Characterization and gene sequencing of a 19-kDa periplasmic protein of *Campylobacter jejuni/coli*. *Research in Microbiology*, 149(2), 95-107.
- Jensen, L. T., & Culotta, V. C. (2002). Regulation of *Saccharomyces cerevisiae* FET4 by oxygen and iron. *Journal of Molecular Biology*, 318(2), 251-260.
- Jeon, B., Itoh, K., Misawa, N., & Ryu, S. (2003). Effects of quorum sensing on *flaA* transcription and autoagglutination in *Campylobacter jejuni*. *Microbiology and immunology*, 47(11), 833-839.
- Jeon, B., Wang, Y., Hao, H., Barton, Y. W., & Zhang, Q. (2010). Contribution of CmeG to antibiotic and oxidative stress resistance in *Campylobacter jejuni*. *Journal of Antimicrobial Chemotherapy*, 66(1), 79-85.
- Jin, S., Joe, A., Lynett, J., Hani, E. K., Sherman, P., & Chan, V. L. (2001). JlpA, a novel surface-exposed lipoprotein specific to *Campylobacter jejuni*, mediates adherence to host epithelial cells. *Molecular Microbiology*, 39, 1225–1236.
- Johnstone, T. C., & Nolan, E. M. (2015). Beyond iron: non-classical biological functions of bacterial siderophores. *Dalton Transactions*, 44(14), 6320-6339.
- Johnson, W. M., & Lior, H. (1988). A new heat-labile cytolethal distending toxin (CLDT) produced by *Campylobacter* Spp. *Microbial Pathogenesis*, 4(2), 115–26.
- Jones, M. A., Marston, K. L., Woodall, C. A., Maskell, D. J., Linton, D., Karlyshev, A. V., ... & Barrow, P. A. (2004). Adaptation of *Campylobacter jejuni* NCTC11168 to high-level colonization of the avian gastrointestinal tract. *Infection and Immunity*, 72(7), 3769-3776.

References

- Jones, T., Spencer, R., & Walsh, C. (1978).** Mechanism and kinetics of iron release from ferritin by dihydroflavins and dihydroflavin analogs. *Biochemistry*, *17*(19), 4011-4017.
- Joubert, L., Derré-Bobillot, A., Gaudu, P., Gruss, A., & Lechardeur, D. (2014).** HrtBA and menaquinones control haem homeostasis in *L. actococcus lactis*. *Molecular Microbiology*, *93*(4), 823-833.
- Kaakoush, N. O., Castaño-Rodríguez, N., Mitchell, H. M., & Man, S. M. (2015).** Global epidemiology of *Campylobacter* infection. *Clinical Microbiology Reviews*, *28*(3), 687-720.
- Kale, A., Phansopa, C., Suwannachart, C., Craven, C. J., Rafferty, J. B., & Kelly, D. J. (2011).** The virulence factor PEB4 (Cj0596) and the periplasmic protein Cj1289 are two structurally related SurA-like chaperones in the human pathogen *Campylobacter jejuni*. *Journal of Biological Chemistry*, *286*(24), 21254-21265.
- Kalmokoff, M., Lanthier, P., Tremblay, T. L., Foss, M., Lau, P. C., Sanders, G., ... & Szymanski, C. M. (2006).** Proteomic analysis of *Campylobacter jejuni* 11168 biofilms reveals a role for the motility complex in biofilm formation. *Journal of Bacteriology*, *188*(12), 4312-4320.
- Kammler, M. E. I. K. E., Schön, C., & Hantke, K. L. A. U. S. (1993).** Characterization of the ferrous iron uptake system of *Escherichia coli*. *Journal of Bacteriology*, *175*(19), 6212-6219.
- Kanjee, U., & Houry, W. A. (2013).** Mechanisms of acid resistance in *Escherichia coli*. *Annual Review of Microbiology*, *67*, 65-81.
- Karlyshev, A. V., Ketley, J. M., & Wren, B. W. (2005).** The *Campylobacter jejuni* glycome. *FEMS Microbiology Reviews*, *29*(2), 377-390.
- Karlyshev, A.V., Linton, D., Gregson, N.A., & Wren, B.W. (2002).** A novel paralogous gene family involved in phase-variable flagella-mediated motility in *Campylobacter jejuni*. *Microbiology*, *148*(Pt 2), 473-480. doi:10.1099/00221287-148-2-473
- Katzav, M., Isohanni, P., Lund, M., Hakkinen, M., & Lyhs, U. (2008).** PCR assay for the detection of *Campylobacter* in marinated and non-marinated poultry products. *Food Microbiology*, *25*(7), 908-914.
- Kelly, D. J. (2001).** The physiology and metabolism of *Campylobacter jejuni* and *Helicobacter pylori*. *Journal of Applied Microbiology*, *90*(S6).
- Kelly, D. J. (2005).** Metabolism, electron transport and bioenergetics of *Campylobacter jejuni*: implications for understanding life in the gut and survival in the environment. *Campylobacter: Molecular and Cellular Biology*, 275-292.
- Kelly, D. J., Hughes, N. J., & Poole, R. K. (2001).** Microaerobic physiology: aerobic respiration, anaerobic respiration, and carbon dioxide metabolism. *Helicobacter Pylori: Physiology and Genetics*, (Dc), 113.

References

- Kendall, J. J., Barrero-Tobon, A. M., Hendrixson, D. R., & Kelly, D. J. (2014).** Hemerythrins in the microaerophilic bacterium *Campylobacter jejuni* help protect key iron-sulphur cluster enzymes from oxidative damage. *Environmental Microbiology*, *16*(4), 1105-1121.
- Kikuchi, H. E., & Suzuki, T. (1984).** An electrophoretic analysis of superoxide dismutase in *Campylobacter* spp. *Journal of General Microbiology*, *130*(11), 2791–2796.
- Kim, H., Lee, H., & Shin, D. (2015a).** Lon-mediated proteolysis of the FeoC protein prevents *Salmonella enterica* from accumulating the Fe (II) transporter FeoB under high-oxygen conditions. *Journal of Bacteriology*, *197*(1), 92-98.
- Kim, J. C., Oh, E., Kim, J., & Jeon, B. (2015b).** Regulation of oxidative stress resistance in *Campylobacter jejuni*, a microaerophilic foodborne pathogen. *Frontiers in Microbiology*, *6*, 751.
- Kim, Y. H., Lee, Y., Kim, S., Yeom, J., Yeom, S., Seok Kim, B., ... & Park, W. (2006).** The role of periplasmic antioxidant enzymes (superoxide dismutase and thiol peroxidase) of the Shiga toxin-producing *Escherichia coli* O157: H7 in the formation of biofilms. *Proteomics*, *6*(23), 6181-6193.
- King, E. O. (1957).** Human infections with *Vibrio fetus* and a closely related vibrio. *The Journal of Infectious Diseases*, 119-128.
- Koch, D., Chan, A. C., Murphy, M. E., Lilie, H., Grass, G., & Nies, D. H. (2011).** Characterization of a dipartite iron uptake system from uropathogenic *Escherichia coli* strain F11. *Journal of Biological Chemistry*, *286*(28), 25317-25330.
- Koenraad, P. M. F. J., Rombouts, F. M., & Notermans, S. H. W. (1997).** Epidemiological aspects of thermophilic *Campylobacter* in water-related environments: a review. *Water Environment Research*, *69*(1), 52-63.
- Kojima, S., & Blair, D. F. (2004).** The bacterial flagellar motor: structure and function of a complex molecular machine. *International Review of Cytology*, *233*, 93-134.
- Konkel, M. E., Christensen, J. E., Keech, A. M., Monteville, M. R., Klena, J. D., & Garvis, S. G. (2005).** Identification of a fibronectin-binding domain within the *Campylobacter jejuni* CadF protein. *Molecular Microbiology*, *57*(4), 1022-1035.
- Konkel, M. E., Garvis, S. G., Tipton, S. L., Anderson, D. E., & Cieplak, W. (1997).** Identification and molecular cloning of a gene encoding a fibronectin-binding protein (CadF) from *Campylobacter jejuni*. *Molecular Microbiology*, *24*, 953–963.
- Konkel, M. E., Kim, B. J., Rivera-Amill, V., & Garvis, S. G. (1999).** Bacterial secreted proteins are required for the internalization of *Campylobacter jejuni* into cultured mammalian cells. *Molecular Microbiology*, *32*(4), 691-701.
- Konkel, M. E., Klena, J. D., Rivera-Amill, V., Monteville, M. R., Biswas, D., Raphael, B., & Mickelson, J. (2004).** Secretion of virulence proteins from *Campylobacter jejuni*

References

- is dependent on a functional flagellar export apparatus. *Journal of Bacteriology*, 186(11), 3296-3303.
- Koolman, L., Whyte, P., Burgess, C., & Bolton, D. (2016).** Virulence gene expression, adhesion and invasion of *Campylobacter jejuni* exposed to oxidative stress (H₂O₂). *International Journal of Food Microbiology*, 220, 33-38.
- Korolik, V. (2019).** The role of chemotaxis during *Campylobacter jejuni* colonisation and pathogenesis. *Current Opinion in Microbiology*, 47, 32-37.
- Kosman, D. J. (2003).** Molecular mechanisms of iron uptake in fungi. *Molecular Microbiology*, 47(5), 1185–1197.
- Kotarski, S. F., Merriwether, T. L., Tkalcevic, G. T., & Gemski, P. (1986).** Genetic studies of kanamycin resistance in *Campylobacter jejuni*. *Antimicrobial Agents and Chemotherapy*, 30(2), 225-230.
- Krewulak, K. D., & Vogel, H. J. (2008).** Structural biology of bacterial iron uptake. *Biochimica et Biophysica Acta (BBA)-Biomembranes*, 1778(9), 1781-1804.
- Krieg, N. R., & Hoffman, P. S. (1986).** Microaerophily and oxygen toxicity. *Annual Review of Microbiology*, 40, 107–130.
- Kuroki, S., Haruta, T., Yoshioka, M., Kobayashi, Y., Nukina, M., & Nakanishi, H. (1991).** Guillain-Barre syndrome associated with *Campylobacter* infection. *The Pediatric Infectious Disease Journal*, 10(2), 149-151.
- Labigne-Roussel, A., Harel, J., & Tompkins, L. (1987).** Gene transfer from *Escherichia coli* to *Campylobacter* species: development of shuttle vectors for genetic analysis of *Campylobacter jejuni*. *Journal of Bacteriology*, 169(11), 5320-5323.
- Lai, C. K., Chen, Y. A., Lin, C. J., Lin, H. J., Kao, M. C., Huang, M. Z., ... & Lin, L. C. (2016).** Molecular mechanisms and potential clinical applications of *Campylobacter jejuni* cytolethal distending toxin. *Frontiers in Cellular and Infection Microbiology*, 6, 9.
- Lara-Tejero, M., & Galán, J. E. (2001).** CdtA, CdtB, and CdtC form a tripartite complex that is required for cytolethal distending toxin activity. *Infection and Immunity*, 69(7), 4358–4365.
- Larrondo, L. F., Canessa, P., Melo, F., Polanco, R., & Vicuna, R. (2007).** Cloning and characterization of the genes encoding the high-affinity iron-uptake protein complex Fet3/Ftr1 in the basidiomycete *Phanerochaete chrysosporium*. *Microbiology*, 153(6), 1772-1780.
- Larson, C. L., Christensen, J. E., Pacheco, S. A., Minnich, S. A., & Konkel, M. E. (2008).** *Campylobacter jejuni* secretes proteins via the flagellar type III secretion system that contribute to host cell invasion and gastroenteritis. In *Campylobacter, Third Edition* (pp. 315-332). American Society of Microbiology.

References

- Lastovica, A. J., On, S. L., and Zhang, L. (2014).** “The family Campylobacteraceae,” in *The Prokaryotes*, eds E. Rosenberg, E. F. DeLong, S. Lory, E. Stackebrandt, and F. Thompson (Berlin: Springer), 307–335.
- Lau, C. K., Krewulak, K. D., & Vogel, H. J. (2016).** Bacterial ferrous iron transport: the Feo system. *FEMS Microbiology Reviews*, 40(2), 273-298.
- Lau, C. K., Ishida, H., Liu, Z., & Vogel, H. J. (2013).** Solution structure of Escherichia coli FeoA and its potential role in bacterial ferrous iron transport. *Journal of Bacteriology*, 195(1), 46-55.
- Lavrrar, J. L., & McIntosh, M. A. (2003).** Architecture of a Fur binding site: a comparative analysis. *Journal of Bacteriology*, 185(7), 2194-2202.
- Lázaro, B., Cárcamo, J., Audicana, A., Perales, I., & Fernández-Astorga, A. (1999).** Viability and DNA maintenance in nonculturable spiral Campylobacter jejuni cells after long-term exposure to low temperatures. *Applied and Environmental Microbiology*, 65(10), 4677-4681.
- Lederberg, E. M., and S. N. Cohen. 1974.** Transformation of *Salmonella typhimurium* by plasmid deoxyribonucleic acid. *Journal of Bacteriology*. 119: 1072-1074.
- Lee, J. W., & Helmann, J. D. (2007).** Functional specialization within the Fur family of metalloregulators. *Biometals*, 20(3-4), 485.
- Lee, L. H., Burg 3rd, E., Baqar, S., Bourgeois, A. L., Burr, D. H., Ewing, C. P., Guerry, P. (1999).** Evaluation of a truncated recombinant flagellin subunit vaccine against Campylobacter jejuni. *Infect Immun*, 67(11), 5799–5805.
- Lee, M. D., & Newell, D. G. (2006).** Campylobacter in poultry: filling an ecological niche. *Avian Diseases*, 50(1), 1-9.
- Lemire, J. A., Harrison, J. J., & Turner, R. J. (2013).** Antimicrobial activity of metals: mechanisms, molecular targets and applications. *Nature Reviews Microbiology*, 11(6), 371.
- Lertsethtakarn, P., Ottemann, K. M., & Hendrixson, D. R. (2011).** Motility and chemotaxis in Campylobacter and Helicobacter. *Annual Review of Microbiology*, 65, 389-410.
- Lewis, L. A., Sung, M. H., Gipson, M., Hartman, K., & Dyer, D. W. (1998).** Transport of intact porphyrin by HpuAB, the hemoglobin-haptoglobin utilization system of Neisseria meningitidis. *Journal of Bacteriology*, 180(22), 6043-6047.
- Line, J. E., Hiett, K. L., Guard-Bouldin, J., & Seal, B. S. (2010).** Differential carbon source utilization by Campylobacter jejuni 11168 in response to growth temperature variation. *Journal of Microbiological Methods*, 80(2), 198-202.

References

- Litrup, E., Torpdahl, M., & Nielsen, E. M. (2007).** Multilocus sequence typing performed on *Campylobacter coli* isolates from humans, broilers, pigs and cattle originating in Denmark. *Journal of Applied Microbiology*, *103*(1), 210–8.
- Litwin, C. M., & Calderwood, S. B. (1993).** Role of iron in regulation of virulence genes. *Clinical Microbiology Reviews*, *6*(2), 137–149.
- Liu, M. M., Boinett, C. J., Chan, A. C., Parkhill, J., Murphy, M. E., & Gaynor, E. C. (2018).** Investigating the *Campylobacter jejuni* Transcriptional Response to Host Intestinal Extracts Reveals the Involvement of a Widely Conserved Iron Uptake System. *MBio*, *9*(4), e01347-18.
- Liu, Y. W., & Kelly, D. J. (2015).** Cytochrome c biogenesis in *Campylobacter jejuni* requires cytochrome c6 (CccA; C j1153) to maintain apocytochrome cysteine thiols in a reduced state for haem attachment. *Molecular Microbiology*, *96*(6), 1298-1317.
- Livak, K. J., & Schmittgen, T. D. (2001).** Analysis of relative gene expression data using real-time quantitative PCR and the $2^{-\Delta\Delta CT}$ method. *Methods*, *25*(4), 402-408.
- Loc Carrillo, C., Atterbury, R.J., el-Shibiny, A., Connerton, P.L., Dillon, E., Scott, A., & Connerton, I.F. (2005).** Bacteriophage therapy to reduce *Campylobacter jejuni* colonization of broiler chickens. *Appl Environ Microbiol*, *71*(11), 6554-6563. doi:10.1128/AEM.71.11.6554-6563.2005
- Loréal, O., Cavey, T., Bardou-Jacquet, E., Guggenbuhl, P., Ropert, M., & Brissot, P. (2014).** Iron, hepcidin, and the metal connection. *Frontiers in pharmacology*, *5*, 128.
- Louwen, R., Heikema, A., Belkum, A. Van, Ott, A., Gilbert, M., Ang, W., van Belkum, A. (2008).** The sialylated lipooligosaccharide outer core in *Campylobacter jejuni* is an important determinant for epithelial cell invasion. *Infection and Immunity*, *76*(10), 4431–4438.
- Louwen, R. P. L., van Belkum, A., Wagenaar, J. A., Doorduyn, Y., Achterberg, R., & Endtz, H. P. (2006).** Lack of association between the presence of the pVir plasmid and bloody diarrhea in *Campylobacter jejuni* enteritis. *Journal of Clinical Microbiology*, *44*(5), 1867-1868.
- Luo, N. & Zhang, Q. (2001).** Molecular characterization of a cryptic plasmid from *Campylobacter jejuni*. *Plasmid* *45*, 127-133.
- MacCallum, A. J., Harris, D., Haddock, G., & Everest, P. H. (2006).** *Campylobacter jejuni*-infected human epithelial cell lines vary in their ability to secrete interleukin-8 compared to in vitro-infected primary human intestinal tissue. *Microbiology*, *152*(12), 3661-3665.
- Malik-Kale, P., Parker, C. T., & Konkel, M. E. (2008).** Culture of *Campylobacter jejuni* with sodium deoxycholate induces virulence gene expression. *Journal of Bacteriology*, *190*(7), 2286-2297.

References

- Man, S. M. (2011).** The clinical importance of emerging *Campylobacter* species. *Nature Reviews Gastroenterology & Hepatology*, 8(12), 669.
- Marlovits, T. C., Haase, W., Herrmann, C., Aller, S. G., & Unger, V. M. (2002).** The membrane protein FeoB contains an intramolecular G protein essential for Fe (II) uptake in bacteria. *Proceedings of the National Academy of Sciences*, 99(25), 16243-16248.
- Marshall, B., & Warren, J. R. (1984).** Unidentified curved bacilli in the stomach of patients with gastritis and peptic ulceration. *The Lancet*, 323(8390), 1311-1315.
- Martin, J. L. (1995).** Thioredoxin—a fold for all reasons. *Structure*, 3(3), 245-250.
- Massé, E., & Gottesman, S. (2002).** A small RNA regulates the expression of genes involved in iron metabolism in *Escherichia coli*. *Proceedings of the National Academy of Sciences*, 99(7), 4620-4625.
- Masse, E., Salvail, H., Desnoyers, G., & Arguin, M. (2007).** Small RNAs controlling iron metabolism. *Current Opinion in Microbiology*, 10(2), 140-145.
- Mathew, A., Eberl, L., & Carlier, A. L. (2014).** A novel siderophore-independent strategy of iron uptake in the genus *Burkholderia*. *Molecular Microbiology*, 91(4), 805-820.
- McCarthy, N. D., Gillespie, I. a, Lawson, a J., Richardson, J., Neal, K. R., Hawtin, P. R., O'Brien, S. J. (2012).** Molecular epidemiology of human *Campylobacter jejuni* shows association between seasonal and international patterns of disease. *Epidemiology and Infection*, 140(12), 2247–55.
- McCrackin, M. A., Helke, K. L., Galloway, A. M., Poole, A. Z., Salgado, C. D., & Marriott, B. P. (2016).** Effect of antimicrobial use in agricultural animals on drug-resistant foodborne campylobacteriosis in humans: a systematic literature review. *Critical Reviews in Food Science and Nutrition*, 56(13), 2115-2132.
- McFadyean, S. J., & Stockman, S. S. (1913).** *Report of the Departmental Committee Appointed by the Board of Agriculture and Fisheries to Inquire Into Epizootic Abortion. Appendix to Part III, Abortion in Sheep.* HM Stationery Office.
- McSweeney, L. A., & Dreyfus, L. A. (2004).** Nuclear localization of the *Escherichia coli* cytolethal distending toxin CdtB subunit. *Cellular Microbiology*, 6(5), 447–58.
- Mead, P. S., Slutsker, L., Dietz, V., McCaig, L. F., Bresee, J. S., Shapiro, C., ... & Tauxe, R. V. (1999).** Food-related illness and death in the United States. *Emerging Infectious Diseases*, 5(5), 607.
- Miethke, M., & Marahiel, M. A. (2007).** Siderophore-based iron acquisition and pathogen control. *Microbiology and Molecular Biology Reviews*, 71(3), 413-451.
- Miethke, M., Monteferrante, C. G., Marahiel, M. A., & van Dijk, J. M. (2013).** The *Bacillus subtilis* EfeUOB transporter is essential for high-affinity acquisition of ferrous and ferric iron. *Biochimica et Biophysica Acta (BBA)-Molecular Cell Research*, 1833(10), 2267-2278.

References

- Miles, A.A., Misra, S.S., & Irwin, J.O. (1938).** The estimation of the bactericidal power of the blood. *The Journal of Hygiene*, 38(6), 732-749.
- Miller, C. E., Rock, J. D., Ridley, K. A., Williams, P. H., & Ketley, J. M. (2008).** Utilization of lactoferrin-bound and transferrin-bound iron by *Campylobacter jejuni*. *Journal of Bacteriology*, 190(6), 1900-1911.
- Miller, C. E., Williams, P. H., & Ketley, J. M. (2009).** Pumping iron: Mechanisms for iron uptake by *Campylobacter*. *Microbiology*, 155(10), 3157–3165.
- Min, T., Vedadi, M., Watson, D. C., Wasney, G. A., Munger, C., Cygler, M., ... & Young, N. M. (2009).** Specificity of *Campylobacter jejuni* adhesin PEB3 for phosphates and structural differences among its ligand complexes. *Biochemistry*, 48(14), 3057-3067.
- Miret, S., Simpson, R. J., & McKie, A. T. (2003).** Physiology and molecular biology of dietary iron absorption. *Annual Review of Nutrition*, 23(1), 283-301.
- Mohammed, K. A. S., Miles, R. J., & Halablab, M. A. (2004).** The pattern and kinetics of substrate metabolism of *Campylobacter jejuni* and *Campylobacter coli*. *Letters in Applied Microbiology*, 39(3), 261-266.
- Monteville, M. R., Yoon, J. E., & Konkel, M. E. (2003).** Maximal adherence and invasion of INT 407 cells by *Campylobacter jejuni* requires the CadF outer-membrane protein and microfilament reorganization. *Microbiology*, 149(1), 153-165.
- Monteville, M. R., & Konkel, M. E. (2002).** Fibronectin-facilitated invasion of T84 eukaryotic cells by *Campylobacter jejuni* occurs preferentially at the basolateral cell surface. *Infection and Immunity*, 70(12), 6665-6671.
- Moore, J. E., Corcoran, D., Dooley, J. S., Fanning, S., Lucey, B., Matsuda, M., ... & O’Riordan, L. (2005).** *Campylobacter*. *Veterinary Research*, 36(3), 351-382.
- Müller, W., Böhland, C., & Methner, U. (2011).** Detection and genotypic differentiation of *Campylobacter jejuni* and *Campylobacter coli* strains from laying hens by multiplex PCR and fla-typing. *Research in Veterinary Science*, 91(3), e48-e52.
- Muraoka, W. T., & Zhang, Q. (2011).** Phenotypic and genotypic evidence for L-fucose utilization by *Campylobacter jejuni*. *Journal of Bacteriology*, 193(5), 1065-1075.
- Murphy, C., Carroll, C., & Jordan, K. N. (2003).** Induction of an adaptive tolerance response in the foodborne pathogen, *Campylobacter jejuni*. *FEMS Microbiology Letters*, 223(1), 89-93.
- Murphy, C., Carroll, C., & Jordan, K. N. (2006).** Environmental survival mechanisms of the foodborne pathogen *Campylobacter jejuni*. *Journal of Applied Microbiology*, 100(4), 623-632.
- Murphy, H. M., Meng, Z., Henry, R., Deletic, A., & McCarthy, D. T. (2017).** Current stormwater harvesting guidelines are inadequate for mitigating risk from *Campylobacter*

References

- during nonpotable reuse activities. *Environmental Science & Technology*, 51(21), 12498-12507.
- Nachamkin, I., Allos, B. M., & Ho, T. (1998).** Campylobacter species and Guillain-Barré syndrome. *Clinical Microbiology Reviews*, 11(3), 555–567.
- Nachamkin, I., Yang, X. H., & Stern, N. J. (1993).** Role of Campylobacter jejuni flagella as colonization factors for three-day-old chicks: analysis with flagellar mutants. *Applied and Environmental Microbiology*, 59(5), 1269–73.
- Naikare, H., Butcher, J., Flint, A., Xu, J., Raymond, K. N., & Stintzi, A. (2013).** Campylobacter jejuni ferric–enterobactin receptor CfrA is TonB3 dependent and mediates iron acquisition from structurally different catechol siderophores. *Metallomics*, 5(8), 988-996.
- Naikare, H., Palyada, K., Panciera, R., Marlow, D., & Stintzi, A. (2006).** Major role for FeoB in Campylobacter jejuni ferrous iron acquisition, gut colonization, and intracellular survival. *Infection and Immunity*, 74(10), 5433–44.
- Nandal, A., Huggins, C. C., Woodhall, M. R., McHugh, J., Rodríguez-Quiñones, F., Quail, M. A., ... & Andrews, S. C. (2010).** Induction of the ferritin gene (ftnA) of Escherichia coli by Fe²⁺–Fur is mediated by reversal of H-NS silencing and is RyhB independent. *Molecular Microbiology*, 75(3), 637-657.
- Narita, S. I., & Tokuda, H. (2017).** Bacterial lipoproteins; biogenesis, sorting and quality control. *Biochimica et Biophysica Acta (BBA)-Molecular and Cell Biology of Lipids*, 1862(11), 1414-1423.
- Neill, S. D., Campbell, J. N., O'brien, J. J., Weatherup, S. T. C., & Ellis, W. A. (1985).** Taxonomic position of Campylobacter cryaerophila sp. nov. *International Journal of Systematic and Evolutionary Microbiology*, 35(3), 342-356.
- Newell, D. G. (2001).** Animal models of Campylobacter jejuni colonization and disease and the lessons to be learned from similar Helicobacter pylori models. *Journal of Applied Microbiology*, 90(S6), 57S-67S.
- Newell, D. G., & Fearnley, C. (2003).** Sources of Campylobacter colonization in broiler chickens. *Applied and Environmental Microbiology*, 69(8), 4343-4351.
- Newell, D. G., McBride, H., Saunders, F., Dehele, Y., & Pearson, A. D. (1985).** The virulence of clinical and environmental isolates of Campylobacter jejuni. *The Journal of Hygiene*, 94(1), 45–54.
- Nielsen, H. L., Ejlersten, T., Engberg, J., & Nielsen, H. (2013).** High incidence of Campylobacter concisus in gastroenteritis in North Jutland, Denmark: a population-based study. *Clinical Microbiology and Infection*, 19(5), 445-450.
- Nikaido, H. (2003).** Molecular basis of bacterial outer membrane permeability revisited. *Microbiol. Mol. Biol. Rev.*, 67(4), 593-656.

References

- Noiraj, N., Guillier, M., Barnard, T. J., & Buchanan, S. K. (2010).** TonB-dependent transporters: regulation, structure, and function. *Annual Review of Microbiology*, *64*, 43-60.
- Nuijten, P. J. M., Van Asten, F. J. a M., Gaastra, W., & Van der Zeijst, B. a M. (1990).** Structural and functional analysis of two *Campylobacter jejuni* flagellin genes. *Journal of Biological Chemistry*, *265*(29), 17798–17804.
- Ó Cróinín, T., & Backert, S. (2012).** Host epithelial cell invasion by *Campylobacter jejuni*: trigger or zipper mechanism? *Frontiers in Cellular and Infection Microbiology*, *2*, 25.
- Oh, E., & Jeon, B. (2014).** Role of alkyl hydroperoxide reductase (AhpC) in the biofilm formation of *Campylobacter jejuni*. *PLoS One*, *9*(1), e87312.
- Okada, U., Yamashita, E., Neuberger, A., Morimoto, M., van Veen, H. W., & Murakami, S. (2017).** Crystal structure of tripartite-type ABC transporter MacB from *Acinetobacter baumannii*. *Nature Communications*, *8*(1), 1336.
- Okuda, S., & Tokuda, H. (2011).** Lipoprotein sorting in bacteria. *Annual Review of Microbiology*, *65*, 239-259.
- Oliver, J. D. (2010).** Recent findings on the viable but nonculturable state in pathogenic bacteria. *FEMS Microbiology Reviews*, *34*(4), 415-425.
- On, S. L. (2001).** Taxonomy of *Campylobacter*, *Arcobacter*, *Helicobacter* and related bacteria: current status, future prospects and immediate concerns. *Journal of Applied Microbiology*, *90*(S6).
- Owen, R. J. (1998).** *Helicobacter*-species classification and identification. *British Medical Bulletin*, *54*(1), 17-30.
- Padgett, P. J., Cover, W. H., & Krieg, N. R. (1982).** The Microaerophile *Spirillum volutans*: Cultivation on Complex Liquid and Solid Media. *Applied and Environmental Microbiology*, *43*(2), 469–77.
- Palyada, K., Sun, Y. Q., Flint, A., Butcher, J., Naikare, H., & Stintzi, A. (2009).** Characterization of the oxidative stress stimulon and PerR regulon of *Campylobacter jejuni*. *BMC Genomics*, *10*(1), 481.
- Palyada, K., Threadgill, D., & Stintzi, A. (2004).** Iron acquisition and regulation in *Campylobacter jejuni*. *Journal of Bacteriology*, *186*(14), 4714-4729.
- Pandey, A., & Sonti, R. V. (2010).** Role of the FeoB protein and siderophore in promoting virulence of *Xanthomonas oryzae* pv. *oryzae* on rice. *Journal of Bacteriology*, *192*(12), 3187-3203.
- Park, S. F. (2002).** The physiology of *Campylobacter* species and its relevance to their role as foodborne pathogens. *International Journal of Food Microbiology*, *74*(3), 177-188.

References

- Parke, D. (1990).** Construction of mobilizable vectors derived from plasmids RP4, pUC18 and pUC19. *Gene*, 93(1), 135-137.
- Parkhill, J., Wren, B. W., Mungall, K., Ketley, J. M., Churcher, C., Basham, D., ... Barrell, B. G. (2000).** The genome sequence of the food-borne pathogen *Campylobacter jejuni* reveals hypervariable sequences. *Nature*, 403(6770), 665–668.
- Parsek, M. R., & Singh, P. K. (2003).** Bacterial biofilms: an emerging link to disease pathogenesis. *Annual Reviews in Microbiology*, 57(1), 677-701.
- Parsons, C. M. (1984).** Influence of caecectomy and source of dietary fibre or starch on excretion of endogenous amino acids by laying hens. *British Journal of Nutrition*, 51(3), 541-548.
- Paster, B. J., Dewhirst, F. E., Seymour, C., Fraser, G. J., & Fox, J. G. (1991).** Helicobacter species isolated from bird and swine feces. *Microbial Ecology in Health and Disease (United Kingdom)*.
- Paul, V. D., & Lill, R. (2015).** Biogenesis of cytosolic and nuclear iron–sulfur proteins and their role in genome stability. *Biochimica Et Biophysica Acta (BBA)-Molecular Cell Research*, 1853(6), 1528-1539.
- Pavlovskis, O. R., Rollins, D. M., Haberberger, R. L., Green, A. E., Habash, L., Strocko, S., & Walker, R. I. (1991).** Significance of flagella in colonization resistance of rabbits immunized with *Campylobacter* spp. *Infection and Immunity*, 59(7), 2259-2264.
- Pearson, B. M., Gaskin, D. J. H., Segers, R. P. a M., Wells, J. M., Nuijten, P. J. M., & Van Vliet, a. H. M. (2007).** The complete genome sequence of *Campylobacter jejuni* strain 81116 (NCTC11828). *Journal of Bacteriology*, 189(22), 8402–8403.
- Philpott, C. C. (2006).** Iron uptake in fungi: a system for every source. *Biochimica et Biophysica Acta (bba)-Molecular Cell Research*, 1763(7), 636-645.
- Phongsisay, V., Perera, V. N., & Fry, B. N. (2007).** Evaluation of eight RNA isolation methods for transcriptional analysis in *Campylobacter jejuni*. *Journal of Microbiological Methods*, 68(2), 427-429.
- Pei, Z., & Blaser, M. J. (1993).** PEB1, the major cell-binding factor of *Campylobacter jejuni*, is a homolog of the binding component in gram-negative nutrient transport systems. *Journal of Biological Chemistry*, 268(25), 18717–18725.
- Pei, Z., Burucoa, C., Grignon, B., Baqar, S., Huang, X. Z., Kopecko, D. J., Blaser, M. J. (1998).** Mutation in the *peb1A* locus of *Campylobacter jejuni* reduces interactions with epithelial cells and intestinal colonization of mice. *Infection and Immunity*, 66(3), 938–43.
- Pei, Z. H., Ellison, R. T., & Blaser, M. J. (1991).** Identification, purification, and characterization of major antigenic proteins of *Campylobacter jejuni*. *Journal of Biological Chemistry*, 266(25), 16363-16369.

References

- Pesci, E. C., Cottle, D. L., & Pickett, C. L. (1994).** Genetic, enzymatic, and pathogenic studies of the iron superoxide dismutase of *Campylobacter jejuni*. *Infection and Immunity*, *62*(7), 2687-2694.
- Pickett, C. L., & Whitehouse, C. A. (1999).** The cytolethal distending toxin family. *Trends in Microbiology*, *7*(7), 292-297.
- Pickett, C. L., Auffenberg, T., Pesci, E. C., Sheen, V. L., & Jusuf, S. S. (1992).** Iron acquisition and hemolysin production by *Campylobacter jejuni*. *Infection and Immunity*, *60*(9), 3872-7.
- Pickett, C. L., Pesci, E. C., Cottle, D. L., Russell, G., Erdem, A. N., & Zeytin, H. (1996).** Prevalence of cytolethal distending toxin production in *Campylobacter jejuni* and relatedness of *Campylobacter* sp. *cdtB* genes. *Infection and Immunity*, *64*(6), 2070-2078.
- Pielsticker, C., Glünder, G., & Rautenschlein, S. (2012).** Colonization properties of *Campylobacter jejuni* in chickens. *European Journal of Microbiology and Immunology*, *2*(1), 61-65.
- Pike, B. L., Guerry, P., & Poly, F. (2013).** Global distribution of *Campylobacter jejuni* Penner serotypes: a systematic review. *PloS One*, *8*(6), e67375.
- Pintar, K. D., Thomas, K. M., Christidis, T., Otten, A., Nesbitt, A., Marshall, B., ... & Ravel, A. (2017).** A comparative exposure assessment of *Campylobacter* in Ontario, Canada. *Risk Analysis*, *37*(4), 677-715.
- Poly, F., & Guerry, P. (2008).** Pathogenesis of campylobacter. *Current Opinion in Gastroenterology*, *24*(1), 27-31.
- Porcheron, G., & Dozois, C. M. (2015).** Interplay between iron homeostasis and virulence: Fur and RyhB as major regulators of bacterial pathogenicity. *Veterinary Microbiology*, *179*(1-2), 2-14.
- Purdy, D., Buswell, C. M., Hodgson, A. E., McAlpine, K., Henderson, I., & Leach, S. A. (2000).** Characterisation of cytolethal distending toxin (CDT) mutants of *Campylobacter jejuni*. *Journal of Medical Microbiology*, *49*(5), 473-479.
- Quiñones, B., Miller, W. G., Bates, A. H., & Mandrell, R. E. (2009).** Autoinducer-2 production in *Campylobacter jejuni* contributes to chicken colonization. *Applied and Environmental Microbiology*, *75*(1), 281-285.
- Rajasekaran, M. B., Nilapwar, S., Andrews, S. C., & Watson, K. A. (2010).** EfeO-cupredoxins: major new members of the cupredoxin superfamily with roles in bacterial iron transport. *Biometals*, *23*(1), 1.
- Rajkumar, M., Ae, N., Prasad, M. N. V., & Freitas, H. (2010).** Potential of siderophore-producing bacteria for improving heavy metal phytoextraction. *Trends in Biotechnology*, *28*(3), 142-149.

References

- Ramos, H. C., Rumbo, M., & Sirard, J. C. (2004). Bacterial flagellins: mediators of pathogenicity and host immune responses in mucosa. *Trends in Microbiology*, *12*(11), 509-517.
- Rao, M. R., Naficy, A. B., Savarino, S. J., Abu-Elyazeed, R., Wierzba, T. F., Peruski, L. F., ... & Clemens, J. D. (2001). Pathogenicity and convalescent excretion of *Campylobacter* in rural Egyptian children. *American Journal of Epidemiology*, *154*(2), 166-173.
- Raphael, B. H., & Joens, L. A. (2003). FeoB is not required for ferrous iron uptake in *Campylobacter jejuni*. *Canadian Journal of Microbiology*, *49*(11), 727-731.
- Ratledge, C., & Dover, L. G. (2000). Iron metabolism in pathogenic bacteria. *Annual Review of Microbiology*, *54*, 881-941.
- Reuter, M., Mallett, A., Pearson, B. M., & van Vliet, A. H. (2010). Biofilm formation by *Campylobacter jejuni* is increased under aerobic conditions. *Applied and Environmental Microbiology*, *76*(7), 2122-2128.
- Reuter, M., Ultee, E., Tan, A., & van Vliet, A. H. (2019). Role of the *Campylobacter jejuni* cheVAWY chemotaxis genes in chemotactic motility and biofilm formation. *BioRxiv*, 449850.
- Richardson, P. T., & Park, S. F. (1995). Enterochelin acquisition in *Campylobacter coli*: Characterization of components of a binding-protein-dependent transport system. *Microbiology*, *141*(12), 3181-3191.
- Ridley, K. A., Rock, J. D., Li, Y., & Ketley, J. M. (2006). Heme utilization in *Campylobacter jejuni*. *Journal of Bacteriology*, *188*(22), 7862-75.
- Ritz, M., Garenaux, A., Berge, M., & Federighi, M. (2009). Determination of *rpoA* as the most suitable internal control to study stress response in *C. jejuni* by RT-qPCR and application to oxidative stress. *Journal of Microbiological Methods*, *76*(2), 196-200.
- Rivera-Amill, V., Kim, B. J., Seshu, J., & Konkel, M. E. (2001). Secretion of the virulence-associated *Campylobacter* invasion antigens from *Campylobacter jejuni* requires a stimulatory signal. *The Journal of Infectious Diseases*, *183*(11), 1607-1616.
- Roop 2nd, R. M., Smibert, R. M., Johnson, J. L., & Krieg, N. R. (1984). Differential characteristics of catalase-positive campylobacters correlated with DNA homology groups. *Can J Microbiol*, *30*(7), 938-951.
- Rotariu, O., Smith-Palmer, A., Cowden, J., Bessell, P. R., Innocent, G. T., Reid, S. W. J., Strachan, N. J. C. (2010). Putative household outbreaks of campylobacteriosis typically comprise single MLST genotypes. *Epidemiology and Infection*, *138*(12), 1744-1747.
- Sahin, O., Kassem, I. I., Shen, Z., Lin, J., Rajashekara, G., & Zhang, Q. (2015). *Campylobacter* in poultry: ecology and potential interventions. *Avian Diseases*, *59*(2), 185-200.

References

- Saha, M., Sarkar, S., Sarkar, B., Sharma, B. K., Bhattacharjee, S., & Tribedi, P. (2016).** Microbial siderophores and their potential applications: a review. *Environmental Science and Pollution Research*, 23(5), 3984-3999.
- Sahin, O., Morishita, T. Y., & Zhang, Q. (2002).** Campylobacter colonization in poultry: sources of infection and modes of transmission. *Animal Health Research Reviews*, 3(2), 95-105.
- Sambrook J., Fritsch F., and Maniatis T. 2001.** Molecular cloning; A Laboratory Manual, *Cold Spring Harbor Laboratory Press. New York.*
- Sambrook J. 1989.** Molecular Cloning; A Laboratory Manual (3rd Edition). *Cold Spring Harbor Laboratory Press. New York.*
- Sanad, Y. M., Kassem, I. I., Abley, M., Gebreyes, W., LeJeune, J. T., & Rajashekara, G. (2011).** Genotypic and phenotypic properties of cattle-associated Campylobacter and their implications to public health in the USA. *PloS One*, 6(10), e25778.
- Sandy, M., & Butler, A. (2009).** Microbial iron acquisition: marine and terrestrial siderophores. *Chemical Reviews*, 109(10), 4580-4595.
- Sanchuki, H. B., Valdameri, G., Moure, V. R., Oliveira, M. A., Pedrosa, F. O., Souza, E. M., ... & Huergo, L. F. (2015).** Purification of the Campylobacter jejuni Dps protein assisted by its high melting temperature. *Protein Expression and Purification*, 111, 105-110.
- Sanyal, S. C., Islam, K. M., Neogy, P. K., Islam, M., Speelman, P., & Huq, M. I. (1984).** Campylobacter jejuni diarrhea model in infant chickens. *Infection and Immunity*, 43(3), 931-936.
- Schalk, I. J., & Guillon, L. (2013).** Fate of ferrisiderophores after import across bacterial outer membranes: different iron release strategies are observed in the cytoplasm or periplasm depending on the siderophore pathways. *Amino Acids*, 44(5), 1267-1277.
- Schmittgen, T. D., Zakrajsek, B. A., Mills, A. G., Gorn, V., Singer, M. J., & Reed, M. W. (2000).** Quantitative reverse transcription-polymerase chain reaction to study mRNA decay: comparison of endpoint and real-time methods. *Analytical Biochemistry*, 285(2), 194-204.
- Schröder, I., Johnson, E., & De Vries, S. (2003).** Microbial ferric iron reductases. *FEMS Microbiology Reviews*, 27(2-3), 427-447.
- Schwyn, B., & Neilands, J. B. (1987).** Universal chemical assay for the detection and determination of siderophores. *Analytical Biochemistry*, 160(1), 47-56.
- Sebald, M., & Veron, M. (1963).** Teneur en bases de l'ADN et classification des vibrions. In *Annales de l'Institut Pasteur* (Vol. 105, No. 5, p. 897). 120 BLVD SAINT-GERMAIN, 75280 PARIS 06, FRANCE: MASSON EDITEUR.

References

- Seo, S. W., Kim, D., Latif, H., O'Brien, E. J., Szubin, R., & Palsson, B. O. (2014). Deciphering Fur transcriptional regulatory network highlights its complex role beyond iron metabolism in *Escherichia coli*. *Nature Communications*, 5, 4910.
- Sestok, A. E., Linkous, R. O., & Smith, A. T. (2018). Toward a mechanistic understanding of Feo-mediated ferrous iron uptake. *Metallomics*, 10(7), 887-898.
- Severance, S., Chakraborty, S., & Kosman, D. J. (2004). The Ftr1p iron permease in the yeast plasma membrane: orientation, topology and structure-function relationships. *Biochemical Journal*, 380(2), 487-496.
- Sheppard, S. K., McCarthy, N. D., Falush, D., & Maiden, M. C. (2008). Convergence of *Campylobacter* species: implications for bacterial evolution. *Science*, 320(5873), 237-239.
- Sheppard, S. K., Didelot, X., Méric, G., Torralbo, A., Jolley, K. A., Kelly, D. J., ... & Falush, D. (2013). Genome-wide association study identifies vitamin B5 biosynthesis as a host specificity factor in *Campylobacter*. *Proceedings of the National Academy of Sciences*, 110(29), 11923-11927.
- Sheppard, S. K., Colles, F. M., McCARTHY, N. D., Strachan, N. J., Ogden, I. D., Forbes, K. J., ... & Maiden, M. C. (2011). Niche segregation and genetic structure of *Campylobacter jejuni* populations from wild and agricultural host species. *Molecular Ecology*, 20(16), 3484-3490.
- Sheppard, S. K., Cheng, L., Méric, G., De Haan, C. P., Llarena, A. K., Marttinen, P., ... & Strachan, N. J. (2014). Cryptic ecology among host generalist *Campylobacter jejuni* in domestic animals. *Molecular Ecology*, 23(10), 2442-2451.
- Sheppard, S. K., & Maiden, M. C. (2015). The evolution of *Campylobacter jejuni* and *Campylobacter coli*. *Cold Spring Harbor perspectives in biology*, 7(8), a018119.
- Silva, J., Leite, D., Fernandes, M., Mena, C., Gibbs, P. A., & Teixeira, P. (2011). *Campylobacter* spp. as a foodborne pathogen: a review. *Frontiers in Microbiology*, 2, 200.
- Skarp, C. P. A., Hänninen, M. L., & Rautelin, H. I. K. (2016). Campylobacteriosis: the role of poultry meat. *Clinical Microbiology and Infection*, 22(2), 103-109.
- Skirrow, M. B. (1977). *Campylobacter* enteritis: a "new" disease. *British Medical Journal*, 2(6078), 9.
- Skirrow, M. B. (1994). Diseases due to *Campylobacter*, *Helicobacter* and related bacteria. *Journal of Comparative Pathology*, 111(2), 113-149.
- Skirrow, M. B. (2006). John McFadyean and the centenary of the first isolation of *Campylobacter* species. *Clinical Infectious Diseases: An Official Publication of the Infectious Diseases Society of America*, 43, 1213-1217.

References

- Smith, C. K., AbuOun, M., Cawthraw, S. A., Humphrey, T. J., Rothwell, L., Kaiser, P., ... & Jones, M. A. (2008).** Campylobacter colonization of the chicken induces a proinflammatory response in mucosal tissues. *FEMS Immunology & Medical Microbiology*, *54*(1), 114-121.
- Sommerlad, S. M., & Hendrixson, D. R. (2007).** Analysis of the roles of FlgP and FlgQ in flagellar motility of *Campylobacter jejuni*. *Journal of Bacteriology*, *189*(1), 179-186.
- Sougakoff, W., Papadopoulou, B., Nordmann, P., & Courvalin, P. (1987).** Nucleotide sequence and distribution of gene *tetO* encoding tetracycline resistance in *Campylobacter coli*. *FEMS Microbiology Letters*, *44*(1), 159-163
- Spiro, S., & Guest, J. R. (1990).** FNR and its role in oxygen-regulated gene expression in *Escherichia coli*. *FEMS microbiology Reviews*, *6*(4), 399-428.
- Stahl, M., Butcher, J., & Stintzi, A. (2012).** Nutrient acquisition and metabolism by *Campylobacter jejuni*. *Frontiers in Cellular and Infection Microbiology*, *2*, 5.
- Stahl, M., Friis, L. M., Nothaft, H., Liu, X., Li, J., Szymanski, C. M., & Stintzi, A. (2011).** L-fucose utilization provides *Campylobacter jejuni* with a competitive advantage. *Proceedings of the National Academy of Sciences*, *108*(17), 7194-7199.
- Stead, D., & Park, S. F. (2000).** Roles of Fe superoxide dismutase and catalase in resistance of *Campylobacter coli* to freeze-thaw stress. *Applied and Environmental Microbiology*, *66*(7), 3110-3112.
- Stern, N. J., Cox, N. A., Bailey, J. S., Berrang, M. E., & Musgrove, M. T. (2001).** Comparison of mucosal competitive exclusion and competitive exclusion treatment to reduce *Salmonella* and *Campylobacter* spp. colonization in broiler chickens. *Poultry Science*, *80*(2), 156-160.
- Stintzi, A., & Whitworth, L. (2003).** Investigation of the *Campylobacter jejuni* cold-shock response by global transcript profiling. *Genome Letters*, *2*(1-2), 18-27.
- Stintzi, A., van Vliet, A. H. M. & Ketley, J. M. (2008).** Iron metabolism, transport and regulation. In *Campylobacter*, 3rd edn, pp. 591-610. Edited by I. Nachamkin, C. Szymanski & M. Blaser. Washington, DC: American Society for Microbiology.
- Stojiljkovic, I., Bäumlner, A. J., & Hantke, K. (1994).** Fur regulon in Gram-negative bacteria: identification and characterization of new iron-regulated *Escherichia coli* genes by a Fur titration assay. *Journal of Molecular Biology*, *236*(2), 531-545.
- Stojiljkovic, I., Cobeljic, M., & Hantke, K. (1993).** *Escherichia coli* K-12 ferrous iron uptake mutants are impaired in their ability to colonize the mouse intestine. *FEMS Microbiology Letters*, *108*(1), 111-115.
- Storz, G., & Imlay, J. A. (1999).** Oxidative stress. *Current Opinion in Microbiology*, *2*(2), 188-194.

References

- Strachan, N. J. C., Gormley, F. J., Rotariu, O., Ogden, I. D., Miller, G., Dunn, G. M., ... Forbes, K. J. (2009).** Attribution of Campylobacter Infections in Northeast Scotland to Specific Sources by Use of Multilocus Sequence Typing. *Journal of Infectious Diseases*, 199(8), 1205–1208.
- Sulaeman, S., Hernould, M., Schaumann, A., Coquet, L., Bolla, J. M., De, E., & Tresse, O. (2012).** Enhanced adhesion of Campylobacter jejuni to abiotic surfaces is mediated by membrane proteins in oxygen-enriched conditions. *PLoS One*, 7(9), e46402.
- Sylte, M. J., Johnson, T. A., Meyer, E. L., Inbody, M. H., Trachsel, J., Looft, T., ... & Zhang, Q. (2019).** Intestinal colonization and acute immune response in commercial turkeys following inoculation with Campylobacter jejuni constructs encoding antibiotic-resistance markers. *Veterinary Immunology and Immunopathology*.
- Szymanski, C. M., & Wren, B. W. (2005).** Protein glycosylation in bacterial mucosal pathogens. *Nature Reviews Microbiology*, 3(3), 225.
- Takagi, H., Shi, D., Ha, Y., Allewell, N. M., & Theil, E. C. (1998).** Localized Unfolding at the Junction of Three Ferritin Subunits A MECHANISM FOR IRON RELEASE? *Journal of Biological Chemistry*, 273(30), 18685-18688.
- Takata, T., Fujimoto, S., & Amako, K. (1992).** Isolation of nonchemotactic mutants of Campylobacter jejuni and their colonization of the mouse intestinal tract. *Infect. Immun.*, 60, 3596–3600.
- Theoret, J. R., Cooper, K. K., Zekarias, B., Roland, K. L., Law, B. F., Curtiss, R., & Joens, L. A. (2012).** The Campylobacter jejuni Dps homologue is important for in vitro biofilm formation and cecal colonization of poultry and may serve as a protective antigen for vaccination. *Clin. Vaccine Immunol.*, 19(9), 1426-1431.
- Thomas, C., Hill, D., & Mabey, M. (2002).** Culturability, injury and morphological dynamics of thermophilic Campylobacter spp. within a laboratory-based aquatic model system. *Journal of Applied Microbiology*, 92(3), 433-442.
- Thomas, M. T., Shepherd, M., Poole, R. K., van Vliet, A. H., Kelly, D. J., & Pearson, B. M. (2011).** Two respiratory enzyme systems in Campylobacter jejuni NCTC 11168 contribute to growth on L-lactate. *Environmental Microbiology*, 13(1), 48-61.
- Tom-Yew, S. A., Cui, D. T., Bekker, E. G., & Murphy, M. E. (2005).** Anion-independent iron coordination by the Campylobacter jejuni ferric binding protein. *Journal of Biological Chemistry*, 280(10), 9283-9290.
- Tonello, F., Dundon, W. G., Satin, B., Molinari, M., Tognon, G., Grandi, G., & Montecucco, C. (1999).** The Helicobacter pylori neutrophil-activating protein is an iron-binding protein with dodecameric structure. *Molecular Microbiology*, 34(2), 238-246.
- Van Asbeck, B. S., Marcelis, J. H., Marx, J. J. M., Struyvenberg, A., Van Kats, J. H., & Verhoef, J. (1983).** Inhibition of bacterial multiplication by the iron chelator

References

- deferoxamine: potentiating effect of ascorbic acid. *European Journal of Clinical Microbiology*, 2(5), 426-431.
- van der Stel, A. X., Van Mourik, A., Heijmen-van Dijk, L., Parker, C. T., Kelly, D. J., van de Lest, C. H., ... & Wösten, M. M. (2015).** The C ampylobacter jejuni RacRS system regulates fumarate utilization in a low oxygen environment. *Environmental Microbiology*, 17(4), 1049-1064.
- van der Wielen, P. W., Biesterveld, S., Notermans, S., Hofstra, H., Urlings, B. A., & van Knapen, F. (2000).** Role of volatile fatty acids in development of the cecal microflora in broiler chickens during growth. *Appl. Environ. Microbiol.*, 66(6), 2536-2540.
- van Mourik, A., Bleumink-Pluym, N. M., van Dijk, L., van Putten, J. P., & Wösten, M. M. (2008).** Functional analysis of a *Campylobacter jejuni* alkaline phosphatase secreted via the Tat export machinery. *Microbiology*, 154(2), 584-592.
- Van Vliet, A. H. M., & Ketley, J. M. (2001).** Pathogenesis of enteric *Campylobacter* infection. *Journal of Applied Microbiology*, 90(S6), 45S-56S.
- Van Vliet, A. H. M., Ketley, J. M., Park, S. F., & Penn, C. W. (2002).** The role of iron in *Campylobacter* gene regulation, metabolism and oxidative stress defence. *FEMS Microbiology Reviews*, 26, 173–186.
- Van Vliet, A. H., Rock, J. D., Madeleine, L. N., & Ketley, J. M. (2000).** The iron-responsive regulator Fur of *Campylobacter jejuni* is expressed from two separate promoters. *FEMS Microbiology Letters*, 188(2), 115-118.
- Van Vliet, A. H., Wooldridge, K. G., & Ketley, J. M. (1998b).** Iron-responsive gene regulation in a *Campylobacter jejuni* fur mutant. *Journal of Bacteriology*, 180(20), 5291-5298.
- Van Vliet, A.H.M., Wood, A.C., Henderson, J., Wooldridge, K.G. and Ketley, J.M. (1998a).** Genetic manipulation of enteric *Campylobacter* species. *Methods in Microbiology* 27, 407±419.
- Van Vliet, A. H., Baillon, M. L. A., Penn, C. W., & Ketley, J. M. (1999).** *Campylobacter jejuni* contains two fur homologs: characterization of iron-responsive regulation of peroxide stress defense genes by the PerR repressor. *Journal of Bacteriology*, 181(20), 6371-6376.
- Vandamme, P. (2000).** Taxonomy of the family *Campylobacteraceae*. *Campylobacter*, 3-26.
- Vandamme, P., & Deley, J. (1991). Proposal for a New Family, *Campylobacteraceae*. *International Journal of Systematic Bacteriology*, 41(3), 451–455.
- VanGuilder, H. D., Vrana, K. E., & Freeman, W. M. (2008).** Twenty-five years of quantitative PCR for gene expression analysis. *Biotechniques*, 44(5), 619-626.
- Varsaki, A., Murphy, C., Barczynska, A., Jordan, K., & Carroll, C. (2015).** The acid adaptive tolerance response in *Campylobacter jejuni* induces a global response, as suggested by proteomics and microarrays. *Microbial Biotechnology*, 8(6), 974-988.

References

- Veeranagouda, Y., Husain, F., Boente, R., Moore, J., Smith, C. J., Rocha, E. R., ... & Wexler, H. M. (2014). Deficiency of the ferrous iron transporter FeoAB is linked with metronidazole resistance in *Bacteroides fragilis*. *Journal of Antimicrobial Chemotherapy*, 69(10), 2634-2643.
- Vegge, C. S., Brøndsted, L., Li, Y. P., Bang, D. D., & Ingmer, H. (2009). Energy taxis drives *Campylobacter jejuni* toward the most favorable conditions for growth. *Appl. Environ. Microbiol.*, 75(16), 5308-5314.
- Vegge, C. S., Jansen van Rensburg, M. J., Rasmussen, J. J., Maiden, M. C., Johnsen, L. G., pDanielsen, M., ... & Kelly, D. J. (2016). Glucose metabolism via the entner-doudoroff pathway in *Campylobacter*: a rare trait that enhances survival and promotes biofilm formation in some isolates. *Frontiers in Microbiology*, 7, 1877.
- Velayudhan, J., & Kelly, D. J. (2002). Analysis of gluconeogenic and anaplerotic enzymes in *Campylobacter jejuni*: an essential role for phosphoenolpyruvate carboxykinase. *Microbiology*, 148(3), 685-694.
- Velayudhan, J., Hughes, N. J., McColm, A. a., Bagshaw, J., Clayton, C. L., Andrews, S. C., & Kelly, D. J. (2000). Iron acquisition and virulence in *Helicobacter pylori*: A major role for FeoB, a high-affinity ferrous iron transporter. *Molecular Microbiology*, 37, 274–286.
- Velayudhan, J., Jones, M. A., Barrow, P. A., & Kelly, D. J. (2004). L-serine catabolism via an oxygen-labile L-serine dehydratase is essential for colonization of the avian gut by *Campylobacter jejuni*. *Infection and Immunity*, 72(1), 260-268.
- Verhoeff-Bakkenes, L., Arends, A. P., Snoep, J. L., Zwietering, M. H., & De Jonge, R. (2008). Pyruvate relieves the necessity of high induction levels of catalase and enables *Campylobacter jejuni* to grow under fully aerobic conditions. *Letters in Applied Microbiology*, 46(3), 377-382.
- Wagenaar, J. A., French, N. P., & Havelaar, A. H. (2013). Preventing *Campylobacter* at the source: why is it so difficult? *Clinical Infectious Diseases*, 57(11), 1600-1606.
- Wagenaar, J. A., Jacobs-Reitsma, W., Hofshagen, M., & Newell, D. (2008). Poultry colonization with *Campylobacter* and its control at the primary production level. In *Campylobacter, Third Edition* (pp. 667-678). American Society of Microbiology.
- Wai, S. N., Nakayama, K., Umene, K., Moriya, T., & Amako, K. (1996). Construction of a ferritin-deficient mutant of *Campylobacter jejuni*: contribution of ferritin to iron storage and protection against oxidative stress. *Molecular Microbiology*, 20(6), 1127-1134.
- Wakeman, C. A., Hammer, N. D., Stauff, D. L., Attia, A. S., Anzaldi, L. L., Dikalov, S. I., ... & Skaar, E. P. (2012). Menaquinone biosynthesis potentiates haem toxicity in *S. taphylococcus aureus*. *Molecular Microbiology*, 86(6), 1376-1392.
- Wang, Y., & Taylor, D. E. (1990). Natural transformation in *Campylobacter* species. *Journal of Bacteriology*, 172(2), 949-955.

References

- Wassenaar, T. M. (1997).** Toxin production by *Campylobacter* spp. *Clinical Microbiology Reviews*, 10(3), 466-476.
- Wassenaar, T. M., van der Zeijst, B. a, Ayling, R., & Newell, D. G. (1993).** Colonization of chicks by motility mutants of *Campylobacter jejuni* demonstrates the importance of flagellin A expression. *Journal of General Microbiology*, 139 Pt 6, 1171–1175.
- Weinberg, E. D. (1997).** The *Lactobacillus* anomaly: total iron abstinence. *Perspectives in Biology and Medicine*, 40(4), 578-583.
- Whiley, H., van den Akker, B., Giglio, S., & Bentham, R. (2013).** The role of environmental reservoirs in human campylobacteriosis. *International Journal of Environmental Research and Public Health*, 10(11), 5886-5907.
- Whitehouse, C. A., Balbo, P. B., Pesci, E. C., Cottle, D. L., Mirabito, P. M., & Pickett, C. L. (1998).** *Campylobacter jejuni* Cytolethal Distending Toxin Causes a G2-Phase Cell Cycle Block. *Infection and Immunity*, 66, 1934–1940.
- Widdel, F., Schnell, S., Heising, S., Ehrenreich, A., Assmus, B., & Schink, B. (1993).** Ferrous iron oxidation by anoxygenic phototrophic bacteria. *Nature*, 362(6423), 834.
- Wigley, P. (2015).** Blurred lines: pathogens, commensals, and the healthy gut. *Frontiers in Veterinary Science*, 2, 40.
- Wilkening, S., & Bader, A. (2004).** Quantitative real-time polymerase chain reaction: methodical analysis and mathematical model. *Journal of Biomolecular Techniques: JBT*, 15(2), 107.
- Williams, L. K., Sait, L. C., Trantham, E. K., Cogan, T. A., & Humphrey, T. J. (2013).** *Campylobacter* infection has different outcomes in fast-and slow-growing broiler chickens. *Avian Diseases*, 57(2), 238-241.
- Wilson, D. J., Gabriel, E., Leatherbarrow, A. J. H., Cheesbrough, J., Gee, S., Bolton, E., ... Diggle, P. J. (2008).** Tracing the source of campylobacteriosis. *PLoS Genetics*, 4(9), e1000203.
- Winer, J., Jung, C. K. S., Shackel, I., & Williams, P. M. (1999).** Development and validation of real-time quantitative reverse transcriptase–polymerase chain reaction for monitoring gene expression in cardiac myocytes in vitro. *Analytical Biochemistry*, 270(1), 41-49.
- Wingstrand, A., Neimann, J., Engberg, J., Nielsen, E.M., Gerner-Smidt, P., Wegener, H.C., & Molbak, K. (2006).** Fresh chicken as main risk factor for campylobacteriosis, Denmark. *Emerg Infect Dis*, 12(2), 280-285. doi:10.3201/eid1202.050936
- Winterbourn, C. C., Hawkins, R. E., Brian, M., & Carrell, R. W. (1975).** The estimation of red cell superoxide dismutase activity. *The Journal of Laboratory and Clinical Medicine*, 85(2), 337-341.

References

- Wirz, S. E., Overesch, G., Kuhnert, P., & Korczak, B. M. (2010).** Genotype and antibiotic resistance analyses of *Campylobacter* isolates from ceca and carcasses of slaughtered broiler flocks. *Applied and Environmental Microbiology*, *76*(19), 6377–86.
- Wooldridge, K. G., & Williams, P. H. (1993).** Iron uptake mechanisms of pathogenic bacteria. *FEMS Microbiology Reviews*, *12*(4), 325–348.
- Wooldridge, K. G., Williams, P. H., & Ketley, J. M. (1994).** Iron-responsive genetic regulation in *Campylobacter jejuni*: cloning and characterization of a fur homolog. *Journal of Bacteriology*, *176*(18), 5852–5856.
- Wright, J. A., Grant, A. J., Hurd, D., Harrison, M., Guccione, E. J., Kelly, D. J., & Maskell, D. J. (2009).** Metabolite and transcriptome analysis of *Campylobacter jejuni* in vitro growth reveals a stationary-phase physiological switch. *Microbiology*, *155*(1), 80–94.
- Wyckoff, E. E., Mey, A. R., Leimbach, A., Fisher, C. F., & Payne, S. M. (2006).** Characterization of ferric and ferrous iron transport systems in *Vibrio cholerae*. *Journal of Bacteriology*, *188*(18), 6515–6523.
- Xu, F., Zeng, X., Haigh, R. D., Ketley, J. M., & Lin, J. (2010).** Identification and characterization of a new ferric enterobactin receptor, CfrB, in *Campylobacter*. *Journal of Bacteriology*, *192*(17), 4425–4435.
- Yakushi, T., Masuda, K., Narita, S. I., Matsuyama, S. I., & Tokuda, H. (2000).** A new ABC transporter mediating the detachment of lipid-modified proteins from membranes. *Nature Cell Biology*, *2*(4), 212.
- Yamanaka, H., Kobayashi, H., Takahashi, E., & Okamoto, K. (2008).** MacAB is involved in the secretion of *Escherichia coli* heat-stable enterotoxin II. *Journal of Bacteriology*, *190*(23), 7693–7698.
- Yamasaki, M., Igimi, S., Katayama, Y., Yamamoto, S., & Amano, F. (2004).** Identification of an oxidative stress-sensitive protein from *Campylobacter jejuni*, homologous to rubredoxin oxidoreductase/rubrerhythrin. *FEMS Microbiology Letters*, *235*(1), 57–63.
- Yang, D. C., Peters, N. T., Parzych, K. R., Uehara, T., Markovski, M., & Bernhardt, T. G. (2011).** An ATP-binding cassette transporter-like complex governs cell-wall hydrolysis at the bacterial cytokinetic ring. *Proceedings of the National Academy of Sciences*, *108*(45), E1052–E1060.
- Yang, H. B., Hou, W. T., Cheng, M. T., Jiang, Y. L., Chen, Y., & Zhou, C. Z. (2018).** Structure of a MacAB-like efflux pump from *Streptococcus pneumoniae*. *Nature Communications*, *9*(1), 196.
- Yao, R., Burr, D. H., & Guerry, P. (1997).** CheY-mediated modulation of *Campylobacter jejuni* virulence. *Molecular Microbiology*, *23*(5), 1021–1031.

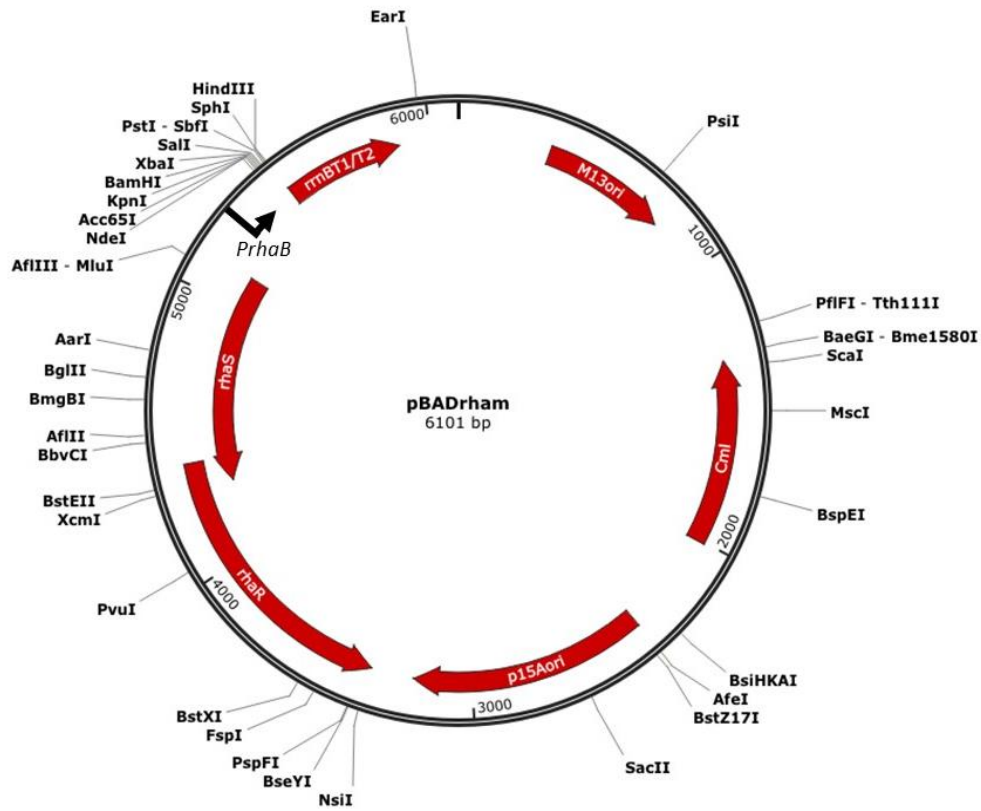
References

- Yao, R., Burr, D. H., Doig, P., Trust, T. J., Niu, H., & Guerry, P. (1994).** Isolation of motile and non-motile insertional mutants of *Campylobacter jejuni*: the role of motility in adherence and invasion of eukaryotic cells. *Molecular Microbiology*, *14*, 883–893.
- Young, J., & Holland, I. B. (1999).** ABC transporters: bacterial exporters-revisited five years on. *Biochimica et Biophysica Acta (BBA)-Biomembranes*, *1461*(2), 177-200.
- Young, K. T., Davis, L. M., & DiRita, V. J. (2007).** *Campylobacter jejuni*: molecular biology and pathogenesis. *Nature Reviews Microbiology*, *5*(9), 665-679.
- Yu, C., & Genco, C. A. (2012).** Fur-mediated activation of gene transcription in the human pathogen *Neisseria gonorrhoeae*. *Journal of Bacteriology*, *194*(7), 1730-1742.
- Yuki, N., & Koga, M. (2006).** Bacterial infections in Guillain-Barre and Fisher syndromes. *Current Opinion in Neurology*, *19*(5), 451-457.
- Yuki, N., Taki, T., Inagaki, F., Kasama, T., Takahashi, M., Saito, K., & Miyatake, T. (1993).** A bacterium lipopolysaccharide that elicits Guillain-Barré syndrome has a GM1 ganglioside-like structure. *The Journal of Experimental Medicine*, *178*(5), 1771-1775.
- Zautner, A. E., Ohk, C., Tareen, A. M., Lugert, R., & Groß, U. (2012).** Epidemiological association of *Campylobacter jejuni* groups with pathogenicity-associated genetic markers. *BMC Microbiology*, *12*(1), 171.
- Zeng, X., Ardeshtna, D., & Lin, J. (2015).** Heat Shock Enhanced Conjugation Efficiency in Standard *Campylobacter jejuni* Strains. *Applied and Environmental Microbiology*, AEM-00346.
- Zeng, X., & Lin, J. (2017).** Characterization of High Affinity Iron Acquisition Systems in *Campylobacter jejuni*. In *Campylobacter jejuni* (pp. 65-78). Humana Press, New York, NY.
- Zeng, X., Mo, Y., Xu, F., & Lin, J. (2013).** Identification and characterization of a periplasmic trilactone esterase, Cee, revealed unique features of ferric enterobactin acquisition in *Campylobacter*. *Molecular Microbiology*, *87*(3), 594-608.
- Zeng, X., Xu, F., & Lin, J. (2009).** Molecular, antigenic, and functional characteristics of ferric enterobactin receptor CfrA in *Campylobacter jejuni*. *Infection and Immunity*, *77*(12), 5437-5448.
- Zhang, C. (2014).** Essential functions of iron-requiring proteins in DNA replication, repair and cell cycle control. *Protein & Cell*, *5*(10), 750-760.
- Zhao, L., Xia, Z., & Wang, F. (2014).** Zebrafish in the sea of mineral (iron, zinc, and copper) metabolism. *Frontiers in Pharmacology*, *5*, 33.
- Zilbauer, M., Dorrell, N., Boughan, P. K., Harris, A., Wren, B. W., Klein, N. J., & Bajaj-Elliott, M. (2005).** Intestinal innate immunity to *Campylobacter jejuni* results in induction of bactericidal human beta-defensins 2 and 3. *Infection and Immunity*, *73*(11), 7281-7289.

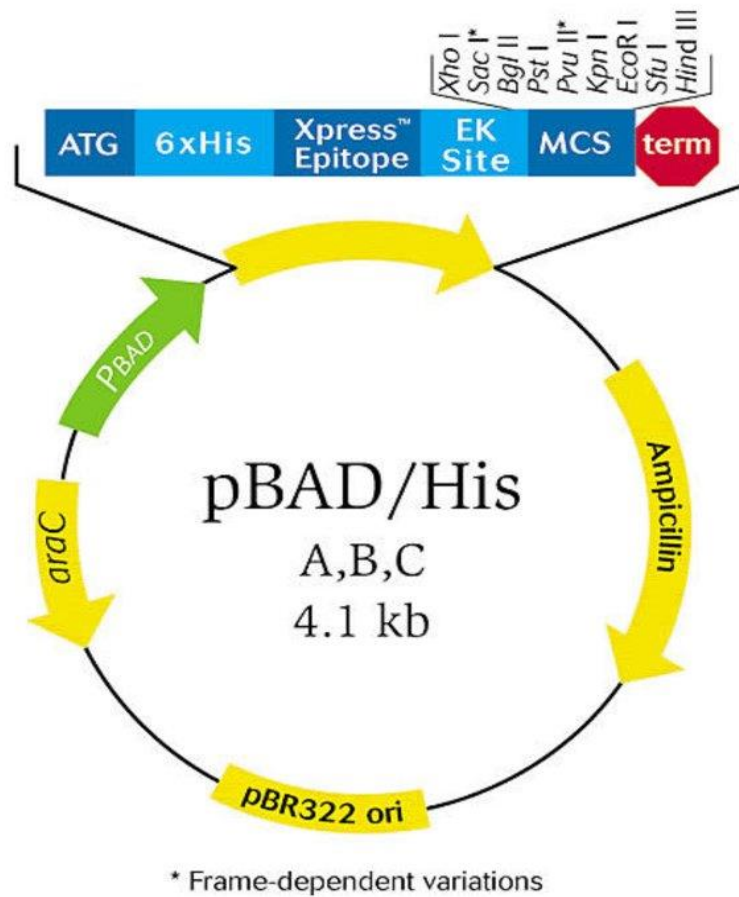
References

- Zipper, H., Brunner, H., Bernhagen, J., & Vitzthum, F. (2004).** Investigations on DNA intercalation and surface binding by SYBR Green I, its structure determination and methodological implications. *Nucleic Acids Research*, 32(12), e103-e103.
- Ziprin, R. L., Young, C. R., Byrd, J. A., Stanker, L. H., Hume, M. E., Gray, S. A., ... & Konkel, M. E. (2001).** Role of *Campylobacter jejuni* potential virulence genes in cecal colonization. *Avian Diseases*, 549-557.
- Ziprin, R. L., Young, C. R., Stanker, L. H., Hume, M. E., & Konkel, M. E. (1999).** The absence of cecal colonization of chicks by a mutant of *Campylobacter jejuni* not expressing bacterial fibronectin-binding protein. *Avian Diseases*, 43(3), 586–589.
- Zückert, W. R. (2014).** Secretion of bacterial lipoproteins: through the cytoplasmic membrane, the periplasm and beyond. *Biochimica et Biophysica Acta (BBA)-Molecular Cell Research*, 1843(8), 1509-1516.

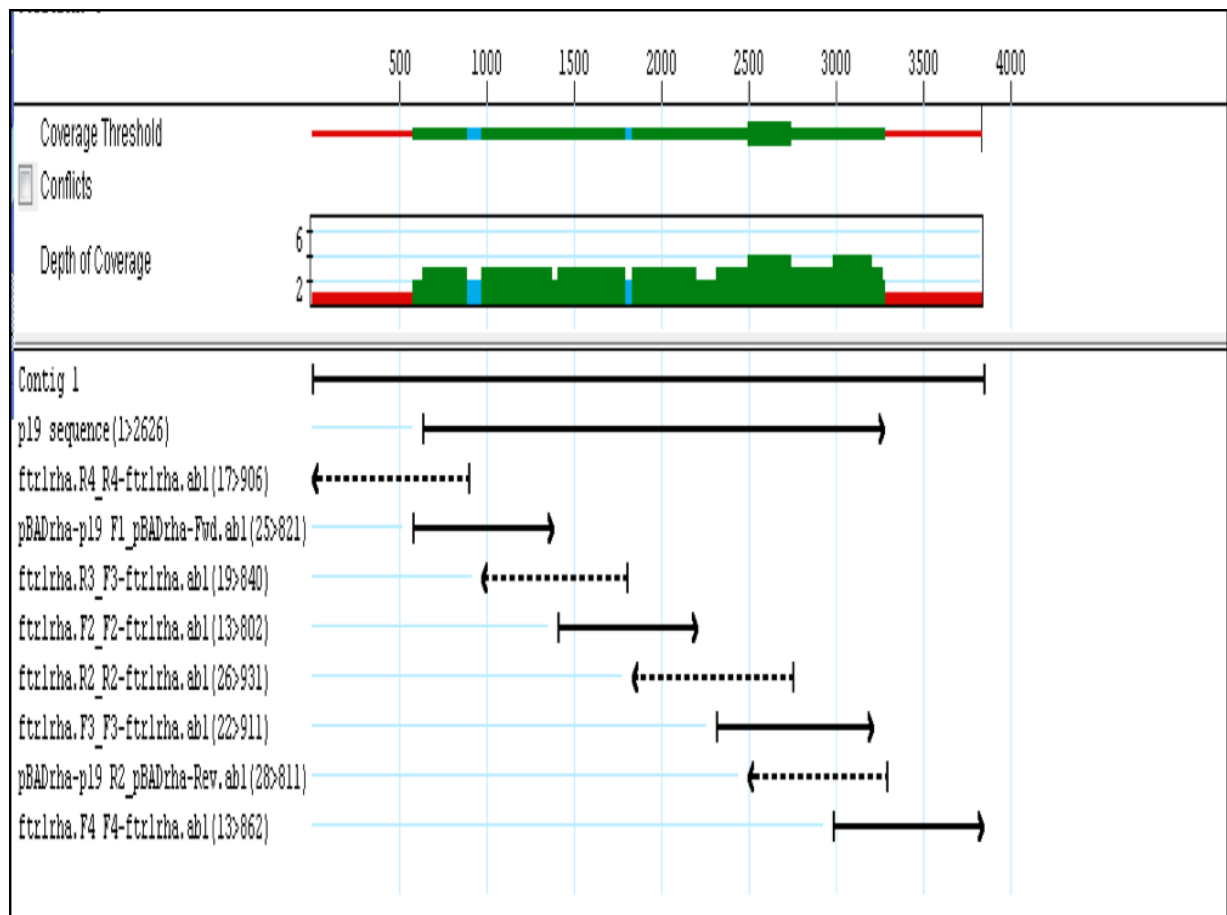
Appendix



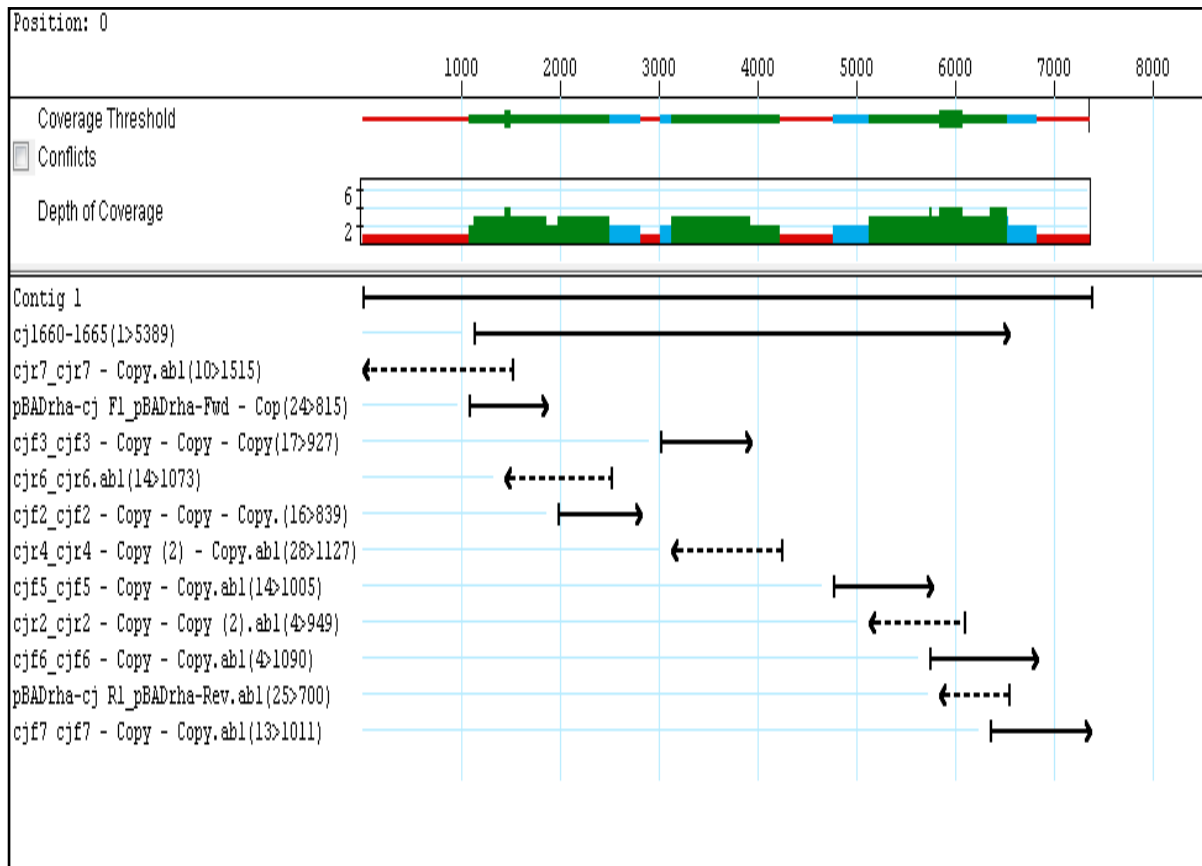
1. Map of rhamnose-inducible plasmid pBAD_{rha}. Rhamnose inducible promoter (P_{rham}). Nucleotide sequence from Genebank. Source: Genebank



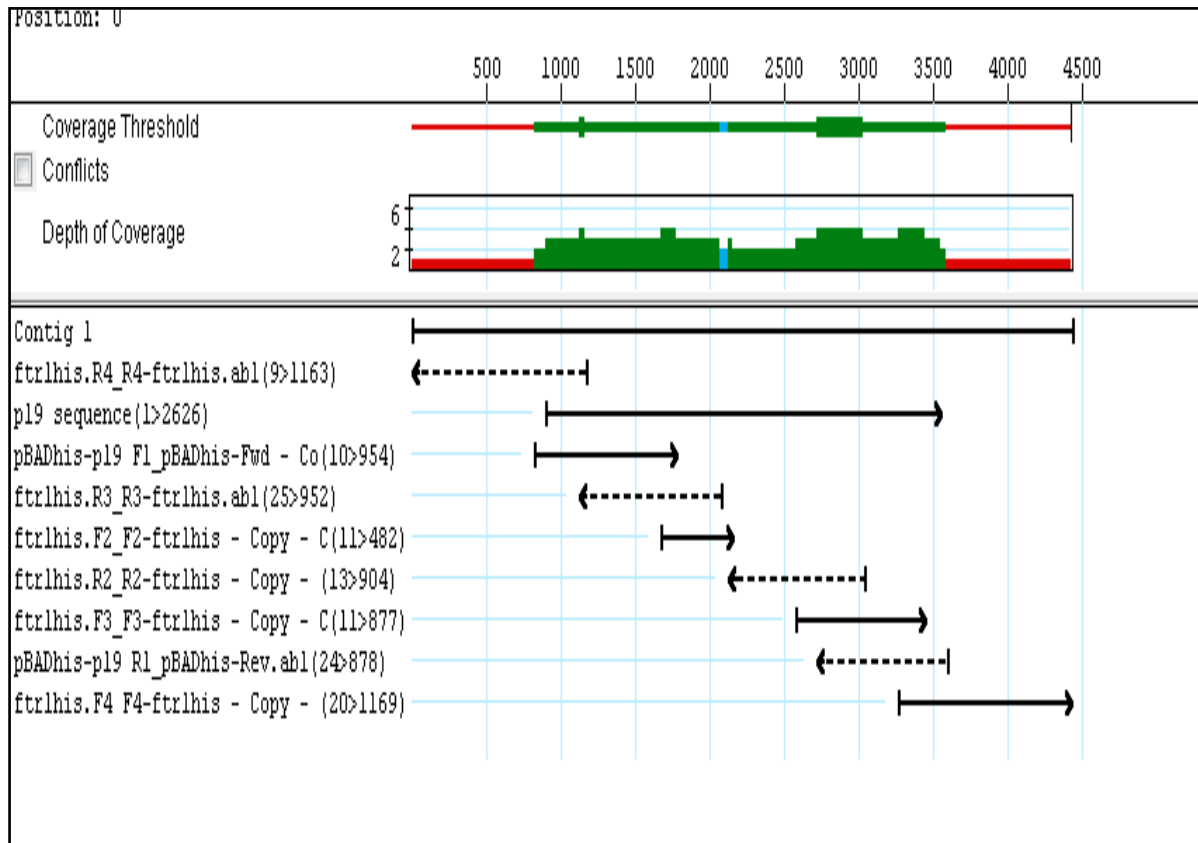
2. **Restriction map of pBAD_{ara}.** The inducible araBAD promoter is shown ('ARA_promoter'). Source: Thermo Fisher Scientific.



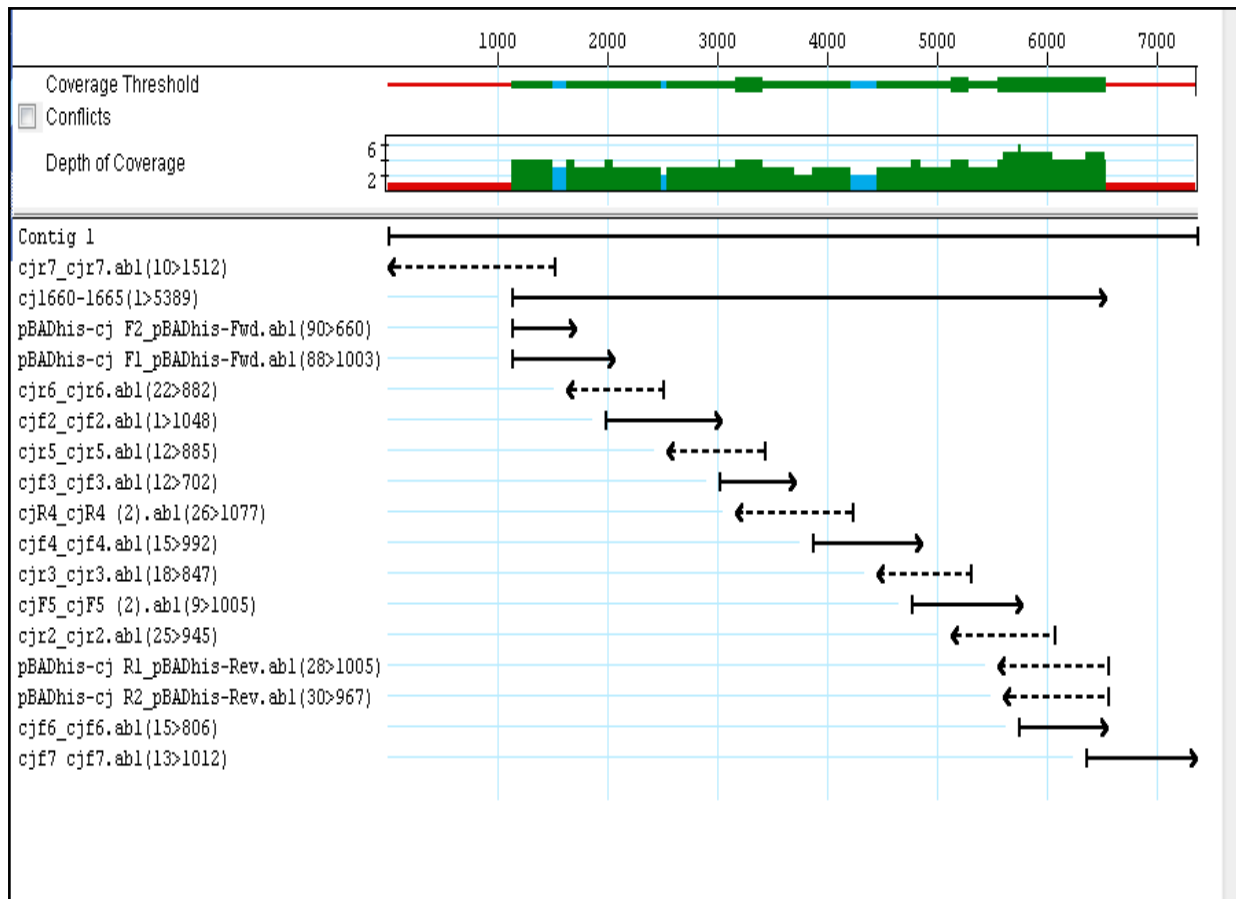
3. Overview of Sanger sequencing assembly of *fetM-P* cloned into pBAD_{rha}. The SeqMan Pro option of the DNASTAR software package was used to assemble eight sets of sequence data derived from the same template (pBAD_{rha}-*fetMP*) using eight primers (F1-4, R1-4; Table 2.4.) designed to provide complete and overlapping sequence data on both strands. All conflicts were resolved by scrutiny of the corresponding chromatograms. The ‘p19 sequence’ represents the original *C. jejuni* sequence (the reference sequence).



4. Overview of Sanger sequencing assembly of *fetA-F* cloned into pBAD_{rha}. The SeqMan Pro option of the DNASTAR software package was used to assemble twelve sets of sequence data derived from the same template (pBAD_{rha}-*fetA-F*) using twelve primers (F1-6, R1-6; Table 2.4.) designed to provide complete and overlapping sequence data on both strands. All conflicts were resolved by scrutiny of the corresponding chromatograms. The ‘*cj 1660-65* sequence’ represents the original *C. jejuni* sequence (the reference sequence).



5. Overview of Sanger sequencing assembly of *fetM-P* cloned into pBAD_{ara}. The SeqMan Pro option of the DNASTAR software package was used to assemble eight sets of sequence data derived from the same template (pBAD_{ara}-*fetMP*) using eight primers (F1-4, R1-4; Table 2.4.) designed to provide complete and overlapping sequence data on both strands. All conflicts were resolved by scrutiny of the corresponding chromatograms. The ‘p19 sequence’ represents the original *C. jejuni* sequence (the reference sequence).



6. Overview of Sanger sequencing assembly of *fetA-F* cloned into pBAD_{ara}. The SeqMan Pro option of the DNASTAR software package was used to assemble twelve sets of sequence data derived from the same template (pBAD_{ara}-*fetA-f*) using twelve primers (F1-6, R1-6; Table 2.4.) designed to provide complete and overlapping sequence data on both strands. All conflicts were resolved by scrutiny of the corresponding chromatograms. The ‘*cj 1660-65* sequence’ represents the original *C. jejuni* sequence (the reference sequence).

pBADrha -*fetMP* forward primer

TCAGCAGGATCACAT**ATG**AAAAATTTTTAAAATTATATTTTTTAATTATAAGTATTTTTTTTATCAAGCTCAGCTTTT
GCTAGGGTAGATGATTATATTAATGAAGCAAATCTTATCAAAGATATGCTAAAACAAAGCATAGAAACTTATAAA
AAGGGCGATAATCTAGGCGCCAAAAAGCTTAGCGAAGATGCGTATTTTCAACATTTTGAAAATATGGAAGGCTCA
ATAGGAAGAAACATAGGAAGAAAAGCTATCACTATGGAGCGTAAATTTGTAAATTTGCGTCGCATGTATAAAGAT
GAAGCTCCTTTGACACAAATTAATGCTTTAATTGATAGTCTTTATTTATGATCTTGATGAAGTAGCTCCGATTTTA
CAAATGGATATCGTTTAAAAGCAGAAGCAAGCGATATAAACTATGATAAGGCTAAAGCTGAAAAATCAAGCCTA
GAAGCCAATGCCAAACGCGAAGCTGATGCAGAAGCTTTAATCGCACAAATGATGGGTGTAGATAAAAAAGATTTA
GCACAAAGCTCTTTAACCAACCAAGCTCCTATACCTATAAAATAATGATACAAGCAAACCTTACAGATGATAATGCA
AGCACTGATTTACAAGCTGCCGCTGCAATGGACGTAAGATTGCAATTTATACTAGATAATATCTCTACCAAATTT
TCACAGGCAGCTAATGCTTTTTAAAGAAAAAACTACCAAAGTAGTAAAGATTTTTTAAATGATGCCTTATTTAGT
GATTATCGCAATACCAAAGTAGAAATTTTAGTAAATAAATTTACCAAAGCAGGAAACGATCAAAAAATTCACAA
GCCATACGCACCCTTATACGCCAAATCAACGATGCAAAAAATAGATGAAAAAGGCTTAAGAGATGGCTTAGATAAC
ATAGAAGAACAAATTTTTGATGTTTTCTTACAAATTCCAAATTCAGAACTTCAAGTTTGCAAATTTGAGGCTTT
AATGATGAAACAAAAGGCAAAGATTATGCCAAAGTTTCTAATGATATCAAACCTTGCTTTAGATGAAATTTTTAAA
AATTATGATGGGTTTAGTGCTTCTATAGTAGATGATTTACAAGGAATTTATCTAGATATTTTTGAAGCAAGCGGT
ATGGAAAATAAATCGGTGCTGTAGATAGCGGCTTAAAACCTAAAATAGAAAGTTTATTTTCCAAAAGCGTAGCT
CTTATCAAAGCAAGTACAGATAAAAAAGAGCTTGAAGCTACTTTTAAATGACTTAGAACAACCTCATAGCCAGCAGC
GTGGATAAAATTCAGATTCTACTCCTTATTCGCTGTTTATATGGGCTTTAGGTATTATTTTGCCTGAAGGCTTG
GAAGCTTTGATTATCGTTGTAGCCATTGTTTCTTATCTTGTGCAAAGTGGCAACAAAAATCGTTTAAATATCGCC
TATAGTGCTCTTTTTACAGGAGTAATTTAAGTTTTGTTACCCTTTTGGAGTTTCTTGGCTATTTAAAGAAAAT
GCAGGACAAAGTAGAGAGCTTATAGAGGGTATTACCATGCTTATAGCCGTATTACTACTCTTTTATGTGGGCTTT
TGGCTACTTTCAAACGCACAAAATAAAAAATGGACAAGCTTTATCAAACAAGGTGCTATAGATGCTATATCAAAC
AATAGTGCAAAAACCCCTTTGGATTACCGTATTTTTAGCTGTTTATAGAGAAGGTGCAGAACTGTGCTTTTTTTAT
CAAGCCTTGCTTTTTGATGCTAAAACAAGCACTGATTTTTGGTGCTGTTTTTGGCGGACTTGGACTTGGAAATTTTA
ATACTTATTGTTTTATATTTTCTTTTAAAAGCAGGAGCCATTCGCATACCTGTAAAACAATTTTCTATATCACT
TCTTACATTATTTTTTACATGGTTTTTGTTTTTACAGGCAAAGGCATAGCCGAACTCATAGAAGGAAAAGTCATC
ATTCCTAGTCTTATACCTATGAATTTTGAACCGATTTTATGGCTTGGAATTTATCCTTACTATGAAACTTTAATC
CCTCAATTTATAGTTTTAATTATGCTAATTATTGGCATTTTAATAACAAAACAAATTTCAAAAAAGGAGTAAAA
TC**ATG**ATAAAAAAGTTTTATCAGTAGTTGCTGCAGCTGCGGTTATTAGTACAAATTTATTTGCAGGCGAAGTGC
CGATCGGCGATCCAAAAGAACTTAATGGCATGGAAAATAGCCGCTGTTTATTTACAACCTATTGAAATGGAGCCAA
GAGGTATTGATTTAGCTGCATCTTTAGCAGATATTCACCTAGAAGCTGACATTCACGCACCTTAAAAACAATCCAA
ATGGTTTTCCAGAAGGTTTTTGGATGCCTTATTTAACTATAGCTTATGAACTTAAAAATACCGACACAGGTGCAA
TTAAACGTGGAACCTTTGATGCCTATGGTGGCTGATGATGGTCCCTCACTATGGTGCAAATATTGCTATGGAAAAAG
ATAAAAAAGGTGGCTTTGGCGTAGGAAATATGAACTTACTTTTTATATCTCAAATCCAGAAAAACAAGTTTTTG
GACGCCATGTTGATGAAGAAACAGGTGTGGGTAAGTGGTTTTGAACCTTTTAAAGTAGATTATAAATTCAAATACA
CAGGCACGCCAAAATAATTTTACGCTCGGATTTTCCGAGTGTTTGAATAT

pBADrha- *fetMP* forward primer

7. Nucleotide sequence of the PCR amplification product of *fetM-P* gene for cloning into pBADrha. The forward and reverse primers (Table 2.4) are underlined and indicated by arrows. Azure highlights indicate sequence matching the Shine-Dalgarno sequence (AGGAGG) likely corresponding to the ribosomal binding sites; bold highlights indicate the start codons of *fetM* and *fetP*; green highlights indicate stop codon of *fetM* and *fetP*. The total fragment size is 2626 bp.

pBADrha *fetA-F* forward primer

CAGCAGGATCACAT**ATG**AGTATATATTTTGTGCATTTTCTTATCAGTGTTTTACC

GCCTAAGTATTTTAATGGCCT
 TTATCACTCCTAATAAAAAATATATTTTTAAAAGTTTTTCGTAGTTTTTTGGGCTTTTATTTGGATATTTG
 CTTTTTTTATCGCAGCACAATTTTTAAAACCGAAAATTTAATCTTTAATTTTGATTTTGTTTTATAGGTTTAT
 TGCTAGTAAGCTTTATATTTTATTTTTGGAAAAAATTTGAAATTTTAAATTTTATTTTATTGGGAATTTAAGTT
 TTTGCACCGCTTTGCATTATTATTTTTTAAGTCAAGATTTCCCTATTTTTACTAGCTCTTTAATCGATAGCGAAG
 GTATAAGTTCTTTAGGTTTTATTGCTTTAGCCTTGCTTGTGTGATTTTGATTTTCTTCTTTTTAAAATGGCAAA
 AAAATTTTAATCAAAAAACAAGCTTTATGCTGTTTTTACTGCTTATCCTTATAGAAAGCGATAAAGCTCTAGCCA
 ATATCTTGCTTACTTTAATGCGAAATTCATCATAGAACTCATGCTTTTTTGGTGAGTTTTGTAGGAAAAAGTA
 ATTATTTTGGTGTTTTTGGAATTTATGTTTATTTAATTTTCATCACTTTTTTAGCATTCTTAAGCTTAAAAATTC
 GCAAAAAAATATAAGCAAAAAACAATTTTAGATATAAATTTATCGCAAAAACGAAGCTAAAACAAGTCTTATTA
 ATCGCTATTTTTCCAGTGTTTTTATCTCCTGTGTGTAAGTTTTTGCATTGTTTTTATACTTTTTTTATGGTAAGCT
 CTAAGCCTTTAACCATAGATGAGCCTAAAGAAATTTTACCCGATAAGAATGGCAAATTTATCTTTGATATAGCTC
 TTTTAAGGGACAACAACTCCACCGCTTTGCTTATATCAGTGCTGAAGGCAAAGTGATAAGGTTTTTTCTTATCA
 ACAAAGAGAAGATAAGGATTCTCCTGTAGCTGTTTTTGATGCTTGTATGATTTGTGGAGATATGGGCTATATCA
 AAAAAGATGGACAACCTCATTTGCATTTCTTGCAATGTGCGTATTTTCTTGCCAAGTGTAGGTAAAAGCGGGGTT
 GCAATCCTATCCCCTCAAATACGAATACGATGGTAACAAAATCACCATAGATGTTAAAGATGTAATAGCAGGAT
 CTAATTATTTTAGTCAAATCAAAGAAATTTGAAGTGCAAGATCCTGTATCAAAAACAAAGTTATAAACACCCAAG
 CTCCTTTTTCTTATAGCTATAAAGGGTTACTTATATTTTTCAAATCAAAACAACATGAAGAATTTAAAAAAG
 ATCCTACAAAATATGTAGAAGAAAACGAAGCCCAATTTTTAATCCAAAGGAGAAATGATGTTGGCTAAAATGATT
 TTTAACTCTATATTTAAAACAATAATCAAAAATTTTTAGCCTTTCTTACTTGTTTTTTAGCCACGCTTTTGCTC
 TCTACTATGCTAAATATTACCCTAAGTATAGGTGATGAAGTAACTAAACAACCTAAAAGCTATGGCTCTAATATC
 CTTGTTTTACCCAAAGGCTCAAGCCTTAGTATAGAAATAGGTAATGAACCTTTATGAACCTTAAAAACAATAAC
 TACCTAGAAGAAAAAATTTATATATGATTTAAAGACATTTATTTGGCGTAACAACATCACCGCACTTGCTCCTTTT
 TTGGAAGGTAAAATCACAATTGAAAACCTCCAGCAAAAAGCACTTATTTATGGTGCCTATTTTTCAAAAAGCCATA
 AAAATTAAAGATGATGATGATTTTATCACAGGTATAAAAAGTCTTTATCCTTATTTAGCAGTGCAAGGAGAATGG
 GCAAAAGATGATAGCAATGAAATCATGCTAGGCGAAGACTTTGCTAAAAACAATAAACTAAAATTAGGAGATACT
 ATCAAATTCATAGGAGAAAACAATCAAAGCAAAGAAGCAAAAATCGTAGGCATTTTACTTCATGCCAATCCTAAA
 ATGTCAAATAAAATCATCGCTCCTTTAAATTTAGCTCAAGATTTACTCAACAAACAAGGGCTTTACTCAAGTACA
 GAAGTAAGAGCTTTTACCATACCTGAATCAGCCCTTTCTGAAAAAGTACGTCGCATGGGCGAAGAAAAATTAGAT
 CAGTTAGAATATGACAAATGGTATTGCTCAGCTTATGTAGGCTCAATCGCTAGTCAAATTAGCGATGGCTTGCCA
 GGTGCTGATGCAAAAGCTCTAAATGCTATAAGCGATGCTCAAAGCTTGGTGGTTAAAAAGATCCAATCCTTAATG

Appendix

GGCATTACTTGCATTATTTGTCTTATTGTTGCAAGTATTGCGATTTCAAGTCTAATGAGTTCTGAAATTCATCGT
AGAAAAAAGAAATAGGACTTTTAAAAGTACTTGGTGCTAATACTTTTCAAATTTATCTCATCTTTGCTAGTGAA
AATTTAATCGTAGCTTTATTTGCTGCTTTACTTGGATTTATTTTTGGCACAGCACTTTCTCAAATCATCAGTCTT
AGTATTTTTGGATATTTTATTGATATAGCCTTTGTAGCTTTACCTTTAAGCTTTATTTTTGCAGGACTTATTGCC
TTACTTGGTTGCTTACTTCTATCAAAAAATATCACACAACCTTTCAGCTGCAGGAGTGCTTTATGGTAGATAAGTT
TTTTCTCAATGAGCTTTTTAAAAGCATTAGCTTTTCTTATCAAAGACTTTTTATTATAGTTTTAAGTGTTTTTAT
AGGAGCACTTACTTGTCTAGCTTTTTTAAATATTTATTTTGATATCGACATCAAACCTTCTAAAGAATTTAAAGC
TTATGGAGCAAATGTAATGATAAGTCCCAAGCAGGATGAAAAATTTATCTCCAATACTGAGTATGAAAAATAAA
AGAAATTTAAAGGCTAGAGCTTTAACTCCTTTTTTGTATGATTTTTTAAATTTAGGCAGTACAAGCGGGGTGGT
TTTAGGCACTGATTTTAGGGCTTTAAAAATCACTAAACCTTTTTTAGAAGTTAAAGAAGGAAGCTTTTCTCTAAA
TGATTTTGATGAAAATTCAGCCTTTTTAGGAGTTAATTTAGCCAAGCAACTAGGCCTTAAAGCAGGCAATGAAC
TCAAATTTATAATCCAAACAACGGAAAAAGCATAAACTTACCATAAAAGGCATACCTTCAAGCAATGATGAATT
TGATAGCATTGTTTTAGCCCCTTTAAAGCGTGGTGCAAAATTTAAGCGATAGAGCCGGTATTAACATGCTAATGC
TGATGTTTATGGAAATTTTGATGAAGTTAAAGCCAAAACACAAGCAATCAGCAATGAATTCATCGATGCAAAACC
TATATCTTCAGTATCCTTAAAGTGAAGTTTTAGTGCTTGAAAAATCAAAGCTTTAATGTTTTTAATCATACTTGT
GGTATTGATCATAGTTACTACTAGCGTTAATACAACCTTTAAGTTCTATTATATTTTTCTCGCAAAAAAGAAATCGC
ACTGCGTTTAGCCTTGGGTGCGAAAAAAGTGAAATTTTTAACTTTTTGCTAGTGAATGCTTTATAGTAAGTTT
TTTTGCTAGTTTAAATCGGAGCTTTTTGTGGGATATTTTTAGCCAATGTCTTTGGTTATTTAATTTTTAATTCAG
TATTGATTTTAGATTTATAGCTGTTTTTATAGCCTTAATCATTTCTTTGATTTTTGCCTTTTTGGCTGCATTTTT
TCCTATAAAAAGAGCATTAAAAATCAATGTGTGTGAAAAATTTGAAAGGTGAATGATGAAAAAGAAGTTATTTAA
ATAAACAATTTAAATAAAGAATTTGGCAAAAGTTAAAGCCTTAAACAATATCAACTTAAGCGTCTATGAAGGAGAA
TGGCTTGCCATCATGGGTCCATCAGGAAGTGGAAAAATCAACACTTTTAAACATACTATCGCTCATGGATACTCCA
AGCTCTGGAGAGTATATCTTGATAATGAAAACCTAGAGCAAATGGATGAAGAGCAAAAAATCACCTTGCCTCGT
GAAAAATAGGGCTTGTCTTTCAACAATTTTATCTTATCCCCTATCTTAACGCCTTAGAAAATGTTATGCTCTCT
CAGTATTATCACTCAAGTGTAGATGAAGAAGATGCCAAAATGGTTCTTGAAAAAGTAGGACTTTTCGCATAGACTC
ACTCATTTACCTAGCCAATTAAGTGGCGGAGAACAACAAGAGTTTGTATAGCAAGAGCTTTAATCAACAACCCA
GAGCTTTTACTCGCAGATGAACCCACAGGAAAATTTAGATGAAGCCAATGAACAAATCGTTCTTCAAACCTTGCAA
AAATTA AAAAATGAAGGTAAAACCATAGTTTAAATCACACACAATCCTGATTTAGCCAAATTCGCAGATCGAAC
CTTATCTTACAACATGGGGTGTAAAAATGAAAAAAGCCTTTTAACTTAAAGCATTGTGTTTTACTCAATGCTT
GTTCTTTTGAAAATTTCAAAGATACTGGAAAAGTTGGAGAAAAAAGCGCTGAAATTTAGCTAAAGATACTTTAG
GAAAAGCTGTAAAACCTTGTGATGATAATACAAGTTTAAAAGTCTTAGTCTTTTTTCAAATGGCTGCCCTTCTT
GCTTAAAAGAAGCTCCCTTCTTTAGATGAATTCATACAAAATCACCCCAATAAAAATCAGTGTTTATGCTATAAATT
CCATCGATAATGCCAATGTGGTTAAGTTTTAGCCGAACAATTTGACTTTAAAAATGTAAAAGTTTTTAAAAGACG
ATCTTAAAATCACCAATGATCGTTACGCTGTGTTTGCAACCCCTACTACCATCATCATTAAGATGGGATGATAA
AAGATAGAATTTTAGGAGAAAAACCATGGGAATTTTTCGAATCCAAGCTTATTTCTTTGCTTAAATCATAGCTTT
ATTTTTTTGTAGCTTGTGATAGTGGAGAAAATTTTAAAGCTTTAAATAGCGATAAAACCTATAATTTTGCTTACAA
TGGTTTTGAAAAAAGCCTAAAACATAAATGATAAAGCACAAAATTTTGCTTAGTATTTTTTCAAAAAGATTGCGG
AGTTTGCAAAGAACAATTCCTATTTTACAGAATTTGGCTAAAAATTTATGATTTTAAATATCTTTGTGGTTTTAGG
CGATGCAAACGATGCAAACGATGCAAAGCTTGGGCTGATGAAAAAGTTTATCTAATTTAGCAATGTTTTATGA
AAAAAGAGCAGCTAAATACCTTTCAAGTGCATTTGGGGAAATATATGGAGTACCTGTGCTTAGTTTTTTTTCAAAGA

Appendix

AGGAAAAATGGATGAAAAATTCATAGGCTTAACTCCTTATAGCATACTTGAAAAAGAAATCAAAAAAGTAAAAAG
CTAAGGATCCTCTAGAGTC



pBADrha *fet A-F* reverse primer

8. Location of pBADrha *-fetA-F* primers. *FetA-F* forward and reverse primers are underline and indicated by arrows. Azure highlight indicates sequence matching the Shine-Dalgarno sequence (AGGAGG) likely corresponding to the ribosomal binding sites, bold highlight indicates the start codon of *fetA-F* and green highlight indicates stop codon of *fetA-F*, the fragment about 5400bp include 6 genes (*cj1660-cj1665*).

pBADara *fetMP* forward primer

GAGGAATTAACCA**ATG**AAAAATTTTTAAATTTATATTTTTAATTATAAGTATTTTTTTATCAAGCTCAGCTTTTGCT
AGGGTAGATGATTATATTAATGAAGCAAATCTTATCAAAGATATGCTAAAACAAAGCATAGAACTTATAAAAAAG
GGCGATAATCTAGGCGCCAAAAAGCTTAGCGAAGATGCGTATTTTCAACATTTTGAAAATATGGAAGGCTCAATA
GGAAGAAACATAGGAAGAAAAGCTATCACTATGGAGCGTAAATTTGTAAATTTGCGTCGCATGTATAAAGATGAA
GCTCCTTTGACACAAATTAATGCTTTAATTGATAGTCTTTATTTATGATCTTGATGAAGTAGCTCCGATTTTACAA
AATGGATATCGTTTTAAAGCAGAAGCAAGCGATATAAACTATGATAAGGCTAAAGCTGAAAAATCAAGCCTAGAA
GCCAATGCCAAACGCGAAGCTGATGCAGAAGCTTTAATCGCACAAATGATGGGTGTAGATAAAAAAGATTTAGCA
CAAAGCTCTTTAACCACCCAAGCTCCTATACCTATAAAATAATGATACAAGCAAACCTTACAGATGATAATGCAAGC
ACTGATTTACAAGCTGCCGCTGCAATGGACGTAAGATTGCAATTTATACTAGATAAATATCTCTACCAAATTTTCA
CAGGCAGCTAATGCTTTTTAAAGAAAAAACTACCAAACCTAGTAAAGATTTTTTAAATGATGCCTTATTTAGTGAT
TATCGCAATACCAAAGTAGAAATTTTAGTAAATAAATTTACCAAAGCAGGAAACGATCAAAAAATTCACAAGCC
ATACGCACCCTTATACGCCAAATCAACGATGCAAAAAATAGATGAAAAAGGCTTAAGAGATGGCTTAGATAACATA
GAAGAACAAATTTTTGATGTTTTCTTACAAATTCCAAATTCAGAACCTTCAAGTTTGCAAATTTCAAGCTTTAAT
GATGAAACAAAAGGCAAAGATTATGCCAAAGTTTCTAATGATATCAAACCTGCTTTAGATGAAATTTAAAAAAT
TATGATGGGTTTTAGTGCTTCTATAGTAGATGATTTACAAGGAATTTATCTAGATATTTTTGAAGCAAGCGGTATG
GAAAATAAAATCGGTGCTGTAGATAGCGGCTTAAAACTTAAAAATAGAAAGTTTATTTTCCAAAAGCGTAGCTCTT
ATCAAAGCAAGTACAGATAAAAAAGAGCTTGAAGCTACTTTTAATGACTTAGAACAACCTCATAGCCAGCAGCGTG
GATAAAATTCAGATTCTACTCCTTATTCGCTGTTTTATATGGGCTTTAGGTATTATTTTGCCTGAAGGCTTGGA
GCTTTGATTATCGTTGTAGCCATTGTTTTCTTATCTTGTGCAAAGTGGAACAAAAATCGTTTAAATATCGCCTAT
AGTGCTCTTTTTACAGGAGTAATTTTAAAGTTTTGTTACCGCTTTTGGAGTTTCTTGGCTATTTAAAGAAAATGCA
GGACAAAGTAGAGAGCTTATAGAGGGTATTACCATGCTTATAGCCGTATTACTACTCTTTTATGTGGGCTTTTGG
CTACTTTCAAACGCACAAAATAAAAAATGGACAAGCTTTATCAAACAAGGTGCTATAGATGCTATATCAAACAAT
AGTGCAAAAACCCTTTGGATTACCGTATTTTTAGCTGTTTTATAGAGAAGGTGCAGAAACTGTGCTTTTTTATCAA
GCCTTGCTTTTTGATGCTAAAACAAGCACTGATTTTTGGTGCTGTTTTTGGCGGACTTGGACTTGAATTTTAATA
CTTATTGTTTTTATATTTTTCTTTTAAAGCAGGAGCCATTCGCATACCTGTAAAACAATTTTTCTATATCACTTCT
TACATTATTTTTTACATGGTTTTTGTTTTTACAGGCAAAGGCATAGCCGAACTCATAGAAGGAAAAGTCATCATT
CCTAGTCTTATACCTATGAATTTTGAACCGATTTTATGGCTTGAATTTATCCTTACTATGAACTTTAATCCCT
CAATTTATAGTTTTAATTATGCTAATTATTGGCATTTTAATAACAAAACAAATTTCAAAAAAGGAGTAAATCA
TGATAAAAAAAGTTTTATCAGTAGTTGCTGCAGCTGCGGTTATTAGTACAAATTTATTTGCAGGCGAAGTGCCGA

Appendix

TCGGCGATCCAAAAGAACTTAATGGCATGGAAATAGCCGCTGTTTATTTACAACCTATTGAAATGGAGCCAAGAG
GTATTGATTTAGCTGCATCTTTAGCAGATATTCACCTAGAAGCTGACATTCACGCACTTAAAAACAATCCAAATG
GTTTTCCAGAAGGTTTTTGGATGCCTTATTTAACTATAGCTTATGAACTTAAAAATACCGACACAGGTGCAATTA
AACGTGGAACCTTTGATGCCTATGGTGGCTGATGATGGTCCCTCACTATGGTGCAAATATTGCTATGGAAAAAGATA
AAAAAGGTGGCTTTGGCGTAGGAAATTATGAACTTACTTTTTATATCTCAAATCCAGAAAAACAAGGTTTTGGAC
GCCATGTTGATGAAGAAACAGGTGTGGGTAAGTGGTTTGAACCTTTTAAAGTAGATTATAAATTCAAATACACAG
GCACGCCAAAATAATTTTACGCTCGGATTTTCCGAGTGTTAAGCTTGGCGTGTGG

pBADara- *fetMP* reverse primer



9. Location of pBADara-*fetM-P* primers. *FetM-P* forward and reverse primers are underline and indicated by arrows. Azure highlight indicates sequence matching the Shine-Dalgarno sequence (AGGAGG) likely corresponding to the ribosomal binding sites, bold highlight indicates the start codon of *FetM-P* and green highlight indicates stop codon of *fetM-P*, the fragment about 2626 bp include 2 genes (*ftr1* and *p19*).

pBADara -*fetA-F* forward primer

GAGGAATTAACCA**ATG**GTATATATTTTTGTGCATTTTCTTATCAGTGTTTTACCGCTAAGTATTTTAAATGGCCTTTA
TCACTCCTAATAAAAAATATATTTTTTAAAAGTTTTTTCGTAGTTTTTTTTGGGCTTTTTATTTGGATATTTTGCTT
TTTTTATCGCAGCACAATTTTTTAAAACCGAAAATTTAATCTTTAATTTTGATTTTGTTTTTATAGGTTTATTGC
TAGTAAGCTTTATATTTTTATTTTTGGAAAAAAATGAAATTTTAAATTTTATTTTATTGGGAATTTTAAAGTTTTT
GCACCGCTTTGCATTATTATTTTTTAAAGTCAAGATTTCCCTATTTTTACTAGCTCTTTAATCGATAGCGAAGGTA
TAAGTTCTTTAGGTTTTTATTGCTTTAGCCTTGCTTGTTTGTATTTTGTATTTTCTTCTTTTTAAAATGGCAAAAA
ATTTTAAATCAAAAAACAAGCTTTATGCTGTTTTTACTGCTTATCCTTATAGAAAGCGATAAAGCTCTAGCCAATA
TCTTGCTTACTTTAATGCGAAATTCATCATAGAACTCATGCTTTTTTGGTGAGTTTTGTAGAAAAAGTAATT
ATTTTGGTGTTTTTGGAAATTTATGTTTATTTAATTTTCATCACTTTTTTAGCATTCTTAAGCTTAAAAATTCGCA
AAAAAATATAAGCAAAAAACAATTTTAGATATAAATTATCGCAAAAAACGAAGCTAAAACAAGTCTTATTAATC
GCTATTTTTCCAGTGTTTTTATCTCCTGTGTTGTAAGTTTTTGCATGTTTTTTATACTTTTTTATGGTAAGCTCTA
AGCCTTTAACCATAGATGAGCCTAAAGAAAATTTACCCGATAAGAATGGCAAATTTATCTTTGATATAGCTCTTT
TAAGGGACAACAACCTCCACCGCTTTGCTTATATCAGTGCTGAAGGCAAAGTGATAAGGTTTTTCTTATCAACA
AAAGAGAAGATAAGGATTCTCCTGTAGCTGTTTTTGGATGCTTGTATGATTTGTGGAGATATGGGCTATATCAAAA
AAGATGGACAACCTCATTTGCATTTCTTGCAATGTGCGTATTTTCTTGCCAAGTGTAGGTAAGCGGGGGTTGCA
ATCCTATCCCACTCAAATACGAATACGATGGTAACAAAAATCACCATAGATGTTAAAGATGTAATAGCAGGATCTA
ATTATTTTAGTCAAATCAAAGAAATGAAGTGCAAGATCCTGTATCAAAAAACAAGGTTATAAACACCCAAGCTC
CTTTTTCTTATAGCTATAAAGGGGTTACTTATTTTCAAATCAAAACAACCTATGAAGAATTTAAAAAGATC
CTACAAAATATGTAGAAGAAAACGAAGCCCAATTTTAAATCAAAGGAGAAATGATGTTGGCTAAAATGATTTTT
AACTCTATATTTAAAAACAATAATTTCAAAAATTTTTAGCCTTTCTTACTTGTTTTTTAGCCACGCTTTTGCTCTCT
ACTATGCTAAATATTACCCTAAGTATAGGTGATGAAGTAACTAAACAACCTCAAAGCTATGGCTCTAATATCCTT
GTTTTACCCAAAGGCTCAAGCCTTAGTATAGAAATAGGTAATGAACTTTATGAACCTTAAAAACAACAACCTAC
CTAGAAGAAAAAATTTATATATGATTAAGACATTTATTGGCGTAACAACATCACCGCACTTGCTCCTTTTTTG

Appendix

GAAGGTAAAATCACAATTGAAAACCTCCAGCAAAAAGCACTTATTTATGGTGCTTATTTTCAAAAAGCCATAAAA
ATTTAAAGATGATGATGATTTTTATCACAGGTATAAAAAGTCTTTATCCTTATTTAGCAGTGCAAGGAGAATGGGCA
AAAGATGATAGCAATGAAATCATGCTAGGCGAAGACTTTGCTAAAAACAATAAACTAAAATTTAGGAGATACTATC
AAATTCATAGGAGAAAAACAATCAAAGCAAAGCAAAAAATCGTAGGCATTTTACTTCATGCCAATCCTAAAATG
TCAAATAAAATCATCGCTCCTTTAAATTTAGCTCAAGATTTACTCAACAAACAAGGGCTTTACTCAAGTACAGAA
GTAAGAGCTTTTACCATACCTGAATCAGCCCTTCTGAAAAAGTACGTCGCATGGGCGAAGAAAAATTAGATCAG
TTAGAATATGACAAATGGTATTGCTCAGCTTATGTAGGCTCAATCGCTAGTCAAATTAGCGATGGCTTGCCAGGT
GCTGATGCAAAAAGCTCTAAATGCTATAAGCGATGCTCAAAGCTTGGTGGTTAAAAAGATCCAATCCTTAATGGGC
ATTACTTGCAATTATTTGTCTTATTGTTGCAAGTATTGCGATTTCAAGTCTAATGAGTTCTGAAATTCATCGTAGA
AAAAAAGAAATAGGACTTTTAAAAGTACTTGGTGCTAATACTTTTCAAATTTATCTCATCTTTGCTAGTGAAAAT
TTAATCGTAGCTTTATTTGCTGCTTTACTTGGATTTATTTTTGGCACAGCACTTTCTCAAATCATCAGTCTTAGT
ATTTTTGGATATTTTATTGATATAGCCTTTGTAGCTTTACCTTTAAGCTTTATTTTTGCAGGACTTATTGCCTTA
CTTGGTTGCTTACTTCCATCAAAAATATCACACAACCTTTCAGCTGCAGGAGTGCTTTATGGTAGATAAGTTTTT
CCTCAATGAGCTTTTTTAAAAGCATTAGCTTTTCTTATCAAAGACTTTTTATTATAGTTTTAAGTGTTTTTATAGG
AGCACTTACTTGCTCAGCTTTTTTAAATATTTATTTTGATATCGACATCAAACCTTCTAAAGAATTTAAAAGCTTA
TGGAGCAAATGTAATGATAAGTCCCAAGCAGGATGAAAATTTTATCTCCAATACTGAGTATGAAAAAATAAAGA
AAATTTAAAGGCTAGAGCTTTAACTCCTTTTTGTATGATTTTTTAAATTTAGGCAGTACAAGCGGGGTGGTTTT
AGGCACTGATTTTAGGGCTTTAAAATCACTAAACCTTTTTTAGAAGTTAAAGAAGGAAGCTTTTCTCTAAATGA
TTTTGATGAAAATTCAGCCTTTTTTAGGAGTTAATTTAGCCAAGCAACTAGGCCTAAAAGCAGGCAATGAACCTCA
AATTTATAATCCAAACAACGGAAAAAGCATAAAAACCTTACCATAAAAAGGCATACTTTCAAGCAATGATGAATTTGA
TAGCATTGTTTTAGCCCTTTAAGCGTGGTGCAAAAATTTAAGCGATAGAGCCGGTATTAAGTATGCTAATGCTGT
AGTTTATGAAAATTTGATGAAGTTAAAGCCAAAAACACAAGCAATCAGCAATGAATTCATCGATGCAAAACCTAT
ATCTTCAGTATCCTTAAGTGAAGGTTTAGTGCTTGAAAAATCAAAGCTTTAATGTTTTTAATCATACTTGTGGT
ATTGATCATAGTTACTACTAGCGTTAATACAACCTTTAAGTCTATTATATTTTTCTCGCAAAAAGAAATCGCACT
GCGTTTTAGCCTTGGGTGCGAAAAAAGTAAAATTTTTAACTTTTTTGCTAGTGAATGCTTTATAGTAAGTTTTTT
TGCTAGTTAATCGGAGCTTTTTGTGGGATATTTTTAGCCAATGCTTTGGTTATTTAATTTTTAATTTCTAGTAT
TGATTTTAGATTTATAGCTGTTTTTATAGCCTTAATCATTTCTTTGATTTTTGCCTTTTTGGCTGCATTTTTTCC
TATAAAAAGAGCATTAAAAATCAATGTGTGTGAAAAATTTGAAAGGTGAATGATGAAAAAGAAGCTTATTTAAATA
AACAATTTAAATAAAGAATTTGGCAAAGTTAAAGCCTTAAACAATATCAACTTAAGCGTCTATGAAGGAGAATGG
CTTGCCATCATGGGTCCATCAGGAAGTGAAAAATCAACACTTTTAAACATACTATCGCTCATGGATACTCCAAGC
TCTGGAGAGTATATCTTTGGATAATGAAAACCTAGAGCAAATGGATGAAGAGCAAAAAATCACCTTGCGTCGTGAA
AAAATAGGGCTTGTCTTTCAACAATTTTCATCTTATCCCCTATCTTAACGCCTTAGAAAATGTTATGCTCTCTCAG
TATTATCACTCAAGTGTAGATGAAGAAGATGCCAAAATGGTTCTTGAAAAAGTAGGACTTTCGCATAGACTCACT
CATTTACCTAGCCAATTAAGTGGCGGAGAACAAACAAAGAGTTTGTATAGCAAGAGCTTTAATCAACAACCCAGAG
CTTTTACTCGCAGATGAACCCACAGGAAATTTAGATGAAGCCAATGAACAAATCGTTCTTCAAACCTTGCAAAA
TTAAAAAATGAAGGTAAAACCATAGTTTTAATCACACACAATCCTGATTTAGCCAAATTCGCAGATCGAACCCTT
ATCTTACAACATGGGGTGTAAAATGAAAAAAGCCTTTTAAATCTTAAGCATTTTGTTTTTACTCAATGCTTGTT
CTTTTGAAAATTCAAAAGATACTGGAAAAAGTTGGAGAAAAAAGCGTGAAATTTAGCTAAAGATACTTTAGGAA
AAGCTGTAAAACCTGCTGATGATAATACAAGTTTAAAAGTCTTAGTCTTTTTTCAAATGGCTGCCCTTCTTGCT
TAAAAGAAGTCCCTTCTTTAGATGAATTCATACAAAATCACCCCAATAAAAATCAGTGTATGCTATAAATTTCCA
TCGATAATGCCAATGTGGTTAAGGTTTTAGCCGAACAATTTGACTTTAAAATGTAAAAGTTTTAAAAGACGATC

Appendix

TTAAAATCACCAATGATCGTTACGCTGTGTTTGAACCCCTACTACCATCATCATTAAGATGGGATGATAAAAG
ATAGAATTTTAGGAGAAAAACCATGGGAATTTTCGAATCCAAGCTTATTTCTTTGCTTTAATCATAGCTTTATT
TTTTGTAGCTTGTGATAGTGGAGAAAAATTTTAAAGCTTTAAATAGCGATAAAACCTATAATTTTGCCTACAATGG
TTTTGAAAAAAGCCTAAAACCTAAATGATAAAGCACAAAATTTTGCCTTAGTATTTTTCACAAAAGATTGCGGAGT
TTGCAAAGAACAAATTCCTATTTTACAGAATTTGGCTAAAAATATGATTTTAATATCTTTGTGGTTTTAGGCCG
TGCAAACGATGCAAACGATGCAAAAGCTTGGGCTGATGAAAAAGGTTTATCTAATTTAGCAATGTTTTATGAAAA
AAGAGCAGCTAAATACCTTTCAAGTGCCATTGGGGAAATATATGGAGTACCTGTGCTTAGTTTTTCAAAGAAGG
AAAAATGGATGAAAAATTCATAGGCTTAACTCCTTATAGCATACTTGAAAAAGAAATCAAAAAAGCTAAAAGCT
TGGCTGTTTTGG



pBADara -*fetA-F* reverse primer

10. Location of pBADara-*fetA-F* primers. *FetA-F* forward and reverse primers are underline and indicated by arrows. Azure highlight indicates sequence matching the Shine-Dalgarno sequence (AGGAGG) likely corresponding to the ribosomal binding sites, bold highlight indicates the start codon of *FetA-F* and green highlight indicates stop codon of *fetA-F*, the fragment about 5400bp include 6 genes (*cj1660-cj1665*).

ATGAAAATTTTTAAAATTATATTTTTAATTATAAGTATTTTTTATCAAGCTCAGCTTTTGCTAGGGTAG
ATGATTATATTAATGAAGCAAATCTTATCAAAGATATGCTAAAACAAAGCATAGAACTTATAAAAAGGG
CGATAATCTAGGCGCCAAAAAGCTTAGCGAAGATGCGTATTTTCAACATTTTGAAAATATGGAAGGCTCA
ATAGGAAGAAACATAGGAAGAAAAGCTATCACTATGGAGCGTAAATTTGTAAATTTGCGTCGCATGTATA
AAGATGAAGCTCCTTTGACACAAATTAATGCTTTAATTGATAGTCTTTATTATGATCTTGATGAAGTAGC
TCCGATTTTACAAAATGGATATCGTTTAAAAGCAGAAGCAAGCGATATAAACTATGATAAGGCTAAAGCT
GAAAAATCAAGCCTAGAAGCCAATGCCAAACGCGAAGCTGATGCAGAAGCTTTAATCGCACAAATGATGG
GTGTAGATAAAAAAGATTTAGCACAAAGCTCTTTAACCACCCAAGCTCCTATACCTATAAATAATGATAC
AAGCAAACCTTACAGATGATAATGCAAGCACTGATTTACAAGCTGCCGCTGCAATGGACGTAAGATTGCAA
TTTATACTAGATAATATCTCTACCAAATTTTACAGGCAGCTAATGCTTTTAAAGAAAAAACTACCAA
CTAGTAAAGATTTTTTAAATGATGCCTTATTTAGTGATTATCGCAATACCAAAGTAGAAATTTTAGTAAA
TAAATTTACCAAAGCAGGAAACGATCAAAAAATTCACAAGCCATACGCACCCTTATACGCCAAATCAAC
GATGCAAAAATAGATGAAAAAGGCTTAAGAGATGGCTTAGATAACATAGAAGAACAAATTTTGTATGTTT
TCTTACAAATTCCAAATTCAGAACTTTCAAGTTTGCAAAATTTCAAGGCTTTAATGATGAAACAAAAGGCAA
AGATTATGCCAAAGTTTCTAATGATATCAAACCTTGCTTTAGATGAAATTTTAAAAAATTTATGATGGGTTT
AGTGCTTCTATAGTAGATGATTTACAAGGAATTTATCTAGATATTTTTGAAGCAAGCGGTATGGAAAATA
AAATCGGTGCTGTAGATAGCGGCTTAAAACCTAAAATAGAAAAGTTATTTTTCCAAAAGCGTAGCTCTTAT
CAAAGCAAGTACAGATAAAAAAGAGCTTGAAGCTACTTTTAAATGACTTAGAACAACTCATAGCCAGCAGC
GTGGATAAAAATTCAGATTCTACTCCTTATTCGCTGTTTATATGGGCTTTAGGTATTATTTGCGTGAAG
GCTTGGAAAGCTTTGATTATCGTTGTAGCCATTGTTTCTTATCTTGTGCAAAGTGGCAACAAAATCGTTT
AAATATCGCCTATAGTGCTCTTTTACAGGAGTAATTTAAGTTTGTACCCTTTTGGAGTTTCTTGG
CTATTTAAAGAAAATGCAGGACAAAGTAGAGAGCTTATAGAGGGTATTACCATGCTTATAGCCGTATTAC
TACTCTTTTATGTGGGCTTTTGGCTACTTTCAAACGCACAAAATAAAAAATGGACAAGCTTTATCAAACA
AGGTGCTATAGATGCTATATCAAACAATAGTGCAAAAACCTTTGGATTACCGTATTTTTAGCTGTTTAT

Appendix

AGAGAAGGTGCAGAACTGTGCTTTTTTATCAAGCCTTGCTTTTTGATGCTAAAACAAGCACTGATTTTG
GTGCTGTTTTTGGCGGACTTGACTTGGAATTTAATACTTATTGTTTTATATTTCTTTTAAAAGCAGG
AGCCATTTCGCATACCTGTAAAACAATTTTTCTATATCACTTCTTACATTATTTTTTACATGGTTTTTGT
TTTACAGGCAAAGGCATAGCCGAACTCATAGAAGGAAAAAGTCATCATTCCTAGTCTTATACCTATGAATT
TTGAACCGATTTTATGGCTTGGAATTTATCCTTACTATGAACTTTAATCCCTCAATTTATAGTTTTAAT
TATGCTAATTATTGGCATTTTAATAACAAAACAAATTTCAAAAAAAGGAGTAAAATCATGATAAAAAAAG
TTTTATCAGTAGTTGCTGCAGCTGCGGTTATTAGTACAAATTTATTTGCAGGCGAAGTGCCGATCGGCGA
TCCAAAAGAACTTAATGGCATGGAAATAGCCGCTGTTTTATTTACAACCTATTGAAATGGAGCCAAGAGGT
ATTGATTTAGCTGCATCTTTAGCAGATATTCACCTAGAAGCTGACATTCACGCCTTAAAAACAATCCAA
ATGGTTTTCCAGAAGGTTTTTGGATGCCTTATTTAACTATAGCTTATGAACTTAAAAATACCGACACAGG
TGCAATTAACGTGGAACCTTTGATGCCTATGGTGGCTGATGATGGTCCCTACTATGGTGCAAATATTGCT
ATGGAAAAAGATAAAAAAGGTGGCTTTGGCGTAGGAAATATGAACTTACTTTTTATATCTCAAATCCAG
AAAAACAAGGTTTTTGGACGCCATGTTGATGAAGAAACAGGTGTGGGTAAGTGGTTTGAACCTTTTAAAGT
AGATTATAAATTCAAATACACAGGCACGCCAAAATAATTTTACGCTCGGATTTTCCGAGTGTGTGAATAT
TTTTATTTTTATTTGAAAAATTAATAAACAATGTTTAAAGAGTAAATTTATGAGTATATATTTTGTGCAT
TTTCTTATCAGTGTTTTACCCTAAGTATTTTAAATGGCCTTTATCACTCCTAATAAAAAATATATTTTTTA
AAAGTTTTTTCGTAGTTTTTTTTGGGCTTTTTATTTGGATATTTTGCTTTTTTTTATCGCAGCACAATTTTT
AAAAACCGAAAATTTAATCTTTAATTTTTGATTTTTGTTTTTATAGTTTTATTGCTAGTAAGCTTTATATTT
TATTTTTTGAAAAAAATTGAAATTTTAAATTTTATTTTATTGGGAATTTTAAAGTTTTTGCACCGCTTTGC
ATTATTATTTTTTAAAGTCAAGATTTCCCTATTTTTACTAGCTCTTTAATCGATAGCGAAGGTATAAGTTC
TTTAGGTTTTTATTGCTTTAGCCTTGCTTGTGTGTTTTGATTTTTCTTCTTTTTTAAAATGGCAAAAAAAT
TTAATCAAAAAACAAGCTTTATGCTGTTTTTACTGCTTATCCTTATAGAAAGCGATAAAGCTCTAGCCA
ATATCTTGCTTACTTTAATGCGAAATTCATCATAGAAACTCATGCTTTTTTGGTGAGTTTTTGTAGGAAA
AAGTAATTATTTTTGGTGTTTTTTGAATTTATGTTTATTTAATTTTCATCACTTTTTTAGCATTCCTAAGC
TTAAAAATTCGCAAAAAAATATAAGCAAAAAACAATTTTAGATATAAATTTATCGCAAAAACGAAGCTA
AAACAAGTCTTATTAATCGCTATTTTTCCAGTGTTTTTATCTCCTGTGTGTAAGTTTTTGCATTGTTTT
ATACTTTTTTATGGTAAGCTCTAAGCCTTTAACCATAGATGAGCCTAAAGAAATTTTACCCGATAAGAAT
GGCAAATTTATCTTTGATATAGCTCTTTTAAAGGGACAACAACCTCCACCGCTTTGCTTATATCAGTGCTG
AAGGCAAAGTGATAAGGTTTTTTCTTATCAACAAAAGAGAAGATAAGGATTCCTCCTGTAGCTGTTTTTGA
TGCTTGTATGATTTGTGGAGATATGGGCTATATCAAAAAAGATGGACAACCTATTTGCATTTCTTGCAAT
GTGCGTATTTTTCTTGCCAAGGTGAGGTAAGCGGGGGTTGCAATCCTATCCCACTCAAATACGAATACG
ATGGTAACAAAATCACCATAGATGTTAAAGATGTAATAGCAGGATCTAATTATTTTAGTCAAATCAAAGA
AATTGAAGTGCAAGATCCTGTATCAAAAAACAAGGTTATAAACACCCAAGCTCCTTTTTCTTATAGCTAT
AAAGGGTTACTTATTATTTTTCAAATCAAAACAACCTATGAAGAATTTAAAAAAGATCCTACAAAATATG
TAGAAGAAAACGAAGCCCAATTTTTAATCCAAAGGAGAAATGATGTTGGCTAAAATGATTTTTAACTCTA
TATTTAAAAACAATTTCAAAAATTTTTAGCCTTTCTTACTTGTTTTTTAGCCACGCTTTTGCTCTCTAC
TATGCTAAATATTACCCTAAGTATAGGTGATGAAGTAACCTAAACAACCTAAAAGCTATGGCTCTAATATC
CTTGTTTTTACCCAAAGGCTCAAGCCTTAGTATAGAAATAGGTAATGAACTTTATGAACCTTAAAAACA
AAAACCTACCTAGAAGAAAAAATTTATATATGATTAAGACATTTATTGGCGTAACAACATCACCGCACT
TGCTCCTTTTTTGAAGGTAAAATCACAATTGAAAACCTCCAGCAAAAAGCACTTATTTATGGTGCTTAT
TTTCAAAAAGCCATAAAAAATTAAGATGATGATGATTTTATCACAGGTATAAAAAAGTCTTTATCCTTATT

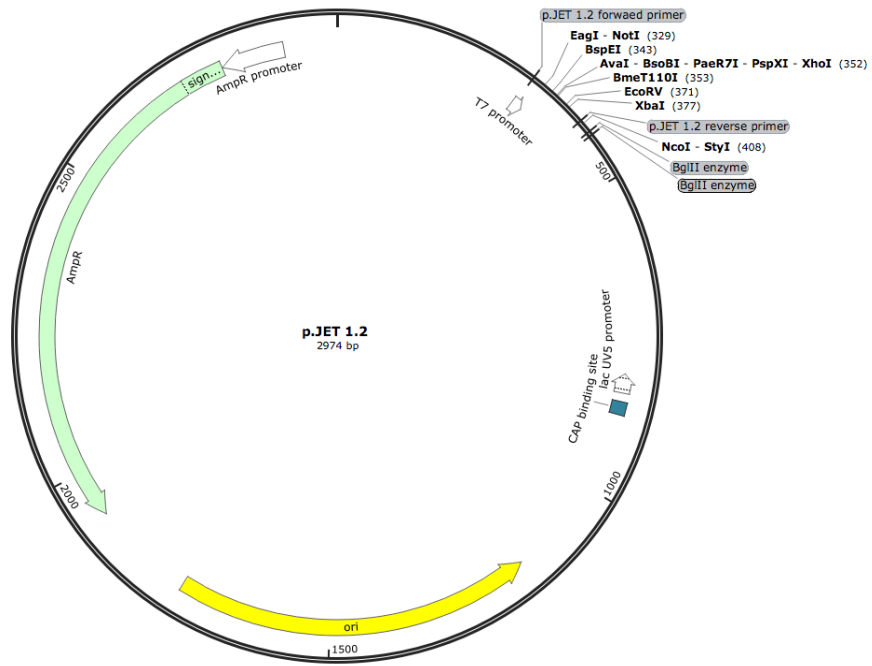
Appendix

TAGCAGTGCAAGGAGAATGGGCAAAAAGATGATAGCAATGAAATCATGCTAGGCGAAGACTTTGCTAAAA
CAATAAACTAAAATTAGGAGATACTATCAAATTCATAGGAGAAAACAATCAAAGCAAAGAAGCAAAAATC
GTAGGCATTTTACTTCATGCCAATCCTAAAATGTCAAATAAAATCATCGCTCCTTTAAATTTAGCTCAAG
ATTTACTCAACAAAACAAGGGCTTTACTCAAGTACAGAAGTAAGAGCTTTTACCATACCTGAATCAGCCCT
TTCTGAAAAAGTACGTTCGCATGGGCGAAGAAAAATTAGATCAGTTAGAATATGACAAAATGGTATTGCTCA
GCTTATGTAGGCTCAATCGCTAGTCAAATTAGCGATGGCTTGCCAGGTGCTGATGCAAAAGCTCTAAATG
CTATAAGCGATGCTCAAAGCTTGGTGGTTAAAAAGATCCAATCCTTAATGGGCATTACTTGCATTATTTG
TCTTATTGTTGCAAGTATTGCGATTTCAAGTCTAATGAGTTCTGAAATTCATCGTAGAAAAAAGAAATA
GGACTTTTAAAAGTACTTGGTGCTAATACTTTTCAAATTTATCTCATCTTTGCTAGTAAAAATTTAATCG
TAGCTTTATTTGCTGCTTTACTTGGATTTATTTTTGGCACAGCACTTTCTCAAATCATCAGTCTTAGTAT
TTTTGGATATTTTATTGATATAGCCTTTGTAGCTTTACCTTTAAGCTTTATTTTTGCAGGACTTATTGCC
TTACTTGGTTGCTTACTTCTATCAAAAATATCACACAACCTTCAGCTGCAGGAGTGCTTTATG**GTAGAT**
AAGTTTTTCTCAATGAGCTTTTTAAAAGCATTAGCTTTTCTTATCAAAGACTTTTTATTATAGTTTTAA
GTGTTTTTATAGGAGCACTTACTTGCTCAGCTTTTTTAAATATTTATTTTGATATCGACATCAAACCTTC
TAAAGAATTTAAAAGCTTATGGAGCAAATGTAATGATAAGTCCCAAGCAGGATGAAAATTTTATCTCCAAT
ACTGAGTATGAAAAATAAAAGAAAAATTTAAAGGCTAGAGCTTTAACTCCTTTTTTGTATGATTTTTTAA
ATTTAGGCAGTACAAGCGGGTGGTTTTAGGCACTGATTTTAGGGCTTTAAAAATCACTAAACCTTTTTT
AGAAGTTAAAGAAGGAAGCTTTTCTCTAAATGATTTTGATGAAAATTCAGCCTTTTTAGGAGTTAATTTA
GCCAAGCAACTAGGCCTAAAAGCAGGCAATGAACTTCAAATTTATAATCCAAACAACGGAAAAAGCATAA
AACTTACCATAAAAAGGCATACTTTCAAGCAATGATGAATTTGATAGCATTGTTTTAGCCCTTTAAGCGT
GGTGCAAAAATTTAAGCGATAGAGCCGGTATTAACATGCTAATGCTGTAGTTTATGGAAATTTTGATGAA
GTTAAAGCCAAAACACAAGCAATCAGCAATGAATTCATCGATGCAAAACCTATATCTTCAGTATCCTTAA
GTGAAGTTTTAGTGCTTGAAAAATCAAAGCTTTAATGTTTTAATCATACTTGTGGTATTGATCATAGT
TACTACTAGCGTTAATACAACCTTTAAGTTCTATTATTTTTCTCGCAAAAAGAAATCGCACTGCGTTTA
GCCTTGGGTGCGAAAAAAGTGAAATTTTTAACTTTTTGCTAGTGAATGCTTTATAGTAAGTTTTTTTTG
CTAGTTTAATCGGAGCTTTTTGTGGGATATTTTTAGCCAATGCTTTGGTTATTTAATTTTTAATTCTAG
TATTGATTTTAGATTTATAGCTGTTTTTATAGCCTTAATCATTTCTTTGATTTTTGCCTTTTTGGCTGCA
TTTTTCTCTATAAAAAGAGCATTAAAAATCAATGTGTGTGAAAAATTTGAAAGGTGAATGAAAAAAGA
ACTTATTTAAAATAAACAATTTAAATAAAGAATTTGGCAAAGTTAAAGCCTTAAACAATATCAACTAAGC
GTCTATGAAGGAGAATGGCTTGCCATCATGGGTCCATCAGGAAGTGAAAAATCAACACTTTTAAACATAC
TATCGCTCATGGATACTCCAAGCTCTGGAGAGTATATCTTGATAATGAAAACCTAGAGCAAATGGATGA
AGAGCAAAAATCACCTTGCGTCGTGAAAAAATAGGGCTTGCTTTCAACAATTTTCATCTTATCCCTAT
CTTAACGCCTTAGAAAATGTTATGCTCTCTCAGTATTATCACTCAAGTGTAGATGAAGAAGATGCCAAAA
TGTTTCTTGAAAAAGTAGGACTTTTCGCATAGACTCACTCATTTACCTAGCCAATTAAGTGGCGGAGAACA
ACAAAGAGTTTGATAGCAAGAGCTTTAATCAACAACCCAGAGCTTTTACTCGCAGATGAACCCACAGGA
AATTTAGATGAAGCCAATGAACAAATCGTTCTTCAAACCTTGCAAAAATTA AAAAATGAAGGTAAAACCA
TAGTTTTAATCACACACAATCCTGATTTAGCCAAATTCGCAGATCGAACCTTATCTTACAACATGGGGT
GTTAAAATGAAAAAAGCCTTTTTAATCTTAAGCATTTTGTTTTTACTCAATGCTTGTCTTTTTGAAAATT
CAAAAGATACTGAAAAAGTTGGAGAAAAAAGCGCTGAAATTTAGCTAAAAGATACTTTAGGAAAAGCTGT
AAAACCTTGCTGATGATAATAACAAGTTAAAAGTCTTAGTCTTTTTTCAAATGGCTGCCCTTCTTGCTTA
AAAGAACTCCCTTCTTTAGATGAATTCATACAAAATCACCCCAATAAAAATCAGTGTATTATGCTATAAATT

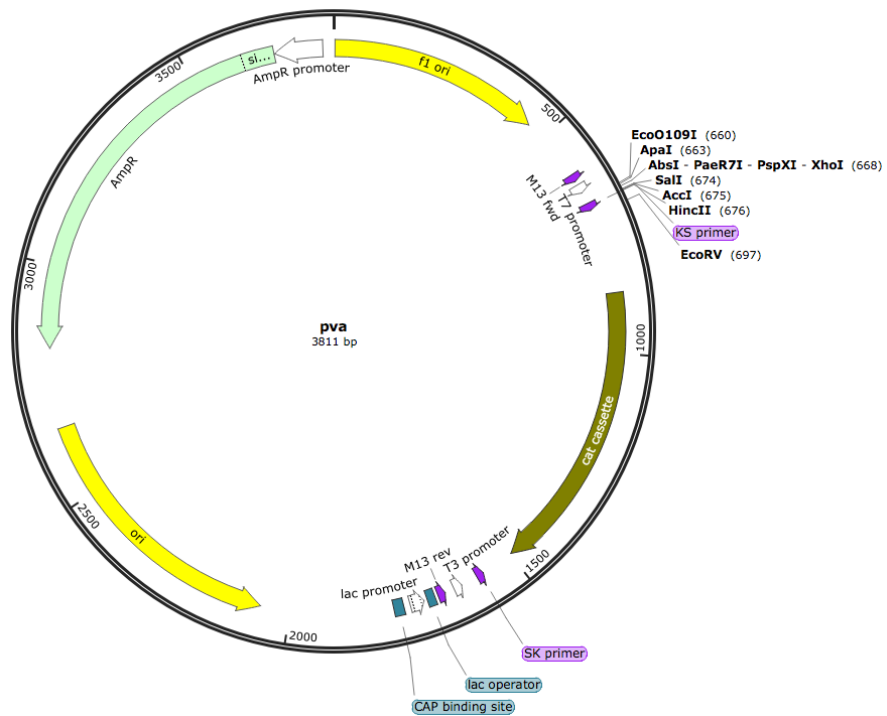
Appendix

CCATCGATAATGCCAATGTGGTTAAGGTTTTAGCCGAACAATTTGACTTTAAAAATGTAAAAGTTTTAAA
AGACGATCTTAAATCACCAATGATCGTTACGCTGTGTTTGCAACCCCTACTACCATCATCATTAAGAT
GGGATGATAAAAGATAGAATTTTAGGAGAAAAACCATGGGAATTTTTTCGAATCCAAGCTTATTTCTTTGC
TTTAATCATAGCTTTATTTTTTGTAGCTTGTGATAGTGGAGAAAAATTTTAAAGCTTTAAATAGCGATAAA
ACCTATAATTTTGCCTACAATGGTTTTGAAAAAGCCTAAAACTAAATGATAAAGCACAAAATTTTGCCT
TAGTATTTTTTACAAAAGATTGCGGAGTTTGCAAAGAACAATTCCTATTTTACAGAATTTGGCTAAAAA
TTATGATTTTAATATCTTTGTGGTTTTAGGCGATGCAAACGATGCAAACGATGCAAAGCTTGGGCTGAT
GAAAAAGGTTTATCTAATTTAGCAATGTTTTATGAAAAAGAGCAGCTAAATACCTTTCAAGTGCCATTG
GGGAAATATATGGAGTACCTGTGCTTAGTTTTTTTCAAAGAAGGAAAAATGGATGAAAAATTCATAGGCTT
AACTCCTTATAGCATACTTGAAAAAGAAATCAAAAAAGTAAAAAGCTAA

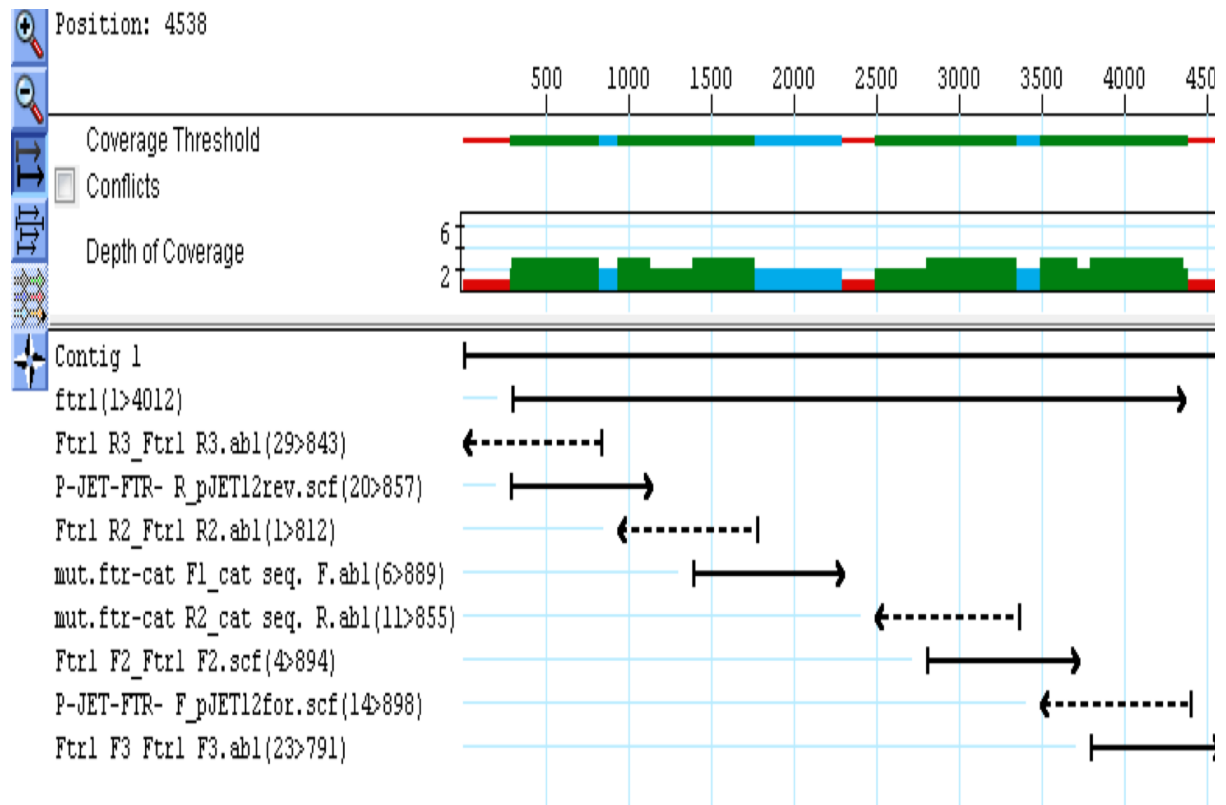
11. Nucleotide sequence of the *fetMP-fetABCDEF* locus of *C. jejuni* NCTC 11168. The locus (from the first start codon to the final stop codon) is 8099 bp. The 82 bp as *fetP-fetA* intergenic region is indicated. Each start codon is indicated by dark green colour, stop codon is indicated by red colour, and regions where orfs overlap are in red font.



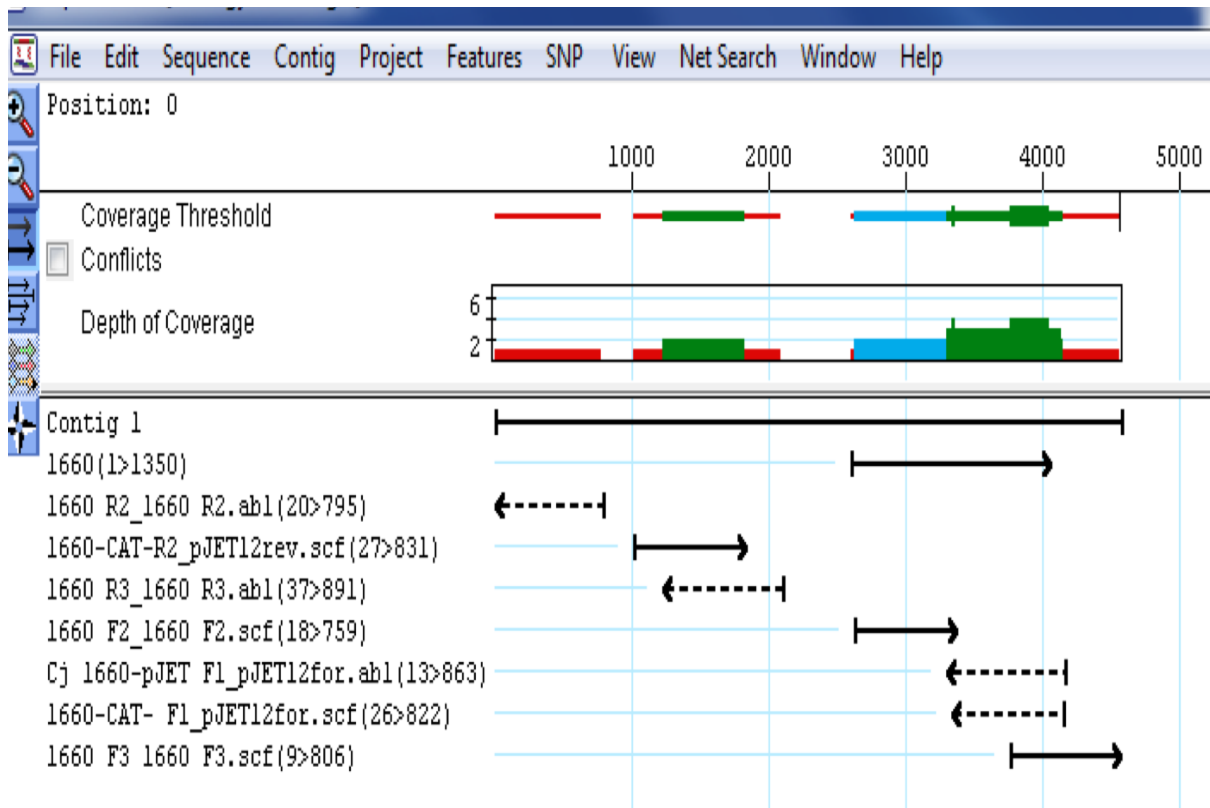
12. Map of pJET1.2 plasmid. Ampicillin resistant with p17 lethal gene. Nucleotide sequence from Genebank.



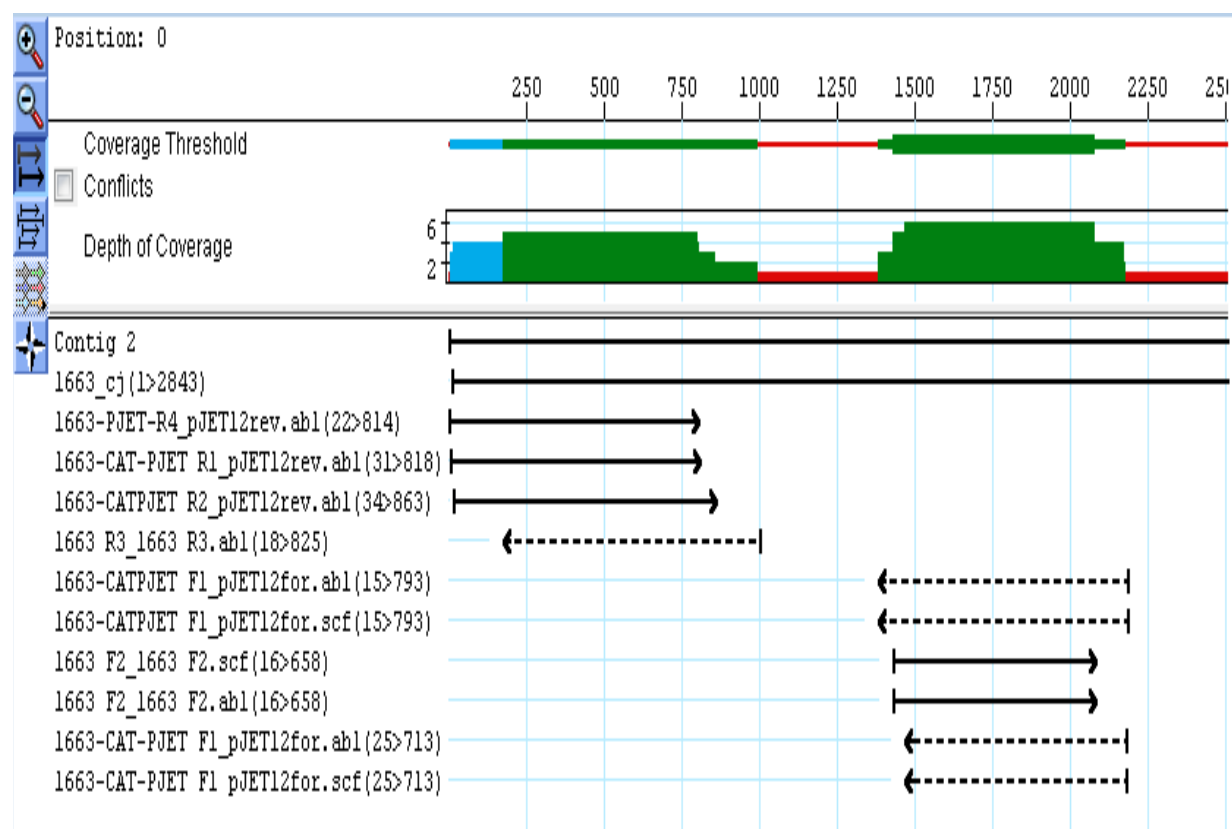
13. pVA35 plasmid map. Light green indicates the ampicillin resistance gene. Yellow arrow indicates origin of replication. Dark yellow is the *cat* cassette gene provides chloramphenicol resistance.



14. Overview of Sanger sequencing assembly of $\Delta ftr1::cat$ cloned into pJET. The SeqMan Pro option of the DNASTar software package was used to assemble eight sets of sequence data derived from the same template (p-JET-*ftr1*) using eight primers (F1-4, R1-4; Table 2.4.) designed to provide complete and overlapping sequence data on both strands. All conflicts were resolved by scrutiny of the corresponding chromatograms. The ‘ftr1 sequence’ represents the original *C. jejuni* sequence (the reference sequence).



15. Overview of Sanger sequencing assembly of $\Delta cj1660::cat$ cloned into pJET. The SeqMan Pro option of the DNASTAR software package was used to assemble eight sets of sequence data derived from the same template (p-JET-*cj1660*) using eight primers (F1-4, R1-4; Table 2.4.) designed to provide complete and overlapping sequence data on both strands. All conflicts were resolved by scrutiny of the corresponding chromatograms. The ‘*cj1660* sequence’ represents the original *C. jejuni* sequence (the reference sequence).



16. Overview of Sanger sequencing assembly of $\Delta cj1663::cat$ cloned into pJET. The SeqMan Pro option of the DNASTAR software package was used to assemble eight sets of sequence data derived from the same template (p-JET-*cj1663*) using eight primers (F1-4, R1-4; Table 2.4.) designed to provide complete and overlapping sequence data on both strands. All conflicts were resolved by scrutiny of the corresponding chromatograms. The ‘*cj1663* sequence’ represents the original *C. jejuni* sequence (the reference sequence).

Appendix

CACCTTCCATACCTTCGATGAGTTCATTCATCAATGCCTCGTTTGTGTCCATAGATTTTTTCAAACCTGA
AGTATTAACAGCAGTCATTAATAACATTACCCATAGAAACATCTGAAACCATACATCCTCCTTTTTAGA
TTGAGTCTTAAGACTTTATTTAAATCGGATGATATTTTTTAAACCTAATATTTTTTACTAACTTTTTTAA
AATTTTTCAAGGGAACCAATATCTGAAATTAATAATCATAAATTTTTTAAAGATAAAATCCTATTTTTAAA
ATTTTTTACACTATGAAACAATAAGCAAAATATAAATGATTGATGCTTTTTAAAAGCGAATTAATGGATAA
AAATTTATTTCAATAAAATTTAAGTTTTATCTTGTTTTTATACAATTTTTAATAATAATCTAAAAATTATAAT
TTAAATGAGAAATCAGGAGCTTGCTAATGTTACTTAAACACGCCTTGCAGGGGGATAATAGATACAAATTT
TGAAAGCAAAAGAATTAGCATAACTTCAACTTTAAAAATTTCAAGAAAAAAGAAAAAGTAGAAGCTAAGG
CTGAGAAAGAAGAAGCAAAATAAAGACAATAGCAATTTCTACAAACACAAAATACCAATAAAAAAGATAAACT
TTTTGGATATATCTGCTTAGTCTAAAATATACTATAGCTATATCTCCTTAAAGAAATACGCAATAAATGATT
TTTTGATTTTTTATTAAGCTTTTTAAAACATCGAAAAAAGAAAAATTAAAAAACAAAAAATAATCCCA
AAGTCCATAGCTTAGAAGAAGACCTTGCATACTTAAAAACAACCCATATTAATCACAATAAAAAATAAATA
TATTTAAATATTTATTAATAATACATTTTTATAATTTAATAAAAAAATATTAACAACATAAAAGCTTATTTTT
TTAGTTCTATTTAAGATTTTTTAGTATTATACTAGCCATTATTTATTTTTGATAATAAATATTTATTTTTATC
AAAAATCAAGGATAATGATAATGAAAAATTTTTAAAAATATATTTTTAATTATAAGTATTTTTTTATCAAG
CTCAGCTTTTTGCTAGGGTAGATGATTATATTAATGAAGCAAACTTATCAAAAGATATGCTAAAACAAAGC
ATAGAACTTATAAAAAAGGGCGATAATCTAGGCGCCAAAAAGCTTAGCGAAGATGCGTATTTTTCAACATT
TTGAAAATATGGAAGGCTCAATAGGAAGAAACATAGGAAGAAAAGCTATCACTATGGAGCGTAAATTTGT
AAATTTGCGTCGCATGTATAAAGATGAAGCTCCTTTGACACAAATTAATGCTTTAATTGATAGTCTTTAT
TATGATCTTGATGAAGTAGCTCCGATTTTTACAAAATGGATATCGTTTAAAAGCAGAAGCAAGCGATATAA
ACTATGATAAAGGCTAAAGCTGAAAAATCAAGCCTAGAAGCCAATGCCAAACGCGAAGCTGATGCAGAAGC
TTTTAATCGCACAAATGATGGGTGTAGATAAAAAAGATTTAGCACAAAGCTCTTTAACCACCCAAGCTCCT
ATACCTATAAATAATGATACAAGCAAACTTACAGATGATAATGCAAGCACTGATTTACAAGCTGCCGCTG
CAATGGACGTAAGATTGCAATTTATACTAGATAATATCTCTACCAAAATTTTCACAGGCAGCTAATGCTTT
TAAAGAAAAAACTACCAACTAGTAAAGATTTTTTAAATGATGCCCTATTTTAGTGATTATCGCAATACC
AAAGTAGAAATTTTAGTAAATAAATTTACCAAAGCAGGAAACGATCAAAAAATTCACAAGCCATACGCA
CCCTTATACGCCAAATCAACGATGCAAAAAATAGATGAAAAAGGCTTAAAGATGGCTTAGATAACATAGA
AGAACAAATTTTTGATGTTTTCTTACAAATTTCCAAATTCAGAACTTTCAAGTTTGCAAATTTCCAGCTTT
AATGATGAAACAAAAGGCAAAGATTATGCCAAAGTTTCTAATGATATCAAACCTTGCCTTAGATGAAATTT
TAAAAAATATGATGGGTTTTAGTGCTTCTATAGTAGATGATTTTACAAGGAATTTATCTAGATATTTTTGA
AGCAAGCGGTATGGAATAAATAAATCGGTGCTGTAGATAGCGGCTTAAAACTTAAAAATAGAAAGTTTTATTT
TCCAAAAGCGTAGCTCTTATCAAAGCAAGTACAGATAAAAAAGAGCTTGAAGCTACTTTTTAATGACTTAG
AACAACCTCATAGCCAGCAGCGTGGATAAAAAATCAAGATTTCTACTCCTTATTCGCTGTTTTATATGGGCTTT
AGGTATTATTTTTGCGTGAAGGCTTGGAAAGCTTTGATTATCGTTGTAGCCATTGTTTCTTATCTTGTGCAA
AGTGGAACAAAAATCGTTTTAAATATCGCTATAGTGCTCTTTTTACAGGAGTAATTTTAAAGTTTTGTTA
CCGCTTTTTGGAGTTTTCTTGGCTATTTAAAGAAAAATGCAGGACAAAGTAGAGAGCTTATAGAGGGTATTAC
CATGCTTATAGCCGTATTACTACTCTTTTTATGTGGGCTTTTTGGCTACTTTCAAACGCACAAAAATAAAAA
TGGACAAGCTTTATCAAACAAGGTGCTATAGATGCTATATCAAACAATAGTGCAAAAACCCTTTTGGATTA
CCGTATTTTTTAGCTGTTTTATAGAGAAGGTGCAGAACTGTGCTTTTTTTATCAAGCCTTGCTTTTTTGATGC
TAAAAACAAGCACTGATTTTTGGTGCTGTTTTTGGCGGACTTGGACTTGGAAATTTAATACTTATTGTTTTTA
TATTTTTCTTTTTAAAAGCAGGAGCCATTCGCATACCTGTAAAACAATTTTTCTATATCACTTCTTACATTA
TTTTTTACATGGTTTTTTGTTTTTACAGGCAAAAGGCATAGCCGAACTCATAGAAGGAAAAGTCATCATTCC
TAGTCTTATACCTATGAATTTTTGAACCGATTTTATGGCTTGGAAATTTATCCTTACTATGAACTTTAATC
CCTCAATTTATAGTTTTAATTATGCTAATTAATGGCATTTTAATAACAAAACAAATTTCAAAAAAAGGAG
TAAAATCATGATAAAAAAAGTTTTTATCAGTAGTTGCTGCAGCTGCGGTTATTAGTACAAATTTTATTTGCA
GGCGAAGTGCCGATCGGCGATCCAAAAGAATTAATGGCATGGAATAGCCGCTGTTTTATTTACAACCTTA
TTGAAATGGAGCCAAGAGGTATTGATTTAGCTGCATCTTTAGCAGATATTCACCTAGAAGCTGACATTTCA
CGCACTTAAAAACAATCCAAATGGTTTTTCCAGAAGGTTTTTGGATGCCCTATTTAACTATAGCTTATGAA
CTTAAAAATACCGACACAGGTGCAATTAAACGTGGAACCTTTGATGCCCTATGGTGGCTGATGATGGTCCCTC
ACTATGGTGCAAAATATTGCTATGGAATAAATAAAGGTTGGCTTTGGCGTAGGAAATTTGAACTTAC
TTTTTATATCTCAAATCCAGAAAAACAAGGTTTTTGGACGCCATGTTGATGAAGAAACAGGTGTGGGTAAG
TGGTTTTGAACCTTTTTAAGTAGATTATAAATTTCAAATACACAGGCACGCCAAAATAATTTTACGCTCGGA
TTTTCCGAGTGTTTTGAATATTTTTATTTTTATTTGAAAAATTAATAACAATGTTTAAAGAGTAAATTA
TGAGTATATATTTTTGTGCATTTTTCTTATCAGTGTTTTACCCTAAGTATTTTAAATGGCCTTTTACTCCTC
TAATAAAAAATATATTTTTTAAAGTTTTTTCGTAGTTTTTTTTGGGCTTTTTATTTGGATATTTTTGCTTTT
TTTTATCGCAGCACAATTTTTTAAAAACCGAAAAATTTAATCTTTAATTTTTGATTTTTGTTTTTATAGGTTTTAT
TGCTAGTAAGCTTTATATTTTTATTTTTGGAAAAAATTTGAAATTTTTAAATTTTTATTTTATTTGGGAATTTT
AAGTTTTTGCACCGCTTTGCATTATTTATTTTTTAAAGTCAAGATTTCCCTATTTTTTACTAGCTCTTTAATC
GATAGCGAAGGTATAAGTTCTTTAGG

17. Nucleotide sequence of the *ptr1* gene of *C. jejuni* NCTC 11168 with 1 kb upstream and downstream regions used in the knockout strategy. The turquoise highlight indicates the primers that used to amplify the region, the red highlight indicates the start and stop codon, the bright green highlight indicates the deleted region from the middle of *ptr1* gene, the dark blue highlight indicates the inverse primers that used to delete the 1kb of the gene.

CACCTTCCATACCTTCGATGAGTTCATTCATCAATGCCTCGTTTGTGTCCATAGATTTTTTCAAACCTGA
 AGTATTAACAGCAGTCATTAAATTAACATTACCCATAGAAACATCTGAAACCATACATCCTCCTTTTAGA
 TTGAGTCTTAAGACTTTATTTAAATCGGATGATATTTTTTAAACTTAATATTTTTTACTAACTTTTTTAA
 AATTTTTCAAGGGAACCAATATCTGAAATTAATAATCATATAATTTTTTAAAGATAAAATCCTATTTTTAAA
 ATTTTTACTATGAAACAATAAGCAAAATATAAATGATTGATGCTTTTTAAAGCGAATTAATGGATAA
 AAATTTATTTCAATAAATTTAAGTTTTATCTTGTTTTATACAATTTTTAATATAATCTAAAATTTAATTT
 TTAATGAGAAATCAGGAGCTTGCTAATGTACTTAACACGCCTTGCAGGGGGATAATAGATACAAATTT
 TGAAAGCAAAGAATTAGCATAACTTCAACTTTAAAATTTCAAGAAAAAAGAAAAAGTAGAAGCTAAGG
 CTGAGAAAAGAAGCAAATAAAGACAATAGCAATCTACAAACACAAATACCAATAAAAAAGATAAACT
 TTTGGATATATCTGCTTAGTCTAAAATATACTATAGCTATATCTCCTTAAAGAATACGCAATAAATGATT
 TTTTGATTTTTATTAAGCTTTTTAAAACATCGAAAAAAGGAAAAATTAAAAAACACAAAAACAATATCCCA
 AAGTCCATAGCTTAGAAGAAGACCTTGCAGATACTTAAAAACAACCCATATTAATCACAAAAATAAATA
 TATTTAAATATTTATTAATAATACATTTTTATAATTTAATAAAAAAATATTTATCAACATAAAAGCTTATTTT
 TTAGTTCTATTTAAGATTTTTAGTATTATACTAGCCATTATTTATTTTGATAATAAATATTTATTTTTATC
 AAAAATCAAGGATAATGATAATGAAAATTTTTAAAATTTATTTTTAATTATAAGTATTTTTTTTATCAAG
 CTCAGCTTTTGTAGGGTAGATGATTATATTAATGAAGCAAATCTTATCAAAGATATGCTAAAACAAAGC
 ATAGAACTTATAAAAAGGGCGATAATCTAGGCGCAAAAAGCTTAGCGAAGATGCGTATTTTCAACATT
 TTGAAAATATGGAAGGCTCAATAGGAAGAAACATAGGAAGAAAAGCTATCACTATGGAGCGTAAATTTGT
 AAATTTGCGTCGCATGTATAAAGATGAAGCTCCTTTGACACAAATTAATGCTTTAATTGATAGTCTTTAT
 TATGATCTTGATGAAGTAGCTCCGATTTTTACAAAATGGATATCGTTTAAAAGCAGAAGCAAGCGATATAA
 ACTATGATAAGGCTAAAGCTGAAAAATCAAGCCTAGAAAGCCAATGCCAAACGCGAAGCTGATGCAGAAGC
 TTTAATCGCACAAATGATGGGTGTAGATAAAAAAGATTTAGCACAAAGCTCTTTAACCACCCAAGCTGCG
 ATCGCCGAATTCCTGCAGCCCGGGGATCCCGGTACCTGCAGAATTCAGCTGCCTCGGCGGTGTTCTTTT
 CCAAGTTAATTGCGTGATATAGATTGAAAAGTGGATAGATTTATGATATAGTGGATAGATTTATGATATAA
 TGAGTTATCAACAAATCGGAATTTACGGAGGATAAATGATGCAATTCACAAAGATTGATATAAATAAATGG
 ACAGAAAAGAGATTTTCGACCCTATTTTGGCAATACGCCCTGCACATATAGTATGACGTTAAAACATCA
 TATTTCTAAGTTGAAAAGGATGGAATAAAGTTATACCCAACTCTTTTATATGGAGTTTACAACGATCATCA
 ATCGACATGAAGAGTTTACGACCATTTAGATGAAAACGGACAGGTAGGCGTTTTTTTCAGAAATGCTGCCT
 TGCTACACAGTTTTTTCATAAGGAAACTGAAACCTTTTTCGAGTATTTGGACTGAGTTTACAGCAGACTATAC
 TGAGTTTCTTCAGAATATCAAAAAGGATATAGACGCTTTTGGTGAACGAAATGGGAATGTCCGCAAAGCCTA
 ATCCTCCGAAAACACTTTCCCTGTTTCTATGATAACGTTGGACAAGCTTTGAAGGCTTTAACTTAAATCTA
 AAAAAAGGATATGACTATCTACTGCCGATATTTACGTTTGGGAAGTATTTATGAGGAGGGCGAAAATACTA
 TATTCCTTATCGATTCAAGTGCATCATGCCGTTTGTGACGGCTTTCATGTTTGCCGTTTTTTGGATGAAT
 TACAAGACTTGCTGAATAAATAAATCCAGTTTGTGCGACTGATAAAAACCTTTAGGAACATAAGGGCG
 CAGCTGAATTCGAGGTACCCGGGATCCACTAGTTCTAGAGCGCCGCGCGATCGCGCTTATAGCCGT
 ATTACTACTCTTTTATGTGGGCTTTTGGCTACTTTCAAACGCACAAAATAAAAAATGGACAAGCTTTATCA
 AACAAGGTGCTATAGATGCTATATCAACAATAGTGCAAAAACCTTTGGATTACCGTATTTTTTAGCTGTT
 TATAGAGAAGGTGCAGAAACTGTGCTTTTTTATCAAGCCTTGCTTTTTTGATGCTAAAACAAGCACTGATTT
 TGGTGTGTTTTTGGCGGACTTGGACTTGGAAATTTAATACTTATTGTTTTTATATTTTTCTTTTAAAAGCAG
 GAGCCATTCGCATACCTGTAAAACAATTTTTCTATATCACTTCTTACATTTATTTTTTACATGGTTTTTGT
 TTTACAGGCAAAGGCATAGCCGAATCATAGAAGGAAAAGTCATCATTCCTAGTCTTATACCTATGAATTT
 TGAACCGATTTTATGGCTTGAATTTATCCTTACTATGAACTTTAATCCCTCAATTTATAGTTTTAATTA
 TGCTAATTATTGGCATTTAATAACAAAAACAATTTCAAAAAAGGAGTAAAATCATGATAAAAAAGTTTT
 TATCAGTAGTTGCTGCAGTTCGCGTTATTAGTACAAATTTATTTGCAGGCGAAGTGCAGTACGGCGATCCCA
 AAAGAACTTAATGGCATGGAATAAGCCGCTGTTTATTACAACTTATGAAATGGAGCCAAGAGGTATTGA
 TTTAGCTGCATCTTTAGCAGATATTCACCTAGAAGCTGACATTCACGCACTTAAAAACAATCCAAATGGTT
 TTCCAGAAGGTTTTTGGATGCCTTATTTAACTATAGCTTATGAACTTAAAAATACCGACACAGGTGCAATTT
 AAACGTGGAACCTTTGATGCCTATGGTGGCTGATGATGGTCCCTCACTATGGTGCAAAATATGCTATGGAAA
 AGATAAAAAAGGTGGCTTTGGCGTAGGAAATATGAACTTACTTTTTATATCTCAAATCCAGAAAAACAAG
 GTTTTGGACGCCATGTTGATGAAGAAACAGGTGTGGGTAAGTGGTTTGAACCTTTTAAAGTAGATTATAAA

TTCAAATACACAGGCACGCCAAAATAATTTTACGCTCGGATTTTCCGAGTGTTTGAATATTTTTATTTTTA
 TTTGAAAAATTAAAATAACAATGTTTAAAGAGTAAATTATGAGTATATATTTTGTGCATTTTCTTATCAGT
 GTTTTACCGCTAAGTATTTTAAATGGCCTTTATCACTCCTAATAAAAAATATATTTTAAAAGTTTTTTCGT
 AGTTTTTTTGGGCTTTTTATTTGGATATTTTGTCTTTTTTATCGCAGCACAAATTTTAAAACCGAAAATT
 TAATCTTTAATTTTGATTTTGTTTTTATAGGTTTATTGCTAGTAAGCTTTATATTTTATTTTTGGAAAAA
 ATTGAAATTTTAAATTTTATTTTATTGGGAATTTTAAAGTTTTTGCACCGCTTTGCATTATTTTAAAG
 TCAAGATTTCCCTATTTTTACTAGCTCTTTAATCGATAGCGAAGGTATAAGTTCTTTAGG

18. Nucleotide sequence of the *Δftr1* gene of *C. jejuni* NCTC 11168 with *cat* cassette gene from pVA35 plasmid. The turquoise highlight indicates the restriction sites of *AsiSI* enzyme used to cut the plasmid and insert the *cat* cassette, the red highlight indicates the start and stop codon, the bright green highlight indicates *cat* cassette gene that inserted in the deletion site of *ftr1* gene. The whole region is about 4 kb.

TCAAGCCTTGCTTTTTGATGCTAAAAACAAGCACTGATTTTGGTGCTGTTTTTGGCGGACTTGGACTTGGAA
 ATTTTAATACTTATTGTTTTATATTTCTTTTAAAAGCAGGAGCCATTCGCATACCTGTAAAACAATTTT
 TCTATATCACTTCTTACATTATTTTTTACATGGTTTTTGTTTTTACAGGCAAAGGCATAGCCGAACATCAT
 AGAAGGAAAAGTCATCATTCTTAGTCTTATACCTATGAATTTTGAACCGATTTTATGGCTTTGGAATTTAT
 CCTTACTATGAAACTTTAATCCCTCAATTTATAGTTTTAATTATGCTAATTATTGGCATTTTAATAACAA
 AACAAATTTCAAAAAAAGGAGTAAAATCATGATAAAAAAGTTTTTATCAGTAGTTGCTGCAGCTGCGGTT
 ATTAGTACAAATTTATTTGCAGGCGAAGTGCCGATCGGCGATCCAAAAGAACCTAATGGCATGGAAATAG
 CCGCTGTTTTATTTACAACCTATTGAAATGGAGCCAAGAGGTATTGATTTAGCTGCATCTTTAGCAGATAT
 TCACCTAGAAGCTGACATTCACGCACTTAAAAACAATCCAAATGGTTTTCCAGAAGGTTTTTGGATGCCT
 TATTTAACTATAGCTTATGAACTTAAAAATACCGACACAGGTGCAATTAACGTGGAACTTTGATGCCTA
 TGGTGGCTGATGATGGTCTCCTACTATGGTGCAATATTGCTATGAAAAAGATAAAAAAGGTGGCTTTGG
 CGTAGGAAATTATGAACTTACTTTTTATATCTCAAATCCAGAAAAACAAGTTTTTGGACGCCATGTTGAT
 GAAGAAACAGGTGTGGGTAAGTGGTTTTGAACCTTTTAAAGTAGATTATAAATTCAAATACACAGGCACGC
 CAAAATAATTTTACGCTCGGATTTTCCGAGTGTTTGAATATTTTTTATTTTTATTTGAAAAATTTAAAATAA
 CAATGTTTTAAAGAGTAAATTTATGAGTATATATTTTGTGCATTTTCTTATCAGTGTTTTTACCGCTAAGTAT
 TTTAATGGCCTTTATCACTCCTAATAAAAAATATATTTTTTAAAAGTTTTTTCGTAGTTTTTTTTGGGCTTT
 TTATTTGGATATTTTGCTTTTTTATCGCAGCACAAATTTTAAAACCGAAAATTTAATCTTTAATTTTG
 ATTTTGTTTTTATAGGTTTATTGCTAGTAAGCTTTATATTTTTATTTTTGGAAAAAATTGAAATTTTAA
 TTTTATTTTATTGGGAATTTTAAAGTTTTTGCACCGCTTTGCATTATTTATTTTTAAGTCAAGATTTCCCT
 ATTTTACTAGCTCTTTAATCGATAGCGAAGGTATAAGTCTTTAGGTTTTTATTGCTTTAGCCTTAGCTTG
 TTTGTATTTGATTTTCTTTTTTAAAATGGCAAAAAATTTTAAATCAAAAAACAAGCTTTTATGCTGTT
 TTTACTGTTTATCTTTATAGAAAGCGATAAAGCTCTAGCCAATATCTTGCTTACTTTTAAATGCGAAATTC
 ATCATAGAAACTCATGCTTTTTTGGTGAGTTTTGTAGGAAAAAGTAATTTATTTTGGTGTTTTTGGAAATTT
 ATGTTTTATTTAATTTTCATCACTTTTTTAGCATTTCTTAAAGCTTAAAAATTCGCAAAAAAATATAAGCAA
 AAAACAATTTTAGATATAAATTTATCGCAAAAAACGAAGCTAAAAACAAGTCTTATTAATCGCTATTTTTCC
 AGTGTTTTTATCTCCTGTGTTGTAAGTTTTTGCATTTGTTTTATACTTTTTTATGGTAAGCTCTAAGCCTT
 TAACCATAGATGAGCCTAAAGAAATTTTACCCGATAAGAATGGCAATTTATCTTTGATATAGCTCTTTT
 AAGGGACAACAACTCCACCGCTTTGCTTATATCAGTGCTGAAGGCAAAGTGATAAGGTTTTTTCTTATC
 AACAAAAGAGAAGATAAGGATTCTCCTGTAGCTGTTTTTGTATGCTTGTATGATTTGTGGAGATATGGGCT
 ATATCAAAAAAGATGGACAACCTCATTTCGATTTCTTGAATGTGCGTATTTTCTTGCCAAGTGTAGGTAA
 AAGCGGGGGTTGCAATCTATCCCCTCAAAATACGAATACGATGGTAACAAAATCACCATAGATGTTAAA
 GATGTAATAGCAGGATCTAATTTATTTAGTCAAAATCAAAAGAAATGAAGTGCAAGATCCTGTATCAAAAA
 CAAAGGTTATAAACACCCAAGCTCCTTTTTCTTATAGCTATAAAAGGGTTACTTATTTATTTTTCAAATCA
 AAACAATATGAAGAATTTAAAAAAGATCTTACAAAATATGTAGAAAGAAAACGAAGCCCAATTTTTAATC
 CAAAGGAGAAATGATGTTGGCTAAAATGATTTTTAACTCTATATTTAAAAACAAAATTTCAAAAATTTTTA
 GCCTTTCTTACTTGTTTTTTAGCCACGCTTTTGTCTCTACTATGCTAAAATATTACCCTAAGTATAGGTG
 ATGAAGTAACTAAACAACCTAAAAGCTATGGCTCTAATATCTTTGTTTTACCCAAAGGCTCAAGCCTTAG
 TATAGAAATAGGTAATGAACCTTTATGAACCTTAAAAAACAACCTACCTAGAAAGAAAAAATTTATAT
 ATGATTAAGACATTTATTGGCGTAACAACATCACCGCACTTGCTCCTTTTTTGGAAAGGTAAAATCACAA
 TTGAAAACCTCCAGCAAAAAAGCACTTATTTATGGTGCTTATTTTTCAAAAAGCCATAAAAAATTAAGATGA
 TGATGATTTTATCACAGGTATAAAAAAGTCTTTATCTTATTTAGCAGTGCAAGGAGAATGGGCAAAAGAT

Appendix

GATAGCAATGAAATCATGCTAGGCGAAGACTTTGCTAAAAACAATAAACTAAAATTAGGAGATACTATCA
AATTCATAGGAGAAAACAATCAAAGCAAAGAAGCAAAAATCGTAGGCATTTTACTTCATGCCAATCCTAA
AATGTCAAATAAAATCATCGCTCCTTTAAATTTAGCTCAAGATTTACTCAACAAACAAGGGCTTTACTCA
AGTACAGAAGTAAGAGCTTTTACCATACCTGAATCAGCCCTTTCTGAAAAAGTACGTGCGATGGGCGAAG
AAAAATTAGATCAGTTAGAATATGACAAATGGTATTGCTCAGCTTATGTAGGCTCAATCGCTAGTCAAAT
TAGCGATGGCTTGCCAGGTGCTGATGCAAAAAGCTCTAAATGCTATAAGCGATGCTCAAAGCTTGGTGGTT
AAAAAGATCCAATCCTTAATGGGCATTACTTGCAATATTTGTCTTATTTGTTGCAAGTATTGCGATTTCAA

19. Nucleotide sequence of the *cj1660* gene of *C. jejuni* NCTC 11168 with 1 kb upstream and downstream regions used in the knockout strategy. The turquoise highlight indicates the primers that used to amplify the region, the red highlight indicates the start and stop codon, the bright green highlight indicates the deleted region from the middle of *cj1660* gene, the dark blue highlight indicates the inverse primers that used to delete the 1 kb of the gene.

TCAAGCCTTGCTTTTTGATGCTAAAAACAAGCACTGATTTTGGTGCTGTTTTTGGCGGACTTGGACTTGGAA
ATTTTAATACTTATTGTTTTATATTTCTTTTAAAAGCAGGAGCCATTCGCATACCTGTA AAAACAATTTT
TCTATATCACTTCTTACATTATTTTTTACATGGTTTTTGTTTTTACAGGCAAAGGCATAGCCGAATCAT
AGAAGGAAAAGTCATCATTCTAGTCTTATACCTATGAATTTTGAACCGATTTTATGGCTTGGAAATTTAT
CCTTACTATGAAACTTTAATCCCTCAATTTATAGTTTTAATTTATGCTAATTATTGGCATTTTAATAACAA
AACAAATTTCAAAAAAAGGAGTAAAATCATGATAAAAAAAGTTTTATCAGTAGTTGCTGCGAGCTGCGGTT
ATTAGTACAAATTTATTTGCGAGGCAAGTGCCGATCGGCGATCCAAAAGAACTTAATGGCATGGAAATAG
CCGCTGTTTTATTTACAACCTATTGAAATGGAGCCAAAGAGGTATTGATTTAGCTGCATCTTTAGCAGATAT
TCACCTAGAAGCTGACATTCACGCACTTAAAAACAATCCAAATGGTTTTCCAGAAGGTTTTTGGATGCCT
TATTTAACTATAGCTTATGAACTTAAAAATACCGACACAGGTGCAATTAACCGTGGAACTTTGATGCCTA
TGGTGGCTGATGATGGTCCCTCACTATGGTGCAATATTTGCTATGGAAAAAGATAAAAAAGGTGGCTTTGG
CGTAGGAAATTTGAACTTACTTTTTATATCTCAAATCCAGAAAAACAAGTTTTTGGACGCCATGTTGAT
GAAGAAACAGGTGTGGGTAAGTGGTTTTGAACCTTTTAAAGTAGATTATAAATTCAAATACACAGGCACGC
CAAAATAATTTTACGCTCGGATTTTCCGAGTGTTTGAATATTTTTATTTTTATTTTAAAAATTAATAA
CAATGTTTTAAAGAGTAAATTATGAGTATATATTTTGTGCATTTTCTTATCAGTGTTTTACCGCTAAGTAT
TTTAATGGCCTTTATCACTCCTGCGATCGCAATTCGAAATTCCTGCAGCCCGGGGGATCCCGGGTACCTGCA
GAATTCAGCTGCTCGGCGGTGTTCCCTTTCCAAGTTAATTGCGTGATATAGATTGAAAAGTGGATAGATTT
ATGATATAGTGGATAGATTTATGATATAATGAGTTATCAACAAAATCGGAATTTACGGAGGATAAATGATG
CAATTCACAAAGATTGATATAAATAATTGGACACGAAAAGAGTATTTGACCACTATTTTGGCAATACGC
CCTGCACATATAGTATGACGGTAAAACCTCGATATTTCTAAGTTGAAAAAGGATGGAAAAAAGTTATACCC
AACTCTTTTATATGGAGTTACAACGATCATCAATCGACATGAAGAGTTCAGGACCGCATTAGATGAAAAC
GGACAGGTAGGCGTTTTTTTTCAGAAATGCTGCCTTGTCTACACAGTTTTTTCATAAGGAACTGAAACTTTT
CGAGTATTTGGACTGAGTTTACAGCAGACTATACTGAGTTTCTTCAGAACTATCAAAGGATATAGACGC
TTTTGGTGAACGAATGGGAATGTCCGCAAAGCCTAATCCTCCGAAAAACACTTTCCCTGTTTCTATGATA
CCGTGGACAAGCTTTGAAGGCTTTAACTTAAATCTAAAAAAGGATATGACTATCTACTGCCGATATTTA
CGTTTTGGGAAGTATTATGAGGAGGGCGGAAAAACTATATTCCTTATCGATTCAAGTGCATCATGCCGT
TTGTGACGGCTTTCATGTTTGCCTTTTTTGGATGAATTACAAGACTTGCTGAATAAATAAAATCCCAGT
TTGTGCACTGATAAAAACCTTTAGGAACTAAAAGGGCGCAGCTGAATTCGCAAGGTACCCGGGATCCAC
TAGTTCTAGAGCGGCCCGCGATCGCAAGCGATCGCAGGTTATAAACACCCAAGCTCCTTTTTCTTAT
AGCTATAAAGGGTTACTTATATTTTTTCAAATCAAAAACAATATGAAGAATTTAAAAAAGATCCTACAA
AATATGTAGAAGAAAACGAAGCCCAATTTTTAATCCAAAGGAGAAATGATGTTGGCTAAAATGATTTTTTA
ACTCTATATTTAAAAACAATAATCAAAAATTTTTAGCCTTTCTTACTTGTTTTTTAGCCACGCTTTTGCT
CTCTACTATGCTAAATATTACCCTAAGTATAGGTGATGAAGTAACTAAACAACCTAAAAGCTATGGCTCT
AATATCCTTGTTTTACCCAAAGGCTCAAGCCTTAGTATAGAAATAGGTAATGAACTTTATGAACCTTAA
AAAACAAAAACCTACCTAGAAGAAAAAATTTATATATGATTTAAAGACATTTTATTGGCGTAACAACATCAC

Appendix

CGCACTTGCTCCTTTTTTGGAAAGGTAAAATCACAATTGAAAACCTCCCAGCAAAAAGCACTTATTTATGGT
GCTTATTTTCAAAAAGCCATAAAAAATTAAGATGATGATGATTTTATCACAGGTATAAAAAGTCTTTATC
CTTATTTAGCAGTGCAAGGAGAATGGGCAAAAAGATGATAGCAATGAAATCATGCTAGGCGAAGACTTTGC
TAAAAACAATAAACTAAAATTAGGAGATACTATCAAATTCATAGGAGAAAAACAATCAAAGCAAAGAAGCA
AAAATCGTAGGCATTTTACTTCATGCCAATCCTAAAATGTCAAATAAAAATCATCGCTCCTTTAAATTTAG
CTCAAGATTTACTCAACAAAACAAGGGCTTTACTCAAGTACAGAAGTAAGAGCTTTTACCATACCTGAATC
AGCCCTTTCTGAAAAAGTACGTCGCATGGGCGAAGAAAAATTAGATCAGTTAGAATATGACAAATGGTAT
TGCTCAGCTTATGTAGGCTCAATCGCTAGTCAAATTAGCGATGGCTTGCCAGGTGCTGATGCAAAAAGCTC
TAAATGCTATAAGCGATGCTCAAAGCTTGGTGGTTAAAAAGATCCAATCCTTAATGGGCATTACTTGCAT
TATTTGTCTTATTGTTGCAAGTATTGCGATTTCAA

20. Nucleotide sequence of the $\Delta cj1660$ gene of *C. jejuni* NCTC 11168 with *cat* cassette gene from pVA35 plasmid. The turquoise highlight indicates the restriction sites of *Asi*SI enzyme used to cut the plasmid and insert the *cat* cassette, the red highlight indicates the start and stop codon, the bright green highlight indicates *cat* cassette gene that inserted in the deletion site of *cj1660* gene. The whole region is about 3.1kb.

AAGTCCCAAGCAGGATGAAAATTTTATCTCCAATACTGAGTATGAAAAATAAAAAGAAAATTTAAAGGCT
AGAGCTTTAACTCCTTTTTTGTATGATTTTTTAAATTTAGGCAGTACAAGCGGGTGGTTTTAGGCACCTG
ATTTTAGGGCTTTAAAAATCACTAAACCTTTTTTAGAAGTTAAAGAAGGAAGCTTTTCTCTAAATGATTT
TGATGAAAATTCAGCCTTTTTAGGAGTTAATTTAGCCAAGCAACTAGGCCATAAAGCAGGCAATGAACCT
CAAATTTATAATCCAAACAACGGAAAAAGCATAAAAACTTACCATAAAAAGGCATACTTTCAAGCAATGATG
AATTTGATAGCATTGTTTTAGCCCTTTAAGCGTGGTGCAAAAATTTAAGCGATAGAGCCGGTATTAACTA
TGCTAATGCTGTAGTTTATGGAAATTTTATGATGAAGTTAAAGCCAAAAACAAGCAATCAGCAATGAATTC
ATCGATGCAAAACCTATATCTTCAGTATCCTTAAGTGAAGGTTTAGTGCTTGAAAAATCAAAGCTTTAA
TGTTTTTAAATCATACTTGTGGTATTGATCATAGTTACTACTAGCGTTAATACAACCTTAAAGTCTATTAT
ATTTTCTCGCAAAAAGAAATCGCACTGCGCTTTAGCCTTGGGTGCGAAAAAAGTAAAATTTTTAACTT
TTTGCTAGTGAATGCTTTATAGTAAGTTTTTTTTGCTAGTTTAAATCGGAGCTTTTTGTGGGATATTTTTAG
CCAATGTCTTTGGTTATTTAATTTTTAATTTCTAGTATTGATTTTAGATTTATAGCTGTTTTTATAGCCTT
AATCATTCTTTGATTTTTGCCTTTTTGGCTGCATTTTTTCCATAAAAAAGAGCATTAAAAATCAATGTG
TGTGAAAATTTGAAAGGTGAATGATGAAAAAGAAGTTATTTAAATAAAACAATTTAAATAAAGAATTTGG
CAAAGTTAAAGCCTTAAACAATATCAACTTAAGCGTCTATGAAGGAGAATGGCTTGCCATCATGGGTCCA
TCAGGAAGTGAAAATCAACACTTTTAAACATACTATCGCTCATGGATACTCCAAGCTCTGGAGAGTATA
TCTTGGATAATGAAAACCTAGAGCAAATGGATGAAGAGCAAAAAATCACCTTGCGTCGTGAAAAAATAGG
GCTTGTCTTTCAACAATTTTATCTTATCCCCTATCTTAACGCCTTAGAAAATGTTATGCTCTCTCAGTAT
TATCACTCAAGTGTAGATGAAGAAGATGCCAAAATGGTTCTTGAAAAAGTAGGACTTTCGCATAGACTCA
CTCATTTACCTAGCCAATTAAGTGGCGGAGAACAACAAGAGTTTGTATAGCAAGAGCTTTAATCAACAA
CCCAGAGCTTTTACTCGCAGATGAACCCACAGGAAAATTTAGATGAAGCCAATGAACAAATCGTTCTTCAA
ACCTTGCAAAAATTTAAAAATGAAGGTAAAACCATAGTTTTAATCACACACAATCCTGATTTAGCCAAT
TCGCAGATCGAACCTTATCTTACAACATGGGGTGTAAAAATGAAAAAAGCCTTTTTAATCTTAAGCATT
TTGTTTTTACTCAATGCTTGTCTTTTGAATTTCAAAAAGATACTGGAAAAGTTGGAGAAAAAAGCGCTG
AAATTTTCAAGTAAAGATACTTTAGGAAAAGCTGTAAGAACTTGCTGATGATAATACAAGTTTAAAGTCTT
AGTCTTTTTTCAAAAATGGCTGCCCTTCTTGTCTTAAAAGAAGTCCCTTCTTTAGATGAATTCATACAAAAT
CACCCCAATAAAAATCAGTGTTTTATGCTATAAATCCATCGATAATGCCAATGTGGTTAAGGTTATAGCCG
AACAATTTGACTTTAAAAATGTAAGGTTTTTAAAAGACGATCTTAAAAATCACCATGATCGTTACGCTGT
GTTTTGCAACCCCTACTACCATCATCATTAAGATGGGATGATAAAAAGATAGAATTTTAGGAGAAAAACCA
TGGGAATTTTTCGAATCCAAGCTTATTTCTTTGCTTTAATCATAGCTTTATTTTTTGTAGCTTGTGATAG
TGGAGAAAATTTTAAAGCTTTAAATAGCGATAAAAACCTATAAATTTGCCTACAATGGTTTTGAAAAAAGC
CTAAAATAAATGATAAAGCACAAAATTTTGCCTTAGTATTTTTTCAAAAAGATTGCGGAGTTTGCAAAG
AACAAATTCCTATTTTACAGAATTTGGCTAAAAATATGATTTTAAATATCTTTGTGGTTTTTAGGCGATGC
AAACGATGCAACGATGCAAAAAGCTTGGGCTGATGAAAAAGTTTATCTAATTTAGCAATGTTTTATGAA
AAAAGAGCAGCTAAATACCTTTCAAGTGCCATTGGGAAAATATATGGAGTACCTGTGCTTAGTTTTTTTCA

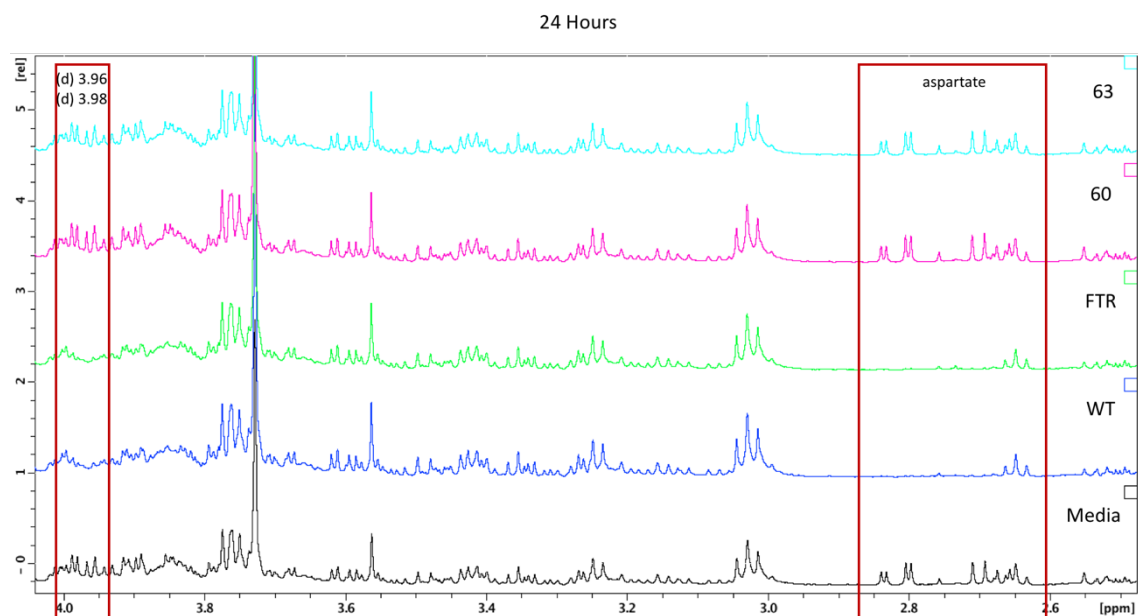
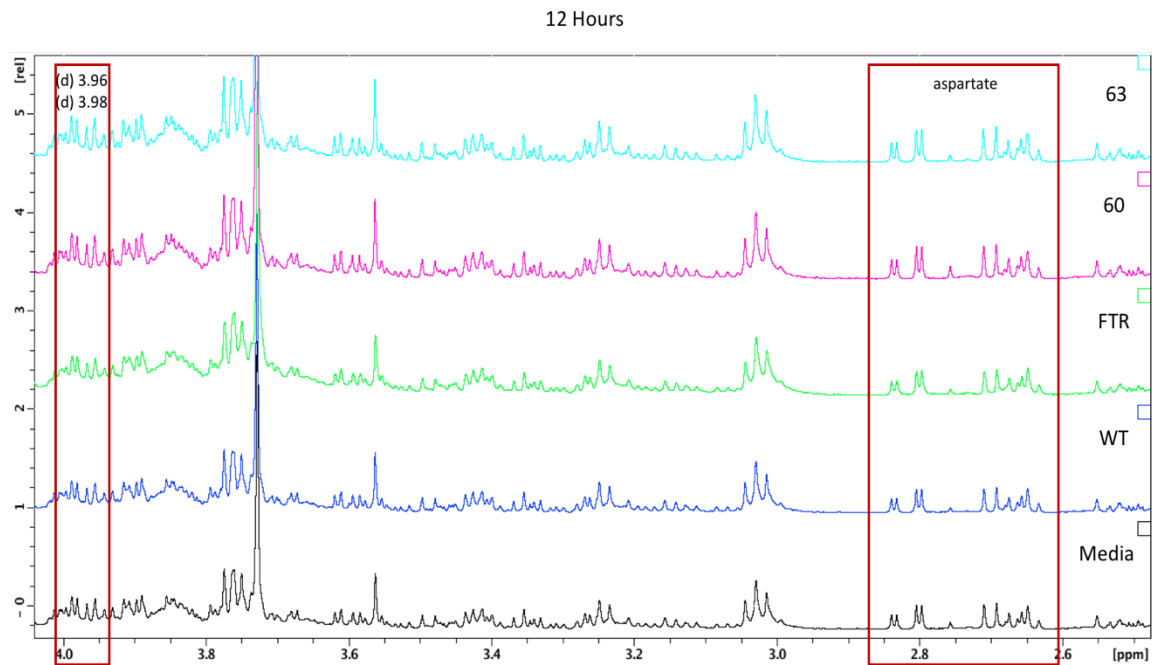
21. Nucleotide sequence of the *cj1663* gene of *C. jejuni* NCTC 11168 with 1 kb upstream and downstream as used in the knockout strategy. The turquoise highlight indicates the primers that used to amplify the region, the red highlight indicates the start and stop codon, the bright green highlight indicates the deleted region from the middle of *cj1663* gene, the dark blue highlight indicates the inverse primers that used to delete the 1 kb of the gene.

AAGTCCCAAGCAGGATGAAAATTTTATCTCCAATACTGAGTATGAAAAAATAAAAAGAAAATTTAAAGGCT
 AGAGCTTTAACTCCTTTTTTGTATGATTTTTTAAATTTAGGCAGTACAAGCGGGGTGGTTTTAGGCCTG
 ATTTTAGGGCTTTAAAAATCACTAAACCTTTTTTAGAAGTTAAAAGAAAGGAGCTTTTCTCTAAATGATTT
 TGATGAAAATTCAGCCTTTTTAGGAGTTAATTTAGCCAAGCAACTAGGCCTAAAAGCAGGCAATGAACCTT
 CAAATTTATAATCCAAACAACGGAAAAAGCATAAAAATTTACCATAAAAAGGCATACTTTCAAGCAATGATG
 AATTTGATAGCATTGTTTTAGCCCCCTTAAGCGTGGTGCAAAAATTTAAGCGATAGAGCCGGTATTAACTA
 TGCTAATGCTGTAGTTTATGGAAAATTTGATGAAGTTAAAGCCAAAACACAAGCAATCAGCAATGAATTC
 ATCGATGCAAAACCTATATCTTCAGTATCCTTAAGTGAAGGTTTAGTGCTTGGAAAAATCAAAGCTTTAA
 TGTTTTTAATCATACTTGTGGTATTGATCATAGTTACTACTAGCGTTAATACAACCTTTAAGTTCTATTAT
 ATTTTCTCGCAAAAAAGAAAATCGCACTGCGTTTAGCCTTGGGTGCGAAAAAAGTGAAATTTTTTAACTT
 TTTGCTAGTGAATGCTTTATAGTAAGTTTTTTGCTAGTTAATCGGAGCTTTTTGTGGGATATTTTTAG
 CCAATGTCTTTGGTTATTTAATTTTTAATTTCTAGTATTTGATTTTAGATTTATAGCTGTTTTTATAGCCTT
 AATCATTCTTTGATTTTTGCCTTTTTGGCTGCATTTTTTCTATAAAAAAGAGCATTAAAAATCAATGTG
 TGTGAAAATTTGAAAGGTGAATGATGAAAAAGAAGTTATTTAAAATAAACAAATTTAAATAAAGAATTTGG
 CAAAGTTAAAGCCTTAAACAATATCAACTTAAGCGTCTGCGATCGCATGCGAATTCCTGCAGCCCGGGG
 ATCCCGGGTACCTGCAGAATTCAGCTGCTCGGCGGTGTTCTTTCCAAGTTAATTGCGTGATATAGATTG
 AAAAGTGGATAGATTTATGATAATAGTGGATAGATTTATGATATAAATGAGTTATCAACAAATCGGAATTTA
 CGGAGGATAAATGATGCAATTCACAAAAGATTGATATAAAATAATTGGACACGAAAAGAGTATTTTCGACCAC
 TATTTTGGCAATACGCCCTGCACATATAGTATGACGGTAAAACTCGATATTTCTAAGTTGAAAAAGGATG
 GAAAAAGTTATAACCAACTCTTTTATATGGAGTTACAACGATCATCAATCGACATGAAGAGTTCAGGAC
 CGCATTAGATGAAAACGGACAGGTAGGCGTTTTTTTTCAGAAATGCTGCCTTGCTACACAGTTTTTTCATAAG
 GAACTGAAACCTTTTTCGAGTATTTGGACTGAGTTTACAGCAGACTATACTGAGTTTCTTCAGAACTATC
 AAAAGGATATAGACGCTTTTTGGTGAACGAATGGGAATGTCCGCAAAGCCTAATCCTCCGAAAAACACTTT
 CCCTGTTTCTATGATACCGTGGACAAGCTTTGAAGGCTTTAACTTAAATCTAAAAAAGGATATGACTAT
 CTAAGTCCGATATTTACGTTTGGGAAGTATTATGAGGAGGGCGGAAAAATACTATATTCCTTTATCGATTC
 AAGTGCATCATGCCGTTTTGTGACGGCTTTTCATGTTTTGCCGTTTTTTTGGATGAATTACAAGACTTGCTGAA
 TAAATAAAATCCCAGTTTGTGCGCACTGATAAAAAACCTTTAGGAACTAAAAGGGCGCAGCTGAATTCGCA
 GGTACCCGGGATCCACTAGTTCTAGAGCGGCCCGCTCGGCGATCGCCAGATCGAACCCTTATCTTACAAC
 ATGGGGTGTAAAATGAAAAAAGCCTTTAATCTTAAGCATTTTGTTTTTACTCAATGCTTGTCTTTTT
 GAAAATTCAAAAGATACTGGAAAAGTTGGAGAAAAAAGCGCTGAAATTTTCAAGTAAAGATACTTTAGGAA
 AAGCTGTAAAAGTGTGATGATAATACAAGTTTAAAAGTCTTAGTCTTTTTTCAAATGGCTGCCCTTC
 TTGCTTAAAAGAACTCCCTTCTTTAGATGAATTCATACAAAATCACCCCAATAAAAATCAGTGTTTATGCT
 ATAAATTCATCGATAATGCCAATGTGGTTAAGGTTTTAGCCGAACAATTTGACTTTAAAAAATGTAAAAG
 TTTTAAAAGACGATCTTAAAATCACCAATGATCGTTACGCTGTGTTTGCACCCTTACTACCATCATCATT
 AAAGATGGGATGATAAAAAGATAGAATTTTAGGAGAAAAACCATGGGAATTTTTTCAAGTCCAAAGCTTATTTT
 TTTGCTTTAATCATAGCTTTATTTTTTGTAGCTTGTGATAGTGGAGAAAAATTTTAAAGCTTTAAATAGCGA
 TAAAACCTATAATTTTGCCTACAATGGTTTTGAAAAAAGCCTAAAACCTAAATGATAAAGCACAAAATTTTG
 CCTTAGTATTTTTTACAAAAGATTGCGGAGTTTGCAAGAACAATTCCTATTTTACAGAATTTGGCTAAA
 AATTATGATTTTAAATATCTTTGTGGTTTTAGGCGATGCAAACGATGCAAACGATGCAAAGCTTGGGCTGA
 TGAAAAAGGTTTTATCTAATTTAGCAATGTTTTATGAAAAAAGAGCAGCTAAATACCTTTCAAGTGCCATTG
 GGGAAATATATGGAGTACCTGTGCTTAGTTTTTTCA

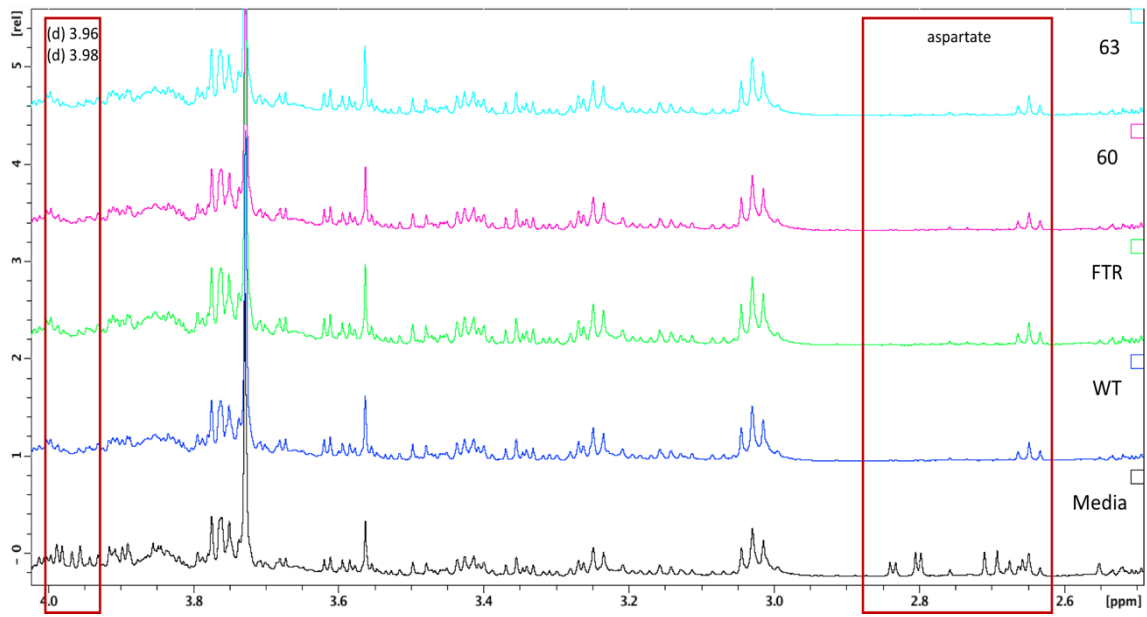
22. Nucleotide sequence of the Δ *cj1663* gene of *C. jejuni* NCTC 11168 with *cat* cassette gene from pVA35 plasmid. The turquoise highlight indicates the restriction sites of *Asi*SI enzyme used to cut the plasmid and insert the *cat* cassette, the red highlight indicates the start

Appendix

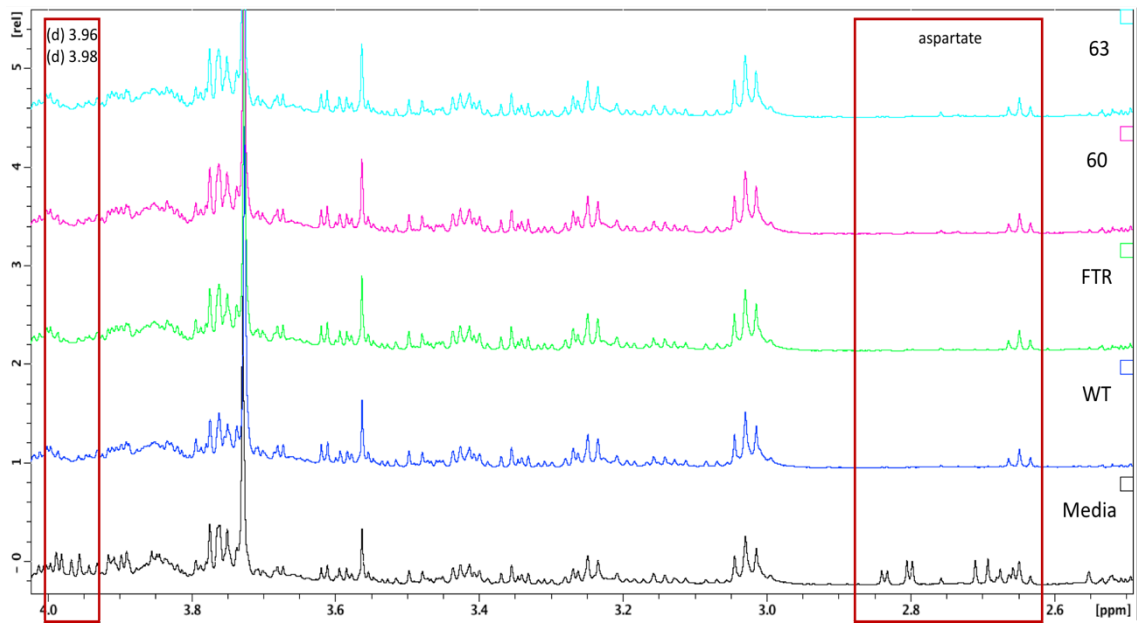
and stop codon, the bright green highlight indicates *cat* cassette gene that inserted in the deletion site of *cj1663* gene. The whole region is about 3.1kb.



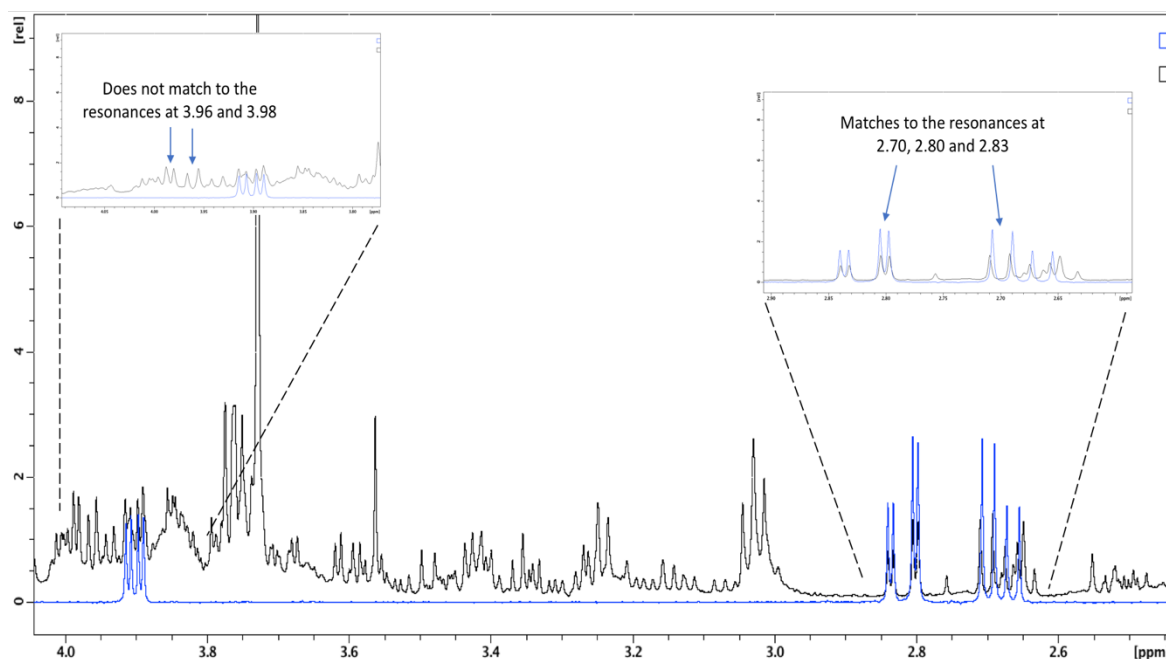
36 Hours



48 Hours



Black = media, Blue = aspartate chemical standard



23. NMR Spectroscopic analysis of the supernatant culture of *C. jejuni*. The analysis is comparison between $\Delta ftr1$, $\Delta cj1660$, and $\Delta cj1663$ mutant strains with the wild type NCTC 11168. There is no difference in the spectra when iron was added, but in the samples without iron there was an interesting change over time. A resonance was expected to be aspartate, was utilised in the W and $\Delta ftr1$ by 24 h but remained in the $\Delta cj1660$, and $\Delta cj1663$ mutants (it was gone at 36 h). The chemical standard of aspartate was run, and it almost entirely matches with what found in the media and the samples except for two resonances which is expected to be aspartate but perhaps attached with something else.